# INSIGHTS IN OBSTETRIC AND PEDIATRIC PHARMACOLOGY: 2021

EDITED BY: Jeffrey Scott Barrett and Catherine M. T. Sherwin
PUBLISHED IN: Frontiers in Pharmacology and Frontiers in Pediatrics

frontiers Research Topics

# frontiers



ISSN 1664-8714
ISBN 978-2-83250-311-9
DOI 10.3389/978-2-83250-311-9

## About Frontiers

Frontiers is more than just an open-access publisher of scholarly articles: it is a pioneering approach to the world of academia, radically improving the way scholarly research is managed. The grand vision of Frontiers is a world where all people have an equal opportunity to seek, share and generate knowledge. Frontiers provides immediate and permanent online open access to all its publications, but this alone is not enough to realize our grand goals.

## Frontiers Journal Series

The Frontiers Journal Series is a multi-tier and interdisciplinary set of open-access, online journals, promising a paradigm shift from the current review, selection and dissemination processes in academic publishing. All Frontiers journals are driven by researchers for researchers; therefore, they constitute a service to the scholarly community. At the same time, the Frontiers Journal Series operates on a revolutionary invention, the tiered publishing system, initially addressing specific communities of scholars, and gradually climbing up to broader public understanding, thus serving the interests of the lay society, too.

## Dedication to Quality

Each Frontiers article is a landmark of the highest quality, thanks to genuinely collaborative interactions between authors and review editors, who include some of the world's best academicians. Research must be certified by peers before entering a stream of knowledge that may eventually reach the public - and shape society; therefore, Frontiers only applies the most rigorous and unbiased reviews.
Frontiers revolutionizes research publishing by freely delivering the most outstanding research, evaluated with no bias from both the academic and social point of view. By applying the most advanced information technologies, Frontiers is catapulting scholarly publishing into a new generation.

## What are Frontiers Research Topics?

Frontiers Research Topics are very popular trademarks of the Frontiers Journals Series: they are collections of at least ten articles, all centered on a particular subject. With their unique mix of varied contributions from Original Research to Review Articles, Frontiers Research Topics unify the most influential researchers, the latest key findings and historical advances in a hot research area! Find out more on how to host your own Frontiers Research Topic or contribute to one as an author by contacting the Frontiers Editorial Office: frontiersin.org/about/contact

# INSIGHTS IN OBSTETRIC AND PEDIATRIC PHARMACOLOGY: 2021

Topic Editors:
**Jeffrey Scott Barrett,** Critical Path Institute, United States
**Catherine M. T. Sherwin,** Wright State University, United States

**Citation:** Barrett, J. S., Sherwin, C. M. T., eds. (2022). Insights in Obstetric and Pediatric Pharmacology: 2021. Lausanne: Frontiers Media SA.
doi: 10.3389/978-2-83250-311-9

# Table of Contents

frontiers | Frontiers in Pharmacology

TYPE Editorial
PUBLISHED 14 September 2022
DOI 10.3389/fphar.2022.995923



OPEN ACCESS

EDITED AND REVIEWED BY
Matitiahu Berkovitch,
Yitzhak Shamir Medical Center, Israel

*CORRESPONDENCE
Jeffrey S. Barrett,
jeff.barrett@aridhia.com

SPECIALTY SECTION
This article was submitted to Obstetric and Pediatric Pharmacology, a section of the journal Frontiers in Pharmacology

RECEIVED 16 July 2022
ACCEPTED 29 July 2022
PUBLISHED 14 September 2022

CITATION
Barrett JS (2022), Editorial: Insights in obstetric and pediatric pharmacology: 2021.
*Front. Pharmacol.* 13:995923.
doi: 10.3389/fphar.2022.995923



# Editorial: Insights in obstetric and pediatric pharmacology: 2021

Jeffrey S. Barrett*

Aridhia Digital Research Environment, Glasgow, United Kingdom

KEYWORDS

**obstetrics, pediatrics, innovation, translational research, collaboaration**

Editorial on the Research Topic
Insights in obstetric and pediatric pharmacology: 2021

Recent years have provided unprecedented opportunities to advance translational science in obstetric and pediatric pharmacology. With our Insights 2021 Research Topic presented herein we also appreciate that there is still much to do. Previous works have pointed out some of the challenges in our domain; many of these relate to the still conservative nature of clinical research in obstetric and pediatric populations and sub-populations (Blehar et al., 2013; Grimsrud et al., 2015) but also include technologies that have yet to expand to accommodate the unique nuances that define these populations (Wancura et al., 2019; Scientific and Technical Advisory Council, 2020) as well as the gaps in physiologic data that needs to be first generated and then shared among the relevant stakeholders (Moya et al., 2014; Chan et al., 2021) in our ecosystem. Fifteen fantastic papers have been accepted in this thematic topic covering a multitude of issues but most highlighting the knowledge gaps that remain and the continued effort required to fill these gaps. Highlighting these submissions are papers that address advances in dried blood spot (DBS) analytical methodologies and their utility in supporting material and fetal sampling in pregnancy studies, physiologically-based PK (PBPK) and population-based PK (PPK) modeling analyses to assess various pregnancy sub-population (e.g., obese pregnant women and pregnant women receiving drug therapy), gene and cell therapy for pediatric patients, and drug metabolism knowledge gaps in pregnant and pediatric populations.

An encouraging theme among these papers is that they not only that they address the aforementioned knowledge gaps, but they all represent building blocks by which future preclinical and clinical investigations in obstetric and pediatric pharmacology can proceed. DBS assays have been around for a long time with many illustrating the benefit in the clinical conduct in obstetric and pediatric clinical trials and still there is a reluctance to invest in the approach prospectively to support new drug research and development due to concerns about transitivity and cross-validation with traditional analytical methodologies and regulatory acceptance (Amini et al., 2021; Blázquez-Gamero et al., 2021). Likewise, PBPK has long been appreciated as a relevant approach to facilitate the design and analysis of obstetric and pediatric pharmacology clinical trials, but few examples have been generated to spur more widespread use and adoption (Gaohua et al., 2012; Zhang et al., 2017) though more recent investigations suggest that their

TABLE 1 Biggest obstacles for obstetric and pediatric pharmacology investigation.

| Obstacle | Current State |
|---|---|
| Empiric dosing practices | While some pediatric centers of excellence are embracing more modern dosing practices including more quantitative approaches to individualized dosing, the default is still empiric-driven at most in-patient settings and certainly the case for outpatients |
| Lack of creative, collaborative, multidisciplinary research approaches | Some positive examples exist but they are typically confined to a few therapeutic areas (e.g., oncology) |
| Reliance on adult drug development experience for dosing, efficacy, and safety expectations for these populations | Clinical development plans for both obstetric and pediatric populations are almost nonexistent unless the target indication is specifically for one or both groups; otherwise plans focus on bridging strategies heavily reliant on the adult (non-pregnant) patient experience |
| Limited consideration of indications that exist only in neonates or during pregnancy | Financial incentives to develop these indications largely do not exist limiting prioritization from would-be developers |
| Lack of biomarkers for these populations | Obviously linked to other factors but despite a well-recognized deficit remains lacking |
| Lagging pharmacoepidemiologic investigations | Access to data challenging; less incentives for planning and operational resources needed |
| Better data bridges to inform decision making | Access and connectivity of data streams not in place; concerns regarding IP and the typical bottlenecks around data sharing |

incorporation into clinical development plans improve both dosing guidance and drug monograph labeling (Coppola et al., 2021; Gill and Jones, 2022). Beyond PBPK, artificial intelligence and machine learning approaches are now being bought to bear in drug development more commonly and regulatory experience is growing with more expanded applications (Liu et al., 2022). Koch et al. remind us that there are opportunities for these newer quantitative approaches to be applied in perinatology, providing an excellent application in the treatment of jaundice in preterm and term neonates.

Therapeutic proteins still represent a gap as a modality for pediatrics and pregnant women though new promising agents in this class provide an opportunity to fill these gaps in addition to benefit patients.

Their development however typically requires some manner of bridging from small molecule experience in these populations. Meibohm paper highlights the knowledge gaps and prioritizes efforts to reduce them for the purpose of accelerating new TP development in these at-risk populations.

Cell and gene therapy for obstetric and pediatric pharmacology populations continues to be an important therapeutic modality requiring additional study. Several critical therapeutic areas including cancer, ischemia, and several rare diseases (Gupta and Anderson, 2014) all represent Frontier areas where translational research is needed for both risk assessment and definition of the therapeutic window for agents under investigation. Currently, there are 3 FDA-approved gene therapies for pediatric patients, but more are in various stages of research and development. Challenges remain including those related to recruiting and educating patients, capital incentives that support the R&D investment, and financial considerations onwhether and how reimbursement of such therapies will be provided. Hence, beyond the drug development challenges, there are concerns about how to appropriately value and benefit from these modalities.

These papers are both timely and clinically relevant in their own right, but they are also likely to be foundational for future work to come. Obstacles remain for obstetric and pediatric pharmacology investigation. Table 1 highlights some of the more commonly identified barriers. Most concerning about the table is that many of the items listed have been identified for some time prompting more serious discussion regarding how we as a community make more substantive progress in some of the core areas centered around education, data sharing, and collaboration. Some progress has been made in fact so we can be encouraged. Recent efforts to support data sharing and collaboration in the rare disease ecosystem bodes well for many of the topics highlighted herein (Larkindale et al., 2022) and recent NICHD grants supporting the collaboration of research projects for obstetric and pediatric patient populations encourage both multidisciplinary collaboration, education, and data sharing (Pawlyk, 2022). Specifically, The Obstetric and Pediatric Pharmacology and Therapeutics Branch of NICHD has established the MPRINT Hub to aggregate, present, and expand the available knowledge, tools, and expertise in maternal and pediatric therapeutics to the broader research, regulatory science, and drug development communities. It will serve as a national resource for conducting and fostering therapeutics-focused research in obstetrics, lactation, and pediatrics while enhancing the inclusion of people with disabilities. Our hope with this Research Topic is that there exists a diverse community of multidisciplinary scientists dedicated to reducing gaps and improving the landscape of obstacles that prohibit progress.

## Author contributions

The author confirms being the sole contributor of this work and has approved it for publication.

## Acknowledgments

Thanks again for the opportunity to present this position to our readership.

## Conflict of interest

Author JB was employed by the company Aridhia Digital Research Environment.

## Publisher's note



## References

Amini, F., Auma, E., Hsia, Y., Bilton, S., Hall, T., Ramkhelawon, L., et al. (2021). Reliability of dried blood spot (DBS) cards in antibody measurement: A systematic review. *PLoS ONE* 16 (3), e0248218. doi:10.1371/journal.pone.0248218

Blázquez-Gamero, D., Sánchez, B., and Folgueira, M. D. (2021). Dried blood spot testing for detection of congenital cytomegalovirus. *JAMA Pediatr.* 175 (8), 865–866. doi:10.1001/jamapediatrics.2021.0755

Blehar, M. C., Spong, C., Grady, C., Goldkind, S. F., Sahin, L., and Clayton, J. A. (2013). Enrolling pregnant women: Issues in clinical research. *Womens Health Issues* 23 (1), e39–45. doi:10.1016/j.whi.2012.10.003

Chan, G. J., Daniel, J., Getnet, M., Kennedy, M., Olowojesiku, R., Hunegnaw, B. M., et al. (2021). Gaps in maternal, newborn, and child health research: A scoping review of 72 years in Ethiopia. *J. Glob. Health Rep.* 5, e2021033. doi:10.29392/001c.22125

Coppola, P., Kerwash, E., and Cole, S. (2021). Physiologically based pharmacokinetics model in pregnancy: A regulatory perspective on model evaluation. *Front. Pediatr.* 9, 687978. doi:10.3389/fped.2021.687978

Gaohua, L., Abduljalil, K., Jamei, M., Johnson, T. N., and Rostami-Hodjegan, A. (2012). A pregnancy physiologically based pharmacokinetic (p-PBPK) model for disposition of drugs metabolized by CYP1A2, CYP2D6 and CYP3A4. *Br. J. Clin. Pharmacol.* 74 (5), 873–885. doi:10.1111/j.1365-2125.2012.04363.x

Gill, K. L., and Jones, H. M. (2022). Opportunities and challenges for PBPK model of mAbs in paediatrics and pregnancy. *AAPS J.* 24, 72. doi:10.1208/s12248-022-00722-0

Grimsrud, K. N., Sherwin, C. M., Constance, J. E., Tak, C., Zuppa, A. F., Spigarelli, M. G., et al. (2015). Special population considerations and regulatory affairs for clinical research. *Clin. Res. Regul. Aff.* 32 (2), 47–56. doi:10.3109/10601333.2015.1001900

Gupta, A., and Anderson, S. (2014). Cell and gene therapy: Overview, current landscape and future trends. *J. Precis. Med.* 11. https://www.thejournalofprecisionmedicine.com/the-journal-of- precision-medicine/cell-and-gene-therapy-overview-current-landscape-and-future-trends/.

Larkindale, J., Betourne, A., Borens, A., Boulanger, V., Theurer Crider, V., Gavin, P., et al. (2022). Innovations in therapy development for rare diseases through the rare disease cures accelerator-data and analytics platform. *Ther. Innov. Regul. Sci.* 56, 768–776. doi:10.1007/s43441-022-00408-x

Liu, Q., Huang, R., Hsieh, J., Zhu, H., Tiwari, M., Liu, G., et al. (2022). Landscape analysis of the application of artificial intelligence and machine learning in regulatory submissions for drug development from 2016 to 2021. *Clin. Pharmacol. Ther.* 2022, 16. Epub ahead of print. PMID: 35707940. doi:10.1002/cpt.2668

Moya, J., Phillips, L., Sanford, J., Wooton, M., Gregg, A., and Schuda, L. (2014). A review of physiological and behavioral changes during pregnancy and lactation: Potential exposure factors and data gaps. *J. Expo. Sci. Environ. Epidemiol.* 24 (5), 449–458. doi:10.1038/jes.2013.92

Pawlyk, A. (2022). *Maternal and pediatric precision in therapeutics (MPRINT) Hub, NIH, obstetric and pediatric pharmacology and therapeutics Branch*. https://www.nichd.nih.gov/about/org/der/branches/opptb/mprint#.

Scientific and technical advisory Council (STAC) of the special journals publisher (SJP): Research design innovations in obstetrics, gynecology, and pediatrics. *Special J. Obstetrics, Gynecol. Pediatr. [SJ-OGPAPR]*, 2020; 1 (1):1–21.

Wancura, M., McCracken, J. M., Steen, E., Cosgriff-Hernandez, E., Keswani, S., and Hakim, J. C. (2019). Emerging technologies in pediatric gynecology: New paradigms in women's health care. *Curr. Opin. Obstet. Gynecol.* 31 (5), 309–316. doi:10.1097/GCO.0000000000000563

Zhang, Z., Imperial, M. Z., Patilea-Vrana, G. I., Wedagedera, J., Gaohua, L., and Unadkat, J. D. (2017). Development of a novel maternal-fetal physiologically based pharmacokinetic model I: Insights into factors that determine fetal drug exposure through simulations and sensitivity analyses. *Drug Metab. Dispos.* 45, 920–938. doi:10.1124/dmd.117.075192

frontiers in Pharmacology

SYSTEMATIC REVIEW
published: 12 August 2021
doi: 10.3389/fphar.2021.725126

# Treatment of Kawasaki Disease: A Network Meta-Analysis of Four Dosage Regimens of Aspirin Combined With Recommended Intravenous Immunoglobulin

*Ying-Hua Huang[1], Yi-Chen Hsin[2], Liang-Jen Wang[3], Wei-Ling Feng[1], Mindy Ming-Huey Guo[1], Ling-Sai Chang[1*†], Yu-Kang Tu[4*†] and Ho-Chang Kuo[1*†]*

[1]Department of Pediatrics and Kawasaki Disease Center, Kaohsiung Chang Gung Memorial Hospital, Chang Gung University College of Medicine, Kaohsiung, Taiwan, [2]Department of Pediatric Allergy, Immunology, and Rheumatology, Division of Pediatrics, Chang Gung Memorial Hospital, Taoyuan, Taiwan, [3]Department of Child and Adolescent Psychiatry, Kaohsiung Chang Gung Memorial Hospital and Chang Gung University College of Medicine, Kaohsiung, Taiwan, [4]Institute of Epidemiology and Preventive Medicine, College of Public Health, National Taiwan University, Taipei, Taiwan

OPEN ACCESS

**Edited by:**
Catherine M. T. Sherwin,
Wright State University, United States

**Reviewed by:**
Elena Y. Enioutina,
The University of Utah, United States
Caren Lee Hughes,
Mayo Clinic Florida, United States

***Correspondence:**
Ling-Sai Chang
joycejohnsyoko@gmail.com
Yu-Kang Tu
yukangtu@ntu.edu.tw
Ho-Chang Kuo
erickuo48@yahoo.com.tw

†These authors have contributed equally to this work

**Specialty section:**
This article was submitted to Obstetric and Pediatric Pharmacology, a section of the journal Frontiers in Pharmacology

**Received:** 14 June 2021
**Accepted:** 03 August 2021
**Published:** 12 August 2021

**Citation:**
Huang Y-H, Hsin Y-C, Wang L-J, Feng W-L, Guo MM-H, Chang L-S, Tu Y-K and Kuo H-C (2021) Treatment of Kawasaki Disease: A Network Meta-Analysis of Four Dosage Regimens of Aspirin Combined With Recommended Intravenous Immunoglobulin. Front. Pharmacol. 12:725126. doi: 10.3389/fphar.2021.725126

Aspirin was once believed to reduce the mortality of Kawasaki disease (KD) due to its effect on the thrombotic occlusion of coronary arteries. However, conflicting evidence has been found regarding aspirin treatment and its benefit in patients with acute KD. We compared the efficacy of different aspirin doses in acute KD. A literature search of PubMed, EMBASE, and Cochrane databases was conducted to identify studies comparing different doses of aspirin for acute KD. The primary outcome of interest was coronary artery lesions (CAL). We used random-effects network meta-analysis. Six retrospective studies, including 1944 patients receiving aspirin in doses of 0, 3–5, 30–50, or 80–100 mg/kg/day, were selected. The risks of CAL were not significantly different for the various doses of aspirin compared to the placebo: odds ratio (OR) was 1.10 [95% confidence interval (CI): 0.70–1.71] for patients with aspirin 3–5 mg/kg/day; OR = 1.23 (95% CI: 0.67–2.26) for aspirin 30–50 mg/kg/day, and OR = 1.59 (95% CI: 0.74, 3.421) for 80–100 mg/kg/day. The P-score ranged from 0.76 for placebo to 0.19 for aspirin 80–100 mg/kg/day. The different doses of aspirin exhibited no significant difference with regard to the efficacy of CAL or with the secondary outcomes of intravenous immunoglobulin resistance or hospital stays for acute KD. Therefore, we found that treatment without any aspirin is not inferior to other doses of aspirin and can also slightly reduce the risk of CAL.

**Keywords: acetylsalicylic acid, aspirin, Kawasaki disease or Kawasaki syndrome, mucocutaneous lymph node syndrome, salicylate**

## INTRODUCTION

Pediatrician Kawasaki Tomisaku first published a report in 1967 on about 50 patients who presented with persistent fever, rash, lymphadenopathy, edema of the limbs, conjunctival injection, redness, and cracking of the lips, strawberry tongue, and convalescent desquamation (Kawasaki, 1967). Since then, acute febrile infantile mucocutaneous lymph node syndrome has also been referred to as Kawasaki disease (KD) because this distinct clinical entity had never been clearly defined before

(Tanaka, 1975). The correlation between KD and coronary vasculitis was later established, with KD being classified as a type of medium vasculitis in a symposium held on systemic vasculitis held at Chapel Hill, North Carolina in 1994 (Burns, 2018). Histopathological investigation of the vascular findings in autopsies of KD patients with sudden cardiac death also demonstrated coronary arteritis (Roberts and Fetterman, 1963; Kushner and Abramowsky, 2010).

The treatment guidelines published by the American Heart Association in 2017 recommend that the standard treatment for acute-phase KD was high-dose intravenous immunoglobulin (IVIG) (level of evidence A) plus acetylsalicylic acid (aspirin) (level of evidence C) (McCrindle et al., 2017). However, the reason for recommending aspirin use is actually because the experimental group and the control group often use the same dose of aspirin in clinical trials, which has prevented clinicians from truly clarifying the aspirin that KD patients genuinely need. Appropriate treatment can reduce coronary artery aneurysm incidence on the 30th day. A single dose of IVIG >1 g/kg is more effective than multiple doses of IVIG for preventing 30 days of coronary artery aneurysm (Durongpisitkul et al., 1995). IVIG >1 g/kg plus ≤ 80 mg/kg/day aspirin is as effective as IVIG >1 g/kg plus aspirin >80 mg/kg/day in preventing coronary artery aneurysm (Durongpisitkul et al., 1995). The effect of preventing coronary artery aneurysm is proportional to the total dose of IVIG, which means that the total dose of 2 g/kg of IVIG is best (Terai and Shulman, 1997). Under the same IVIG dose, no statistical difference has been found in the effectiveness of aspirin at 30–50 mg/kg/day and aspirin at 80–120 mg/kg/day in preventing coronary artery abnormalities (Terai and Shulman, 1997). Due to the continued recommendation of aspirin, analysis in the relevant literature regarding aspirin not being used in the acute phase of KD is lacking.

In contrast, despite a lack of evidence provided by randomized control trials (RCT), traditional high-dose aspirin was considered to have no significant therapeutic effect in a 10-years retrospective study of 260 KD children (Platt et al., 2020). However, understanding the preventive effect of low-dose aspirin on coronary artery lesions (CAL) is still necessary (Chiang et al., 2020). Kuo et al. are currently conducting a comparative study on the effectiveness of IVIG alone and high-dose aspirin (80–100 mg/kg/day) as treatment in the acute phase of KD. The study has been designed as a multi-center, prospective, randomized controlled double-blind trial with two parallel groups to determine whether IVIG alone as the main treatment for acute KD is as effective as the combined treatment with high-dose aspirin. The endpoint of said trial is the formation of CAL observed at 6–8 weeks (Kuo et al., 2018).

According to previous studies by Kuo et al., using high-dose aspirin (80–100 mg/kg/day) in the acute phase of KD has demonstrated no significant benefit, and the incidence of CAL and the number of days of hospitalization between high and low-dose aspirin also showed no significant difference. However, high-dose aspirin has affected the recovery of hemoglobin. The results of this study revealed the controversy over high-dose aspirin use in the acute phase of KD (Kuo et al., 2015). In a retrospective study with a large sample size, the use of aspirin was most prone to side effects related to the digestive system (5.3% among 910 KD patients) (Huang et al., 2018). Bleeding in the upper and lower gastrointestinal tract and abnormal liver function have been reported, and symptoms of abdominal discomfort may also appear in patients treated with aspirin (Matsubara et al., 1996; Zheng et al., 2019; Mammadov et al., 2020). Asthma caused by aspirin was also a suspected reason for the increase in the risk of asthma following KD (Kawane et al., 1996; Van Bever et al., 2004; Huang et al., 2020).

In the plan of a RCT, due to sample size considerations, designing multiple arms with four commonly used doses (placebo, 3–5, 30–50, 80–100 mg/kg/day) was impractical and not feasible. Furthermore, several meta-analysis comparisons consisted primarily of low- and high-dose comparisons (Zheng et al., 2019; Chiang et al., 2020; Jia et al., 2020). We still do not know whether aspirin is necessary for treating KD in the acute phase or the best dose of treatment, so the diagnosis and treatment guidelines are currently incapable of providing appropriate recommendations based on evidence (McCrindle et al., 2017). Therefore, it is necessary to use network meta-analysis to compare the effects of various commonly used treatment doses of aspirin administered in conjunction with 2 g/kg IVIG.

## MATERIALS AND METHODS

This network meta-analysis was reported in accordance with the general principles of the Preferred Reporting Items for Systematic Reviews and Meta-Analysis (PRISMA) extension to network meta-analysis (Hutton et al., 2015). We adopted a population–intervention–comparison–outcome framework for study inclusion in order to describe the treatment of acute Kawasaki disease, the impact of aspirin by dose plus 2 g/kg IVIG in the therapeutic outcomes of CAL, IVIG resistance, and hospital stays.

### Search Strategy

For our comprehensive search, we systematically scanned the following databases from inception to April 30, 2021: Cochrane Database of Systematic Reviews ($n$ = 3), Embase ($n$ = 3,573), and Pubmed ($n$ = 973). Our search strategy was developed in Pubmed with input from the review team. The Medical Subject Headings (MeSH) used in the search strategy included [Mucocutaneous Lymph Node Syndrome (MeSH Terms) OR Kawasaki disease OR Kawasaki syndrome] AND [aspirin (MeSH Terms) OR acetylsalicylic acid OR salicylate]. Searches were not limited by language or study design. The Pubmed strategy was also applied to all the other resources searched. Search results were imported into EndNote X9 (Clarivate Analytics, Philadelphia, PA, United States) and de-duplicated.

We carried out a search for studies of different aspirin doses and updated searches as necessary. In view of limitations on time and resources, we decided to identify studies by specifically searching relevant systematic reviews and meta-analyses.

Studies were initially assessed for relevance using titles and abstracts. When possible, we obtained full manuscripts of any titles/abstracts that appeared to be relevant, and two reviewers independently assessed the relevance of each study.

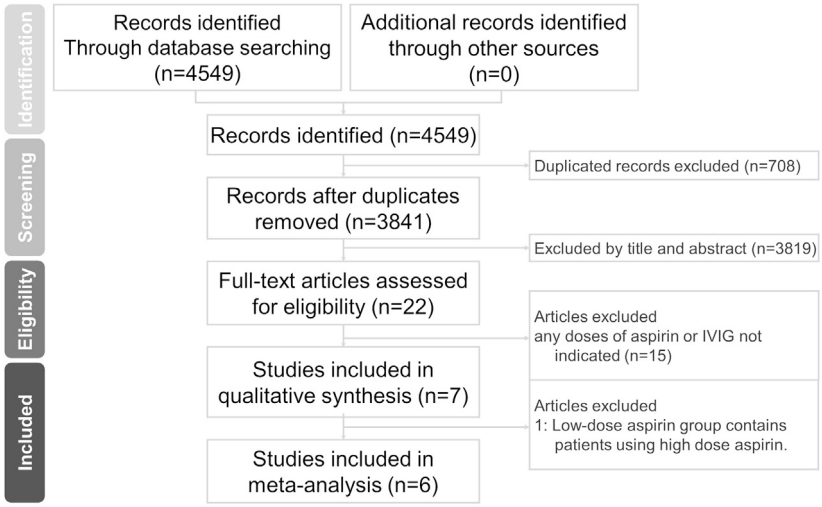


**FIGURE 1 |** Preferred Reporting Items for Systematic Reviews and Meta-Analyses (PRISMA) flow diagram of the study search and selection process. IVIG, intravenous immunoglobulin.

Relevant studies were evaluated for quality, and key outcome data were extracted. The outcome measures to be considered included the incidence of CAL as the primary outcome, with IVIG resistance and hospital stays as secondary outcomes. The incidence of CAL was assessed through echocardiograph. All coronary artery abnormalities, including either small aneurysm or dilatation, were considered CAL. If the same study had two CAL definition methods, we recorded the stricter and more consolidated one. Using a standardized data form in Microsoft Excel, two reviewers (LSC and YHH) independently extracted and tabulated data for study quality, intervention characteristics, participants, and outcomes from the final list of selected eligible studies. If any discrepancies were observed between the studies selected by the same investigators, a third investigator (YCH) was involved through consensus.

## Selection Criteria and Data Analysis

When sufficient data were available for quantitative assessment, we applied a network meta-analysis (NMA). The population of interest focused on human studies in which all subjects were diagnosed with KD. For all doses of aspirin in the acute phase of KD, we performed a NMA for relevant comparators among aspirin 0, 3–5, 30–50, and 80–100 mg/kg/day. Evidence on combined treatments (e.g., 2 g/kg IVIG plus indicated aspirin doses) was considered for inclusion. The acute phase of KD was defined as the period that started at the febrile phase after KD was diagnosed and ended with defervescence according to the American Heart Association (McCrindle et al., 2017). We did not consider other studies using any doses of aspirin or IVIG that were not indicated as part of the NMA.

We conducted random effects NMA by using R software's "netmeta" package. The estimates of effectiveness relative to the reference treatment were summarized using odds ratio with accompanying 95% confidence intervals (CI) for CAL and IVIG resistance. The estimates of effectiveness were measured using mean differences with accompanying 95% CI for our NMA on days of hospital stays. The treatments were ranked using P-score. Where possible, consistency between direct and indirect estimates of treatment effect in the NMA was assessed using the design-by-treatment interaction model and node-splitting model (Yu-Kang, 2016). The quality of the nonunionized studies included in the meta-analyses was determined using the Newcastle-Ottawa Scale (NOS) (Baumer et al., 2006). Using said scale, studies that scored at least five stars were considered to have moderate to high methodological quality. Quality assessment was undertaken by one investigator and then independently checked by a second investigator.

$I^2$ values can range from 0 to 100%; a value greater than 75% represents high heterogeneity, while one less than 25% suggests low heterogeneity (Jia et al., 2020).

# RESULTS

The electronic database searches and manual search of reference lists from published reviews for clinical effectiveness evidence on different aspirin doses (i.e., 0, 3–5, 30–50, 80–100 mg/kg/day) yielded a total of 3,841 abstracts published between 1978 and 2021 after de-duplication between databases (**Figure 1**). We had obtained full papers and checked reference lists from records that were potentially relevant systematic reviews or meta-analyses (Durongpisitkul et al., 1995; Terai and Shulman, 1997; Baumer et al., 2006; Ho and Curtis, 2017; Zheng et al., 2019; Chiang et al., 2020; Jia et al., 2020). A total of 3,819 studies were ruled out after screening the titles and abstracts.

Of these, 22 studies underwent a further full-text review for eligibility, and six retrospective comparative studies ultimately met our inclusion criteria. The study by Dallaire was eliminated from the analysis since it included 24/365 subjects with aspirin dose >10 mg/kg/day in the low-dose aspirin group after excluding patients without IVIG (Dallaire et al., 2017). A small number of patients also received steroid or infliximab treatment. Ito et al.

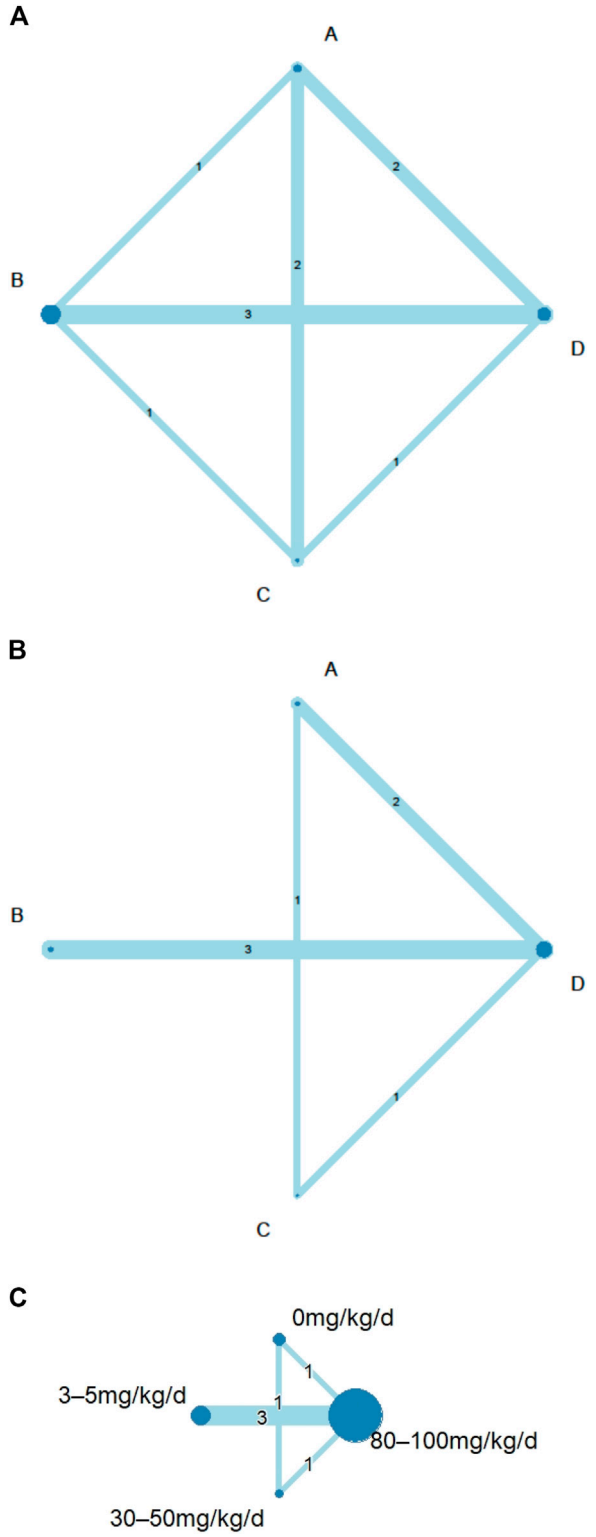


**FIGURE 2 |** Network geometry of eligible comparisons among different doses of aspirin for: **(A)** consistency analyses of coronary artery lesions (CAL) rate by node-split model; **(B)** intravenous immunoglobulin (IVIG) resistance rate; **(C)** length of hospital stays. Network diagrams were produced with

(*Continued*)

**FIGURE 2 |** node size corresponding to the number of included studies and the line width representing the number of included studies comparing the interventions. The number of direct comparisons was expressed as a number in the middle of a line between nodes. **(A)** aspirin 0 mg/kg/day; **(B)**, 3–5 mg/kg/day; **(C)**, 30–50 mg/kg/day; **(D)**, 80–100 mg/kg/day; d, day.

compared aspirin 30 mg/kg/day along with 2 g/kg IVIG to 50 mg/kg/day combined the same IVIG dose (Ito et al., 2020). Kim et al. compared two groups between KD patients with aspirin 3–5 and ≥30 mg/kg/day (Kim et al., 2017). All subjects were prescribed 2 g/kg IVIG. Kuo et al. defined high-dose aspirin >30 mg/kg/day and compared it with no aspirin use (Kuo et al., 2015). The patients were treated with a single dose of IVIG (2 g/kg). Another dual-center retrospective study by Kuo et al. compared the therapeutic effects of high-dose aspirin >50 mg/kg/day and low-dose 3–5 mg/kg/day (Kuo et al., 2012). All patients in both groups were treated with the standard care of IVIG. In the study by Platt et al., 10 mg/kg/day was regarded as the cut-off value for high and low doses of aspirin (Platt et al., 2020). Most patients received the Privigen brand of IVIG. Studies by Akagi, Koren, Saulsbury, Wang, and others all had KD patients treated with IVIG at doses other than 2 g/kg (Koren et al., 1985a; Akagi et al., 1990; Akagi et al., 1991; Saulsbury, 2002; Wang et al., 2020). Akagi et al. investigated the therapeutic efficacy of 100 vs. 30 mg/kg/day aspirin (Akagi et al., 1990). Koren et al. compared whether KD patients with and without aspirin 80–180 mg/kg/day developed coronary artery aneurysms (Koren et al., 1985a). In the study by Saulsbury et al., patients receiving IVIG were divided into 400 mg/kg for four consecutive days or a single infusion of 2 g/kg, and aspirin treatment was divided into 80–100 or 3–5 mg/kg/day (Saulsbury, 2002). The retrospective study of Wang et al. divided aspirin into the following three groups: 20–29, 30–39, and 40–50 mg/kg/day (Wang et al., 2020). Migally et al. did not clearly define what dose patients without high-dose aspirin received, while patients who did not receive IVIG were also included in the study (Migally et al., 2018). Studies performed before the beginning or suggestion of IVIG treatment were excluded (Yokoyama et al., 1980; Koren et al., 1985b; Ichida et al., 1987). This study did not exclude any papers from its analysis for the reason that the full-text data was not available.

In total, the included studies consisted of 1944 participants that we divided into four unique doses (**Figure 2**). The list of the final subset is summarized in **Table 1**. The studies were conducted primarily in Asia, with the following breakdown: Korea ($n$ = 2), Japan ($n$ = 1), China ($n$ = 1), Iran ($n$ = 1), and Canada ($n$ = 1) (Lee et al., 2013; Rahbarimanesh et al., 2014; Amarilyo et al., 2017; Dhanrajani et al., 2018; Huang et al., 2018; Kwon et al., 2020). Two of the studies investigated three different doses, whereas the other studies investigated only two different doses.

## Coronary Artery Lesions

All doses of aspirin had a similar effect on CAL outcome. We did not detect significant inconsistencies in the evidence networks for any of the secondary outcomes. Applying a random-effects model, the results for all the individual treatment comparisons

**TABLE 1 |** Study characteristics and information of the six included studies.

| References first author year published | Country and number of centers | Study characteristic | Endpoints | Total number of patients | Aspirin mg/kg/day | Age (months) | Male (%) | NOS |
|---|---|---|---|---|---|---|---|---|
| Kwon et al., 2020 (Kwon et al., 2020) | Korea One | retrospective cohort | CAL<br>IVIG R<br>Hospital stays | 323 | 0<br>30–50<br>80–100 | 39.6<br>34.2<br>32.8 | 55.6<br>59.3<br>68 | 7 |
| Huang et al., 2018 (Huang et al., 2018) | China One | retrospective cohort | CAL | 910 | 0<br>3–5<br>30–50 | 22.8<br>23.7<br>25.8 | 67<br>63<br>69 | 8 |
| Dhanrajani et al., 2018 (Dhanrajani et al., 2018) | Canada Two | retrospective chart review | CAL<br>IVIG R<br>Hospital stays | 242 | 3–5<br><br>80–100 | 33<br><br>36 | 59<br><br>58.3 | 7 |
| Amarilyo et al., 2017 (Amarilyo et al., 2017) | Israel<br>Six | retrospective, cohort study | CAL<br>IVIG R<br>Hospital stays | 220 | 3–5<br><br>80–100 | 34.8<br><br>28.8 | 65.1<br><br>63.5 | 6 |
| Rahbarimanesh et al., 2014 (Rahbarimanesh et al., 2014) | Iran One | Not reported | CAL<br>IVIG R<br>Hospital stays | 69 | 3–5<br>80–100 | — | — | 4 |
| Lee et al., 2013 (Lee et al., 2013) | Korea One | Not reported | CAL<br>IVIG R | 180 | 0<br>80–100 | 30.7<br>30.2 | 58.82<br>55.81 | 6 |

*CAL, coronary artery lesions; IVIG R, resistance to intravenous immunoglobulin; NOS, Newcastle-Ottawa Scale.*

(both direct and indirect), are shown in **Figure 3**. No significant difference was noted between 30–50 mg/kg/day (compared to placebo, OR = 1.23, 95% CI: 0.67–2.26) and between 80–100 mg/kg/day and placebo (OR = 1.59, 95% CI: 0.74–3.42). An $I^2$ statistic of 0% indicated that heterogeneity was low for the included studies. No inconsistency was observed between direct and indirect comparisons in the loop-specific analysis of CAL ($p$ = 0.8072). Furthermore, one of the retrospective comparative studies was rated as four stars and was considered to be of low quality, while the other five reports were awarded ≧ six stars and qualified as having high quality.

## IVIG Resistance

IVIG-resistant KD patients are defined as patients that need to be treated again. Possible options are a second dose of IVIG, infliximab, or intravenous pulse methylprednisolone (Chan et al., 2019). Re-treatment prolongs the length of hospital stay and costs and is also a risk factor for CAL (Chang et al., 2020). The evidence basis of our NMA consisted of five studies involving 1,179 children (**Figure 2**). Compared to placebo, any aspirin given to KD patients, such as 3–5, 30–50, and 80–100 mg/kg/day, showed a decreasing trend in the prevalence of IVIG resistance, but its CI overlapped with the null effect of one. Regarding IVIG resistance, no meaningful risk difference was identified among these four groups. Aspirin 3–5, 30–50, and 80–100 mg/kg/day were found to be comparable to placebo (**Figure 3**). We conducted pairwise meta-analysis for the different aspirin regimens based on dosing (**Supplementary Table S1**). Among the interventions, aspirin 30–50 mg/kg/day ranked highest for the prevention of IVIG resistance, followed by 80–100, 3–5 mg/kg/day, and the placebo. An $I^2$ statistic of 75.5% indicated substantial heterogeneity in this model. Visual inspection for publication bias, which was detected using funnel plots, demonstrated asymmetry in **Figure 4**.

## Length of Hospitalization

Four studies with a total of 999 participants reported the duration of hospital stay (**Figure 2**). The mean duration of hospital stays ranged from 7.3 days in the aspirin 80–100 group compared to the 3–5 mg/kg/day group in the study by Amarilyo et al. to 4.1 days in the 3–5 mg/kg/day group compared to aspirin 80–100 in the study by Dhanrajani et al. (**Supplementary Table S2**). KD patients using aspirin 3–5 mg/kg/day showed the shortest hospital stays. Compared to placebo, the combination of aspirin 3–5 mg/kg/day and IVIG showed a mean difference (MD) of −0.22 days (95% CI: −3.62, 3.18) for hospital stays. Upon analyzing the individual studies, the MD in length of hospitalization was not statistically significant for any of the direct comparisons; by evaluating the MD values for each comparison, all confidence intervals crossed the zero value (**Figure 3** and **Supplementary Table S3**). Evaluating the P-score, the values ranged from 0.6853 for aspirin 30–50 mg/kg/day to 0.2840 for aspirin 3–5 mg/kg/day (**Supplementary Table S4**). After applying a random-effects model, the results for all the individual treatment comparisons (both direct and indirect), are shown in **Figure 3**, **Supplementary Table S3**, and **Supplementary Figure S1**. Visual inspection of the symmetrical funnel plot of hospital stays indicated no publication bias (**Figure 4**).

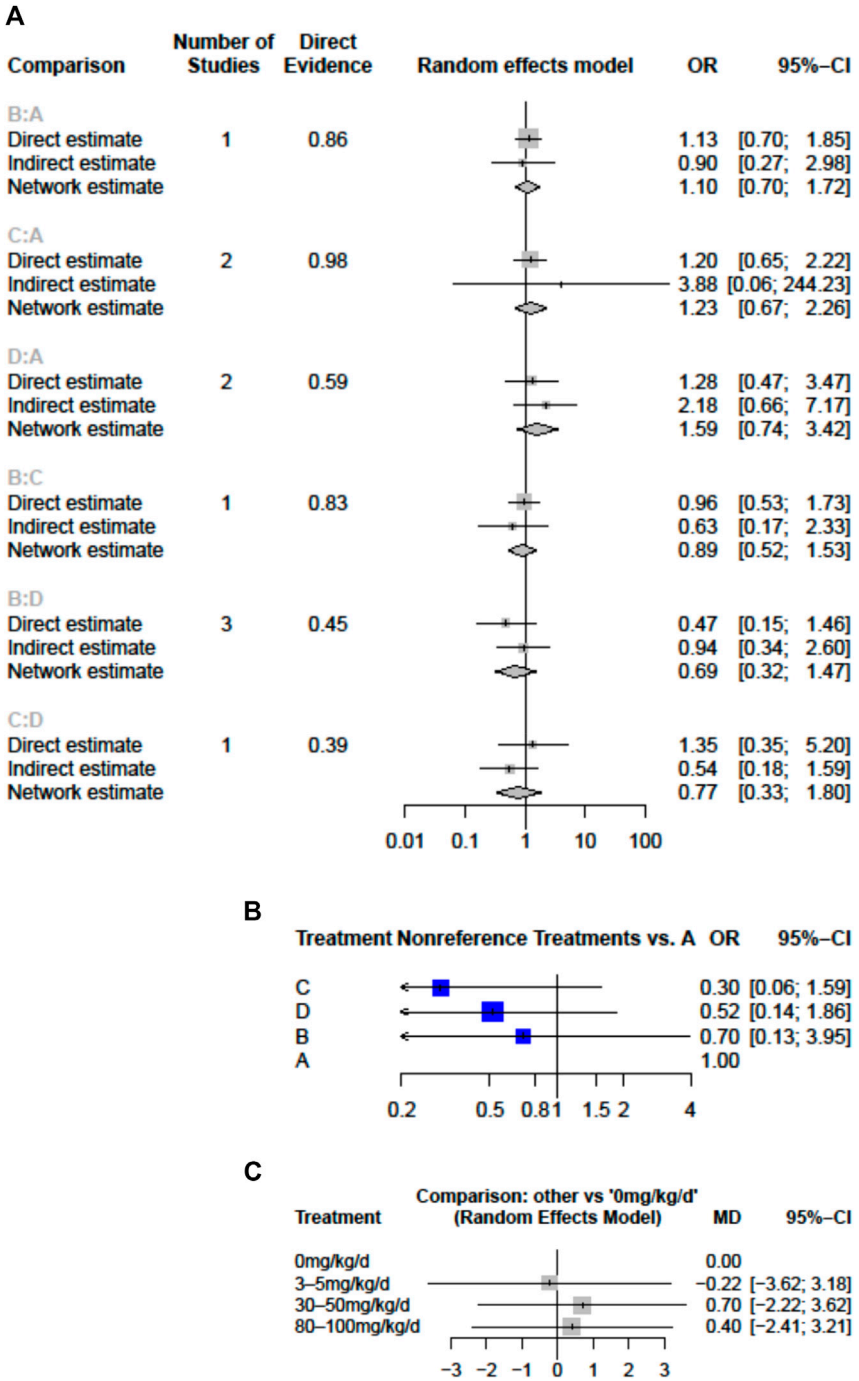


**FIGURE 3 |** Forest plots of network meta-analysis for the effects of aspirin doses on **(A)** the risk of coronary artery lesions (CAL) **(B)** the risk of intravenous immunoglobulin (IVIG) resistance **(C)** hospital stays (mean difference in days) **(A)**, aspirin 0 mg/kg/day **(B)**, 3–5 mg/kg/day **(C)**, 30–50 mg/kg/day; D, 80–100 mg/kg/day; CI, confidence interval; d, day; OR, odds ratio.

In comparing moderate doses (30–50 mg/kg/day) and high doses (80–100), the length of hospital stay at a moderate dose was slightly higher by MD 0.30 (−2.22–2.82) (**Supplementary Table S3**). However, the risk of CAL (OR, 0.77; 95% CI 0.33–1.80) and the chance of needing to be treated again due to IVIG resistance (**Supplementary Table S1**) were both slightly lower in KD patients who received moderate-dose aspirin treatment. The comparison of 0 and 3–5 mg/kg/day (low dose) and 30–50 and 80–100 mg/kg/day (high dose) of aspirin found that the risks of CAL and IVIG resistance did not differ significantly.

In summary, from P-scores and forest plots, 3–5 mg/kg/day aspirin can numerically reduce the length of hospital stays.

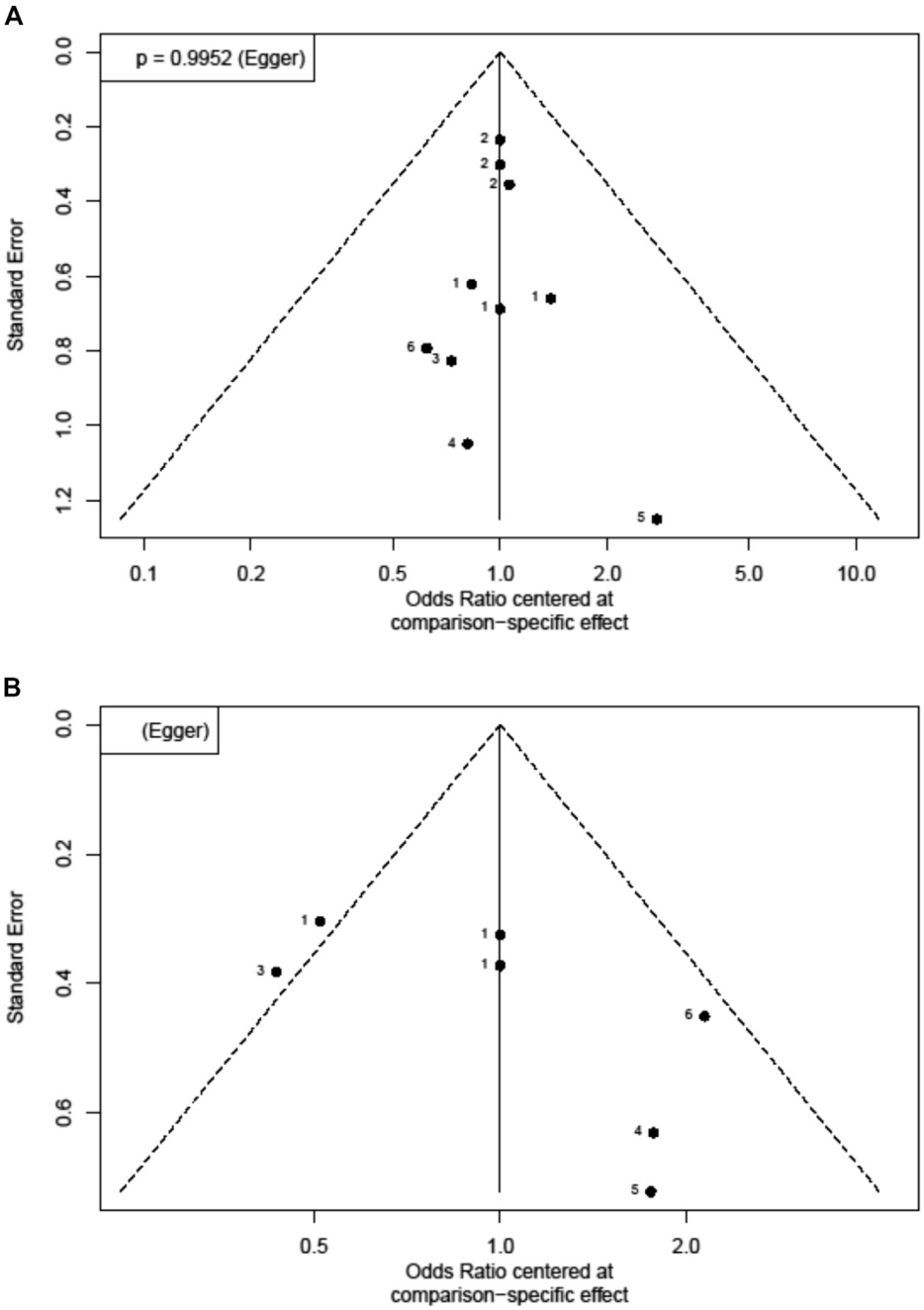


**FIGURE 4 |** Funnel plots for each outcome. Each dot reflects a study; the *y*-axis reflects the sample size or standard error, and the *x*-axis reflects the effect size of each study. Large studies are distributed in the top of the plot, and smaller studies are scattered toward the bottom of the plot **(A)** risk of coronary artery lesions (CAL) **(B)** risk of intravenous immunoglobulin (IVIG) resistance **(C)** length of hospital stays.

However, the data did not reach statistical differences. The mean difference of the length of hospital stay was small, i.e., less than 1 day.

## DISCUSSION

To the best of our knowledge, this study is the first to identify effects of different aspirin doses with regard to CAL, IVIG resistance, and hospital stays in KD using NMA. Although aspirin has been widely used in the treatment of KD, no optimal dose has yet been confirmed. Studies have found that KD children with aspirin 80–100 mg/kg/day had a lower risk of developing refractory KD and tend to have shorter fever duration (Lee et al., 2013; Dhanrajani et al., 2018). Ito and his colleague investigated KD outcomes for aspirin 30 and 50 mg/kg/day, respectively. The risk of refractory KD in the 30 mg/kg/day

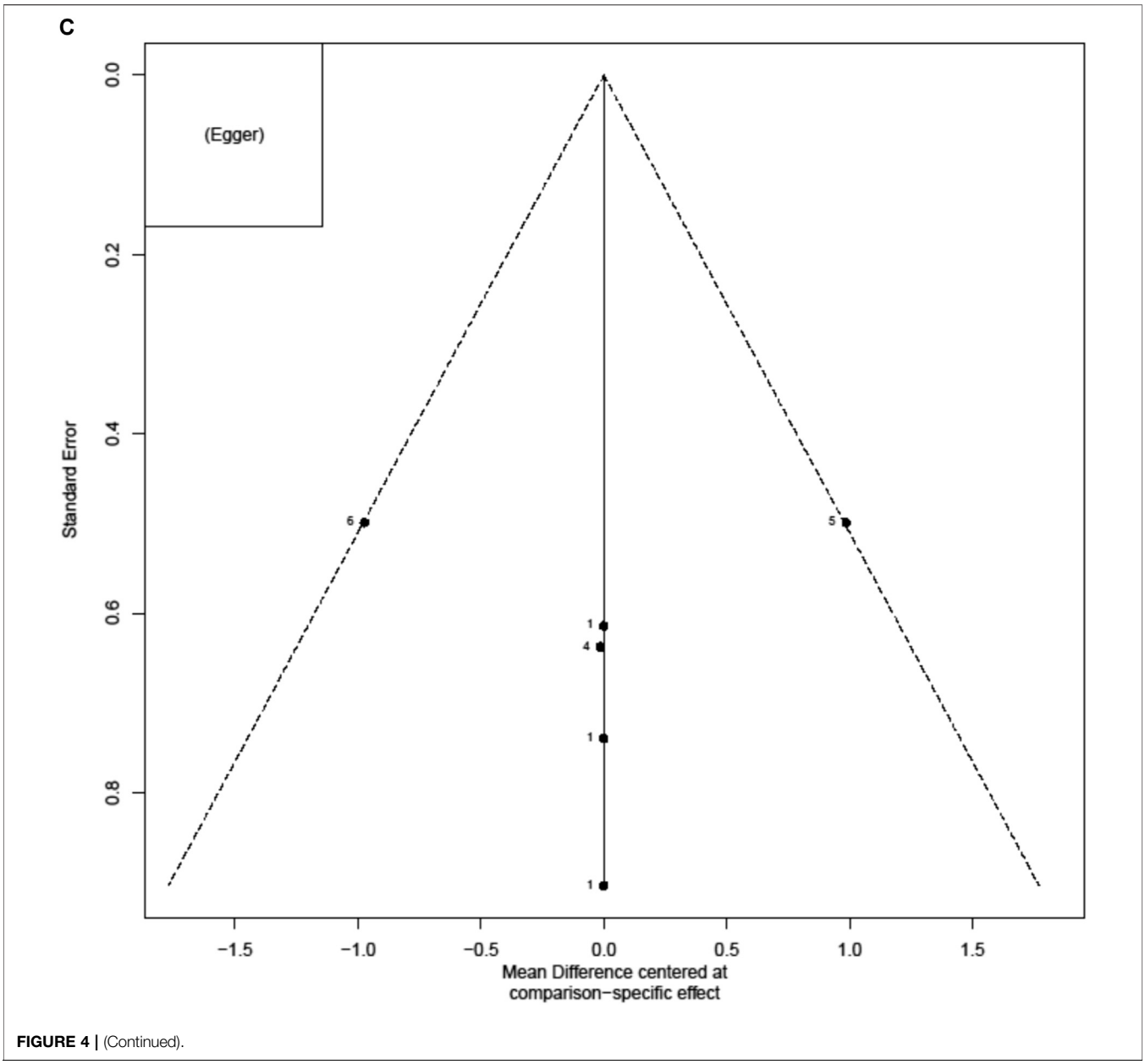


**FIGURE 4 |** (Continued).

aspirin group was significantly higher than the 50 mg/kg/day aspirin (odds ratio 1.379, $p = 0.021$). Even when the difference in aspirin is only 20 mg/kg/day, different therapeutic effects may be obtained. Because many studies have not strictly defined the dose of aspirin, a robust comparison of these different doses remains incomplete.

In previous studies, results showing aspirin efficacy for KD have varied. The use of moderate-dose aspirin has been recommended because no aspirin may be associated with a higher chance of receiving a second treatment, and 80–100 mg/kg/day aspirin may have life-threatening side effects (One patient complicated with Reye's syndrome died) (Kwon et al., 2020). Moderate or high-dose aspirin was unable to reduce the CAL risk in KD children compared to 3–5 mg/kg/day aspirin in the retrospective Korean nationwide survey (Kim et al., 2017). In accordance with our analysis, it has been suggested that aspirin <10 mg/kg/day combined with IVIG may be as effective as aspirin ≥10 or >30 mg/kg/day plus IVIG (Jia et al., 2020; Platt et al., 2020). In addition, prescribing low-dose 3–5 mg/kg/day or no aspirin for the initial treatment of KD may be associated with a decreased incidence of CAL compared to aspirin ≥30 mg/kg/day (Zheng et al., 2019; Chiang et al., 2020; Jia et al., 2020).

The mechanism of action of low-dose aspirin is anti-platelet aggregation, which employs the irreversible inhibition of platelet cyclooxygenase to prevent arachidonic acid from converting into thromboxane A2, thus reducing platelet aggregation and release response. Regarding KD treatment, high-dose aspirin was administered from 80 to 100 mg/kg/day in the US to

30–50 mg/kg/day in Japan and then changed to low-dose aspirin, 3–5 mg/kg/day, 48 h after defervescence for 6–8 weeks (Chang et al., 2017). The mechanisms of action of high-dose aspirin greater than 30 mg/kg/day are anti-inflammatory, analgesic, and antipyretic (Kato et al., 1979). Aspirin inhibits cyclooxygenase in a similar manner as other NSAIDs, while high-dose aspirin in particular inhibits the cyclooxygenase vinylation of the arterial wall and interferes with the production of powerful vasodilators and platelet aggregation inhibitor prostacyclin. Prostaglandin and thromboxane B2 (TxB2) were significantly decreased after treatment with an aspirin dose of 30 mg/kg/day (Sasai, 1988; Tanoshima et al., 2019). The TxB2/6-keto- prostaglandin F1 (PGF1) ratio was decreased with the aspirin dose of 2–5 mg/kg ($p < 0.05$) (Tanoshima et al., 2019). Akagi et al. found that high-dose aspirin therapy (100 mg/kg/day) may be disadvantageous as anti-thrombotic treatment because the surveyed plasma TxB2 production, which was completely blocked in patients with aspirin doses of 30 or 100 mg/kg/day, and plasma 6-keto-PGF1 alpha levels in patients with 100 mg/kg/day on day 14 were lower than those in patients with an aspirin does of 30 mg/kg/day (Akagi et al., 1990). An investigation of eicosanoid metabolism identified significantly lower TxB2 in KD patients with aspirin doses of 30 or 60 mg/kg/kg compared with no aspirin (Fulton et al., 1988). Salicylate bioavailability correlated to serum concentrations was impaired during the acute phase and then significantly increased during the subacute phase. Remarkably lower serum albumin concentrations resulted in decreased protein binding in the acute phase and more free salicylates (Koren et al., 1988; Koren et al., 1991). Aspirin doses lower than 80 mg/kg/day could not reach the therapeutic concentration; meanwhile, more than a quarter of patients with aspirin >120 mg/kg/day exceeded toxic concentration (Koren and MacLeod, 1984). Another route of aspirin dose above 100 mg/kg/day with intravenous administration posed a beneficial anti-inflammatory effect (Umezawa et al., 1992). However, aspirin may cause stomach bleeding, especially when combined with alcoholic beverages. Combined with chickenpox or influenza, aspirin can cause Reye's syndrome, which has a mortality rate of up to 30% (Matsumoto et al., 2020). Furthermore, in patients with favism, aspirin may cause hemolytic anemia (Chen et al., 2014).

This NMA had several limitations. First, due to the different definitions of fever reduction (calculated from the beginning of IVIG treatment or the end of treatment), the comparison of the NMA was not possible (Lee et al., 2013; Rahbarimanesh et al., 2014; Kwon et al., 2020). Second, due to the retrospective study design, estimating the adverse effects of aspirin was difficult, so this NMA could not compare the adverse effects of different doses of aspirin. Furthermore, pharmacogenomic differences among patients of different races could have been a confounding variable (Mallah et al., 2020).

The body of evidence on the clinical effectiveness and safety of different aspirin doses is small, especially with regard to a lack of RCT, but our NMA indicates similar effects among different aspirin doses in their influence of KD prognosis. Our review does not support using low-dose (3–5 mg/kg/day), moderate (30–50 mg/kg/day), or high-dose (80–100 mg/kg/day) aspirin in the acute phase of KD. Similar to the conclusion of Hsieh et al., no aspirin is not inferior to other doses of aspirin and can also slightly reduce the risk of CAL (Hsieh et al., 2004). Further prospective RCT studies are warranted to confirm the efficacy and adverse events of different doses of aspirin treatment for acute KD.

## DATA AVAILABILITY STATEMENT

The original contributions presented in the study are included in the article/**Supplementary Material**, further inquiries can be directed to the corresponding authors.

## AUTHOR CONTRIBUTIONS

Conceptualization, L-SC and H-CK; Methodology, Y-KT; Validation, Y-KT; Formal Analysis, L-SC, W-LF, and Y-HH; Writing – Original Draft Preparation, Y-HH; Writing – Review & Editing, M-HG., H-CK, and Y-KT; Visualization, Y-CH; Supervision, L-JW; Funding Acquisition, L-SC and Y-HH. All authors have drafted the work or substantively revised it, have approved the submitted version, and agree to be personally accountable for the authors' own contributions and for ensuring resolution of questions related to the accuracy or integrity of any part of the work.

## FUNDING

This study was supported in part by the Chang Gung Memorial Hospital (CFRPG8J0141, CMRPG8K0642) and the Ministry of Science and Technology, Taiwan (110-2635-B-182A-004). However, these institutions had no role in the study design, data collection and analysis, decision to publish, or preparation of the manuscript. Thanks to Chih-Wei Hsu for providing the PRISMA picture.

## SUPPLEMENTARY MATERIAL

The Supplementary Material for this article can be found online at: https://www.frontiersin.org/articles/10.3389/fphar.2021.725126/full#supplementary-material

## REFERENCES

Akagi, T., Kato, H., Inoue, O., and Sato, N. (1990). A Study on the Optimal Dose of Aspirin Therapy in Kawasaki Disease. Clinical Evaluation and Arachidonic Acid Metabolism. *Kurume Med. J.* 37, 203–208. doi:10.2739/kurumemedj.37.203

Akagi, T., Kato, H., Inoue, O., and Sato, N. (1991). Salicylate Treatment in Kawasaki Disease: High Dose or Low Dose?. *Eur. J. Pediatr.* 150, 642–646. doi:10.1007/bf02072625

Amarilyo, G., Koren, Y., Brik Simon, D., Bar-Meir, M., Bahat, H., Helou, M. H., et al. (2017). High-dose Aspirin for Kawasaki Disease: Outdated Myth or Effective Aid?. *Clin. Exp. Rheumatol.* 35 Suppl 103 (Suppl. 103), 209–212.

Baumer, J. H., Love, S., Gupta, A., Haines, L., Maconochie, I. K., and Dua, J. S. (2006). Salicylate for the Treatment of Kawasaki Disease in Children. *Cochrane database Syst. Rev.*, Cd004175. doi:10.1002/14651858.CD004175.pub2

Burns, J. C. (2018). History of the Worldwide Emergence of Kawasaki Disease. *Int. J. Rheum. Dis.* 21, 13–15. doi:10.1111/1756-185x.13214

Chan, H., Chi, H., You, H., Wang, M., Zhang, G., Yang, H., et al. (2019). Indirect-comparison Meta-Analysis of Treatment Options for Patients with Refractory Kawasaki Disease. *BMC Pediatr.* 19, 158. doi:10.1186/s12887-019-1504-9

Chang, L.-S., Hsu, Y.-W., Lu, C.-C., Lo, M.-H., Hsieh, K.-S., Li, S.-C., et al. (2017). CYP2E1 Gene Polymorphisms Related to the Formation of Coronary Artery Lesions in Kawasaki Disease. *Pediatr. Infect. Dis. J.* 36, 1039–1043. doi:10.1097/inf.0000000000001657

Chang, L.-S., Lin, Y.-J., Yan, J.-H., Guo, M. M.-H., Lo, M.-H., and Kuo, H.-C. (2020). Neutrophil-to-lymphocyte Ratio and Scoring System for Predicting Coronary Artery Lesions of Kawasaki Disease. *BMC Pediatr.* 20, 398. doi:10.1186/s12887-020-02285-5

Chen, C.-H., Lin, L.-Y., Yang, K. D., Hsieh, K.-S., and Kuo, H.-C. (2014). Kawasaki Disease with G6PD Deficiency-Report of One Case and Literature Review. *J. Microbiol. Immunol. Infect.* 47, 261–263. doi:10.1016/j.jmii.2012.05.002

Chiang, M.-H., Liu, H. E., and Wang, J.-L. (2020). Low-dose or No Aspirin Administration in Acute-phase Kawasaki Disease: a Meta-Analysis and Systematic Review. *Arch. Dis. Child.* 106, 662–668. doi:10.1136/archdischild-2019-318245

Dallaire, F., Fortier-Morissette, Z., Blais, S., Dhanrajani, A., Basodan, D., Renaud, C., et al. (2017). Aspirin Dose and Prevention of Coronary Abnormalities in Kawasaki Disease. *Pediatrics* 139, e20170098. doi:10.1542/peds.2017-0098

Dhanrajani, A., Chan, M., Pau, S., Ellsworth, J., Petty, R., and Guzman, J. (2018). Aspirin Dose in Kawasaki Disease: The Ongoing Battle. *Arthritis Care Res.* 70, 1536–1540. doi:10.1002/acr.23504

Durongpisitkul, K., Gururaj, V. J., Park, J. M., and Martin, C. F. (1995). The Prevention of Coronary Artery Aneurysm in Kawasaki Disease: a Meta-Analysis on the Efficacy of Aspirin and Immunoglobulin Treatment. *Pediatrics* 96, 1057–1061.

Fulton, D. R., Meissner, H. C., and Peterson, M. B. (1988). Effects of Current Therapy of Kawasaki Disease on Eicosanoid Metabolism. *Am. J. Cardiol.* 61, 1323–1327. doi:10.1016/0002-9149(88)91177-0

Ho, L. G. Y., and Curtis, N. (2017). What Dose of Aspirin Should Be Used in the Initial Treatment of Kawasaki Disease?. *Arch. Dis. Child.* 102, 1–1182. doi:10.1136/archdischild-2017-313538

Hsieh, K.-S., Weng, K.-P., Lin, C.-C., Huang, T.-C., Lee, C.-L., and Huang, S.-M. (2004). Treatment of Acute Kawasaki Disease: Aspirin's Role in the Febrile Stage Revisited. *Pediatrics* 114, e689–e693. doi:10.1542/peds.2004-1037

Huang, P.-Y., Huang, Y.-H., Guo, M. M.-H., Chang, L.-S., and Kuo, H.-C. (2020). Kawasaki Disease and Allergic Diseases. *Front. Pediatr.* 8, 614386. doi:10.3389/fped.2020.614386

Huang, X., Huang, P., Zhang, L., Xie, X., Xia, S., Gong, F., et al. (2018). Is Aspirin Necessary in the Acute Phase of Kawasaki Disease?. *J. Paediatr. Child. Health* 54, 661–664. doi:10.1111/jpc.13816

Hutton, B., Salanti, G., Caldwell, D. M., Chaimani, A., Schmid, C. H., Cameron, C., et al. (2015). The PRISMA Extension Statement for Reporting of Systematic Reviews Incorporating Network Meta-Analyses of Health Care Interventions: Checklist and Explanations. *Ann. Intern. Med.* 162, 777–784. doi:10.7326/m14-2385

Ichida, F., Fatica, N. S., Engle, M. A., O'Loughlin, J. E., Klein, A. A., Snyder, M. S., et al. (1987). Coronary Artery Involvement in Kawasaki Syndrome in Manhattan, New York: Risk Factors and Role of Aspirin. *Pediatrics* 80, 828–835.

Ito, Y., Matsui, T., Abe, K., Honda, T., Yasukawa, K., Takanashi, J.-i., et al. (2020). Aspirin Dose and Treatment Outcomes in Kawasaki Disease: A Historical Control Study in Japan. *Front. Pediatr.* 8, 249. doi:10.3389/fped.2020.00249

Jia, X., Du, X., Bie, S., Li, X., Bao, Y., and Jiang, M. (2020). What Dose of Aspirin Should Be Used in the Initial Treatment of Kawasaki Disease? A Meta-Analysis. *Rheumatology (Oxford, England)* 59, 1826–1833. doi:10.1093/rheumatology/keaa050

Kato, H., Koike, S., and Yokoyama, T. (1979). Kawasaki Disease: Effect of Treatment on Coronary Artery Involvement. *Pediatrics* 63, 175–179.

Kawane, H., Tamaoki, J., Chiyotani, A., Sakai, A., Takemura, H., and Konno, K. (1996). Menthol and Aspirin-Induced Asthma. *Respir. Med.* 90, 247. doi:10.1016/S0954-6111(96)90300-5

Kawasaki, T. (1967). [Acute Febrile Mucocutaneous Syndrome with Lymphoid Involvement with Specific Desquamation of the Fingers and Toes in Children]. *Arerugi* 16, 178–222.

Kim, G. B., Yu, J. J., Yoon, K. L., Jeong, S. I., Song, Y. H., Han, J. W., et al. (2017). Medium- or Higher-Dose Acetylsalicylic Acid for Acute Kawasaki Disease and Patient Outcomes. *J. Pediatr.* 184, 125–129. doi:10.1016/j.jpeds.2016.12.019

Koren, G., and MacLeod, S. M. (1984). Difficulty in Achieving Therapeutic Serum Concentrations of Salicylate in Kawasaki Disease. *J. Pediatr.* 105, 991–995. doi:10.1016/S0022-3476(84)80097-9

Koren, G., Rose, V., Lavi, S., and Rowe, R. (1985). Probable Efficacy of High-Dose Salicylates in Reducing Coronary Involvement in Kawasaki Disease. *Jama* 254, 767–769. doi:10.1001/jama.254.6.767

Koren, G., Rose, V., Lavi, S., and Rowe, R. (1985). Probable Efficacy of High-Dose Salicylates in Reducing Coronary Involvement in Kawasaki Disease. *J. Am. Med. Assoc.* 254, 767–769. doi:10.1001/jama.254.6.767

Koren, G., Schaffer, F., Silverman, E., Walker, S., Duffy, C., Stein, L., et al. (1988). Determinants of Low Serum Concentrations of Salicylates in Patients with Kawasaki Disease. *J. Pediatr.* 112, 663–667. doi:10.1016/s0022-3476(88)80194-x

Koren, G., Silverman, E., Sundel, R., Edney, P., Newburger, J. W., Klein, J., et al. (1991). Decreased Protein Binding of Salicylates in Kawasaki Disease. *J. Pediatr.* 118, 456–459. doi:10.1016/s0022-3476(05)82168-7

Kuo, H.-C., Guo, M. M.-H., Lo, M.-H., Hsieh, K.-S., and Huang, Y.-H. (2018). Effectiveness of Intravenous Immunoglobulin Alone and Intravenous Immunoglobulin Combined with High-Dose Aspirin in the Acute Stage of Kawasaki Disease: Study Protocol for a Randomized Controlled Trial. *BMC Pediatr.* 18, 200. doi:10.1186/s12887-018-1180-1

Kuo, H.-C., Lo, M.-H., Hsieh, K.-S., Guo, M. M.-H., and Huang, Y.-H. (2015). High-Dose Aspirin Is Associated with Anemia and Does Not Confer Benefit to Disease Outcomes in Kawasaki Disease. *PloS one* 10, e0144603, doi:10.1371/journal.pone.0144603

Kuo, H. C., Liang, C. D., Yang, K. D., Huang, S. M., Hwang, D. C., Lin, C. C., et al. (2012). High-dose Aspirin in Acute Kawasaki Disease. *Pediatr. Int.* 54, 115. doi:10.1111/j.1442-200X.2012.03535.x

Kushner, H. I., and Abramowsky, C. R. (2010). An Old Autopsy Report Sheds Light on a "new" Disease: Infantile Polyarteritis Nodosa and Kawasaki Disease. *Pediatr. Cardiol.* 31, 490–496. doi:10.1007/s00246-009-9625-9

Kwon, J. E., Roh, D. E., and Kim, Y. H. (2020). The Impact of Moderate-Dose Acetylsalicylic Acid in the Reduction of Inflammatory Cytokine and Prevention of Complication in Acute Phase of Kawasaki Disease: The Benefit of Moderate-Dose Acetylsalicylic Acid. *Children* 7, 185. doi:10.3390/children7100185

Lee, G., Lee, S. E., Hong, Y. M., and Sohn, S. (2013). Is High-Dose Aspirin Necessary in the Acute Phase of Kawasaki Disease?. *Korean Circ. J.* 43, 182–186. doi:10.4070/kcj.2013.43.3.182

Mallah, N., Zapata-Cachafeiro, M., Aguirre, C., Ibarra-García, E., Palacios–Zabalza, I., Macías-García, F., et al. (2020). Influence of Polymorphisms Involved in Platelet Activation and Inflammatory Response on Aspirin-Related Upper Gastrointestinal Bleeding: A Case-Control Study. *Front. Pharmacol.* 11, 860. doi:10.3389/fphar.2020.00860

Mammadov, G., Liu, H. H., Chen, W. X., Fan, G. Z., Li, R. X., Liu, F. F., et al. (2020). Hepatic Dysfunction Secondary to Kawasaki Disease: Characteristics, Etiology and Predictive Role in Coronary Artery Abnormalities. *Clin. Exp. Med.* 20, 21–30. doi:10.1007/s10238-019-00596-1

Matsubara, T., Mason, W., Kashani, I. A., Kligerman, M., and Burns, J. C. (1996). Gastrointestinal Hemorrhage Complicating Aspirin Therapy in Acute Kawasaki Disease. *J. Pediatr.* 128, 701–703. doi:10.1016/S0022-3476(96)80140-5

Matsumoto, K., Hasegawa, S., Nakao, S., Shimada, K., Mukai, R., Tanaka, M., et al. (2020). Assessment of Reye's Syndrome Profile with Data from the US Food and Drug Administration Adverse Event Reporting System and the Japanese Adverse Drug Event Report Databases Using the Disproportionality Analysis. *SAGE Open Med.* 8, 205031212097417. doi:10.1177/2050312120974176

McCrindle, B. W., Rowley, A. H., Newburger, J. W., Burns, J. C., Bolger, A. F., Gewitz, M., et al. (2017). Diagnosis, Treatment, and Long-Term Management of Kawasaki Disease: A Scientific Statement for Health Professionals from the

American Heart Association. *Circulation* 135, e927–e999. doi:10.1161/cir.0000000000000484

Migally, K., Braunlin, E. A., Zhang, L., and Binstadt, B. A. (2018). Duration of High-Dose Aspirin Therapy Does Not Affect Long-Term Coronary Artery Outcomes in Kawasaki Disease. *Pediatr. Res.* 83, 1136–1145. doi:10.1038/pr.2018.44

Platt, B., Belarski, E., Manaloor, J., Ofner, S., Carroll, A. E., John, C. C., et al. (2020). Comparison of Risk of Recrudescent Fever in Children with Kawasaki Disease Treated with Intravenous Immunoglobulin and Low-Dose vs High-Dose Aspirin. *JAMA Netw. Open* 3, e1918565, doi:10.1001/jamanetworkopen.2019.18565

Rahbarimanesh, A., Taghavi-Goodarzi, M., Mohammadinejad, P., Zoughi, J., Amiri, J., and Moridpour, K. (2014). Comparison of High-Dose versus Low-Dose Aspirin in the Management of Kawasaki Disease. *Indian J. Pediatr.* 81, 1403. doi:10.1007/s12098-014-1437-0

Roberts, F. B., and Fetterman, G. H. (1963). POLYARTERITIS NODOSA IN INFANCY. *J. Pediatr.* 63, 519–529. doi:10.1016/s0022-3476(63)80361-3

Sasai, K. (1988). [Plasma PGE2, TXB2 and 6-keto PGF1 Alpha Levels in Patients with Kawasaki Disease]. *Arerugi* 37, 952–958.

Saulsbury, F. T. (2002). Comparison of High-Dose and Low-Dose Aspirin Plus Intravenous Immunoglobulin in the Treatment of Kawasaki Syndrome. *Clin. Pediatr. (Phila)* 41, 597–601. doi:10.1177/000992280204100807

Tanaka, N. (1975). Kawasaki Disease (Acute Febrile Infantile Muco-Cutaneous Lymph Node Syndrome) in Japan: Relationship with Infantile Periarteritis Nodosa. *Pathologia et microbiologia* 43, 204–218. doi:10.1159/000162822

Tanoshima, R., Hashimoto, R., Suzuki, T., Ishiguro, A., and Kobayashi, T. (2019). Effectiveness of Antiplatelet Therapy for Kawasaki Disease: a Systematic Review. *Eur. J. Pediatr.* 178, 947–955. doi:10.1007/s00431-019-03368-x

Terai, M., and Shulman, S. T. (1997). Prevalence of Coronary Artery Abnormalities in Kawasaki Disease Is Highly Dependent on Gamma Globulin Dose but Independent of Salicylate Dose. *J. Pediatr.* 131, 888–893. doi:10.1016/s0022-3476(97)70038-6

Umezawa, T., Matsuo, N., and Saji, T. (1992). Treatment of Kawasaki Disease Using the Intravenous Aspirin Anti-inflammatory Effect of Salicylate. *Pediatr. Int.* 34, 584–588. doi:10.1111/j.1442-200x.1992.tb01013.x

Van Bever, H. P., Quek, S. C., and Lim, T. (2004). Aspirin, Reye Syndrome, Kawasaki Disease, and Allergies; a Reconsideration of the Links. *Arch. Dis. Child.* 89, 1178. doi:10.1136/adc.2004.055681

Wang, J., Chen, H., Shi, H., Zhang, X., Shao, Y., Hang, B., et al. (2020). Effect of Different Doses of Aspirin on the Prognosis of Kawasaki Disease. *Pediatr. Rheumatol.* 18, 48. doi:10.1186/s12969-020-00432-x

Yokoyama, T., Kato, H., and Ichinose, E. (1980). Aspirin Treatment and Platelet Function in Kawasaki Disease. *Kurume Med. J.* 27, 57–61. doi:10.2739/kurumemedj.27.57

Yu-Kang, T. (2016). Node-Splitting Generalized Linear Mixed Models for Evaluation of Inconsistency in Network Meta-Analysis. *Value in Health* 19, 957–963. doi:10.1016/j.jval.2016.07.005

Zheng, X., Yue, P., Liu, L., Tang, C., Ma, F., Zhang, Y., et al. (2019). Efficacy between Low and High Dose Aspirin for the Initial Treatment of Kawasaki Disease: Current Evidence Based on a Meta-Analysis. *PloS one* 14, e0217274, doi:10.1371/journal.pone.0217274

**Conflict of Interest:** The authors declare that the research was conducted in the absence of any commercial or financial relationships that could be construed as a potential conflict of interest.

**Publisher's Note:** All claims expressed in this article are solely those of the authors and do not necessarily represent those of their affiliated organizations, or those of the publisher, the editors and the reviewers. Any product that may be evaluated in this article, or claim that may be made by its manufacturer, is not guaranteed or endorsed by the publisher.

frontiers in Pharmacology

BRIEF RESEARCH REPORT
published: 22 September 2021
doi: 10.3389/fphar.2021.752022

# Neonatal Feeding Trajectories in Mothers With Bipolar Disorder Taking Lithium: Pharmacokinetic Data

*Maria Luisa Imaz[1,2], Klaus Langohr[3], Mercè Torra[4], Dolors Soy[5], Luisa García-Esteve[1,2] and Rocio Martin-Santos[1,2]**

[1]Perinatal Mental Health Clinic-BCN Unit, Department of Psychiatry and Psychology, Hospital Clínic, Centro de Investigación Biomédica en Red en Salud Mental (CIBERSAM), Institut D'Investigacions Biomèdiques August Pi I Sunyer (IDIBAPS), University of Barcelona (UB), Barcelona, Spain, [2]Department of Medicine, Institute of Neuroscience, University of Barcelona (UB), Barcelona, Spain, [3]Departament of Statistics and Operations Research, Universitat Politècnica de Catalunya, Barcelona, Spain, [4]Pharmacology and Toxicology Laboratory, Biochemistry and Molecular Genetics Service, Biomedical Diagnostic Center (CBD), Hospital Clínic, IDIBAPS, and Department of Medicine, UB, Barcelona, Spain, [5]Division of Medicine, Pharmacy Service, Hospital Clínic, IDIBAPS, UB, Barcelona, Spain

**Purpose:** Women who take lithium during pregnancy and continue after delivery may choose to breastfeed, formula feed, or mix these options. The aim of the study was to evaluate the neonatal lithium serum concentrations based on these three feeding trajectories.

**Methods:** We followed 24 women with bipolar disorder treated with lithium monotherapy during late pregnancy and postpartum (8 per trajectory). Lithium serum concentrations were determined by an AVL 9180 electrolyte analyser with a 0.10 mEq/L detection limit and a 0.20 mEq/L limit of quantification (LoQ).

**Results:** There was complete lithium placental passage at delivery, with a mean ratio of lithium concentration in the umbilical cord to maternal serum of 1.12 ± 0.17. The median times to LoQ were 6–8, 7–8, and 53–60 days for formula, mixed, and exclusive breastfeeding respectively. The generalized log-rank testing indicated that the median times to LoQ differ according to feeding trajectory ($p = 0.037$). According to the multivariate analysis-adjusted lithium serum concentrations at birth, times to LoQ are, on average, longer under exclusive breastfeeding (formula, $p = 0.015$; mixed, $p = 0.012$). No lithium accumulation was observed in infants under either exclusive or mixed breastfeeding. During the lactation follow-up, there was no acute growth or developmental delays in any neonate or infant. Indeed, lithium concentrations in the three trajectories declined in all cases. However, the time needed to reach the LoQ was much longer for those breastfeeding exclusively.

**Conclusions:** In breastfeed infant no sustained accumulation of lithium and no adverse effects on development or growth were observed.

**Keywords: bipolar disorder, lithium, breastfeeding, exclusive maternal breastfeeding, mixed breastfeeding, formula feeding, pharmacokinetics, mother-infant dyad**

OPEN ACCESS

***Edited by:***
*Catherine M. T. Sherwin, Wright State University, United States*

***Reviewed by:***
*Robert Ward, The University of Utah, United States*
*Karel Allegaert, University Hospitals Leuven, Belgium*

****Correspondence:***
*Rocio Martin-Santos*
*rmsantos@clinic.cat*

***Specialty section:***
*This article was submitted to Obstetric and Pediatric Pharmacology, a section of the journal Frontiers in Pharmacology*

***Received:*** *02 August 2021*
***Accepted:*** *07 September 2021*
***Published:*** *22 September 2021*

***Citation:***
*Imaz ML, Langohr K, Torra M, Soy D, García-Esteve L and Martin-Santos R (2021) Neonatal Feeding Trajectories in Mothers With Bipolar Disorder Taking Lithium: Pharmacokinetic Data. Front. Pharmacol. 12:752022. doi: 10.3389/fphar.2021.752022*

## INTRODUCTION

Breastfeeding is an important public health issue because it promotes health, prevents disease, and contributes to reducing health inequalities in mothers and nursing infants (US Surgeon, 2011). Human milk is tailored to meet the nutritional needs of human newborns and infants, including those who are premature and sick; it provides an optimal balance of nutrients in an easily digestible and bioavailable form (James et al., 2009). Ideally, breastfeeding should be used for the first 6 months of life where possible, followed by a combination of breast milk with appropriate complementary foods until at least 1–2 years (WHO/UNICEF, 2003; AAP, 2012). For this purpose, exclusive breastfeeding is defined as the baby receiving breast milk, with the possible inclusion of vitamins or minerals through drops and syrups (Labbock et al., 2012). Exclusive breastfeeding is the reference model against which all alternative feeding methods should be measured regarding growth, health, development, and other short- and long-term outcomes. However, a common reason for not starting or for interrupting breastfeeding is medication transfer and risk of infant toxicity. Evidence-based perinatal psychopharmacology is driven by the need to balance the disease-related risks (i.e., the natural course of the bipolar disorder) and any risks to the mother, fetus or infant related to the exposure to medication.

Lithium is an effective first-line treatment for bipolar disorder (Yatham et al., 2018). Women who discontinue treatment during the perinatal period are at high risk of relapse (Vigera et al., 2007). Continued lithium prophylaxis during pregnancy may not only maintain mood stability during pregnancy but also prevent postpartum relapse (Poels et al., 2018). Lithium is a monovalent cation that is absorbed rapidly after oral intake, and it is not metabolized or bound to proteins, being eliminated almost exclusively *via* the kidneys (Granjean and Aubry, 2009). Anatomic and physiological changes during pregnancy may progressively alter the pharmacokinetics of lithium over the course of the three trimesters (Feghali et al., 2015; Westin et al., 2017; Allegaert, 2020; ). In the third trimester, lithium clearance has been found to rise by 30–50%, which may require an adjustment of the dose guided by therapeutical drug monitoring (Granjean and Aubry, 2009; Wesseloo et al., 2017). Lithium has complete placental passage, with an ion equilibration across placental barrier that is remarkably uniform across a wide range of maternal concentrations (0.2–2.6 mEq/L) (Newport et al., 2005). Due to the very low molecular weight and lack of protein binding, lithium is readily transferred to breastmilk (Hale and Rowe, 2017). Lithium excreted in human breast milk is highly variable, being approximately 50% (range 0.17–1.07%) of the mother serum concentration (Imaz et al., 2019; Newmark et al., 2019). The amount of lithium that receives the infant depends on several factors, such as the volume of milk transfer to the infant, the concentration of the lithium in the milk, and the infant's ability to absorb (Lawrence, 1994). On the other hand, lithium is excreted almost entirely by the kidneys and is freely filtered by the glomeruli. Fractional excretion of lithium is 20%, and 60% of the filtered lithium is reabsorbed in the proximal tubule and 20% in the loop of Henle and the collecting duct (Zhuo and Li, 2013). The tubular secretion is immature at birth and approaches adult values by 7–12 months of age (Zhang et al., 2019). However, the glomerular filtration rate matures more rapidly than tubular secretion, resulting in a glomerutubular imbalance in neonates.

Lithium use while breastfeeding is a controversial topic, due to the potential risk to the neonate of lithium accumulation and secondary toxicity, especially among those who are preterm and sick (Malhi et al., 2017; Galbally et al., 2018). Two systematic reviews of clinical studies into lithium use during breastfeeding found limited evidence about whether one should initiate, maintain, or discontinue lithium during breastfeeding (Imaz et al., 2019; Newmark et al., 2019).

At present, a woman who takes lithium during pregnancy and continues after delivery may choose either breastfeeding or formula feed, or may combine these options. Given the paucity of clinical data on side effects in the infant, pharmacokinetic data may help to assess the safety of breast milk. Infant exposure to lithium is most accurately determined by measuring the drug concentration in an infant's serum (FDA, 2005).

In this study, we hypothesized that lithium would not be accumulated in infants under either exclusive or partial breastfeeding. Our aim was to evaluate neonatal lithium concentrations in different feeding trajectories to help clinicians and patients make informed decisions about lithium use and breastfeeding during lactation.

## METHODS

### Subjects and Assessments

We included data from 24 women with bipolar disorder who received lithium monotherapy and were clinically stable in late pregnancy in our university hospital between 2006 and 2018. Among these, eight women each were included into three groups, as defined by the World Health Organization (WHO, 2008): exclusive breastfeeding, mixed breastfeeding (i.e., 50–80% breastfeeding) or formula feeding. The participants were required to meet the DSM-IV-R or DSM-V criteria for bipolar I, bipolar II, or bipolar NOS. We also ensured that they were not taking concomitant medication that could interact with lithium (e.g., ibuprofen). The study was approved by the Ethics Committee for Drugs Research of the Institution (CEIm: HCD/2020/1305).

At a prenatal visit (33–35 gestational weeks), consistent with current best practice, all women were informed of the risks and benefits of lithium use during lactation. The patient and psychiatrist then collaborated to write a birth and breastfeeding plan that included clinical management, lithium monitoring in the mother and infant, and strategies to minimise postpartum sleep disruption (i.e., partner/parent support overnight for infant care) (Doan et al., 2014). All women were taking lithium twice a day to maintain constant serum lithium concentrations (Malhi and Tanious, 2011). Women were advised to suspend lithium administration at the onset of labour in the event of spontaneous deliveries, or 12 h before a scheduled caesarean section or induction. Lithium was then restarted at the same dose 6 h after vaginal delivery and 12 h after caesarean section. During subsequent follow-up visits, a senior psychiatrist evaluated the

psychopathological state of the mothers, and adjusted the dose of lithium if necessary.

The neonate underwent standard follow-up. At 12–24 h of life, a neonatologist performed a systematic physical examination; at 48 h, a paediatric nurse performed a screening assessment; and, after hospital discharge, infants were evaluated regularly by a paediatrician (e.g., for weight, length, cranial circumference, neurodevelopment, and vaccination schedule) according to the standard clinical protocol of the Public Health Agency of Catalonia (ASPCAT, 2019).

## Blood Sample Collection

At delivery, we collected 10 ml paired samples of cord blood and maternal venous blood. During lactation, two paediatric nurse phlebotomists simultaneously collected venous blood from mothers (5 ml) and infants (2 ml), at 10–11 am, before the mother took her first daily dose of lithium. To study the behaviour of serum lithium concentrations during the lactation period we tried to collect samples on days 2, 7 ± 2, 15 ± 2, 30 ± 5, and 60 ± 5 postpartum; however, this was not always possible due to the technical difficulty involved and the postpartum schedules, and so the time intervals were irregular. There were no adverse incidents in the mothers or neonates/infants during blood extraction. We stopped neonatal/infant blood analysis at the request of the mother, and if serum lithium concentrations were below the limit of quantification (LoQ) of 0.20 mEq/L on two consecutive occasions. The sample at 48 h postpartum was obtained during the newborn screening assessment.

## Serum Lithium Analysis

For lithium analysis, we collected maternal, cord, and neonatal/infant venous blood samples in BD Vacutainer® no-additive Z plus tubes (BD Diagnostics, Preanalytical Systems, Franklin Lakes, NJ07417). After allowing the blood to clot in an upright position for at least 30 min, serum was separated by centrifugation at approximately 3,000 rpm for 10 min and analysed as soon as possible. If storage was required, the serum samples were capped and refrigerated at 4°C–8°C until analysis. Lithium concentrations were determined by an AVL 9180 electrolyte analyser based on the ion-selective electrode measurement principle (Roche Diagnostics 9,115 Hague Road Indianapolis, IN46256). Two-point calibration was performed every 4 h with a measurement range between 0.1 and 6 mEq/L. The limit of detection was 0.10 mEq/L and the LoQ was 0.20 mEq/L. Expressed as a percentage (coefficient of variation), the within-day precision was 0.97–4.1% and the between-day precision was 1.3–6.4%.

## Lithium Concentration Analysis

The ratio of lithium concentration in the umbilical cord to that in the maternal serum was calculated for each maternal-infant pair as the lithium placental passage index. The infant serum lithium concentration was monitored from birth until the time when the serum lithium concentration reached the LoQ or below. Since lithium could be taken at arbitrary times, the time of interest was interval-censored between the last day that the lithium level was above the LoQ and the first day that it was equal to or below the LoQ.

## Statistical Analysis

All data were analysed using SPSS for Windows (Version 25; IBM Corp., Armonk, NY, United States) and the statistical software package R (V4.0.2; The R Foundation for Statistical Computing, Vienna, Austria). A descriptive analysis was performed to characterize the sample and the placental passage of lithium, using either absolute and relative frequencies or means, standard deviations, and ranges as appropriate.

For the analysis of the interval-censored data, we used the Turnbull estimator to estimate the probability that the LoQ was reached as a function of time (Turnbull, 1976). The generalized log-rank test for interval-censored data based on a vector distribution was used to test whether the median times until the LoQ differ among feeding trajectories (Fay and Shaw, 2010; Oller and Langohr, 2017).

To adjust the comparison of the feeding trajectories for the lithium concentrations at birth, the Weilbull regression model was applied. This parametric model models the logarithm of the times of interest assuming that these times follow a Weibull distribution (Gómez et al., 2009). Following, post-hoc comparisons were carried out to compare the feeding trajectories in the frame of this model and the corresponding confidence intervals and *p*-values were adjusted for multiple comparisons.

# RESULTS

## Characteristics of the Samples

Most participants were Caucasian (96%; $n = 23$), the mean (±SD) age was 33 ± 3.8 years, around half (54%; $n = 13$) had university level education, and all were married or had a partner. Obstetrically, 19 (80%) of the mothers were primiparous and 9 (37.5%) had deliveries by caesarean section. The three study groups (exclusive breastfeeding, mixed breastfeeding, and formula feeding) were similar with respect to sociodemographic and obstetric characteristics.

Two women relapsed postpartum. One woman in the exclusive breastfeeding group needed a brief hospitalization at day 45 postpartum for a manic episode with psychotic features despite having a therapeutic lithium concentration (0.91 mEq/L). Another woman in the mixed breastfeeding group had a manic relapse at 36 days, but with subtherapeutic serum levels (0.21 mEq/L), and her levels improved with outpatient therapy. Breastfeeding was stopped in both patients.

All neonates were full-term newborns (37.4–41.2 weeks) and had an adequate weight for gestional age, mean ± SD (range) 3,478 ± 455 g (2,500–4,400 g). **Table 1** shows the gender and lithium concentrations at delivery for the 24 full-term neonates by their feeding trajectory. As shown, the three study groups were similar with respect to gender and the umbilical cord and maternal lithium concentrations. There was complete lithium placental passage at delivery: the mean ratio of lithium concentration between the umbilical cord and maternal serum was 1.12 ± 0.17. Although most neonates at delivery did not show signs of lithium toxicity or other adverse clinical events, adverse effects were recorded in six (25%). In the exclusive breastfeeding group, there were two cases (25%) of transient hypotonia and one

**TABLE 1 |** Descriptive statistics of neonates according to feeding trajectory.

| | All *N* = 24 | Exclusive *N* = 8 | Mixed *N* = 8 | Formula *N* = 8 |
|---|---|---|---|---|
| **Gender** | | | | |
| Female | 12 (50%) | 4 (50%) | 5 (62.5%) | 3 (37.5%) |
| Male | 12 (50%) | 4 (50%) | 3 (37.5%) | 5 (62.5%) |
| **Intrapartum serum lithium concentration[a]** | | | | |
| Umbilical cord | 0.48 (0.22) (0.23–0.96) | 0.44 (0.16) (0.23–0.76) | 0.58 (0.29) (0.26–0.96) | 0.42 (0.17) (0.25–0.68) |
| Maternal serum | 0.43 (0.20) (0.19–0.95) | 0.39 (0.16) (0.19–0.72) | 0.50 (0.27) (0.22–0.95) | 0.40 (0.15) (0.25–0.64) |
| Ratio | 1.12 (0.17) (0.63–1.53) | 1.13 (0.11) (1.02–1.30) | 1.16 (0.16) (1–1.53) | 1.06 (0.22) (0.63–1.28) |

*Data are presented as either N (%) or Mean (SD) (range).*
[a]*mEq/L, including the ratio of umbilical cord to maternal serum levels.*

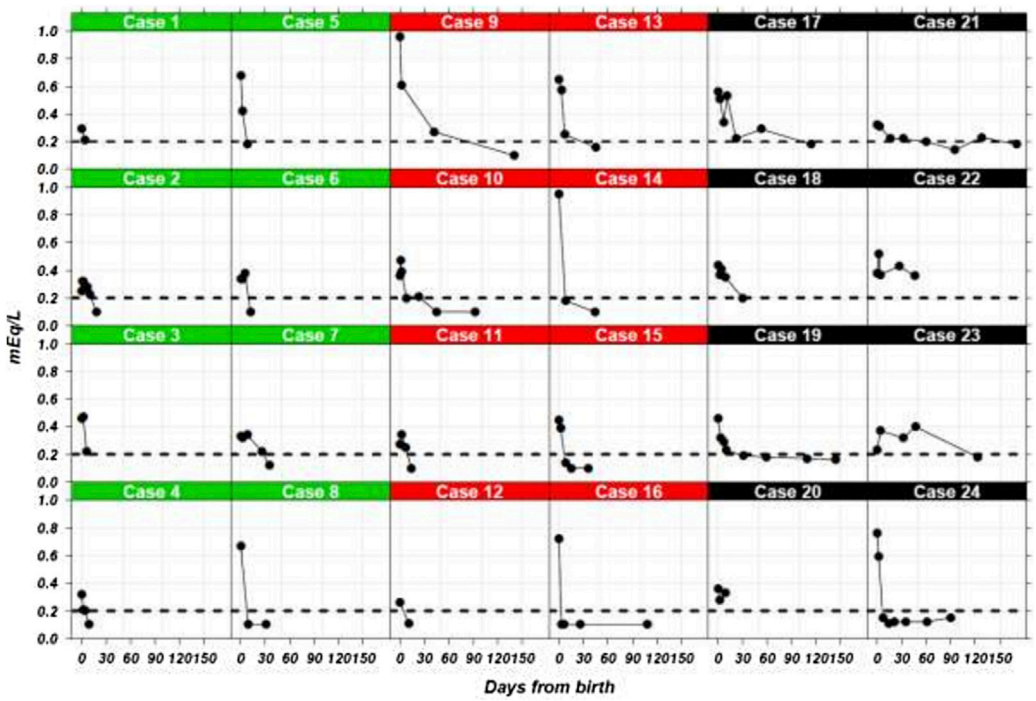


**FIGURE 1 |** Lithium serum concentrations in 24 neonates from birth. Three groups of neonates are shown by type of feeding. Cases 1–8 (green), 9–16 (red), and 17–24 (black) show the results formula-fed, mixed-fed, and exclusive breastfed neonates, respectively. The dotted line indicates the 0.20 mEq/L limit of quantification.

case (12.5%) of isolated low-set ears. In the mixed breastfeeding group, three (37.5%) had respiratory distress following operative delivery (i.e., forceps or caesarean): one needed neonatal resuscitation in the delivery room (cord lithium, 0.95 mEq/L) and two required admission to the neonatal intensive care unit for 24 h (cord lithium, 0.55 and 0.96 mEq/L). In the formula feeding group, there was a single case (12.5%) of transient hypertonia.

The 48 h newborn screening assessment was in all cases normal. Postpartum neonatal thyroid function (TSH) was between the normal ranges (0.10–5.65 mU/mL) in all cases. Neonatal bilirubinemia results (by transcutaneous bilirubinometers) were below 12 mg/dl (2.50–11.50 mg/dl) in all cases. The physiological weight loss in the first 48 h was 9.3% (8.86–9.76%).

The mean ± SD (range) hospitalisation period was 2.83 ± 0.86 days (2–4 days).

Finally, paediatricians observed no growth or developmental delays in any of the infants during follow-up.

## Lithium Concentrations

We collected a total of 138 lithium serum samples, 24 samples from mother-infant pairs at delivery, and 90 samples from neonates during lactation.

**Figure 1** shows the time course data of the serum lithium concentrations for each of the 24 neonates, where the dotted line represents the limit of quantification (LoQ) of 0.20 mEq/L. However, seven cases [fourth in formula group (cases 2, 3, 6 and 7), two in the mixed breastfeeding group (cases 10 and 11), and one case in the exclusive breastfeeding group (case 22)] showed a transient increase of serum lithium concentration (<0.15 mEq/L; range: 0.01–0.14) probably associated to the physiological weight loss. In the exclusive

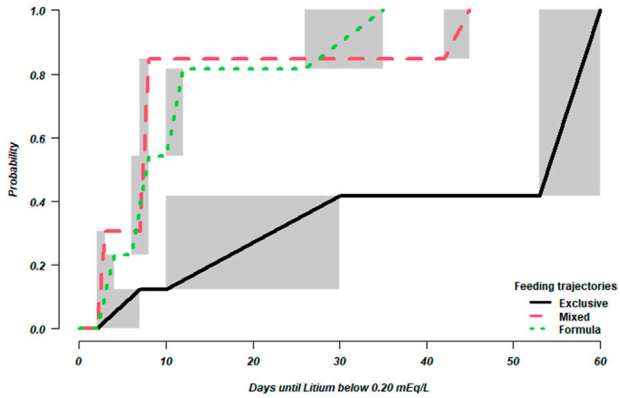


**FIGURE 2 |** Estimated cummulative probability that lithium serum concentrations falls below LoQ. Shaded areas indicate that the estimation of the probability is not defined in the corresponding intervals, but only known to increase monotonically.

breastfeeding group, one case (case 23) showed also a transient increase (0.14 mEq/L) because of physiological weight loss and drastic increase in maternal level of lithium concentration (0.19 mEq/L to 1.09 mEq/L); and another (case 17) showed an increase of 0.19 mEq/L on the 11th day of life because the infant's serum sample was hemolyzed.

**Supplementary Figure S1** presents the interval-censored times until the time when lithium levels fell below the LoQ; the exact moment was not observed and was only known to lie in these intervals. After 40 days, the lithium serum concentration of only 4 neonates with exclusive breastfeeding was definitely below the LoQ, compared to 7 neonates with mixed feeding and 6 with formula feeding.

## Univariate Nonparametric Analysis

**Figure 2** (and **Supplementary Table 1)** shows the estimated probabilities that the lithium levels falls below the LoQ as a function of time from birth according to the Turnbull estimator. The median times until LoQ lay between 6–8 days (formula feeding), 7–8 days (mixed), and 53–60 days (exclusive breastfeeding). According to the results of the generalized log-rank test to compare the lactation types ($\chi 2 = 6.8$, df = 2, $p = 0.037$) times to LoQ differed between the feeding trajectories.

## Multivariate Analysis

**Table 2** provides the parameter estimates of the Weibull regression model, which was used to compare the feeding trajectories while adjusting for the lithium concentrations at birth, and shows the results of the pairwise post-hoc comparisons. The differences observed among breastfeeding trajectories are not explained by different lithium levels at birth and we can therefore state that, on average, the times to LoQ were longest under exclusive breastfeeding; no statistically significant differences were found between the mixed and the formula trajectory.

# DISCUSSION

As far as we know, this is the first study to compare serum lithium concentrations during three feeding trajectories after delivery: namely, exclusive breastfeeding, formula feeding, and a mixed approach. Notably, no lithium sustained accumulation was found in infants under either exclusive or mixed breastfeeding. As expected, however, we found significant differences in the time taken to reach or exceed the LoQ between the feeding trajectories. All in all, the results provide substantial support for recommending maternal breastfeeding in women with lithium-responsive bipolar disorder in whom lithium prophylaxis helps to prevent postpartum affective relapse.

In a preliminary study of exclusive breastfeeding in the neonatal period, we found that lithium clearance in nursing infants was independent of maternal lithium levels, and that infant serum lithium concentrations fell over time from delivery to the third month postpartum, by 43.80% (95%CI: −38.45% to −43.88%) in the first month and by 58.52% (95%CI: −38.22% to −78.90%) at 3 months (Imaz et al., 2021). In women who had taken lithium weeks before delivery, it was shown that infant

**TABLE 2 |** Parameter estimates of the Weibull regression model for time until lithium serum concentrations falls below LoQ and pairwise post-hoc comparisons of feeding trajectories.

| **Weibull regression model** | | | | |
|---|---|---|---|---|
| — | **Value** | **SE** | **Z** | **p** |
| (Intercept) | 3.566 | 0.582 | 6.126 | 0.000 |
| Lithium concentration[a] at birth | 0.851 | 1.117 | 0.762 | 0.446 |
| Mixed *vs* exclusive breastfeeding | −1.593 | 0.637 | −2.501 | 0.012 |
| Formula *vs* exclusive breastfeeding | −1.357 | 0.555 | −2.444 | 0.015 |
| **Pairwise comparisons** | | | | |
| — | **Differences** | **Lower 95%CI** | **Upper 95%CI** | **p** |
| Mixed *vs* exclusive breastfeeding | −1.593[b] | −3.085 | −0.102 | 0.033 |
| Formula *vs* exclusive breastfeeding | −1.357[b] | −2.656 | −0.057 | 0.038 |
| Formula *vs* mixed breastfeeding | 0.237 | −1.284 | 1.757 | 0.929 |

*Abbreviations: CI, confidence interval; SE, standard error*

[a]*mEq/L.*

[b]*The negative sign indicates larger times until lithium serum concentrations falls below LoQ under exclusive breastfeeding.*

serum concentrations in the first week postpartum may reflect transplacental passage rather than intake *via* breast milk (Hale and Rowe, 2017). In the present study, we compared the pharmacokinetics of serum lithium concentrations from delivery during three feeding trajectories. The analysis of the formula feeding trajectory (in which the last infant exposure to lithium was at delivery) provided us with a reference point with which to compare the course of the exclusive and mixed breastfeeding trajectories in the first 7–10 days postpartum. Although serum lithium concentrations declined in all three trajectories, the time needed to reach the LoQ was longest in the exclusive breastfeeding trajectory. The non accumulation of lithium in breastfeeding infant could be explained by 1) the decrease of transport of lithium into the milk with age; and 2) because the neonatal lithium renal excretion increases with maturation of renal tubular transport, even though tubular function matures more slowly than glomerular function after birth (Zhang et al., 2019).

Previous systematic reviews have failed to address clinical symptoms of lithium toxicity in infants for levels <0.30 mEq/L (Pacchiarotti et al., 2016; Imaz et al., 2019; Newmark et al., 2019). We decided to stop monitoring lithium concentrations in infants when levels reached ≤0.20 mEq/L in two consecutive determinations (i.e., the LoQ) (Armbruster and Pry, 2008). We chose the time to reach the LoQ as our outcome variable because the three groups had different lithium exposures: the last exposure was at delivery in the formula group, but it continued in different proportions in the mixed and exclusive breastfeeding groups. However, neonates in all groups shared the problems of an immature renal system and the physiological loss of fluids, which may affect lithium concentrations.

With regard to the effects of transplacental lithium exposure at birth, six neonates in this sample suffered mild and transient complications that resolved before hospital discharge. During the follow-up period, paediatricians found no observable growth or developmental delay in neonates or infants in any of the three trajectories.

The postpartum period is associated with the highest lifetime risk of hospitalisation for women with bipolar disorder (Munk-Olsen et al., 2009). Lithium has proven to be an effective preventive treatment during the postpartum period (Berking et al., 2015). A systematic review and meta-analysis showed a relapse rate during postpartum in women with bipolar disorder of 37% (Wesseloo et al., 2016). In the first month postpartum, the recommended therapeutical range is ≥0.80 mEq/L (Wesseloo et al., 2017). In our sample of bipolar disorder patients under lithium monotherapy during lactation, only two patients out of 24 (fewer than 10%) relapsed during follow-up (at 36 and 45 days postpartum respectively): one with a subtherapeutic serum lithium concentration, and the other within the therapeutic range.

The study has several strengths and limitations. The strengths include its assessment of the three breastfeeding trajectories from delivery in groups with similar obstetrical and demographic characteristics. As for to limitations, the study was performed in a selected sample of bipolar women receiving lithium monotherapy during pregnancy and lactation, all of whom had full-term newborns. As such, our findings may be not generalizable to more heterogeneous populations (i.e. pre-term neonates; sick infants; lithium in polytherapy, and so on). The amount of lithium transferred to breastfed infant could be measure directly in infant serum or estimated on the basis of pharmacokinetics parameters [i.e. milk to maternal plasma drug concentration ratio (M/P ratio), the relative infant dose (RID)]. The infant serum concentration provides information regarding the fraction of drug that is systematically available to the breastfed child (Begg et al., 2002). It is the most direct measure for risk assessment (FDA, 2005). We decided to use the infant serum lithium concentration as direct measure. Having to obtain a blood sample to analyze the infant serum lithium concentration may be a limitation, as this is an invasive method that may cause pain and may be rejected by some parents. Because of this, the determination of lithium in saliva has been proposed; however, from the pre-analytical point of view, obtaining saliva in infants between 0 and 2 months is especially challenging, and in addition the therapeutic range of lithium in this matrix has not been yet defined (Murru et al., 2017). We were also aware of the limit of detectability of the assay used to measure lithium concentration, especially for values below the LoQ.

## CONCLUSIONS

We conclude that bipolar women treated with lithium monotherapy during late pregnancy (with a brief peripartum discontinuation) and postpartum may continue lithium use during breastfeeding, since it is safe and does not cause infant harm or accumulation of lithium in our sample. Lithium concentrations in the three lactation trajectories (exclusive, mixed and formula) fell in all cases. However, the time needed to reach the LoQ was much longer in the case of mothers who breastfed exclusively.

Clinical follow-up is required throughout the postpartum period to ensure the safety of both the mother and infant. We recommend that infant lithium serum concentrations be monitored peripartum at 2 days and 1 week postpartum for all trajectories, with additional monitoring at 1 and 2 months postpartum for those who exclusively breastfeed. Later on, if infant lithemia is < 0.20 mEq/, lithium monitoring may only be necessary in the case of fever, unusual behaviour, increased sedation, hypotonia, dehydration, difficulty feeding, or abnormal growth or development.

Finally, more standardized and collaborative studies are needed in larger cohorts to better elucidate the extent of maternal-infant lithium transfer and the effects of breast milk exposure on infant health and development.

## DATA AVAILABILITY STATEMENT

The raw data supporting the conclusion of this article will be made available by the authors, without undue reservation.

## ETHICS STATEMENT

The studies involving human participants were reviewed and approved by the Ethics committee of drugs research of Hospital Clinic de Barcelona, Spain. Written informed consent from the participants' legal guardian/next of kin was not required to participate in this study in accordance with the national legislation and the institutional requirements.

## AUTHOR CONTRIBUTIONS

All authors (MLI, KL, MT, DS, LG-E, and RM-S) gave substantial contributions to the interpretation of the data, revised the manuscript critically and approved the final version. MLI and RM-S designed the study and wrote the first draft of the paper. Specific contribution: MLI recorded the retrospective data of the patients. KL implemented the statistical methods. KL, MLI, and RM-S performed the data analysis.

## ACKNOWLEDGMENTS

The study was supported by the Generalitat de Catalunya/ Support a les activitats dels Grups de Recerca, SGR 2017/1798 (RM-S) and SGR 2017/622 (KL), the CIBER en Salud Mental (CIBERSAM), Barcelona, and by the Ministerio de Ciencia e Innovación (Spain) (PID 2019-104830RB-I00).

## SUPPLEMENTARY MATERIAL

The Supplementary Material for this article can be found online at: https://www.frontiersin.org/articles/10.3389/fphar.2021.752022/full#supplementary-material

## REFERENCES

Allegaert, K. (2020). Perinatal Pharmacology and Safety Profiles. In: *Handbook of Clinical Neurology Vol 171 (3rd Series)*, ed. E. A. P. Steegers, M. J. Cipolla, and E. C. Miller. Amsterdam: Elsevier BV:161–178. doi:10.1016/b978-0-444-64239-4.00008-4

Armbruster, D. A., and Pry, T. (2008). Limit of Blank, Limit of Detection and Limit of Quantitation. *Clin. Biochem. Rev.* 29 Suppl 1, S49–S52.

Begg, E. J., Duffull, S. B., Hackett, L. P., and Ilett, K. F. (2002). Studying Drugs in Human Milk: Time to Unify the Approach. *J. Hum. Lact* 18, 323–332. doi:10.1177/089033402237904

Bergink, V., Burgerhout, K. M., Koorengevel, K. M., Kamperman, A. M., Hoogendijk, W. J., Lambregtse-van den Berg, M. P., et al. (2015). Treatment of Psychosis and Mania in the Postpartum Period. *Am. J. Psychiatry* 172, 115–123. doi:10.1176/appi.ajp.2014.13121652

Doan, T., Gay, C. L., Kennedy, H. P., Newman, J., and Lee, K. A. (2014). Nighttime Breastfeeding Behavior Is Associated with More Nocturnal Sleep Among First-Time Mothers at One Month Postpartum. *J. Clin. Sleep Med.* 10, 313–319. doi:10.5664/jcsm.3538

Fay, M. P., and Shaw, P. A. (2010). Exact and Asymptotic Weighted Logrank Tests for Interval Censored Data: The Interval R Package. *J. Stat. Softw.* 36, 1–34. doi:10.18637/jss.v036.i02

Feghali, M., Venkataramanan, R., and Caritis, S. (2015). Pharmacokinetics of Drugs in Pregnancy. *Semin. Perinatol* 39, 512–519. doi:10.1053/j.semperi.2015.08.003

Food and Drug Administration (FDA) (2005). Clinical Lactation Studies-Study Design, Data Analysis and Recommendations for Labelling. Avabilable at: www.fda.gov/RegulatoryInformation/Guidances/ucm127484.htm.

Galbally, M., Bergink, V., Vigod, S. N., Buist, A., Boyce, P., Chandra, P., et al. (2018). Breastfeeding and Lithium: Is Breast Always Best?. *Lancet Psychiatry* 5, 534–536. doi:10.1016/S2215.0366(18)30085-3

Gómez, G., Calle, M. L., Oller, R., and Langohr, K. (2009). Tutorial on Methods for Interval-Censored Data and Their Implementation in R. *Stat. Model.* 9, 259–297. doi:10.1177/1471082x0900900402

Grandjean, E. M., and Aubry, J.-M. (2009). Lithium: Updated Human Knowledge Using an Evidence-Based Approach. *CNS Drugs* 23, 331–349. doi:10.2165/00023210-200923040-00005

Hale, T. W., and Howe, H. E. (2017). *Medications and Mother's Milk*. New York: Springer, 568–571.

Imaz, M. L., Torra, M., Soy, D., García-Esteve, L., and Martin-Santos, R. (2019). Clinical Lactation Studies of Lithium: a Systematic Review. *Front. Pharmacol.* 10, 1005. doi:10.3389/fphar.2019.01005

Imaz, M. L., Soy, D., Torra, M., Garcia-Esteve, L., Soler, C., and Martin-Santos, R. (2021). Case Report: Clinical and Pharmacokinetic Profile of Lithium Monotherapy in Exclusive Breastfeeding. A Follow-Up Case Series. *Front. Pharmacol.* 10, 1005. doi:10.1007/s10096-019-03695-9

James, D. C., and Lessen, R. (2009). Position of the American Dietetic Association: Promoting and Supporting Breastfeeding. *J. Am. Diet. Assoc.* 109, 1926–1942. doi:10.1016/j.jada.2009.09.018

Labbock, M. H., and Starling, A. (2012). Definition of Breastfeeding: Call for the Development and Use of Consistent Definitions in Research and Peer-Reviewed Literature. *Breastfeed. Med.* 7, 397–402. doi:10.1089/bfm.2012.9975

Lawrence, R. A. (1994). *Breastfeeding: A Guide for the Medical Profession*. St Louis, Mo: Mosby.

Malhi, G. S., Gessler, D., and Outhred, T. (2017). The Use of Lithium for the Treatment of Bipolar Disorder: Recommendations from Clinical Practice Guidelines. *J. Affect. Disord.* 217, 266–280. doi:10.1016/j.jad.2017.03.052

Malhi, G. S., and Tanious, M. (2011). Optimal Frequency of Lithium Administration in the Treatment of Bipolar Disorder: Clinical and Dosing Considerations. *CNS Drugs* 25, 289–298. doi:10.2165/11586970-000000000-0000

Munk-Olsen, T., Laursen, T. M., Mendelson, T., Pedersen, C. B., Mors, O., and Mortensen, P. B. (2009). Risks and Predictors of Readmission for a Mental Disorder during the Postpartum Period. *Arch. Gen. Psychiatry* 66, 189–195. doi:10.1001/archgenpsychiatry.2008.528

Murru, A., Torra, M., Callari, A., Pacchiarotti, I., Romero, S., Gonzalez de la Presa, B., et al. (2017). A Study on the Bioequivalence of Lithium and Valproate Salivary and Blood Levels in the Treatment of Bipolar Disorder. *Eur. Neuropsychopharmacol.* 27, 744–750. doi:10.1016/j.euroneuro.2017.06.003

Newmark, R. L., Bogen, D. L., Wisner, K. L., Isaac, M., Ciolino, J. D., and Clark, C. T. (2019). Risk-Benefit Assessment of Infant Exposure to Lithium through Breast Milk: a Systematic Review of the Literature. *Int. Rev. Psychiatry* 31, 295–304. doi:10.1080/09540261.2019.1586657

Newport, D. J., Viguera, A. C., Beach, A. J., Ritchie, J. C., Cohen, L. S., and Stowe, Z. N. (2005). Lithium Placental Passage and Obstetrical Outcome: Implications for Clinical Management during Late Pregnancy. *Am. J. Psychiatry* 162, 2162–2170. doi:10.1176/appi.ajp.162.11.2162

Oller, R., and Langohr, K. (2017). FHtest: An R Package for the Comparison of Survival Curves with Censored Data. *J. Stat. Softw.* 81, 1–25. doi:10.18637/jss.v081.i15

Pacchiarotti, I., León-Caballero, J., Murru, A., Verdolini, N., Furio, M. A., Pancheri, C., et al. (2016). Mood Stabilizers and Antipsychotics during Breastfeeding: Focus on Bipolar Disorder. *Eur. Neuropsychopharmacol.* 26, 1562–1578. doi:10.1016/j.euroneuro.2016.08.008

Poels, E. M. P., Bijma, H. H., Galbally, M., and Bergink, V. (2018). Lithium during Pregnancy and after Delivery: a Review. *Int. J. Bipolar Disord.* 6, 26. doi:10.1186/s40345-018-0135-7

Public Health Agency of Catalonia (ASPCAT) Agència de Salut Pública de Catalunya (ASPCAT). Protocol d'activitats preventives i de promoció de la

salut a l'edat pediàtrica. Avabilable at: http://salutpublica.gencat.cat/ca/ambits/promocio_salut/Infancia-i-adolescencia/Infancia/infancia-amb-salut/. (Accessed December 10, 2019).

The American Academy of Pediatrics (AAP) (2012). Breastfeeding and the Use of Human Milk. *Pediatrics* 129, 827–841. doi:10.1542/peds.2012-0755f

Turnbull, B. W. (1976). The Empirical Distribution Function with Arbitrarily Grouped, Censored and Truncated Data. *J. R. Stat. Soc. Ser. B (Methodological)* 38, 290–295. doi:10.1111/j.2517-6161.1976.tb01597.x

U.S. Department of Health and Human Services (2011). *The Surgeon General's Call to Action to Support Breastfeeding*. Washington, DC: Department of Health and Human Services, Office of the Surgeon General U.S.

Viguera, A. C., Newport, D. J., Ritchie, J., Stowe, Z., Whitfield, T., Mogielnicki, J., et al. (2007). Lithium in Breast Milk and Nursing Infants: Clinical Implications. *Am. J. Psychiatry* 164, 342–345. doi:10.1176/ajp.2007.164.2.342

Wesseloo, R., Kamperman, A. M., Munk-Olsen, T., Pop, V. J., Kushner, S. A., and Bergink, V. (2016). Risk of Postpartum Relapse in Bipolar Disorder and Postpartum Psychosis: a Systematic Review and Meta-Analysis. *Am. J. Psychiatry* 173, 117–127. doi:10.1178/appi.ajp.2015.15010124

Wesseloo, R., Wierdsma, A. I., van Kamp, I. L., Munk-Olsen, T., Hoogendijk, W. J. G., Kushner, S. A., et al. (2017). Lithium Dosing Strategies during Pregnancy and the Postpartum Period. *Br. J. Psychiatry* 211, 31–36. doi:10.1192/bjp.bp.116.192799

Westin, A. A., Brekke, M., Molden, E., Skogvoll, E., Aadal, M., and Spigset, O. (2017). Changes in Drug Disposition of Lithium during Pregnancy: a Retrospective Observational Study of Patient Data from Two Routine Therapeutic Drug Monitoring Services in Norway. *BMJ Open* 7 (7), e015738. doi:10.1136/bmjopen-2016-015738

World Health Organization (WHO) (2008). *Indications for Assessing Infant and Young Child Feeding Practice: Conclusions of a Consensus Meeting Held 6-8 November 2007*. Washington. D.C., USAGeneva: World Health Organization.

World Health Organization/UNICEF (2003). Global Strategy for Infant and Young Child Feeding. Avabilable at: https://www.who.int/nutrition/publications/infantsfeeding/9241562218/3n/. (Accessed 02 14, 20).

Yatham, L. N., Kennedy, S. H., Parikh, S. V., Schaffer, A., Bond, D. J., Frey, B. N., et al. (2018). Canadian Network for Mood and Anxiety Treatments (CANMAT) and International Society for Bipolar Disorders (ISBD) 2018 Guidelines for the Management of Patients with Bipolar Disorder. *Bipolar Disord.* 20, 97–170. doi:10.1111/bdi.12609

Zhang, Y., Mehta, N., Muhari-Stark, E., Burckart, G. J., van den Anker, J., and Wang, J. (2019). Pediatric Renal Ontogeny and Applications in Drug Development. *J. Clin. Pharmacol.* 59 Suppl 1 (S1), S9–S20. doi:10.1002/jcph.1490

Zhuo, J. L., and Li, X. C. (2013). Proximal Nephron. *Proximal Nephron. Compr. Physiol.* 3, 1079–1123. doi:10.1002/cphy.c110061

**Conflict of Interest:** The authors declare that the research was conducted in the absence of any commercial or financial relationships that could be construed as a potential conflict of interest.

**Publisher's Note:** All claims expressed in this article are solely those of the authors and do not necessarily represent those of their affiliated organizations, or those of the publisher, the editors and the reviewers. Any product that may be evaluated in this article, or claim that may be made by its manufacturer, is not guaranteed or endorsed by the publisher.

frontiers in Pharmacology

CASE REPORT
published: 25 November 2021
doi: 10.3389/fphar.2021.756056

# Case Report: Persistent Pulmonary Hypertension of the Newborn and Narrowing of the Ductus Arteriosus After Topical Use of Non-Steroidal Anti-Inflammatory During Pregnancy

*Kévin Le Duc[1,2]*, Sixtine Gilliot[3,4], Jean Benoit Baudelet[5], Sébastien Mur[1], Mohamed Riadh Boukhris[1], Olivia Domanski[5], Pascal Odou[3,4] and Laurent Storme[1,2]*

[1]Department of Neonatology, Jeanne de Flandre Hospital, University Hospital of Lille, Lille, France, [2]ULR2694 Metrics–Perinatal Environment and Health, University of Lille, Lille, France, [3]ULR 7365–GRITA–Groupe de Recherche sur Les Formes Injectables et Les Technologies Associées, Université de Lille, CHU Lille, Lille, France, [4]Institut de Pharmacie, CHU Lille, Lille, France, [5]Department of Pediatric Cardiology, Institut Coeur Poumon, University Hospital of Lille, Lille, France

OPEN ACCESS

**Edited by:**
Catherine M. T. Sherwin,
Wright State University, United States

**Reviewed by:**
Tamorah Rae Lewis,
Children's Mercy Hospital,
United States
Candice Fike,
The University of Utah, United States

***Correspondence:**
Kévin Le Duc
kevin.leduc@chru-lille.fr

**Specialty section:**
This article was submitted to Obstetric and Pediatric Pharmacology, a section of the journal Frontiers in Pharmacology

**Received:** 09 August 2021
**Accepted:** 28 October 2021
**Published:** 25 November 2021

**Citation:**
Le Duc K, Gilliot S, Baudelet JB, Mur S, Boukhris MR, Domanski O, Odou P and Storme L (2021) Case Report: Persistent Pulmonary Hypertension of the Newborn and Narrowing of the Ductus Arteriosus After Topical Use of Non-Steroidal Anti-Inflammatory During Pregnancy. Front. Pharmacol. 12:756056. doi: 10.3389/fphar.2021.756056

**Background:** The use of non-steroidal anti-inflammatory drugs (NSAIDs) during the third trimester of pregnancy can cause premature constriction of the ductus arteriosus. This report describes a case of *in utero* narrowing of the ductus arteriosus (DA) diagnosed postnatally in a baby with Persistent Pulmonary Hypertension of the Newborn (PPHN), after maternal use of Diclofenac-Epolamine 140 mg patch during the second and third trimester.

**Case Presentation:** A fetal ultrasounds revealed an enlarged hypertrophic right ventricle at 32 weeks of gestation. Detailed questioning of the mother highlighted that topical Diclofenac (FLECTOR®) had been used at 26 and at 31 weeks of gestation. An echocardiography performed 8 h postnatally showed supra-systemic pulmonary hypertension, a restrictive ductus arteriosus and a dilated right ventricle. The newborn was treated by inhaled nitric oxide and oral Sildenafil and was discharged from hospital on day 24. He had a complete normalization of his pulmonary vascular resistance on day 48.

**Conclusion:** This case illustrates the potential fetal and neonatal complications associated with maternal topical Diclofenac medication during pregnancy resulting in antenatal closure of the DA.

**Keywords: PPHN (persistent pulmonary hypertension of the newborn), NSAID (non-steroidal anti-inflammatory drug), ductus arteriosus, NICU (neonatal intensive care unit), pregnancy, neonate**

## INTRODUCTION

During pregnancy, the right ventricular output is mostly directed from the pulmonary artery to the aorta, which contributes to systemic circulation (Rasanen et al., 1996). Patency of the ductus arteriosus is maintained during gestation by an elevated concentration of prostaglandin ($PGE_2$) and a low fetal blood partial pressure of $O_2$ (Clyman, 2006).

The use of non-steroidal anti-inflammatory drugs (NSAIDs) during the third trimester of pregnancy can cause premature constriction of the ductus arteriosus by inhibiting cyclo-oxygenase 2 (COX-2) (Van Marter et al., 1996; Gewillig et al., 2009; Storme et al., 2013).

Diclofenac, a NSAID, was found to show the greatest potency for inhibition of phorbol ester-induced $PGE_2$ production (reflecting inflammation induced COX-2 activity) compared with a similar range of NSAIDs in human fibroblasts *in vitro*. It has also been classified as one of the most potent inducers of ductus arteriosus constriction in rats (Momma et al., 1984; Cordero et al., 2001). Diclofenac is a low molecular weight molecule of 318.15 Da which crosses trophoblastic membranes easily, with a mean maternal/fetal drug ratio that is inferior to one, indicating the drug may accumulate in fetal tissue over time (Siu et al., 2000). The placental transport of NSAIDs involves specific transports including monocarboxylate transporter 4 -a proton dependent transporter, which transports L-lactic acid as a substrate (Emoto et al., 2002). This case report highlights the importance of informing pregnant women about the risk of self-medication and topical NSAID use during pregnancy.

## CASE DESCRIPTION

We report the case of a newborn infant with persistent pulmonary hypertension of the newborn (PPHN) resulting from antenatal narrowing of the ductus arteriosus related to maternal application of topical Diclofenac during the second trimester of pregnancy. The infant was born to a 35-year-old mother both the course of the pregnancy–the mother's second–and antenatal blood tests were unremarkable. As recommended by the French National technical Committee on Prenatal Ultrasound Screening, three antenatal echography were performed during the first, second were described as normal. The third revealed cardiac ventricular asymmetry and a right ventricle cardiac hypertrophy (**Figure 1**).

A male infant weighing 3,470 g (50th-90th percentile) was delivered at 39 weeks of gestation by a planned cesarean section for breech presentation. Apgar scores were 10 at both 1 and 5 min. A pediatrician examined the baby 8 h after birth for moderate dyspnea. Cardiac auscultation revealed a systolic ejection murmur loudest over the pulmonary valve Pre-ductal oxygen saturation was 88% in room air, which increased to 98% with high flow nasal cannula at 2 L/Kg/min and $O_2$ supplementation (from 30 to 100% $FiO_2$). The newborn was admitted to the Neonatal Intensive Care Unit where an echocardiography showed supra-systemic pulmonary hypertension with tricuspid regurgitation blood flow velocities of 60 mmHg (**Figure 2**), whereas systolic blood pressure was 54 mmHg. An accelerated right-to-left shunting was recorded across a restrictive DA. No cardiac malformation was found.

Our hypotheses were therefore:

- a premature closure of the ductus arteriosus during pregnancy,
- a premature closure of the foramen ovale,
- or an alveolar capillary dysplasia.

A CT scan with contrast was performed 5 days after birth, showing an aneurysm of the inter-atrial septum without shunting, a dilated right ventricle and a markedly dilated main pulmonary artery.

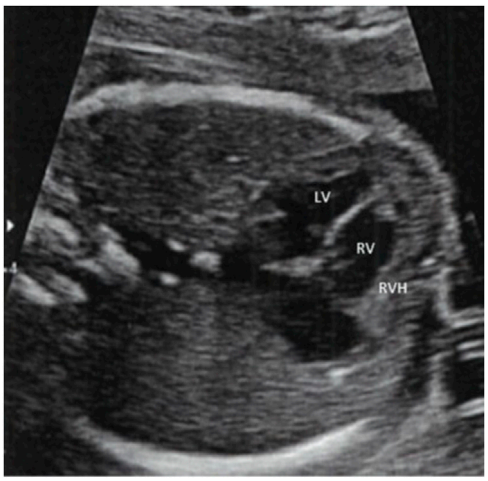


**FIGURE 1 |** Apical 4 chamber during fetal echocardiography at 32 weeks of gestation. Cardiac ventricular asymmetry and right ventricle cardiac hypertrophy. LV: Left Ventricle; RV: Right Ventricle; RVH: Right Ventricle Hypertrophy.

The newborn was managed by inhaled NO (20 ppm), alprostadil infusion (0.02 $\mu g^{-1}$ kg.$min^{-1}$) and high-flow oxygen supplementation through nasal cannulas for 18 days. Oral Sildenafil was started on day 3 due to the persistence of pulmonary hypertension. Symptoms improved on day 17, the ductus arteriosus was closed at day 20 and the infant was discharged from hospital on day 24 with normalization of pulmonary pressures (**Figure 3**). Sildenafil was stopped on day 157. At the age of 1 year, the infant presented no symptoms, a normal neuro-developmental outcome and a normal echocardiography.

Rigorous and repeated anamnestic determined that the mother applied Flector® (Diclofenac-Epolamine 140 mg patch, GENEVRIER SA Laboratory) on her lumbar area for back pain at 26 and 31 weeks of gestational age. In order to further reduce the pain, a hot water bottle was also applied to the area at the same time as the patch.

## DISCUSSION

This case reveals the risk of a sustained narrowing of the ductus arteriosus resulting in prolonged persistent pulmonary hypertension in the postnatal period after maternal use of topical diclofenac during the second trimester.

Besides NSAIDs, other causes of fetal ductal constriction and PPHN have previously been reported. Acetaminophen may increase the risk of prenatal ductus arteriosus constriction, through inhibition of prostaglandin G2 synthesis. Growing body of evidence suggests a role of maternal consumption of polyphenols-rich food (green tea, orange juice, coco bean, spring vegetables), which interfere with prostaglandin metabolism, in

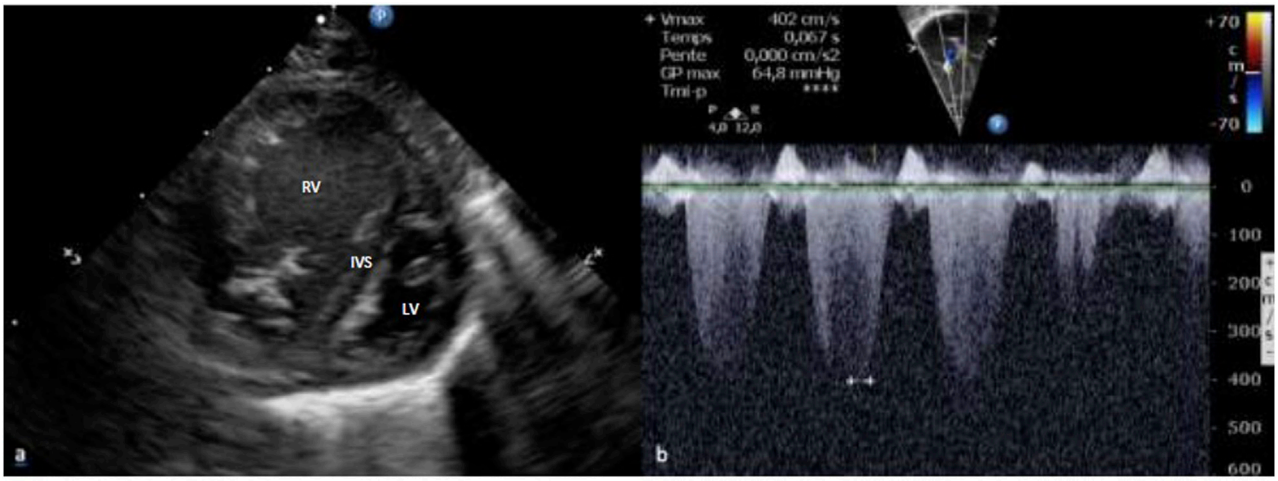


**FIGURE 2 |** Supra-systemic pulmonary hypertension was assessed on echocardiography. Parasternal short axis ventricles **(A)**: Bowing of the interventricular septum into the left ventricle. Apical 4 chamber **(B)**: Tricuspid regurgitation blood flow velocities higher than 4 $m.s^{-1}$. RV: Right Ventricle; LV: Left Ventricle; IVS: Interventricular Septum.

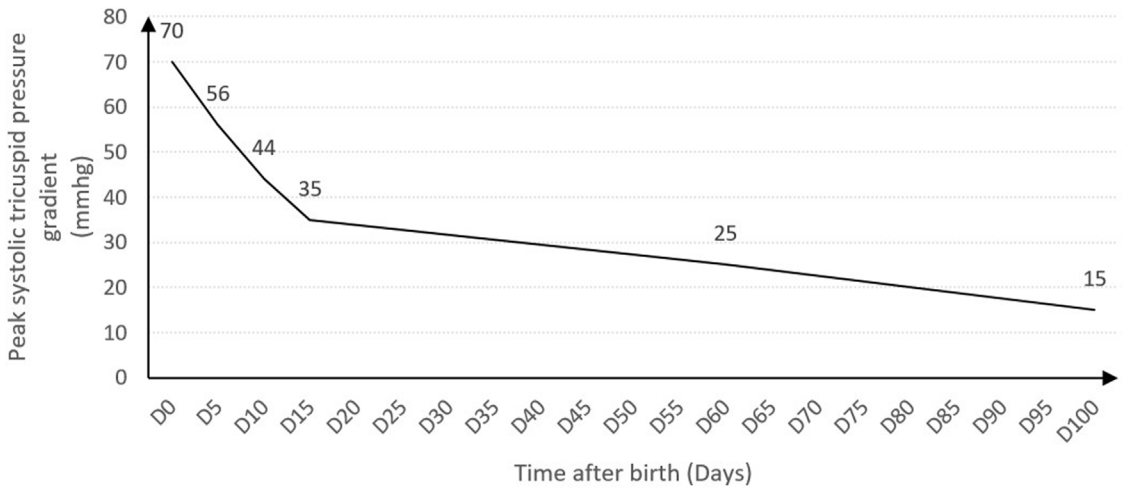


**FIGURE 3 |** Change of pulmonary artery systolic pressures (mmHg) estimated by measuring peak systolic tricuspid regurgitation velocity. PAPs normalized 2 months after birth. D, Day.

prenatal ductus arteriosus narrowing (Zielinsky and Busato, 2013). After rigorous questioning of the mother, no paracetamol treatment or excessive polyphenol-rich food intake were recorded.

Antenatal narrowing of the DA results in increased pulmonary artery pressure, which in turn mediates a remodeling of the vascular wall through sustained elevation of vascular stretch stress, leading to structural pulmonary hypertension (Storme et al., 2002; Larrue et al., 2005; Shima et al., 2011).

Previous studies clearly showed that DA sensitivity to constricting factors increases during the last trimester of pregnancy (Van den Veyver and Moise, 1993). The risk of indomethacin-induced fetal ductal constriction increases with advancing gestational age (Luchese et al., 2003). Second trimester fetal adverse events have been reported after prolonged NSAID exposure of at least 7 days while our case reports the occurrence of DA narrowing after two topical applications of a daily NSAID patch (48 h of total application) (Dathe et al., 2019).

Only one previous case of antenatal DA closure has been reported after maternal topical use of diclofenac during the third trimester of pregnancy. In that case, diclofenac has been applied at 35 weeks gestational age and the constriction of the ductus arteriosus was rapidly reversible at birth (Torloni et al., 2006). In this latter case report, the formulation of diclofenac incriminated in DA narrowing was a gel formulation of diclofenac

diethlyamine (Cataflam Rmugel 11.6 mg/g, Novartis). It is of current knowledge that topical NSAIDs, including diclofenac diethylamine, are associated with systemic effects (Evans et al., 1995). The patch delivery in diclofenac-epolamine (DI-EP) was developed more recently to prevent the acute release of NSAIDS to the bloodstream and control the amount of active substance delivered through the skin, in contrast to that from application of bioequivalent gels or ointments of diclofenac (Goh and Lane, 2014). The pharmacokinetics parameters of diclofenac patches are expected to lengthen the time of product release in the central comportment, to reach a maximal plasmatic concentration of about 20 ng/ml (Rainsford et al., 2008). Previous studies on transplacental pharmacokinetics of diclofenac reported that the fetal peak plasma concentration was estimated to be one-tenth of the maternal value (Shintaku et al., 2012). Concerning pharmacodynamics, an animal predictive model performed on rats revealed that the concentration–response (response being DA narrowing) relationship in rat fetus was characterized by an EC50 of 1.4 ng/ml, reinforcing the plausibility of the link between diclofenac patch application and DA narrowing in our case report (Shintaku et al., 2012). Furthermore, it is likely that the use of hot water bottle for back pain may have promoted skin absorbance of the drug (Park et al., 2008; Panda et al., 2019).

There are no reports on the occurrence of systemic side effects related to a single topical NSAIDs application, when applied in conformity with recommendations of us, in current literature. The risk of occurrence is often related to misuse; in our case, the application of heat to the same area as the patch led to an increase of the drug's absorption and the modification of the delivery profile of diclofenac.

Regarding these elements, the implication of the DI-EP patch (Flector®) in the occurrence of pulmonary hypertension in newborn infants cannot be excluded. Furthermore, it is likely that the use of a hot water bottle for back pain may have promoted skin absorbance of the drug (Park et al., 2008; Panda et al., 2019). In light of this evidence, the role of the DI-EP patch (Flector®) on pulmonary hypertension in newborns in must be highly considered.

Cases of antenatal closure of the DA after oral use of diclofenac during the third trimester of pregnancy have more commonly been reported (Auer et al., 2004). According to the summary of product characteristics, the use of FLECTOR® patch must be avoided during the five first months of pregnancy and is strictly contraindicated during the 3rd trimester of pregnancy. Many other patches containing diclofenac as the main active substance are available on the market (Voltarenplast®, Antacalm®, Flectoreffigel®). They differ in the salt of diclofenac they contain and must be responsible for an equivalent risk of DA narrowing. Patches containing diclofenac salts are over-the-counter medications in many countries and their use does not require any medical prescription, enhancing the risk of misuse in pregnant women.

Our findings suggest that maternal educational programs should include information pertaining to topical treatments in order to prevent potentially harmful self-medication in pregnant women.

## DATA AVAILABILITY STATEMENT

The raw data supporting the conclusions of this article will be made available by the authors, without undue reservation.

## ETHICS STATEMENT

Ethical review and approval was not required for the study on human participants in accordance with the local legislation and institutional requirements. Written informed consent to participate in this study was provided by the participants' legal guardian/next of kin.

## AUTHOR CONTRIBUTIONS

KL, SG, SM, MB, OD, JB, PO, and LS were involved in drafting the manuscript. All authors read and approved the final version of the manuscript.

## ACKNOWLEDGMENTS

The authors thank Kelly Saint Denny for English editing.

## REFERENCES

Auer, M., Brezinka, C., Eller, P., Luze, K., Schweigmann, U., and Schwärzler, P. (2004). Prenatal Diagnosis of Intrauterine Premature Closure of the Ductus Arteriosus Following Maternal Diclofenac Application. *Ultrasound Obstet. Gynecol.* 23, 513–516. doi:10.1002/uog.1038

Clyman, R. I. (2006). Mechanisms Regulating the Ductus Arteriosus. *Neonatology* 89, 330–335. doi:10.1159/000092870

Cordero, J. A., Camacho, M., Obach, R., Domenech, J., and Vila, L. (2001). *In Vitro* based index of Topical Anti-inflammatory Activity to Compare a Series of NSAIDs. *Eur. J. Pharm. Biopharm.* 51, 135–142. doi:10.1016/S0939-6411(00)00149-1

Dathe, K., Hultzsch, S., Pritchard, L. W., and Schaefer, C. (2019). Risk Estimation of Fetal Adverse Effects after Short-Term Second Trimester Exposure to Non-steroidal Anti-inflammatory Drugs: a Literature Review. *Eur. J. Clin. Pharmacol.* 75, 1347–1353. doi:10.1007/s00228-019-02712-2

Emoto, A., Ushigome, F., Koyabu, N., Kajiya, H., Okabe, K., Satoh, S., et al. (2002). H(+)-linked Transport of Salicylic Acid, an NSAID, in the Human Trophoblast Cell Line BeWo. *Am. J. Physiol. Cel Physiol* 282, C1064–C1075. doi:10.1152/ajpcell.00179.2001

Evans, J. M., McMahon, A. D., McGilchrist, M. M., White, G., Murray, F. E., McDevitt, D. G., et al. (1995). Topical Non-steroidal Anti-inflammatory Drugs and Admission to Hospital for Upper Gastrointestinal Bleeding and Perforation: a Record Linkage Case-Control Study. *BMJ* 311, 22–26. doi:10.1136/bmj.311.6996.22

Gewillig, M., Brown, S. C., De Catte, L., Debeer, A., Eyskens, B., Cossey, V., et al. (2009). Premature Foetal Closure of the Arterial Duct: Clinical Presentations and Outcome. *Eur. Heart J.* 30, 1530–1536. doi:10.1093/eurheartj/ehp128

Goh, C. F., and Lane, M. E. (2014). Formulation of Diclofenac for Dermal Delivery. *Int. J. Pharm.* 473, 607–616. doi:10.1016/j.ijpharm.2014.07.052

Larrue, B., Jaillard, S., Lorthioir, M., Roubliova, X., Butrous, G., Rakza, T., et al. (2005). Pulmonary Vascular Effects of Sildenafil on the Development of Chronic Pulmonary Hypertension in the Ovine Fetus. *Am. J. Physiol. Lung Cel Mol Physiol* 288, L1193–L1200. doi:10.1152/ajplung.00405.2004

Luchese, S., Mânica, J. L., and Zielinsky, P. (2003). Intrauterine Ductus Arteriosus Constriction: Analysis of a Historic Cohort of 20 Cases. *Arq Bras Cardiol.* 81, 405–404. doi:10.1590/S0066-782X2003001200007

Momma, K., Hagiwara, H., and Konishi, T. (1984). Constriction of Fetal Ductus Arteriosus by Non-steroidal Anti-inflammatory Drugs:study of Additional 34 Drugs. *Prostaglandins* 28, 527–536. doi:10.1016/0090-6980(84)90241-7

Panda, A., Sharma, P. K., and Narasimha Murthy, S. (2019). Effect of Mild Hyperthermia on Transdermal Absorption of Nicotine from Patches. *AAPS PharmSciTech* 20, 77. doi:10.1208/s12249-019-1299-x

Park, J. H., Lee, J. W., Kim, Y. C., and Prausnitz, M. R. (2008). The Effect of Heat on Skin Permeability. *Int. J. Pharm.* 359, 94–103. doi:10.1016/j.ijpharm.2008.03.032

Rainsford, K. D., Kean, W. F., and Ehrlich, G. E. (2008). Review of the Pharmaceutical Properties and Clinical Effects of the Topical NSAID Formulation, Diclofenac Epolamine. *Curr. Med. Res. Opin.* 24, 2967–2992. doi:10.1185/03007990802381364

Rasanen, J., Wood, D. C., Weiner, S., Ludomirski, A., and Huhta, J. C. (1996). Role of the Pulmonary Circulation in the Distribution of Human Fetal Cardiac Output during the Second Half of Pregnancy. *Circulation* 94, 1068–1073. doi:10.1161/01.CIR.94.5.1068

Shima, Y., Ishikawa, H., Matsumura, Y., Yashiro, K., Nakajima, M., and Migita, M. (2011). Idiopathic Severe Constriction of the Fetal Ductus Arteriosus: a Possible Underestimated Pathophysiology. *Eur. J. Pediatr.* 170, 237–240. doi:10.1007/s00431-010-1295-3

Shintaku, K., Hori, S., Satoh, H., Tsukimori, K., Nakano, H., Fujii, T., et al. (2012). Prediction and Evaluation of Fetal Toxicity Induced by NSAIDs Using Transplacental Kinetic Parameters Obtained from Human Placental Perfusion Studies. *Br. J. Clin. Pharmacol.* 73, 248–256. doi:10.1111/j.1365-2125.2011.03921.x

Siu, S. S., Yeung, J. H., and Lau, T. K. (2000). A Study on Placental Transfer of Diclofenac in First Trimester of Human Pregnancy. *Hum. Reprod.* 15, 2423–2425. doi:10.1093/humrep/15.11.2423

Storme, L., Aubry, E., Rakza, T., Houeijeh, A., Debarge, V., Tourneux, P., et al. (2013). Pathophysiology of Persistent Pulmonary Hypertension of the Newborn: Impact of the Perinatal Environment. *Arch. Cardiovasc. Dis.* 106, 169–177. doi:10.1016/j.acvd.2012.12.005

Storme, L., Parker, T. A., Kinsella, J. P., Rairigh, R. L., and Abman, S. H. (2002). Chronic Hypertension Impairs Flow-Induced Vasodilation and Augments the Myogenic Response in Fetal Lung. *Am. J. Physiol. Lung Cel Mol Physiol* 282, L56–L66. doi:10.1152/ajplung.2002.282.1.L56

Torloni, M. R., Cordioli, E., Zamith, M. M., Hisaba, W. J., Nardozza, L. M., Santana, R. M., et al. (2006). Reversible Constriction of the Fetal Ductus Arteriosus after Maternal Use of Topical Diclofenac and Methyl Salicylate. *Ultrasound Obstet. Gynecol.* 27, 227–229. doi:10.1002/uog.2647

Van den Veyver, I. B., and Moise, K. J. (1993). Prostaglandin Synthetase Inhibitors in Pregnancy. *Obstet. Gynecol. Surv.* 48, 493–502. doi:10.1097/00006254-199307000-00026

Van Marter, L. J., Leviton, A., Allred, E. N., Pagano, M., Sullivan, K. F., Cohen, A., et al. (1996). Persistent Pulmonary Hypertension of the Newborn and Smoking and Aspirin and Nonsteroidal Antiinflammatory Drug Consumption during Pregnancy. *Pediatrics* 97, 658–663. doi:10.1097/00006254-199611000-00010

Zielinsky, P., and Busato, S. (2013). Prenatal Effects of Maternal Consumption of Polyphenol-Rich Foods in Late Pregnancy upon Fetal Ductus Arteriosus. *Birth Defects Res. C Embryo Today* 99, 256–274. doi:10.1002/bdrc.21051

**Conflict of Interest:** The authors declare that the research was conducted in the absence of any commercial or financial relationships that could be construed as a potential conflict of interest.

**Publisher's Note:** All claims expressed in this article are solely those of the authors and do not necessarily represent those of their affiliated organizations, or those of the publisher, the editors and the reviewers. Any product that may be evaluated in this article, or claim that may be made by its manufacturer, is not guaranteed or endorsed by the publisher.

frontiers in Pharmacology

ORIGINAL RESEARCH
published: 09 December 2021
doi: 10.3389/fphar.2021.768599

# Metabolomic Profiling Identifies Exogenous and Microbiota-Derived Metabolites as Markers of Methotrexate Efficacy in Juvenile Idiopathic Arthritis

*Ryan Sol Funk*[1]* *and Mara L. Becker*[2]

[1]Department of Pharmacy Practice, University of Kansas Medical Center, Kansas City, KS, United States, [2]Department of Pediatrics, Division of Rheumatology, Duke University School of Medicine, Durham, NC, United States

Variability in methotrexate (MTX) efficacy represents a barrier to early and effective disease control in the treatment of juvenile idiopathic arthritis (JIA). This work seeks to understand the impact of MTX on the plasma metabolome and to identify metabolic biomarkers of MTX efficacy in a prospective cohort of children with JIA. Plasma samples from a cohort of children with JIA ($n$ = 30) collected prior to the initiation of MTX and after 3 months of therapy were analyzed using a semi-targeted global metabolomic platform detecting 673 metabolites across a diversity of biochemical classes. Disease activity was measured using the 71-joint count juvenile arthritis disease activity score (JADAS-71) and clinical response to MTX was based on achievement of ACR Pedi 70 response. Metabolomic analysis identified 50 metabolites from diverse biochemical classes that were altered following the initiation of MTX ($p < 0.05$) with 15 metabolites reaching a false-discovery rate adjusted p-value (q-value) of less than 0.05. Enrichment analysis identified a class-wide reduction in unsaturated triglycerides following initiation of MTX (q = 0.0009). Twelve of the identified metabolites were significantly associated with disease activity by JADAS-71. Reductions in three metabolites were found to be associated with clinical response by ACR Pedi 70 response criteria and represented several microbiota and exogenously derived metabolites including: dehydrocholic acid, biotin, and 4-picoline. These findings support diverse metabolic changes following initiation of MTX in children with JIA and identify metabolites associated with microbial metabolism and exogenous sources associated with MTX efficacy.

**Keywords: juvenile idiopathic arthritis, methotrexate, metabolomic, biomarker, pediatric, pharmacology**

OPEN ACCESS

***Edited by:***
*Catherine M. T. Sherwin, Wright State University, United States*

***Reviewed by:***
*Diederik De Cock, Division of Skeletal Tissue Engineering, Belgium*
*Stuart MacLeod, University of British Columbia, Canada*

***Correspondence:**
*Ryan Sol Funk*
*ryanfunk@kumc.edu*

***Specialty section:***
*This article was submitted to Obstetric and Pediatric Pharmacology, a section of the journal Frontiers in Pharmacology*

***Received:*** *31 August 2021*
***Accepted:*** *18 November 2021*
***Published:*** *09 December 2021*

***Citation:***
*Funk RS and Becker ML (2021) Metabolomic Profiling Identifies Exogenous and Microbiota-Derived Metabolites as Markers of Methotrexate Efficacy in Juvenile Idiopathic Arthritis. Front. Pharmacol. 12:768599. doi: 10.3389/fphar.2021.768599*

## INTRODUCTION

Rapid control of disease activity to prevent irreversible joint damage and improve long-term outcomes continues to be a major therapeutic goal in the treatment of juvenile idiopathic arthritis (JIA) (Consolaro et al., 2012). Response to drug therapy is currently characterized by a variable and unpredictable course, which commonly necessitates a trial-and-error treatment approach to identify an effective treatment regimen (Becker, 2012). In the management of JIA, methotrexate (MTX) has continued to be a cornerstone of therapy since the establishment of its

efficacy in the early 1990s (Giannini et al., 1992). However, MTX is characterized by a delayed onset of action with approximately one in three patients failing to adequately respond to initial treatment (Ruperto et al., 2004). At this time, no reliable biomarkers exist to guide drug selection and optimization and the current approach wastes precious time and jeopardizes the overarching goal of early disease control (Funk and Becker, 2016). As a result, there exists a need to apply novel analytical approaches to further understand the pharmacology of MTX and to identify biomarkers to guide clinicians in the selection and optimization of drug therapy.

Efforts to identify clinical biomarkers of MTX response in JIA have predominately focused on targeted analyses related to the disposition of MTX, its intracellular metabolism to form polyglutamated metabolites, and its pharmacological effects on folate and folate-dependent biochemical pathways (Funk et al., 2014; Calasan et al., 2015). A major limitation to this targeted approach has been the biased nature of these studies, which often limit that analysis to only a handful of metabolites representing a limited number of biochemical pathways. As an -omics approach, metabolomics offers a relatively unbiased method to investigate the effect of MTX on a diversity of biochemicals and biochemical pathways towards an improved understanding of the pharmacological basis for response to MTX and to identify potential metabolic biomarkers of MTX response in JIA (Funk et al., 2020).

The metabolome is the complete set of low-molecular weight chemicals within a biological system and represents not only the activities of genetically encoded metabolic pathways, but also reflects exogenous exposures (e.g., diet, drugs, vitamins, toxins, microbiota) (Fiehn, 2002). Metabolomics is the study of these molecules within that system. In the case of patients, the plasma or serum metabolome is commonly measured because of the relative ease of collection, preparation, and storage (Beger et al., 2016). Metabolomic studies have been conducted in patients with rheumatoid arthritis (RA) and other autoimmune diseases and have identified several metabolites and metabolic pathways associated with disease activity and drug response (Wang et al., 2012; Jiang et al., 2013; Kapoor et al., 2013; Young et al., 2013; Guma et al., 2016). However, this work represents the first to evaluate metabolomic changes resulting from the initiation of MTX in JIA and the association of these changes with the drug's early clinical efficacy.

In this exploratory study, a semi-targeted global metabolomics approach is applied to evaluate metabolomic changes associated with the initiation of MTX in a prospective cohort of children with JIA. The resulting metabolomic data is subsequently used to identify potential metabolic biomarkers of MTX response in these patients and novel biochemical pathways relevant to MTX efficacy in JIA. The metabolomic profiles are evaluated using chemometric and network enrichment analyses to interpret the impact of MTX on the plasma metabolome and they are then further integrated with the clinical response data to identify putative metabolomic markers of MTX response in JIA.

# MATERIALS AND METHODS

## Patients

Plasma samples were acquired from a single-center prospective cohort of JIA patients. The study included patients diagnosed with JIA requiring initiation of MTX monotherapy as deemed appropriate by their treating provider. Patients who required a concurrent biologic disease modifying antirheumatic drug (DMARD) were excluded. Diagnosis of JIA was established based on the Edmonton 2001 International League of Associations of Rheumatology (ILAR) criteria for JIA (Petty et al., 2004). Patients were initiated on a standardized MTX dose of 15 mg/m$^2$ weekly along with 1 mg folic acid daily. MTX route of administration for the study was standardized to subcutaneous, however due to a national shortage of MTX for injection, oral MTX was permitted ($n$ = 12). All patients completed 3 months of full and consistent dosing of 15 mg/m$^2$ of MTX weekly prior to their follow up sample collection. Concurrent medications allowed included nonsteroidal anti-inflammatory drugs (NSAIDs) and daily low-dose corticosteroids (the lesser of 0.2 mg/kg/day or 10 mg of prednisone). Intra-articular corticosteroid injections (IASI) were allowed, however injected joints were counted as "active" at follow up to reduce the potential bias resulting from IASI. Venous blood samples (10 ml) were collected in K2-EDTA containing tubes prior to initiation of MTX and at the patient's routine 3-months follow up clinic visit along with routine laboratory blood draws. Parental/patient (>18 years of age) written informed consent and patient written informed assent for patients ages 7–18 years were collected from all participants in accordance with approval from the Children's Mercy Hospital Pediatric Institutional Review Board.

## Clinical Data

Clinical response data collected at 3 months included the American College of Rheumatology (ACR) Pediatric 30, 50, and 70 response, which is a composite score comprised of: 1) physician global assessment of disease activity (MD-VAS), 2) patient/parent assessment of overall well-being (PT-VAS), 3) functional ability (Childhood Health Assessment Questionnaire, CHAQ), 4) number of joints with active arthritis, 5) number of joints with limited range of motion, and 6) erythrocyte sedimentation rate (ESR) (Giannini et al., 1997). We also utilized the validated continuous Juvenile Arthritis disease Activity Score (JADAS-71) compiled from the normalized ESR, the active joint count, PT-VAS, and MD-VAS (Consolaro et al., 2009). Additional variables collected included age, sex, serum c-reactive protein (CRP) levels, MTX route of administration, NSAID use, and oral corticosteroid use.

## Metabolomics Analysis

Plasma was isolated from venous blood samples by centrifugation at 2,000 RPM in a Beckman tabletop centrifuge for 10 min. The resulting plasma supernatant was separated into aliquots and stored at -80°C prior to analysis. Samples were shipped on dry ice to the NIH West Coast Metabolomics Center at the University of California, Davis (Davis, CA) for global semi-targeted analysis

utilizing three independent standardized analytical methods to measure intermediates of primary metabolism, biogenic amines, and lipids (Cajka and Fiehn, 2016; Fiehn, 2016). Samples were thawed and prepared for analysis using a biphasic liquid-liquid extraction method developed for metabolomic analysis using plasma and serum samples across the three analytical platforms, which includes automated liner exchange-cold injection system gas chromatography time-of-flight mass spectrometry, charged surface hybrid chromatography electrospray ionization quadropole time-of-flight mass spectrometry, and hydrophilic interaction liquid chromatography electrospray ionization quadropole time-of-flight mass spectrometry. The resulting peaks were identified based on retention times and mass spectra from MassBank of North America and reported as peak height intensities. Peak height intensity tables were curated by the NIH West Coast Metabolomics Center and submitted to Metabolomics Workbench (https://www.metabolomicsworkbench.org/) under Project ID PR001148. Raw peak intensity data from each analytical platform underwent a standardized normalization procedure. The normalization ratio was calculated as the ratio of the sum of peak heights for all identified metabolites (mTIC) for each sample to the total average mTIC for all samples. Peak heights for each metabolite were divided by the normalization ratio to arrive at the normalized peak height intensity. Metabolites measured in more than one analytical platform were combined by mean normalization to give equal weighting to each platform and averaged. The resulting normalized peak height intensities for identified compounds were uploaded into MetaboAnalyst 3.0 and normalized by logarithmic transformation and Pareto scaling (Xia et al., 2015; Xia and Wishart, 2016). The resulting data were analyzed for fold-change and non-parametric paired analysis and visualized using volcano plots to identify metabolites significantly altered following the initiation of MTX.

## Enrichment Analysis

The fold-change and p-values for each identified metabolite were extracted and used to conduct chemical and metabolic network enrichment analysis. Visualization of chemometric and biochemical networks altered following the initiation of MTX was conducted using MetaMapp to generate a network map based on chemical similarity utilizing the Kyoto Encyclopedia of Genes and Genomes (KEGG) metabolic network database and Tanimoto substructure similarity coefficients (Barupal et al., 2012). The resulting mapping data was uploaded into Cytoscape 3.7.1 for visualization. Enrichment analysis based on chemical similarity was also conducted using the open-source software Chemical Similarity Enrichment Analysis for Metabolomics (ChemRICH) (Barupal and Fiehn, 2017). The ChemRICH analysis uses Tanimoto substructure similarity coefficients and medical subject headings ontology to generate non-overlapping clusters of metabolites into distinct chemical classes and is independent of biochemical pathway assignments.

## Statistical Analysis

Analysis of changes in individual metabolites following the initiation of MTX was conducted in MetaboAnalyst 3.0 using paired non-parametric univariate analysis. All metabolites achieving a raw p-value less than 0.05 were used in the chemometric and metabolic network enrichment analyses. Statistical testing within the chemometric analysis using the ChemRICH platform was determined by Kolmogorv-Smirnov testing and an FDR adjusted p-value (q-value) of less than 0.05 was considered significant. Individual metabolites achieving a q-value less than 0.05 were selected for individual analysis for their relationship with disease activity and clinical response to MTX. The Wilcoxon rank-sum test was used to compare changes in metabolites levels over the treatment period between patient groups based on clinical response based on ACR Pedi 70 or JADAS-71. Spearman's correlations were used to evaluate the relationships between metabolite levels and disease activity by JADAS-71 and active joint counts. A multivariate nominal regression model analysis was used to explore multivariate associations with MTX response. Analyses were performed using JMP software version 11 (SAS Institute, Cary, NC).

**TABLE 1 |** Patient demographic and clinical data. Following 3-months of MTX therapy, patients meeting the ACR Pedi 70 response criteria (ACR Pedi >70) were considered responsive to MTX and patients failing to meet ACR Pedi 30 response criteria were considered non-responsive to MTX. The demographics, concomitant medications, route of MTX administration, and baseline and 3-months measures of disease activity are included and compared between the two groups (comparisons resulting in a *p-value* < 0.05 are italicized). Baseline clinical data are representative of the larger cohort from which these samples were chosen (data not shown).

| | **ACR pedi < 30** | **ACR pedi > 70** | **p-value** |
|---|---|---|---|
| Patients, no | 15 | 15 | NA |
| Female, no. (%) | 10 (67) | 11 (73) | 1.0 |
| Age, years | 10 [6,15] | 9 [5,13] | 0.48 |
| NSAID, no. (%) | 14 (93) | 11 (73) | 0.33 |
| Corticosteroids, no. (%) | 2 (13.3) | 0 (0) | 0.48 |
| MTX, subcutaneous, no. (%) | 7 (47) | 11 (73) | 0.26 |
| ***Baseline*** | **ACR Pedi < 30** | **ACR Pedi > 70** | **p-value** |
| Active joints, no | 6 [2,11] | 6 [2,13] | 1.0 |
| PT-VAS | 6 [3,8] | 6 [3,8] | 0.80 |
| MD-VAS | 4 [3,7] | 5 [3,6] | 0.97 |
| CHAQ | 0.4 [0.1.6] | 0.7 [0.3.1.2] | 0.36 |
| ESR, mm/hr | 10 [9,23] | 16 [10,57] | 0.10 |
| CRP | 0.6 [0.5.1.5] | 1.5 [0.5.3.2] | 0.10 |
| JADAS-71 | 16 [13.24.6] | 18.7 [10.6.34] | 0.85 |
| ***3-months*** | **ACR Pedi < 30** | **ACR Pedi > 70** | **p-value** |
| Active joints, no | 5 [1,9] | 0 [0,5] | *0.02* |
| PT-VAS | 5 [3,7] | 0 [0,2] | *<0.0001* |
| MD-VAS | 3.5 [1.8.5] | 0 [0,1] | *<0.0001* |
| CHAQ | 0.4 [0.1.1] | 0 [0,0] | *0.003* |
| ESR, mm/hr | 9 [7.8.17.8] | 9 [7,14] | 0.76 |
| CRP | 0.5 [0.5.1.1] | 0.5 [0.5.1.2] | 0.31 |
| JADAS-71 | 14.2 [7.8.17] | 2 [0,7] | *0.0002* |

# RESULTS

## Patient Demographic and Clinical Data

Subjects were identified for inclusion in this analysis from an ongoing prospective cohort study on biomarkers of MTX

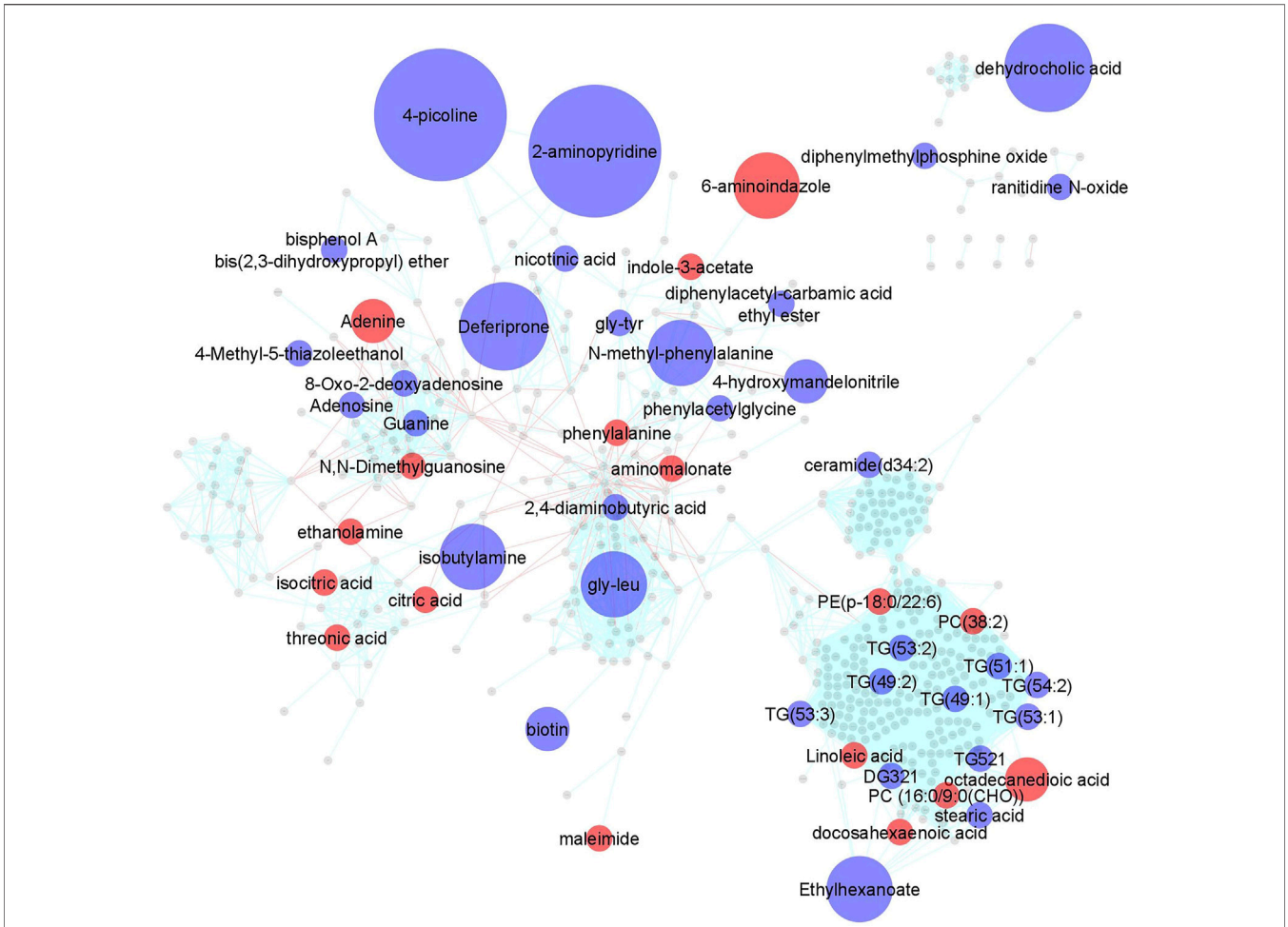


**FIGURE 1 |** Changes in the plasma metabolomic profile in children with JIA following the initiation of MTX. Metabolite levels were determined at baseline and after 3 months of MTX therapy. Changes in metabolite levels were determined by paired analysis and metabolic changes were mapped using MetaMapp and visualized in Cytoscape 3.7.1. Metabolites found to significantly change based on a p-value < 0.05 were color coded and indicate either an increase (red) or decrease (blue) following initiation of MTX. Node size is proportional to measured fold-change. Red lines between nodes represent KEGG reaction pairs, while blue-green lines represent pairing based on chemical similarity.

efficacy in JIA. Subject selection was based on the availability of plasma samples both at baseline and after 3 months of MTX therapy at a stable dose of 15 mg/m$^2$, as well as the availability of clinical response data defined using the ACR Pedi response criteria. To optimize discrimination, 2 groups comprised of extreme response phenotypes were selected. Specifically, 15 subjects were selected based on the achievement of ACR Pedi 70 response criteria by 3 months and were classified as "responders", and 15 subjects were selected based on their failure to achieve ACR Pedi 30 response criteria by 3 months and were classified as "non-responders". The demographics of each of the two groups are provided for comparison (**Table 1**). The cohort consisted of 30 subjects with a median age of 9.9 years (range: 1.8–17 years), with 21 females, 25 subjects on concomitant NSAID therapy, 2 receiving corticosteroids, and 18 receiving MTX *via* subcutaneous injection. No significant differences in baseline demographic characteristics nor baseline measures of disease activity were found between the groups. Of note, there were also no significant differences in baseline clinical characteristics with the remaining portion of the cohort excluded from this work ($n$ = 38) including JIA subtype, age, gender, MTX route of administration, MD-VAS, PT-VAS, CHAQ, baseline active joint count, baseline JADAS-71, ESR or CRP. As expected, multiple measures of disease activity were significantly lower at the 3-months visit in the responder group compared to the non-responders, including: JADAS-71, active joint count, PT-VAS, MD-VAS, and CHAQ.

Impact of MTX on the plasma metabolome in JIA. Using a semi-targeted global metabolomics approach, 673 identified metabolites were measured in plasma samples collected for each patient at baseline and at their 3-months visit. A paired analysis was conducted to evaluate metabolic changes over the treatment period and a metabolic network map was created

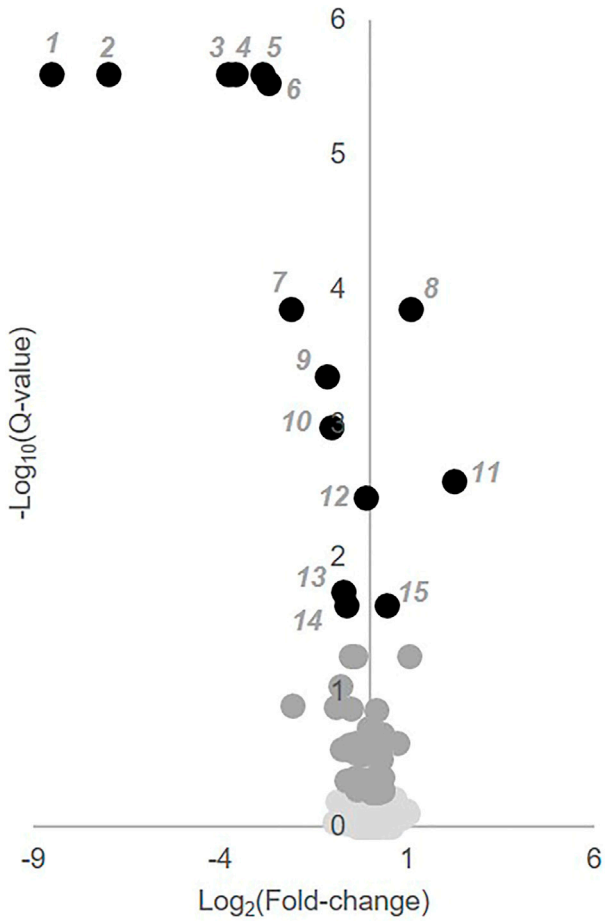


**FIGURE 2 |** Identification of key metabolites altered following the initiation of MTX. Semi-quantitative data from 673 identified metabolites measured at baseline and after 3 months of MTX therapy were compared by paired univariate analysis. Metabolomics data was analyzed using MetaboAnalyst 3.0 and the resulting volcano plot of key metabolites based on a q-value < 0.05 are presented. In the volcano plot, black numbered metabolites represent those found to be altered following the initiation of MTX.

using MetaMapp and visualized in Cytoscape 3.7.1 (**Figure 1**). As highlighted, 50 metabolites across a diversity of biochemical classes were impacted by MTX ($p < 0.05$). Further chemometric enrichment analysis by chemical class clustering was conducted using the ChemRICH platform and identified a class effect of MTX on unsaturated triglycerides. MTX treatment was found to be associated with a reduction in plasma levels of unsaturated triglycerides (q = 0.0009).

## Identification of Plasma Metabolic Markers Responsive to MTX Therapy in JIA

To identify individual metabolic markers that are responsive to MTX therapy, metabolites found to change over the treatment period with a q-value less than 0.05 were selected for further analysis (**Figure 2**). A total of 15 metabolites met these criteria and are listed along with their chemical class, fold-change, direction of change, coefficient of variation for both baseline and 3-months measurements, and q-value (**Table 2**). Plots for the semi-quantitative measurement of each of the identified metabolites based on log normalized peak intensity is provided for visual comparison (**Figure 3**).

## Association of Metabolic Markers With Disease Activity in JIA

Metabolites significantly impacted following the initiation of MTX were then evaluated for their association with disease activity using metabolite levels and JADAS-71 scores combined from both the baseline and 3-months visit (**Figure 4**). Lower disease activity scores were found to be significantly associated with lower levels of 2-aminopyridine (q = 0.002), biotin (q = 0.002), dehydrocholic acid (q = 0.002), isobutylamine (q = 0.002), glycine-leucine (gly-leu) (q = 0.002), 4-picoline (q = 0.002), deferiprone (0.002), triacylglycerol 53:2 (TG 53:2) (q = 0.004), nicotinic acid (q = 0.007), 4-hydroxymandelonitrile (q = 0.007), and higher levels of adenine (q = 0.005) and 6-aminoindazole (q = 0.007). For comparison, the correlation of the identified metabolites with JADAS-71 were stronger than those observed for serum CRP levels ($\rho = 0.31$, $p = 0.31$) and similar to those seen with the ESR ($\rho = 0.45$, $p = 0.0004$), which is a component of the JADAS-71 composite score calculation.

Similarly, the total number of active joint counts at baseline and 3-months were evaluated for their association with the identified metabolic markers. Lower active joint counts were associated with lower levels of 2-aminopyridine ($\rho = 0.27$, $p = 0.03$, q = 0.096), biotin ($\rho = 0.33$, $p = 0.01$, q = 0.06), dehydrocholic acid ($\rho = 0.34$, $p = 0.007$, q = 0.06), gly-leu ($\rho = 0.26$, $p = 0.05$, q = 0.096), and higher levels of adenine ($\rho = -0.26$, $p = 0.05$, q = 0.096) and 6-aminoindazole ($\rho = -0.35$, $p = 0.006$, q = 0.06). In contrast, active joint counts were not found to be significantly correlated with either serum CRP levels ($\rho = 0.11$, $p = 0.41$), or the ESR ($\rho = 0.18$, $p = 0.17$).

## Metabolic Markers Associated With MTX Efficacy in JIA

MTX efficacy in this study was defined as achieving a 70% improvement in disease activity based on the ACR Pedi 70 response criteria by 3 months. Non-responders were defined as those not even achieving ACR Pedi 30 response criteria. Changes in metabolite concentrations over 3 months following the initiation of MTX were compared between patients classified as responders and non-responders. Of the metabolites found to be significantly altered following the initiation of MTX, only changes in three of these metabolites were found to be associated with MTX response and included: dehydrocholic acid (q = 0.0003), 4-picoline (q = 0.05), and biotin (q = 0.24) (**Figure 5**). Low disease activity at 3 months, defined as a JADAS-71 score of ≤2.5, was used as a secondary measure of MTX response. Of the metabolites found to be significantly associated with ACR Pedi 70 response at 3 months, only changes in dehydrocholic acid were found to be significantly

**TABLE 2 |** Plasma metabolites altered following 3-months of MTX therapy. The table of metabolites are identified by number from the volcano plot in **Figure 2**. The metabolite name, chemical class, fold-change color coded based on whether the metabolite increased (red) or decrease (blue), the coefficient of variation (CV) for the metabolite at the baseline and 3-months timepoint, and the q-value are provided.

| # | Name | Class | Fold-change | Baseline CV | 3-months CV | q-value |
|---|---|---|---|---|---|---|
| 1 | 2-Aminopyridine | Pyridine | 370 | 0.38 | 2.82 | $2.5 \times 10^{-6}$ |
| 2 | 4-Picoline | Picoline | 125 | 0.26 | 2.65 | $2.5 \times 10^{-6}$ |
| 3 | Dehydrocholic Acid | Bile Acid | 14 | 0.39 | 1.83 | $2.5 \times 10^{-6}$ |
| 4 | Deferiprone | Pyridine | 12 | 1.74 | 1.51 | $2.5 \times 10^{-6}$ |
| 5 | Isobutylamine | Butylamine | 7.1 | 0.43 | 1.11 | $2.5 \times 10^{-6}$ |
| 6 | Ethylhexanoate | Fatty Acid | 6.3 | 4.45 | 2.67 | $3.0 \times 10^{-6}$ |
| 7 | Gly-Leu | Dipeptide | 4.3 | 0.70 | 1.02 | $1.4 \times 10^{-4}$ |
| 8 | Adenine | Purine | 2.1 | 0.50 | 0.39 | $1.4 \times 10^{-4}$ |
| 9 | Biotin | Imidazole | 2.2 | 0.34 | 0.55 | $4.5 \times 10^{-4}$ |
| 10 | 4-Hydroxymandelonitrile | Acetonitrile | 2.0 | 0.40 | 0.64 | 0.0011 |
| 11 | 6-Aminoimidazole | Indazole | 4.8 | 1.45 | 0.67 | 0.0027 |
| 12 | Ceramide (d34:2) | Ceramide | 1.1 | 0.29 | 0.21 | 0.0036 |
| 13 | Nicotinic Acid | Pyridine | 1.6 | 1.79 | 3.88 | 0.018 |
| 14 | TG (53:2) | Triglyceride | 1.5 | 0.51 | 0.75 | 0.023 |
| 15 | Maleimide | Maleimide | 1.40 | 0.33 | 0.33 | 0.023 |

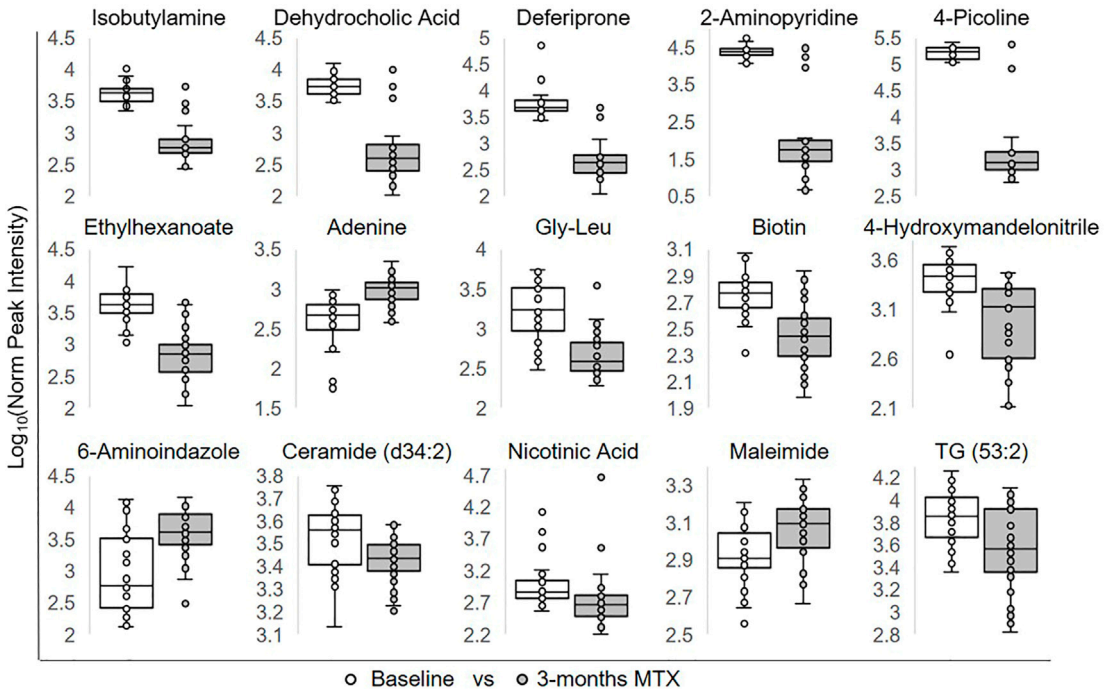


**FIGURE 3 |** Relative plasma levels of metabolites significantly altered following the initiation of MTX. The log normalized peak ion intensity plots for the eight metabolites identified by univariate analyses are presented. Data points and representative box and whisker plots are shown based on metabolomics analysis at baseline and following the 3-months MTX treatment period. Log normalized peak ion intensities were compared between groups using paired non-parametric analysis with unequal variances.

associated with achieving a JADAS-71 ≤ 2.5 (q = 0.06) (**Figure 5D**). Further, percent change from baseline in JADAS-71 was found to be positively associated with the observed reduction in dehydrocholic acid (**Figure 5E**).

Although there was no statistically significant association of route of administration with clinical response (**Table 1**), MTX route of administration has previously been demonstrated to impact clinical response to MTX (Visser and Van der Heijde, 2009). As a result, the JIA population was further stratified by dosing route to investigate if the observed metabolic changes associated with response varied by route of administration. Among patients receiving MTX orally, ACR Pedi 70 response at 3 months continued to be associated with greater reductions in dehydrocholic acid ($p$ = 0.009), 4-picoline ($p$ = 0.04), and biotin

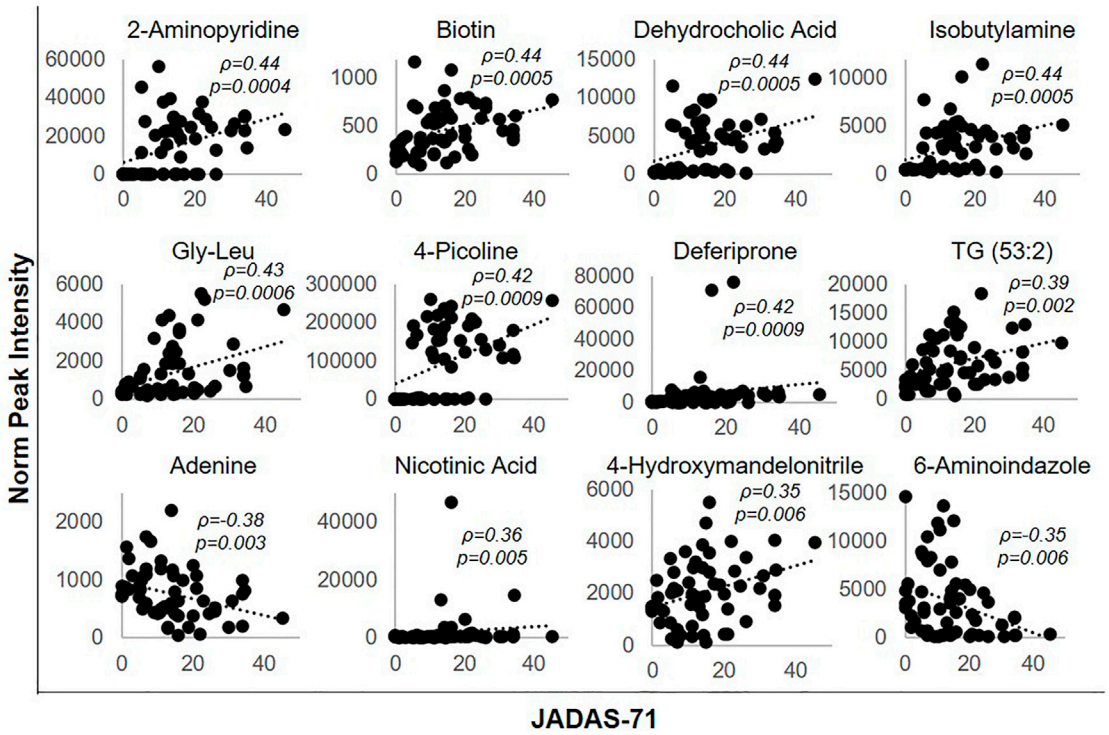


**FIGURE 4 |** Association of disease activity with metabolite levels over the 3-months treatment period. The normalized peak ion intensity for each of the identified metabolites was evaluated for its relationship with JADAS-71 scores by Spearman's rank correlation analysis. The resulting Spearman's correlation coefficient (ρ) and associated p-values are provided.

($p$ = 0.04). However, among patients receiving MTX by the subcutaneous route, ACR Pedi 70 response at 3 months was only associated with greater reductions in dehydrocholic acid ($p$ = 0.009). A nominal logistic regression model for MTX response by ACR Pedi 70 criteria was built using route of administration and change in dehydrocholic acid levels as the independent variables to evaluate if the relationship of dehydrocholic acid levels with clinical response were independent of differences in response based on route of administration. MTX route of administration was not found to be significantly associated with response, but greater reductions in dehydrocholic acid continued to demonstrate a significant association with response ($p$ = 0.03) in the model.

## DISCUSSION

In this work, the initiation of MTX in children with JIA is found to be associated with a diversity of changes in the plasma metabolome. Visualization by metabolic network mapping highlights these changes (**Figure 1**). Alterations in the plasma metabolome reflect direct effects of MTX on these metabolic pathways, or alternatively may reflect alterations in the immunoinflammatory disease process. Metabolic pathways predicted to be impacted based on the known pharmacological activity of MTX include pathways related to folate metabolism, including intermediates of nucleotide metabolism and methylation (Cronstein and Aune, 2020). In our study, treatment with MTX was found to be associated with altered nucleotide metabolism, including increased plasma adenine and N,N-dimethylguanosine levels, and decreased levels of adenosine, guanine, and 8-oxo-2-deoxyadenosine. In contrast to previous work that found no difference in adenosine concentrations in the blood of children with JIA receiving MTX (Dolezalova et al., 2005), this work found a 40% reduction in plasma adenosine levels following the initiation of MTX. This finding is contradictory to those expected based on the hypothesis that MTX mediates its anti-inflammatory activity through the indirect inhibition of adenosine deaminase resulting in an increase in extracellular adenosine concentrations (Nalesnik et al., 2011). However, it must be noted that adenosine is unstable in plasma and these samples were not prepared in such a manner to control for this rapid degradation (Lofgren et al., 2018). MTX treatment was also associated with an increase in the amino acid phenylalanine with a corresponding reduction in its N-methylated product, which represents a potential indicator of reduced methyltransferase activity. However, no significant reduction in plasma levels of the universal methyl donor S-adenosyl-methionine were observed (Wang and Chiang, 2012).

The majority of metabolites identified as significantly altered following the initiation of MTX haven't been previously identified as pharmacological targets of MTX. It is possible that changes in many of these metabolites are reflective of metabolic changes related to the underlying immunoinflammatory process. The

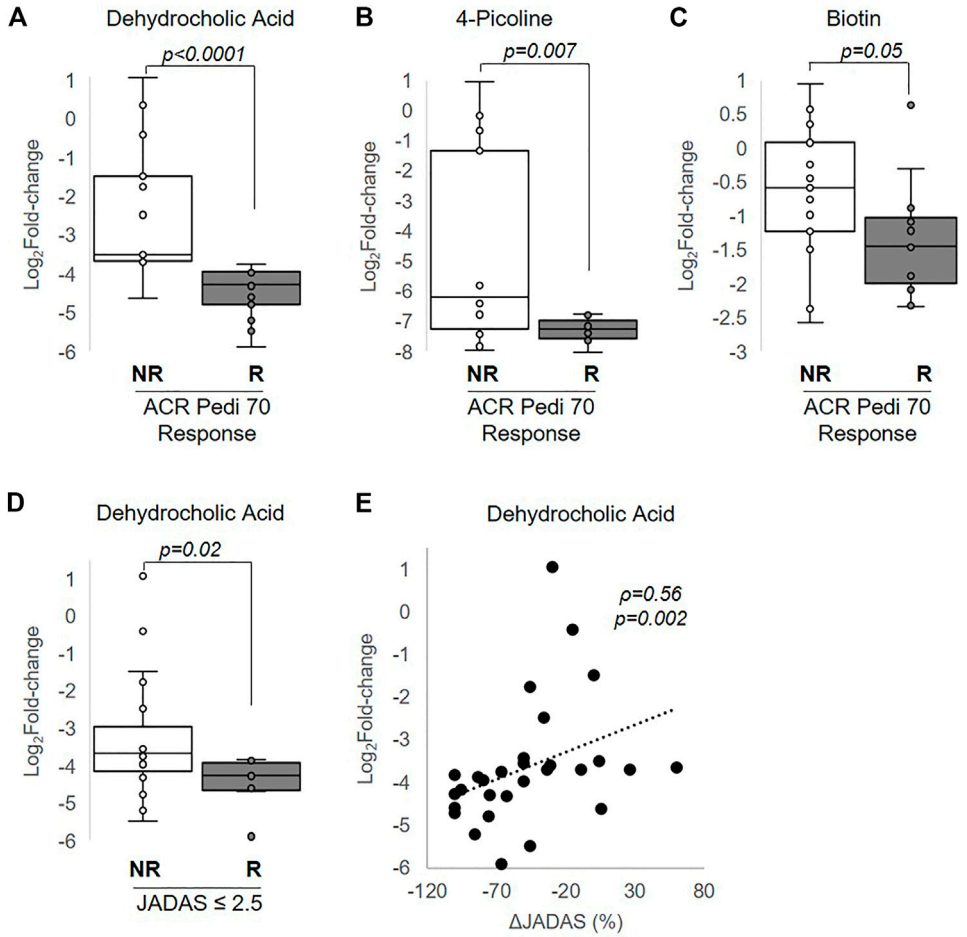


**FIGURE 5 |** Association of changes in metabolite levels with MTX efficacy at 3 months. The fold-change in **(A)** dehydrocholic acid, **(B)** 4-picoline, and **(C)** biotin are compared between responders and non-responders based on achievement of ACR Pedi 70 response criteria. **(D)** The fold-change in dehydrocholic acid over the 3-months treatment period is compared between responders and non-responders based on achievement of a JADAS ≤2.5. **(E)** The association between fold-change in dehydrocholic acid and percentage change in JADAS-71 was evaluated by Spearman's rank correlation analysis. The resulting Spearman's correlation coefficient (ρ) and associated p-values are provided. Unpaired analysis in **(A–D)** were conducted by Wilcoxon rank-sum analysis and the resulting p-values are provided.

chemical enrichment analysis found that the only class-wide metabolic effect associated with MTX treatment was a reduction in unsaturated triglycerides. This finding is in agreement with previous studies demonstrating that children with active JIA had, on average, 37–59% higher plasma triglyceride concentrations compared to healthy control subjects, and that inactive disease was associated with normalization of these levels (Ilowite et al., 1989; Tselepis et al., 1999). Elevated triglycerides represent a component of a broader dyslipoproteinemia of autoimmunity attributed to reduced lipase activity related to pro-inflammatory signaling and associated with increased atherogenic risk (Wang et al., 2020). Our work also found MTX therapy was associated with increases in plasma concentrations of several unsaturated fatty acids, including docosahexanoic acid and linoleic acid. Previous work has similarly found lower unsaturated fatty acid levels in the serum of JIA patients with active disease, and found that unsaturated fatty acid concentrations were inversely associated with markers of disease activity (Gorczyca et al., 2017). The omega-3 unsaturated fatty acids have been proposed to alter eicosanoid metabolism in favor of an anti-inflammatory state and potentially alter innate and adaptive immune cell function, as well as cytokine and reactive oxygen species production (Miles and Calder, 2012) (Gheita et al., 2012).

In evaluating potential metabolic biomarkers associated with MTX response, only metabolites achieving an FDR-adjusted p-value (i.e., q-value) less than 0.05 were considered. The resulting metabolites represented a diversity of biochemical classes, with many representing metabolites that fail to map to endogenous metabolic pathways. Several of these metabolites were found to be significantly associated with JADAS-71 scores and active joint counts resulting in associations that were stronger than those observed with ESR and CRP, which represent the inflammatory markers commonly used as measures of active disease in practice. In comparing changes in metabolite levels based on the ACR Pedi response criteria, changes in

dehydrocholic acid, 4-picoline, and biotin were found to be significantly different between responders and non-responders; and in subjects who achieved a JADAS ≤2.5, changes in dehydrocholic acid were found to be significantly different. Furthermore, changes in dehydrocholic acid were found to be significantly associated with changes in JADAS over the treatment period and remained significant after controlling for MTX administration. None of these metabolites have been previously associated with the efficacy of MTX and therefore represent potential novel biomarkers of response.

Dehydrocholic acid is a secondary bile acid and is an oxidation product of cholic acid (Navarro Suarez et al., 2018). Recognizing that secondary bile acids are primarily formed through enterohepatic recirculation of primary bile acids with metabolism occurring *via* the gut microbiota (Staley et al., 2017), changes in dehydrocholic acid levels secondary to MTX therapy support the findings that MTX efficacy in autoimmune arthritis may be related to its effect on the gut microbiota (Artacho et al., 2020; Scher et al., 2020; Nayak et al., 2021; Wu, 2021). This potential relationship is further supported by the identification of biotin as a metabolite associated with MTX efficacy, as systemic biotin is at least partially generated through gut microbial metabolism (Rowland et al., 2018). 4-picoline is within the class of compounds known as methylpyridines and is an aromatic compound found in food stuffs and its presence may represent consumption of foods containing this compound (Arn and Acree, 1998). The basis for the relationship between MTX efficacy and 4-picoline levels will require further investigation, as its role in metabolism is unknown and has only been speculated to represent a potential biomarker of foods enriched in this metabolite, such as tea.

This is the first study to evaluate the relationship between the effect of MTX on the plasma metabolome in relation to its clinical effect. Previous metabolic studies have been conducted in RA and have identified a number of metabolites and metabolic pathways associated with clinical response to MTX, however these studies were largely based on metabolomic analysis at a single timepoint. An NMR-based metabolomics analysis of serum samples from 38 RA patients found significant differences in the concentrations of 11 metabolites between MTX responders and non-responders when measured after 24 weeks of therapy (Wang et al., 2012). This list included markers of nucleotide (uric acid, uracil, hypoxanthine), amino acid (aspartate, methionine, histidine, glycine, tryptophan, taurine), TCA cycle (α-oxoglutarate) and microbial (TMAO) metabolism. The same metabolic pathways were also found to be impacted by MTX in our study, however the metabolites representing these changes differed in our pediatric cohort. This may reflect differences in the study design, in that the previous study only evaluated metabolite concentrations at the 24-weeks timepoint, while our study focused only on metabolites that changed in response to MTX therapy over a 12-week period. Similar efforts have focused on using baseline metabolomic profiling to identify predictors of drug response (Gosselt et al., 2020). Responders were found to have significantly lower concentrations of several markers of nucleotide and amino acid metabolism (guanosine diphosphate, adenosine triphosphate, uric acid, taurine, homocysteine) and higher concentrations of intermediates of glycolysis (glycerol-3-phosphate, diphosphoglycerate, phosphoenolpyruvate). These findings suggested that pretreatment variability in amino acid metabolism and cellular respiration may predict future response to MTX therapy, but the work did not explore how MTX impacted the metabolome and whether the impact on the metabolome was associated with its efficacy. In fact, the authors highlighted the need for future longitudinal metabolomic studies to investigate the impact of MTX on metabolism in relation to efficacy with a goal of improving our understanding of the mechanism of action of MTX, as done here. Another study focused on an untargeted approach that measured over 3,000 lipid metabolites at baseline and after 4 weeks of therapy to predict MTX response at 6 months in RA (Maciejewski et al., 2021). The study failed to identify any lipid species, alone or in combination, that predicted response to MTX. Again, this study focused on predictive markers of MTX response and used an untargeted approach limited to lipid metabolites. Ultimately, our study confirms that MTX has a significant impact on the plasma metabolome in children with JIA, and that some of these changes differentiate patients responding to MTX from those not responding to MTX. Specifically, the metabolites identified here implicate exogenous and microbiota metabolites, and highlight the potential role of environmental and gastrointestinal microbial metabolism as important mediators in the clinical response to MTX.

The limitations of this study include an exploratory study design with a limited sample size of 30 JIA patients that was further divided into two groups based on clinical response. This sample size was in line with previous metabolomics studies and power was increased through the use of a paired approach to the analysis using both baseline and 3-months follow up samples from the same patients. Choosing extreme response phenotypes intended to clearly delineate the clinical response differences between groups and minimize the known heterogeneity in JIA. The baseline clinical features however did not differ from the larger cohort. In addition, the identification of statistically significant metabolomic changes and metabolic biomarkers demonstrates that the study was adequately powered for these analytes. Another limitation of the study is the variation in the route of MTX administration in the study cohort. This could result in potential confounding variables related to variation in MTX bioavailability, metabolomic changes, and clinical response. Although the subcutaneous route is preferred, especially for higher doses of MTX, such as the 15 $mg/m^2$ dose used in this study, a national shortage of injectable MTX resulted in the use of oral MTX in 12 of our patients. Although we did not find a statistically significant difference in response based on route of administration, there was increased use of subcutaneous MTX in responders (73%) compared to non-responders (47%). We attempted to control for route of administration in our sub-analysis, which ultimately resulted in a reduction in power, but we were able to confirm the relationship of reductions in dehydrocholic with clinical response by both routes of administration. Similarly, although use of NSAIDs and corticosteroids did not statistically differ between responders

and non-responders, it must be acknowledged that these therapeutic agents can also impact the plasma metabolome and may represent potential confounding factors in this analysis. Only 2 subjects received corticosteroids in this cohort, but were not actively on corticosteroids at the time of baseline or 3-months sampling (i.e., they received and were discontinued on corticosteroids within the 3-month sampling window). In addition, recognizing that several of the metabolites that we found were associated with the gut microbiota, it may have been helpful to collect information on antibiotic use prior to initiation of the study and any prospective dietary changes throughout the study. The effect of diet and diurnal variation on the plasma metabolome may represent additional confounding variables, as samples were collected as part of routine care and were not controlled for either diet or time of day. However, recent work investigating the impact of season, time of day, fasting status, tobacco, alcohol, and NSAID use failed to demonstrate a significant impact of these potential confounding variables on the metabolome, but did find that the metabolome was sensitive to sex and age (Hardikar et al., 2020). Although we were not able to capture all potentially confounding variables in our analysis, our responder and non-responder groups were found to be similar in both sex and age. The study is also limited by the semi-quantitative approach to measuring metabolite levels that lack authentic internal standards for the absolute quantitation of each of the identified metabolites. However, this is the standard approach in global metabolomics analyses. Although multiple analytical platforms were used to capture a diverse representation of the plasma metabolome, there remains a multitude of unidentified metabolites that were not included in this analysis. However, this limitation applies to all metabolomics studies.

## CONCLUSION

Metabolomics represents an unbiased and untargeted approach to improve our understanding of the underlying biochemical changes associated with MTX therapy and the relationship of these changes with its clinical efficacy in JIA. As a result, metabolomics serves as a tool for hypothesis generation that holds the possibility of both identifying novel drug target pathways for the treatment of JIA as well as the identification of potential metabolic biomarkers to guide clinicians in the optimization of MTX therapy in JIA. The findings in this study support a robust and diverse change in the plasma metabolome following the initiation of MTX in children with JIA. In particular, MTX therapy is associated with a class-wide reduction in plasma triglycerides that is likely reflective of the previously described dyslipoproteinemia of autoimmunity that is at least partially corrected following the initiation of MTX. Although a number of individual metabolites representing a diversity of chemical classes were found to be significantly associated with disease activity, only a few metabolites were found to discriminate between patients based on clinical response to MTX. These metabolites included dehydrocholic acid, biotin, and 4-picoline, and are all likely related to exogenous sources and possibly related to gut microbial metabolism. Subsequent targeted and functional metabolic studies are needed to further evaluate these putative biomarkers of MTX response in JIA.

## DATA AVAILABILITY STATEMENT

The datasets presented in this study can be found in online repositories. The names of the repository/repositories and accession number(s) can be found at: https://www.metabolomicsworkbench.org/ under Project ID: PR001148.

## ETHICS STATEMENT

The studies involving human participants were reviewed and approved by Children's Mercy Hospital Pediatric Institutional Review Board. Written informed consent to participate in this study was provided by the participant and/or the participants' legal guardian/next of kin.

## AUTHOR CONTRIBUTIONS

RF and MB. conceived and designed the study. MB. collected the patient samples and clinical data. RF. collected and analysed the data. RF and MB. wrote and revised the manuscript.

## FUNDING

This work was supported by the University of Kansas and a CTSA grant from NCATS awarded to the University of Kansas for Frontiers: University of Kansas Clinical and Translational Science Institute (# KL2TR002367) and the Kansas Institute of Precision Medicine Centers of Biomedical Research Excellence grant from NIGMS awarded to the University of Kansas Medical Center (# P20GM130423). Funding for this work was through the Rheumatology Research Foundation Rheumatology Investigator Award and R Bridge Award (PI Becker).

## ACKNOWLEDGMENTS

The authors would like to acknowledge Kelly Paglia and members of the Fiehn Laboratory at the NIH West Coast Metabolomics Center for their help in the design and conduct of this metabolomics analysis. We would also like to acknowledge Chelsey Smith for her assistance in patient recruitment and coordination of the study.

## REFERENCES


Arn, H., and Acree, T. E. (1998). Flavornet: A Database of Aroma Compounds Based on Odor Potency in Natural Products. *Dev. Food Sci.* 40, 27. doi:10.1016/s0167-4501(98)80029-0

Artacho, A., Isaac, S., Nayak, R., Flor-Duro, A., Alexander, M., Koo, I., et al. (2020). The Pretreatment Gut Microbiome Is Associated with Lack of Response to Methotrexate in New-Onset Rheumatoid Arthritis. *Arthritis Rheumatol.* 73 (6), 931–942. doi:10.1002/art.41622

Barupal, D. K., and Fiehn, O. (2017). Chemical Similarity Enrichment Analysis (ChemRICH) as Alternative to Biochemical Pathway Mapping for Metabolomic Datasets. *Sci. Rep.* 7, 14567. doi:10.1038/s41598-017-15231-w

Barupal, D. K., Haldiya, P. K., Wohlgemuth, G., Kind, T., Kothari, S. L., Pinkerton, K. E., et al. (2012). MetaMapp: Mapping and Visualizing Metabolomic Data by Integrating Information from Biochemical Pathways and Chemical and Mass Spectral Similarity. *BMC Bioinformatics* 13, 99. doi:10.1186/1471-2105-13-99

Becker, M. L. (2012). Optimization of Pediatric Rheumatology Therapeutics. *Clin. Pharmacol. Ther.* 91, 597–606. doi:10.1038/clpt.2011.293

Beger, R. D., Dunn, W., Dunn, W., Schmidt, M. A., Gross, S. S., Kirwan, J. A., et al. (2016). Metabolomics Enables Precision Medicine: "A White Paper, Community Perspective"Metabolomics Enables Precision Medicine: "A White Paper, Community Perspective. *Metabolomics* 12, 149. doi:10.1007/s11306-016-1094-6

Cajka, T., and Fiehn, O. (2016). Toward Merging Untargeted and Targeted Methods in Mass Spectrometry-Based Metabolomics and Lipidomics. *Anal. Chem.* 88, 524–545. doi:10.1021/acs.analchem.5b04491

Ćalasan, M. B., Den Boer, E., De Rotte, M. C., Vastert, S. J., Kamphuis, S., De Jonge, R., et al. (2015). Methotrexate Polyglutamates in Erythrocytes Are Associated with Lower Disease Activity in Juvenile Idiopathic Arthritis Patients. *Ann. Rheum. Dis.* 74, 402–407. doi:10.1136/annrheumdis-2013-203723

Consolaro, A., Ruperto, N., Bazso, A., Pistorio, A., Magni-Manzoni, S., Filocamo, G., et al. (2009). Ravelli, A., and Paediatric Rheumatology International Trials, ODevelopment and Validation of a Composite Disease Activity Score for Juvenile Idiopathic Arthritis. *Arthritis Rheum.* 61, 658–666. doi:10.1002/art.24516

Consolaro, A., Negro, G., Lanni, S., Solari, N., Martini, A., and Ravelli, A. (2012). Toward a Treat-To-Target Approach in the Management of Juvenile Idiopathic Arthritis. *Clin. Exp. Rheumatol.* 30, S157–S162.

Cronstein, B. N., and Aune, T. M. (2020). Methotrexate and its Mechanisms of Action in Inflammatory Arthritis. *Nat. Rev. Rheumatol.* 16, 145–154. doi:10.1038/s41584-020-0373-9

Dolezalová, P., Krijt, J., Chládek, J., Nemcová, D., and Hoza, J. (2005). Adenosine and Methotrexate Polyglutamate Concentrations in Patients with Juvenile Arthritis. *Rheumatology (Oxford)* 44, 74–79. doi:10.1093/rheumatology/keh401

Fiehn, O. (2002). Metabolomics--the Link between Genotypes and Phenotypes. *Plant Mol. Biol.* 48, 155–171. doi:10.1007/978-94-010-0448-0_11

Fiehn, O. (2016). Metabolomics by Gas Chromatography-Mass Spectrometry: Combined Targeted and Untargeted Profiling. *Curr. Protoc. Mol. Biol.* 114, 30–32. doi:10.1002/0471142727.mb3004s114

Funk, R. S., and Becker, M. L. (2016). Disease Modifying Anti-rheumatic Drugs in Juvenile Idiopathic Arthritis: Striving for Individualized Therapy. *Expert Rev. Precision Med. Drug Develop.* 1, 53–68. doi:10.1080/23808993.2016.1133234

Funk, R. S., Van Haandel, L., Leeder, J. S., and Becker, M. L. (2014). Folate Depletion and Increased Glutamation in Juvenile Idiopathic Arthritis Patients Treated with Methotrexate. *Arthritis Rheumatol.* 66, 3476–3485. doi:10.1002/art.38865

Funk, R. S., Singh, R. K., and Becker, M. L. (2020). Metabolomic Profiling to Identify Molecular Biomarkers of Cellular Response to Methotrexate *In Vitro*. *Clin. Transl. Sci.* 13, 137–146. doi:10.1111/cts.12694

Gheita, T., Kamel, S., Helmy, N., El-Laithy, N., and Monir, A. (2012). Omega-3 Fatty Acids in Juvenile Idiopathic Arthritis: Effect on Cytokines (IL-1 and TNF-α), Disease Activity and Response Criteria. *Clin. Rheumatol.* 31, 363–366. doi:10.1007/s10067-011-1848-5

Giannini, E. H., Brewer, E. J., Kuzmina, N., Shaikov, A., Maximov, A., Vorontsov, I., et al. (1992). Methotrexate in Resistant Juvenile Rheumatoid Arthritis. Results of the U.S.A.-U.S.S.R. Double-Blind, Placebo-Controlled Trial. The Pediatric Rheumatology Collaborative Study Group and the Cooperative Children's Study Group. *N. Engl. J. Med.* 326, 1043–1049. doi:10.1056/NEJM199204163261602

Giannini, E. H., Ruperto, N., Ravelli, A., Lovell, D. J., Felson, D. T., and Martini, A. (1997). Preliminary Definition of Improvement in Juvenile Arthritis. *Arthritis Rheum.* 40, 1202–1209. doi:10.1002/1529-0131(199707)40:7<1202:AID-ART3>3.0.CO;2-R

Gorczyca, D., Postępski, J., Czajkowska, A., Paściak, M., Prescha, A., Olesińska, E., et al. (2017). The Profile of Polyunsaturated Fatty Acids in Juvenile Idiopathic Arthritis and Association with Disease Activity. *Clin. Rheumatol.* 36, 1269–1279. doi:10.1007/s10067-017-3586-9

Gosselt, H. R., Muller, I. B., Jansen, G., Van Weeghel, M., Vaz, F. M., Hazes, J. M. W., et al. (2020). Identification of Metabolic Biomarkers in Relation to Methotrexate Response in Early Rheumatoid Arthritis. *J. Pers Med.* 10, 271. doi:10.3390/jpm10040271

Guma, M., Tiziani, S., and Firestein, G. S. (2016). Metabolomics in Rheumatic Diseases: Desperately Seeking Biomarkers. *Nat. Rev. Rheumatol.* 12, 269–281. doi:10.1038/nrrheum.2016.1

Hardikar, S., Albrechtsen, R. D., Achaintre, D., Lin, T., Pauleck, S., Playdon, M., et al. (2020). Impact of Pre-blood Collection Factors on Plasma Metabolomic Profiles. *Metabolites* 10, 213. doi:10.3390/metabo10050213

Ilowite, N. T., Samuel, P., Beseler, L., and Jacobson, M. S. (1989). Dyslipoproteinemia in Juvenile Rheumatoid Arthritis. *J. Pediatr.* 114, 823–826. doi:10.1016/s0022-3476(89)80148-9

Jiang, M., Chen, T., Feng, H., Zhang, Y., Li, L., Zhao, A., et al. (2013). Serum Metabolic Signatures of Four Types of Human Arthritis. *J. Proteome Res.* 12, 3769–3779. doi:10.1021/pr400415a

Kapoor, S. R., Filer, A., Fitzpatrick, M. A., Fisher, B. A., Taylor, P. C., Buckley, C. D., et al. (2013). Metabolic Profiling Predicts Response to Anti-tumor Necrosis Factor α Therapy in Patients with Rheumatoid Arthritis. *Arthritis Rheum.* 65, 1448–1456. doi:10.1002/art.37921

Löfgren, L., Pehrsson, S., Hägglund, G., Tjellström, H., and Nylander, S. (2018). Accurate Measurement of Endogenous Adenosine in Human Blood. *PLoS One* 13, e0205707. doi:10.1371/journal.pone.0205707

Maciejewski, M., Sands, C., Nair, N., Ling, S., Verstappen, S., Hyrich, K., et al. (2021). Prediction of Response of Methotrexate in Patients with Rheumatoid Arthritis Using Serum Lipidomics. *Sci. Rep.* 11, 7266. doi:10.1038/s41598-021-86729-7

Miles, E. A., and Calder, P. C. (2012). Influence of marine N-3 Polyunsaturated Fatty Acids on Immune Function and a Systematic Review of Their Effects on Clinical Outcomes in Rheumatoid Arthritis. *Br. J. Nutr.* 107 (Suppl. 2), S171–S184. doi:10.1017/S0007114512001560

Nalesnik, M., Nikolić, J. M., and Jandrić, S. (2011). Adenosine Deaminase and C-Reactive Protein in Diagnosing and Monitoring of Rheumatoid Arthritis. *Med. Glas (Zenica)* 8, 163–168.

Navarro Suarez, L., Brückner, L., and Rohn, S. (2018). Electrochemical Oxidation of Primary Bile Acids: A Tool for Simulating Their Oxidative Metabolism? *Int. J. Mol. Sci.* 19, 2491. doi:10.3390/ijms19092491

Nayak, R. R., Alexander, M., Deshpande, I., Stapleton-Gray, K., Rimal, B., Patterson, A. D., et al. (2021). Methotrexate Impacts Conserved Pathways in Diverse Human Gut Bacteria Leading to Decreased Host Immune Activation. *Cell Host Microbe* 29, 362–e11. doi:10.1016/j.chom.2020.12.008

Petty, R. E., Southwood, T. R., Manners, P., Baum, J., Glass, D. N., Goldenberg, J., et al. (2004). International League of Associations for Rheumatology Classification of Juvenile Idiopathic Arthritis: Second Revision, Edmonton, 2001. *J. Rheumatol.* 31, 390–392.

Rowland, I., Gibson, G., Heinken, A., Scott, K., Swann, J., Thiele, I., et al. (2018). Gut Microbiota Functions: Metabolism of Nutrients and Other Food Components. *Eur. J. Nutr.* 57, 1–24. doi:10.1007/s00394-017-1445-8

Ruperto, N., Murray, K. J., Gerloni, V., Wulffraat, N., De Oliveira, S. K., Falcini, F., et al. (2004). A Randomized Trial of Parenteral Methotrexate Comparing an Intermediate Dose with a Higher Dose in Children with Juvenile Idiopathic Arthritis Who Failed to Respond to Standard Doses of Methotrexate. *Arthritis Rheum.* 50, 2191–2201. doi:10.1002/art.20288

Scher, J. U., Nayak, R. R., Ubeda, C., Turnbaugh, P. J., and Abramson, S. B. (2020). Pharmacomicrobiomics in Inflammatory Arthritis: Gut Microbiome as Modulator of Therapeutic Response. *Nat. Rev. Rheumatol.* 16, 282–292. doi:10.1038/s41584-020-0395-3

Staley, C., Weingarden, A. R., Khoruts, A., and Sadowsky, M. J. (2017). Interaction of Gut Microbiota with Bile Acid Metabolism and its Influence on Disease States. *Appl. Microbiol. Biotechnol.* 101, 47–64. doi:10.1007/s00253-016-8006-6

Tselepis, A. D., Elisaf, M., Besis, S., Karabina, S. A., Chapman, M. J., and Siamopoulou, A. (1999). Association of the Inflammatory State in Active Juvenile Rheumatoid Arthritis with Hypo-High-Density Lipoproteinemia and Reduced Lipoprotein-Associated Platelet-Activating Factor Acetylhydrolase Activity. *Arthritis Rheum.* 42, 373–383. doi:10.1002/1529-0131(199902)42:2<373:AID-ANR21>3.0.CO;2-3

Visser, K., and Van Der Heijde, D. (2009). Optimal Dosage and Route of Administration of Methotrexate in Rheumatoid Arthritis: a Systematic Review of the Literature. *Ann. Rheum. Dis.* 68, 1094–1099. doi:10.1136/ard.2008.092668

Wang, Y. C., and Chiang, E. P. (2012). Low-dose Methotrexate Inhibits Methionine S-Adenosyltransferase *In Vitro* and *In Vivo*. *Mol. Med.* 18, 423–432. doi:10.2119/molmed.2011.00048

Wang, Z., Chen, Z., Yang, S., Wang, Y., Yu, L., Zhang, B., et al. (2012). (1)H NMR-Based Metabolomic Analysis for Identifying Serum Biomarkers to Evaluate Methotrexate Treatment in Patients with Early Rheumatoid Arthritis. *Exp. Ther. Med.* 4, 165–171. doi:10.3892/etm.2012.567

Wang, Y., Yu, H., and He, J. (2020). Role of Dyslipidemia in Accelerating Inflammation, Autoimmunity, and Atherosclerosis in Systemic Lupus Erythematosus and Other Autoimmune Diseases. *Discov. Med.* 30, 49–56.

Wu, H. J. (2021). Methotrexate Works Remotely, from the Gut. *Cell Host Microbe* 29, 325–326. doi:10.1016/j.chom.2021.02.016

Xia, J., and Wishart, D. S. (2016). Using MetaboAnalyst 3.0 for Comprehensive Metabolomics Data Analysis. *Curr. Protoc. Bioinformatics* 55, 14–91. doi:10.1002/cpbi.11

Xia, J., Sinelnikov, I. V., Han, B., and Wishart, D. S. (2015). MetaboAnalyst 3.0--making Metabolomics More Meaningful. *Nucleic Acids Res.* 43, W251–W257. doi:10.1093/nar/gkv380

Young, S. P., Kapoor, S. R., Viant, M. R., Byrne, J. J., Filer, A., Buckley, C. D., et al. (2013). The Impact of Inflammation on Metabolomic Profiles in Patients with Arthritis. *Arthritis Rheum.* 65, 2015–2023. doi:10.1002/art.38021

**Conflict of Interest:** The authors declare that the research was conducted in the absence of any commercial or financial relationships that could be construed as a potential conflict of interest.

**Publisher's Note:** All claims expressed in this article are solely those of the authors and do not necessarily represent those of their affiliated organizations, or those of the publisher, the editors and the reviewers. Any product that may be evaluated in this article, orclaim that may be made by its manufacturer, is not guaranteed or endorsed by the publisher.

frontiers in Pharmacology

ORIGINAL RESEARCH
published: 20 December 2021
doi: 10.3389/fphar.2021.771818

# Organic Anion Transporting Polypeptide 2B1 in Human Fetal Membranes: A Novel Gatekeeper for Drug Transport During Pregnancy?

*Esha Ganguly*[1†], *Ananth Kumar Kammala*[1†], *Meagan Benson*[1], *Lauren S. Richardson*[1,2], *Arum Han*[2] *and Ramkumar Menon*[1*]

[1]*Division of Basic and Translational Research, Department of Obstetrics and Gynecology, The University of Texas Medical Branch at Galveston, Galveston, TX, United States,* [2]*Department of Electrical and Computer Engineering, Texas A&M University, College Station, TX, United States*

Current intervention strategies have not been successful in reducing the risks of adverse pregnancy complications nor maternal and fetal morbidities associated with pregnancy complications. Improving pregnancy and neonatal outcomes requires a better understanding of drug transport mechanisms at the feto-maternal interfaces, specifically the placenta and fetal membrane (FM). The role of several solute carrier uptake transporter proteins (TPs), such as the organic anion transporting polypeptide 2B1 (OATP2B1) in transporting drug across the placenta, is well-established. However, the mechanistic role of FMs in this drug transport has not yet been elucidated. We hypothesize that human FMs express OATP2B1 and functions as an alternate gatekeeper for drug transport at the feto-maternal interface. We determined the expression of OATP2B1 in term, not-in-labor, FM tissues and human FM cells [amnion epithelial cell (AEC), chorion trophoblast cell (CTC), and mesenchymal cells] using western blot analyses and their localization using immunohistochemistry. Changes in OATP2B1 expression was determined for up to 48 h after stimulation with cigarette smoke extract (CSE), an inducer of oxidative stress. The functional role of OATP2B1 was determined by flow cytometry using a zombie violet dye substrate assay. After OATP2B1 gene silencing, its functional relevance in drug transport through the feto-maternal interface was tested using a recently developed feto-maternal interface organ-on-a-chip (OOC) system that contained both FM and maternal decidual cells. Propagation of a drug (Rosuvastatin, that can be transported by OATP2B1) within the feto-maternal interface OOC system was determined by mass spectrometry. FMs express OATP2B1 in the CTC and AEC layers. In FM explants, OATP2B1 expression was not impacted by oxidative stress. Uptake of the zombie violet dye within AECs and CTCs showed OATP2B1 is functionally active. Silencing OATP2B1 in CTCs reduced Rosuvastatin propagation from the decidua to the fetal AEC layer within the feto-maternal interface-OOC model. Our data suggest that TPs in FMs may function as a drug transport system at the feto-maternal interface, a function that was previously thought to be performed exclusively by the placenta. This new knowledge will help improve drug delivery testing during pregnancy and contribute to designing drug delivery strategies to treat adverse pregnancy outcomes.

OPEN ACCESS

***Edited by:***
*Catherine M. T. Sherwin,*
*Wright State University, United States*

***Reviewed by:***
*Loic Blanchon,*
*Université Clermont Auvergne, France*
*Tamas Zakar,*
*The University of Newcastle, Australia*

****Correspondence:***
*Ramkumar Menon*
*ram.menon@utmb.edu*

*[†]These authors have contributed equally to this work*

***Specialty section:***
*This article was submitted to Obstetric and Pediatric Pharmacology, a section of the journal Frontiers in Pharmacology*

***Received:*** *07 September 2021*
***Accepted:*** *18 November 2021*
***Published:*** *20 December 2021*

***Citation:***
*Ganguly E, Kammala AK, Benson M, Richardson LS, Han A and Menon R (2021) Organic Anion Transporting Polypeptide 2B1 in Human Fetal Membranes: A Novel Gatekeeper for Drug Transport During Pregnancy? Front. Pharmacol. 12:771818. doi: 10.3389/fphar.2021.771818*

Keywords: transporter protein, drug transport, pregnancy, human fetal membranes, organ-on-a-chip

## INTRODUCTION

More than one in six pregnancies are affected by various pregnancy-related complications, including preterm birth, fetal growth restrictions, or preeclampsia, which are associated with substantial maternal, fetal, and neonatal morbidity and mortality (Collier and Molina, 2019). Despite the rising trend in pregnancy-related complications within the past decades in the United States, current treatment strategies have not been successful in reducing adverse pregnancy outcomes (D'Alton et al., 2019). Moreover, the current lack of knowledge about the effect of maternally administered drugs on the developing fetus is a major public healthcare concern worldwide (Sachdeva et al., 2009).

Unfortunately, and justifiably, concerns about fetal safety have limited pharmacotherapy and drug studies during pregnancy (Costantine, 2014). For example, maternal treatment with antiepileptic drugs results in fetal teratogenicity, such as intrauterine growth restriction, congenital anomalies, and infant mortality (Güveli et al., 2017). Given that therapy during pregnancy-related complications may expose the fetus to adverse effects *in utero*, a proper understanding of the passage of drugs across the feto-maternal interface will guide the development of more accurate and safer pharmacotherapy during pregnancy. The feto-maternal interface is comprised of the placenta-decidua basalis interface and the fetal membrane (FM) (i.e., amniochorion)-decidua parietalis interface, both acting as protective barriers throughout pregnancy while maintaining communication between the mother and the fetus (Menon et al., 2021). Disruption of these interfaces leads to various pregnancy complications, including preterm birth, which can have long-term adverse effects on maternal and fetal health (Menon et al., 2019). Thus, understanding the role of the feto-maternal interfaces in drug transport is critical to advancing clinical treatment strategies during pregnancy.

Drug transporter proteins play an essential role in regulating the transport of drugs across a variety of tissues such as intestinal enterocytes, kidneys (proximal tubule), hepatocytes, and brain (International Transporter et al., 2010). The distribution, substrate specificity, and activities of the membrane transporters are essential determinants of drug absorption, excretion, and in many cases, the extent of drug entry into target organs (Al-Enazy et al., 2017). The placenta-decidua basalis interface is the only region studied for drug transportation functions during pregnancy due to its direct interaction with maternal blood (Dallmann et al., 2019). Gestational age-dependent expression of transporter proteins in the placenta is crucial in limiting fetal toxicities by preventing entry or facilitating the active efflux of endogenous waste products and xenobiotics out of the fetal compartment (Anoshchenko et al., 2020). For example, ATP-Binding Cassette (ABC) efflux transporters such as breast cancer resistance protein (BCRP; ABCG2) and P-glycoprotein (P-gp; ABCB1) are among one of the highly expressed transporters in the placenta, and can transport diverse therapeutic drugs (such as antihypertensive, antivirals, and antibiotics), thus protecting the fetus from the effects of the treatment (Staud et al., 2012; Han et al., 2018). In addition to the ABC efflux transporters, the organic anionic transporters (OATs) and organic anion transporting polypeptides (OATPs) also play a critical role in the transport of various endogenous molecules and xenobiotics (Staud et al., 2012). OATs and OATPs mediate the transport of steroid sulfates, thyroid hormones, and drugs (e.g., statins), as well as the transport of waste products (Roth et al., 2012). An essential member of the OATP family is OATP2B1. In human placenta, OATP2B1 is expressed on the basal membrane of the syncytiotrophoblast (Grube et al., 2007). However, the physiological and pharmacological role of OATP2B1 is poorly understood, which is one of the focus of our study.

Despite being structurally and functionally different from the placental interface, the role of FM-decidua parietalis interface in drug transportation and function remains unclear. Of note, drugs have to pass through both placenta-decidua basalis and the FM-decidua parietalis to reach the fetus. Thus, it is important to understand whether drugs can indeed pass through the FM-decidua parietalis interface to reach the fetus. An ideal strategy will be the simultaneous testing of drug transporter expression and function at both interfaces to have a complete understanding of drug kinetics (i.e., absorption, distribution, metabolism, elimination) and its associated effects on the fetus. We hypothesize that human FMs express transporter proteins, such as OATP2B, which function as an alternate gatekeeper for drug transport at the feto-maternal interface.

## METHODS

### IRB Ethics Committee Approval Statement

Placental samples used for this study were collected after normal term cesarean deliveries from John Sealy hospital [University of Texas Medical Branch (UTMB)] at Galveston, Texas, United States in accordance with the relevant guidelines and regulations of approved protocols for various studies (UTMB 11-251). As discarded placentas after delivery were used for the study, no subject recruitment or consent was required.

### Placental and FM Explant Culture

Placental and FM (i.e., amniochorion) tissues from term, not in labor, cesarean deliveries (TNIL) ($n = 5$) were used for this project and prepared as previously described by our laboratory ($n = 6$ tissues for western blotting and $n = 5$ tissues for explant culture) (Ayad et al., 2018; Sheller-Miller et al., 2020). Briefly, the FM was dissected from the placenta, washed three times in normal saline, cleaned with sterile saline-moistened gauze to clear any adherent blood clots and all the decidua, and washed in Hank's balanced solution (HBSS) with penicillin 100 U/mL and streptomycin 100 μg/ml. Using a skin biopsy punch, the membranes were cut into 6-mm disks. Sections were taken from midzone of the

fetal membranes, avoiding the regions overlying the cervix or placenta. Four disks of the amniochorion membranes were placed in each well of a 24-well tissue culture plate with 0.4 ml of Dulbecco's modified Eagle's medium (DMEM) with Ham F12 nutrient mixture 1:1; antibiotics: penicillin (100 IU/ml), streptomycin (100 μg/ml), and amphotericin B (2.5 μg/ml); glutamine (2 mmol/L); and 15% heat-inactivated fetal bovine serum. Cultures were incubated at 37°C with 5% $CO_2$. The medium was changed at 24 h (hrs.) when the study reagents were added.

Placental explants were prepared as described previously (Behnia et al., 2016; Arita et al., 2018). Briefly, placental tissues were washed with sterile saline. After removal of the blood clots by gentle blotting, segments of the maternal part of the placental villi were isolated by sharp dissection, and subsequently washed and cut 3–5 times. Chopped tissues were washed in DMEM supplemented with 5% fetal bovine serum (v/v), penicillin (100 U/mL), and streptomycin (100 μg/ml). Placental tissue (0.1 gm) was placed in each well of a 24-well tissue culture plate in 0.5 ml DMEM with Ham F12 nutrient mixture 1:1; antibiotics: penicillin (100 IU/ml), streptomycin (100 μg/ml), and amphotericin B (2.5 μg/ml); glutamine (2 mmol/L); and 10% heat-inactivated fetal bovine serum. The medium was changed at 24 h when the study reagents were added.

## Culture of Immortalized Human FM Cells

Maternal decidual and FM cells [amnion epithelial cells (AECs); amnion mesenchymal cells (AMCs), chorionic trophoblast cells (CTCs)] were isolated from term, not-in-labor, cesarean-delivered FM and immortalized by a standard HPV16 E6E7 retrovirus protocol (Halbert et al., 1991). Retroviruses were obtained from the PA317 LXSN 16E6E7 (ATCC® CRL-2203™) cell line. Cells derived from healthy FM tissues were seeded in 6-well plates. The next day, cells were infected with 500 μL of the mixture containing 50 μL of retrovirus supernatant, 5 μg of protamine sulfate in serum-free culture medium, and incubated at 37°C for 6 h. Culture medium was replaced with fresh media, and 48 h after the viral infection, antibiotic selection was started. Five days after the antibiotic selection process, the immortalized cells were expanded and passaged several times (up to passage 8) before using them in the experiments. AMCs and maternal decidual cells were cultured and maintained in complete media consisting of Dulbecco's modified Eagle's medium (DMEM) with Ham F12 nutrient mixture 1:1; antibiotics: penicillin (100 IU/ml), streptomycin (100 μg/ml), and amphotericin B (2.5 μg/ml); and 5% heat-inactivated fetal bovine serum. AECs were cultured in complete keratinocyte serum-free media (KSFM), a culture highly selective for epithelial cells, supplemented with human recombinant epidermal growth factor (0.1 ng/ml), bovine pituitary extract (30 μg/ml), and primocin (0.5 mg/ml) (ant-pm-1; Invivogen). Supplements were added to the media immediately before use. CTCs were cultured in Dulbecco's modified Eagle's medium (DMEM) with Ham F12 nutrient mixture 1:1 supplemented with the following: fetal bovine serum, penicillin, streptomycin, bovine serum albumin, ITS-X, CHIR99021, A83-01, SB431542, L-ascorbic acid, epidermal growth factor, VPA, and Y27632 (ROCK inhibitor). Cells used for all experiments were within 10 passages.

## Stimulation of FM and Placental Explant Culture With Cigarette Smoke Extract

Cigarette smoke extract (CSE) was prepared as previously reported by our laboratory (Menon et al., 2013; Sheller et al., 2016; Richardson et al., 2020a). Briefly, smoke drawn from a single lit commercial cigarette (unfiltered Camel™, R.J. Reynolds Tobacco Co.; Winston Salem, NC) was bubbled through 50 ml of tissue culture medium (DMEM: F12 Ham's mixture with antimicrobial agents and FBS). Each cigarette is reported to contain 26 mg of tar and 1.7 mg of nicotine. The stock CSE was filter-sterilized using a 0.25 μm pore Millipore filter (Millipore, Bedford, MA) to remove insoluble particles. Fetal membrane and placental explants were then stimulated with CSE (diluted 1:10 in culture media) for 0, 4, 8, 24 and 48 h. CSE was prepared freshly for each experiment. After the treatments, the explants (placental and FM) were removed and processed for western blotting for OATP2B1. Both placental and FM explants were used to better understand the expression levels of OATP2B1 in response to CSE stimulation.

## Immunohistochemistry for OATP2B1

Immunohistochemistry (IHC) for OATP2B1 was performed on FM tissues using methods previously described by our laboratory (Kammala et al., 2020). Briefly, FM sections were fixed in 4% paraformaldehyde for 48 h and embedded in paraffin. Tissue sections were cut to 5 μm thickness, placed on a positively charged slide, and attached by keeping them at 50°C for 45 min. Slides were deparaffinized using xylene, and then rehydrated with 100% alcohol, 95% alcohol, and normal saline (pH 7.4), followed by staining. Tissue sections were probed with the antihuman OATP2B1 antibody (1:500, ab222094, Abcam, Cambridge, United Kingdom) overnight at 4°C, and IHC anti-rabbit/anti-mouse secondary antibody (Mouse and Rabbit Specific HRP/DAB (ABC) Detection IHC kit, ab64264, Abcam, Cambridge, United Kingdom) was added for 45 min at room temperature, followed by adding DAB as a chromogen for 15 s, and then hematoxylin as a counterstain for color development. Bright-field microscopy images were captured using a Nikon Eclipse TS100 microscope (20x and 100x) (Nikon).

## Flow Cytometry for Surface Expression of Fluorophore Conjugated OATP2B1 in FM Cells

Firstly, anti-human OATP2B1 antibody (ab222094, Abcam, Cambridge, United Kingdom) was labeled using the CF® Dye and Biotin Protein Labeling Kits (Biotium, Fremont, CA) along with Rabbit IgG (AB_2532938, Invitrogen) as per the manufacturer's protocol. The next day, the conjugated

OATP2B1 antibody was used for flow cytometry analysis. Briefly, FM cells (AEC, AMC, and CTC), maternal decidua, and BeWo cells (used as a surrogate for placental cells) were harvested, washed in ice-cold PBS, 10% FCS, 1% sodium azide and centrifuged at 3,000 rpm for 10 min. Cell pellets were incubated with specific fluorophore conjugated antihuman OATP2B1 antibody (1:50) and propidium iodide dye (BioLegend, San Diego, CA) for 30 min at 4°C in dark. Cells were washed three times by centrifugation at 400 g for 5 min and resuspended in 500 µL of ice-cold PBS, 10% FCS, 1% sodium azide, and analyzed immediately on a CytoFLEX flow cytometer (Beckman Coulter, Brea, CA).

## Fluorescent Zombie Violet Dye Uptake Determined by Flow Cytometry in FM Cells

Based on our IHC and western blotting data, we chose AECs and CTCs to further study the uptake function of cell surface OATP2B1 by flow cytometry. Previous studies have demonstrated that intracellular accumulation of zombie violet dye is increased explicitly by OATPs (Patik et al., 2015; Patik et al., 2018). OATP2B1 is known to function almost exclusively at acidic extracellular pH (Patik et al., 2018). Based on these criteria, we chose the zombie violet dye uptake assay to determine the functional capacity of OATP2B1 in FM cells. Briefly, cells were washed in uptake buffer (125 mM NaCl, 4.8 mM KCl, 1.2 mM $CaCl_2$, 1.2 mM $KH_2PO_4$, 12 mM $MgSO_4$, 25 mM MES, and 5.6 mM glucose, with the pH adjusted to 5.5 using 1 M HEPES and 1 N NaOH). After washing $5 \times 10^5$ cells were incubated for 15 min at 37°C with Zombie violet (BioLegend®, San Diego, CA, United States; 0.4 µL zombie violet/$5 \times 10^5$ cell) and propidium iodide dye (BioLegend, San Diego, CA) in a final volume of 100 µL. The reaction was stopped by adding 1 ml ice-cold PBS and the fluorescence of 10,000 living cells was immediately determined on a CytoFLEX flow cytometer (Beckman Coulter, Brea, CA). Dead cells were excluded by propidium iodide labeling.

## Protein Extraction and Western Blotting

Placental and FM explants as well as immortalized maternal DECs and FM cells (AECs, AMCs, CTCs) were lysed with radioimmunoprecipitation lysis buffer [50 mM Tris (pH 8.0), 150 mM NaCl, 1% Triton X-100, 1.0 mM EDTA (pH 8.0), and 0.1% SDS] supplemented with a protease and phosphatase inhibitor cocktail and also phenyl methyl sulfonyl fluoride. Human FM were homogenized as previously described (Richardson et al., 2020a). After centrifugation at 12,000 g for 20 min, the supernatant was collected and protein concentrations were determined using the Pierce bicinchoninic acid kit (Thermo Scientific, Waltham, MA, United States). The protein samples were separated using SDS-polyacrylamide gel electrophoresis on a gradient (4–15%) Mini-PROTEAN TGX Precast Gel (Bio-Rad, Hercules, CA, United States) and transferred to the membrane using a Bio-Rad Gel Transfer Device (Bio-Rad). Membranes were blocked in 5% non-fat milk in 1× Tris-buffered saline-Tween 20 for a minimum of 1 h at room temperature and then probed overnight at 4°C using primary antibody overnight. The membranes were then incubated with secondary antibody conjugated with horseradish peroxidase, and immunoreactive proteins were visualized using chemiluminescence reagents ECL WB detection system (Amersham Piscataway, NJ, United States). The following anti-human antibodies were used for western blot: OATP2B1 (1:1,000 for tissues and 1:250 for FM cells, ab245246, Abcam, United States) and β-actin (1: 15,000, Sigma- Aldrich, St. Louis, MO, United States). Protein band quantification were normalized to β-actin expression in each lane, and the expression levels were densitometrically determined using the Bio-Rad Image Lab 6.0 software.

## Short-Interfering RNA-Mediated Gene Silencing of OATP2B1 in CTCs

CTCs were found to have maximum levels of OATP2B1 compared to all other cell types in FMs. Therefore, we chose CTCs to further study the role of OATP2B1 in the uptake of fluorescent zombie violet dye and substrate (Rosuvastatin) propagation across the FM layers based on our immunohistochemistry western blot analyses. CTCs were cultured to 50-60% confluency in DMEM/F12 medium supplemented with 10% FBS and antimicrobial agents (penicillin, streptomycin, and amphotericin), and then transfected with 15 µL of 20 µM oligos (Dharmacon, Lafayette, CO, United States) directed against OATP2B1 or nontarget scrambled (control) siRNAs using RNAimax lipofectamine as per the manufacturer's instructions (Thermo Fisher Scientific, Waltham, MA, United States). After 24 h, OATP2B1 knockdown CTCs were separately used for the fluorescent zombie violet uptake assay BeWo cells was used as a surrogate of placental cells. BeWo cells is a commonly used *in vitro* model for studying the placental barrier. BeWo cells emulate a term human placental barrier in culture conditions because of its ability to fuse and form a syncytium *in vitro*. In another set of experiments, control and knockdown CTCs were loaded into the feto-maternal interface OOC device as previously described (Radnaa et al., 2021), as further described in the following section.

## Use of the Four-co-culture-chamber Feto-Maternal Interface OOC Device to Monitor the Propagation of Rosuvastatin Across Fetal Membrane Cells

The development and validation of the feto-maternal interface -OOC device have been previously reported by our laboratory (Richardson et al., 2019; Richardson et al., 2020b; Richardson et al., 2020c; Radnaa et al., 2021). In brief, the microfluidic feto-maternal interface -OOC is composed of four concentric cell culture compartments (one for maternal cells and three for fetal cells) interconnected through arrays of microfluidic channels to allow co-cultivation of four different cell types. Chamber one, the central chamber is for maternal DECs, chamber two is for fetal CTCs, chamber three is for AMCs, and the outermost

chamber is for AECs. Each cell chamber is 250 μm in height, and the width of each chamber was designed to mimic the differences in thickness of each maternal and fetal layer as seen *in utero*. The chambers are interconnected through an array of 24 microchannels (all width: 35 μm; length: 600 μm for CTCs to DECs and AMCs to CTCs, 300 μm for AECs to AMCs; all height: 5 μm) that performed several functions, such as preventing the flow of cells between compartments during the initial cell loading process, allowing independent localized biochemical treatments to each compartment, enabling independent elution of supernatant from each cell compartment, and allowing biochemicals to diffuse between the chambers to enable cell-cell communication. The number of microchannels, along with the height and width, remained same throughout all experiments as to not affect the diffusion rate of molecules. The device contains an on-chip reservoir block placed on top of the cell culture chamber layer and is comprised of multiple 4 mm diameter and 2 mm deep reservoirs, where each reservoir is aligned in such a way that they are placed on top of the inlets and outlets of each cell culture chamber in the main cell culture layer. The center culture chamber has one reservoir on top of it and the outermost culture chamber has four reservoirs on top of it, while the two middle culture chambers have two reservoirs each on top of them, to provide sufficient cell culture medium to all parts of the cell culture chambers evenly. The feto-maternal interface -OOC was fabricated in polydimethyl siloxane (PDMS, 1:10 mixture, Sylgard 184; DowDuPont, Midland, MI, United States) using a two-step photolithography master mold fabrication process, followed by a soft lithography process of replica-molding the final PDMS device from the master mold (Park et al., 2010). The bonding of the PDMS layer onto the glass substrate was improved by treating the PDMS layers with oxygen plasma (Harrick Plasma, Ithaca, NY, United States), followed by bonding the layer onto a glass substrate. This process was repeated to bond the PDMS reservoir layer on top of the device. The feto-maternal interface -OOC device was stored dry (for up to 1 month) and before using the feto-maternal interface -OOC, the devices were sterilized with 70% ethanol for 15 min.

## Type IV Collagen Loading Into the Feto-Maternal Interface-OOC Microchannels

Before using the feto-maternal interface-OOC, the devices were washed three times with PBS, filled with type IV basement membrane collagen Matrigel (Corning Matrigel basement membrane matrix, DEV-free; 1:25 in media), and incubated at 37°C with 5% $CO_2$ overnight. Diluted type IV collagen basement membrane Matrigel was used to fill the microfluidic channels between the AMC and the CTC compartments, mimicking the amnion and chorion basement membranes *in utero*. These Matrigel-filled microchannels will allow localized drug treatment of each cell layer and independently take supernatant from each layer. These channels also allow biochemical to diffuse between the layers and permit cell migration and transition, as seen in the fetal membrane-decidua feto-maternal interface.

## Cell Seeding and Culture in the Feto-Maternal Interface-OOC Device

After Matrigel loading, the cell chambers were rinsed two times with PBS to remove extra Matrigel, and the devices were loaded with immortalized cells in the different culture chambers. Immortalized cells were then trypsinized and loaded into the device, starting from the center chamber to the outside. Cell loading concentration in each chamber mimicked those of *in utero* cell ratios of the FM tissue (60,000 DECs for chamber one, 200,000 CTCs + 5% primary collagen + 25% Matrigel for chamber two, 62,500 AMCs + 20% primary collagen + 25% Matrigel for chamber three, and 120,000 AECs for chamber four). Following cell seeding, both the feto-maternal interface-OOC devices and the 24-well plates were incubated at 37°C with 5% $CO_2$ overnight before Rosuvastatin treatment.

## Rosuvastatin Treatment Preparation

Rosuvastatin was obtained from Sigma-Aldrich (St Louis, MO). Rosuvastatin calcium salt was prepared as a stock of 10 mg/ml in serum-free media, and was added in a concentration of 200 nmol/L. The dose of rosuvastatin was chosen based on the maximum concentrations achievable in tissues after therapeutic doses, as previously reported by our laboratory (Ayad et al., 2018). Next day, rosuvastatin (200 ng/ml) was added to the maternal DEC chamber, and the supernatant from each chamber (AEC, AMC, CTC, and maternal DEC) was collected after 4 h. We chose this time point because previous studies from our laboratory have observed propagation of rosuvastatin from the maternal decidual chamber to the AEC chamber of the feto-maternal interface-OOC within 4 h after introducing the drug (unpublished data). To confirm the kinetics of Rosuvastatin in OATP2B1 knockdown CTCs, the concentration of rosuvastatin in the media collected from each of the chamber was analyzed by mass spectrometry (see below for details).

## Mass Spectrometry for Analysis of Rosuvastatin Propagation in the Feto-Maternal Interface -OOC

Targeted liquid chromatography tandem mass spectrometry (LC-QQQ) analysis was performed on a TSQ Altis mass spectrometer (Thermo Scientific, Waltham, MA) coupled to a binary pump UHPLC (Vanquish, Thermo Scientific). Scan parameters for target ions as per the Selective Reaction Monitoring (SRM Table) for Rosuvastatin were used. The injection volume was 10 μL. Chromatographic separation was achieved on a Hypersil GOLD™ C18 HPLC column (Dimensions: Particle size: 5 μm; Diameter: 50 mm; and Length: 2.1 mm) (Thermo Scientific) maintained at 30°C using a solvent gradient method. Solvent A was 0.1% formic acid in water. Solvent B was 0.1% formic acid in acetonitrile. The gradient method used was 0–1 min (20% B to

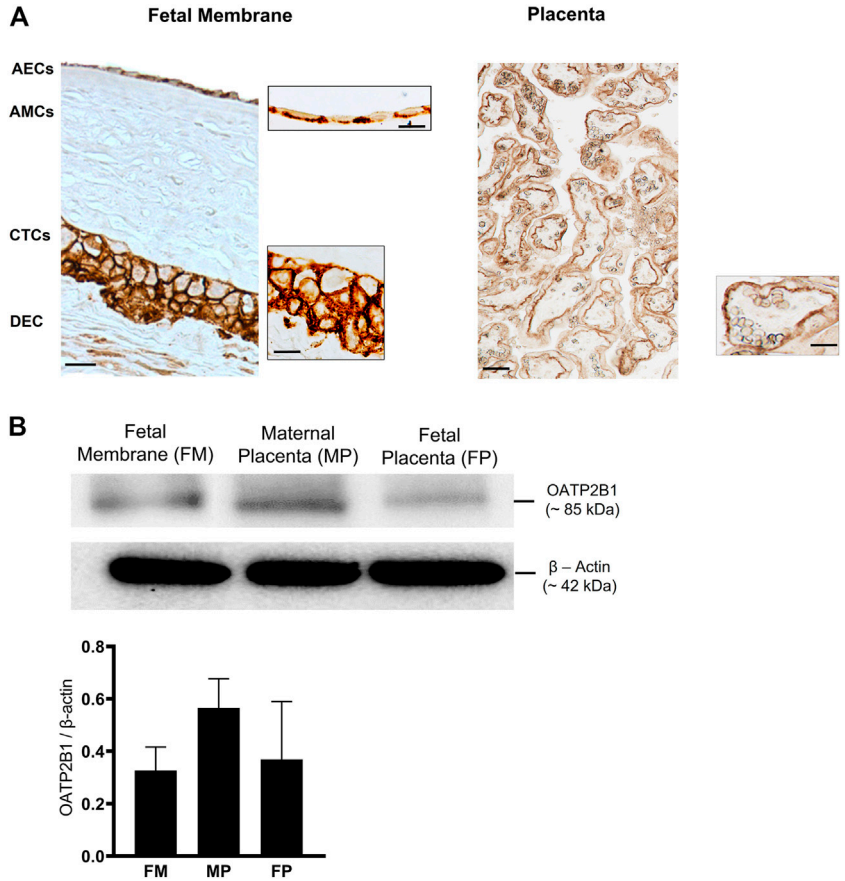


**FIGURE 1 |** Localization and expression of OATP2B1 transporter protein in fetal membrane tissues and human placenta. **(A)** Bright field microscopy showing localization of OATP2B1 (brown) in human fetal membrane AECs and CTCs (left image) at a magnification of 20x (main image) and 100x (inset image) and placental syncytiotrophoblast at a magnification of 20x (main and inset image (right image). 20x and 100x images were taken in different regions of the tissue. Images are representative of three biological replicates. Scale bar = 30 μM. **(B)** Western blot analysis and quantification of OATP2B1 in human fetal membranes and placenta (maternal and fetal side). β-Actin is used as a loading control. Representative western blots are shown. $n$ = 6 biological replicates. Error bars represent mean ±SEM.

60% B), 1-2 min (60% B to 95% B), 2-4 min (95% B), 4–4.1 min (95% B to 20% B), and 4.1–5 min (20% B). The flow rate was 0.5 ml $min^{-1}$. Sample acquisition and data analysis was performed using the Trace Finder 4.1 software (Thermo Scientific).

## Statistical Analysis

Statistical analysis and significance were determined by using the Prism 9 software (Graph Pad, San Diego, CA). Statistical analyses for normally distributed data were performed using analysis of variance (ANOVA) with the Tukey Multiple Comparisons Test. Significance is shown as $^{*}p < 0.05$ and $^{**}p < 0.01$. All data are shown as mean ± standard error of the mean (SEM).

# RESULTS

## OATP2B1 Localization in FMs

FMs are divided into morphologically distinct amnion and chorion membranes, each with its own well-defined microarchitecture (Menon et al., 2019). First, OATP2B1 localization was confirmed in different layers of FMs by IHC ($n$ = 3). OATP2B1 expression was localized on the basolateral surface of AECs and on both the apical and basolateral surfaces of CTCs (**Figure 1A**). In line with previous studies, OATP2B1 was also localized on the basolateral surface of placental syncyiotrophoblasts (**Figure 1A**). Next, we determined the protein expression of OATP2B1 in FMs by western blotting ($n$ = 6). The expression level of OATP2B1 was similar in FMs as in both maternal and fetal sides of the placenta (used as a positive control in our experiment) (**Figure 1B**). These results show that OATP2B1 location and expression are relatively similar in the FM and placenta.

## Surface Expression of OATP2B1 in FM Cells

To test whether OATP2B1 is expressed on the surface of fetal membrane cells, flow cytometry analysis was performed on AECs, CTCs, AMCs, and maternal DECs. As shown in **Figure 2A**, cells expressing OATP2B1 receptor bind to a conjugated antibody and show a distinct shift in flow peak towards right (blue) from the

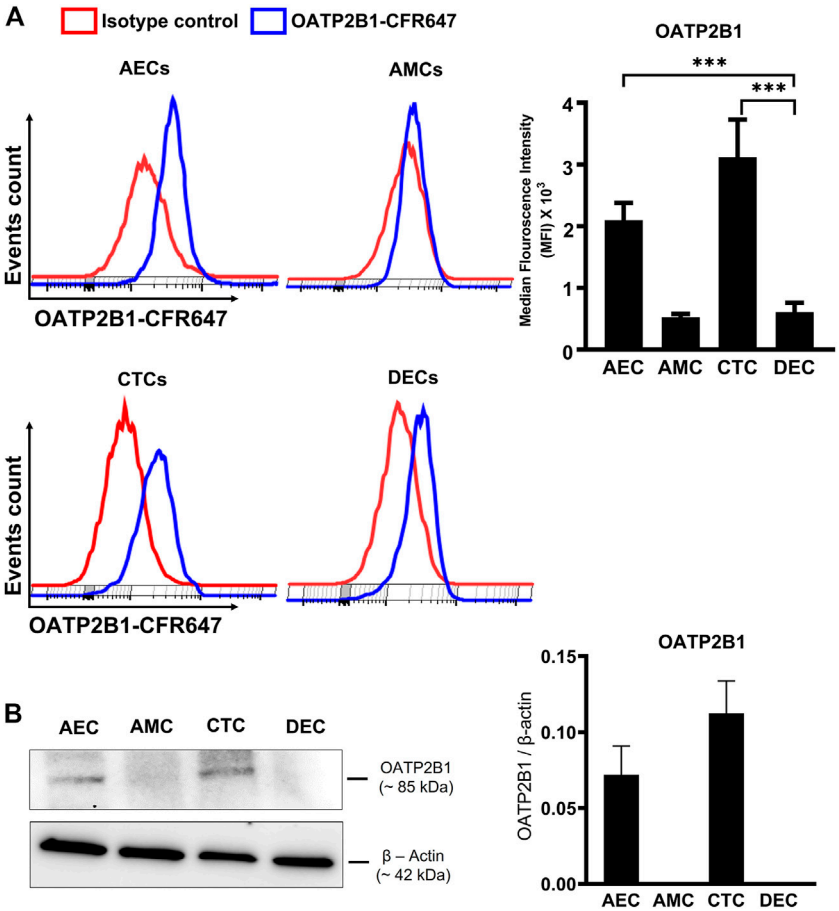


**FIGURE 2 |** Expression of OATP2B1 transporter protein in human fetal membrane cells. **(A)** Cell surface expression of OATP2B1 in fetal membrane cells (AECs, AMCs, CTCs) and maternal decidual cells (DECs) using primary antibody conjugated with CFR647. Representative histograms of stained samples are shown. The mean fluorescence of these histograms was calculated using the FlowJo Software. **(B)** Western blot analysis and quantification of OATP2B1 in fetal membrane AECs, AMC, CTCs, and maternal DECs. Actin was used as a loading control. Representative blots are shown. Error bars represent mean ± SEM. *n* = 4 biological replicates.

Isotype control stained cells (red). In line with our IHC data, flow cytometry analyses showed differential expression of OATP2B1 on the surface of FM cells (**Figure 2A**). The surface expression of OATP2B1 on the CTCs was significantly higher compared to the maternal DECs ($p < 0.5$) (**Figure 2A**). Furthermore, western blot analysis showed OATP2B1 expression in only AECs and CTCs of the FM, but not in AMCs and DECs (**Figure 2B**).

## Functional Activity of OATP2B1 in FM AECs and CTCs

Next, the zombie violet uptake assay was used to determine the functional role of OATP2B1 in FM cells (Patik et al., 2018; Patik et al., 2015). Zombie violet is a fluorescent viability dye that is taken up by dead cells; however, the presence of OATP can mediate uptake of zombie violet dye in living cells at an extracellular pH of 5.5 (Patik et al., 2018). As an internal control, we have used the propidium iodide (PI) which will stain also dead cells. As shown in **Figure 3A**, uptake of the zombie violet dye by OATP2B1 receptor showed a distinct shift in flow peak towards right (blue) from the live cells (red). The uptake of zombie violet dye by fetal membrane AECs and CTCs was comparable to the dye uptake observed in the placental BeWo cells (**Figures 3A,B**). Uptake of the dye by the FM and placental cells suggest that OATP2B1 expressed on cell surfaces of AECs, CTCs and BeWo are functional.

## Oxidative Stress Suppresses OATP2B1 Expression at the Feto-Maternal Interface

Previous reports show that CSE-induced oxidative stress promotes cellular senescence, cellular transitions, and a pro-inflammatory environment (increased concentrations of pro-inflammatory cytokines) (Polettini et al., 2018; Richardson et al., 2020a). Moreover, a pro-inflammatory environment at the feto-maternal interface has been reported in preterm birth, preeclampsia, and fetal growth restriction (Aouache et al., 2018). Therefore, to determine the effect of CSE-induced oxidative stress on OATP2B1 expression at the feto-maternal interface, FM and placenta explants were exposed to CSE for up to 24 h (0, 4, 8, 24,

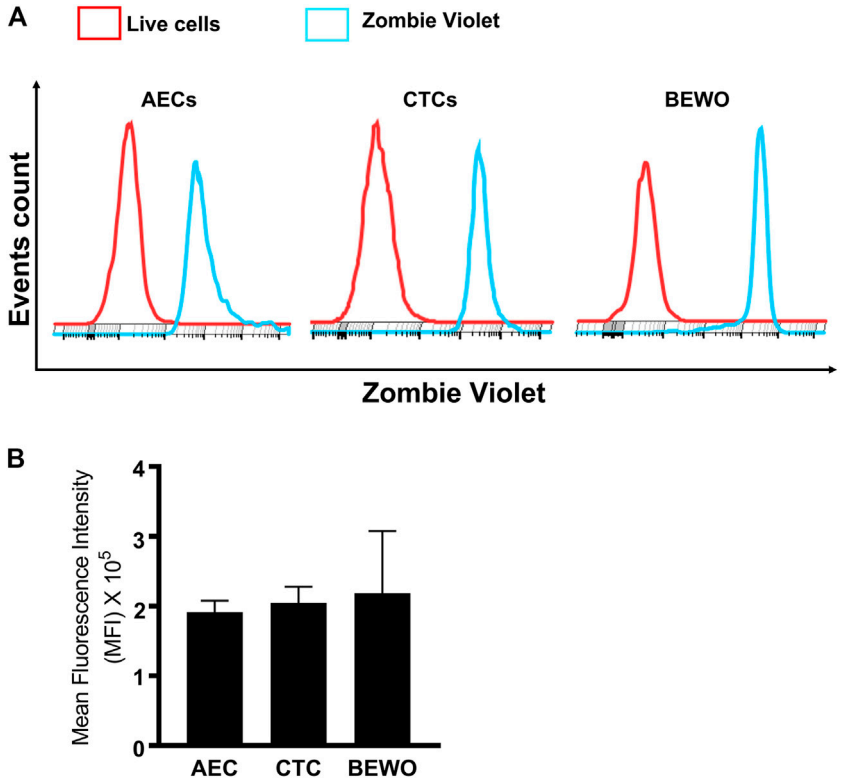


**FIGURE 3 |** Functional validation of OATP2B1 in fetal membrane and placental cells. **(A)** Functional activity of OATP2B1 in fetal membrane (AECs and CTCs) and placental (BeWo) cells was determined by flow cytometry. Representative histograms of zombie violet dye uptake are shown. **(B)** The mean fluorescence intensity of these histograms was calculated using the FlowJo software. $n$ = 4 biological replicates. Error bars represent mean ± SEM.

48 h) and analyzed for OATP2B1 expression by western blotting. Oxidative stress did not have a significant impact on OATP2B1 expression in the FM (**Figure 4A**); however, CSE led to a significant decrease in OATP2B1 expression in placental explants ($p < 0.05$) (**Figure 4B**). These results suggest that oxidative stress or a pro-inflammatory *in utero* environment during pregnancy can lead to differential OATP2B1 expression at the FM-decidua parietalis interface and the placenta-decidua basalis interface.

## Silencing OATP2B1 in CTCs Reduces Drug Transport

To validate the contribution of OATP2B1 in drug transport, the zombie violet uptake assay was conducted after silencing OATP2B1. A reduction in OATP2B1 expression was determined by western blot analysis in CTCs and BEWO cells (**Figure 5A**). Knocking down OATP2B1 in CTCs reduced the uptake of zombie violet dye (as indicated by the zombie violet-stained blue peak overlapping with the unstained red peak), suggesting that OATP2B1 in CTCs could play an essential role in the uptake of substrates within the FM (**Figure 5B**). Interestingly, silencing OATP2B1 had little to no effect on the zombie violet dye uptake in BeWo cells (**Figure 5B**). We speculate that the differences in uptake results between the FM and placental cells after OXTP2B1 knockdown indicate that possibly in placental BeWo cells other uptake receptors (such as OATP1B1) may also contribute to substrate uptake, whereas in FM CTCs OATP2B1 may play a more predominant role in the uptake of substrates from the maternal DEC.

To confirm OATP2B1's role in drug transport, especially in CTCs, the feto-maternal interface-OOC device was used to study the contribution of OATP2B1 in the transport of rosuvastatin through the FM layers. Here, OATP2B1-silenced CTCs were used and compared to normal CTCs. We used stain as the model drug, since they are competitive inhibitors of 3-hydroxy-3-methylglutaryl-coenzyme-A reductase (HMG-CoA reductase) and have been tested in multiple models of pregnancy complications, such as preterm birth and preeclampsia (Istvan, 2003; Basraon et al., 2012). Specifically, we selected rosuvastatin because it is more hydrophilic than other statins (such as pravastatin) and requires protein transporters such as OATP2B1 to enter the cell to inhibit the HMG-CoA reductase enzyme (Climent et al., 2021). This drug was loaded into the DEC chamber (innermost chamber) and its propagation throughout the FM layers measured using mass spectrometry (**Figure 6A**). Mass spectrometry data suggests that 18.45% of rosuvastatin propagated from the maternal decidual chamber to the fetal CTC chamber under control conditions. siRNA-mediated silencing of OATP2B1 in CTCs however resulted in only

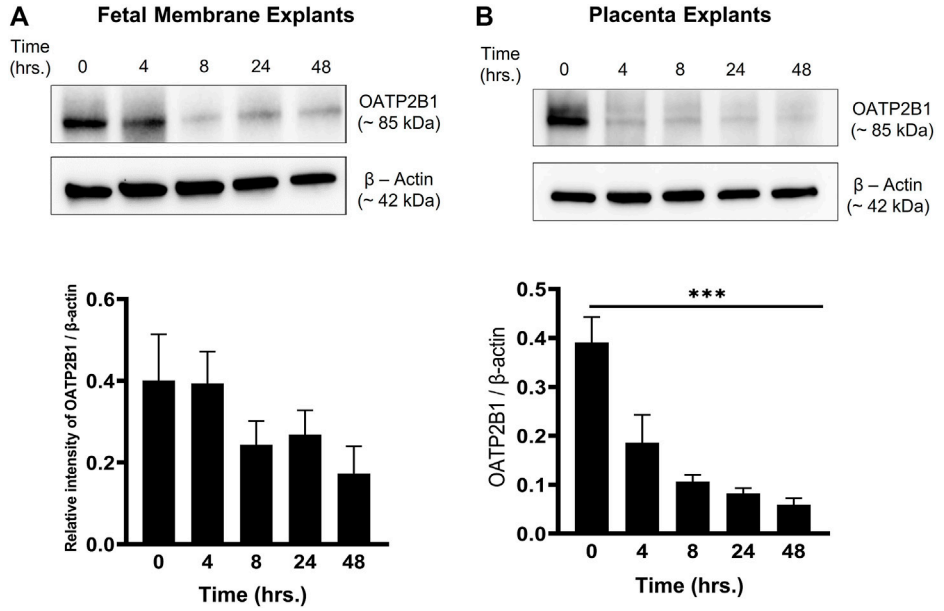


**FIGURE 4 |** Expression of OATP2B1 in fetal membrane and placenta explants upon stimulation with CSE-induced oxidative stress. **(A)** Western blot analysis and quantification of OATP2B1 in CSE-treated fetal membrane explants shows no significant effect on OATP2B1 expression. **(B)** Western blot analysis and quantification of OATP2B1 in CSE-treated placental explants shows a time-dependent reduction in OATP2B1 expression (***$p < 0.001$). β-Actin was used as a loading control. Representative blots are shown. $n = 5$ biological replicates. Error bars represent mean ± SEM.

2.57% of rosuvastatin propagating from the DEC chamber to the CTC chamber (**Figure 6B**). Furthermore, OATP2B1 silencing also reduced rosuvastatin propagation from the DEC chamber to the AEC chamber, where only 0.32% of rosuvastatin was detected in the AEC chamber from OATP2B1 knockdown CTCs compared to 1.73% in non-targeted siRNA control CTCs (**Figure 6B**). These data further confirm our findings that OATP2B1 could potentially act as one of the most significant drug transport receptors in FM CTCs.

## DISCUSSION

The feto-maternal interfaces are critical for the transport of numerous endogenous substrates, including hormones, steroids, metabolites, neurotransmitters, and exogenous substrates, including drugs (i.e., statins, glycosides, and antivirals) between the mother and the fetus (Menon and Richardson, 2017; Richardson and Menon, 2018). Drug transport across the placental interface is well studied. In contrast, there is a lack of knowledge regarding the contribution of the other feto-maternal interface, namely the FM-decidual interface, as a path for drug transport during pregnancy. The FM provides mechanical, immune, endocrine, transportation, and antimicrobial functions during pregnancy (Menon, 2016). Despite its importance in maintaining pregnancy and fetal growth, research focusing on the role of FM cells in the transport of exogenous and/or endogenous substrates is lacking compared to that of placenta. This is partly because of the avascular nature of FMs, although chorion trophoblast lines with vascular maternal decidua. We report for the first time, to the best of our knowledge, that human FM express functionally intact transporter proteins that can transport drugs. The significance of these findings are: 1) OATP2B1 is expressed in fetal membranes and is mainly localized in the CTC and AEC layers; 2) CTC and AEC cell layers show functionally active cell surface expression of the OATP2B1 transporter; 3) CSE-induced oxidative stress and pro-inflammatory conditions resulted in a time-dependent decrease in the expression of OATP2B1 in the placental explants but not in the FM, and 4) using a four-chambered feto-maternal interface-OOC device, we showed that silencing of OATP2B1 in CTCs significantly reduced drug (rosuvastatin) propagation from the maternal decidua through the CTCs and AMCs to the AECs. In summary, our findings suggest that transporter proteins expressed in the FM-decidual interface can play an important role in drug transport at a similar level, if not more, than the placenta.

OATP2B1 is predominantly involved in the tissue uptake of endogenous (i.e., steroid hormones, metabolites, and neurotransmitters) and exogenous (i.e., statins, glycosides, and antivirals) substrates, and has a sizeable substrate-specific difference in affinity of substrate compared to other OATP transporters because of its multiple substrate binding sites (Ogura et al., 2020). In line with the previous studies, we found that OATP2B1 is expressed on the placental syncyiotrophoblasts basal membrane (fetal-facing). Because of its localization, OATP2B1 plays an important role in drug transport and uptake of sulfates (such as dehydroepiandrosterone; DHEA) from the fetal circulation (Grube et al., 2007). New to the field, OATP2B1 was also

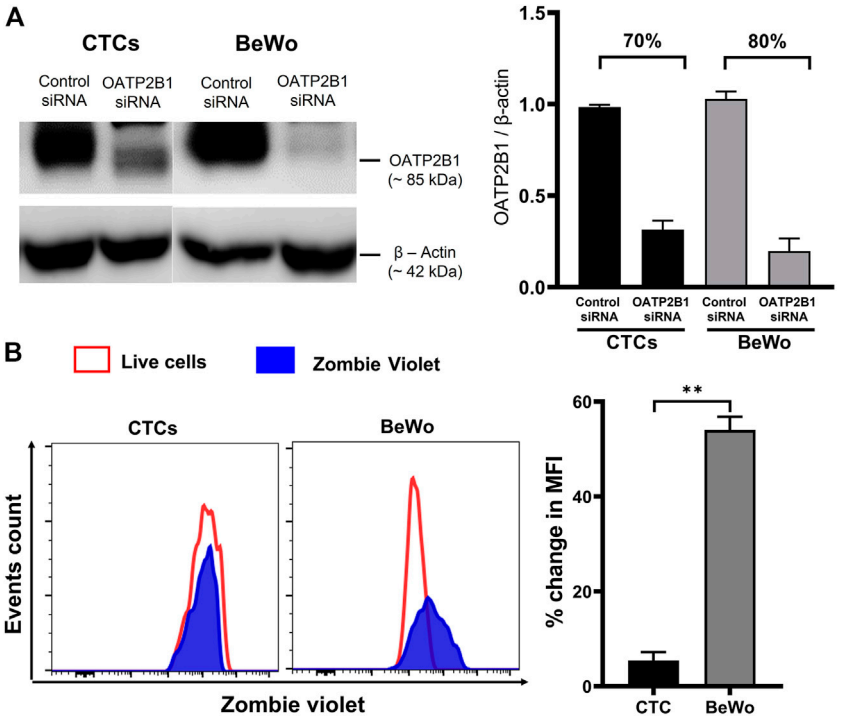


**FIGURE 5 |** Effect of OATP2B1 silencing on zombie violet dye uptake assay in placental BeWo cells and fetal membrane CTCs. **(A)** Western blot analysis and quantification of OATP2B1 in siRNA-treated BeWo cells and CTCs to determine the efficiency of knockdown. OATP2B1 was silenced in BeWo cells (70%) and CTCs (80%) using short-interfering RNA (siRNA). Non-targeted scrambled siRNA is used as control siRNA. β-Actin was used as a loading control. Representative blots are shown. Error bars represent mean ± SEM. **(B)** OATP2B1 siRNA-treated BeWo cells and CTCs were subjected to the zombie violet dye uptake assay. The data shows that the uptake of zombie violet dye (as indicated by the percent change in mean fluorescence intensity compared to the unstained controls) was reduced to a greater extent in OATP2B1 siRNA-treated CTCs compared to the siRNA treated BeWo cells. Representative histograms of the dye uptake determined by flow cytometry analysis are shown. The percent change in mean fluorescence intensity (MFI) in OATP2B1 knockdown CTCs and BeWo cells (**p < 0.01*) compared to their respective controls was calculated using the FlowJo software. *n* = 4 biological replicates. Error bars represent mean ± SEM.

identified on the basolateral surface of AECs as well as on the apical and basolateral surfaces of CTCs. Our functional data suggest that OATP2B1 activity on AECs and CTCs is comparable to that seen in placental BeWo cells. Although active OATP2B1 receptors were detected on the surface of FM cells, the transport directionality in each cell types remains to be confirmed, which we plan to conduct as future studies. The presence of OATP2B1 on the surface of AECs and CTCs suggests that fetal membranes can also allow transport and/or diffusion of drugs and their metabolites to reach the intraamniotic cavity, amniotic fluid, and the fetus. Furthermore, the absence of OATP2B1 transporters in the AMCs and maternal decidua denotes different cell-type specificity that may have distinct functions in drug transport mechanisms across fetal membranes. As reported by Richardson et al., AMCs are not necessarily constituents of fetal membranes, but they are transient AECs undergoing a recycling process through cyclic epithelial-to-mesenchymal and mesenchymal-to-epithelial state (Richardson et al., 2020a), a process required to maintain FM integrity. Hence, AMCs are not expected to perform tasks such as transportation of materials between the feto-maternal compartment. Therefore, lack of functional transporters such as OATP2B1 in AMCs are justified.

Interestingly, oxidative stress and inflammation can also affect OATP2B1 expression (Kojovic et al., 2020). For example, a study by Kojovic et al., reported that OATP2B1 expression was increased in placentae obtained from women with preeclampsia (a pregnancy-specific disorder often characterized by increased oxidative stress and increased pro-inflammatory cytokines) (Kojovic et al., 2020). An alteration in the expression of functionally essential transporters (such as OATP2B1) suggests that placental function is compromised during pregnancy complications. However, the impact of oxidative stress and inflammation on OATP2B1 expression in FMs remained unknown. In our study, OATP2B1 expression remained unaffected following CSE treatment, whereas in the placental explants OATP2B1 decreased in a time-dependant manner following CSE treatment. This finding is contrary to previous findings (Kojovic et al., 2020), where OATP2B1 expression was increased in preeclamptic placentae (Kojovic et al., 2020). This could be due to differences between explant phenotypes used, as Kojovic et al., utilized placental tissues obtained from preeclamptic women and here cesarian-derived placental explants were stimulated with CSE. A reduction in the expression of placental OATP2B1 transporter under oxidative stress conditions could potentially lead to a greater risk of

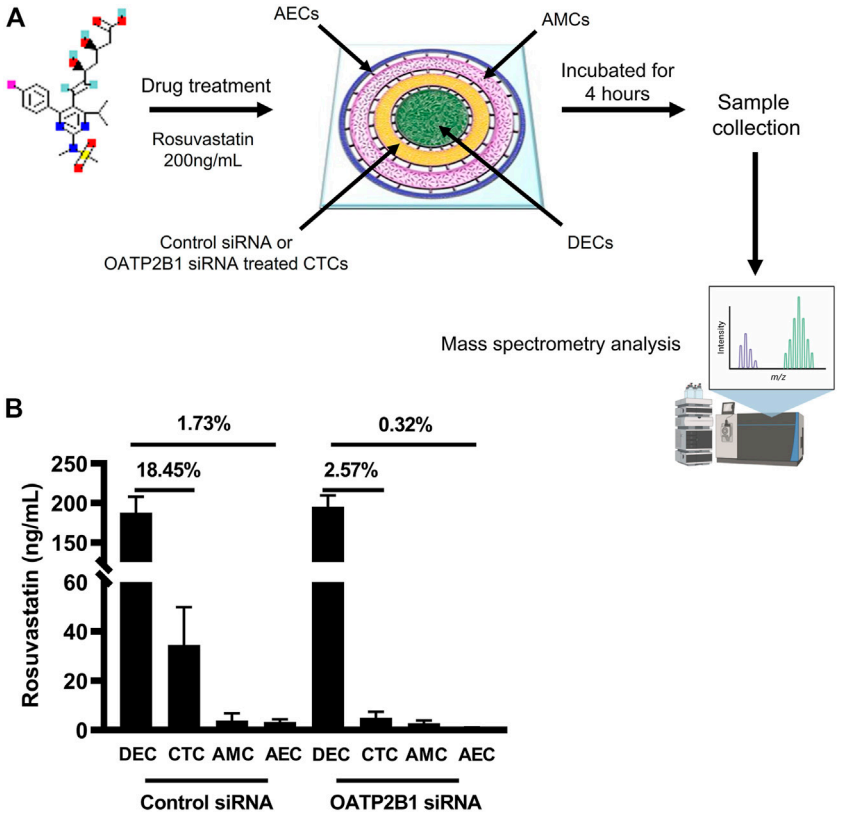


**FIGURE 6 |** Role of OATP2B1 in rosuvastatin transport across the feto-maternal interface-OOC. **(A)** Schematic showing the four concentric cell culture chambers of the feto-maternal interface-OOC used to determine the role of OATP2B1 in transporting drug across the different fetal membrane chambers [AECs (blue, chamber 1), AMCs (pink, chamber 2), CTCs (yellow, chamber 3), and maternal DECs (green, chamber 4)]. Rosuvastatin (200 ng/ml) was introduced in the decidual chamber of the feto-maternal interface-OOC with either control mock siRNA or OATP2B1-knockdowned CTCs. Following incubation for 4 h, media was collected from different chambers of feto-maternal interface-OOC for mass spectrometry analysis. **(B)** Under control siRNA conditions, 18.45 and 1.73% of rosuvastatin propagated from the maternal DEC to the CTC chamber as well as to the AEC chamber, respectively. OATP2B1 silencing in OATP2B1 resulted in only 2.57% rosuvastatin propagation from the maternal DEC chamber to the CTC chamber, and only 0.32% of rosuvastatin propagation from the DEC chamber to the AEC chamber, and then zero to the CTC chamber. Data is represented as mean ± SEM. Rosuvastatin propagation across the feto-maternal interface -OOC was confirmed from six independent experiments.

substrate accumulation, thus resulting in fetal toxicity. The apparent lack of change of OATP2B1 in fetal membrane explants under similar conditions suggests that fetal membranes can act to transport drugs from fetal circulation under oxidative stress conditions when placental drug transporters may be less functional, providing a new avenue for drug delivery to the fetus.

We further validated the functional role of OATP2B1 in crossing the feto-maternal interface by using an exogenous substrate (rosuvastatin) and siRNA silencing of OATP2B1 in CTCs in our previously developed feto-maternal interface-OOC device. Rosuvastatin is more hydrophilic than other statins (such as pravastatin) and requires protein transporters such as OATP2B1 to enter the cell to inhibit the HMG-CoA reductase enzyme (Climent et al., 2021). Therefore, it is an ideal candidate to use as a substrate for characterizing the functions of transporter proteins. Additionally, rosuvastatin has been reported to reduce oxidative stress-driven inflammation in fetal membranes and has lesser side effects and more effectiveness in regulating inflammatory conditions (Ayad et al., 2018; Kim et al., 2019). Our study found that rosuvastatin propagates from the maternal decidua to the AEC layer of fetal membranes. Interestingly, under control conditions we found substantial rosuvastatin propagation (18.45%) from maternal DEC to CTC chamber, of which only 1.73% of rosuvastatin propagated from CTC to the AEC chamber. We speculated that the marked decrease in rosuvastatin propagation from CTC to AEC chamber as evidenced by reduced rosuvastatin concentration could be due to the fact that we measured only the parent rosuvastatin compound by mass spectrometry, and it is highly plausible that rosuvastatin could be metabolized by the enzymes in the CTC layer. However, if the reduction in rosuvastatin propagation into the AEC chamber could be due to metabolism of rosuvastatin in the chorionic layer remains to be confirmed. Furthermore, siRNA-mediated knockdown of OATP2B1 in CTCs resulted in a significant decrease in rosuvastatin propagation into the CTC chamber and a subsequent reduction into the AEC chamber. Our findings further elucidate the role of human FM in drug transport. Additionally, we have determined that CTCs within the FM, a

layer that forms the barrier between mother and the fetus, play a vital role in propagating maternal drugs through the fetal membrane cell layers to reach the amniotic fluid and the fetus.

As noted above, our study provides novel insights into drug transport mechanisms during pregnancy. The discovery of FM as an alternate gatekeeper for drug transport across the feto-maternal interface has broad clinical implications: 1) Designing novel drug delivery systems that could cross not only the placenta, but also FM to improve their pharmacokinetics and therapeutic application; 2) The presence of transport proteins on fetal membranes is expected to expand pharmacologic research during pregnancy, as barrier functions of this second entrance point need to be evaluated thoroughly for currently used and future drugs; The utilization of feto-maternal interface-OOC devices for investigating the role of transporter proteins in drug propagation can be translated to studying drug kinetics during pregnancy and could potentially reduce the time and cost associated with clinical and pre-clinical trials.

Strengths of our study include using an innovative four-chamber microfluidic organ-on-chip device containing different cellular layers of FM and maternal DECs (representing feto-maternal interface) developed and validated in our laboratory. Our feto-maternal interface-OOC can maintain cellular interactions of the amniochorion-decidual interface as seen *in vivo*, mimics the physiological state of feto-maternal interactions during pregnancy, and is fully compatible with various analyses methods such as microscopy and biochemical analyses. Our findings are not without limitations, however. We were limited in testing OATP2B1 substrate (rosuvastatin) propagation only from the maternal decidua through the fetal CTC layer and matrix into the AEC chamber. More importantly, OATPs have differential affinity towards transport substrates, such as steroid sulfates, thyroid hormones, xenobiotics, and drugs; therefore, to fully delineate the functional role of OATP2B1, propagation of various substrates *via* OATP2B1 needs to be further explored. Moreover, substrate propagation from the AEC chamber to the maternal decidua could provide an additional understanding of the transport directionality of OATP2B1s present in AEC and CTC layers of the fetal membranes, which will be explored in future studies.

In summary, we found that FMs can function as a gatekeeper for drug transport. The transporter protein, OATP2B1, expressed on AECs and CTCs, plays an important functional role in drug transportation across the feto-maternal interface. The use of the feto-maternal interface-OOC further confirms, that in addition to the placenta, the FM-decidual interface can transport drugs during pregnancy. Hence, the FM barrier functions need to be evaluated thoroughly for current and future clinical use. This knowledge will improve drug delivery testing during pregnancy and can contribute to designing new drug delivery strategies to better treat adverse pregnancy outcomes.

## DATA AVAILABILITY STATEMENT

The raw data supporting the conclusion of this article will be made available by the authors, without undue reservation.

## ETHICS STATEMENT

The studies involving human participants were reviewed and approved by the UTMB 11-251. Written informed consent for participation was not required for this study in accordance with the national legislation and the institutional requirements.

## AUTHOR CONTRIBUTIONS

EG performed experiments, analyzed data, and drafted the manuscript. AK conceived the study, performed experiments, analyzed data, and drafted the manuscript. MB and LR designed experiments and edited the manuscript. AH provided funding and edited the manuscript. RM conceived the study, provided funding, and edited the manuscript. All authors have read and agreed to the published version of the manuscript.

## FUNDING

This study was supported by funding from the National Institutes of Health/Eunice Kennedy Shriver National Institute of Child Health and Human Development (NIH/NICHD) grant #R01 HD100729 and National Center for Advancing Translational Sciences (NCATS) grant # 1UG3TR003283 to RM and AH.

## REFERENCES

Al-Enazy, S., Ali, S., Albekairi, N., El-Tawil, M., and Rytting, E. (2017). Placental Control of Drug Delivery. *Adv. Drug Deliv. Rev.* 116, 63–72. doi:10.1016/j.addr.2016.08.002

Anoshchenko, O., Prasad, B., Neradugomma, N. K., Wang, J., Mao, Q., and Unadkat, J. D. (2020). Gestational Age-dependent Abundance of Human Placental Transporters as Determined by Quantitative Targeted Proteomics. *Drug Metab. Dispos* 48 (9), 735–741. doi:10.1124/dmd.120.000067

Aouache, R., Biquard, L., Vaiman, D., and Miralles, F. (2018). Oxidative Stress in Preeclampsia and Placental Diseases. *Int. J. Mol. Sci.* 19 (5), 1496. doi:10.3390/ijms19051496

Arita, Y., Pressman, M., Getahun, D., Menon, R., and Peltier, M. R. (2018). Effect of Tetrabromobisphenol A on Expression of Biomarkers for Inflammation and Neurodevelopment by the Placenta. *Placenta* 68, 33–39. doi:10.1016/j.placenta.2018.06.306

Ayad, M. T., Taylor, B. D., and Menon, R. (2018). Regulation of P38 Mitogen-Activated Kinase-Mediated Fetal Membrane Senescence by Statins. *Am. J. Reprod. Immunol.* 80 (4), e12999. doi:10.1111/aji.12999

Basraon, S. K., Menon, R., Makhlouf, M., Longo, M., Hankins, G. D., Saade, G. R., et al. (2012). Can Statins Reduce the Inflammatory Response Associated with Preterm Birth in an Animal Model. *Am. J. Obstet. Gynecol.* 207 (3), 224–227. doi:10.1016/j.ajog.2012.06.020

Behnia, F., Sheller, S., and Menon, R. (2016). Mechanistic Differences Leading to Infectious and Sterile Inflammation. *Am. J. Reprod. Immunol.* 75 (5), 505–518. doi:10.1111/aji.12496

Climent, E., Benaiges, D., and Pedro-Botet, J. (2021). Hydrophilic or Lipophilic Statins. *Front. Cardiovasc. Med.* 8, 687585. doi:10.3389/fcvm.2021.687585

Collier, A. Y., and Molina, R. L. (2019). Maternal Mortality in the United States: Updates on Trends, Causes, and Solutions. *Neoreviews* 20 (10), e561–e74. doi:10.1542/neo.20-10-e561

Costantine, M. M. (2014). Physiologic and Pharmacokinetic Changes in Pregnancy. *Front. Pharmacol.* 5, 65. doi:10.3389/fphar.2014.00065

D'Alton, M. E., Friedman, A. M., Bernstein, P. S., Brown, H. L., Callaghan, W. M., Clark, S. L., et al. (2019). Putting the "M" Back in Maternal-Fetal Medicine: A 5-year Report Card on a Collaborative Effort to Address Maternal Morbidity and Mortality in the United States. *Am. J. Obstet. Gynecol.* 221 (4), 311–e1. doi:10.1016/j.ajog.2019.02.055

Dallmann, A., Liu, X. I., Burckart, G. J., and van den Anker, J. (2019). Drug Transporters Expressed in the Human Placenta and Models for Studying Maternal-Fetal Drug Transfer. *J. Clin. Pharmacol.* 59 (Suppl. 1), S70–S81. doi:10.1002/jcph.1491

Grube, M., Reuther, S., Meyer Zu Schwabedissen, H., Köck, K., Draber, K., Ritter, C. A., et al. (2007). Organic Anion Transporting Polypeptide 2B1 and Breast Cancer Resistance Protein Interact in the Transepithelial Transport of Steroid Sulfates in Human Placenta. *Drug Metab. Dispos* 35 (1), 30–35. doi:10.1124/dmd.106.011411

Güveli, B. T., Rosti, R. Ö., Güzeltaş, A., Tuna, E. B., Ataklı, D., Sencer, S., et al. (2017). Teratogenicity of Antiepileptic Drugs. *Clin. Psychopharmacol. Neurosci.* 15 (1), 19–27. doi:10.9758/cpn.2017.15.1.19

Halbert, C. L., Demers, G. W., and Galloway, D. A. (1991). The E7 Gene of Human Papillomavirus Type 16 Is Sufficient for Immortalization of Human Epithelial Cells. *J. Virol.* 65 (1), 473–478. doi:10.1128/JVI.65.1.473-478.1991

Han, L. W., Gao, C., and Mao, Q. (2018). An Update on Expression and Function of P-gp/ABCB1 and BCRP/ABCG2 in the Placenta and Fetus. *Expert Opin. Drug Metab. Toxicol.* 14 (8), 817–829. doi:10.1080/17425255.2018.1499726

International Transporter, C., Giacomini, K. M., Huang, S. M., Tweedie, D. J., Benet, L. Z., Brouwer, K. L., et al. (2010). Membrane Transporters in Drug Development. *Nat. Rev. Drug Discov.* 9 (3), 215–236. doi:10.1038/nrd3028

Istvan, E. (2003). Statin Inhibition of HMG-CoA Reductase: a 3-dimensional View. *Atheroscler. Suppl.* 4 (1), 3–8. doi:10.1016/s1567-5688(03)00003-5

Kammala, A. K., Sheller-Miller, S., Radnaa, E., Kechichian, T., Subramanian, H., and Menon, R. (2020). Sodium Hydrogen Exchanger Regulatory Factor-1 (NHERF1) Regulates Fetal Membrane Inflammation. *Int. J. Mol. Sci.* 21 (20), 7747. doi:10.3390/ijms21207747

Kim, S. W., Kang, H. J., Jhon, M., Kim, J. W., Lee, J. Y., Walker, A. J., et al. (2019). Statins and Inflammation: New Therapeutic Opportunities in Psychiatry. *Front. Psychiatry* 10, 103. doi:10.3389/fpsyt.2019.00103

Kojovic, D., V Workewych, N., and Piquette-Miller, M. (2020). Role of Elevated SFLT-1 on the Regulation of Placental Transporters in Women with Pre-eclampsia. *Clin. Transl Sci.* 13 (3), 580–588. doi:10.1111/cts.12742

Menon, R., Boldogh, I., Urrabaz-Garza, R., Polettini, J., Syed, T. A., Saade, G. R., et al. (2013). Senescence of Primary Amniotic Cells via Oxidative DNA Damage. *PLoS One* 8 (12), e83416. doi:10.1371/journal.pone.0083416

Menon, R. (2016). Human Fetal Membranes at Term: Dead Tissue or Signalers of Parturition. *Placenta* 44, 1–5. doi:10.1016/j.placenta.2016.05.013

Menon, R., Lappas, M., and Zakar, T. (2021). Editorial: The Role of the Fetal Membranes in Pregnancy and Birth. *Front. Physiol.* 12, 653084. doi:10.3389/fphys.2021.653084

Menon, R., Richardson, L. S., and Lappas, M. (2019). Fetal Membrane Architecture, Aging and Inflammation in Pregnancy and Parturition. *Placenta* 79, 40–45. doi:10.1016/j.placenta.2018.11.003

Menon, R., and Richardson, L. S. (2017). Preterm Prelabor Rupture of the Membranes: A Disease of the Fetal Membranes. *Semin. Perinatol* 41 (7), 409–419. doi:10.1053/j.semperi.2017.07.012

Ogura, J., Yamaguchi, H., and Mano, N. (2020). Stimulatory Effect on the Transport Mediated by Organic Anion Transporting Polypeptide 2B1. *Asian J. Pharm. Sci.* 15 (2), 181–191. doi:10.1016/j.ajps.2019.10.004

Park, J., Li, J., and Han, A. (2010). Micro-macro Hybrid Soft-Lithography Master (MMHSM) Fabrication for Lab-On-A-Chip Applications. *Biomed. Microdevices* 12 (2), 345–351. doi:10.1007/s10544-009-9390-9

Patik, I., Kovacsics, D., Német, O., Gera, M., Várady, G., Stieger, B., et al. (2015). Functional Expression of the 11 Human Organic Anion Transporting Polypeptides in Insect Cells Reveals that Sodium Fluorescein Is a General OATP Substrate. *Biochem. Pharmacol.* 98 (4), 649–658. doi:10.1016/j.bcp.2015.09.015

Patik, I., Székely, V., Német, O., Szepesi, Á., Kucsma, N., Várady, G., et al. (2018). Identification of Novel Cell-Impermeant Fluorescent Substrates for Testing the Function and Drug Interaction of Organic Anion-Transporting Polypeptides, OATP1B1/1B3 and 2B1. *Sci. Rep.* 8 (1), 2630. doi:10.1038/s41598-018-20815-1

Polettini, J., Richardson, L. S., and Menon, R. (2018). Oxidative Stress Induces Senescence and Sterile Inflammation in Murine Amniotic Cavity. *Placenta* 63, 26–31. doi:10.1016/j.placenta.2018.01.009

Radnaa, E., Richardson, L. S., Sheller-Miller, S., Baljinnyam, T., de Castro Silva, M., Kumar Kammala, A., et al. (2021). Extracellular Vesicle Mediated Feto-Maternal HMGB1 Signaling Induces Preterm Birth. *Lab. Chip* 21 (10), 1956–1973. doi:10.1039/d0lc01323d

Richardson, L., Jeong, S., Kim, S., Han, A., and Menon, R. (2019). Amnion Membrane Organ-On-Chip: an Innovative Approach to Study Cellular Interactions. *FASEB J.* 33 (8), 8945–8960. doi:10.1096/fj.201900020RR

Richardson, L., Kim, S., Menon, R., and Han, A. (2020). Organ-On-Chip Technology: The Future of Feto-Maternal Interface Research. *Front. Physiol.* 11, 715. doi:10.3389/fphys.2020.00715

Richardson, L., and Menon, R. (2018). Proliferative, Migratory, and Transition Properties Reveal Metastate of Human Amnion Cells. *Am. J. Pathol.* 188 (9), 2004–2015. doi:10.1016/j.ajpath.2018.05.019

Richardson, L. S., Kim, S., Han, A., and Menon, R. (2020). Modeling Ascending Infection with a Feto-Maternal Interface Organ-On-Chip. *Lab. Chip* 20 (23), 4486–4501. doi:10.1039/d0lc00875c

Richardson, L. S., Taylor, R. N., and Menon, R. (2020). Reversible EMT and MET Mediate Amnion Remodeling during Pregnancy and Labor. *Sci. Signal.* 13 (618), eaay1486. doi:10.1126/scisignal.aay1486

Roth, M., Obaidat, A., and Hagenbuch, B. (2012). OATPs, OATs and OCTs: the Organic Anion and Cation Transporters of the SLCO and SLC22A Gene Superfamilies. *Br. J. Pharmacol.* 165 (5), 1260–1287. doi:10.1111/j.1476-5381.2011.01724.x

Sachdeva, P., Patel, B. G., and Patel, B. K. (2009). Drug Use in Pregnancy; a point to ponder!. *Indian J. Pharm. Sci.* 71 (1), 1–7. doi:10.4103/0250-474X.51941

Sheller, S., Papaconstantinou, J., Urrabaz-Garza, R., Richardson, L., Saade, G., Salomon, C., et al. (2016). Amnion-Epithelial-Cell-Derived Exosomes Demonstrate Physiologic State of Cell under Oxidative Stress. *PLoS One* 11 (6), e0157614. doi:10.1371/journal.pone.0157614

Sheller-Miller, S., Radnaa, E., Arita, Y., Getahun, D., Jones, R. J., Peltier, M. R., et al. (2020). Environmental Pollutant Induced Cellular Injury Is Reflected in Exosomes from Placental Explants. *Placenta* 89, 42–49. doi:10.1016/j.placenta.2019.10.008

Staud, F., Cerveny, L., and Ceckova, M. (2012). Pharmacotherapy in Pregnancy; Effect of ABC and SLC Transporters on Drug Transport across the Placenta and Fetal Drug Exposure. *J. Drug Target.* 20 (9), 736–763. doi:10.3109/1061186X.2012.716847

**Conflict of Interest:** The authors declare that the research was conducted in the absence of any commercial or financial relationships that could be construed as a potential conflict of interest.

**Publisher's Note:** All claims expressed in this article are solely those of the authors and do not necessarily represent those of their affiliated organizations, or those of the publisher, the editors and the reviewers. Any product that may be evaluated in this article, or claim that may be made by its manufacturer, is not guaranteed or endorsed by the publisher.

frontiers in Pharmacology

PERSPECTIVE
published: 10 February 2022
doi: 10.3389/fphar.2022.847021

# Knowledge Gaps in the Pharmacokinetics of Therapeutic Proteins in Pediatric Patients

*Bernd Meibohm* *

*Department of Pharmaceutical Sciences, College of Pharmacy, The University of Tennessee Health Science Center, Memphis, TN, United States*

Therapeutic proteins such as monoclonal antibodies and their derivatives, fusions proteins, hormone analogs and enzymes for replacement therapy are an ever-growing mainstay in our pharmacopoeia. While a growing number of these medications are developed for and used in younger and younger pediatric patients, knowledge gaps in the basic understanding of the molecular and physiologic processes governing the disposition of these compounds in the human body and their modulation by age and childhood development are a hindrance to the effective and timely development and clinical use of these compounds, especially in very young pediatric patient populations. This is particularly the case for the widespread lack of information on the ontogeny and age-associated expression and function of receptor systems that are involved in the molecular processes driving the pharmacokinetics of these compounds. This article briefly highlights three receptor systems as examples, the neonatal Fc receptor, the asialoglycoprotein receptor, and the mannose receptor. It furthermore provides suggestions on how these gaps should be addressed and prioritized to provide the field of pediatric clinical pharmacology the urgently needed tools for a more effective development and clinical utilization of this important class of drugs with rapidly evolving importance as cornerstone in pediatric pharmacotherapy.

**Keywords: pediatrics, therapeutic proteins, pharmacokinetics, pediatric extrapolation, ontogeny, neonatal Fc receptor, mannose receptor, asialoglycoprotein receptor**

OPEN ACCESS

***Edited by:***
*Catherine M. T. Sherwin, Wright State University, United States*

***Reviewed by:***
*Honghui Zhou, Janssen Research and Development (United States), United States*

***Correspondence:**
*Bernd Meibohm*
*bmeibohm@uthsc.edu*

***Specialty section:***
*This article was submitted to Obstetric and Pediatric Pharmacology, a section of the journal Frontiers in Pharmacology*

***Received:*** *31 December 2021*
***Accepted:*** *24 January 2022*
***Published:*** *10 February 2022*

***Citation:***
*Meibohm B (2022) Knowledge Gaps in the Pharmacokinetics of Therapeutic Proteins in Pediatric Patients. Front. Pharmacol. 13:847021. doi: 10.3389/fphar.2022.847021*

## INTRODUCTION

Over the past 25 years, therapeutic proteins such as monoclonal antibodies (mAbs) and their derivatives, fusions proteins, hormone analogs and enzymes for replacement therapy have gained major roles in the armamentarium to treat numerous conditions and diseases (Crommelin et al., 2019). More recently, constructs that are the result of advanced protein engineering such as bispecifics and similar innovative molecules have been added to this group of molecules and are receiving major attention in drug development programs (Rathi and Meibohm, 2015; Brinkmann and Kontermann, 2017). While these protein-based medications are typically first developed and approved for adult patient populations, extensions of regulatory approval for use in pediatric populations is frequently pursued after initial market introduction (Zhang et al., 2015; Temrikar et al., 2020). These efforts have been further spurred and formalized by regulatory incentives and regulatory requirements that have been established over the past 3 decades in Europe and North America (Zisowsky et al., 2010; Zhang et al., 2015). In this context, there is an ever growing need to

establish dosage regimens and dosing recommendations that address the specific needs of different age groups of pediatric patients to ensure a safe and effective pharmacotherapy in these patient populations (Xu et al., 2013; Malik et al., 2021).

While pediatric dosing may be affected by differences in pharmacokinetic as well as pharmacodynamic processes but also differences in disease etiology and progression, particular interest has often been directed towards pharmacokinetic differences. This is based on the notion that full and partial extrapolation approaches of efficacy from adults to children frequently rely on exposure-matching where dosing regimens of the drug in question in different pediatric populations are selected in such a way that they achieve drug exposures in the pediatric patients "similar" to those having shown to be efficacious and safe in adults (Mulugeta et al., 2016). This approach of course relies on the assumption that the course of the disease and the response to the drug are sufficiently similar between adults and the considered pediatric population, a prerequisite that needs to be supported by adequate data.

## KEY MECHANISMS OF DRUG DISPOSITION PROCESSES FOR THERAPEUTIC PROTEINS

The pharmacokinetic processes of distribution and elimination of therapeutic proteins are governed by combinations of physicochemical, physiologic and receptor-mediated processes and have been reviewed in detail elsewhere (Tang et al., 2004; Mould and Meibohm, 2016; Ryman and Meibohm, 2017; Meibohm, 2019). In brief, distribution is largely determined by molecule size and charge. Large therapeutic proteins such as mAbs with a molecular weight of 150 kDa are largely confined to the vascular space with only limited distribution into the interstitial space of extravascular organs and tissues. Distribution for these molecules is largely driven by convective extravasation that is, determined by the number and size of pores between endothelial cells lining the blood and lymphatic vessels and pressure gradients between hydrostatic and colloid osmotic pressure in vascular, interstitial and lymphatic spaces and capillaries.

Elimination processes can broadly be distinguished into unspecific proteolytic degradation that can either be receptor-mediated or non-receptor-mediated (Meibohm, 2019). Non-receptor-mediated processes are usually initiated by pinocytosis, a fluid-phase endocytotic cellular uptake of the therapeutic protein molecule followed by intracellular lysosomal degradation to small peptides and amino acids. This degradation process is performed by phagocytic cells of the reticuloendothelial system as well as endothelial cells lining blood and lymph capillaries. Organs with major capillary beds such as muscle, skin and to lesser degree the intestine as well as organs with high number of phagocytic cells are thus major contributors to this nonspecific proteolytic degradation (Eigenmann et al., 2017). In case of receptor-mediated proteolysis, the intracellular uptake may be mediated by membrane-standing promiscuous receptor systems, for example, the LDL-receptor, or sugar-recognizing receptors such as the mannose receptor. Usually, receptor-mediated uptake processes are substantially faster and more efficient than pinocytosis, and proteins using these pathways are more rapidly eliminated. In the specific case where the membrane receptor that facilitates the intracellular uptake is the pharmacologic target, one refers to target-mediated elimination. Due to the usually high binding affinity of the therapeutic protein for its pharmacologic target, the target-mediated elimination process is usually substantially faster than the elimination processes relying on pinocytosis or "unspecific" receptor-mediated endocytosis (Tang et al., 2004). For mAbs and antibody-derivatives, interaction with immunoglobulin-specific receptors such as the neonatal Fc-receptor (FcRn) and Fcγ receptors may also affect the clearance of these therapeutic proteins. Interaction with FcRn in the acidified lysosome after intracellular uptake may prevent IgG molecules and thus mAbs from proteolytic degradation, thereby leading to an increased residence time and thus decreased clearance of these molecules in the systemic circulation (Ryman and Meibohm, 2017). Interaction between mAbs and Fcγ-receptors expressed on immune cells, while highly relevant for processing and removal of immune complexes, may constitute additional elimination pathways, although their overall contribution seems to be limited for the majority of mAbs (Thomas and Balthasar, 2019). For small therapeutic proteins below the glomerular filtration cutoff of approximately 60 kDa, proteolytic degradation in proximal tubular cells after glomerular filtration in the kidneys may also contribute to their clearance (Meibohm and Zhou, 2012).

## DIFFERENCES IN THERAPEUTIC PROTEIN DISPOSITION BETWEEN CHILDREN AND ADULTS AND RELATED KNOWLEDGE GAPS

Pediatric extrapolation efforts to establish dosing regimens for therapeutic proteins are hampered by a lack of a comprehensive understanding of the differences in drug distribution and elimination mechanisms between children and adults, particularly young pediatric patients such as full term and premature neonates and infants, i.e., in the range younger than 1 year of age. While many disposition processes based on physicochemical and physiologic processes are reasonably well understood, those related to receptor-mediated processes remain in many instances unclear or elusive. In more general terms, size-related differences between children and adults have relatively well been characterized, while knowledge on pediatric maturation-related differences remains spotty.

The distribution processes of most therapeutic proteins, as described in the previous section, are largely driven by conserved physicochemical processes together with physiologic differences between adults and different pediatric age groups and can thus usually be well predicted for pediatric populations. Therefore, allometric scaling approaches accounting for body size

differences between children and adults usually characterize the distribution of therapeutic proteins well. Only for very young pediatric patients such as newborns and infants, further differences may need to be considered. These include the well-known higher total and extracellular tissue water content, larger capillary beds and thus capillary surface area per tissue volume, and higher perfusion rates (Friis-Hansen, 1983; Malik and Edginton, 2018). All these processes together would be expected to result in faster extravasation of therapeutic proteins, lower concentration differences between the vascular and the extravascular space, and overall larger extravascular distribution volumes per volume unit of tissue (Temrikar et al., 2020). While an allometric exponent of 1 has widely been used to scale distribution volumes between children and adults based on body weight (Meibohm et al., 2005), more recent analyses considering a diverse set of protein-based therapeutics suggest that an exponent of 0.8 might be more appropriate (Malik et al., 2021).

Similar to distribution volumes, clearance values for non-receptor-mediated proteolytic degradation processes of therapeutic proteins in children can also relatively well be derived from adult values based on allometric scaling with allometric exponents of 0.75 or 0.85 accounting solely for body size-based differences between children and adults (Malik et al., 2021). Only for children younger than 1 year of age, maturation-related differences also have to be considered. For example, young infants, newborns and particularly low-birth weight infants have been reported to exhibit a 2–3 times higher lysosomal protein turnover normalized for body weight (Beaufrere, 1994), which would be expected to affect unspecific proteolytic degradation and result in an increased protein clearance (Temrikar et al., 2020).

For receptor-mediated elimination processes, however, the available knowledgebase on age- and maturation-related differences between children and adults is very scarce. For FcRn, for example, data have been limited to rodent studies. While messenger RNA (mRNA) expression of the α-chain of FcRn in rats suggested an age-associated increase (Tian et al., 2014), more recent results on age-associated expression at the protein level in mice suggest no relevant differences in expression from newborn through juvenile animals to adults in skin and spleen tissues (Limothai, 2015), which may be interpreted as more definitive due to the often limited mRNA-to-functional protein correlation for many endogenous proteins including FcRn (Li and Balthasar, 2018; Temrikar et al., 2020). There are currently no human data yet available on the ontogeny of FcRn, especially in very young pediatric patients. A more likely age-associated effect on FcRn recycling of mAbs and their derivatives are the well documented substantially lower reference values for endogenous IgG subclasses in infants compared to older children and adults (Plebani et al., 1989) that would be expected to lead to less endogenous competition for FcRn and thus a more efficient recycling process with potentially reduced clearance for protein molecules interacting with FcRn (Temrikar et al., 2020).

An example for a promiscuous membrane receptor facilitating the uptake of therapeutic proteins for subsequent lysosomal degradation is the asialoglycoprotein receptor (ASGPR) (Stockert, 1995). It is expressed on hepatocytes and facilitates the uptake of proteins that carry a glycan chain with a terminal galactose or galactose derivative. Examples are erythropoietin, reteplase, lanoteplase and clotting factor VIII (Lunghi et al., 2021). ASGPR has also been implicated in the glycoform selective clearance of therapeutic proteins with complex N- or O-linked glycosylation structures (Jones et al., 2007; Stefanich et al., 2008). More recently, ASGPR has also been utilized to facilitate hepatic targeting of N-acetylgalactosamine-conjugated RNA interference therapeutics (Li et al., 2021). Data on ASGPR expression and activity in children is very limited. While ASGPR has been detected in human fetal liver (Yoshida et al., 1999), age-related expression levels are limited to mice where activity increased postpartum and reached adult levels after 5 days (Collins et al., 1984). Additional knowledge has been inferred by physiologic pharmacokinetic modelling of pharmacokinetic data for known ASGPR substrates from different species (Poulin, 2011).

Similar to ASGPR, the mannose receptor is a highly effective endocytic receptor that is expressed on selected populations of macrophages and dendritic cells, and that recognizes glycoproteins with mannosylated glycan chains (Martinez-Pomares, 2012). High-mannose glycoforms of mAbs have increased clearance compared to mAbs with other glycans due to interaction with the mannose receptor (Falck et al., 2021). The age-associated expression of the mannose receptor is largely unknown. In mice, the mannose receptor was first detected on macrophages on day 10 in the embryonic stage and persisted postnatally thereafter (Takahashi et al., 1998). This may imply that mannose receptor activity has already reached adult levels at birth. The major role of FcRn, ASGPR, and the mannose receptor om the disposition of therapeutic proteins are summarized in **Table 1**.

For target-mediated drug disposition processes, data are even more scarce than for those elimination processes related to less specific receptor systems such as ASGPR or the mannose receptor. One might expect that each target has its own specific ontogeny with age- and maturation-associated differences in target receptor abundance, turnover and internalization kinetics (Temrikar et al., 2020). This becomes especially challenging when new therapeutic targets and/or novel indications are pursued. In addition, individual pediatric patients usually follow different temporal developmental trajectories that further complicate and individualize their dose requirements for a specific therapeutic protein (Barrett et al., 2012).

## DISCUSSION AND PERSPECTIVES

The selection of safe and efficacious dosing regimens for drug development and applied pharmacotherapy of therapeutic proteins in pediatric patients is severely hampered by substantial knowledge gaps on the ontogeny and age-associated expression and function of receptor systems that are involved in the molecular processes driving the pharmacokinetics of these compounds. This is particularly relevant for newborns

**TABLE 1 |** Examples of receptor systems affecting the pharmacokinetics of therapeutic proteins with unknown ontogeny.

| Receptor system | Tissues with high expression | Recognized molecular structure | Examples for affected therapeutic proteins |
|---|---|---|---|
| Asialoglycoprotein receptor (ASGPR) | Hepatocytes (sinusoidal surface) | Glycan chains with terminal galactose or N-acetylgalactosamine residues | Erythropoietin; FSH; clotting factors VII, VIII, IX; reteplase, lanoteplase |
| Mannose receptor | Macrophages, immature dendritic cells, and liver sinusoidal endothelial cells | Glycan chains with high mannose content (M5-M9) | High mannose forms for IgG monoclonal antibodies and their derivatives |
| Neonatal Fc receptor (FcRn) | Vascular endothelial cells and phagocytic cells as well as other cell types, particularly in liver, spleen, intestine, lungs and lymph nodes | FcRn pH-dependent binding site on the constant domain of IgG molecule and albumin | Monoclonal antibodies; antibody-derivatives and fusion proteins with intact FcRn-binding site on the Fc domain; albumin fusion proteins |

and infants where differences in therapeutic protein pharmacokinetics cannot be fully explained by size differences between children and adults and where additional maturation processes need to be considered. This article briefly highlighted three receptor systems as examples, FcRn, ASGPR and the mannose receptor, but numerous others may be involved in the disposition process of specific therapeutic proteins as well. Priorities for filling these knowledge gaps should be initially directed towards those receptor systems that are more broadly relevant to the largest number of therapeutic proteins, for example, FcRn for all mAbs and mAb derivatives with intact FcRn binding site.

Population pharmacokinetic modeling (PopPK) and physiological pharmacokinetic modeling (PBPK) have been widely used in support of pediatric extrapolation exercises based on exposure-matching approaches for traditional small molecule drugs (Conklin et al., 2019). While PopPK is a data-driven, deductive modeling approach, PBPK can be viewed as an inductive approach based on the integrated prior knowledge of drug- and system-specific parameters and structures (Barrett et al., 2012). A recent analysis of FDA approval data for the 20 monoclonal antibodies and Fc-fusion proteins approved at the time in both adult and pediatric indications revealed that while 19 of the 20 projects included PopPK based modeling and simulation in support of the selected pediatric dosing regimens, only one of them included a PBPK approach (Liu et al., 2019). This lack of use of PBPK for therapeutic proteins in pediatric indications may partially be related to the highlighted knowledge gaps in understanding pediatric disposition of these molecules as PBPK rather than PopPK is largely dependent on an intrinsic understanding of the drug disposition mechanisms and pathways that underlie a therapeutic protein's pharmacokinetic behavior.

There have recently been elegant attempts to impute the lack of age-associated function of receptor systems such as FcRn through PBPK modeling frameworks using known PK data of endogenous and therapeutic proteins (Hardiansyah and Ng, 2018; Pan et al., 2020). While these approaches are pragmatic in the current situation, they still cannot overcome the residual uncertainty associated with the arbitrary assignment of age-associated disposition behavior to one unmeasured model component. This underlines the need for basic molecular pharmacology investigations in the age groups of interest to fill our existing knowledge gaps with high quality data. The gained knowledge would likely not only benefit one specific development project or compound but would likely be more broadly applicable. These opportunities to add to the collective pediatric drug disposition knowledgebase will be crucial to advance the reliability and reduce the uncertainty of pediatric extrapolation efforts (Laer et al., 2009; Temrikar et al., 2020). Only then will the currently existing uncertainties in extrapolation of therapeutic proteins to pediatric patients be overcome and a more widespread application of prospective modeling frameworks in this area be possible.

## DATA AVAILABILITY STATEMENT

The original contributions presented in the study are included in the article/supplementary material, further inquiries can be directed to the corresponding author.

## AUTHOR CONTRIBUTIONS

The author confirms being the sole contributor of this work and has approved it for publication.

## REFERENCES


Barrett, J. S., Della Casa Alberighi, O., Läer, S., and Meibohm, B. (2012). Physiologically Based Pharmacokinetic (PBPK) Modeling in Children. *Clin. Pharmacol. Ther.* 92, 40–49. doi:10.1038/clpt.2012.64

Beaufrère, B. (1994). Protein Turnover in Low-Birth-Weight (LBW) Infants. *Acta Paediatr. Suppl.* 405, 86–92. doi:10.1111/j.1651-2227.1994.tb13404.x

Brinkmann, U., and Kontermann, R. E. (2017). The Making of Bispecific Antibodies. *MAbs* 9, 182–212. doi:10.1080/19420862.2016.1268307

Collins, J. C., Stockert, R. J., and Morell, A. G. (1984). Asialoglycoprotein Receptor Expression in Murine Pregnancy and Development. *Hepatology* 4, 80–83. doi:10.1002/hep.1840040114

Conklin, L. S., Hoffman, E. P., and Van Den Anker, J. (2019). Developmental Pharmacodynamics and Modeling in Pediatric Drug Development. *J. Clin. Pharmacol.* 59 (Suppl. 1), S87–S94. doi:10.1002/jcph.1482

Crommelin, D. J. A., Sindelar, R. D., and Meibohm, B. (2019). *Pharmaceutical Biotechnology: Fundamentals and Applications*. New York: Springer.

Eigenmann, M. J., Fronton, L., Grimm, H. P., Otteneder, M. B., and Krippendorff, B. F. (2017). Quantification of IgG Monoclonal Antibody Clearance in Tissues. *MAbs* 9, 1007–1015. doi:10.1080/19420862.2017.1337619

Falck, D., Thomann, M., Lechmann, M., Koeleman, C. A. M., Malik, S., Jany, C., et al. (2021). Glycoform-resolved Pharmacokinetic Studies in a Rat Model Employing Glycoengineered Variants of a Therapeutic Monoclonal Antibody. *MAbs* 13, 1865596. doi:10.1080/19420862.2020.1865596

Friis-Hansen, B. (1983). Water Distribution in the Foetus and Newborn Infant. *Acta Paediatr. Scand. Suppl.* 305, 7–11. doi:10.1111/j.1651-2227.1983.tb09852.x

Hardiansyah, D., and Ng, C. M. (2018). Effects of the FcRn Developmental Pharmacology on the Pharmacokinetics of Therapeutic Monoclonal IgG Antibody in Pediatric Subjects Using Minimal Physiologically-Based Pharmacokinetic Modelling. *MAbs* 10, 1144–1156. doi:10.1080/19420862.2018.1494479

Jones, A. J., Papac, D. I., Chin, E. H., Keck, R., Baughman, S. A., Lin, Y. S., et al. (2007). Selective Clearance of Glycoforms of a Complex Glycoprotein Pharmaceutical Caused by Terminal N-Acetylglucosamine Is Similar in Humans and Cynomolgus Monkeys. *Glycobiology* 17, 529–540. doi:10.1093/glycob/cwm017

Läer, S., Barrett, J. S., and Meibohm, B. (2009). The In Silico Child: Using Simulation to Guide Pediatric Drug Development and Manage Pediatric Pharmacotherapy. *J. Clin. Pharmacol.* 49, 889–904. doi:10.1177/0091270009337513

Li, J., Liu, J., Zhang, X., Clausen, V., Tran, C., Arciprete, M., et al. (2021). Nonclinical Pharmacokinetics and Absorption, Distribution, Metabolism, and Excretion of Givosiran, the First Approved N-Acetylgalactosamine-Conjugated RNA Interference Therapeutic. *Drug Metab. Dispos* 49, 572–580. doi:10.1124/dmd.121.000381

Li, T., and Balthasar, J. P. (2018). FcRn Expression in Wildtype Mice, Transgenic Mice, and in Human Tissues. *Biomolecules* 8, 115. doi:10.3390/biom8040115

Limothai, W. (2015). "Challenges in the Pharmacokinetics of Therapeutic Proteins," in *Theses and Dissertations (ETD)*. Paper 396. Memphis: University of Tennessee Health Science Center. doi:10.21007/etd.cghs.2015.0184

Liu, X. I., Dallmann, A., Wang, Y. M., Green, D. J., Burnham, J. M., Chiang, B., et al. (2019). Monoclonal Antibodies and Fc-Fusion Proteins for Pediatric Use: Dosing, Immunogenicity, and Modeling and Simulation in Data Submitted to the US Food and Drug Administration. *J. Clin. Pharmacol.* 59, 1130–1143. doi:10.1002/jcph.1406

Lunghi, B., Morfini, M., Martinelli, N., Balestra, D., Linari, S., Frusconi, S., et al. (2021). The Asialoglycoprotein Receptor Minor Subunit Gene Contributes to Pharmacokinetics of Factor VIII Concentrates in Hemophilia A. *Thromb. Haemost*. doi:10.1055/a-1591-7869

Malik, P., and Edginton, A. (2018). Pediatric Physiology in Relation to the Pharmacokinetics of Monoclonal Antibodies. *Expert Opin. Drug Metab. Toxicol.* 14, 585–599. doi:10.1080/17425255.2018.1482278

Malik, P. R. V., Temrikar, Z. H., Chelle, P., Edginton, A. N., and Meibohm, B. (2021). Pediatric Dose Selection for Therapeutic Proteins. *J. Clin. Pharmacol.* 61 (Suppl. 1), S193–S206. doi:10.1002/jcph.1829

Martinez-Pomares, L. (2012). The Mannose Receptor. *J. Leukoc. Biol.* 92, 1177–1186. doi:10.1189/jlb.0512231

Meibohm, B., Läer, S., Panetta, J. C., and Barrett, J. S. (2005). Population Pharmacokinetic Studies in Pediatrics: Issues in Design and Analysis. *AAPS J.* 7, E475–E487. doi:10.1208/aapsj070248

Meibohm, B., and Zhou, H. (2012). Characterizing the Impact of Renal Impairment on the Clinical Pharmacology of Biologics. *J. Clin. Pharmacol.* 52, 54S–62S. doi:10.1177/0091270011413894

Meibohm, B. (2019). "Pharmacokinetics and Pharmacodynamics of Therapeutic Peptides and Proteins," in *Pharmaceutical Biotechnology: Fundamentals and Applications*. Editors D.J.A. Crommelin, R.D. Sindelar, and B. Meibohm (New York: Spinger), 105–137. doi:10.1007/978-3-030-00710-2_6

Mould, D. R., and Meibohm, B. (2016). Drug Development of Therapeutic Monoclonal Antibodies. *BioDrugs* 30, 275–293. doi:10.1007/s40259-016-0181-6

Mulugeta, Y., Barrett, J. S., Nelson, R., Eshete, A. T., Mushtaq, A., Yao, L., et al. (2016). Exposure Matching for Extrapolation of Efficacy in Pediatric Drug Development. *J. Clin. Pharmacol.* 56, 1326–1334. doi:10.1002/jcph.744

Pan, X., Stader, F., Abduljalil, K., Gill, K. L., Johnson, T. N., Gardner, I., et al. (2020). Development and Application of a Physiologically-Based Pharmacokinetic Model to Predict the Pharmacokinetics of Therapeutic Proteins from Full-Term Neonates to Adolescents. *AAPS J.* 22, 76. doi:10.1208/s12248-020-00460-1

Plebani, A., Ugazio, A. G., Avanzini, M. A., Massimi, P., Zonta, L., Monafo, V., et al. (1989). Serum IgG Subclass Concentrations in Healthy Subjects at Different Age: Age normal Percentile Charts. *Eur. J. Pediatr.* 149, 164–167. doi:10.1007/BF01958271

Poulin, P. (2011). A Single-Species Approach Considering Additional Physiological Information for Prediction of Hepatic Clearance of Glycoprotein Derivate Therapeutics. *Clin. Pharmacokinet.* 50, 665–674. doi:10.2165/11592610-000000000-00000

Rathi, C., and Meibohm, B. (2015). Clinical Pharmacology of Bispecific Antibody Constructs. *J. Clin. Pharmacol.* 55 (Suppl. 3), S21–S28. doi:10.1002/jcph.445

Ryman, J. T., and Meibohm, B. (2017). Pharmacokinetics of Monoclonal Antibodies. *CPT Pharmacometrics Syst. Pharmacol.* 6, 576–588. doi:10.1002/psp4.12224

Stefanich, E. G., Ren, S., Danilenko, D. M., Lim, A., Song, A., Iyer, S., et al. (2008). Evidence for an Asialoglycoprotein Receptor on Nonparenchymal Cells for O-Linked Glycoproteins. *J. Pharmacol. Exp. Ther.* 327, 308–315. doi:10.1124/jpet.108.142232

Stockert, R. J. (1995). The Asialoglycoprotein Receptor: Relationships between Structure, Function, and Expression. *Physiol. Rev.* 75, 591–609. doi:10.1152/physrev.1995.75.3.591

Takahashi, K., Donovan, M. J., Rogers, R. A., and Ezekowitz, R. A. (1998). Distribution of Murine Mannose Receptor Expression from Early Embryogenesis through to Adulthood. *Cell Tissue Res* 292, 311–323. doi:10.1007/s004410051062

Tang, L., Persky, A. M., Hochhaus, G., and Meibohm, B. (2004). Pharmacokinetic Aspects of Biotechnology Products. *J. Pharm. Sci.* 93, 2184–2204. doi:10.1002/jps.20125

Temrikar, Z. H., Suryawanshi, S., and Meibohm, B. (2020). Pharmacokinetics and Clinical Pharmacology of Monoclonal Antibodies in Pediatric Patients. *Paediatr. Drugs* 22, 199–216. doi:10.1007/s40272-020-00382-7

Thomas, V. A., and Balthasar, J. P. (2019). Understanding Inter-individual Variability in Monoclonal Antibody Disposition. *Antibodies (Basel)* 8, 56. doi:10.3390/antib8040056

Tian, Z., Sutton, B. J., and Zhang, X. (2014). Distribution of Rat Neonatal Fc Receptor in the Principal Organs of Neonatal and Pubertal Rats. *J. Recept Signal. Transduct Res.* 34, 137–142. doi:10.3109/10799893.2013.865745

Xu, Z., Davis, H. M., and Zhou, H. (2013). Rational Development and Utilization of Antibody-Based Therapeutic Proteins in Pediatrics. *Pharmacol. Ther.* 137, 225–247. doi:10.1016/j.pharmthera.2012.10.005

Yoshida, S., Furuhashi, M., and Suganuma, N. (1999). Expression of Asialoglycoprotein Receptor in Human Fetal Liver. *Endocr. J.* 46, 67–73. doi:10.1507/endocrj.46.67

Zhang, Y., Wei, X., Bajaj, G., Barrett, J. S., Meibohm, B., Joshi, A., et al. (2015). Challenges and Considerations for Development of Therapeutic Proteins in Pediatric Patients. *J. Clin. Pharmacol.* 55 (Suppl. 3), S103–S115. doi:10.1002/jcph.382

Zisowsky, J., Krause, A., and Dingemanse, J. (2010). Drug Development for Pediatric Populations: Regulatory Aspects. *Pharmaceutics* 2, 364–388. doi:10.3390/pharmaceutics2040364

**Conflict of Interest:** The author declares that the research was conducted in the absence of any commercial or financial relationships that could be construed as a potential conflict of interest.

frontiers in Pharmacology

REVIEW
published: 15 February 2022
doi: 10.3389/fphar.2022.828010

# The Blind Spot of Pharmacology: A Scoping Review of Drug Metabolism in Prematurely Born Children

*Mette Louise Mørk*[1], *Jón Trærup Andersen*[1], *Ulrik Lausten-Thomsen*[2] *and Christina Gade*[1]*

[1]Department of Clinical Pharmacology, Copenhagen University Hospital Bispebjerg and Frederiksberg, Copenhagen, Denmark, [2]Department of Neonatology, Copenhagen University Hospital Rigshospitalet, Copenhagen, Denmark

The limit for possible survival after extremely preterm birth has steadily improved and consequently, more premature neonates with increasingly lower gestational age at birth now require care. This specialized care often include intensive pharmacological treatment, yet there is currently insufficient knowledge of gestational age dependent differences in drug metabolism. This potentially puts the preterm neonates at risk of receiving sub-optimal drug doses with a subsequent increased risk of adverse or insufficient drug effects, and often pediatricians are forced to prescribe medication as off-label or even off-science. In this review, we present some of the particularities of drug disposition and metabolism in preterm neonates. We highlight the challenges in pharmacometrics studies on hepatic drug metabolism in preterm and particularly extremely (less than 28 weeks of gestation) preterm neonates by conducting a scoping review of published literature. We find that >40% of included studies failed to report a clear distinction between term and preterm children in the presentation of results making direct interpretation for preterm neonates difficult. We present summarized findings of pharmacokinetic studies done on the major CYP sub-systems, but formal meta analyses were not possible due the overall heterogeneous approaches to measuring the phase I and II pathways metabolism in preterm neonates, often with use of opportunistic sampling. We find this to be a testament to the practical and ethical challenges in measuring pharmacokinetic activity in preterm neonates. The future calls for optimized designs in pharmacometrics studies, including PK/PD modeling-methods and other sample reducing techniques. Future studies should also preferably be a collaboration between neonatologists and clinical pharmacologists.

**Keywords: infant, premature, pharmacokinetics, cytochrome P-450 enzyme system, pharmaceutical preparations**

OPEN ACCESS

***Edited by:***
*Catherine M. T. Sherwin, Wright State University, United States*

***Reviewed by:***
*Kathleen Job, The University of Utah, United States*
*Karel Allegaert, University Hospitals Leuven, Belgium*

***Correspondence:**
*Christina Gade*
*Christina.gade@regionh.dk*

***Specialty section:***
*This article was submitted to Obstetric and Pediatric Pharmacology, a section of the journal Frontiers in Pharmacology*

***Received:*** *02 December 2021*
***Accepted:*** *25 January 2022*
***Published:*** *15 February 2022*

***Citation:***
*Mørk ML, Andersen JT, Lausten-Thomsen U and Gade C (2022) The Blind Spot of Pharmacology: A Scoping Review of Drug Metabolism in Prematurely Born Children. Front. Pharmacol. 13:828010. doi: 10.3389/fphar.2022.828010*

## 1 INTRODUCTION

Prematurely born children represent a very fragile subset of neonates, as they often present a complex and challenging pathophysiological condition associated with increased risk of long-term morbidity and mortality. Treatment includes various pharmaceutical agents, yet there is currently insufficient knowledge of gestational age dependent differences in drug metabolism. This potentially puts the preterm at risk of receiving suboptimal drug doses with a subsequent increased risk of adverse or insufficient drug effects (Kearns et al., 2003; O'Hara et al., 2015; van den Anker and Allegaert, 2021).

Although the need for clinical research to identify optimal drug dosing in term and preterm neonates has long been acknowledged as indispensable (Tayman et al., 2011; O'Hara et al., 2015; van

den Anker and Allegaert, 2021), the progress has been slow. Recently, data on premature neonates have begun to emerge, and particularly pharmacometric modeling-approaches have added available information on this pediatric subgroup (Smits et al., 2019). However, data is still scarce, and pediatricians are often forced to prescribe medication as off-label or even off-science (Barr et al., 2002; Al-Turkait et al., 2020; Schrier et al., 2020).

## 2 PREMATURITY

The average human gestation is 40 weeks, and prematurity is defined as being born before 37 weeks of gestation (Engle et al., 2004). The global prematurity rates are approximately 10% but vary from 4 to 5% in some European countries to 15–18% in some parts of Africa and Asia (Blencowe et al., 2012; Chawanpaiboon et al., 2019). It is a complex and challenging pathophysiological condition associated with increased risk of long-term morbidity and mortality (Saigal and Doyle, 2008) and it is the leading cause of death in children under 5 years of age (Harrison and Goldenberg, 2016; Chawanpaiboon et al., 2019). Prematurity can be considered a continuum of organ immaturity with huge differences in presentation, morbidity, and need for treatment at either end of the spectrum and is often sub-categorized in moderate to late preterm (32–36 weeks of gestation), very preterm (28–32 weeks of gestation), and extremely preterm (before 28 weeks of gestation) (Engle, 2004). Neonates can equally be classified per birth weight as low birth, (LBW, <2500 g), very low birth weight (VLBW, <1500 g) and extremely low birth weight (ELBW, <1000 g) (World Health Organization, 2004, 10), but although LBW often is caused by prematurity, it cannot be used directly as a marker of the degree of prematurity as LBW can be caused by intrauterine growth restriction (IUGR).

Although there are wide variations in prematurity survival rates across regions and countries (Helenius et al., 2017), overall survival rates for premature and particularly extremely premature neonates have hugely improved since the 1980s (Glass et al., 2015). Importantly, the limit for early human viability, defined as the earliest gestational age an infant can potentially survive being born at, has steadily dropped and some babies delivered at 24, 23, and even 22 weeks of gestation are now able to survive. A recent study from Sweden reports a 20% survival rate in children born at 22 weeks (Norman et al., 2019) and a Japanese study has found a survival rate of 36% in children born at 22 weeks (Ishii et al., 2013). Case reports of children surviving being born at 21 weeks (Sung et al., 2018; Tiniest Babies Registry) or with birth weight below 250 g have emerged, but survival remains low (Brumbaugh et al., 2019). Whereas the reasons for this progress in prematurity survival certainly are multifactorial, the improvement is believed to be linked to overall improvement in neonatal intensive care, such as development of increasingly better artificial airways and breathing circuits and rational application of mechanical ventilation and airway distending pressure (Glass et al., 2015; Pierrat et al., 2021).

Another major driving factor for the improvement in premature survival rates has been pharmacological advancements, both prenatal, immediately post-natal and post-natal. Antenatally, the administering of a course of corticosteroids to women prior to anticipated preterm birth has been demonstrated to have a marked positive effect of subsequent preterm mortality and morbidity ever since the first randomized controlled trial of betamethasone for the prevention of respiratory distress syndrome in preterm neonates in 1972 (Liggins and Howie, 1972). Subsequently, many clinical trials have demonstrated the effect of antenatal corticosteroids before preterm birth, as summarized in a recent systematic Cochrane review demonstrating its effect on reducing neonatal mortality (RR 0.78, 95% CI 0.70–0.87), respiratory distress syndrome (RR 0.71, 95% CI 0.65–0.78), and cerebral intraventricular hemorrhage (RR 0.58, 95% CI 0.45–0.75) (McGoldrick et al., 2020). Antenatal corticosteroid is a pharmacological cornerstone of prophylactic treatment in preterm birth.

A huge leap in pharmacological treatment of preterm children, and possibly one of the single greatest breakthroughs in treatment of premature children, was the development of exogenous surfactant administration techniques in the 1980s and early 1990s. Since the first successful attempts in 1980 (Fujiwara et al., 1980) using the first artificial preparations, this therapy has become the definitive standard treatment for neonatal respiratory distress syndrome and is believed to be one of the most effective medicines in the health system (Hentschel et al., 2020). As respiratory distress syndrome is the single most important cause of illness and death in preterm children (Stevens et al., 2007; Sardesai et al., 2017), surfactant administration has led to a marked increase in survival and helped lower the limit for early human viability (Rojas-Reyes et al., 2012; Sweet et al., 2019; Hentschel et al., 2020).

Pharmacological treatment remains a cornerstone in postnatal care in preterm children, as demonstrated by a recent review of drug utilization studies in neonatal units that found a high mean number of drugs per infant, with eight studies reporting a very high burden (>30 drugs per infant). Drug use patterns were found to be generally uniform with antibiotics being the most frequently prescribed drug in the neonatal department (Al-Turkait et al., 2020). Naturally, trends in general drug prescription have changed over the years but off-label drug use in premature children is still very common: of the top 50 medications of extremely low birth weight premature infants, only 40% were FDA-labeled for use in infants (Stark et al., 2021). This represents a relative lack of proper pharmacokinetic (PK) studies in premature children and remedying this will likely be a long haul due to the difficulties of conducting clinical PK studies in preterm children.

## 3 DRUG DISPOSITION IN PREMATURE NEONATES

Accurate dosing is essential for a safe and effective pharmacological treatment of premature neonates. An in-depth knowledge of the anatomical and physiological particularities of preterm neonates is therefore crucial for the understanding of the drug pharmacokinetics in this population. Herein, the differences in ontogeny between the extremely, the

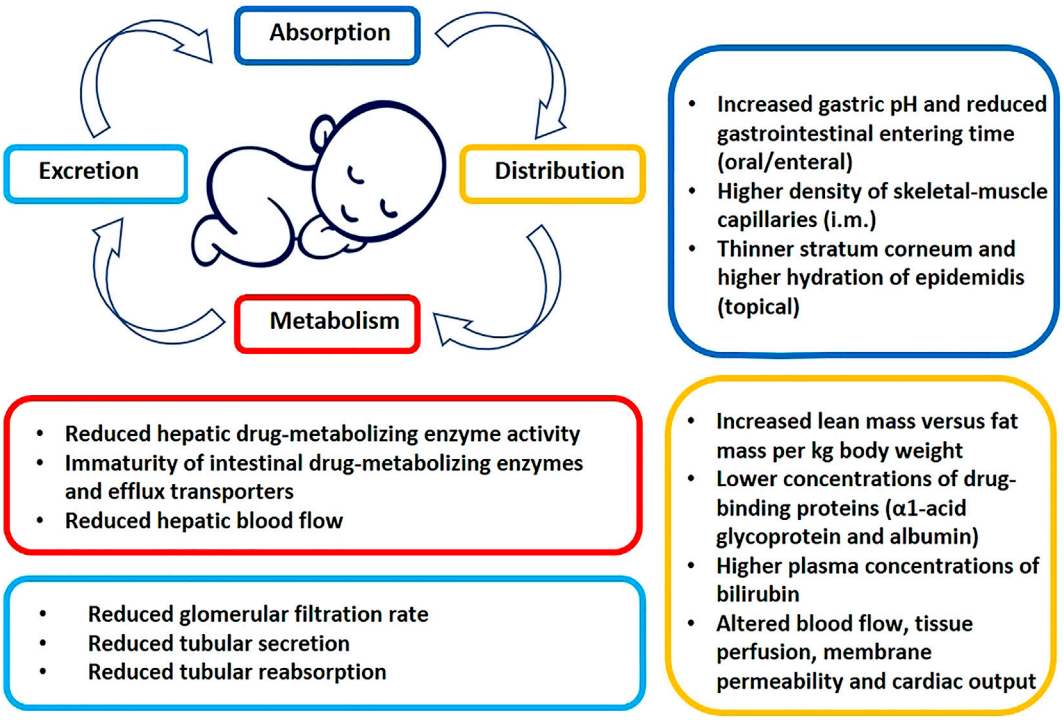


**FIGURE 1 |** Prematurity associated pato-physiological conditions potentially altering the pharmacokinetics of drugs (see text for details).

very and the late preterm neonate should be taken into consideration (Barker et al., 2018; van den Anker et al., 2018).

Also, most aspects of drug disposition are subject to change in case of co-morbidities, which unfortunately relatively often occurs in premature neonates. Sepsis, surgery, and (for moderate and late preterm neonates where such treatment is possible) advanced treatment such as whole body hypothermia (Smith et al., 2019), extracorporeal membrane oxygenation (ECMO), or hemo-dialysis may all significantly alter drug distribution and metabolism.

A summary of the most important prematurity associated characteristics of pharmacokinetics in preterm neonates is presented in **Figure 1** and below.

## 3.1 Absorption

In preterm neonates, the immaturity of absorptive surfaces may influence drug exposure (O'Hara et al., 2015). At present, there is no clear consensus describing the ontogeny of gastric pH and its impact on drug absorption, and gastric emptying time has not been found age dependent (Bonner et al., 2015). However, gastrointestinal abnormalities and dysfunctions in preterm neonates can affect transit time and enteral absorption (Johnson, 2011; van den Anker and Allegaert, 2021). Developmental differences in the activity of intestinal drug-metabolizing enzymes and efflux transporters will most likely affect the exposure of several drugs in preterm neonates, but this area is still not well understood (Kearns et al., 2003; van den Anker and Allegaert, 2021).

The exposure of drugs after rectal administration is generally increased in preterm neonates, e.g., paracetamol, most likely due to developmental immaturity of the hepatic metabolism rather than increased mucosal translocation (Kafetzis et al., 1979; Ruggiero et al., 2014). Due to the relatively higher density of skeletal-muscle capillaries in neonates, water-soluble drugs show an increased intramuscular absorption, e.g., absorption of amikacin (Kafetzis et al., 1979). Whether this is also the case for preterm neonates is unknown, but the example of intramuscular administration of vitamin E acetate in a lipophilic preparation, showed that the ester was never systematically detectable in premature neonates as opposed to E-vitamin delivered in an aqueous preparation (Italian Collaborative Group on Preterm Delivery, 1991).

The presence of a thinner stratum corneum in preterm neonates, a higher body surface area-to-weight ratio as well as higher cutaneous perfusion and hydration of the epidermis places preterm neonates at risk of adverse effects from topical exposures due to an increased absorption e.g. corticosteroids (Borzyskowski et al., 1976; Munro, 1976) and chlorhexidine (Cowen et al., 1979). Application of antiseptic solutions containing alcohols has led to severe burns in premature infants (Brayer et al., 2004). Pulmonary, sublingual, and buccal absorption are not well studied in preterm or term neonates (O'Hara et al., 2015; van den Anker and Allegaert, 2021).

## 3.2 Distribution

In the extremely preterm neonate, total body fat content can be as low as 1% of the total body weight and total body water is decreasing from 85% in preterm neonates to 75% in term

neonates (Tetelbaum et al., 2005; Ford and Calvert, 2008) (Sharma et al., 2008). Due to the lower percentage of fat and muscle mass in preterm neonates, drugs that are normally rapidly distributed into the muscle tissue, like fentanyl, will remain in the plasma compartment for a longer time (O'Hara et al., 2015). Significant changes in intra/extracellular body fluid distribution per concurrent weight occurs postnatally during the first week of life. Thus, both gestational age (GA) at birth and postnatal age (PNA) influences total body water content and distribution, and this should ideally be taken into consideration when optimizing individual drug doses (van den Anker and Allegaert, 2021).

At the time of birth, neonates have lower concentrations of the drug-binding proteins α1-acid glycoprotein and albumin when compared to older children (Ehrnebo et al., 1971; Windorfer et al., 1974; Ku and Smith, 2015). The amount of free drug available for distribution will therefore be increased for highly protein bound drugs, e.g., theophylline (Aranda et al., 1976). Effects and toxicity may therefore be obtained at lower total plasma concentrations. Also elevated plasma levels of bilirubin can increase the concentration of unbound drugs by displacing highly bound drugs from protein-binding sites, e.g., ampicillin, benzodiazepine and phenytoin (Fredholm et al., 1975; Tayman et al., 2011; Zwart et al., 2021).

Higher CNS drug concentrations may occur in preterm neonates due to reduced outward drug transport, however, this area still needs to be elaborated (Painter et al., 1981; Liu et al., 2008; Ku and Smith, 2015). Changes in the volume of distribution are also related to changes in blood flow, tissue perfusion, membrane permeability and cardiac output (Kearns et al., 2003; O'Hara et al., 2015; van den Anker and Allegaert, 2021). Furthermore, it should be noticed that pathological circulatory conditions, e.g., a hemodynamically significant persistent ductus arteriosus can also alter the volume of distribution of drugs in preterm neonates (Ku and Smith, 2015; O'Hara et al., 2015).

## 3.3 Metabolism

The major site of drug metabolism is the liver and the drug metabolizing enzymes are broadly divided into phase I and phase II enzymes. The phase I enzymes are responsible for primary oxidation, reduction and hydrolysis processes. The most important group of enzymes involved in phase I metabolism are cytochrome (CYP) P450 enzymes with a major contribution of cytochrome P450 3A4 (Hines and McCarver, 2002). However, while CYP3A4 constitutes 30–40% of the total liver CYP content in adult, CYP3A7 is found to be the major form in human embryonic, fetal and newborn liver (Gow et al., 2001; Hines and McCarver, 2002). In the period from late fetal to early neonatal life, there appears to be a peak in CYP3A7 activity, then a transition in expression and catalytic activity from predominant CYP3A7 to CYP3A4 (de Wildt et al., 1999; Gow et al., 2001).

Phase II enzymes are responsible for conjugate drug molecules to allow excretion. Phase II drug metabolizing enzymes are mostly transferases and include: UDP-glucuronosyltransferases (UGTs), sulfotransferases (SULTs), N-acetyltransferases (NATs), glutathione S-transferases (GSTs) and various methyltransferases (Xu et al., 2005; O'Hara et al., 2015).

A lack of activity of metabolizing enzymes can be responsible for extreme toxicity syndromes (O'Hara et al., 2015). Severe toxicity syndromes in premature infants have been described due to reduced capacity of their metabolic systems, e.g., grey baby syndrome, which is caused by diminished ability to conjugate chloramphenicol and to excrete the active form in the urine (Craft et al., 1974). In addition, gasping syndrome with benzyl alcohol, where benzoic acid cannot be conjugated but is accumulated, causing metabolic acidosis in premature neonates (Gershanik et al., 1982).

Similarly to many other physiological and metabolic processes in newborns, pharmacokinetics also exhibit a relative immaturity that changes postnatally, and for the CYP450 system, it is believed that some CYP450 enzymes are active *in utero* while others do not active until after birth (Gow et al., 2001; O'Hara et al., 2015). When corrected for weight the content of CYP enzymes in fetal livers is 30–60% of adult values and full CYP activity is usually achieved by 2 years of age. Yet, the many physiological and metabolic processes depend not only on postnatal age, but also on gestational age, i.e., degree of maturation, at the time of birth (Gow et al., 2001; Kearns et al., 2003; O'Hara et al., 2015).

Knowledge of maturation of drug metabolizing enzymes is therefore an important factor in determining drug selection in neonates. This is further complicated as various elements of the drug metabolism pathways do not mature at the same rate postnatally (Hines and McCarver, 2002). For example, use of codeine is not appropriate during the first month of life as conversion to morphine *via* CYP2D6 is low resulting in very limited effectiveness (O'Hara et al., 2015). Midazolam is metabolized by CYP3A4 at a slower rate causing increased duration of sedation and early exposure to opioid infusion in the first 3 days was associated with higher risk of adverse outcomes in extremely preterm infants (de Wildt et al., 2010; Shah et al., 2011; Ng et al., 2012; O'Hara et al., 2015). Contrarily, CYP1A2 is induced rapidly after birth with post-natal age rather than post-menstrual age correlating with changes in half-life and clearance (Hines and McCarver, 2002; Schmidt et al., 2006). This rapid induction fits clinically with the lack of toxicity to caffeine seen in even the most premature infants started on caffeine for the prevention or treatment of apnea of prematurity (Schmidt et al., 2006). However, the pattern and timing of post-natal CYP1A2 induction remain unclear.

Maturation rates are difficult to generalize, and enzyme-specific information needs to be determined for an accurate estimate of drug metabolism including clinical conditions such as sepsis and complex surgery, nutritional state and diet (infant formula versus breast milk), polymorphism and even antenatal exposure to cigarette smoke (Czekaj et al., 2005; Blake et al., 2006; Allegaert, 2017; Li et al., 2021).

## 3.4 Excretion

Water soluble drugs with low molecular weight are primarily eliminated by renal excretion. The glomerular filtration rate (GFR) is highly dependent on gestational age and is ranging

from 0.6–0.8 to 2–4 ml per minute per 1.73 $m^2$ in preterm neonates and term neonates, respectively (Hayton, 2000; Ali et al., 2012). For example, gentamycin is therefore necessitating dosing intervals of 36–48 h in preterm newborns but reduced to 24 h in term newborns (Ali et al., 2012; Fuchs et al., 2014). Also, tubular secretion and reabsorption is reduced in preterm neonates. Tubular secretion has importance for the renal elimination of, e.g., penicillins, cephalosporins, and digoxin (Kearns et al., 2003).

# 4 CHALLENGES IN PHARMACOKINETIC STUDIES IN PREMATURE NEONATES

## 4.1 Blind Spots

As the anatomical and physiological characteristics of preterm neonates differ significantly from older children and adults, the process of neonatal pharmacological development becomes very complex. Furthermore, neonatology represents a small sub-field of pharmacology, and as a small target population, neonates are often overlooked.

Pharmaceutical companies largely refrain from proactively investing in the pediatric sector due to both economic and practical considerations, as reported by the EMA (European Medicines Agency and its Paediatric Committee, 2016; Van Driest and Choi, 2019). Even academia-driven research in the population of preterm neonates is limited and often focused on various other areas of clinical research than pharmacology.

## 4.2 Ethical Considerations

The ethical principles of pediatric research are well known (Roth-Cline et al., 2011), but the challenges are even more pronounced in the preterm population. Overall, inclusion of newborns in research should comprise a minimal risk and/or have a potential for direct benefits for the trial participant to be considered ethically acceptable (Barker et al., 2018).

Due to the stressful situation of becoming a parent to a premature child, the required informed parental consent for neonates participating in research, can be difficult to obtain. The process may require repeated discussions with the families, and thus complicate recruitment for studies during the first hours/days of life (O'Hara et al., 2020).

Failure of recruitment of a sufficient number of premature neonates within the planned study period may force investigators to facilitate costly prolongations of the study or even to a premature study termination without reaching the target sample size. Failed drug trials and the general lack of pediatric clinical trials contribute to the high prevalence of off-label use in neonates.

## 4.3 Practical Challenges

Fortunately, relatively few children are born very or extremely preterm, but the scarcity of premature neonates makes it challenging to include this population in PK studies. Traditional PK study designs involve multiple blood samples at fixed intervals and generally require the same number of samples from all subjects taken at the same time (O'Hara et al., 2020). This approach presents practical difficulties in preterm neonates, as repeated blood sampling quickly exceeds the regulated (EMA, 2018; Barker et al., 2018) maximum of 1% at any one time, or 3% within 1 month, amounting to 400 µl or 1.2 ml respectively for a neonate weighing 500 g. Also, the sampling procedure may prove challenging, as even something as mundane as drawing blood often requires experience in the extremely preterm children. Likewise, urine sampling may prove difficult to collect in a standardized manner (Van Driest and Choi, 2019).

# 5 EXPLORING THE AVAILABLE DATA ON PREMATURE NEONATES: AN EXAMPLE USING HEPATIC DRUG METABOLISM

## 5.1 Methods

A PubMed search was performed on 3 January 2022 for the terms phase I and phase II metabolism in premature children using the following search string: {"Infant, Premature" (mesh) OR "Infant, Extremely Premature" (mesh) OR "Infant, Low Birth Weight" (mesh) OR "Infant, Very Low Birth Weight" (mesh) OR "Infant, Premature, Diseases" (mesh) OR [(preterm OR prematurity OR premature OR prematurely) AND (infant* OR infancy OR baby OR babies OR neonat* OR newborn*)] OR preemi* OR premi OR preterm OR "very low birth weight" OR VLBW OR "low birth weight" OR LBW OR "very low birthweight" OR "low birthweight"} AND {["Cytochrome P-450 Enzyme System" (mesh) OR "Cytochromes" OR Cytochrome* OR "P450"] OR ["Methyltransferases" (mesh) OR "Sulfotransferases" (mesh) OR "Acetyltransferases" (mesh) OR "Acyltransferases" (mesh) OR "Glucuronosyltransferase" (mesh) OR glucuronidation* OR Methyltransferase* OR Sulfotransferase* OR Acetyltransferase*)]} AND {[humans (Filter)] AND [newborn (Filter)]}.

Manuscripts were reviewed for relevance to the topic of this review, as well as for citations related to the topic of the review by two independent reviewers (MLM and CG). In case of disagreement, a third author (ULT) would arbitrate. This review should however be considered a scoping rather than a systematic review.

## 5.2 Findings

Our search resulted in 1206 hits, of which a total of 70 manuscripts were found relevant to the scoping review (Aranda et al., 1976; Loughnan et al., 1977; Windorfer and Pringsheim, 1977; Pitlick et al., 1978; Onishi et al., 1979; Grygiel and Birkett, 1980; Brazier et al., 1981; Kawade and Onishi, 1981; Mulhall et al., 1983; Tserng et al., 1983; Ribon et al., 1984; Grasela and Donn, 1985; Choonara et al., 1989; RJ et al., 1990; Fujii et al., 1993; Hartley et al., 1993, 1994; Reiter and Stiles, 1993; Brammer and Coates, 1994; Vauzelle-Kervroedan et al., 1996; Sato et al., 1997; Treluyer et al., 1997; Wenzl et al., 1998; Lee et al., 1999; Touw et al., 2000; de Wildt et al., 2001, 2002, 2010; Lowry et al., 2001; Allegaert et al., 2008a, 2008b, 2015; Wade et al., 2008, 2009, 2009; Knibbe et al., 2009; Mugabo et al., 2011; George et al., 2012; Ince et al., 2013; Kim et al., 2013; Le Doare et al., 2013; Wang et al., 2013; Bekker et al., 2014; de Waal

et al., 2014; Krekels et al., 2015; Mahmood, 2015, 2017; Ogawa et al., 2015; Pain et al., 2015; Auriti et al., 2016; Cook et al., 2016; Momper et al., 2016; Flint et al., 2017; Hwang et al., 2017; Sohn et al., 2017; Völler et al., 2017; JM et al., 2018, 2018; Anderson and Holford, 2018; Brussee et al., 2018; Leroux et al., 2018; Michelet et al., 2018; Neyro et al., 2018; Tsakiri et al., 2018; Gerhart et al., 2019; Gonzalez et al., 2019; Smith et al., 2019; van Groen et al., 2019).

Overall, the large heterogeneity of the studies with regards to both scope, methodology, and particularly the detail of reporting results, precludes any formal comparison, let alone meta-analyses. In particular, many studies examined neonates, but failed to distinguish between term and preterm neonates. This was the case in more than 40% of the studies. The full spectrum of prematurity was found to be explored from 22 gestational weeks and onwards. Extreme premature neonates (born before 28 GA weeks) were included in less than 55% of these studies.

Furthermore, the age of the children at the time of inclusion and/or sampling (postnatal age, PNA) was unclear in approximately 30% of the studies. In the remaining articles the PNA varied from a few hours to 1 year. The overall mean age at the time of inclusion varied from 4 days to 1.5 months. Keeping in mind that prematurity is defined as being born before 37 weeks of gestation, this logically reduces the actual number of included neonates, who were extremely, very or even late preterm at the time of sampling. These findings elucidate how most PK studies in the youngest pediatric populations are not sufficiently transparent in the presentation of data contributions.

Generally, the gestational- and postnatal ages are displayed in intervals, making an accurate estimation of the degree of prematurity impossible. Additionally, the interpretation of the strength of the contributing data becomes very difficult, as, e.g., a 2 weeks old child that was born at 26 weeks gestational age and a newborn child born at 28 weeks gestational age are not necessarily equal in terms of metabolic maturation.

Most studies (approximately 70%) focused on the phase I metabolism, and the most studied CYP subclasses were CYP3A4, CYP1A2, CYP2E1, CYP2C19, and CYP2C9 either as individual or contributing enzymes. The phase II metabolism systems were studied in approximately 35% of the articles identified [with glucuronidation (notably UDP-Glucuronosyltransferase-2B7)] and sulfation being the most studied.

### 5.2.1 Phase I Metabolism in Preterm Neonates

In **Tables 1–3** we summarize the Cytochrome P450 subclasses, we found to be the most studied *in vivo* in preterm neonates, i.e., 3A4, 1A2, and 2C9/2C19.

### 5.2.2 CYP3A4

Identified studies of CYP3A4 activity are displayed in **Table 1**. Midazolam was predominantly reported as an *in vivo* probe for CYP3A4 activity, and the clearance values reported illustrated a clear tendency towards reduced CYP3A4 activity in preterm neonates as compared to full born neonates and older children (Burtin et al., 1994; Vauzelle-Kervroedan et al., 1996; Lee et al., 1999; de Wildt et al., 2001, 2002; Ogawa et al., 2015; Brussee et al., 2018; JM et al., 2018; van Groen et al., 2019). The largest study identified was a population-based study (Burtin et al., 1994) included plasma samples from 197 neonates (gestational age 26–42 weeks, postnatal age 0–10 days) on artificial ventilation. Here clearance was found to be directly proportional to birth weight and gestational age, but not postnatal age (between 0 and 10 days).

### 5.2.3 CYP 2C9 and - 2C19

Identified studies of CYP2C19 and CYP2C9 activity are displayed in **Table 2**. Only phenobarbital was found reported as an *in vivo* probe for CYP2C9 (Pitlick et al., 1978; Ribon et al., 1984; Grasela and Donn, 1985; MP et al., 1989; Touw et al., 2000; Völler et al., 2017), although additional minor metabolism occurs *via* CYP2C19 and CYP2E1 (approximately 5%). A general trend towards reduced phenobarbital clearance was observed in premature neonates. In a recent population study, a PK model was developed based on data sharing from former studies, and the maturation of clearance was predicted to be dependent on both body weight and postnatal age in preterm neonates.

The activity of CYP2C19 was investigated by use of the substrate's phenytoin and pantoprazole (Loughnan et al., 1977; Ward et al., 2010). Latest was investigated by Ward et al., in 2010, who found oral clearance of pantoprazole reduced in preterm neonates. Oral clearance increased with increased postnatal age, but no apparent trend was seen for postmenstrual age.

### 5.2.4 CYP1A2

Primarily theophylline was used as substrate in all the identified *in vivo* studies investigating CYP1A2 activity in preterm neonates (Grygiel and Birkett, 1980; Brazier et al., 1981; Tserng et al., 1983; Lowry et al., 2001; Kim et al., 2013; Sohn et al., 2017; Jiang et al., 2021), which are displayed in **Table 3**. CYP1A2 was generally found associated to postnatal age rather than postmenstrual age and to birth weight. Furthermore, well-known genetic polymorphism-associated differences in CYP1A2 activity were not yet found expressed in the preterm population.

### 5.2.5 CYP2E1

Three studies investigating the *in vivo* CYP2E1 activity were identified. Isoniazid (Bekker et al., 2014) and paracetamol (Cook et al., 2016; Flint et al., 2017) were the substrates studied. A markedly reduced isoniazid clearance was noted in neonates with low GA and LBW. None of the studies using paracetamols as substrate succeeded in defining the CYP2E1 maturity, probably because the contribution of the CYP2E1 pathway is minimal, albeit important due to formation of the toxic metabolite NAPQI, for the metabolism of paracetamol.

### 5.2.6 CYP2D6

*In vivo* CYP2D6 metabolism has been investigated in premature neonates using tramadol as substrate (Allegaert et al., 2008a; 2008b). Here, PMA and CYP2D6 polymorphisms (Li et al., 2021) was found to determine the O-demethylation activity in the preterm neonates.

### 5.2.7 Phase II Metabolism in Premature Neonates

Twenty studies investigating the *in vivo* phase II metabolism were identified (Windorfer and Pringsheim, 1977; Mulhall et al.,

**TABLE 1 |** Summary of studies exploring CYP3A (4/5) activity in preterm neonates.

| References | Premature (N) | GA, range | PNA, range | BW, range | Substrate | Dose | Clearance parameter | Clearance | Clearance premature |
|---|---|---|---|---|---|---|---|---|---|
| Burtin et al. (1994) | Min. 96* | 26–42 | 0–10 | 700–5200 | Midazolam | 0.032–1.6 mg/kg (IV bolus) | Total CL | Mean 1.2 (SD ± 0.96) ml/kg/min | ↓ |
| Vauzelle-Kervroedan et al. (1996) | 7 | 31.4–36.5 | 1–14 | 1540–2700 | Cortisol | - (endogenous) | 6 βOHF/FF ratio | Mean 7.2 (SD ± 1.5) | (↑) |
| Lee et al. (1999) | 60 | 24–31 | 2–15 | 523–1470 | Midazolam | 0.1 mg/kg (IV bolus) | Total CL | Mean 1.0 (SD ± 0.2) ml/kg/min | ↓ |
| De Wildt et al. (2001) | 24 | 26–34 | 3–11 | 760–1630 | Midazolam | 0.1 mg/kg (IV bolus) | Total CL and 1-OH-M/M ($AUC_{0-t}$) ratio | Mean 2.3 (SD ± 1.5) ml/kg/min and 0.09 (<0.001–1) | ↓ |
| De Wildt et al. (2002) | 15 | 26–31 | 3–13 | Mean 1076 (SD ± 240) | Midazolam | 0.1 mg/kg (PO or IV bolus) | CL/F and 1-OH-M/M ($AUC_{0-t}$) ratio | 2.7 (range 0.7–15.5) ml/kg/min and 0.03 (<0.01–0.96) | ↓ |
| Brussee et al. (2018) | Min. 55* | ND | 1–44 | 770–3700 | Midazolam | 0.1 mg/kg (IV 30 min infusion) | Total CL | ** | ** |
| Ogawa et al. (2015) | 34 | 24–32.9 | 1–37 | 598–1868 | Doxapram | 0.2 mg/kg (IV) | Total CL | 0.698 L/kg/h | ↓ |
| Brussee et al. (2018) | 37 | 26–34 | 3–11 | 770–2030[1] | Midazolam | 0.1 mg/kg (PO or IV) | Hepatic CL | 1.62 L/h | ↓ |
| Groen et al., 2019 | Unclear* | 23.9–41.4 | 4.2–343.7 | 2600–8900[1] | Midazolam ($^{14}$C-marked) | 111 Bq/kg; 37.6 ng/kg (IV) | Total CL | Median 1.8 (range 0.7–6.7) ml/kg/min | ↓ |

[1]*Weight at sample time.*

**Exact number of premature children included has not been specified.*

***The model over-estimated clearance and was not found applicable to predict midazolam CL in critical ill preterm neonates.*

*BW, birth weight in grams; Bq, Becquerel; CL, clearance; GA, gestational age at birth in weeks; IV, intravenous; N, number of included premature neonates; ND, not defined; PNA, postnatal age at start of sampling in days; PO, orally.*

**TABLE 2 |** Summary of studies exploring CYP2C9 (rows 1–6) and CYP2C19 (rows 7–8) activity in preterm neonates.

| References | Premature (N) | GA, range | PNA, range | BW, range | Substrate | Dose | Clearance parameter | Clearance | Clearance premature |
|---|---|---|---|---|---|---|---|---|---|
| Pitlick et al. (1978) | Unclear* | 30–40 | <2 | 1350–2850 | Phenobarbital | LD, 20 mg/kg (IV) MD, 5 mg/kg/day | Total CL ($T_{1/2}$) | - | ↓ |
| Ribon et al. (1984) | 17 | 28–37 | <1 | 1250–3000 | Phenobarbital | 5 mg/kg (IM) or 10 mg/kg (IV) | Total CL ($T_{1/2}$) | - | ↓ |
| De Carolis et al., 1989 | Unclear* | 27–37 | ND | 800–3090 | Phenobarbital | LD 20 mg/kg (IV) MD 5 mg/kg/15 h | Total CL ($T_{1/2}$) | - | ↓ |
| Grasela and Donn, (1985) | Min 46* | 24–42 | 1–16 | 600–3620 | Phenobarbital | LD, 20 mg/kg MD, 5 mg/kg | Total CL | Mean 0.0047 (±19%) L/h/kg | ↔ |
| Touw et al. (2000) | Unclear* | 26 + 6–41 + 4 | ND | 590–4070 | Phenobarbital | LD 23 ± 11 mg/kg MD 51 mg/kg/day | Total CL/total CL per kg body weight | Mean 9.3 (SD ± 4.9) ml/h/mean 4.3 (SD ± 1.1) | ↑ |
| Völler et al. (2017) | Min. 25* | 24–42 | 0–22 | 450–4400 | Phenobarbital | LD 20 mg/kg MD 3.9 mg/kg | Total CL | Mean 0.0091 (±9%) L/h | ↓ |
| Loughnan et al. (1977) | 4 | 32–36 | 2–18 | 760–2950 | Phenytoin | 12 mg/kg (IV) | Total CL ($T_{1/2}$) | - | ↓ |
| Ward et al. (2010) | 37 | 23–41 | 9.1–137.2 | 2018–4550 | Pantoprazol | 0.6 or 1.2 mg/kg/ day (PO) | CL/F | Mean 0.21 (SD ± 0.12) L/h/kg (1.25 mg) Mean 0.23 (SD ± 0.21) L/h/kg (2.5 mg) | ↓ |

**Exact number of premature children included has not been specified.*

*BW, birth weight in grams; CL, clearance; GA, gestational age at birth in weeks; IM, intramuscular; IV, intravenous; LD, loading dose; MD, maintenance dose; N, number of included premature neonates; ND, not defined; PNA, postnatal age at start of sampling in days; PO, orally.*

**TABLE 3 |** Summary of studies exploring CYP1A2 activity in preterm neonates.

| References | Premature (N) | GA, range | PNA, range | BW, range | Substrate | Dose | Clearance parameter | Clearance | Clearance premature |
|---|---|---|---|---|---|---|---|---|---|
| Grygiel and Birkett. (1980) | 6 | 28–32 | ND | 800–1620 | Theophylline | 4.5 (±0.04) mg/day (PO) | Theophylline urin metabolite ratio | - | ↓ |
| Brazier et al. (1981) | 2 | 32 | 1–9 | 1360, 1380 | Theophylline | 3 mg/kg/8 h (PO) | Total CL and Theophylline urin metabolite ratio | - | ↓ |
| Tserng et al. (1983) | 9 | 26–32 | 4–39 | 780–2050 | Theophylline | LD 6.6 mg/kg (IV) MD 2.6 mg/kg/8 h | Theophylline urin metabolite ratio | - | ↓ |
| Lowry et al. (2001) | 3 | 24, 28, 31 | 56, 21, 0 | 880, 1060 and 1800 | Theophylline | 2 mg/kg/12 h and 2.5 mg/kg/12 h (all overdoses) | Total CL | 0.01, 0.02 and 0.05 L/h/kg | ↓ |
| Kim et al. (2013) | 100 | 24.3–35.7 | 2.8–79.1 | 500–2900[1] | Theophylline | Dose not specified | Total CL | 0.16 (SD ± 20%) L/h | ↓ |
| Sohn et al. (2017) | 104 | 24 + 2–35 + 5 | 5–74 | 540–2500 | Amiphylline Theophylline | LD 8 mg/kg (IV/PO) | Total CL, Theophylline urin metabolite ratio | 0.5 (SD ± 0.29) ml/min/kg | ↓ |
| | | | | 540–2900[1] | | MD 1,3–3 mg/kg/8 or 12th h | | 0.34 (SD ± 0.28) ml/min/kg | |
| Jiang et al. (2021) | 17 | 26–32 | 4–43 | 750–2400 | Caffeine | 5.01 ± 0.56 mg/kg | Total CL | 7.3 (SD ± 2.5) ml/h | ↓ |

[1]*Weight at sample time.*

*BW, birth weight in grams; CL, clearance; GA, gestational age at birth in weeks; IV, intravenous; LD, loading dose; MD, maintenance dose; N, number of included premature neonates; ND, not defined; PNA, postnatal age at start of sampling in days; PO, orally.*

1983a; Choonara et al., 1989; Hartley et al., 1993, 1994; H et al., 1993; Reiter and Stiles, 1993; Brammer and Coates, 1994; Sato et al., 1997; Wenzl et al., 1998; Wade et al., 2008, 2009; Knibbe et al., 2009; Krekels et al., 2015; Mahmood, 2015; Auriti et al., 2016; Cook et al., 2016; Flint et al., 2017; MF et al., 2017; Leroux et al., 2018; Gerhart et al., 2019). A large heterogenitet was found and several substrates were used and included chloramphenicol, morphine, fluconazole, lorazepam, micafungin, paracetamol, and mefenamic acid. Overall, the activity of the phase II metabolis, pathways were found reduced in preterm neonates. Herein, morphine metabolism by UGT2B7 was found closely related to body weight as opposed and post-natal age (day 1–10) (Knibbe et al., 2009), and fluconazol clearance by UGTB7was found to increase with increase with BGA, PNA and PMA (Wade et al., 2008).

## 5.3 Interpretation

The understanding of developmental pharmacology in infants and children has increased significantly since the seminal review by Kearns et al. (2003) and new data have been added in both neonates in general (Allegaert, 2017) and in premature neonates (van den Anker and Allegaert, 2021). Furthermore, pharmacometrics modelling approaches are now, despite limited data, being used to support neonatal and pediatric drug development as well as commonly used off-label drugs. The insight into ontogeny of, e.g., the phase I metabolism of extreme premature neonates has previously been based on, e.g., fetal samples (Kearns et al., 2003). However, with a limit of early human viability, that is, constantly improving, PK data on the extreme premature neonates remain unreasonable scarce.

The results from the present study illustrate the difficulties in obtaining data from the very youngest and smallest neonates. Particularly, it is challenging to explore include patients shortly after birth and consequently the early stages of xenobiotic biotransformation ontogeny remain relatively underexplored.

This is exemplified by our findings, as most studies lacked detailed information, e.g., on the number of very and extremely preterm neonates. Importantly, the post-natal age at sampling for the included patients were often not specified, making definitive interpretation of these early stages of xenobiotic biotransformation very difficult. Finally, details on the number of samples deriving from the preterm neonates was also seldom reported.

As expected, we did find an overall clear tendency of an immature, and thus reduced, drug metabolism in the preterm infants when compared to term neonates and older children. This was the case for virtually all reported enzyme-systems. However, as we also found a large heterogeneity in the studies, including methodological differences in the studies pathways and the use of both non-compartmental- and population PK methods, we cannot perform any direct comparison or formal meta-analysis of the reported findings.

# 6 POSSIBLE SOLUTIONS AND FUTURE DIRECTIONS

Neonatology has been fortunate to experience some major leaps in pharmacology treatments for premature children but game-changing drugs like surfactant are rare. However, new therapeutic products are increasingly being studied for neonatal diseases and advances are constantly being made. These current and future advances must integrate the increased knowledge of the ontogeny of organ and enzyme systems in premature children. Thereby we can construct optimized models that takes into consideration the

normal maturation of neonates (van den Anker and Allegaert, 2021).

As illustrated, there is still a lack of data from extremely premature children sampled shortly after birth, a testament to the practical and ethical challenges. Neonatal pharmacological research could benefit from increased representation of multidisciplinary neonatal clinicians on relevant committees to streamlining of ethics and governance procedures for multi-site studies. This will likely require dedicated time and support as clinician time for additional service outside of clinical care is often unfunded and burdensome. Similarly, the practicalities of inclusion of extremely premature children immediately after birth may be tackled by increased use of antenatal parental consent (Memon et al., 2020).

Obviously, the development of sparse plasma/blood sampling and analyzing techniques improve the feasibility of including the very small preterm neonates. This fact, and the use of left-over or opportunistic samples from routine sampling will yield a higher inclusion rate. Pharmacometric modeling approaches have reduced the high number of samples needed, but by combining these modern techniques with a higher inclusion rate, a high level of detailing will be possible By use of already existing modeling methods and optimal sampling design, parameter estimation with maximal precision is possible (Smits et al., 2021). However, refinement of these methods will be important for the future.

From a regulatory point of view, it would be highly desirable if continued improvements on targeted and efficient clinical trial designs in neonates became standard in pediatric drug development. Herein, PK and PD characterization in the pediatric subgroup of neonatology should be considered from the earliest drug development stages.

Furthermore, development of microdosing studies present an attractive alternative to overcome ethical and analytical challenges in phenotyping studies. Microdoses are subtherapeutic doses (typically < 100th of therapeutic dose) that are unlikely to elicit any pharmaceutical response or side effects. The microdosing approach has been validated for, e.g., midazolam in preterm neonates (van Groen et al., 2019).

The use of international multicenter studies, pediatric trial networks, diverse databases, biomarkers, and integration of Real-world Data, use of artificial intelligence and machine learning such as text mining and deep-learning models to extract relevant information from electronic patient records is likely to further advance neonatal pharmacology (Mulugeta et al., 2018; Goulooze et al., 2020; Smits et al.). However, models of any kind should be developed wisely, bearing in mind that the risk of poor performance is particularly high if certain age groups such as preterm neonates are underrepresented or absent in the data set used to develop the model (Mulugeta et al., 2018; Goulooze et al., 2020; Smits et al.).

## 7 CONCLUSION

This review highlights the insufficiencies in the current knowledge of the maturation of drug metabolizing enzymes in preterm neonates, and particularly in the very or extremely preterm neonates. We illustrate the overall heterogeneous approach to measuring and presenting the phase I and II pathways metabolism in preterm neonates, often with use of exclusively opportunistic sampling—a testament to the practical and ethical challenges in measuring pharmacokinetic activity in preterm neonates.

With the advances in overall neonatal intensive care, the limit for possible survival in extremely preterm neonates has improved. Consequently, neonates with increasingly lower gestational age at birth now require care, including intensive pharmacological treatment. This calls for optimized designs of future pharmacometrics studies, preferably as multi-site/international collaboration between neonatologists and clinical pharmacologists that will allow for integration of all available techniques, including low volume plasma/blood analysis techniques, pharmacokinetic modeling, “Big Data”, and even machine learning.

The understanding of the impact of growth, development, and organ maturation on the absorption, distribution, metabolism, and excretion of drugs in neonates, infants, children, and adolescents has progressed tremendously in recent decades, but it has mainly been driven by a few, but dedicated researchers; it is now time for the broader pharmacological scientific community to turn its gaze toward the most premature children.

## AUTHOR CONTRIBUTIONS

MM: Project coordinator, drafted the initial manuscript, collected data, and approved the final manuscript as submitted, CG: conceptualized and designed the study, drafted the initial manuscript, designed the data collections instrument, and approved the final manuscript as submitted. UL-T: conceptualized and designed the study, drafted the initial manuscript, designed the data collection instrument, and approved the final manuscript as submitted, JA: conceptualized and designed the study, designed the data collection instrument, reviewed and revised the manuscript, and approved the final manuscript as submitted.

## REFERENCES

Al-Turkait, A., Szatkowski, L., Choonara, I., and Ojha, S. (2020). Review of Drug Utilization Studies in Neonatal Units: A Global Perspective. *Int. J. Environ. Res. Public Health* 17, E5669. doi:10.3390/ijerph17165669

Ali, A. S., Farouq, M. F., and Al-Faify, K. A. (2012). Pharmacokinetic Approach for Optimizing Gentamicin Use in Neonates during the First Week of Life. *Indian J. Pharmacol.* 44, 36–40. doi:10.4103/0253-7613.91864

Allegaert, K. (2017). Better Medicines for Neonates: Improving Medicine Development, Testing, and Prescribing. *Early Hum. Dev.* 114, 22–25. doi:10.1016/j.earlhumdev.2017.09.007

Allegaert, K., Holford, N., Anderson, B. J., Holford, S., Stuber, F., Rochette, A., et al. (2015). Tramadol and O-Desmethyl Tramadol Clearance Maturation and Disposition in Humans: a Pooled Pharmacokinetic Study. *Clin. Pharmacokinet.* 54, 167–178. doi:10.1007/s40262-014-0191-9

Allegaert, K., van den Anker, J. N., de Hoon, J. N., van Schaik, R. H. N., Debeer, A., Tibboel, D., et al. (2008a). Covariates of Tramadol Disposition in the First Months of Life. *Br. J. Anaesth.* 100, 525–532. doi:10.1093/bja/aen019

Allegaert, K., van Schaik, R. H. N., Vermeersch, S., Verbesselt, R., Cossey, V., Vanhole, C., et al. (2008b). Postmenstrual Age and CYP2D6 Polymorphisms Determine Tramadol O-Demethylation in Critically Ill Neonates and Infants. *Pediatr. Res.* 63, 674–679. doi:10.1203/PDR.0b013e31816ff712

Anderson, B. J., and Holford, N. H. G. (2018). Negligible Impact of Birth on Renal Function and Drug Metabolism. *Paediatr. Anaesth.* 28, 1015–1021. doi:10.1111/pan.13497

EMA (2018). Investigation of Medicinal Products in the Term and Preterm Neonate. *Eur. Med. Agency*. Available at: https://www.ema.europa.eu/en/investigation-medicinal-products-term-preterm-neonate (Accessed December 1, 2021).

Aranda, J. V., Sitar, D. S., Parsons, W. D., Loughnan, P. M., and Neims, A. H. (1976). Pharmacokinetic Aspects of Theophylline in Premature Newborns. *N. Engl. J. Med.* 295, 413–416. doi:10.1056/NEJM197608192950803

Auriti, C., Falcone, M., Ronchetti, M. P., Goffredo, B. M., Cairoli, S., Crisafulli, R., et al. (2016). High-Dose Micafungin for Preterm Neonates and Infants with Invasive and Central Nervous System Candidiasis. *Antimicrob. Agents Chemother.* 60, 7333–7339. doi:10.1128/AAC.01172-16

Barker, C. I. S., Standing, J. F., Kelly, L. E., Hanly Faught, L., Needham, A. C., Rieder, M. J., et al. (2018). Pharmacokinetic Studies in Children: Recommendations for Practice and Research. *Arch. Dis. Child.* 103, 695–702. doi:10.1136/archdischild-2017-314506

Barr, J., Brenner-Zada, G., Heiman, E., Pareth, G., Bulkowstein, M., Greenberg, R., et al. (2002). Unlicensed and Off-Label Medication Use in a Neonatal Intensive Care Unit: a Prospective Study. *Am. J. Perinatol.* 19, 67–72. doi:10.1055/s-2002-23557

Bekker, A., Schaaf, H. S., Seifart, H. I., Draper, H. R., Werely, C. J., Cotton, M. F., et al. (2014). Pharmacokinetics of Isoniazid in Low-Birth-Weight and Premature Infants. *Antimicrob. Agents Chemother.* 58, 2229–2234. doi:10.1128/AAC.01532-13

Blake, M. J., Abdel-Rahman, S. M., Pearce, R. E., Leeder, J. S., and Kearns, G. L. (2006). Effect of Diet on the Development of Drug Metabolism by Cytochrome P-450 Enzymes in Healthy Infants. *Pediatr. Res.* 60, 717–723. doi:10.1203/01.pdr.0000245909.74166.00

Blencowe, H., Cousens, S., Oestergaard, M. Z., Chou, D., Moller, A.-B., Narwal, R., et al. (2012). National, Regional, and Worldwide Estimates of Preterm Birth Rates in the Year 2010 with Time Trends since 1990 for Selected Countries: a Systematic Analysis and Implications. *Lancet Lond. Engl.* 379, 2162–2172. doi:10.1016/S0140-6736(12)60820-4

Bonner, J. J., Vajjah, P., Abduljalil, K., Jamei, M., Rostami-Hodjegan, A., Tucker, G. T., et al. (2015). Does Age Affect Gastric Emptying Time? A Model-Based Meta-Analysis of Data from Premature Neonates through to Adults. *Biopharm. Drug Dispos.* 36, 245–257. doi:10.1002/bdd.1937

Borzyskowski, M., Grant, D. B., and Wells, R. S. (1976). Cushing's Syndrome Induced by Topical Steroids Used for the Treatment of Non-bullous Ichthyosiform Erythroderma. *Clin. Exp. Dermatol.* 1, 337–342. doi:10.1111/j.1365-2230.1976.tb01440.x

Brammer, K. W., and Coates, P. E. (1994). Pharmacokinetics of Fluconazole in Pediatric Patients. *Eur. J. Clin. Microbiol. Infect. Dis. Off. Publ. Eur. Soc. Clin. Microbiol.* 13, 325–329. doi:10.1007/BF01974613

Brayer, C., Micheau, P., Bony, C., Tauzin, L., Pilorget, H., Sampériz, S., et al. (2004). Neonatal Accidental Burn by Isopropyl Alcohol. *Arch. Pediatr. Organe Off. Soc. Francaise Pediatr.* 11, 932–935. doi:10.1016/j.arcped.2004.04.023

Brazier, J. L., Salle, B., Ribon, B., Desage, M., and Renaud, H. (1981). *In Vivo* N7 Methylation of Theophylline to Caffeine in Premature Infants. Studies with Use of Stable Isotopes. *Dev. Pharmacol. Ther.* 2, 137–144. doi:10.1159/000481025

Brumbaugh, J. E., Hansen, N. I., Bell, E. F., Sridhar, A., Carlo, W. A., Hintz, S. R., et al. (2019). Outcomes of Extremely Preterm Infants with Birth Weight Less Than 400 G. *JAMA Pediatr.* 173, 434–445. doi:10.1001/jamapediatrics.2019.0180

Brussee, J. M., Yu, H., Krekels, E. H. J., de Roos, B., Brill, M. J. E., van den Anker, J. N., et al. (2018). First-Pass CYP3A-Mediated Metabolism of Midazolam in the Gut Wall and Liver in Preterm Neonates. *CPT Pharmacomet. Syst. Pharmacol.* 7, 374–383. doi:10.1002/psp4.12295

Burtin, P., Jacqz-Aigrain, E., Girard, P., Lenclen, R., Magny, J. F., Betremieux, P., et al. (1994). Population Pharmacokinetics of Midazolam in Neonates. *Clin. Pharmacol. Ther.* 56, 615–625. doi:10.1038/clpt.1994.186

Chawanpaiboon, S., Vogel, J. P., Moller, A.-B., Lumbiganon, P., Petzold, M., Hogan, D., et al. (2019). Global, Regional, and National Estimates of Levels of Preterm Birth in 2014: a Systematic Review and Modelling Analysis. *Lancet Glob. Health* 7, e37–e46. doi:10.1016/S2214-109X(18)30451-0

Choonara, I. A., McKay, P., Hain, R., and Rane, A. (1989). Morphine Metabolism in Children. *Br. J. Clin. Pharmacol.* 28, 599–604. doi:10.1111/j.1365-2125.1989.tb03548.x

Cook, S. F., Stockmann, C., Samiee-Zafarghandy, S., King, A. D., Deutsch, N., Williams, E. F., et al. (2016). Neonatal Maturation of Paracetamol (Acetaminophen) Glucuronidation, Sulfation, and Oxidation Based on a Parent-Metabolite Population Pharmacokinetic Model. *Clin. Pharmacokinet.* 55, 1395–1411. doi:10.1007/s40262-016-0408-1

Cowen, J., Ellis, S. H., and McAinsh, J. (1979). Absorption of Chlorhexidine from the Intact Skin of Newborn Infants. *Arch. Dis. Child.* 54, 379–383. doi:10.1136/adc.54.5.379

Craft, A. W., Brocklebank, J. T., Hey, E. N., and Jackson, R. H. (1974). The "Grey Toddler". Chloramphenicol Toxicity. *Arch. Dis. Child.* 49, 235–237. doi:10.1136/adc.49.3.235

Czekaj, P., Wiaderkiewicz, A., Florek, E., and Wiaderkiewicz, R. (2005). Tobacco Smoke-dependent Changes in Cytochrome P450 1A1, 1A2, and 2E1 Protein Expressions in Fetuses, Newborns, Pregnant Rats, and Human Placenta. *Arch. Toxicol.* 79, 13–24. doi:10.1007/s00204-004-0607-7

de Waal, R., Kroon, S. M., Holgate, S. L., Horn, A. R., Tooke, L. J., Norman, J., et al. (2014). Nevirapine Concentrations in Preterm and Low Birth Weight HIV-Exposed Infants: Implications for Dosing Recommendations. *Pediatr. Infect. Dis. J.* 33, 1231–1233. doi:10.1097/INF.0000000000000453

de Wildt, S. N., Kearns, G. L., Hop, W. C. J., Murry, D. J., Abdel-Rahman, S. M., and van den Anker, J. N. (2002). Pharmacokinetics and Metabolism of Oral Midazolam in Preterm Infants. *Br. J. Clin. Pharmacol.* 53, 390–392. doi:10.1046/j.1365-2125.2002.01223.x

de Wildt, S. N., Kearns, G. L., Hop, W. C., Murry, D. J., Abdel-Rahman, S. M., and van den Anker, J. N. (2001). Pharmacokinetics and Metabolism of Intravenous Midazolam in Preterm Infants. *Clin. Pharmacol. Ther.* 70, 525–531. doi:10.1067/mcp.2001.120683

de Wildt, S. N., Kearns, G. L., Leeder, J. S., and van den Anker, J. N. (1999). Cytochrome P450 3A: Ontogeny and Drug Disposition. *Clin. Pharmacokinet.* 37, 485–505. doi:10.2165/00003088-199937060-00004

de Wildt, S. N., Kearns, G. L., Murry, D. J., Koren, G., and van den Anker, J. N. (2010). Ontogeny of Midazolam Glucuronidation in Preterm Infants. *Eur. J. Clin. Pharmacol.* 66, 165–170. doi:10.1007/s00228-009-0741-5

Ehrnebo, M., Agurell, S., Jalling, B., and Boréus, L. O. (1971). Age Differences in Drug Binding by Plasma Proteins: Studies on Human Foetuses, Neonates and Adults. *Eur. J. Clin. Pharmacol.* 3, 189–193. doi:10.1007/BF00565004

Engle, W. A. (2004). American Academy of Pediatrics Committee on Fetus and NewbornAge Terminology during the Perinatal Period. *Pediatrics* 114, 1362–1364. doi:10.1542/peds.2004-1915

European Medicines Agency and its Paediatric Committee (2016). 10-year Report to the European Commission - General Report on the Experience Acquired as a Result of the Application of the Paediatric Regulation. Available at: https://ec.europa.eu/health/sites/health/files/files/paediatrics/2016_pc_report_2017/ema_10_year_report_for_consultation.pdf (Accessed December 16, 2018).

Flint, R. B., Roofthooft, D. W., van Rongen, A., van Lingen, R. A., van den Anker, J. N., van Dijk, M., et al. (2017). Exposure to Acetaminophen and All its Metabolites upon 10, 15, and 20mg/kgintravenous Acetaminophen in Very -preterminfants. *Pediatr. Res* 82, 678–684. doi:10.1038/pr.2017.129

Ford, S., and Calvert, J. (2008). Adaptation for Life: A Review of Neonatal Physiology. *Anaesth. Intensive Care Med.* 12, 93–98. doi:10.1016/j.mpaic.2008.01.009

Fredholm, B. B., Rane, A., and Persson, B. (1975). Diphenylhydantoin Binding to Proteins in Plasma and its Dependence on Free Fatty Acid and Bilirubin Concentration in Dogs and Newborn Infants. *Pediatr. Res.* 9, 26–30. doi:10.1203/00006450-197501000-00005

Fuchs, A., Guidi, M., Giannoni, E., Werner, D., Buclin, T., Widmer, N., et al. (2014). Population Pharmacokinetic Study of Gentamicin in a Large Cohort of Premature and Term Neonates. *Br. J. Clin. Pharmacol.* 78, 1090–1101. doi:10.1111/bcp.12444

Fujii, R., Matsumoto, S., Sakiyama, Y., Ishikawa, Y., Takeda, T., Hatae, Y., et al. (1993). A Clinical Study of Fluconazole-Granules and -injectable in Pediatric Patients with Deep-Seated Mycoses. *Jpn. J. Antibiot.* 46, 654–685. doi:10.11553/antibiotics1968b.46.654

Fujiwara, T., Maeta, H., Chida, S., Morita, T., Watabe, Y., and Abe, T. (1980). Artificial Surfactant Therapy in Hyaline-Membrane Disease. *Lancet Lond. Engl.* 1, 55–59. doi:10.1016/s0140-6736(80)90489-4

George, M., Kitzmiller, J. P., Ewald, M. B., O'Donell, K. A., Becter, M. L., and Salhanick, S. (2012). Methadone Toxicity and Possible Induction and Enhanced Elimination in a Premature Neonate. *J. Med. Toxicol. Off. J. Am. Coll. Med. Toxicol.* 8, 432–435. doi:10.1007/s13181-012-0249-8

Gerhart, J. G., Watt, K. M., Edginton, A., Wade, K. C., Salerno, S. N., Benjamin, D. K., et al. (2019). Physiologically-Based Pharmacokinetic Modeling of Fluconazole Using Plasma and Cerebrospinal Fluid Samples from Preterm and Term Infants. *CPT Pharmacomet. Syst. Pharmacol.* 8, 500–510. doi:10.1002/psp4.12414

Gershanik, J., Boecler, B., Ensley, H., McCloskey, S., and George, W. (1982). The Gasping Syndrome and Benzyl Alcohol Poisoning. *N. Engl. J. Med.* 307, 1384–1388. doi:10.1056/NEJM198211253072206

Glass, H. C., Costarino, A. T., Stayer, S. A., Brett, C. M., Cladis, F., and Davis, P. J. (2015). Outcomes for Extremely Premature Infants. *Anesth. Analg.* 120, 1337–1351. doi:10.1213/ANE.0000000000000705

Gonzalez, D., Laughon, M. M., Smith, P. B., Ge, S., Ambalavanan, N., Atz, A., et al. (2019). Population Pharmacokinetics of Sildenafil in Extremely Premature Infants. *Br. J. Clin. Pharmacol.* 85, 2824–2837. doi:10.1111/bcp.14111

Goulooze, S. C., Zwep, L. B., Vogt, J. E., Krekels, E. H. J., Hankemeier, T., van den Anker, J. N., et al. (2020). Beyond the Randomized Clinical Trial: Innovative Data Science to Close the Pediatric Evidence Gap. *Clin. Pharmacol. Ther.* 107, 786–795. doi:10.1002/cpt.1744

Gow, P. J., Ghabrial, H., Smallwood, R. A., Morgan, D. J., and Ching, M. S. (2001). Neonatal Hepatic Drug Elimination. *Pharmacol. Toxicol.* 88, 3–15. doi:10.1034/j.1600-0773.2001.088001003.x

Grasela, T. H., and Donn, S. M. (1985). Neonatal Population Pharmacokinetics of Phenobarbital Derived from Routine Clinical Data. *Dev. Pharmacol. Ther.* 8, 374–383. doi:10.1159/000457062

Grygiel, J. J., and Birkett, D. J. (1980). Effect of Age on Patterns of Theophylline Metabolism. *Clin. Pharmacol. Ther.* 28, 456–462. doi:10.1038/clpt.1980.188

Saxén, H., Hoppu, K., and Pohjavuori, M., (1993). Pharmacokinetics of Fluconazole in Very Low Birth Weight Infants during the First Two Weeks of Life. *Clin. Pharmacol. Ther.* 54, 269–277. doi:10.1038/clpt.1993.147

Harrison, M. S., and Goldenberg, R. L. (2016). Global burden of Prematurity. *Semin. Fetal Neonatal. Med.* 21, 74–79. doi:10.1016/j.siny.2015.12.007

Hartley, R., Green, M., Quinn, M. W., Rushforth, J. A., and Levene, M. I. (1994). Development of Morphine Glucuronidation in Premature Neonates. *Biol. Neonate* 66, 1–9. doi:10.1159/000244083

Hartley, R., Quinn, M., Green, M., and Levene, M. I. (1993). Morphine Glucuronidation in Premature Neonates. *Br. J. Clin. Pharmacol.* 35, 314–317. doi:10.1159/000244083

Hayton, W. L. (2000). Maturation and Growth of Renal Function: Dosing Renally Cleared Drugs in Children. *AAPS PharmSci* 2, E3. doi:10.1208/ps020103

Helenius, K., Sjörs, G., Shah, P. S., Modi, N., Reichman, B., Morisaki, N., et al. (2017). Survival in Very Preterm Infants: An International Comparison of 10 National Neonatal Networks. *Pediatrics* 140, e20171264. doi:10.1542/peds.2017-1264

Hentschel, R., Bohlin, K., van Kaam, A., Fuchs, H., and Danhaive, O. (2020). Surfactant Replacement Therapy: from Biological Basis to Current Clinical Practice. *Pediatr. Res.* 88, 176–183. doi:10.1038/s41390-020-0750-8

Hines, R. N., and McCarver, D. G. (2002). The Ontogeny of Human Drug-Metabolizing Enzymes: Phase I Oxidative Enzymes. *J. Pharmacol. Exp. Ther.* 300, 355–360. doi:10.1124/jpet.300.2.355

Hwang, M. F., Beechinor, R. J., Wade, K. C., Benjamin, D. K., Smith, P. B., Hornik, C. P., et al. (2017). External Evaluation of Two Fluconazole Infant Population Pharmacokinetic Models. *Antimicrob. Agents Chemother.* 61, e01352–17. doi:10.1128/AAC.01352-17

Ince, I., de Wildt, S. N., Wang, C., Wang, C., Peeters, M. Y. M., Burggraaf, J., et al. (2013). A Novel Maturation Function for Clearance of the Cytochrome P450 3A Substrate Midazolam from Preterm Neonates to Adults. *Clin. Pharmacokinet.* 52, 555–565. doi:10.1007/s40262-013-0050-0

Ishii, N., Kono, Y., Yonemoto, N., Kusuda, S., and Fujimura, M.Neonatal Research Network, Japan (2013). Outcomes of Infants Born at 22 and 23 Weeks' Gestation. *Pediatrics* 132, 62–71. doi:10.1542/peds.2012-2857

Italian Collaborative Group on Preterm Delivery (1991). Absorption of Intramuscular Vitamin E in Premature Babies. *Dev. Pharmacol. Ther.* 16, 13–21. doi:10.1159/000480550

Jiang, Z., Gao, X., Liang, J., and Ni, S. (2021). Simultaneous Quantitation of Serum Caffeine and its Metabolites by Ultra-high-performance Liquid Chromatography–Tandem Mass Spectrometry for CYP1A2 Activity Prediction in Premature Infants. *Biomed. Chromatogr.* 35, e5141. doi:10.1002/bmc.5141

Jm, B., Nj, V., Ehj, K., Aj, V., E, J.-A., Jma, van. G., et al. (2018). Predicting CYP3A-Mediated Midazolam Metabolism in Critically Ill Neonates, Infants, Children and Adults with Inflammation and Organ Failure. *Br. J. Clin. Pharmacol.* 84, 358–368. doi:10.1111/bcp.13459

Johnson, P. J. (2011). Neonatal Pharmacology-Ppharmacokinetics. *Neonatal. Netw. NN* 30, 54–61. doi:10.1891/0730-0832.30.1.54

Kafetzis, D. A., Sinaniotis, C. A., Papadatos, C. J., and Kosmidis, J. (1979). Pharmacokinetics of Amikacin in Infants and Pre-school Children. *Acta Paediatr. Scand.* 68, 419–422. doi:10.1111/j.1651-2227.1979.tb05030.x

Kawade, N., and Onishi, S. (1981). The Prenatal and Postnatal Development of UDP-Glucuronyltransferase Activity towards Bilirubin and the Effect of Premature Birth on This Activity in the Human Liver. *Biochem. J.* 196, 257–260. doi:10.1042/bj1960257

Kearns, G. L., Abdel-Rahman, S. M., Alander, S. W., Blowey, D. L., Leeder, J. S., and Kauffman, R. E. (2003). Developmental Pharmacology-Ddrug Disposition, Action, and Therapy in Infants and Children. *N. Engl. J. Med.* 349, 1157–1167. doi:10.1056/NEJMra035092

Kim, S. E., Kim, B.-H., Lee, S., Sohn, J. A., Kim, H.-S., Cho, J.-Y., et al. (2013). Population Pharmacokinetics of Theophylline in Premature Korean Infants. *Ther. Drug Monit.* 35, 338–344. doi:10.1097/FTD.0b013e3182866695

Knibbe, C. A. J., Krekels, E. H. J., van den Anker, J. N., DeJongh, J., Santen, G. W. E., van Dijk, M., et al. (2009). Morphine Glucuronidation in Preterm Neonates, Infants and Children Younger Than 3 Years. *Clin. Pharmacokinet.* 48, 371–385. doi:10.2165/00003088-200948060-00003

Krekels, E. H. J., van Ham, S., Allegaert, K., de Hoon, J., Tibboel, D., Danhof, M., et al. (2015). Developmental Changes rather Than Repeated Administration Drive Paracetamol Glucuronidation in Neonates and Infants. *Eur. J. Clin. Pharmacol.* 71, 1075–1082. doi:10.1007/s00228-015-1887-y

Ku, L. C., and Smith, P. B. (2015). Dosing in Neonates: Special Considerations in Physiology and Trial Design. *Pediatr. Res.* 77, 2–9. doi:10.1038/pr.2014.143

Le Doare, K., Barber, N., Doerholt, K., and Sharland, M. (20132013). Rifampicin Pharmacokinetics in Extreme Prematurity to Treat Congenital Tuberculosis. *BMJ Case Rep.*, bcr2012008207. doi:10.1136/bcr-2012-008207

Lee, T. C., Charles, B. G., Harte, G. J., Gray, P. H., Steer, P. A., and Flenady, V. J. (1999). Population Pharmacokinetic Modeling in Very Premature Infants Receiving Midazolam during Mechanical Ventilation: Midazolam Neonatal Pharmacokinetics. *Anesthesiology* 90, 451–457. doi:10.1097/00000542-199902000-00020

Leroux, S., Jacqz-Aigrain, E., Elie, V., Legrand, F., Barin-Le Guellec, C., Aurich, B., et al. (2018). Pharmacokinetics and Safety of Fluconazole and Micafungin in Neonates with Systemic Candidiasis: a Randomized, Open-Label Clinical Trial. *Br. J. Clin. Pharmacol.* 84, 1989–1999. doi:10.1111/bcp.13628

Li, Q., Wu, Y.-E., Wang, K., Shi, H.-Y., Zhou, Y., Zheng, Y., et al. (2021). Developmental Pharmacogenetics of CYP2D6 in Chinese Children: Loratadine as a Substrate Drug. *Front. Pharmacol.* 12, 1396. doi:10.3389/fphar.2021.657287

Liggins, G. C., and Howie, R. N. (1972). A Controlled Trial of Antepartum Glucocorticoid Treatment for Prevention of the Respiratory Distress Syndrome in Premature Infants. *Pediatrics* 50, 515–525. doi:10.1542/peds.50.4.515

Liu, X., Chen, C., and Smith, B. J. (2008). Progress in Brain Penetration Evaluation in Drug Discovery and Development. *J. Pharmacol. Exp. Ther.* 325, 349–356. doi:10.1124/jpet.107.130294

Loughnan, P. M., Greenwald, A., Purton, W. W., Aranda, J. V., Watters, G., and Neims, A. H. (1977). Pharmacokinetic Observations of Phenytoin Disposition in the Newborn and Young Infant. *Arch. Dis. Child.* 52, 302–309. doi:10.1136/adc.52.4.302

Lowry, J. A., Jarrett, R. V., Wasserman, G., Pettett, G., and Kauffman, R. E. (2001). Theophylline Toxicokinetics in Premature Newborns. *Arch. Pediatr. Adolesc. Med.* 155, 934–939. doi:10.1001/archpedi.155.8.934

Mahmood, I. (2017). Prediction of Clearance, Volume of Distribution, and Half-Life of Drugs in Extremely Low to Low Birth Weight Neonates: An Allometric Approach. *Eur. J. Drug Metab. Pharmacokinet.* 42, 601–610. doi:10.1007/s13318-016-0372-z

Mahmood, I. (2015). Prediction of Glucuronidated Drug Clearance in Pediatrics (≤5 Years): An Allometric Approach. *Eur. J. Drug Metab. Pharmacokinet.* 40, 53–59. doi:10.1007/s13318-014-0178-9

McGoldrick, E., Stewart, F., Parker, R., and Dalziel, S. R. (2020). Antenatal Corticosteroids for Accelerating Fetal Lung Maturation for Women at Risk of Preterm Birth. *Cochrane Database Syst. Rev.* 12, CD004454. doi:10.1002/14651858.CD004454.pub4

Memon, N., Griffin, I. J., Lee, C. W., Herdt, A., Weinberger, B. I., Hegyi, T., et al. (2020). Developmental Regulation of the Gut-Liver (FGF19-Cyp7a1) axis in Neonates. *J. Matern.-Fetal Neonatal. Med. Off. J. Eur. Assoc. Perinat. Med. Fed. Asia Ocean. Perinat. Soc. Int. Soc. Perinat. Obstet.* 33, 987–992. doi:10.1080/14767058.2018.1513483

Hwang, M. F., Beechinor, R. J., Wade, K. C., Benjamin, D. K., Jr, Smith, P. B., et al. (2017). External Evaluation of Two Fluconazole Infant Population Pharmacokinetic Models. *Antimicrob. Agents Chemother.* 61. doi:10.1128/AAC.01352-17

Michelet, R., Van Bocxlaer, J., Allegaert, K., and Vermeulen, A. (2018). The Use of PBPK Modeling across the Pediatric Age Range Using Propofol as a Case. *J. Pharmacokinet. Pharmacodyn.* 45, 765–785. doi:10.1007/s10928-018-9607-8

Momper, J. D., Capparelli, E. V., Wade, K. C., Kantak, A., Dhanireddy, R., Cummings, J. J., et al. (2016). Population Pharmacokinetics of Fluconazole in Premature Infants with Birth Weights Less Than 750 Grams. *Antimicrob. Agents Chemother.* 60, 5539–5545. doi:10.1128/AAC.00963-16

De Carolis, M. P., Muzii, U., Romagnoli, C., Zuppa, A. A., Zecca, E., and Tortorolo, G. (1989). Phenobarbital for Treatment of Seizures in Preterm Infant: a New Administration Scheme. *Dev. Pharmacol. Ther.* 14, 84–89. doi:10.1159/000480923

Mugabo, P., Els, I., Smith, J., Rabie, H., Smith, P., Mirochnick, M., et al. (2011). Nevirapine Plasma Concentrations in Premature Infants Exposed to Single-Dose Nevirapine for Prevention of Mother-To-Child Transmission of HIV-1. *South. Afr. Med. J. Suid-afr. Tydskr. Vir Geneeskd.* 101, 655–658.

Mulhall, A., de Louvois, J., and Hurley, R. (1983a). Chloramphenicol Toxicity in Neonates: its Incidence and Prevention. *Br. Med. J. Clin. Res. Ed.* 287, 1424–1427. doi:10.1136/bmj.287.6403.1424

Mulugeta, L. Y., Yao, L., Mould, D., Jacobs, B., Florian, J., Smith, B., et al. (2018). Leveraging Big Data in Pediatric Development Programs: Proceedings from the 2016 American College of Clinical Pharmacology Annual Meeting Symposium. *Clin. Pharmacol. Ther.* 104, 81–87. doi:10.1002/cpt.975

Munro, D. D. (1976). The Effect of Percutaneously Absorbed Steroids on Hypothalamic--pituitary--adrenal function after intensive use in in-patients. *Br. J. Dermatol.* 94 (Suppl. 12), 67–76. doi:10.1111/j.1365-2133.1976.tb02272.x

Neyro, V., Elie, V., Médard, Y., and Jacqz-Aigrain, E. (2018). mRNA expression of drug metabolism enzymes and transporter genes at birth using human umbilical cord blood. *Fundam. Clin. Pharmacol.* 32, 422–435. doi:10.1111/fcp.12357

Ng, E., Taddio, A., and Ohlsson, A. (2012). Intravenous midazolam infusion for sedation of infants in the neonatal intensive care unit. *Cochrane Database Syst. Rev.* 13, CD002052. doi:10.1002/14651858.CD002052.pub2

Norman, M., Hallberg, B., Abrahamsson, T., Björklund, L. J., Domellöf, M., Farooqi, A., et al. (2019). Association Between Year of Birth and 1-Year Survival Among Extremely Preterm Infants in Sweden During 2004-2007 and 2014-2016. *JAMA* 321, 1188–1199. doi:10.1001/jama.2019.2021

Ogawa, Y., Irikura, M., Kobaru, Y., Tomiyasu, M., Kochiyama, Y., Uriu, M., et al. (2015). Population pharmacokinetics of doxapram in low-birth-weight Japanese infants with apnea. *Eur. J. Pediatr.* 174, 509–518. doi:10.1007/s00431-014-2416-1

O'Hara, K., Martin, J. H., and Schneider, J. J. (2020). Barriers and Challenges in Performing Pharmacokinetic Studies to Inform Dosing in the Neonatal Population. *Pharm. Basel Switz.* 8, E16. doi:10.3390/pharmacy8010016

O'Hara, K., Wright, I. M. R., Schneider, J. J., Jones, A. L., and Martin, J. H. (2015). Pharmacokinetics in neonatal prescribing: evidence base, paradigms and the future. *Br. J. Clin. Pharmacol.* 80, 1281–1288. doi:10.1111/bcp.12741

Onishi, S., Kawade, N., Itoh, S., Isobe, K., and Sugiyama, S. (1979). Postnatal development of uridine diphosphate glucuronyltransferase activity towards bilirubin and 2-aminophenol in human liver. *Biochem. J.* 184, 705–707. doi:10.1042/bj1840705

Pain, J. B., Lê, M. P., Caseris, M., Amiel, C., Lassel, L., Charpentier, C., et al. (2015). Pharmacokinetics of dolutegravir in a premature neonate after HIV treatment intensification during pregnancy. *Antimicrob. Agents Chemother.* 59, 3660–3662. doi:10.1128/AAC.00173-15

Painter, M. J., Pippenger, C., Wasterlain, C., Barmada, M., Pitlick, W., Carter, G., et al. (1981). Phenobarbital and phenytoin in neonatal seizures: metabolism and tissue distribution. *Neurology* 31, 1107–1112. doi:10.1212/wnl.31.9.1107

Pierrat, V., Marchand-Martin, L., Marret, S., Arnaud, C., Benhammou, V., Cambonie, G., et al. (2021). Neurodevelopmental outcomes at age 5 among children born preterm: EPIPAGE-2 cohort study. *BMJ* 373, n741. doi:10.1136/bmj.n741

Pitlick, W., Painter, M., and Pippenger, C. (1978). Phenobarbital pharmacokinetics in neonates. *Clin. Pharmacol. Ther.* 23, 346–350. doi:10.1002/cpt1978233346

Reiter, P. D., and Stiles, A. D. (1993). Lorazepam toxicity in a premature infant. *Ann. Pharmacother.* 27, 727–729. doi:10.1177/106002809302700611

Ribon, B., Brazier, J. L., Claris, O., Cortambert, F., Chouchane, N., Bannier, A., et al. (1984). Pharmacokinetic study in the premature newborn of a lyophilized form of phenobarbital. *Dev. Pharmacol. Ther.* 7 (Suppl. 1), 177–184. doi:10.1159/000457250

Rj, K., Tl, C., P, G., Jl, R., and Rl, W. (1990). Effect of phenobarbital administration on theophylline clearance in premature neonates. *Ther. Drug Monit.* 12, 139–143. doi:10.1097/00007691-199003000-00005

Rojas-Reyes, M. X., Morley, C. J., and Soll, R. (2012). Prophylactic versus selective use of surfactant in preventing morbidity and mortality in preterm infants. *Cochrane Database Syst. Rev.* 14, CD000510. doi:10.1002/14651858.CD000510.pub2

Roth-Cline, M., Gerson, J., Bright, P., Lee, C. S., and Nelson, R. M. (2011). Ethical considerations in conducting pediatric research. *Handb. Exp. Pharmacol.* 205, 219–244. doi:10.1007/978-3-642-20195-0_11

Ruggiero, S., Clavenna, A., Reale, L., Capuano, A., Rossi, F., and Bonati, M. (2014). Guanfacine for attention deficit and hyperactivity disorder in pediatrics: a systematic review and meta-analysis. *Eur. Neuropsychopharmacol. J. Eur. Coll. Neuropsychopharmacol.* 24, 1578–1590. doi:10.1016/j.euroneuro.2014.08.001

Saigal, S., and Doyle, L. W. (2008). An overview of mortality and sequelae of preterm birth from infancy to adulthood. *Lancet Lond. Engl.* 371, 261–269. doi:10.1016/S0140-6736(08)60136-1

Sardesai, S., Biniwale, M., Wertheimer, F., Garingo, A., and Ramanathan, R. (2017). Evolution of surfactant therapy for respiratory distress syndrome: past, present, and future. *Pediatr. Res.* 81, 240–248. doi:10.1038/pr.2016.203

Sato, J., Kudo, N., Owada, E., Ito, K., Niida, Y., Umetsu, M., et al. (1997). Urinary excretion of mefenamic acid and its metabolites including their esterglucuronides in preterm infants undergoing mefenamic acid therapy. *Biol. Pharm. Bull.* 20, 443–445. doi:10.1248/bpb.20.443

Schmidt, B., Roberts, R. S., Davis, P., Doyle, L. W., Barrington, K. J., Ohlsson, A., et al. (2006). Caffeine therapy for apnea of prematurity. *N. Engl. J. Med.* 354, 2112–2121. doi:10.1056/NEJMoa054065

Schrier, L., Hadjipanayis, A., Stiris, T., Ross-Russell, R. I., Valiulis, A., Turner, M. A., et al. (2020). Off-label use of medicines in neonates, infants, children, and adolescents: a joint policy statement by the European Academy of Paediatrics and the European society for Developmental Perinatal and Pediatric Pharmacology. *Eur. J. Pediatr.* 179, 839–847. doi:10.1007/s00431-019-03556-9

Shah, P. S., Dunn, M., Lee, S. K., Allen, A. C., and Singhal, N.Canadian Neonatal Network (2011). Early opioid infusion and neonatal outcomes in preterm neonates ≤28 weeks' gestation. *Am. J. Perinatol.* 28, 361–366. doi:10.1055/s-0030-1270112

Sharma, A., Ford, S., and Calvert, J. (2008). Adaptation for life: a review of neonatal physiology. *Anaesth. Intensive Care Med.* 9 (3), 93–98. doi:10.1016/j.mpaic.2008.01.009

Smith, P. B., Cotten, C. M., Hudak, M. L., Sullivan, J. E., Poindexter, B. B., Cohen-Wolkowiez, M., et al. (2019). Rifampin Pharmacokinetics and Safety in Preterm and Term Infants. *Antimicrob. Agents Chemother.* 63, e00284–19. doi:10.1128/AAC.00284-19

Smits, A., Annaert, P., Cavallaro, G., De Cock, P. A. J. G., de Wildt, S. N., Kindblom, J. M., et al. (2021). Current knowledge, challenges and innovations in developmental pharmacology: A combined conect4children Expert Group and European Society for Developmental, Perinatal and Paediatric Pharmacology White Paper. *Br. J. Clin. Pharmacol. N/a.* Online ahead of print doi:10.1111/bcp.14958

Sohn, J. A., Kim, H.-S., Oh, J., Cho, J.-Y., Yu, K.-S., Lee, J., et al. (2017). Prediction of serum theophylline concentrations and cytochrome P450 1A2 activity by analyzing urinary metabolites in preterm infants. *Br. J. Clin. Pharmacol.* 83, 1279–1286. doi:10.1111/bcp.13211

Stark, A., Smith, P. B., Hornik, C. P., Zimmerman, K. O., Hornik, C. D., Pradeep, S., et al. (2021). Medication Use in the Neonatal Intensive Care Unit and Changes from 2010 to 2018. *J. Pediatr.* S0022-3476 (21), 00860–X. doi:10.1016/j.jpeds.2021.08.075

Stevens, T. P., Harrington, E. W., Blennow, M., and Soll, R. F. (2007). Early surfactant administration with brief ventilation vs. selective surfactant and continued mechanical ventilation for preterm infants with or at risk for respiratory distress syndrome. *Cochrane Database Syst. Rev.* 17, CD003063. doi:10.1002/14651858.CD003063.pub3

Sung, S. I., Ahn, S. Y., Yoo, H. S., Chang, Y. S., and Park, W. S. (2018). The Youngest Survivor with Gestational Age of $21^{5}/_{7}$ Weeks. *J. Korean Med. Sci.* 33, e22. doi:10.3346/jkms.2018.33.e22

Sweet, D. G., Carnielli, V., Greisen, G., Hallman, M., Ozek, E., Te Pas, A., et al. (2019). European Consensus Guidelines on the Management of Respiratory Distress Syndrome - 2019 Update. *Neonatology* 115, 432–450. doi:10.1159/000499361

Tayman, C., Rayyan, M., and Allegaert, K. (2011). Neonatal pharmacology: extensive interindividual variability despite limited size. *J. Pediatr. Pharmacol. Ther. JPPT Off. J. PPAG* 16, 170–184. doi:10.5863/1551-6776-16.3.170

Tetelbaum, M., Finkelstein, Y., Nava-Ocampo, A. A., and Koren, G. (2005). Back to basics: understanding drugs in children: pharmacokinetic maturation. *Pediatr. Rev.* 26, 321–328. doi:10.1542/pir.26-9-321

Tiniest Babies Registry. University of Iowa.Available at: https://webapps1.healthcare.uiowa.edu/TiniestBabies/getInfantList.aspx (Accessed January 8, 2022).

Touw, D. J., Graafland, O., Cranendonk, A., Vermeulen, R. J., and van Weissenbruch, M. M. (2000). Clinical pharmacokinetics of phenobarbital in neonates. *Eur. J. Pharm. Sci. Off. J. Eur. Fed. Pharm. Sci.* 12, 111–116. doi:10.1016/s0928-0987(00)00145-7

Treluyer, J. M., Gueret, G., Cheron, G., Sonnier, M., and Cresteil, T. (1997). Developmental expression of CYP2C and CYP2C-dependent activities in the human liver: in-vivo/in-vitro correlation and inducibility. *Pharmacogenetics* 7, 441–452. doi:10.1097/00008571-199712000-00002

Tsakiri, S., Aneji, C., Domonoske, C., Mazur, L., Benjamin, D. K., and Wootton, S. H. (2018). Voriconazole Treatment for an Infant With Intractable Candida glabrata Meningitis. *Pediatr. Infect. Dis. J.* 37, 999–1001. doi:10.1097/INF.0000000000002073

Tserng, K. Y., Takieddine, F. N., and King, K. C. (1983). Developmental aspects of theophylline metabolism in premature infants. *Clin. Pharmacol. Ther.* 33, 522–528. doi:10.1038/clpt.1983.71

van den Anker, J., and Allegaert, K. (2021). Considerations for Drug Dosing in Premature Infants. *J. Clin. Pharmacol.* 61 (Suppl. 1), S141. –S151. doi:10.1002/jcph.1884

van den Anker, J., Reed, M. D., Allegaert, K., and Kearns, G. L. (2018). Developmental Changes in Pharmacokinetics and Pharmacodynamics. *J. Clin. Pharmacol.* 58 (Suppl. 10), S10. doi:10.1002/jcph.1284

Van Driest, S. L., and Choi, L. (2019). Real-World Data for Pediatric Pharmacometrics: Can We Upcycle Clinical Data for Research Use. *Clin. Pharmacol. Ther.* 106, 84–86. doi:10.1002/cpt.1416

van Groen, B. D., Vaes, W. H., Park, B. K., Krekels, E. H. J., van Duijn, E., Kõrgvee, L.-T., et al. (2019). Dose-linearity of the pharmacokinetics of an intravenous [14C]midazolam microdose in children. *Br. J. Clin. Pharmacol.* 85, 2332–2340. doi:10.1111/bcp.14047

Vauzelle-Kervroedan, F., Rey, E., Pariente-Khayat, A., Bienvenu, T., Badoual, J., Olive, G., et al. (1996). Non invasive *In Vivo* study of the maturation of CYP IIIA in neonates and infants. *Eur. J. Clin. Pharmacol.* 51, 69–72. doi:10.1007/s002280050162

Völler, S., Flint, R. B., Stolk, L. M., Degraeuwe, P. L. J., Simons, S. H. P., Pokorna, P., et al. (2017). Model-based clinical dose optimization for phenobarbital in neonates: An illustration of the importance of data sharing and external validation. *Eur. J. Pharm. Sci. Off. J. Eur. Fed. Pharm. Sci.* 109S, S90. –S97. doi:10.1016/j.ejps.2017.05.026

Wade, K. C., Benjamin, D. K., Kaufman, D. A., Ward, R. M., Smith, P. B., Jayaraman, B., et al. (2009). Fluconazole dosing for the prevention or treatment of invasive candidiasis in young infants. *Pediatr. Infect. Dis. J.* 28, 717–723. doi:10.1097/INF.0b013e31819f1f50

Wade, K. C., Wu, D., Kaufman, D. A., Ward, R. M., Benjamin, D. K., Sullivan, J. E., et al. (2008). Population pharmacokinetics of fluconazole in young infants. *Antimicrob. Agents Chemother.* 52, 4043–4049. doi:10.1128/AAC.00569-08

Wang, C., Sadhavisvam, S., Krekels, E. H. J., Dahan, A., Tibboel, D., Danhof, M., et al. (2013). Developmental changes in morphine clearance across the entire paediatric age range are best described by a bodyweight-dependent exponent model. *Clin. Drug Investig.* 33, 523–534. doi:10.1007/s40261-013-0097-6

Ward, R. M., Tammara, B., Sullivan, S. E., Stewart, D. L., Rath, N., Meng, X., et al. (2010). Single-dose, multiple-dose, and population pharmacokinetics of pantoprazole in neonates and preterm infants with a clinical diagnosis of gastroesophageal reflux disease (GERD). *Eur. J. Clin. Pharmacol.* 66, 555–561. doi:10.1007/s00228-010-0811-8

Wenzl, T. G., Schefels, J., Hörnchen, H., and Skopnik, H. (1998). Pharmacokinetics of oral fluconazole in premature infants. *Eur. J. Pediatr.* 157, 661–662. doi:10.1007/s004310050906

Windorfer, A., Kuenzer, W., and Urbanek, R. (1974). The influence of age on the activity of acetylsalicylic acid-esterase and protein-salicylate binding. *Eur. J. Clin. Pharmacol.* 7, 227–231. doi:10.1007/BF00560385

Windorfer, A., and Pringsheim, W. (1977). Studies on the concentrations of chloramphenicol in the serum and cerebrospinal fluid of neonates, infants, and small children. Reciprocal reactions between chloramphenicol, penicillin and phenobarbitone. *Eur. J. Pediatr.* 124, 129–138. doi:10.1007/BF00477548

World Health Organization (2004). ICD-10 : international statistical classification of diseases and related health problems : tenth revision. Available at: https://apps.who.int/iris/handle/10665/42980 (Accessed January 10, 2022).

Xu, C., Li, C. Y.-T., and Kong, A.-N. T. (2005). Induction of phase I, II and III drug metabolism/transport by xenobiotics. *Arch. Pharm. Res.* 28, 249–268. doi:10.1007/BF02977789

Zwart, L. D., Snoeys, J., Jacobs, F., Li, L. Y., Poggesi, I., Verboven, P., et al. (2021). Prediction of the drug-drug interaction potential of the alpha-acid glycoprotein bound, CYP3A4/CYP2C9 metabolized oncology drug. *Erdafitinib. CPT Pharmacomet. Syst. Pharmacol. N/a.* 10, 1107–1118. doi:10.1002/psp4.12682

**Conflict of Interest:** The authors declare that the research was conducted in the absence of any commercial or financial relationships that could be construed as a potential conflict of interest.

**Publisher's Note:** All claims expressed in this article are solely those of the authors and do not necessarily represent those of their affiliated organizations, or those of the publisher, the editors and the reviewers. Any product that may be evaluated in this article, or claim that may be made by its manufacturer, is not guaranteed or endorsed by the publisher.

frontiers in Pharmacology

PERSPECTIVE
published: 25 February 2022
doi: 10.3389/fphar.2022.833217

# Selective Serotonin Reuptake Inhibitor Pharmacokinetics During Pregnancy: Clinical and Research Implications

*Ethan A. Poweleit*[1,2,3,4], *Margaret A. Cinibulk*[5], *Sarah A. Novotny*[6], *Melissa Wagner-Schuman*[7], *Laura B. Ramsey*[3,4] *and Jeffrey R. Strawn*[3,7,8]*

[1]Division of Biomedical Informatics, Cincinnati Children's Hospital Medical Center, Cincinnati, OH, United States, [2]Department of Biomedical Informatics, University of Cincinnati College of Medicine, Cincinnati, OH, United States, [3]Department of Pediatrics, Division of Clinical Pharmacology, Cincinnati Children's Hospital Medical Center, University of Cincinnati College of Medicine, Cincinnati, OH, United States, [4]Department of Pediatrics, Division of Research in Patient Services, Cincinnati Children's Hospital Medical Center, University of Cincinnati College of Medicine, Cincinnati, OH, United States, [5]Department of Psychiatry and Behavioral Sciences, University of Southern California, Los Angeles, CA, United States, [6]Department of Obstetrics and Gynecology, Division of Maternal-Fetal Medicine, University of Mississippi, Jackson, MS, United States, [7]Department of Psychiatry and Behavioral Neuroscience, University of Cincinnati, Cincinnati, OH, United States, [8]Department of Pediatrics, Division of Child and Adolescent Psychiatry, Cincinnati Children's Hospital Medical Center, Cincinnati, OH, United States

Pregnancy and associated physiologic changes affect the pharmacokinetics of many medications, including selective serotonin reuptake inhibitors—the first-line pharmacologic interventions for depressive and anxiety disorders. During pregnancy, SSRIs exhibit extensive pharmacokinetic variability that may influence their tolerability and efficacy. Specifically, compared to non-pregnant women, the activity of cytochrome P450 (CYP) enzymes that metabolize SSRIs drastically changes (e.g., decreased CYP2C19 activity and increased CYP2D6 activity). This perspective examines the impact of pharmacokinetic genes—related to CYP activity on SSRI pharmacokinetics during pregnancy. Through a simulation-based approach, plasma concentrations for SSRIs metabolized primarily by CYP2C19 (e.g., escitalopram) and CYP2D6 (e.g., fluoxetine) are examined and the implications for dosing and future research are discussed.

**Keywords: anxiety, depression, pharmacokinctics, pregnancy, SSRI (selective serotonergic reuptake inhibitors)**

OPEN ACCESS

***Edited by:***
*Catherine M. T. Sherwin, Wright State University, United States*

***Reviewed by:***
*Andy Eugene, Medical University of Lublin, Poland*

***Correspondence:**
*Jeffrey R. Strawn*
*strawnjr@uc.edu*

***Specialty section:***
*This article was submitted to Obstetric and Pediatric Pharmacology, a section of the journal Frontiers in Pharmacology*

***Received:*** *10 December 2021*
***Accepted:*** *24 January 2022*
***Published:*** *25 February 2022*

***Citation:***
*Poweleit EA, Cinibulk MA, Novotny SA, Wagner-Schuman M, Ramsey LB and Strawn JR (2022) Selective Serotonin Reuptake Inhibitor Pharmacokinetics During Pregnancy: Clinical and Research Implications. Front. Pharmacol. 13:833217. doi: 10.3389/fphar.2022.833217*

## INTRODUCTION

Selective Serotonin Reuptake Inhibitors (SSRIs) are commonly used to treat depression and anxiety across the lifespan, including during pregnancy (Mesches et al., 2020). Among these SSRIs, citalopram, escitalopram, sertraline, fluvoxamine and fluoxetine are most commonly used during pregnancy, while paroxetine is used less frequently secondary to concerns related to the risk of congenital malformations including cardiac malformations (Bérard et al., 2016). In general, when SSRIs are used in pregnancy, there is a consideration of their benefits and risks, including the transient syndrome of neonatal SSRI withdrawal (Moses-Kolko et al., 2005), longer term developmental outcomes of fluoxetine-exposed children and reassuring data suggesting that *in utero* SSRI exposure does not affect IQ and language development (Nulman et al., 1997). Importantly, during pregnancy, plasma SSRI concentrations vary considerably—in part because of a surfeit of pregnancy-related changes in cytochrome P450 (CYP) activity. This variation in SSRI exposure may alter efficacy and tolerability, and necessitate dose adjustment in pregnant people.

Physiologic changes during pregnancy substantially alter SSRI pharmacokinetics **Table 1**. Pregnancy is associated with delayed gastric emptying, increased gastric pH, increased cardiac

output, increased total body water and extracellular fluid space, increased fat compartment, increased renal blood flow and glomerular filtration rate (GFR), decreased plasma albumin concentration, and altered cytochrome P450 activity (Pariente et al., 2016). Further, enhanced elimination and associated decreases in drug exposure (lower peak/trough plasma concentrations) decrease the availability of some medications during pregnancy (Pariente et al., 2016). Yet, despite pregnancy related variation in concentrations of multiple medications—including SSRIs—guidance on SSRI dosing during pregnancy is scarce, with only recommendations from the American College of Obstetrics and Gynecology that a single medication at a higher dose be used rather than multiple medications in treating depression during pregnancy (Tseng et al., 2015; Arnold and Flint, 2017). Further confounding drug metabolism in pregnancy is the potential metabolic contribution of the fetus and placenta. While predominately located in the liver, CYP enzymes are present in a variety of tissues including the human placenta. The fetal liver itself has potential to contribute to maternal drug metabolism, however a significant contribution is unlikely due to the relatively small mass (Hakkola et al., 1998).

Herein, we will focus on pregnancy-related changes in SSRI pharmacokinetics and how variation is influenced by maternal CYP2C19 and CYP2D6, two cytochrome enzymes whose activity is not only affected by pregnancy, but also affected by genetic variation in the genes that encode these enzymes. Additionally, we will briefly review variation in SSRI exposure during pregnancy using pharmacokinetic modeling simulations and propose next steps in understanding how variation in SSRI pharmacokinetics potentially affect clinical management of pregnant patients in terms of relapse, tolerability and withdrawal symptoms.

## VARIATION IN SSRI PHARMACOKINETICS

In contemporary clinical practice, treatment guidelines for anxiety or depressive disorders rarely incorporate factors that influence antidepressant exposure (other than dose). Moreover, intrinsic factors that affect SSRI concentrations are rarely considered in clinical trials of SSRIs. As such, the current approach to dosing SSRIs is to typically initiate antidepressant therapy at a 'starting dose' and to titrate based on response and tolerability. However, variation in SSRI exposure contributes to differences in efficacy and tolerability (Sakolsky et al., 2011; Strawn et al., 2020). Understanding this variation in pregnancy has important implications given the prevalence of drug discontinuation due to non-response and the burden of depressive and anxiety disorders during pregnancy.

SSRI exposure is affected by many factors (*e.g.*, age, concomitant medications, and CYP activity), as well as medication dose, amount, and dosing frequency. Further, CYP activity is influenced by genetic polymorphisms affecting the amount and/or function of the protein, age-related changes in the maturation of the enzyme and altered enzyme activity due to specific diseases, as well as inflammation. For some SSRIs, CYP activity—which varies among pregnancy—substantially impacts exposure (Area Under the Curve, AUC), maximum concentrations ($C_{MAX}$), and half-life ($t_{½}$). Pharmacogenetic factors that influence CYP activity are rarely included in current pharmacokinetic models yet understanding these contributions could enhance understanding of differences in SSRI pharmacokinetics, particularly during pregnancy, which itself accentuates this variation in exposure. Such interactions of pharmacogenetics as well as auto- or drug-based enzyme inhibition/induction, must be considered to develop precision dosing algorithms, especially during pregnancy.

## SSRI PHARMACOKINETICS AND PHARMACOGENETICS

Relationships between pharmacokinetically-relevant genes (e.g., *CYP2D6* and *CYP2C19*) and SSRI exposure have been established over the past 2 decades. Recently, a meta-analysis of 94 unique studies, revealed significant relationships between CYP2D6 and CYP2C19 metabolizer status and escitalopram, fluvoxamine, fluoxetine, paroxetine and sertraline exposure and reciprocal apparent total drug clearance (Milosavljević et al., 2021). Further, in non-pregnant patients, modeling studies and guidelines from the Clinical Pharmacogenetics Information Consortium (CPIC) and The Dutch Pharmacogenetics Working Group recommend that dosing for some SSRIs should consider variation in CYP2D6 and CYP2C19 (Hicks et al., 2015; Brouwer et al., 2021). Recommendations from the Food and Drug Administration (FDA) as well as the European Medicine Agency (EMA) are mixed with regard to variation in CYP2D6 and CYP2C19 and SSRIs. For example, the FDA recommends that coadministration of CYP2D6-metabolized medications with paroxetine should be approached with caution (GlaxoSmithKline, 2012), whereas for fluoxetine, the agency recommends, because fluoxetine inhibits CYP2D6 activity, "individuals with normal CYP2D6 metabolic activity resemble a poor metabolizer… [*eo ipso*] coadministration of fluoxetine with other drugs that aremetabolized by CYP2D6 should be approached with caution (Eli Lilly and Company, 2019)." Additionally, the package insert for fluoxetine notes that concentrations of s-fluoxetine are significantly higher in patients who are CYP2D6 poor metabolizers compared to normal metabolizers. However, the package inserts do not contain specific dosing guidance for either paroxetine or fluoxetine (GlaxoSmithKline, 2012; Eli Lilly and Company, 2019). For citalopram, the FDA-approved package insert recommends, based on an AUC increase of 68% in CYP2C19 poor metabolizers that these individuals not be treated with more than 20 mg/day given the risk of QT prolongation (Allergan USA, 2017). This guidance is reiterated in multiple sections of the document, including the dosing, arming and dosage/administration sections of the document. Further, the document also advises patients with CYP2C19 inhibitors not be treated with doses >20 mg/day (Allergan USA, 2017). Finally, the package inserts for escitalopram and sertraline do not provide any guidance regarding the impact of CYP2C19 phenotype on

dosing (Forest Pharmaceuticals, 2009). It is important to note that the FDA labels for most medications were approved before pharmacogenetic associations were well established, and inclusion of pharmacogenetic information occurred retroactively. For example, the anti-coagulant clopidogrel, which was approved in 1997 and had a boxed warning added in 2010 warning "diminished antiplatelet effect in patients with two loss-of-function alleles of the CYP2C19 gene" (Bristol-Myers Squibb and Sanofi Pharmaceuticals Partnership, 2021) However, the drug label still does not require pharmacogenetic testing (Roden and Shuldiner, 2010), which could place the manufacturer at legal risk.

## CYP2D6 and CYP2C19 Activity During Pregnancy

Pregnancy alters the activity of CYP2D6 and CYP2C19. Implicated in the metabolism of approximately 25% of all CYP-metabolized medications, CYP2D6 contributes to the metabolism of multiple SSRIs (e.g., fluoxetine, paroxetine, fluvoxamine). Further, genetic polymorphisms in the *CYP2D6* gene produce phenotypic differences: ultrarapid, normal, intermediate, and poor metabolizers (Caudle et al., 2020). However, during pregnancy, CYP2D6 activity across all phenotypes, except poor metabolizers, increases (Wadelius et al., 1997; Tracy et al., 2005; Ryu et al., 2016). CYP2D6 poor metabolizers have no enzymatic activity given the combination of two no function alleles, so increases in activity for patients with this phenotype may be negligible to nonexistent during pregnancy.

CYP2C19 is the primary enzyme involved in the metabolism of escitalopram, citalopram, and sertraline, as well as many other medications (e.g., proton pump inhibitors, clopidogrel). Similar to CYP2D6, polymorphisms in the CYP2C19 gene produce phenotypes of ultrarapid, rapid, normal, intermediate, and poor metabolizers (Caudle et al., 2017). Small studies have reported CYP2C19 activity decreases during pregnancy (McGready et al., 2003). Like CYP2D6 poor metabolizers, we suspect CYP2C19 poor metabolizers to have trivial decreases in activity, if any at all, during pregnancy due to individuals with this phenotype having two CYP2C19 no function alleles. For several medications, this pregnancy-related variation in CYP2D6 and CYP2C19 activity has been associated with increased clearance of metoprolol (Hogstedt et al., 1985), clonidine, anti-retrovirals and glyburide. Moreover, several lines of evidence suggest the need to titrate several medications during pregnancy (Tasnif et al., 2016).

# SSRI PHARMACOKINETICS DURING PREGNANCY

Fewer than a dozen *in vivo* and modeling studies have examined SSRI pharmacokinetics in pregnant women (Heikkinen et al., 2002; Heikkinen et al., 2003; Freeman et al., 2008; Sit et al., 2008; Ververs et al., 2009; Sit et al., 2011; Westin et al., 2017), in addition to two modeling-based explorations of SSRI pharmacokinetics in pregnant women (Almurjan et al., 2020; Almurjan et al., 2021). To extend these findings and to illustrate how baseline phenotypic variation in CYP enzymes may affect pregnancy-associated changes in SSRI pharmacokinetics, we simulated escitalopram and fluoxetine concentrations at steady state during pregnancy and compared to a non-pregnant state across metabolizer phenotypes. We estimated the pregnancy-associated changes using MwPharm (version 3.82, Mediware, Czech Republic), a pharmacokinetic modeling program that enables users to approximate a patient's clearance, volume of distribution, exposure, and concentration of individual medications (e.g., escitalopram and fluoxetine + norfluoxetine) based on previously published parameters (Schenker et al., 1988; Søgaard et al., 2005). A one-compartment and two-compartment model were used for escitalopram and fluoxetine + norfluoxetine, respectively. CYP2C19- and CYP2D6-related differences in clearance for escitalopram and fluoxetine + norfluoxetine, respectively, were determined based on previously published studies (Chang et al., 2014; Steere et al., 2015; Magalhães et al., 2020). Model parameters for each medication were entered, in addition to patient characteristics, including age, body size, sex, and medication/dosing history. Considering patient and medication information, the program simulates a time course of medication plasma concentrations for a patient, in addition to their estimated effects. Physiological changes during pregnancy (e.g., total body weight, creatinine clearance) were based on published parameters (Abduljalil et al., 2012) and NHANES data (Fryar et al., 2021); these parameters were reviewed by a board-certified maternal-fetal medicine physician (SAN) and complete model parameters can be found in the supplement (**Supplementary Table S1-S3**).

For a non-pregnant woman treated with escitalopram (20 mg/day), escitalopram concentrations vary significantly across CYP2C19 phenotypes, with rapid and ultrarapid metabolizers having steady state trough concentrations below the lower therapeutic reference range of 15 ng/ml (**Figure 1**). By trimesters 2 (week 20) and 3 (week 33), there is an estimated decrease in CYP2C19 activity by 62 and 68%, respectively, resulting in trough concentrations for all metabolizer phenotypes within the therapeutic range (McGready et al., 2003; Ke et al., 2014) (**Figure 1**). CYP2C19 poor, intermediate, and normal metabolizers are expected to have similar escitalopram concentrations by trimester 2 due to activity levels bottoming out, with poor metabolizers having slightly lower concentrations compared to pre-pregnancy due to increases in weight and creatinine clearance (Abduljalil et al., 2012). Escitalopram simulated data are available in the supplement (**Supplementary Material**).

We also evaluated the influence of CYP2D6 phenotypes on the pharmacokinetics of fluoxetine and its active metabolite, norfluoxetine. Steady state concentrations were within the expected therapeutic reference range at a dose of 40 mg/day during a non-pregnant state (Hiemke et al., 2018) (**Figure 2**). By trimester 2 (week 20), CYP2D6 activity is estimated to increase by 131% compared to a non-pregnancy, and trough concentrations of the active moiety for all metabolizer phenotypes are within the therapeutic reference range (Tracy et al., 2005; Abduljalil et al., 2012; Hiemke et al., 2018) (**Figure 2**). CYP2D6 activity is increased by 137% by trimester 3 (week 33), with trough concentrations still within the therapeutic reference range for all phenotypes (**Figure 2**). Fluoxetine + norfluoxetine simulated data are available in the supplement (**Supplementary Material**).

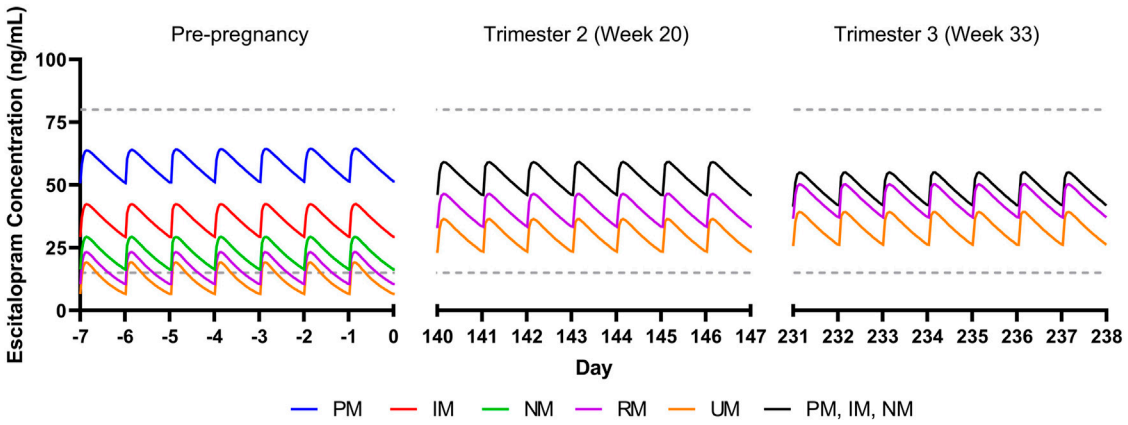


**FIGURE 1 |** Modeled escitalopram concentrations in pregnancy for CYP2C19 phenotypes. PM, poor metabolizer; IM, intermediate metabolizer, NM, normal metabolizer; RM, rapid metabolizer, UM, ultrarapid metabolizer. Dashed gray lines represent therapeutic trough concentrations (Hiemke et al., 2018).

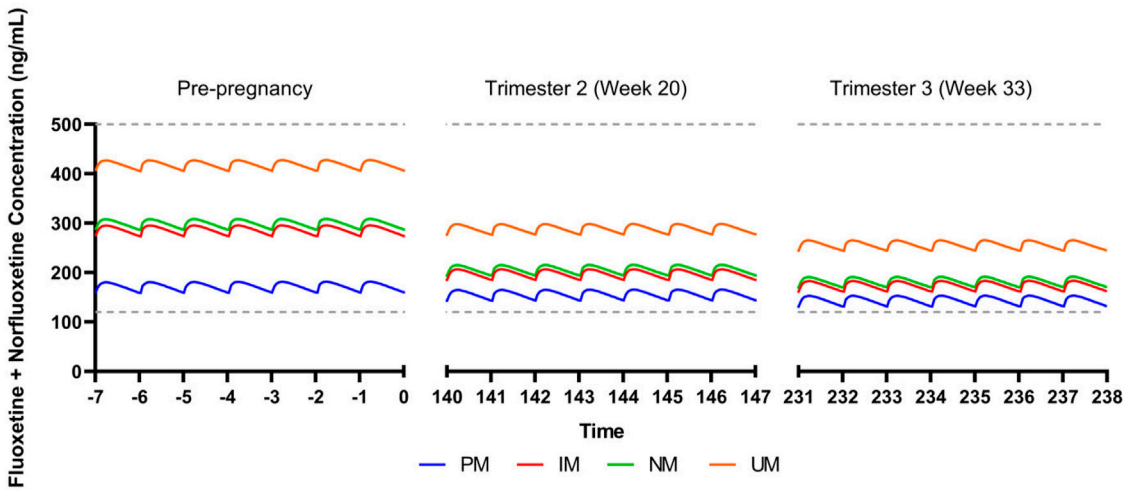


**FIGURE 2 |** Modeled fluoxetine and norfluoxetine concentrations in pregnancy for patients treated with fluoxetine 40 mg/day. CYP2D6 phenotypes are shown as follows: PM, poor metabolizer; IM, intermediate metabolizer; NM, normal metabolizer; RM, rapid metabolizer; UM, ultrarapid metabolizer. Dashed gray lines represent therapeutic trough concentrations (Hiemke et al., 2018).

Our simulations reflect differences in escitalopram and fluoxetine pharmacokinetics while accounting for each drug's primary metabolizing enzyme (CYP2C19 and CYP2D6, respectively), in addition to changes in total body weight and creatinine clearance. While this perspective precludes extensive physiological-based pharmacokinetic modeling that account for additional parameters that are relevant during pregnancy, these simulations reveal significant heterogeneity in SSRI concentrations due to CYP enzymes. Of note, our escitalopram model demonstrates an increase in concentrations for CYP2C19 intermediate, normal, rapid, and ultrarapid metabolizers relative to pre-pregnancy, which contrasts literature showing an overall decrease in escitalopram concentrations throughout gestation (Sit et al., 2008). Whereas we only accounted for CYP2C19, induction of CYP3A4 and CYP2D6 during pregnancy may partially mitigate in CYP2C19 activity, thereby decreasing escitalopram concentrations in later pregnancy (Desta et al., 2002; Tracy et al., 2005). Further, despite trough concentrations being within the therapeutic window for escitalopram and fluoxetine + norfluoxetine, clinicians should monitor changes in target symptoms and tolerability, especially later in pregnancy where SSRI concentrations differ significantly. Models accounting for multiple CYP enzymes involved in the metabolic pathway of these medications, among other pertinent parameters, are needed to further understand the complexity of SSRI pharmacokinetics during pregnancy (Betcher and George, 2020). This may be particularly important in some specific populations and, as an example, in Chinese individuals, CYP2C19 poor metabolizers had a mean 46% increase in fluoxetine $C_{MAX}$ and similar increases

**TABLE 1 |** Selective serotonin reuptake inhibitors (SSRIs) and cytochrome P450 enzymes responsible for their metabolism, as well as changes in the activity of these cytochromes during pregnancy.

| SSRI | Relative change in concentration | References | Enzymes | Activity in pregnancy |
|---|---|---|---|---|
| Citalopram | ↓ | Heikkinen et al. (2002) | CYP2C19 | Decrease |
| | ↓ | Sit et al. (2008) | CYP2D6 | Increase |
| | ↓ | Westin et al. (2017) | CYP3A4 | Increase |
| Escitalopram | ↓ | Sit et al. (2008) | CYP2C19 | Decrease |
| | ↔ | Westin et al. (2017) | CYP2D6 | Increase |
| | | | CYP3A4 | Increase |
| Paroxetine | ↕ | Ververs et al. (2009) | CYP2D6 | Increase |
| | ↓ | Westin et al. (2017) | CYP3A4 | Increase |
| Fluvoxamine | ↓ | Westin et al. (2017) | CYP2D6 | Increase |
| | | | CYP1A2 | Decrease |
| Fluoxetine | ↓ | Heikkinen et al. (2003) | CYP2D6 | Increase |
| | ↓ | Sit et al., 2010 | CYP2C9 | Increase |
| | ↔ | Westin et al. (2017) | | |
| Sertraline | ↓ | Sit et al. (2008) | CYP2C19 | Decrease |
| | ↓ | Freeman et al. (2008) | CYP2B6 | Increase |
| | ↑ | Westin et al. (2017) | CYP2C9 | Increase |
| | ↓ | Heinonen et al. (2021) | CYP2D6 | Increase |

*Abbreviations: SSRI, selective serotonin reuptake inhibitor.*

*↓, decrease in concentration. ↑, increase in concentration. ↕, dependent on the CYP2D6 metabolizer phenotype. ↔, no significant change across pregnancy.*

in $AUC_{(0,\infty)}$ compared to normal metabolizers (Liu et al., 2001). Thus, future investigations of fluoxetine and paroxetine pharmacokinetics, including those in pregnancy, may benefit from including non-CYP2D6 phenotypes. Finally, no studies (or models) have examined the impact of transcription regulators of CYP450 activity in pregnancy, although these transcription regulators (e.g., testis-specific Y-encoded-like protein [TSPYLs]) affect the activity of CYP2C19 and other P450 enzymes (Qin et al., 2018). Recent studies suggest that some single nucleotide polymorphisms may decrease suppression of CYP2C19 expression and boost metabolism of some CYP2C19-metabolized SSRIs, including escitalopram and citalopram, and even alter improvement trajectories in escitalopram and citalopram-treated adults with depressive disorders (Qin et al., 2020).

Beyond these models, two population pharmacokinetic modeling studies previously examined pregnancy-related changes in paroxetine (Almurjan et al., 2020) and sertraline (Almurjan et al., 2021) concentrations with regard to CYP2D6 and CYP2C19 metabolizer status, respectively. These studies aimed to identify "appropriate dose titration strategies to stabilize" medication concentrations within therapeutic ranges during pregnancy. For paroxetine, a significant number of pregnant ultrarapid metabolizers had trough concentrations < 20 ng/ml compared to normal metabolizers and this study suggested that for most phenotypes, pregnant women may require doses >20 mg day to maintain an exposure comparable to 20 mg daily pre-pregnancy (Almurjan et al., 2020). In a virtual modeling study of sertraline pharmacokinetics in pregnancy, trough sertraline concentrations decreased throughout pregnancy. Some of this decreased exposure was related to expansion in maternal volume and decreased albumin. However, titration of sertraline was needed for patients of all CYP2C19 phenotypes. Normal and ultrarapid metabolizers needed doses between 100 and 150 mg daily (throughout the pregnancy). However, poor metabolizers needed a dose of 50 mg daily during the first trimester and then required titration to 100 mg daily during the second and third trimester (Almurjan et al., 2021).

## THERAPEUTIC DRUG MONITORING OF SSRIS DURING PREGNANCY

Given temporal variation in physiology and drug metabolism throughout pregnancy, therapeutic drug monitoring could facilitate understanding of differences in SSRI exposure and remission during gestation. Though most women take one or more medications during pregnancy, clinical trials often exclude pregnant women, so exposure data are lacking for many medications in pregnant women (NICHD Obstetric and Pediatric Pharmacology and Therapeutics Branch, 2021). Recently, the Eunice Kennedy Shriver National Institute of Child Health and Human Development (NICHD) Obstetric and Pediatric Pharmacology and Therapeutics Branch recognized the knowledge gaps in the use of therapeutics in children, pregnant, and lactating people. The resulting strategic plan that aims to advance safe and effective therapeutics for pregnant and lactating people acknowledges that "a key requirement for the advancement of therapeutics that can restore the foundation for healthy pregnancies is understanding how drug action is altered during normal

pregnancy, the post-partum period, and lactation" (NICHD Obstetric and Pediatric Pharmacology and Therapeutics Branch, 2021). Drug action may change during pregnancy because of myriad mechanisms, including pharmacokinetic and pharmacodynamic effects. The NICHD Obstetric and Pediatric Pharmacology and Therapeutics Branch established the Maternal and Pediatric Precision in Therapeutics Hub to aggregate knowledge about maternal and pediatric therapeutics (NICHD Obstetric and Pediatric Pharmacology and Therapeutics Branch, 2021). We look forward to seeing this hub and the research projects funded by this mechanism advance precision therapeutics in pregnancy.

## CONCLUSION AND FUTURE DIRECTIONS

Pregnancy is associated with induction of many enzymes, including CYP2D6, CYP2C9 (as well as CYP3A4, CYP2E1) and these shifts subtend differences in SSRI metabolism during pregnancy. However, pharmacokinetic data from prospective studies in pregnant women are rare and infrequently consider intrinsic variation in cytochromes activity. Importantly, several approaches may address the dearth of pharmacokinetic data in pregnancy and extend model-based recommendations that have been developed for sertraline and paroxetine (Almurjan et al., 2020; Almurjan et al., 2021). Phlebotomy performed during usual care permits opportunistic sampling, an approach that has been used to examine developmental pharmacokinetics of many medications—including SSRIs—in children (Girdwood et al., 2021). Additionally, population PK studies may provide additional information regarding the pregnancy-related pharmacokinetic changes as they relate to variation in CYP phenotypes. These simulation studies also have the potential to examine the impact of dose changes which may normalize exposure related to pregnancy-related shifts in pharmacokinetic parameters and CYP phenotypes (Almurjan et al., 2020; Almurjan et al., 2021). While understanding the effects of this variation in SSRI pharmacokinetics and the underlying differences in pharmacokinetic genes on SSRI exposure in pregnancy is in its early stages, multiple applications can already be imagined. These include identifying patients at risk of symptomatic worsening as result of decreased SSRI exposure, recognizing SSRI withdrawal symptoms related to increased SSRI metabolism in previously stably treated patients and correctly attributing side effect to pregnancy-related shifts in SSRI exposure. Further, the increasing prevalence of obesity and morbid obesity and effects on adequate medication exposure is poorly understood in pregnancy. Weight may play a significant role in treating depression and anxiety in pregnancy, particularly given that several studies have demonstrated relationships between body mass index and response in antidepressant-treated patients. Incorporating the contribution of obesity on CYP enzyme activity in future models could further enhance our understanding of variation in exposure and thereby decreasing treatment failure. Concomitant medications—which are common in pregnancy—may produce phenoconversion for several CYP enzymes. In pregnant people, the effects of phenoconversion, or even its magnitude throughout pregnancy, are poorly understood. Finally, future studies must examine factors that contribute to pregnancy-related variation in exposure. These factors include changes in renal clearance, which increases during the first trimester, peaks in the second trimester, and diminishes at the end of pregnancy as well as changes in target engagement (e.g., pharmacodynamics).

## DATA AVAILABILITY STATEMENT

The original contributions presented in the study are included in the article/**Supplementary Material**, further inquiries can be directed to the corresponding author.

## AUTHOR CONTRIBUTIONS

Conceptualization, EP, MC, SN, JS, and LR; methodology, EP, LR; resources, JS and LR; writing—original draft preparation, MC, EP, JS, and LR; writing—review and editing, all authors; visualization, EP, LR; supervision, LR and JS.; project administration, LR and JS funding acquisition, LR and JS All authors have read and agreed to the published version of the manuscript.

## FUNDING

This research was funded by the Eunice Kennedy Shriver National Institute of Child Health and Development (LR and JS), Grant number R01HD099775, R01HD098757 (JRS). This work was also supported by the Young Family Foundation (JRS).

## ACKNOWLEDGMENTS

The authors thank Ashley Specht, BBA (University of Cincinnati, Department of Psychiatry and Behavioral Neuroscience, Anxiety Disorders Research Program) for her review and editorial assistance.

## SUPPLEMENTARY MATERIAL

The Supplementary Material for this article can be found online at: https://www.frontiersin.org/articles/10.3389/fphar.2022.833217/full#supplementary-material

## REFERENCES


Abduljalil, K., Furness, P., Johnson, T. N., Rostami-Hodjegan, A., and Soltani, H. (2012). Anatomical, Physiological and Metabolic Changes with Gestational Age during normal Pregnancy: A Database for Parameters Required in Physiologically Based Pharmacokinetic Modelling. *Clin. Pharmacokinet.* 51 (6), 365–396. doi:10.2165/11597440-000000000-00000

Allergan USA (2017). Citalopram [package Insert]. Irvine, CA. Available at: https://www.accessdata.fda.gov/drugsatfda_docs/label/2017/020822s047lbl.pdf (Accessed February 5, 2022).

Almurjan, A., Macfarlane, H., and Badhan, R. K. S. (2020). Precision Dosing-Based Optimisation of Paroxetine during Pregnancy for Poor and Ultrarapid CYP2D6 Metabolisers: a Virtual Clinical Trial Pharmacokinetics Study. *J. Pharm. Pharmacol.* 72 (8), 1049–1060. doi:10.1111/jphp.13281

Almurjan, A., Macfarlane, H., and Badhan, R. K. S. (2021). The Application of Precision Dosing in the Use of Sertraline throughout Pregnancy for Poor and Ultrarapid Metabolizer CYP 2C19 Subjects: A Virtual Clinical Trial Pharmacokinetics Study. *Biopharm. Drug Dispos.* 42 (6), 252–262. doi:10.1002/bdd.2278

Arnold, K. C., and Flint, C. J. (2017). "Use of Psychiatric Medications during Pregnancy and Lactation," in *Obstetrics Essentials* Washington, DC: Springer, 75–81. doi:10.1007/978-3-319-57675-6_12

Bérard, A., Iessa, N., Chaabane, S., Muanda, F. T., Boukhris, T., and Zhao, J. P. (2016). The Risk of Major Cardiac Malformations Associated with Paroxetine Use during the First Trimester of Pregnancy: a Systematic Review and Meta-Analysis. *Br. J. Clin. Pharmacol.* 81 (4), 589–604. doi:10.1111/bcp.12849

Betcher, H. K., and George, A. L. (2020). Pharmacogenomics in Pregnancy. *Semin. Perinatol* 44 (3), 151222. doi:10.1016/j.semperi.2020.151222

Bristol-Myers Squibb and Sanofi Pharmaceuticals Partnership (2021). Plavix [Package Insert]. Bridgewater, NJ. Available at: https://www.accessdata.fda.gov/drugsatfda_docs/label/2021/020839s074lbl.pdf (Accessed February 5, 2022).

Brouwer, J. M. J. L., Nijenhuis, M., Soree, B., Guchelaar, H.-J., Swen, J. J., van Schaik, R. H. N., et al. (2021). Dutch Pharmacogenetics Working Group (DPWG) Guideline for the Gene-Drug Interaction between CYP2C19 and CYP2D6 and SSRIs. *Eur. J. Hum. Genet.* [Epub ahead of print]. doi:10.1038/s41431-021-01004-7

Caudle, K. E., Dunnenberger, H. M., Freimuth, R. R., Peterson, J. F., Burlison, J. D., Whirl-Carrillo, M., et al. (2017). Standardizing Terms for Clinical Pharmacogenetic Test Results: Consensus Terms from the Clinical Pharmacogenetics Implementation Consortium (CPIC). *Genet. Med.* 19 (2), 215–223. doi:10.1038/gim.2016.87

Caudle, K. E., Sangkuhl, K., Whirl-Carrillo, M., Swen, J. J., Haidar, C. E., Klein, T. E., et al. (2020). Standardizing CYP2D6 Genotype to Phenotype Translation: Consensus Recommendations from the Clinical Pharmacogenetics Implementation Consortium and Dutch Pharmacogenetics Working Group. *Clin. Transl. Sci.* 13 (1), 116–124. doi:10.1111/cts.12692

Chang, M., Tybring, G., Dahl, M.-L., and Lindh, J. D. (2014). Impact of Cytochrome P450 2C19 Polymorphisms on Citalopram/Escitalopram Exposure: A Systematic Review and Meta-Analysis. *Clin. Pharmacokinet.* 53, 801–811. doi:10.1007/s40262-014-0162-1

Desta, Z., Zhao, X., Shin, J. G., and Flockhart, D. A. (2002). Clinical Significance of the Cytochrome P450 2C19 Genetic Polymorphism. *Clin. Pharmacokinet.* 41 (12), 913–958. doi:10.2165/00003088-200241120-00002

Eli Lilly and Company (2019). Fluoxetine [package Insert]. Indianapolis. Available at: https://www.accessdata.fda.gov/drugsatfda_docs/label/2017/018936s108lbl.pdf (Accessed February 5, 2022).

Forest Pharmaceuticals (2009). Escitalopram [package Insert]. St. Louis. Available at: https://www.accessdata.fda.gov/drugsatfda_docs/label/2009/021323s032,021365s023lbl.pdf (Accessed February 5, 2022).

Freeman, M. P., Nolan, P. E., Davis, M. F., Anthony, M., Fried, K., Fankhauser, M., et al. (2008). Pharmacokinetics of Sertraline across Pregnancy and Postpartum. *J. Clin. Psychopharmacol.* 28 (6), 646–653. doi:10.1097/JCP.0b013e31818d2048

Fryar, C. D., Gu, Q., Ogden, C. L., Flegal, K. M., and Ogden, C. L. (2021). Anthropometric Reference Data for Children and Adults: United States, 2011-2014. *Vital Health Stat. 3* (36), 1–46.

Girdwood, S. T., Kaplan, J., and Vinks, A. A. (2021). Methodologic Progress Note: Opportunistic Sampling for Pharmacology Studies in Hospitalized Children. *J. Hosp. Med.* 16 (1), 35–37. doi:10.12788/jhm.3380

GlaxoSmithKline (2012). Paroxetine Hydrochloride [package Insert]. Research Triangle Park. Available at: https://www.accessdata.fda.gov/drugsatfda_docs/label/2012/020031s067%2C020710s031.pdf (Accessed February 5, 2022).

Hakkola, J., Pelkonen, O., Pasanen, M., and Raunio, H. (1998). Xenobiotic-Metabolizing Cytochrome P450 Enzymes in the Human Feto-Placental Unit: Role in Intrauterine Toxicity. *Crit. Rev. Toxicol.* 28, 35–72. doi:10.1080/10408449891344173

Heikkinen, T., Ekblad, U., Kero, P., Ekblad, S., and Laine, K. (2002). Citalopram in Pregnancy and Lactation. *Clin. Pharmacol. Ther.* 72 (2), 184–191. doi:10.1067/mcp.2002.126181

Heikkinen, T., Ekblad, U., Palo, P., and Laine, K. (2003). Pharmacokinetics of Fluoxetine and Norfluoxetine in Pregnancy and Lactation. *Clin. Pharmacol. Ther.* 73 (4), 330–337. doi:10.1016/S0009-9236(02)17634-X

Heinonen, E., Blennow, M., Blomdahl-Wetterholm, M., Hovstadius, M., Nasiell, J., Pohanka, A., et al. (2021). Sertraline Concentrations in Pregnant Women are Steady and the Drug Transfer to their Infants is Low. *Eur. J. Clin. Pharmacol.* 77 (9), 1323–1331.

Hicks, J. K., Bishop, J. R., Sangkuhl, K., Müller, D. J., Ji, Y., Leckband, S. G., et al. (2015). Clinical Pharmacogenetics Implementation Consortium (CPIC) Guideline for CYP2D6 and CYP2C19 Genotypes and Dosing of Selective Serotonin Reuptake Inhibitors. *Clin. Pharmacol. Ther.* 98 (2), 127–134. doi:10.1002/cpt.147

Hiemke, C., Bergemann, N., Clement, H. W., Conca, A., Deckert, J., Domschke, K., et al. (2018). Consensus Guidelines for Therapeutic Drug Monitoring in Neuropsychopharmacology: Update 2017. *Pharmacopsychiatry* 51 (1–2), e1. doi:10.1055/s-0037-1600991

Högstedt, S., Lindberg, B., Peng, D. R., Regårdh, A., Deckert, C. G., Rane, A., et al. (1985). Pregnancy-Induced Increase in Metoprolol Metabolism. *Clin. Pharmacol. Ther.* 37 (6), 688–92. doi:10.1055/s-0037-1600991

Ke, A. B., Nallani, S. C., Zhao, P., Rostami-Hodjegan, A., and Unadkat, J. D. (2014). Expansion of a PBPK Model to Predict Disposition in Pregnant Women of Drugs Cleared via Multiple CYP Enzymes, Including CYP2B6, CYP2C9 and CYP2C19. *Br. J. Clin. Pharmacol.* 77 (3), 554–570. doi:10.1111/bcp.12207

Liu, Z. Q., Cheng, Z. N., Huang, S. L., Chen, X. P., Ou-Yang, D. S., Jiang, C. H., et al. (2001). Effect of the CYP2C19 Oxidation Polymorphism on Fluoxetine Metabolism in Chinese Healthy Subjects. *Br. J. Clin. Pharmacol.* 52 (1), 96–99. doi:10.1046/j.0306-5251.2001.01402.x

Magalhães, P., Alves, G., Fortuna, A., Llerena, A., and Falcão, A. (2020). Pharmacogenetics and Therapeutic Drug Monitoring of Fluoxetine in a Real-World Setting: A PK/PD Analysis of the Influence of (Non-)genetic Factors. *Exp. Clin. Psychopharmacol.* 28 (5), 589–600. doi:10.1037/pha0000334

McGready, R., Stepniewska, K., Seaton, E., Cho, T., Cho, D., Ginsberg, A., et al. (2003). Pregnancy and Use of Oral Contraceptives Reduces the Biotransformation of Proguanil to Cycloguanil. *Eur. J. Clin. Pharmacol.* 59 (7), 553–557. doi:10.1007/s00228-003-0651-x

Mesches, G. A., Wisner, K. L., and Betcher, H. K. (2020). A Common Clinical Conundrum: Antidepressant Treatment of Depression in Pregnant Women. *Semin. Perinatol.* 44 (3), 151229. doi:10.1016/j.semperi.2020.151229

Milosavljevic, F., Bukvic, N., Pavlovic, Z., Miljevic, C., Pešic, V., Molden, E., et al. (2021). Association of CYP2C19 and CYP2D6 Poor and Intermediate Metabolizer Status with Antidepressant and Antipsychotic Exposure. *JAMA Psychiatry* 78, 270. doi:10.1001/jamapsychiatry.2020.3643

Moses-Kolko, E. L., Bogen, D., Perel, J., Bregar, A., Uhl, K., Levin, B., et al. (2005). Neonatal Signs after Late In Utero Exposure to Serotonin Reuptake Inhibitors. *JAMA* 293, 2372. doi:10.1001/jama.293.19.2372

NICHD Obstetric and Pediatric Pharmacology and Therapeutics Branch (2021). Maternal and Pediatric Precision in Therapeutics (MPRINT) Hub. Available at: https://www.nichd.nih.gov/about/org/der/branches/opptb/mprint#overview (Accessed December 5, 2021).

Nulman, I., Rovet, J., Stewart, D. E., Wolpin, J., Gardner, H. A., Theis, J. G., et al. (1997). Neurodevelopment of Children Exposed In Utero to Antidepressant Drugs. *N. Engl. J. Med.* 336 (4), 258–262. doi:10.1056/nejm199701233360404

Pariente, G., Leibson, T., Carls, A., Adams-Webber, T., Ito, S., and Koren, G. (2016). Pregnancy-Associated Changes in Pharmacokinetics: A Systematic Review. *Plos Med.* 13 (11), e1002160. doi:10.1371/journal.pmed.1002160

Qin, S., Liu, D., Kohli, M., Wang, L., Vedell, P. T., Hillman, D. W., et al. (2018). TSPYL Family Regulates CYP17A1 and CYP3A4 Expression: Potential Mechanism Contributing to Abiraterone Response in Metastatic Castration-Resistant Prostate Cancer. *Clin. Pharmacol. Ther.* 104 (1), 201–210. doi:10.1002/cpt.907

Qin, S., Eugene, A. R., Liu, D., Zhang, L., Neavin, D., Biernacka, J. M., et al. (2020). Dual Roles for the TSPYL Family in Mediating Serotonin Transport and the Metabolism of Selective Serotonin Reuptake Inhibitors in Patients with Major Depressive Disorder. *Clin. Pharmacol. Ther.* 107 (3), 662–670. doi:10.1002/cpt.1692

Roden, D. M., and Shuldiner, A. R. (2010). Responding to the Clopidogrel Warning by the US Food and Drug Administration. *Circulation* 122, 445–448. doi:10.1161/CIRCULATIONAHA.110.973362

Ryu, R. J., Eyal, S., Easterling, T. R., Caritis, S. N., Venkataraman, R., Hankins, G., et al. (2016). Pharmacokinetics of Metoprolol during Pregnancy and Lactation. *J. Clin. Pharmacol.* 56 (5), 581–589. doi:10.1002/jcph.631

Sakolsky, D. J., Perel, J. M., Emslie, G. J., Clarke, G. N., Wagner, K. D., Vitiello, B., et al. (2011). Antidepressant Exposure as a Predictor of Clinical Outcomes in the Treatment of Resistant Depression in Adolescents (TORDIA) Study. *J. Clin. Psychopharmacol.* 31, 92. doi:10.1097/jcp.0b013e318204b117

Schenker, S., Bergstrom, R. F., Wolen, R. L., and Lemberger, L. (1988). Fluoxetine Disposition and Elimination in Cirrhosis. *Clin. Pharmacol. Ther.* 44 (3), 353–359. doi:10.1038/clpt.1988.161

Sit, D. K., Perel, J. M., Helsel, J. C., and Wisner, K. L. (2008). Changes in Antidepressant Metabolism and Dosing across Pregnancy and Early Postpartum. *J. Clin. Psychiatry* 69 (4), 652–658. doi:10.4088/jcp.v69n0419

Sit, D., Perel, J. M., Luther, J. F., Wisniewski, S. R., Helsel, J. C., and Wisner, K. L. (2010). Disposition of Chiral and Racemic Fluoxetine and Norfluoxetine Across Childbearing. *J. Clin. Psychopharmacol.* 30 (4), 381–6.

Sit, D., Perel, J. M., Wisniewski, S. R., Helsel, J. C., Luther, J. F., and Wisner, K. L. (2011). Mother-infant Antidepressant Concentrations, Maternal Depression, and Perinatal Events. *J. Clin. Psychiatry* 72 (7), 994–1001. doi:10.4088/JCP.10m06461

Søgaard, B., Mengel, H., Rao, N., and Larsen, F. (2005). The Pharmacokinetics of Escitalopram after Oral and Intravenous Administration of Single and Multiple Doses to Healthy Subjects. *J. Clin. Pharmacol.* 45 (12), 1400–1406. doi:10.1177/0091270005280860

Steere, B., Baker, J. A., Hall, S. D., and Guo, Y. (2015). Prediction of *In Vivo* Clearance and Associated Variability of CYP2C19 Substrates by Genotypes in Populations Utilizing a Pharmacogenetics-Based Mechanistic Model. *Drug Metab. Dispos.* 43 (6), 870–883. doi:10.1124/dmd.114.061523

Strawn, J. R., Mills, J. A., Schroeder, H., Mossman, S. A., Varney, S. T., Ramsey, L. B., et al. (2020). Escitalopram in Adolescents with Generalized Anxiety Disorder: A Double-Blind, Randomized, Placebo-Controlled Study. *J. Clin. Psychiatry* 81 (5), e1–e9. doi:10.4088/JCP.20m13396

Tasnif, Y., Morado, J., and Hebert, M. F. (2016). Pregnancy-related Pharmacokinetic Changes. *Clin. Pharmacol. Ther.* 100 (1), 53–62. doi:10.1002/cpt.382

Tracy, T. S., Venkataramanan, R., Glover, D. D., and Caritis, S. N. (2005). Temporal Changes in Drug Metabolism (CYP1A2, CYP2D6 and CYP3A Activity) during Pregnancy. *Am. J. Obstet. Gynecol.* 192 (2), 633–639. doi:10.1016/j.ajog.2004.08.030

Tseng, D., Hvidding, J., and Ona, C. (2015). International Comparison of Current Guidelines for Use of Psychotropic Medications during Pregnancy and Lactation (2015 Updates). *J. Obstet. Gynaecol. Res.* 41 (Suppl. 1), 113.

Ververs, F. F., Voorbij, H. A., Zwarts, P., Belitser, S. V., Egberts, T. C., Visser, G. H., et al. (2009). Effect of Cytochrome P450 2D6 Genotype on Maternal Paroxetine Plasma Concentrations during Pregnancy. *Clin. Pharmacokinet.* 48 (10), 677–683. doi:10.2165/11318050-000000000-00000

Wadelius, M., Darj, E., Frenne, G., and Rane, A. (1997). Induction of CYP2D6 in Pregnancy. *Clin. Pharmacol. Ther.* 62 (4), 400–407. doi:10.1016/S0009-9236(97)90118-1

Westin, A. A., Brekke, M., Molden, E., Skogvoll, E., and Spigset, O. (2017). Selective Serotonin Reuptake Inhibitors and Venlafaxine in Pregnancy: Changes in Drug Disposition. *PLoS ONE* 12 (7), e0181082. doi:10.1371/journal.pone.0181082

**Conflict of Interest:** The authors declare that the research was conducted in the absence of any commercial or financial relationships that could be construed as a potential conflict of interest.

**Publisher's Note:** All claims expressed in this article are solely those of the authors and do not necessarily represent those of their affiliated organizations, or those of the publisher, the editors, and the reviewers. Any product that may be evaluated in this article, or claim that may be made by its manufacturer, is not guaranteed or endorsed by the publisher.

frontiers in Pediatrics

ORIGINAL RESEARCH
published: 02 March 2022
doi: 10.3389/fped.2022.837492

# Pharmacometric Analysis of Intranasal and Intravenous Nalbuphine to Optimize Pain Management in Infants

*Miriam Pfiffner[1]*, Eva Berger-Olah[2], Priska Vonbach[1,3], Marc Pfister[4†] and Verena Gotta[4†]*

*[1] Hospital Pharmacy, University Children's Hospital Zurich, Zurich, Switzerland, [2] Emergency Unit, University Children's Hospital Zurich, Zurich, Switzerland, [3] PEDeus, A Subsidiary of the University Children's Hospital Zurich, Zurich, Switzerland, [4] Pediatric Pharmacology and Pharmacometrics Research Center, University Children's Hospital Basel (UKBB), Basel, Switzerland*

**Objectives:** The objective of this pharmacometric (PMX) study was to (i) characterize population pharmacokinetics (PPK) and exposure-pain response associations following intranasal (0.1 mg/kg) or intravenous (IV, 0.05 mg/kg) administration of nalbuphine, with the goal to (ii) evaluate strategies for optimized dosing and timing of painful interventions in infants 1–3 months old.

**Methods:** PPK analysis of nalbuphine serum concentrations, prospectively collected 15, 30, and between 120 and 180 min post-dose, utilizing the software package Monolix. The final PPK model was applied to derive individual time-matched concentration predictions for each pain assessment (Neonatal Infant Pain Score, NIPS) after establishment of venous access and urinary catheterization or lumbar puncture. Drug exposure-pain response simulations were performed to evaluate potential benefits of higher doses with respect to a previously proposed target concentration of 12 mcg/L (efficacy threshold).

**Results:** Thirty-eight of 52 study subjects receiving nalbuphine had at least one concentration measurement and were included in the pharmacometric analysis. A two-compartment model with allometric scaling was applied to describe population PK data, with intranasal bioavailability estimated to be 41% (95%CI: 26–56%). Model-based simulations showed that the proposed efficacy threshold (12 mcg/L) is expected to be exceeded with an IV dose of 0.05 mg/kg for 6 min, with 0.1 mg/kg for 30 min and with 0.2 mg/kg for 80 min. This efficacy threshold is not achieved with intranasal doses of 0.1 and 0.2 mg/kg, whereas an intranasal dose of 0.4 mg/kg is expected to exceed such threshold for 30 to 100 min.

**Conclusion:** This PMX study confirmed that bioavailability of intranasal nalbuphine is close to 50%. Exposure-pain response simulations indicated that an intranasal dose of 0.4 mg/kg is required to provide a comparable pain control as achieved with an IV dose of 0.1–0.2 mg/kg. The optimal time window for painful procedures appears to be within

OPEN ACCESS

***Edited by:***
*Catherine M. T. Sherwin, Wright State University, United States*

***Reviewed by:***
*Pavla Pokorna, Charles University, Czechia*
*Jonathan Michael Davis, Tufts University, United States*

****Correspondence:***
*Miriam Pfiffner*
*miriam.pfiffner@kispi.uzh.ch*

*† These authors share last authorship*

***Specialty section:***
*This article was submitted to Obstetric and Pediatric Pharmacology, a section of the journal Frontiers in Pediatrics*

***Received:*** *16 December 2021*
***Accepted:*** *24 January 2022*
***Published:*** *02 March 2022*

***Citation:***
*Pfiffner M, Berger-Olah E, Vonbach P, Pfister M and Gotta V (2022) Pharmacometric Analysis of Intranasal and Intravenous Nalbuphine to Optimize Pain Management in Infants. Front. Pediatr. 10:837492. doi: 10.3389/fped.2022.837492*

the first 30 min after IV administration of 0.1 mg/kg nalbuphine, whereas such procedures should be scheduled 30 min after an intranasal dose of 0.4 mg/kg nalbuphine. Additional clinical studies are warranted to confirm these PMX based recommendations and to further optimize pain management in this vulnerable infant population.

**Keywords: nalbuphine, opioid analgesics, pharmacokinetics, pharmacodynamics, exposure response, infants, pediatrics**

## INTRODUCTION

Nalbuphine is an opioid analgesic agent that is used for the treatment of moderate to severe pain. Due to its unique mixed agonist and partial antagonist properties (on kappa and mu opioid receptors, respectively), it shows a lower ceiling effect on respiratory depression compared to mu receptor agonists such as morphine or fentanyl (1–3). For this reason it is frequently used in pediatric patients, including infants and neonates (4–6). Although nalbuphine has been approved more than 20 years ago, pharmacokinetic data on the drug remain limited, especially in children and optimal dosing is not well characterized in infants and young children (4–10). As the drug undergoes extensive and variable first-pass metabolism, nalbuphine is usually given parenterally (1, 4, 8). The metabolism of nalbuphine involves phase I oxidation–reduction *via* Cytochrome P450 to 25% (*via* CYP2C9 and CYP2C19) and phase II glucuronidation *via* UDP-glucuronosyltransferases to 75% (UGT2B7, UGT1A3, and UGT1A9) (11).

We have previously investigated whether intranasal administration could be a non-invasive alternative route of administration in infants 1–3 months of age for interventional pain management, as establishing venous access can be particularly time-consuming, difficult and stressful in this age group (12–16). Despite expected different pharmacokinetic profiles after intravenous (IV) and intranasal administration, we observed overall comparable tolerability and exposure coverage in terms of area under the concentration time curve during the first 2.5 h following single administration of 0.1 mg/kg intranasal vs. 0.05 mg/kg IV nalbuphine. However, a relatively high proportion of study subjects exhibited severe pain as assessed by neonatal infant pain score (NIPS), and a previously proposed target concentration of 12 mcg/L (in children >1 years under continuous infusion) (4), was achieved neither by IV nor intranasal administration in this study.

Population pharmacokinetic and exposure-pain response modeling are pharmacometric (PMX) tools that can facilitate evaluation and optimization of current dosing in young children with the goal to further improve pain control and optimize timing of interventions (17, 18). As such, key objectives of this PMX study were (i) to characterize population pharmacokinetics after single IV and intranasal administration in infants 1–3 months of age, (ii) to explore exposure-pain response associations in these pediatric patients, and (iii) to perform PMX-based simulations to evaluate and optimize dosing strategies in this vulnerable pediatric patient population.

**Abbreviations:** IV, intravenous; PMX, pharmacometric; PPK, population pharmacokinetics; NIPS, neonatal infant pain score; CL, clearance; Q, intercompartmental clearance; V, volume of distribution; V1, central compartment volume; $C_{max}$, maximum serum concentration; $t_{max}$, time to reach maximum serum concentration; $t_{1/2}$, terminal half-life; AUC, area under the concentration time curve; IQR, interquartile range; $k_a$, rate constant; CYPs, cytochrome P450s; UGTs, UDP-glucuronosyltransferases.

## TRIAL DESIGN, PARTICIPANTS AND INTERVENTIONS

Data used for this analysis originates from a prospective, single center, open-label pharmacokinetic and safety study performed in the interdisciplinary emergency department at the University Children's Hospital Zurich between 2017 and 2018 (ClinicalTrials.gov Identifier: NCT03059511). Briefly, infants aged 29 days to 3 months with a minimum body weight of 3.0 kg and fever without a source requiring interventional pain management for diagnostic procedures were eligible, while preterm infants with kidney or liver disease were excluded.

After parental informed consent was obtained, study participants were alternately allocated to either 0.05 mg/kg IV or 0.1 mg/kg intranasal nalbuphine (Nalbuphin OrPha® 20 mg/2 ml, OrPha Swiss, Kuesnacht, Switzerland). The relative intranasal dosage was based on intranasal bioavailability reported for other opioids; according to lipophilicity and molecular weight we expected nalbuphine intranasal bioavailability between 50 and 80% (15, 19). It should be noted that the Swiss health authority Swissmedic defined the upper limit of nalbuphine doses to be investigated in our pediatric study (0.05 mg/kg IV compared to 0.1 mg/kg intranasal nalbuphine). To create ideal conditions to enhance nasal absorption, a nasal device [Mucosal Atomization Device (MAD 300) Teleflex, USA] was used to atomize the drug particles and each nostril was cleaned before drug administration. With the expected volume of 0.03–0.1 ml we expected minimal run-off (14, 15, 19).

Blood samples [0.5 ml blood, in line with recommendations (20)] for nalbuphine serum concentration measurement were obtained 15, 30, and 120 to 180 min post-dose. Painful diagnostic interventions, including establishment of venous access for blood sampling, urinary catheterization and lumbar puncture were carried out 5 min before, 20 and 35 min after drug administration in the IV study group and 5, 20 and 35 min after drug administration in the intranasal study group, respectively. Pain score during each painful intervention was assessed by NIPS (in-house standard) (21, 22).

## Serum Drug Analysis

Nalbuphine serum levels were measured using liquid chromatography coupled to tandem mass spectrometry. The lower limit of quantification was 0.1 mcg/L, the upper limit of quantification 2,500 mcg/L. Intra- and interday assay precision was $< 8.15\%$ and $< 5.3\%$, respectively.

## Pharmacometric Modeling and Simulation

### PMX Based Pharmacokinetic Analyses

Data were analyzed by population pharmacokinetic (PPK) modeling, including all study subjects for whom at least one serum concentration sample was obtained. Implausible serum concentrations were defined as rising concentrations after iv administration, or concentrations >60 mcg/L (>200 mcg/L in a sensitivity analysis), corresponding to a theoretical distribution volume of <0.83 L/kg (<0.25 L/kg respectively), i.e., much lower than estimated from previously reported volume of distribution of $3.62 \pm 1.77$ L/kg in children 1.5–5 years (6), and were excluded from the primary analysis.

PPK model development was conducted using the software Monolix (version 2018R2, Antony, France: Lixoft SAS, 2018). IV data was modeled separately in a first step, and then fitted simultaneously with intranasal data to estimate average intranasal bioavailability. Monolix version 2020R1 was used to refit the final model and to perform model simulations in combination with Simulx in R (R Core Team, https://www.R-project.org/). Further statistics and figures were also created using R.

#### Structural Model

Both one- and two-compartment models were tested to describe the distribution kinetics of nalbuphine after IV administration. According to literature the elimination was assumed to follow first-order elimination kinetics (4, 7). Several models were tested for description of the absorption kinetics following inclusion of intranasal data, such as simple first- and zero order absorption, with/without lag-time, using one or several transit-compartments, with/without accidental enteral absorption (23).

#### Statistical Model

Inter-individual variability of model parameters was assumed to be log-normally distributed. For the residual error, both proportional and mixed error models were tested for both iv and intranasal data.

#### Covariate Analysis

Standard allometric scaling was used to account for the expected relationship between body size and clearance (CL) and/or volume of distribution (V), respectively (fixed exponents of 0.75 and 1) (24). The association of model parameters with further potential covariates (age and gender) was guided by visual inspection of scatter plots of individual random effects vs. covariates (for parameters with small eta-shrinkage), by statistical testing (likelihood ratio test of model with vs. without covariate included) and decrease in random inter-individual variability.

#### Model Evaluation

Non-nested models were compared by their Akaike information criterion and nested models by the likelihood ratio test, based on comparison of the objective function value (corresponding to $-2 \times$ log-likelihood). Further model selection criteria were the decrease in inter-individual variability and residual error, relative standard error of parameters (target: ≤30% to maximal 50%) and state-of-the-art goodness of fit plots (observations vs. predictions, residual diagnostics, visual predictive check).

#### Sensitivity Analyses

Two sensitivity analyses were performed by refitting the final model to the dataset including implausible serum concentrations >200 mcg/L and >60 mcg/L (see methods section), while excluding rising concentrations after IV administration.

#### PMX Based Predictions and Simulations

For each individual, predicted maximum serum concentration ($C_{max}$), time to reach maximum serum concentration ($t_{max}$) (derived from individual concentration-time profile predictions) and terminal half-life ($t_{1/2}$) (derived from individual model parameters) were calculated, and summarized by median (interquartile range IQR) for each study group.

Expected overall exposure range was summarized by median simulated concentration-time profiles with 90% prediction intervals (5 and 95th percentile) for each study group. Those prediction intervals were derived from simulations for 5,000 hypothetical individuals with identical weight distribution as in the analysis dataset, and model-predicted random inter-individual variability and residual error. In addition, median concentration-time profiles with 2- or 4- fold higher dosing were simulated assuming dose proportionality. Simulated exposure range was compared to previously proposed target concentration of 12 mcg/L (i.e. efficacy threshold) under continuous iv infusion in children >1 years for treatment of postoperative pain (4), with a special focus on duration >12 mcg/L as possible indicator of duration of effect.

#### PMX Based Exposure-Pain Response Analyses

Individual concentration-time profile predictions derived from the final PPK model were further used to derive time-matched concentration predictions to investigate the association between drug exposure and severe pain (defined as NIPS >4), and expected duration of pain relief (i.e., NIPS ≤4). Initial descriptive analysis included a summary and boxplots of drug exposure per intervention and treatment group (median, IQR). Data from all pain assessments under nalbuphine exposure were then pooled for a model-based analysis. Fixed and mixed-effect (random intercept) logistic regression models were applied, considering linear, log-linear and non-linear relationships (Emax- and sigmoid Emax concentration-response models) with serum nalbuphine. The predicted concentration-pain response (pharmacodynamic) curve was contrasted for model evaluation with a non-parametric regression line (loess). The predicted pain response-over-time (pharmacokinetic/pharmacodynamic) curve was evaluated by comparison of predicted proportions with severe pain under median drug exposure (and 5/95th

**TABLE 1 |** Characteristics of study subjects included in primary population pharmacokinetic and exposure-response analysis.

| Group | Nalbuphine 0.05 mg/kg iv | Nalbuphine 0.1 mg/kg intranasal | All, iv | All, intranasal |
|---|---|---|---|---|
| Number of study subjects | 15 | 23 | 26 | 26 |
| Male | 9 (60%) | 14 (61%) | 16 (62%) | 16 (62%) |
| Age [days] | 56 (37–68.5) | 55 (39–62.5) | 56 (40–70) | 55 (39–63) |
| Weight [kg] | 4.7 (4.3–6.0) | 5.0 (4.7–5.5) | 5.0 (4.5–5.9) | 5.0 (4.7–5.5) |

*Continuous variables are given as median (IQR), categorical variables as number (percent).*

percentiles, according to PPK model predictions) with observed proportions of severe pain (mean, 95% confidence interval; all patients with NIPS assessments included irrespective of concentration measurements).

# RESULTS

## Data

Out of 52 study subjects who were included in the study and received nalbuphine, 48 study subjects (92%) had at least one serum concentration measured. According to criteria specified above, concentrations from 10 study subjects were excluded from the primary PPK analyses: three concentrations because rising values after iv administration and seven implausible concentrations (>60 mcg/L; see definition in methods section). As such a total of 38 study subjects were retained for primary PPK analysis and exposure-pain response analysis. **Table 1** shows patient characteristics (flowchart is provided as **Supplementary Figure 1**). Considering detailed patient numbers per intervention with available NIPS assessments under nalbuphine exposure, assessments of 20 patients during establishment of venous access (intranasal group only), 30 patients during urinary catheterization and 21 patients during lumbar puncture (intranasal and IV group combined) were available for exposure-pain response analysis. Corresponding NIPS assessments for calculation of observed proportions with severe pain were available for a total of 21 study subjects during establishment of venous access (intranasal group), 42 study subjects during urinary catheterization, and 25 study subjects during lumbar puncture (25).

## PMX Modeling and Simulation

### PMX Based Pharmacokinetic Analyses

IV nalbuphine data were well described by a two-compartmental model with the peripheral compartment volume fixed to 2 × central compartment volume (V1) as reported by Jaillon et al. (6), and weight-based allometric scaling (26). Given weight distribution in dataset, weight was centered to 5 kg. To further enhance model stability in the combined intranasal/IV model we fixed intercompartmental clearance ($Q_{5kg}$) to 15.4 L/h (as estimated in the IV model), $CL_{5kg}$ was estimated to 10.3 L/h and $V1_{5kg}$ to 12.2 L. Between-subject variability was included on CL and V1 (estimated to 77 and 118%, respectively). Given available data, inclusion of age and sex as covariates did not reduce inter-individual variability nor improved model fit ($P > 0.05$) (correlation with individual random effects illustrated in **Supplementary Figure 2**). A simple first-order absorption model was utilized to describe intranasal absorption kinetics [rate constant ($k_a$) estimated to 0.81/h]. Lag-time, one or several transit-compartments did not improve the model fit. Intranasal bioavailability was estimated to be 0.41 (95%CI: 0.26–0.56).

Sensitivity analyses (details: **Table 2**) resulted in similar estimates for bioavailability (0.47 to 0.36, with overlapping 95% CI). In sensitivity analysis I, CL/V1 estimates were 60/63% lower with largely increased inter-individual variability. In sensitivity analysis II CL/V1 estimates remained within the 95%CI of the reported estimates. Visual predictive checks for model evaluation are provided as **Supplementary Figure 3**.

### PMX Based Predictions and Simulations

Median (IQR) individual $C_{max}$ was 3.4 (3.0–4.8) mcg/L after intranasal administration [at $t_{max}$ = 50 (39–64) min] vs. 17.9 (7.5–32.8) mcg/L after intranasal administration (at time = 0 h). Median terminal $t_{1/2}$ was estimated to be 3.3 h (IQR: 2.1–6.1 h), the initial $t_{1/2}$ to be 0.12 h (0.09–0.29 h).

**Figure 1A** (upper panel) shows model-predicted median concentration-time profiles and 95% prediction intervals, which matched the observed concentrations well. The expected median concentration following 2- or 4-fold higher dosing is shown in **Figure 1B** (upper panel). The proposed target concentration of 12 mcg/L was exceeded after IV administration by the median predicted exposure for 6 min after the studied dose of 0.05 mg/kg (solid line), for 30 min after double dose of 0.1 mg/kg (dashed line), and for 80 min after 4-fold dose of 0.2 mg/kg (dotted line). Following intranasal administration, the proposed target was exceeded by the median predicted exposure only after 4-fold increased dose (dotted line), between 30 and 100 min.

### PMX Based Exposure-Pain Response Analyses

**Table 3** gives a summary of drug exposure during the different medical interventions in study subjects with low-moderate (NIPS ≤ 4) vs. severe pain (NIPS > 4). Exposure tended to be higher during establishment of IV access ($P = 0.052$) and urinary catheterization ($P = 0.189$) in study subjects with low-moderate pain than in study subjects with severe pain, but less during lumbar puncture ($P = 0.885$).

A logistic random intercept model with a log-linear concentration-pain response relationship on the logit scale described the pooled data best (lowest bias over concentration and over time, $P < 0.05$). The corresponding predicted probability of severe pain (NIPS > 4) vs. plasma exposure is contrasted with observed mean proportions (as captured by a loess) in **Figure 2**. The baseline probability of severe pain (NIPS > 4) at a concentration of 1 mcg/L was predicted to 79.5% (95% CI: 54–96%; interindividual variability expressed as ±standard deviation of estimated random effects = 53.8–92.8%), the odds ratio for doubling nalbuphine exposure was estimated to 0.49 (95% CI: 0.21–0.86). Non-linear exposure-response relationships could not be estimated with good confidence.

**TABLE 2 |** Population pharmacokinetic parameter estimates of the primary analysis, as well as sensitivity analyses.

| | **Primary analysis ($n$ = 38 individuals)** | | **Sensitivity analysis I (all data, except rising concentration after iv administration) ($n$ = 45)** | | **Sensitivity analysis II (all data, except serum concentration > 200 mcg/L and rising concentration after iv administration) ($n$ = 42)** | |
|---|---|---|---|---|---|---|
| **Parameter** | **Value** | **R.s.e. [%]** | **Value** | **R.s.e. [%]** | **Value** | **R.s.e. [%]** |
| F | 0.41 (0.26–0.56)* | 18.5 | 0.405 (0.23–0.58)* | 21.6 | 0.36 (0.23–0.49)* | 18.2 |
| ka [$h^{-1}$] | 0.81 (0.53–1.09)* | 17.6 | 0.684 | 23 | 0.744 | 24.1 |
| CL [L/h] for 5 kg infant | 10.3 (6.2–14.4)* | 20.2 | 4.6 (0.98–8.2)* | 40.2 | 8.86 (5.4–12.3)* | 20 |
| V1 [L] for 5 kg infant | 12.2 (5.8–18.6)* | 26.7 | 5.02 (0.98–9.1)* | 41.1 | 8.36 (3.7–13.0)* | 28.5 |
| V2 [L] | Fixed to 2 × V1 | | Fixed to 2 × V1 | | Fixed to 2 × V1 | |
| Q [L/h] for 5 kg infant | 15.4 fix | | 15.4 fix | | 15.4 fix | |
| omega_CL | 0.679 (CV = 77%) | 21.9 | 1.72 (CV = 427.4%) | 14.5 | 0.718 (CV = 82.1%) | 19.7 |
| omega_V1 | 0.936 (CV = 118%) | 15.3 | 2.12 (CV = 940.8%) | 12.2 | 1.16 (CV = 168.5%) | 14 |
| Res. Error | 0.353 | 10.1 | 0.396 | 10.2 | 0.39 | 10.6 |

*R.s.e., relative standard error; F, Bioavailability; ka, rate constant; CL, Clearance; V1, central compartment volume; V2, peripheral compartment volume; Q, intercompartmental clearance; omega, standard deviation of random-effect; CV, coefficient of variation (inter-individual variability); calculated as* $\sqrt{\exp^{omega^2} - 1}$ *Res. error, residual error (intra-individual variability); *95% Confidence Interval.*

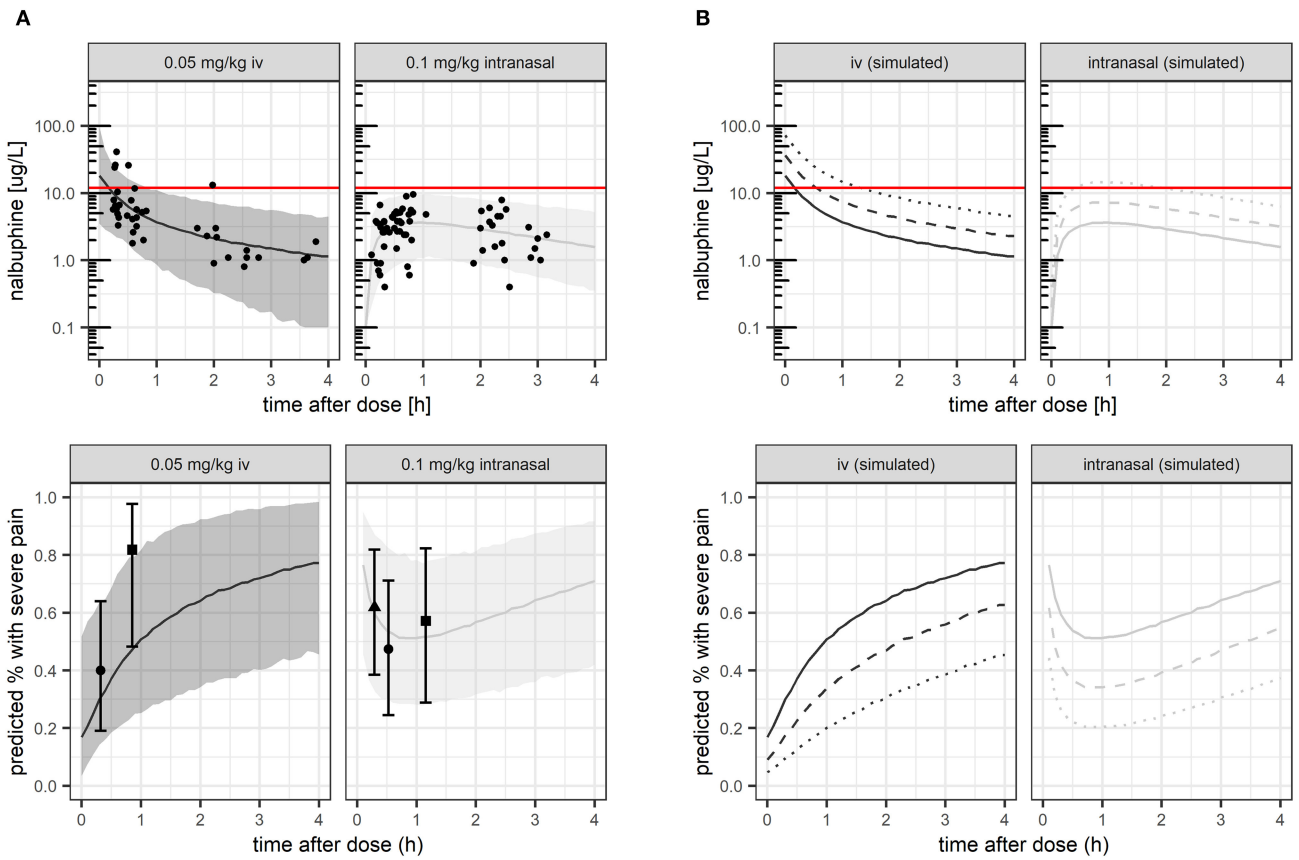


**FIGURE 1 |** Nalbuphine exposure (**A,B** upper panels) and corresponding proportion of patients with severe pain (**A,B** lower panels). **(A)** studied nalbuphine dose of 0.05 mg/kg IV and 0.1 mg/kg intranasally, respectively. **(B)** studied nalbuphine dose compared with simulated 2–4 × higher dose. *Lines*: model-predicted median (*solid*: studied dose, *dashed*: 2 × higher dose, d*otted*: 4 × higher dose). *Dots*: observed exposure (upper panel **A**) and observed proportion with severe pain, respectively (lower panel A, shown with 95% confidence intervals). *Shaded area*: 5 and 95th exposure percentiles.

**TABLE 3 |** Summary of model-predicted individual nalbuphine concentration during the different medical interventions (establishment of venous access, urinary catheterization and lumbar puncture) in study subjects with low-moderate (NIPS ≤ 4) vs. severe pain (NIPS > 4).

| | Median [IQR] serum concentration nalbuphine (mcg/L) Patients with NIPS ≤ 4 | Median (IQR) serum concentration nalbuphine (mcg/L) Patients with NIPS >4 | *p*-value* |
|---|---|---|---|
| Establishing venous access (intransal group only) | 2.93 [2.53, 3.63] $n = 7$ | 1.81 [0.73, 2.78] $n = 13$ | 0.052 |
| Catheterization | 3.23 [2.76, 9.11] $n = 19$ | 3.24 [1.65, 6.10] $n = 11$ | 0.189 |
| Lumbar puncture | 4.17 [3.16, 5.02] $n = 8$ | 4.12 [2.92, 5.43] $n = 13$ | 0.885 |

*n, number of study subjects. *Wilcoxon-test.*

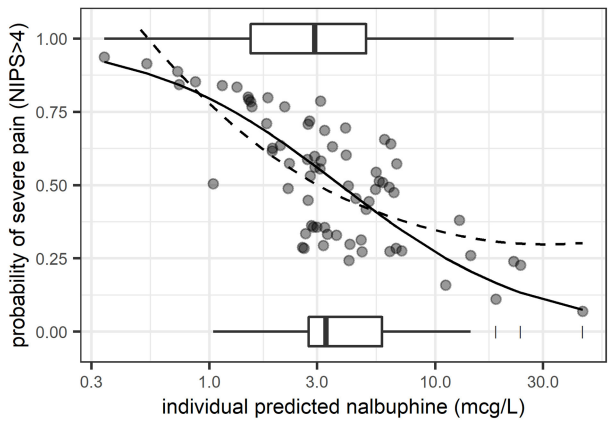


**FIGURE 2 |** Predicted probability of severe pain (NIPS > 4) from logistic regression (random intercept model) vs. plasma exposure. *Solid line*: mean model prediction. *Dashed line*: observed mean proportions as captured by a non-parametric regression line (loess). *Boxplots*: exposure distribution for observations with severe pain (plotted at a probability of 1) and those with low to moderate pain (plotted at a probability of 0). *Dots*: individual predicted probabilities.

Pharmacometric simulations illustrating predicted probability of severe pain over time, compared with observed proportions under the given dose for model evaluation are shown in **Figure 1A** (lower panel). Model-based simulations for 2- or 4-fold higher doses are shown for predicted median exposure (**Figure 1B**). At median predicted $C_{max}$ values, the mean probability of severe pain would be predicted to 17% (IV, at $t =$ 0 h) and 53% (intranasal) under the studied dose, respectively, decreasing by 2-fold/4-fold higher doses to 9%/5% (IV), and 36%/22% (intranasal).

## DISCUSSION

This is the first study reporting population pharmacokinetics of nalbuphine in infants 1–3 months of age, characterizing IV and intranasal kinetic profiles after single doses of 0.05 and 0.1 mg/kg, respectively. The model allowed to derive individual kinetic predictions for investigation of exposure-pain response associations, and to evaluate the potential benefit of 2-or 4-fold higher dosing by pharmacometric simulations. Output from this simulation suggested that doubling studied intranasal dose with respect to IV dosing may not be sufficient to achieve optimal pain control, despite a relative bioavailability estimated to be close to 50% (point estimate: 41%, 95%CI: 26–56%). Due to different kinetic profile after intranasal administration, simulations indicate that intranasal doses of 0.4 mg/kg would be required to exceed a previously proposed target concentration in 50% of the patients, achieved *after* 30 min of drug administration. On the other hand, a standard IV dose of 0.1 mg/kg is expected to exceed this target concentration *within* the first 30 min after drug administration. This finding has important implications for optimal timing of interventions and supports clinical usefulness of current IV doses of 0.1–0.2 mg/kg in this age group. Our PPK model parameters are consistent with previous pediatric and adult papers (4, 6, 27). For example, our average weight-normalized CL estimate would calculate to 2.28 L/kg/h (for a 5 kg infant) which is close to estimates of 2.89 L/kg/h [reported for 1.5–5 year old children (6)] to approximately 3.0 L/kg/h [1-year old infants, (4)], but significantly higher than reported in neonates (0.5 L/kg/h) (5). This suggests that maturation of nalbuphine metabolic pathways is almost complete at the age of 1–3 months. Human *in vivo* experiments had shown that the ratio of metabolite production in nalbuphine *via* CYPs and UGTs is ∼23:77 (11). However, no general developmental pattern for the individual UGT isoforms is currently available. UGT2B7 activity seemed to reach adult values between 2 and 6 months, which is more or less in accordance with our assumption (28). In addition, no age-effect could be observed in our analysis, with the possible limitation of small patient numbers. That our weight-normalized clearance is slightly higher than 1.78 L/kg/h reported in young men (6) is expected for a drug with clearance well characterized by standard allometric scaling, an approach that has successfully been used for nalbuphine previously (4). In fact, our scaled "adult" drug clearance estimate would calculate to 75 L/h for 70 kg $[=10.3\cdot(70/5)^{0.75}]$, which is in agreement with 90 L/h (range: 49–137 L/h) reported in adults after 20 mg IV (7). Estimated intranasal bioavailability of 41% appears much higher than oral bioavailability reported in adults [12% Aitkenhead et al. (7) or 16.4–17.4% Lo et al. (29)] (7, 29), and suggests that much of the drug after intranasal administration was well absorbed by the nasal mucosa in infants, allowing avoidance of gastrointestinal and hepatic first-pass metabolism.

Our PPK model-predicted median (IQR) individual $C_{max}$ of 3.4 (3.0–4.8) mcg/L after intranasal administration at $t_{max} = 50$ (39–64) min was similar to measured $C_{max}$ of 4.5 (3.5–5.6) mcg/L after 37 (32–65) min previously reported (25). The estimated bioavailability of 41% further confirms the previous observation that 2-fold higher intranasal than IV doses result in similar exposure coverage in terms of area under the concentration time curve (AUC). Our model-based concentration prediction after IV administration however shows large differences between median measured "$C_{max}$" after 15 min (6.5 mcg/L) and actually expected median $C_{max}$ immediately after IV dosing (17.9 mcg/L). It also revealed that even a 4-fold higher intranasal dose (i.e., 0.4 mg/kg

intranasal) is not expected to achieve observed $C_{max}$ comparable with an IV dose of 0.05 mg/kg.

An IV dose of 0.1 mg/kg is exceeding a previously proposed target concentration of 12 mcg/L (efficacy threshold) for at least 30 min. To achieve such target exposure an intranasal dose of 0.4 mg/kg is required. Performed simulations allowed us to identify an optimal time frame for interventions. Target concentrations are achieved during the first 30 min after 0.1 mg/kg IV administration, whereas efficacy threshold is exceeded 30 to almost 120 min after 0.4 mg/kg intranasal administration. The duration of analgesic effect was not formally assessed in our study, but pharmacokinetic and pharmacodynamic indicators of duration of effect [duration of concentration $>$ 12 mcg/L (4) and duration of NIPS $\leq$ 4, respectively] could be derived by model-based simulations. In line with this model-based simulations and target exposure, exposure response associations suggested greater benefit of intranasal dose increase compared to IV dose increase. Potential maximal reduction of probability of severe pain was up to −31% following 0.4 mg/kg intranasal dosing vs. up to −12% with 0.2 mg/kg IV dosing.

Our PMX study has a several limitations. With this model-based analysis, we cannot conclude about the safety of simulated higher intranasal doses up to 0.4 mg/kg; the safety and tolerability of studied doses was not subject of this analysis, but is reported separately, manuscript submitted (25). In our PPK model not all distribution parameters could be estimated from data given tailored sampling design in young children. Incorporating literature values resulted however in unbiased model predictions with suitable extrapolation properties as discussed above. Inter-individual pharmacokinetic variability was large (CL = 77% and V1 = 118%) despite including weight as covariate for allometric scaling, and could not be further explained by age and/or sex. While this may point to almost mature metabolic pathways as discussed above, it must be noted that included infants were in a similar physiologic age group and of course prepubertal, and variability associated with immature metabolic pathways can hence not fully be excluded. As discussed separately (25), large variability and unusually high drug concentrations may partly be attributed to practical considerations, like imprecision of dosing associated with small drug volumes (between 0.02 and 0.10 ml), possible intranasal swallowing with intranasal drug administration and likely variable line flushing in context of IV drug administration. This illustrates some of the practical challenges of intravenous and intranasal drug administration in infants. Also pharmacodynamic inter-individual variability was large. This is pharmacologically not uncommon, but also here practical considerations need to be considered, as pain assessments in nonverbal children, especially infants are challenging, and may be subject to inter-observer variability (22). NIPS measured can only be considered as a surrogate indicator of pain, as other distress like hunger or positioning may falsely be interpreted as pain by the score. Use of alternative scores such as the Neonatal Facial Coding System (NFCS) may have been of interest (22), but would have decreased feasibility of the study as not standardly used in our emergency department. Also pooling NIPS assessments under different interventions may further have contributed to intra-individual variability. In this context we acknowledge the exploratory nature of the pharmacodynamic analysis, as the study was not specifically designed to investigate exposure-response relationships. As such we did not evaluate potential benefits of more complex modeling strategies, e.g., to account for a possible "placebo effect" in the absence of nalbuphine exposure in the IV group during establishment of venous access. Still, despite these limitations and large variability, a pharmacologically plausible trend toward higher exposure in patients with mild to moderate NIPS was observed during different interventions, which was significant after pooling data for exposure response analysis. We may note again that we had initially planned to study a usual dose of 0.1 mg/kg iv (as compared to 0.2 mg/kg intranasal), which was however refused by the Swiss medical authority due to safety concerns. The relatively low dose studied (0.05 mg/kg IV) may have finally facilitated the detection of a significant exposure-response relationship, suggesting optimal clinical efficacy and plateau effect at usual iv doses of 0.1–0.2 mg/kg.

This is the first study characterizing intranasal and IV population pharmacokinetics in infants 1–3 months, including evaluation of target exposure achievement and exposure-pain response associations. While relative bioavailability of intranasal nalbuphine is close to 50%, a different kinetic profile requires a higher intranasal dose of 0.4 mg/kg to achieve target exposures observed with intravenous doses of 0.1–0.2 mg/kg. A clinically relevant finding is that painful interventions are best done within first 30 min after IV administration, while with intranasal administration such interventions should be scheduled at least 30 min after dosing. Because the proposed 4 fold intranasal dose of 0.4 mg/kg may also increase the risk of adverse drug reactions, additional clinical studies are warranted to confirm these recommendations in this vulnerable pediatric patient population.

## DATA AVAILABILITY STATEMENT

The datasets generated during the current study are available from the corresponding author on reasonable request.

## ETHICS STATEMENT

The studies involving human participants were reviewed and approved by Local Ethics Committee Swissmedic. Written informed consent to participate in this study was provided by the participants' legal guardian/next of kin.

## AUTHOR CONTRIBUTIONS

MPfif: conceptualization/design, methodology, investigation, data curation, investigation, formal analysis, and writing—drafting the initial manuscript. EB-O: conceptualization/design, methodology, data curation, investigation, supervision/oversight, resources, and writing—review or editing of the manuscript. PV: conceptualization/design, funding acquisition, methodology, supervision/oversight, resources, and writing—review or editing of the manuscript. MPfis: conceptualization/design, funding acquisition, methodology, supervision/oversight, resources, and writing—review or editing of the manuscript.

VG: supervision/oversight, data curation, investigation, formal analysis, and writing—review or editing of the manuscript. All authors contributed to the article and approved the submitted version.

## FUNDING

This study was supported by internal funds of the University Children's Hospital Zurich.

## ACKNOWLEDGMENTS

The authors would like to thank the whole team of the Children's Hospital Zurich emergency unit for their great commitment. We also thank Martin Volleberg Institute of Clinical Chemistry, Children's Hospital Zurich, Dr. Daniel Müller Institute of Clinical Chemistry, University Hospital Zurich and Dr. Andrew Atkinson statistician, Pediatric Pharmacology and Pharmacometrics Research Center, University Children's Hospital Basel. We also would like to thank pediatric patients and their parents for their participation in this study.

## SUPPLEMENTARY MATERIAL

The Supplementary Material for this article can be found online at: https://www.frontiersin.org/articles/10.3389/fped.2022.837492/full#supplementary-material

## REFERENCES

1. Swissmedicinfo.ch. *Fachinformation Nalbuphin*. Swissmedicinfo Online Access Februar 2016.
2. FDA. Reference ID: 4500827. FDA-Approved Drugs (2019). Silver Spring, MD: U.S. Food and Drug Administration. Available online at: https://www.accessdata.fda.gov/scripts/cder/daf/index.cfm?event=overview.process&ApplNo=018024
3. Fachinformationsverzeichnis Deutschland. Nubain ® 10 mg / ml Injektionslösung. Nubain® 10 mg/ml Injektionslösung (2020). p. 1–3. Available online at: https://www.fachinfo.de/api/fachinfo/pdf/023086
4. Bressolle F, Khier S, Rochette A, Kinowski JM, Dadure C, Capdevila X. Population pharmacokinetics of nalbuphine after surgery in children. *Br J Anaesth*. (2011) 106:558–65. doi: 10.1093/bja/aer001
5. Jacqz-Aigrain E, Debillon T, Daoud P, Boithias C, Hamon I, Rayet I, et al. Population Pharmacokinetics of Nalbuphine in Neonates. *Paediat Perinat Drug Ther*. 2003. 5:190–8. doi: 10.1185/146300903774115793
6. Jaillon P, Gardin ME, Lecocq B, Richard MO, Meignan S, Blondel Y, et al. Pharmacokinetics of nalbuphine in infants, young healthy volunteers, and elderly patients. *Clin Pharmacol Ther*. (1989) 46:226–33. doi: 10.1038/clpt.1989.130
7. Aitkenhead A, Lin E, Achola K. The pharmacokinetics of oral and intravenous nalbuphine in healthy volunteers. *Br J Clin Pharmacol*. (1988) 25:264–8. doi: 10.1111/j.1365-2125.1988.tb03300.x
8. Nicolle E, Veitl S, Guimier C, Bessard G. Modified method of nalbuphine determination in plasma: validation and application to pharmacokinetics of the rectal route. *J Chromatogr B Biomed Appl*. (1997) 690:89–97. doi: 10.1016/S0378-4347(96)00369-6
9. Cai LJ, Zhang J, Wang XM, Zhu RH, Yang J, Zhang QZ, et al. Validated LC-MS/MS assay for the quantitative determination of nalbuphine in human plasma and its application to a pharmacokinetic study. *Biomed Chromatogr*. (2011) 25:1308–14. doi: 10.1002/bmc.1601
10. Thigpen JC, Odle BL, Harirforoosh S. Opioids : a review of pharmacokinetics and pharmacodynamics in neonates , infants , and children. *Eur J Drug Metab Pharmacokinet*. (2019) 44:591–609. doi: 10.1007/s13318-019-00552-0
11. Liang R, Shih Y, Chen Y, Liu W, Yang W. European journal of pharmaceutical sciences a dual system platform for drug metabolism : nalbuphine as a model compound. *Eur J Pharm Sci*. (2020) 141:105093. doi: 10.1016/j.ejps.2019.105093
12. Ruest S, Anderson A. Management of acute pediatric pain in the emergency department. *Curr Opin Pediatr*. (2016) 28:298–304. doi: 10.1097/MOP.0000000000000347
13. Del Pizzo J, Callahan JM. Intranasal medications in pediatric emergency medicine. *Pediatr Emerg Care*. (2014) 30:496–501. doi: 10.1097/PEC.0000000000000171
14. Corrigan M, Wilson SS, Hampton J. Safety and efficacy of intranasally administered medications in the emergency department and prehospital settings. *Am J Heal Pharm*. (2015) 72:1544–54. doi: 10.2146/ajhp140630
15. Grassin-Delyle S, Buenestado A, Naline E, Faisy C, Blouquit-Laye S, Couderc L-JJ, et al. Intranasal drug delivery: an efficient and non-invasive route for systemic administration-focus on opioids. *Pharmacol Ther*. (2012) 134:366–79. doi: 10.1016/j.pharmthera.2012.03.003
16. Pansini V, Curatola A, Gatto A, Lazzareschi I, Ruggiero A, Chiaretti A. Intranasal drugs for analgesia and sedation in children admitted to pediatric emergency department: a narrative review. *Ann Transl Med*. (2021) 9:189–189. doi: 10.21037/atm-20-5177
17. Ziesenitz VC, Rodieux F, Atkinson A, Borter C, Bielicki JA, Haschke M, et al. Dose evaluation of intravenous metamizole (dipyrone) in infants and children: a prospective population pharmacokinetic study. *Eur J Clin Pharmacol*. (2019) 75:1491–502. doi: 10.1007/s00228-019-02720-2
18. Ziesenitz VC, Zutter A, Erb TO, van den Anker JN. Efficacy and Safety of Ibuprofen in Infants Aged Between 3 and 6 Months. *Pediatr Drugs*. (2017) 19:277–90. doi: 10.1007/s40272-017-0235-3
19. Fortuna A, Alves G, Serralheiro A, Sousa J, Falcão A. Intranasal delivery of systemic-acting drugs: small-molecules and biomacromolecules. *Eur J Pharm Biopharm*. (2014) 88:8–27. doi: 10.1016/j.ejpb.2014.03.004
20. Heidmets L, Ilmoja M, Pisarev H. Blood Loss Related to Participation in Pharmacokinetic Study in Preterm. *Neonatology*. (2011) 100:111–5. doi: 10.1159/000323699
21. Pain Assessment and Management Initiative C of MJ. Neonatal Infant Pain Scale (NIPS) (2015). p. 1–27. Available online at: https://com-jax-emergency-pami.sites.medinfo.ufl.edu/files/2015/02/Neonatal-Infant-Pain-Scale-NIPS-pain-scale.pdf
22. Giordano V, Edobor J, Deindl Ph, Wildner B, Goeral K, Steinbauer Ph, et al. Pain and sedation scales for neonatal and pediatric patients in a preverbal stage of development a systematic review. *JAMA Pediatr*. (2019) 173(12):1186–97. doi: 10.1001/jamapediatrics.2019.3351
23. Savic RM, Jonker DM, Kerbusch T, Karlsson MO. Implementation of a transit compartment model for describing drug absorption in pharmacokinetic studies. *J Pharmacokinet Pharmacodyn*. (2007) 34:711–26. doi: 10.1007/s10928-007-9066-0
24. Utesch T, Rack A, Von M. *Allometrie und Skalierung von Modellparametern Übersicht Einleitung Allometrie ( Populations- ) Pharmakokinetik Zusammenfassung*.
25. Pfiffner M, Verena Gotta, Pfister M, Vonbach P, Berger Olah E. *Pharmacokinetics and tolerability of intranasal or intravenous administration of nalbuphine in infants*, manuscript submitted.
26. Germovsek E, Barker CIS, Sharland M, Standing JF. Pharmacokinetic–pharmacodynamic modeling in pediatric drug development, and the importance of standardized scaling of clearance. *Clin Pharmacokinet*. (2019) 58:39–52. doi: 10.1007/s40262-018-0659-0
27. Bessard G, Alibeu JP, Cartal M, Nicolle E, Serre Debeauvais F, Devillier P. Pharmacokinetics of intrarectal nalbuphine in children undergoing general anaesthesia. *Fundam Clin Pharmacol*. (1997) 11:133–7. doi: 10.1111/j.1472-8206.1997.tb00180.x
28. Wildt SN De, Kearns GL, Leeder JS, Anker JN, Van Den. Glucuronidation in humans pharmacogenetic and developmental aspects. *Clin*

*Pharmacokinet*. (1999) 36:439–52. doi: 10.2165/00003088-199936060-00005

29. Lo M-W, Schary WL Jr., Whitney CC. The disposition and bioavailability of intravenous and oral nalbuphine in healthy volunteers. *J Clin Pharmacol.* (1987) 27:866–73. doi: 10.1002/j.1552-4604.1987.tb05581.x

**Conflict of Interest:** The authors declare that the research was conducted in the absence of any commercial or financial relationships that could be construed as a potential conflict of interest.

**Publisher's Note:** All claims expressed in this article are solely those of the authors and do not necessarily represent those of their affiliated organizations, or those of the publisher, the editors and the reviewers. Any product that may be evaluated in this article, or claim that may be made by its manufacturer, is not guaranteed or endorsed by the publisher.

frontiers in Pharmacology

REVIEW
published: 10 March 2022
doi: 10.3389/fphar.2022.818726

# Characterizing Pharmacokinetics in Children With Obesity—Physiological, Drug, Patient, and Methodological Considerations

*Jacqueline G. Gerhart*[1], *Stephen Balevic*[1,2,3], *Jaydeep Sinha*[1,4], *Eliana M. Perrin*[5], *Jian Wang*[6], *Andrea N. Edginton*[7] *and Daniel Gonzalez*[1]*

[1]Division of Pharmacotherapy and Experimental Therapeutics, UNC Eshelman School of Pharmacy, The University of North Carolina at Chapel Hill, Chapel Hill, NC, United States, [2]Department of Pediatrics, Duke University Medical Center, Durham, NC, United States, [3]Duke Clinical Research Institute, Durham, NC, United States, [4]Department of Pediatrics, UNC School of Medicine, The University of North Carolina at Chapel Hill, Chapel Hill, NC, United States, [5]Department of Pediatrics, Johns Hopkins University Schools of Medicine and School of Nursing, Baltimore, MD, United States, [6]Office of Drug Evaluation IV, Center for Drug Evaluation and Research, US Food and Drug Administration, Silver Spring, MD, United States, [7]School of Pharmacy, University of Waterloo, Waterloo, ON, Canada

Childhood obesity is an alarming public health problem. The pediatric obesity rate has quadrupled in the past 30 years, and currently nearly 20% of United States children and 9% of children worldwide are classified as obese. Drug distribution and elimination processes, which determine drug exposure (and thus dosing), can vary significantly between patients with and without obesity. Obesity-related physiological changes, such as increased tissue volume and perfusion, altered blood protein concentrations, and tissue composition can greatly affect a drug's volume of distribution, which might necessitate adjustment in loading doses. Obesity-related changes in the drug eliminating organs, such as altered enzyme activity in the liver and glomerular filtration rate, can affect the rate of drug elimination, which may warrant an adjustment in the maintenance dosing rate. Although weight-based dosing (i.e., in mg/kg) is commonly practiced in pediatrics, choice of the right body size metric (e.g., total body weight, lean body weight, body surface area, etc.) for dosing children with obesity still remains a question. To address this gap, the interplay between obesity-related physiological changes (e.g., altered organ size, composition, and function), and drug-specific properties (e.g., lipophilicity and elimination pathway) needs to be characterized in a quantitative framework. Additionally, methodological considerations, such as adequate sample size and optimal sampling scheme, should also be considered to ensure accurate and precise top-down covariate selection, particularly when designing opportunistic studies in pediatric drug development. Further factors affecting dosing, including existing dosing recommendations, target therapeutic ranges, dose capping, and formulations constraints, are also important to consider when undergoing dose selection for children with obesity. Opportunities to bridge the dosing knowledge gap in children with obesity include modeling and simulating techniques (i.e., population pharmacokinetic and physiologically-based pharmacokinetic [PBPK] modeling), opportunistic clinical data, and real world data. In this review, key considerations related to physiology, drug

OPEN ACCESS

**Edited by:**
*Catherine M. T. Sherwin, Wright State University, United States*

**Reviewed by:**
*Viera Lukacova, Simulations Plus, United States*
*Jeannine S. McCune, Beckman Research Institute, United States*

***Correspondence:**
*Daniel Gonzalez*
*daniel.gonzalez@unc.edu*

**Specialty section:**
*This article was submitted to Obstetric and Pediatric Pharmacology, a section of the journal Frontiers in Pharmacology*

**Received:** *19 November 2021*
**Accepted:** *24 January 2022*
**Published:** *10 March 2022*

**Citation:**
*Gerhart JG, Balevic S, Sinha J, Perrin EM, Wang J, Edginton AN and Gonzalez D (2022) Characterizing Pharmacokinetics in Children With Obesity—Physiological, Drug, Patient, and Methodological Considerations. Front. Pharmacol. 13:818726. doi: 10.3389/fphar.2022.818726*

parameters, patient factors, and methodology that need to be accounted for while studying the influence of obesity on pharmacokinetics in children are highlighted and discussed. Future studies will need to leverage these modeling opportunities to better describe drug exposure in children with obesity as the childhood obesity epidemic continues.

**Keywords: obesity, pediatrics, drug development, pharmacokinetics, physiologically-based pharmacokinetics**

## INTRODUCTION

Almost 20% of children in the United States (US) and 10% of children worldwide are currently classified as obese (World Health Organization, 2016; NCD-RisC, 2017; Skinner et al., 2018). The prevalence of pediatric obesity is growing, with obesity rates quadrupling in children in the US in the past quarter-century. This is an imperative public health issue, as children with obesity are at increased risk of developing comorbidities, such as cardiovascular disease and type 2 diabetes (Skinner et al., 2015). This means that children with obesity require more prescription drugs than those without obesity, and children with obesity often experience worse outcomes with clinically-used dosing (Scherrer et al., 2015; Solmi and Morris, 2015) In adults, obesity is defined as an abnormally high body size for a given height, measured by body mass index (BMI). A generally accepted reference BMI limit is 30 $kg/m^2$, beyond which an adult will be classified as obese. Such a fixed reference body size metric does not apply to children because of the baseline changes in the body size to height ratio due to continuous growth and development (Kuczmarski et al., 2000). In children, BMI overall increases naturally as the child matures, and also undulates, particularly in the age from 3–8 years when there is a physiological "BMI dip" (Kuczmarski et al., 2000). Therefore, to characterize childhood obesity, an age- and sex-specific reference BMI limit is generally considered. The US Centers for Disease Control and Prevention (CDC) has recommended the 95th percentile of the BMI-to-age curve as the reference limit, with a BMI percentile ≥95 but <120% of the 95th percentile indicating Class 1 obesity, a BMI from 120–140% of the 95th percentile indicating Class II obesity, and a BMI >140% of the 95th percentile indicating Class III obesity (Gulati et al., 2012). Many additional body size measures have been proposed to measure obesity, which are summarized in **Table 1**. While these body size measures are often more accurate in describing fat and lean body size in children, they can be more challenging to calculate in a clinical setting (Freedman and Sherry, 2009; Anderson and Holford, 2017; Sinha et al., 2018; Green et al., 2020).

Unfortunately, despite the frequent use of prescription drugs in children with obesity, the data to inform their specific dosing is lacking (Solmi and Morris, 2015). While US legislation in recent years has increased the amount of pediatric data submitted to the FDA, this has not bridged the gap in studies conducted in children with obesity (Harskamp-van Ginkel et al., 2015; Mulugeta et al., 2016; Sun et al., 2017). Although data for four drugs submitted to the FDA emphasized the effect of body size on pharmacokinetics (PK) in children, only one FDA label to date provides dosing information in children with obesity (Vaughns et al., 2018; Cleocin Phosphate, 2020). Currently, the best body size descriptor to use and whether to cap dosing is unknown for many drugs dosed in patients with obesity. Thus, there is a lack of standard dosing practice, with clinicians using different body weight measures or simply capping at the adult recommended dose. Many ethical and logistical barriers to conducting clinical PK studies in children with obesity contribute to this data gap. Pharmacokinetic studies in general traditionally require intensive sampling to adequately characterize drug disposition to determine dosing that is both safe and efficacious, which is not always feasible in pediatric populations. A stigma surrounding obesity can depress enrollment rates of these children. Lower enrollment of children with obesity relative to those without obesity means that they are often underrepresented in all-comer trials, and that these trials may thus be underpowered to detect differences in exposure between children with and without obesity. The additional enrollment time and trial cost might hugely limit

**TABLE 1 |** Selected direct and indirect measures of body size for children.

**Total body weight (TBW)**

$TBW\ [kg] = Measured\ weight\ of\ child\ [kg]$

**Body mass index (BMI)**

$$BMI\ [\tfrac{kg}{m^2}] = \frac{TBW\ [kg]}{Height\ [m]^2}$$

**Body surface area (BSA)**[a]

$$BSA\ [m^2] = 0.024265 * TBW\ [kg]^{0.5378} * Height\ [cm]^{0.3964}$$

**Ideal body weight (IBW)**[b]

$$IBW\ [kg] = BMI_{50}\ [\tfrac{kg}{m^2}] * Height\ [m]^2$$

$$BMI_{50}\,(boys)\ [\tfrac{kg}{m^2}] = 24.27 - \frac{8.91}{1+(\frac{Age\ [y]}{15.78})^{4.40}}$$

$$BMI_{50}\,(girls)\ [\tfrac{kg}{m^2}] = 22.82 - \frac{7.51}{1+(\frac{Age\ [y]}{13.46})^{4.44}}$$

**Fat-free mass (FFM)**[c]

$$FFM\,(boys)\ [kg] = [0.88 + (\frac{1-0.88}{1+(\frac{Age\ [y]}{13.4})^{-12.7}})][\frac{9270*TBW\ [kg]}{6680+(216*BMI\ [\frac{kg}{m^2}])}]$$

$$FFM\,(girls)\ [kg] = [1.11 + (\frac{1-1.11}{1+(\frac{Age\ [y]}{7.1})^{-1.1}})][\frac{9270*TBW\ [kg]}{8780+(244*BMI\ [\frac{kg}{m^2}])}]$$

**Body fat percent (BFP)**[d]

$$BFP\,(boys)\ [\%] = \frac{0.647*0.0598*e^{2.050*BMI_{95}\ [\frac{kg}{m^2}]}}{0.647+0.0598*(e^{2.050*BMI_{95}\ [\frac{kg}{m^2}]}-1)} + 0.1140 - 0.00890 * Age\ [y]$$

$$BFP\,(girls)\ [\%] = \frac{1.080*0.1930*e^{0.897*BMI_{95}\ [\frac{kg}{m^2}]}}{1.080+0.1930*(e^{0.897*BMI_{95}\ [\frac{kg}{m^2}]}-1)} - 0.0856 + 0.00682 * Age\ [y]$$

[a]*See (Haycock et al., 1978),* n = *81 subjects.*
[b]*See (Pai and Paloucek, 2000; Callaghan and Walker, 2015),* n = *108 subjects.*
[c]*See (Janmahasatian et al., 2005; Al-Sallami et al., 2015),* n = *1,011 subjects.*
[d]*See (Green et al., 2020),* n = *4,274 subjects.*

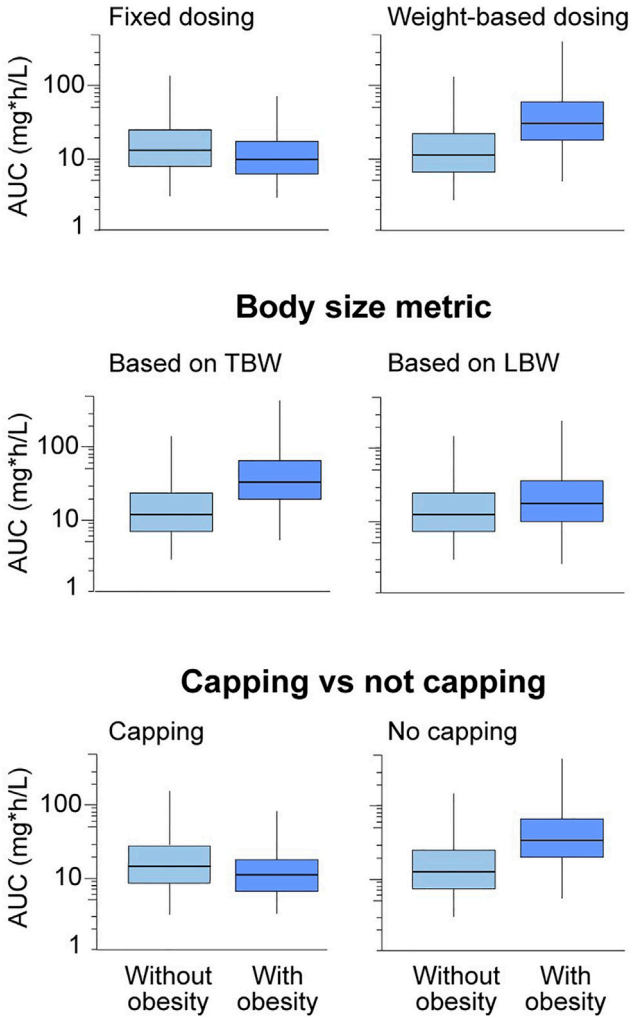


**FIGURE 1 |** Trends in drug exposure in children with versus without obesity will depend on different types of dosing considerations, including fixed versus weight-based dosing, total body weight versus a lean body weight size descriptor, and capping versus not capping. Boxplots show relative drug exposure in children with versus without obesity for a theoretical drug under these various dosing scenarios with hypothetical drug exposure. Note that these are expected trends with obesity for different dosing constraints, and the magnitude of the change may vary depending on drug properties. Additional constraints on dosing include available formulations and dosing routes, as well as previously established therapeutic ranges. AUC, area under the plasma concentration-versus-time curve; LBW, lean body weight; TBW, total body weight.

the inclusion of the full age and body size range of children required to characterize drug disposition in children with obesity.

Many dosing considerations contribute to confusion around dosing in children with obesity (**Figure 1**). Dosing guidance in children with and without obesity is typically bucketed into subgroups by age, though the age bounds on these subgroups may differ by drug. Typically used age subgroups include 2—< 6 years, 6—< 12 years, 12—< 18 years, and 18—< 21 years describing early childhood, middle childhood, early adolescence, and late adolescence, respectively (Williams et al., 2012; U. S. Food and Drug Administration, 2014). PK may differ between these pediatric age subgroups due to differences in growth and maturation, or obesity onset and the physiologically healthy BMI variations within these subgroups. However, these age classifications might not fit neatly within a particular drug's indication, or enrollment challenges may preclude subgrouping. Most pediatric clinically used dosing is weight-based (i.e., using total body weight or a measure of lean body weight), but may vary in terms of what body size metric is used to calculate the absolute dose. Fixed dosing can also be considered, particularly if the drug is dosed primarily in older pediatric populations or has a wide therapeutic window. Dose capping, or implementing a maximum total dose, is common in children who receive weight-based dosing. Often, the adult recommended dose or dose cap is also used in children with obesity, as is best clinical practice in the absence of further dosing guidance in these children. The Medication Dosing in Overweight and Obese Children report issued by the Pediatric Pharmacy Advocacy Group states that the regular adult dose for any particular drug should be considered for children with obesity exceeding 40 kg in total body weight (Matson et al., 2017). It is not recommended to exceed the recommended adult maximum dose in these children (Matson et al., 2017). However, extrapolating dosing guidance from adults, with or without obesity, is not scientifically advised given that differences in PK may exist due to maturation or obesity disease progression. The reality of how a drug is currently formulated (e.g., formulation route, fixed co-administration ratio, or pre-filled syringes) may constrain actual use of the ideal dosing. In this case, it is important to consider how a drug realistically be dosed in clinical practice.

In order to evaluate and choose appropriate doses for children with obesity, it is necessary to understand the PK drivers of dosing, including clearance and volume of distribution. Specifically, studying the change in PK of drugs in children with versus without obesity is imperative. By altering body size and composition, obesity can also influence drug disposition that already has a baseline influence from age-related growth and development. One prior review found that 65% of drugs studied in children, including those with obesity, demonstrated altered PK with obesity (Harskamp-van Ginkel et al., 2015). However, none of these drugs have dosing guidance that would account for altered body size and composition with obesity (Harskamp-van Ginkel et al., 2015). By mechanism, the PK differences are the combined effect of obesity-related structural and functional changes in physiology (e.g., organ size, composition, and function) and the drug-related properties (e.g., physicochemical and absorption, distribution, metabolism, and elimination [ADME] properties). Therefore, the effect of obesity on drug disposition depends on the particular drug in question, which needs separate assessment. This also highlights the fact that a universal dosing scheme for obesity is unlikely to exist. Instead, it should be developed based on separate evaluations for obesity's effect on a particular drug's disposition. In

reality, characterizing these effects of obesity is not straightforward in children. First, unlike adults, pediatric PK studies are conducted in patient populations, which potentially confounds the effect of obesity by other pathological influences. Further, because of methodological constraints, pediatric PK studies are often suboptimal to characterize these effects accurately and precisely. Therefore, apart from the drug-related properties, understanding the patient-related and methodology-related aspects are also equally important to consider while elucidating the effect of obesity in children. In this review, we explore how these four considerations—physiology, drug parameters, patient population characteristics, and methodological considerations (**Figure 2**)—can impact the assessment of PK in children with obesity. We conclude by exploring opportunities to bridge the dosing knowledge gap in these children.

## PHYSIOLOGICAL CONSIDERATIONS

The following equation can characterize the impact of various factors on PK parameters:

$$PK_i = PK_{standard} * f_{size} * f_{function} * f_{age}$$

where $PK_i$ is an individual's PK parameter, $PK_{standard}$ is the typical value of the PK parameter, and $f_{size}$, $f_{function}$, and $f_{age}$ are the effects of body size, organ function, and age (i.e., growth and maturation) on the PK parameter, respectively (Anderson and Holford, 2009). For children with obesity, the effects of both increased body size and age are important for characterizing PK. In this section, we consider the physiological effect of obesity as the effect of increased body size and fat mass alone, rather than pathological changes in renal or hepatic function, for example.

Many physiological variables that directly influence the volume and composition of plasma and tissues compartments can impact a drug's volume of distribution ($V_{ss}$) during obesity. $V_{ss}$ can be defined using the equation below:

$$V_{ss} = V_{plasma} + V_{tissue} * \frac{f_{u,p}}{f_{u,t}}$$

where $V_{plasma}$ is plasma volume, $V_{tissue}$ is tissue water volume, $f_{u,p}$ is fraction unbound in plasma, and $f_{u,t}$ is fraction unbound in tissue. Increased $V_{plasma}$ and $V_{tissue}$ (given more distribution space) can increase cardiac output during obesity (Vasan, 2003; Colles et al., 2006; Gerhart et al., 2021), potentially increasing the $V_{ss}$ on an absolute scale. However, the extent of increase in $V_{ss}$ is also dependent on the drug binding to plasma protein (that determines $f_{u,p}$) as well as to the tissue components (that determines $f_{u,t}$), which are potentially altered due to altered composition during obesity. While studies have shown that plasma composition with respect to serum albumin and hematocrit are largely unaffected by obesity, it changes with respect to $\alpha$1-acid glycoprotein (AAG), which increases approximately 2-fold with obesity in adults (Benedek et al., 1983, 1984; Blouin et al., 1987; Gerhart et al., 2021). However, this increase in AAG has not yet been identified in pediatric populations with obesity due to limited studies (Gerhart et al., 2021).

An increase in body fat with obesity is also accompanied by an increase in lean mass to provide additional structural (e.g., increased skeletal strength) and functional (e.g., increased metabolic need) support due to extra weight gain from adiposity. For example, key clearance organs such as the kidney and liver increase 19% and 18% in mass on average, respectively, with obesity (Nawaratne et al., 1998; Gerhart et al., 2021). These organ mass increases were determined by a series of magnetic resonance imaging and dual x-ray absorptiometry studies in adults and ultrasound scans in pediatric populations with and without obesity (Hwaung et al., 2019; Gerhart et al., 2021). Unlike body fat, these increases in non-fat organs do not increase proportionately with obesity. As a result, both the lean mass and body fat fractions (percent of total body weight) can be different between two children with the same body weight, but one with and one without obesity. Such alteration in body composition (i.e., the relative content of fat and non-fat tissues) between the two children may cause their individual $V_{ss}$ to differ, especially for drugs that do not uniformly distribute into the fat and non-fat tissues (i.e., drugs with varying lipophilicities). See **Figure 3** for a summary of observed obesity-induced physiological changes relevant to PK for adults and children with obesity.

In general, the rate-limiting physiological variables of drug elimination do not change proportionately with increasing body size associated with obesity, raising concerns about the applicability of the conventional mg/kg dosing with obesity (Nawaratne et al., 1998; Young et al., 2009). For hepatic clearance, the key variables are functional liver size, hepatic blood flow, and activity and abundance of drug-metabolizing enzymes (DMEs). Liver size and blood flow are both increased with obesity, as mentioned above. Inflammatory cytokines such as interleukin 6, often associated with obesity, have been shown to down-regulate activity of cytochrome P450 (CYP) enzymes and hepatic drug transporters in mice and humans (Richardson and Morgan, 2005; Schmitt et al., 2011; Cayot et al., 2014; Morgan et al., 2018; Abualsunun et al., 2020). There is additional evidence of some obesity-associated alterations in activity of DMEs and transporters in adult clinical studies. Evidence was available mainly for CYP3A4 and CYP2E1, where up to a 40% decrease and a 140% increase in DME activity was reported (Ulvestad et al., 2013; Krogstad et al., 2021). However, such evidence is lacking in children with obesity, as it is challenging to obtain biopsy samples from these children. There are very few clinical studies reported in children that extrapolate metabolic enzyme activity from drug clearance or metabolite formation rate. For example, a pediatric study of the CYP3A4 substrate midazolam reported a 38% increase in absolute clearance with obesity, possibly conflicting with adult reports due to lower comorbidity rates in pediatric obesity (van Rongen et al., 2018). There is even less evidence to inform potential changes in transporter activity in children with obesity. While some studies of adults with nonalcoholic steatohepatitis, a common obesity-related fibro-inflammatory disease of the liver, show altered transport by organic anion transporting polypeptide (OATP) and multidrug resistance-associated protein (MRP), such investigations have yet to be explored in adults or

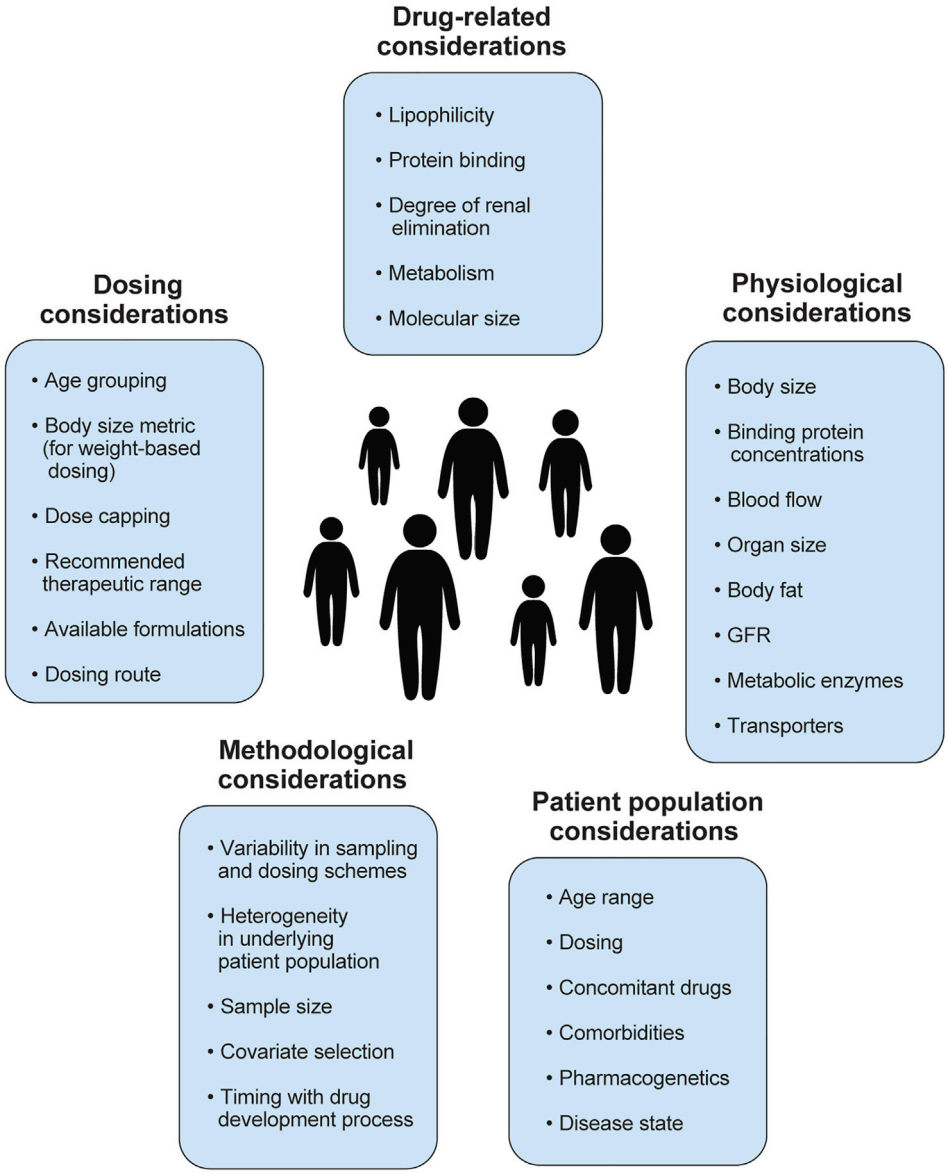


**FIGURE 2 |** Summary of factors to consider when studying pharmacokinetics in children with obesity, including physiological, drug-related, patient population, methodological considerations. Several factors to consider in dose selection are also included. GFR, glomerular filtration rate.

children with obesity specifically (Pierre et al., 2017; Ali et al., 2018; Sjöstedt et al., 2021).

For renal clearance, key variables include glomerular filtration rate (GFR) and tubular secretion and reabsorption. While absolute GFR is 12–29% higher in children 2–18 years of age with obesity, the more typically reported body surface area-normalized GFR is 1–3% lower on average (Correia-Costa et al., 2016; Gerhart et al., 2021). Increases in kidney size and GFR can impact the clearance of drugs with significant renal elimination. Changes in tubular reabsorption and secretion have not yet been explored in children with obesity. However, studies of drugs that are preferentially reabsorbed (e.g., lithium) and secreted (e.g., procainimide, ciprofloxacin, and cimetidine) in the renal tubule in adults suggest both increased tubular reabsorption and secretion with obesity (Christoff et al., 1983; Reiss et al., 1994; Blouin and Warren, 1999). Decreased renal clearance of these drugs supports the theory that tubular reabsorption and secretion is altered in these cases (Christoff et al., 1983; Reiss et al., 1994; Blouin and Warren, 1999).

## DRUG-RELATED CONSIDERATIONS

### Physicochemical Properties

The volume of distribution is important because it influences the selection of loading doses. Comparing the weight-normalized volume of distribution using total versus lean body weight measures helps illustrate how obesity impacts this PK

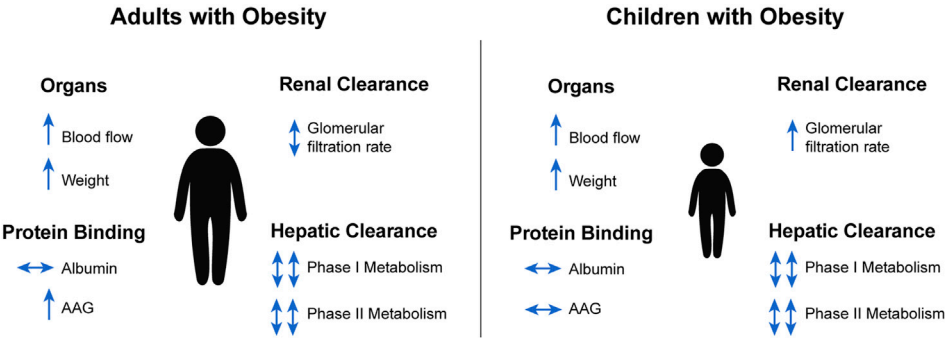


**FIGURE 3 |** Summary of obesity-induced physiological changes relevant to pharmacokinetics in adults and children (Ghobadi et al., 2011; Gerhart et al., 2021). AAG, alpha-1 acid glycoprotein.

parameter. If total body weight-normalized volume of distribution is similar between children with and without obesity, this suggests that the drug experiences high distribution into the additional fat mass. If total body weight-normalized volume of distribution is less in children with obesity, then there is not full distribution of the drug into excess fat mass. See **Table 2** for a selection of drugs previously studied in children with obesity. One review evaluating this across several prior studies found that total body weight was the best metric for characterizing volume of distribution in adults with obesity (for 40% of drugs). In contrast, lean body weight was the best metric for clearance (for 35% of drugs) (Green and Duffull, 2004). This meta-analysis also found that total body weight dosing for moderate to high lipophilic drugs best described the data empirically, whereas lean body weight-based dosing best described low lipophilic drugs (Green and Duffull, 2004). A similar empirical analysis is lacking for children with obesity. However, no single body size metric has been found to describe the overall impact of obesity on these PK parameters, as the best metric varies depending on the drug under study. Note that while drug concentration in the blood is easily measured, actual sites of distribution cannot be determined without directly sampling various tissues. Thus, it is challenging to evaluate changes in tissue distribution of a drug with obesity.

## Elimination Routes

The degree to which a drug is eliminated via renal excretion (e.g., by GFR) versus hepatic metabolism can also impact the degree to which the drug's clearance is altered with obesity. Vancomycin is a commonly used drug cleared entirely by GFR. Two studies evaluating vancomycin clearance differences in age-matched children with or without obesity observed a decrease (~25% or less) in weight-normalized clearance with obesity, with the magnitude of the difference declining in younger age groups (Le et al., 2015; Nassar et al., 2015). This is in-line with assumptions based on physiological changes, which suggest that absolute GFR increases only 12–29% on average with obesity, not proportionally with increased total body weight with obesity (Correia-Costa et al., 2016; Gerhart et al., 2021).

A drug's metabolism profile can also make a drug more susceptible to changes with obesity depending on which DMEs are responsible. For example, one pediatric study of chlorzoxazone, a CYP2E1 substrate, found that overall systemic clearance normalized to weight was significantly higher in children with versus without obesity, while the renal elimination remained unchanged (Gade et al., 2018). This suggests a potential increase in CYP2E1 activity and/or expression in children with obesity that drove two-fold higher absolute clearance (Gade et al., 2018). Studies of CYP3A substrates are mixed. Weight-normalized clearance decreased with obesity in children receiving clindamycin and in one study of midazolam, but was similar or slightly elevated relative to children without obesity in a study of fentanyl and two other midazolam studies (Harskamp-van Ginkel et al., 2015; van Rongen et al., 2015; Gade et al., 2020; Gerhart et al., 2021; Maharaj et al., 2021). This is likely also influenced by the degree to which liver blood flow impacts the hepatic clearance of these drugs based on their differing extraction ratios, or possibly differences in relative affinity for CYP3A5, 3A4, and/or 3A7. This also contrasts with midazolam studies in adults with obesity, which suggest a decrease in CYP3A4 metabolism (van Rongen et al., 2018). More studies are needed to confirm reduced CYP3A metabolism observed in adults with obesity. While these changes in drugs with a primary elimination route can be straightforward, these elimination-driven changes might be less clear for drugs with mixed elimination pathways.

## Biologics

Compared to small molecule drugs, biologics have several unique considerations with respect to drug absorption, distribution, metabolism, and excretion. Although biologics represent a heterogeneous drug class, including vaccines and blood products, we will specifically focus on therapeutic proteins.

Biologics are characterized by complex quaternary structures and very large molecular weights (1.3–251 kDa), which are susceptible to degradation in the gastrointestinal tract, and thus not suitable for oral administration (Vugmeyster et al., 2012; Meibohm, 2019). Accordingly, all currently used biologics are given parenterally, either intravenously,

**TABLE 2 |** Representative sample of reported pharmacokinetic changes with obesity for drugs dosed in children.

| Drug | Patient population | Sample size | Age | Body size | Dosing | PK conclusions | Dosing conclusion |
|---|---|---|---|---|---|---|---|
| Acetaminophen Barshop et al. (2011) | Case-control study of children with NAFLD | Without NAFLD: *n* = 12 boys<br>With NAFLD: *n* = 12 boys | Without NAFLD: 14.4 (4.5) years<br>With NAFLD: 14.8 (1.8) years | Without NAFLD: 26.22 (10.95) kg/m$^2$ BMI; 1.21 (1.42) BMI z-score<br>With NAFLD: 34.00 (6.14) kg/m$^2$ BMI; 2.30 (0.43) BMI z-score | Single 5 mg/kg oral dose capped at 325 mg | Children with NAFLD had higher concentrations of the glucuronide metabolite but no significant differences in PK parameters | --- |
| Busulfan Browning et al. (2011) | Children undergoing hematopoietic stem cell transplant conditioning | BMI percentile <25%: *n* = 17 (25.0%)<br>25-<85%: *n* = 29 (42.6%)<br>≥85%: *n* = 22 (32.4%) | Mean 7.1 (6.1) [0–21] years | 30.6 [2.5–117.8] kg TBW | BMI percentile <25%: 3.6 (0.7) mg/kg IV<br>25-<85%: 4.0 (1.1) mg/kg IV<br>≥85%: 2.9 (1.1) mg/kg IV; based on TBW | Children with high BMIs had higher AUCs after TBW dosing compared to children with mid-range or low BMIs. 53% of children with high BMIs would have AUCs ≥20% outside the target using AIBW dosing | Children with higher BMIs require a lower dose (2.9 mg/kg TBW) to match AUC to children with mid-range (4.0 mg/kg TBW) or low (3.6 mg/kg TBW) BMIs. Therapeutic drug monitoring is recommended |
| Clindamycin Smith et al. (2017) | Children receiving drug per standard of care | 420 total PK samples from 220 children (76 with obesity) | [range 0.01–20.5] years | BMI percentile <95%: *n* = 144 (65.4%)<br>≥95–99%: *n* = 46 (20.0%)<br>>99%: *n* = 30 (13.6%) | Drug dosed per standard of care | Obesity status did not explain inter-individual variability after accounting for TBW in PK parameters | Results support TBW-based dosing for all children |
| Doxorubicin Thompson et al. (2009) | Children with cancer | 22 children (6 with body fat >30%) | 15 [3.3–21.5] years | 51.5 [12.4–80] kg TBW<br>19.7 [13.2–30.0] kg/m$^2$ BMI<br>25 [15–36] body fat % | Any infusion <24 h on 1,2 days schedule not based on IBW or capped | Doxorubinol, but not doxorubicin, clearance was lower in patients with body fat >30% | --- |
| Fentanyl Maharaj et al. (2021) | Children receiving drug per standard of care | 53 samples from 32 children (31 with obesity) | 13 [2–19] years | 52 [16–164] kg TBW | Drug dosed per standard of care | The risk of achieving $C_{ss}$ values above the target increased with increasing body weight. Use of a theoretical allometric relationship between weight and CL described the PK in children with obesity | A proposed model-derived continuous infusion strategy based on TBW maximized the probability of achieving the target $C_{ss}$ range |
| Gentamicin Choi et al. (2011) | Case-control study of children with and without obesity | 25 children without obesity and 25 children with obesity | [2–18] years | --- | Without obesity: 2.25 (0.41) mg/kg TBW<br>With obesity: 1.86 (0.43) mg/kg TBW | Children with obesity had significantly higher peak and trough concentrations despite receiving significantly lower mg/kg TBW doses | Empirical dose reduction and therapeutic drug monitoring is necessary for children with obesity |
| Midazolam Gade et al. (2020) | --- | 67 adolescents (36 with obesity) with 13 plasma samples each | Without obesity: 14 [11–17] years<br>With obesity: 14 [11–17] years | Without obesity: 55 [33–76] kg TBW<br>With obesity: 77 [46–124] kg TBW | Single 1 μg IV bolus microdose | Faster inter-compartmental CL and a greater peripheral $V_d$ were observed in adolescents with obesity | Current dosing guidelines using TBW may lead to supra- or sub-therapeutic dosing in adolescents with obesity |

(Continued on following page)

**TABLE 2 |** (*Continued*) Representative sample of reported pharmacokinetic changes with obesity for drugs dosed in children.

| Drug | Patient population | Sample size | Age | Body size | Dosing | PK conclusions | Dosing conclusion |
|---|---|---|---|---|---|---|---|
| Midazolam van Rongen et al. (2015) | Adolescents undergoing surgery | 19 children with obesity or who were overweight (BMI percentile ≥85%) | Mean 15.9 [12.5–18.9] years | Mean 102.7 [62–149.8] kg TBW Mean 36.1 [24.8–55.0] kg/m$^2$ BMI | Either 2 or 3 mg IV | TBW did not influence CL but did affect peripheral $V_d$. This was explained by excess weight rather than maturational growth | Results suggest a potential need for higher initial infusion rates in adolescents with obesity |
| Vancomycin Le et al. (2015) | Case-control study of children with and without obesity | 87 matched pairs with 389 total plasma samples | Without obesity: 10.0 [IQR 4.8–15.2] years<br>With obesity: 10.2 [IQR 4.5–14.8] years | Without obesity: 44.0 [IQR 23.4–78.1] kg TBW<br>With obesity: 31.3 [IQR 16.8–47.1] kg TBW | Without obesity: mean 47.4 (13.0) [IQR 39.9–53.3] mg/kg/d TBW<br>With obesity: mean 41.9 (12.0) [IQR 33.4–50.1] mg/kg/d TBW | TBW and allometric weight were reasonable estimations of differences in CL and $V_d$ | PK differences are small and not likely clinically relevant in dose variation |
| Vancomycin Nassar et al. (2015) | Case-control study of children with and without obesity | 77 peak and trough concentrations from 51 children | 5 [0.5–18] years | 17.6 [3.5–83.0] kg TBW; Children were divided into underweight, normal weight, and overweight groups | 20 mg/kg TBW IV BID | PK parameters for all weight groups were similar | --- |

*Values reported as mean (standard deviation) or median [range] unless otherwise specified.*
*AIBW, adjusted ideal body weight; AUC, area under the plasma concentration-versus-time curve; BID, twice daily; BMI, body mass index; CL, clearance; $C_{ss}$, steady-state plasma concentration; IBW, ideal body weight; IQR, interquartile range; IV, intravenous; NAFLD, nonalcoholic fatty liver disease; PK, pharmacokinetic; TBW, total body weight; $V_d$, volume of distribution.*

subcutaneously, or intramuscularly. Biologics generally have volumes of distribution that approximate plasma volume, although molecular size, charge, and the presence of certain components (e.g., Fc fragments) can impact the drug's volume (Vugmeyster et al., 2012). Following subcutaneous or intramuscular administration, small biologics (<1 kDa) diffuse readily into blood, whereas large proteins generally reach systemic circulation through convective transport into lymphatic vessels. However, monoclonal antibodies (mAbs) or other drugs with an Fc component can undergo transcellular transport to the systemic circulation (Meibohm, 2019). Lastly, drug clearance for biologics can occur via multiple mechanisms, including proteolysis, intracellular catabolism through the reticuloendothelial system, or target-mediated drug disposition (TMDD) by binding to therapeutic targets (Vugmeyster et al., 2012). As a result, some biologics (e.g., mAbs) often show both linear and non-linear elimination processes. In addition, some patients may develop anti-drug antibodies against therapeutic proteins, often accelerating drug clearance (Mould, 2015).

The impact of obesity on the PK of biologics has not been extensively studied, but population pharmacokinetic (PopPK) modeling in adults suggests that body weight is a significant covariate on PK parameters for patients with and without obesity for many biologics. Using the most commonly prescribed biologics as an example, larger body weight is associated with higher clearance for etanercept, rituximab, and adalimumab; and higher volume of distribution for adalimumab and infliximab (Lee et al., 2003; Fasanmade et al., 2009; Nader et al., 2017; Rozman et al., 2017). Moreover, the impact of body size on biologics PK may be one potential mechanism that explains why patients with rheumatic diseases and with obesity have a substantially higher risk of failing treatment with anti-cytokine biologics (Singh et al., 2018).

Although the mechanisms by which biologics PK is altered by body size are not fully understood, several theories have been proposed. First, subcutaneous blood flow is reduced in individuals with obesity, potentially reducing or delaying the absorption of therapeutic proteins administered subcutaneously (Frayn and Karpe, 2014). Second, adipose tissue may have reduced expression of the neonatal Fc receptor (FcRn), which is responsible for recycling mAbs and other biologics with an Fc fragment (Hodkinson, 2017). Third, proteolytic clearance is higher with body weight (Mould, 2015). And lastly, obesity results in a state of chronic inflammation through increased expression of multiple inflammatory cytokines (Kern et al., 2001; Gremese et al., 2014; Schmidt et al., 2015). The inflammatory state could potentially increase biologics drug clearance through either increased protein catabolism or elevation of the baseline level of the target cytokine itself, causing enhanced TMDD. For example, both high pre-

treatment C-reactive protein (CRP) and tumor necrosis factor alpha (TNFα) levels (i.e., target baseline) are inversely correlated with infliximab trough levels (Wolbink et al., 2005; Takeuchi et al., 2011). Moreover, infliximab's half-life decreases from 14 to 8 days when CRP increases from 0.1 mg/L to 14 mg/L (Ternant et al., 2013).

Until the impact of obesity on biologics PK is better understood, it is difficult to provide definitive guidance on dosage adjustment for this drug class. However, because total blood volume relative to body size is reduced in patients with obesity, intravenous biologics that are dosed on a mg/kg basis (i.e., intravenous immune globulin [IVIG]) could potentially result in higher plasma concentrations when absolute body weight is used (Hodkinson, 2017). Accordingly, IVIG is often dosed using adjusted or ideal body weight (Anderson and Olson, 2015; Ameratunga, 2017). Conversely, differences in drug exposure were not different when subcutaneous immune-globulin was administered in patients with and without obesity, underscoring the heterogeneous effect that obesity may have on drug PK depending on the drug, route of administration, and possibly other unobserved patient characteristics (Shapiro, 2013).

## PATIENT POPULATION CONSIDERATIONS

Due to physiologic BMI undulations, physiologic developmental body fat changes, and other developmental changes, children over a wide range of ages (i.e., children ≥2 years of age through adulthood) should be enrolled to fully understand changes in PK. Unlike adults, for children the effect of obesity on PK can vary with age groups since age itself has a baseline influence on PK. This means that the difference in PK between children with and without obesity at one age group may be different within another age group (particularly after the onset of adolescence), and extrapolation without accounting for the age effect may lead to bias (van Rongen et al., 2018). For example, in a PK study of vancomycin in 87 age-matched pairs of children with and without obesity, weight-normalized clearance was similar between these two groups for children 2–12 years of age. In contrast, weight-normalized clearance decreased with obesity for those >12 years (Le et al., 2015). This observation may reflect the magnitude of the difference not being large enough to be detected by the study's sample size, or perhaps because a longer duration of obesity in older children leads to more pronounced obesity-induced changes or different BMI changes (fat-free mass, etc.) amongst these age groups.

Patient-related factors other than age can also affect PK and drug exposure, such as differences in dosing (e.g., weight-based dosing using different body size measures or drug formulations), concomitant drug administration, or pharmacogenetic variation in DMEs and transporters. Pediatric PK trials are commonly done by opportunistic sampling during standard of care treatment. Therefore, co-administration of certain drugs (e.g., enzyme-inducing antiepileptic drugs) interacting with an elimination pathway (e.g., CYP metabolism) of the drug in question potentially confounds the impact of obesity on clearance. The same confounding effect can come from pharmacogenetic alteration (i.e., gain or loss of function) in DMEs and transporters. Unfortunately, drug-drug interaction and pharmacogenetic studies are less commonly conducted in children, and these effects (if present) would potentially confound the assessment of obesity on PK (Gonzalez and Sinha, 2021). Obesity-focused pediatric trials should consider such potential effects of these patient-related factors (beyond just age) during trial design.

Further, an inherent issue with studying populations with obesity is the presence of comorbidities affecting PK, potentially confounding the influence of obesity (although these comorbidities are usually less prevalent in children than in adults with obesity). The common comorbidities associated with pediatric obesity include prediabetes and diabetes mellitus, dyslipidemia, prehypertension and hypertension, non-alcoholic fatty liver disease (NAFLD), polycystic ovary syndrome (PCOS), obstructive sleep apnea, and psychiatric conditions (Styne et al., 2017). NAFLD, which is estimated to occur in 38% of US children with obesity, has been shown to alter transport and clearance of hepatically eliminated drugs in adults (Schwimmer et al., 2006; Merrell and Cherrington, 2011). Reductions in kidney function with prolonged duration of diabetes, for example, may also impair drug clearance. These factors can change the fraction eliminated by a given elimination route, resulting in different obesity-induced changes. Conversely, for drugs studied for indications primarily in populations with obesity (e.g., metformin), there may be limited subjects without obesity to fully evaluate pharmacokinetic trends across a range of body sizes.

## METHODOLOGICAL CONSIDERATIONS

Typical PK studies in adults with obesity often involve a case-control matched noncompartmental analysis (NCA), in which PK parameters are calculated from individual concentration-versus-time profiles. However, the rich sampling scheme required to generate these profiles is difficult to collect in children, for whom generally only sparse samples are available. Even if rich pediatric sampling is available for children with obesity, it is still challenging to use NCA outside of a phase I study in the face of PK confounders. Due to the nature of pediatric studies, there is often significant inter-patient variability around sampling (including number and timing of sampling) and dosing regimens in addition to patient heterogeneity in terms of age, disease state, organ function, etc., which precludes the use of a naïve-pooled approach for PK parameter estimation.

Modeling and simulations tools can greatly aid understanding of PK in children with obesity and were recommended for consideration in all pediatric drug development programs by the FDA's Advisory Committee for Pharmaceutical Science and Clinical Pharmacology in 2012 (Food and Drug Administration, 2019). PopPK models are commonly used in PK analysis of drugs in children owing to sparse sampling requirements (Tremoulet et al., 2014; Standing et al., 2018). PopPK is a useful modeling tool because it can be used to analyze even sparse real-world data and

assess the effect of different body size metrics on PK parameters. However, PopPK is very data-driven and heavily reliant on study design. To evaluate the effect of obesity status (or age or organ function), data from a full age, size, or organ function range is required, and thus a robust study design is needed. In PopPK models, allometric scaling using plausible body size metrics (e.g., total body weight or fat-free mass) should be explored instead of a fixed *a priori* scaling with total body weight raised to the power of 0.75 (Sinha et al., 2019). An additional effect of age on clearance and volume of distribution (i.e., separate from body size) should also be tested (Germovsek et al., 2019). Simulations of target PK metrics (e.g., AUC or steady-state trough concentration) from the PopPK model should be used to find optimal dosing scalars (e.g., total body weight) and dosing regimens that would achieve equivalent exposure in children with and without obesity for a given age group.

Conversely, physiologically-based pharmacokinetic (PBPK) modeling is a bottom-up PK modeling approach that does not require extensive data, and thus it is not reliant on the PopPK constraints mentioned above. PBPK models account for changes in physiology and body composition in children to accurately guide dosing in children with obesity, all while requiring minimal data to develop. These models integrate physiological parameters (i.e., organ size and blood flow), drug parameters (i.e., physicochemical properties and metabolism), and known efficacy targets to describe drug disposition mechanistically and inform dosing (Cao and Jusko, 2012; Kuepfer et al., 2016). PBPK models offer advantages over traditional methods, such as PopPK models, by 1) describing developmental and physiological changes in children to capture the effect of age and body size on disposition, 2) providing prediction of concentrations in any tissue to allow for assessment of drug disposition at the target site, and 3) incorporating mechanistic information that is required to understand differences in PK. However, because of their foundations in physiology, these PBPK models require significant physiological information on the population under study, some of which is still unknown in children with obesity. This bottom-up approach can also require *in vitro* and physicochemical information not yet available, particularly for newer drugs under study. Nevertheless, PBPK modeling represents a useful tool for simulating PK and exposure of drugs dosed in children with obesity, even in the face of little data.

## OPPORTUNITIES AND FUTURE DIRECTIONS

A better understanding of the effect of obesity on PK for drugs commonly dosed in children with obesity is an urgent public health need, particularly as the already high prevalence of obesity in children grows. While the PK of many drugs has been shown to be altered in both adults and children as described herein, the impact of excess body size on drugs' clearance and volume of distribution has not been determined. To improve the safety and efficacy of drugs dosed in children, clinical PK studies need to enroll a more representative cohort of children across a wide range of body sizes. While there are numerous ethical and logistical constraints to be overcome in the enrollment of children with obesity, there are opportunities to bridge this PK data gap. This is supported by a new regulatory requirement for clinical trials to consider diversity and inclusion, including children with obesity.

Sparse sampling typical in pediatric PK studies may be supplemented with opportunistic or electronic health record (EHR) data. Opportunistic data involves collecting data from routine laboratory blood draws from pediatric patients receiving a particular drug under study per standard of care. Further clinical data documented in a pediatric patient's chart, such as demographics (e.g., age, BMI) and laboratory values (e.g., albumin, serum creatinine), can be easily collected. Similarly, drug concentration and dosing information from therapeutically monitored drugs, such as enoxaparin, can be collected retrospectively from EHR data for PK analysis (Richard et al., 2013). Consent rates for these types of data collection are typically higher, as it minimizes risk to the pediatric patient. However, opportunistic and EHR data have more inherent variability, putting additional pressure on sample sizes. Additionally, EHR data collection will only be feasible for the few drugs that undergo therapeutic drug monitoring.

PBPK modeling has tremendous potential for bottom-up prediction of PK in a target population without the need for data. Therefore, in the absence of data in this special population of children with obesity, PBPK modeling should be applied to complement PopPK analysis, especially in finding the likely effective dose for children with obesity. This approach has been previously used in adults with obesity to successfully predict drug clearance of eight drugs, including alprazolam, caffeine, chlorzoxazone, cyclosporine, midazolam, phenytoin, theophylline, and triazolam (Ghobadi et al., 2011). This approach has also recently been used to predict clearance and volume of distribution differences in children with versus without obesity receiving clindamycin and trimethoprim/sulfamethoxazole (Gerhart et al., 2021). There is an opportunity to continue applying this PBPK modeling approach to other drugs while evaluating the virtual population's underlying assumptions as new data becomes available about the physiological changes altered by obesity in children.

With the rise in popularity of biologics, there is an urgent need to address existing knowledge gaps in the optimal use of these drugs in children, particularly those with obesity. For example, researchers are still investigating the precise mechanisms that govern biologics drug disposition, such as anti-drug antibody-mediated clearance, factors affecting absorption, and the role of FcRn on biologics distribution, among others (Vugmeyster et al., 2012). Moreover, there is an ongoing need to understand the impact of genetic polymorphisms that affect both disposition processes (e.g., mutations in FcRn) and drug response (e.g., mutations in the TNFα receptor) (Jančić et al., 2015; Billiet et al., 2016). Accordingly, it will be increasingly important to support translational pharmacokinetic/pharmacodynamic (PK/PD) studies for modeling and simulation. By leveraging data from these mechanistic PK/PD studies, PBPK models were successfully scaled from adults to children for several biologics, including infliximab, palivizumab, and bevacizumab (Malik and Edginton, 2019; Basu et al., 2020). Lastly, clinical studies are needed to identify optimal target concentrations before the promise of

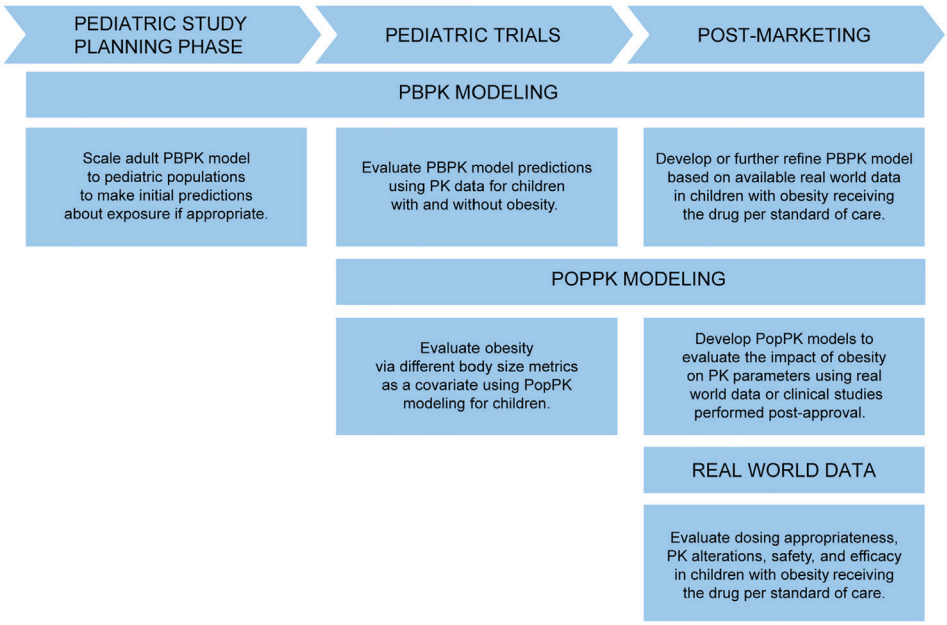


**FIGURE 4 |** Approaches to evaluate PK in children with obesity throughout pediatric drug development and into the post-marketing phase. PBPK, physiologically-based pharmacokinetic; PK, pharmacokinetics; PopPK, population pharmacokinetic.

PBPK model-guided dosing becomes a reality in children with obesity (Balevic and Sagcal-Gironella, 2022).

Ultimately, considering PK in children with obesity should be a part of pediatric drug development and considered as early in the pediatric drug development process as possible. This is especially true when the drug under study is particularly likely to be indicated in children with obesity (e.g., a diabetes or statin drug). PBPK modeling can be used at the beginning of a pediatric drug development program as part of the pediatric investigation plan (PIP) to estimate PK changes and inform dosing in children with versus without obesity *a priori*, then evaluated prospectively in pediatric studies (**Figure 4**). In this way, PBPK is used to make initial predictions until pediatric data becomes available. When these pediatric studies are performed, the impact of body size on PK can be further evaluated using PopPK modeling. If a drug is already approved, investigating dosing in children with obesity using opportunistic and EHR data can occur.

## CONCLUSION

Children with obesity are a rapidly growing patient population with a large knowledge gap in PK and dosing. Studies of children with obesity must consider obesity-induced changes in physiology relevant to PK, such as increased organ size and elimination mechanisms. Drug properties, such as lipophilicity or elimination route, can impact the degree to which these obesity-induced changes affect PK. Additional patient factors, particularly age range, concomitant drug administration, and comorbidities, must also be considered for a particular drug under study. Methodological factors like variability in sampling and dosing schemes and the underlying patient population and sample size must be accounted for when studying PK in children with obesity.

Children with obesity are susceptible to altered PK due to obesity-related physiological changes, such as increased organ size and drug elimination capacity. The extent to which obesity affects PK depends on the drug properties, such as lipophilicity and elimination pathway(s). However, several other factors that are mainly related to patient population, such as age group, concomitant drug administration, and comorbidities, can confound obesity-related changes in PK. Methodological constraints in pediatric trials like limited sample size and sparse sampling scheme impose further challenges in characterizing PK changes in children with obesity. This review has highlighted the key considerations related to physiology, drug parameters, patient factors, and methodology that need to be accounted for while studying the influence of obesity on PK in children. A well-designed study and appropriate use of modeling and simulation techniques can ensure appropriate dosing in children with obesity, thereby delivering safe and effective therapies to this vulnerable group of patients.

## AUTHOR CONTRIBUTIONS

JG and SB wrote the manuscript with guidance from JS and DG. EP, JW, and AE reviewed the manuscript critically. All authors approved the final version of the manuscript to be published.

## FUNDING

JG received research support from a Fred Eshelman Pre-Doctoral Fellowship in Pharmaceutical Sciences from the American Foundation for Pharmaceutical Education (AFPE). DG received research support from the Eunice Kennedy Shriver National Institute of Child Health and Human Development (NICHD) (5R01HD096435-04 and 1R01HD102949-01A1). The content is solely the authors' responsibility and does not necessarily represent the official views of the National Institutes of Health. The funders were not involved in the study design, collection, analysis, interpretation of data, the writing of this article, or the decision to submit it for publication. All authors declare no other competing interests.

## ACKNOWLEDGMENTS

We thank Catherine Laplace for her contributions to the aesthetic creation of our figures.

## REFERENCES

Abualsunun, W. A., Sahin, C., Cummins, C. L., and Piquette-Miller, M. (2020). Essential Role of STAT-3 Dependent NF-Kb Activation on IL-6-mediated Downregulation of Hepatic Transporters. *Eur. J. Pharm. Sci.* 143, 105151. doi:10.1016/j.ejps.2019.105151

Al-Sallami, H. S., Goulding, A., Grant, A., Taylor, R., Holford, N., and Duffull, S. B. (2015). Prediction of Fat-free Mass in Children. *Clin. Pharmacokinet.* 54, 1169–1178. doi:10.1007/s40262-015-0277-z

Ali, I., Slizgi, J. R., Kaullen, J. D., Ivanovic, M., Niemi, M., and Stewart, P. W. (2018). Transporter-mediated Alterations in Patients with NASH Increase Systemic and Hepatic Exposure to an OATP and MRP2 Substrate. *Clin. Pharmacol. Ther.* 104, 749–756. doi:10.1002/cpt.997

Ameratunga, R. (2017). Initial Intravenous Immunoglobulin Doses Should Be Based on Adjusted Body Weight in Obese Patients with Primary Immunodeficiency Disorders. *Allergy Asthma Clin. Immunol.* 13, 1–5. doi:10.1186/s13223-017-0220-y

Anderson, B. J., and Holford, N. H. G. (2009). Mechanistic Basis of Using Body Size and Maturation to Predict Clearance in Humans. *Drug Metab. Pharmacokinet.* 24, 25–36. doi:10.2133/dmpk.24.25

Anderson, B. J., and Holford, N. H. G. (2017). What Is the Best Size Predictor for Dose in the Obese Child? *Paediatr. Anaesth.* 27, 1176–1184. doi:10.1111/pan.13272

Anderson, C. R., and Olson, J. A. (2015). Correlation of Weight-Based i.V. Immune Globulin Doses with Changes in Serum Immunoglobulin G Levels. *Am. J. Heal. Pharm.* 72, 285–289. doi:10.2146/ajhp140171

Balevic, S., and Sagcal-Gironella, A. C. P. (2022). Precision Medicine: Towards Individualized Dosing in Pediatric Rheumatology. *Rheum. Dis. Clin. North. Am.* 48, 305–330. doi:10.1016/j.rdc.2021.09.010

Barshop, N. J., Capparelli, E. V., Sirlin, C. B., Schwimmer, J. B., and Lavine, J. E. (2011). Acetaminophen Pharmacokinetics in Children with Nonalcoholic Fatty Liver Disease. *J. Pediatr. Gastroenterol. Nutr.* 52, 198–202. doi:10.1097/MPG.0b013e3181f9b3a0

Basu, S., Lien, Y. T., Vozmediano, V., Schlender, J.-F., Eissing, T., Schmidt, S., et al. (2020). Physiologically Based Pharmacokinetic Modeling of Monoclonal Antibodies in Pediatric Populations Using PK-Sim. *Front. Pharmacol.* 11, 1–14. doi:10.3389/fphar.2020.00868

Benedek, I., Blouin, R., and McNamara, P. (1984). Serum Protein Binding and the Role of Increased α1-acid Glycoprotein in Moderately Obese Male Subjects. *Br. J. Clin. Pharmacol.* 18, 941–946. doi:10.1111/j.1365-2125.1984.tb02567.x

Benedek, I., Fiske, W., III, Griffen, W., Bell, R., Blouin, R., and McNamara, P. (1983). Serum α1-acid Glycoprotein and the Binding of Drugs in Obesity. *Br. J. Clin. Pharmacol.* 16, 751–754. doi:10.1111/j.1365-2125.1983.tb02258.x

Billiet, T., Dreesen, E., Cleynen, I., Wollants, W. J., Ferrante, M., van Assche, G., et al. (2016). A Genetic Variation in the Neonatal Fc-Receptor Affects Anti-TNF Drug Concentrations in Inflammatory Bowel Disease. *Am. J. Gastroenterol.* 111, 1438–1445. doi:10.1038/ajg.2016.306

Blouin, R. A., and Warren, G. W. (1999). Pharmacokinetic Considerations in Obesity. *J. Pharm. Sci.* 88, 1–7. doi:10.1021/js980173a

Blouin, R., Kolpek, J., and Mann, H. (1987). Influence of Obesity on Drug Disposition. *Clin. Pharmacol.* 6, 706–714.

Browning, B., Thormann, K., Donaldson, A., Halverson, T., Shinkle, M., and Kletzel, M. (2011). Busulfan Dosing in Children with BMIs ≥85% Undergoing HSCT: A New Optimal Strategy. *Biol. Blood Marrow Transpl.* 17, 1383–1388. doi:10.1016/j.bbmt.2011.01.013

Callaghan, L. C., and Walker, J. D. (2015). An Aid to Drug Dosing Safety in Obese Children: Development of a New Nomogram and Comparison with Existing Methods for Estimation of Ideal Body Weight and Lean Body Mass. *Anaesthesia* 70, 176–182. doi:10.1111/anae.12860

Cao, Y., and Jusko, W. J. (2012). Applications of Minimal Physiologically-Based Pharmacokinetic Models. *J. Pharmacokinet. Pharmacodyn.* 39, 711–723. doi:10.1007/s10928-012-9280-2

Cayot, A., Laroche, D., Disson-Dautriche, A., Arbault, A., Maillefert, J. F., and Ornetti, P. (2014). Cytochrome P450 Interactions and Clinical Implication in Rheumatology. *Clin. Rheumatol.* 33, 1231–1238. doi:10.1007/s10067-014-2710-3

Choi, J. J., Moffett, B. S., McDade, E. J., and Palazzi, D. L. (2011). Altered Gentamicin Serum Concentrations in Obese Pediatric Patients. *Pediatr. Infect. Dis. J.* 30, 347–349. doi:10.1097/INF.0b013e31820013d210.1097/INF.0b013e3181ff023e

Christoff, P. B., Conti, D. R., Naylor, C., and Jusko, W. J. (1983). Procainamide Disposition in Obesity. *Drug Intell. Clin. Pharm.* 17, 516–522. doi:10.1177/106002808301700704

Cleocin Phosphate (2020). (clindamycin Injection, USP) and (Clindamycin Injection in 5% Dextrose). Available at: https://www.accessdata.fda.gov/drugsatfda_docs/label/2008/050441s055,050639s016lbl.pdf (Accessed November 14, 2020).

Colles, S. L., Dixon, J. B., Marks, P., Strauss, B. J., and O'Brien, P. E. (2006). Preoperative Weight Loss with a Very-Low-Energy Diet: Quantitation of Changes in Liver and Abdominal Fat by Serial Imaging. *Am. J. Clin. Nutr.* 84, 304–311. doi:10.1093/ajcn/84.2.30410.1093/ajcn/84.1.304

Correia-Costa, L., Schaefer, F., Afonso, A. C., Bustorff, M., Guimarães, J. T., Guerra, A., et al. (2016). Normalization of Glomerular Filtration Rate in Obese Children. *Pediatr. Nephrol.* 31, 1321–1328. doi:10.1007/s00467-016-3367-8

Fasanmade, A. A., Adedokun, O. J., Ford, J., Hernandez, D., Johanns, J., Hu, C., et al. (2009). Population Pharmacokinetic Analysis of Infliximab in Patients with Ulcerative Colitis. *Eur. J. Clin. Pharmacol.* 65, 1211–1228. doi:10.1007/s00228-009-0718-4

Food and Drug Administration (2019). Center for Drug Evaluation and Research Summary Minutes of the Advisory Committee for Pharmaceutical Science and Clinical Pharmacology. Available at: https://wayback.archive-it.org/7993/20170404154933/https:/www.fda.gov/downloads/AdvisoryCommittees/CommitteesMeetingMaterials/Drugs/AdvisoryCommitteeforPharmaceuticalScienceandClinicalPharmacology/UCM306989.pdf (Accessed Oct 07, 2021).

Frayn, K. N., and Karpe, F. (2014). Regulation of Human Subcutaneous Adipose Tissue Blood Flow. *Int. J. Obes.* 38, 1019–1026. doi:10.1038/ijo.2013.200

Freedman, D. S., and Sherry, B. (2009). The Validity of BMI as an Indicator of Body Fatness and Risk Among Children. *Pediatrics* 124, S23–S34. doi:10.1542/peds.2008-3586e

Gade, C., Dalhoff, K., Peterson, T. S., Riis, T., Schmeltz, C., Chabanova, E., et al. (2018). Higher Chlorzoxazone Clearance in Obese Children Compared with Nonobese Peers. *Br. J. Clin. Pharmacol.* 84, 1738–1747. doi:10.1111/bcp.13602

Gade, C., Sverrisdóttir, E., Dalhoff, K., Sonne, J., Johansen, M. Ø., Christensen, H. R., et al. (2020). Midazolam Pharmacokinetics in Obese and Non-obese Children and Adolescents. *Clin. Pharmacokinet.* 59, 643–654. doi:10.1007/s40262-019-00838-1

Gerhart, J. G., Carreño, F. O., Edginton, A. N., Sinha, J., Perrin, E. M., Kumar, K. R., et al. (2021). Development and Evaluation of a Virtual Population of Children with Obesity for Physiologically Based Pharmacokinetic Modeling. *Clin. Pharmacokinet.* Published online ahead of print. doi:10.1007/s40262-021-01072-4

Germovsek, E., Barker, C. I. S., Sharland, M., and Standing, J. F. (2019). Pharmacokinetic-pharmacodynamic Modeling in Pediatric Drug Development, and the Importance of Standardized Scaling of Clearance. *Clin. Pharmacokinet.* 58, 39–52. doi:10.1007/s40262-018-0659-0

Ghobadi, C., Johnson, T. N., Aarabi, M., Almond, L. M., Allabi, A. C., Rowland-Yeo, K., et al. (2011). Application of a Systems Approach to the Bottom-Up Assessment of Pharmacokinetics in Obese Patients: Expected Variations in Clearance. *Clin. Pharmacokinet.* 50, 809–822. doi:10.2165/11594420-000000000-00000

Gonzalez, D., and Sinha, J. (2021). Pediatric Drug-Drug Interaction Evaluation: Drug, Patient Population, and Methodological Considerations. *J. Clin. Pharmacol.* 61, S175–S187. doi:10.1002/jcph.1881

Green, B., and Duffull, S. B. (2004). What Is the Best Size Descriptor to Use for Pharmacokinetic Studies in the Obese? *Br. J. Clin. Pharmacol.* 58, 119–133. doi:10.1111/j.1365-2125.2004.02157.x

Green, T. P., Binns, H. J., Wu, H., Ariza, A. J., Perrin, E. M., Quadri, M., et al. (2020). Estimation of Body Fat Percentage for Clinical Pharmacokinetic Studies in Children. *Clin. Transl. Sci.*, 1–9. doi:10.1111/cts.12896

Gremese, E., Tolusso, B., Gigante, M. R., and Ferraccioli, G. (2014). Obesity as a Risk and Severity Factor in Rheumatic Diseases (Autoimmune Chronic Inflammatory Diseases). *Front. Immunol.* 5, 1–10. doi:10.3389/fimmu.2014.00576

Gulati, A. K., Kaplan, D. W., and Daniels, S. R. (2012). Clinical Tracking of Severely Obese Children: A New Growth Chart. *Pediatrics* 130, 1136–1140. doi:10.1542/peds.2012-0596

Harskamp-van Ginkel, M. W., Hill, K. D., Becker, K., Testoni, D., Cohen-Wolkowiez, M., Gonzalez, D., et al. (2015). Drug Dosing in Obese Children: A Systematic Review of Current Pharmacokinetic Data. *J. Am. Med. Assoc. Pediatr.* 169, 678–685. doi:10.1016/j.bbamem.2015.02.010.Cationic10.1001/jamapediatrics.2015.132

Haycock, G. B., Schwartz, G. J., and Wisotsky, D. H. (1978). Geometric Method for Measuring Body Surface Area: A Height-Weight Formula Validated in Infants, Children, and Adults. *J. Pediatr.* 93, 62–66. doi:10.1016/S0022-3476(78)80601-5

Hodkinson, J. P. (2017). Considerations for Dosing Immunoglobulin in Obese Patients. *Clin. Exp. Immunol.* 188, 353–362. doi:10.1111/cei.12955

Hwaung, P., Bosy-Westphal, A., Muller, M. J., Geisler, C., Heo, M., Thomas, D. M., et al. (2019). Obesity Tissue: Composition, Energy Expenditure, and Energy Content in Adult Humans. *Obesity* 27, 1472–1481. doi:10.1002/oby.22557

Jančić, I., Šefik-Bukilica, M., Živojinović, S., Damjanov, N., Spasovski, V., Kotur, N., et al. (2015). Influence of Promoter Polymorphisms of the TNF-α (-308g/A) and IL-6 (-174g/C) Genes on Therapeutic Response to Etanercept in Rheumatoid Arthritis. *J. Med. Biochem.* 34, 414–421. doi:10.2478/jomb-2014-0060

Janmahasatian, S., Duffull, S. B., Ash, S., Ward, L. C., Byrne, N. M., and Green, B. (2005). Quantification of Lean Bodyweight. *Clin. Pharmacokinet.* 44, 1051–1065. doi:10.2165/00003088-200544100-00004

Kern, P. A., Ranganathan, S., Li, C., Wood, L., and Ranganathan, G. (2001). Adipose Tissue Tumor Necrosis Factor and Interleukin-6 Expression in Human Obesity and Insulin Resistance. *Am. J. Physiol. Endocrinol. Metab.* 280, 745–751. doi:10.1152/ajpendo.2001.280.5.E745

Krogstad, V., Peric, A., Robertsen, I., Kringen, M. K., Vistnes, M., Hjelmesæth, J., et al. (2021). Correlation of Body Weight and Composition with Hepatic Activities of Cytochrome P450 Enzymes. *J. Pharm. Sci.* 110, 432–437. doi:10.1016/j.xphs.2020.10.027

Kuczmarski, R. J., Ogden, C. L., Guo, S. S., Grummer-Strawn, L. M., Flegal, K. M., Mei, Z., et al. (2000). *2000 CDC Growth Charts for the United States: Methods and Development*. Washington, DC: National Center for Health Statistics. doi:10.1001/jamaoncol.2020.2822

Kuepfer, L., Niederalt, C., Wendl, T., Schlender, J. F., Willmann, S., Lippert, J., et al. (2016). Applied Concepts in PBPK Modeling: How to Build a PBPK/PD Model. *CPT Pharmacometrics Syst. Pharmacol.* 5, 516–531. doi:10.1002/psp4.12134

Le, J., Capparelli, E. V., Wahid, U., Wu, Y. S. S., Romanowski, G. L., Tran, T. M., et al. (2015). Bayesian Estimation of Vancomycin Pharmacokinetics in Obese Children: Matched Case-Control Study. *Clin. Ther.* 37, 1340–1351. doi:10.1016/j.clinthera.2015.05.006

Lee, H., Kimko, H. C., Rogge, M., Wang, D., Nestorov, I., and Peck, C. C. (2003). Population Pharmacokinetic and Pharmacodynamic Modeling of Etanercept Using Logistic Regression Analysis. *Clin. Pharmacol. Ther.* 73, 348–365. doi:10.1016/S0009-9236(02)17635-1

Maharaj, A. R., Wu, H., Zimmerman, K. O., Speicher, D. G., Sullivan, J. E., Watt, K., et al. (2021). Dosing of Continuous Fentanyl Infusions in Obese Children: A Population Pharmacokinetics Analysis. *J. Clin. Pharmacol.*, 1–24.

Malik, P. R. V., and Edginton, A. N. (2019). Physiologically-based Pharmacokinetic Modeling vs. Allometric Scaling for the Prediction of Infliximab Pharmacokinetics in Pediatric Patients. *CPT Pharmacometrics Syst. Pharmacol.* 8, 835–844. doi:10.1002/psp4.12456

Matson, K. L., Horton, E. R., and Capino, A. C. (2017). Medication Dosage in Overweight and Obese Children. *J. Pediatr. Pharmacol. Ther.* 22, 81–83. doi:10.5863/1551-6776-22.1.81

Meibohm, B. (2019). "Pharmacokinetics and Pharmacodynamics of Therapeutic Peptides and Proteins,". *Meibohm Pharmaceutical Biotechnology*. Editors D. Crommelin and R. Sindelar (Cham: Springer). doi:10.1007/978-3-030-00710-2_6

Merrell, M. D., and Cherrington, N. J. (2011). Drug Metabolism Alterations in Nonalcoholic Fatty Liver Disease. *Drug Metab. Rev.* 43, 317–334. doi:10.3109/03602532.2011.577781

Morgan, E. T., Dempsey, J. L., Mimche, S. M., Lamb, T. J., Kulkarni, S., Cui, J. Y., et al. (2018). Physiological Regulation of Drug Metabolism and Transport: Pregnancy, Microbiome, Inflammation, Infection, and Fasting. *Drug Metab. Dispos.* 46, 503–513. doi:10.1124/dmd.117.079905

Mould, D. R. (2015). The Pharmacokinetics of Biologics: A Primer. *Dig. Dis.* 33, 61–69. doi:10.1159/000437077

Mulugeta, Y., Barrett, J. S., Nelson, R., Eshete, A. T., Mushtaq, A., Yao, L., et al. (2016). Exposure Matching for Extrapolation of Efficacy in Pediatric Drug Development. *J. Clin. Pharmacol.* 56, 1326–1334. doi:10.1002/jcph.744

Nader, A., Beck, D., Noertersheuser, P., Williams, D., and Mostafa, N. (2017). Population Pharmacokinetics and Immunogenicity of Adalimumab in Adult Patients with Moderate-To-Severe Hidradenitis Suppurativa. *Clin. Pharmacokinet.* 56, 1091–1102. doi:10.1007/s40262-016-0502-4

Nassar, L., Hadad, S., Gefen, A., Shachor-Meyouhas, Y., Mashiach, T., Krivoy, N., et al. (2015). Prospective Evaluation of the Dosing Regimen of Vancomycin in Children of Different Weight Categories. *Curr. Drug Saf.* 7, 375–381. doi:10.2174/1574886311207050009l0.2174/157488612805076606

Nawaratne, S., Brien, J. E., Seeman, E., Fabiny, R., Zalcberg, J., Cosolo, W., et al. (1998). Relationships Among Liver and Kidney Volumes, Lean Body Mass and Drug Clearance. *Br. J. Clin. Pharmacol.* 46, 447–452. doi:10.1046/j.1365-2125.1998.00812.x

NCD-RisC (2017). Worldwide Trends in Body-Mass index, Underweight, Overweight, and Obesity from 1975 to 2016: a Pooled Analysis of 2416 Population-Based Measurement Studies in 128·9 Million Children, Adolescents, and Adults. *Lancet* 390, 2627–2642. doi:10.1016/S0140-6736(17)32129-3

Pai, M. P., and Paloucek, F. P. (2000). The Origin of the "Ideal" Body Weight Equations. *Ann. Pharmacother.* 34, 1066–1069. doi:10.1345/aph.19381

Pierre, V., Johnston, C. K., Ferslew, B. C., Brouwer, K. L. R., and Gonzalez, D. (2017). Population Pharmacokinetics of Morphine in Patients with Nonalcoholic Steatohepatitis (NASH) and Healthy Adults. *CPT Pharmacometrics Syst. Pharmacol.* 6, 331–339. doi:10.1002/psp4.12185

Reiss, R. A., Haas, C. E., Karki, S. D., Gumbiner, B., Welle, S. L., and Carson, S. W. (1994). Lithium Pharmacokinetics in the Obese. *Clin. Pharmacol. Ther.* 55, 392–398. doi:10.1038/clpt.1994.47

Richard, A. A., Kim, S., Moffett, B. S., Bomgaars, L., Mahoney, D., and Yee, D. L. (2013). Comparison of Anti-xa Levels in Obese and Non-obese Pediatric Patients Receiving Treatment Doses of Enoxaparin. *J. Pediatr.* 162, 293–296. doi:10.1016/j.jpeds.2012.07.047

Richardson, T. A., and Morgan, E. T. (2005). Hepatic Cytochrome P450 Gene Regulation during Endotoxin-Induced Inflammation in Nuclear Receptor Knockout Mice. *J. Pharmacol. Exp. Ther.* 314, 703–709. doi:10.1124/jpet.105.085456

Rozman, S., Grabnar, I., Novaković, S., Mrhar, A., and Jezeršek Novaković, B. (2017). Population Pharmacokinetics of Rituximab in Patients with Diffuse Large B-Cell Lymphoma and Association with Clinical Outcome. *Br. J. Clin. Pharmacol.* 83, 1782–1790. doi:10.1111/bcp.13271

Scherrer, P. D., Mallory, M. D., Cravero, J. P., Lowrie, L., Hertzog, J. H., and Berkenbosch, J. W. (2015). The Impact of Obesity on Pediatric Procedural Sedation-Related Outcomes: Results from the Pediatric Sedation Research Consortium. *Pediatr. Anesth.* 25, 689–697. doi:10.1111/pan.12627

Schmidt, F. M., Weschenfelder, J., Sander, C., Minkwitz, J., Thormann, J., Chittka, T., et al. (2015). Inflammatory Cytokines in General and central Obesity and Modulating Effects of Physical Activity. *PLoS One* 10, 1–17. doi:10.1371/journal.pone.0121971

Schmitt, C., Kuhn, B., Zhang, X., Kivitz, A. J., and Grange, S. (2011). Disease-drug-drug Interaction Involving Tocilizumab and Simvastatin in Patients with Rheumatoid Arthritis. *Clin. Pharmacol. Ther.* 89, 735–740. doi:10.1038/clpt.2011.35

Schwimmer, J. B., Deutsch, R., Kahen, T., Lavine, J. E., Stanley, C., and Behling, C. (2006). Prevalence of Fatty Liver in Children and Adolescents. *Pediatrics* 118, 1388–1393. doi:10.1542/peds.2006-1212

Shapiro, R. (2013). Subcutaneous Immunoglobulin (16 or 20%) Therapy in Obese Patients with Primary Immunodeficiency: A Retrospective Analysis of Administration by Infusion Pump or Subcutaneous Rapid Push. *Clin. Exp. Immunol.* 173, 365–371. doi:10.1111/cei.12099

Singh, S., Facciorusso, A., Singh, A. G., Casteele, N. V., Zarrinpar, A., Prokop, L. J., et al. (2018). Obesity and Response to Anti-tumor Necrosis Factor-α Agents in Patients with Select Immune-Mediated Inflammatory Diseases: A Systematic Review and Meta-Analysis. *PLoS One* 13, 1–26. doi:10.1371/journal.pone.0195123

Sinha, J., Al-Sallami, H. S., and Duffull, S. B. (2019). Choosing the Allometric Exponent in Covariate Model Building. *Clin. Pharmacokinet.* 58, 89–100. doi:10.1007/s40262-018-0667-0

Sinha, J., Duffull, S. B., and Al-Sallami, H. S. (2018). A Review of the Methods and Associated Mathematical Models Used in the Measurement of Fat-free Mass. *Clin. Pharmacokinet.* 57, 781–795. doi:10.1007/s40262-017-0622-5

Sjöstedt, N., Neuhoff, S., and Brouwer, K. L. R. (2021). Physiologically-based Pharmacokinetic Model of Morphine and Morphine-3-Glucuronide in Nonalcoholic Steatohepatitis. *Clin. Pharmacol. Ther.* 109, 676–687. doi:10.1002/cpt.2037

Skinner, A. C., Perrin, E. M., Moss, L. A., and Skelton, J. A. (2015). Cardiometabolic Risks and Severity of Obesity in Children and Young Adults. *N. Engl. J. Med.* 373, 1307–1317. doi:10.1056/NEJMoa1502821

Skinner, A. C., Ravanbakht, S. N., Skelton, J. A., Perrin, E. M., and Armstrong, S. C. (2018). Prevalence of Obesity and Severe Obesity in US Children. *Pediatrics* 141, 1999–2016. doi:10.1542/peds.2017-3459

Smith, M. J., Gonzalez, D., Goldman, J. L., Yogev, R., Sullivan, J. E., Reed, M. D., et al. (2017). Pharmacokinetics of Clindamycin in Obese and Nonobese Children. *Antimicrob. Agents Chemother.* 61, 1–12. doi:10.1128/aac.02014-16

Solmi, F., and Morris, S. (2015). Association between Childhood Obesity and Use of Regular Medications in the UK: Longitudinal Cohort Study of Children Aged 5 – 11 Years. *Br. Med. J. Open* 5, 1–10. doi:10.1136/bmjopen-2014-007373

Standing, J. F., Ongas, M. O., Ogwang, C., Kagwanja, N., Murunga, S., Mwaringa, S., et al. (2018). Dosing of Ceftriaxone and Metronidazole for Children with Severe Acute Malnutrition. *Clin. Pharmacol. Ther.* 104, 1165–1174. doi:10.1002/cpt.1078

Styne, D. M., Arslanian, S. A., Connor, E. L., Farooqi, I. S., Murad, M. H., Silverstein, J. H., et al. (2017). Pediatric Obesity-Assessment, Treatment, and Prevention: An Endocrine Society Clinical Practice Guideline. *J. Clin. Endocrinol. Metab.* 102, 709–757. doi:10.1210/jc.2016-2573

Sun, H., Temeck, J., Chambers, W., Perkins, G., Bonnel, R., and Murphy, D. (2017). Extrapolation of Efficacy in Pediatric Drug Development and Evidence-Based Medicine: Progress and Lessons Learned. *Ther. Innov. Regul. Sci.*, 1–7. doi:10.1177/2168479017725558.Extrapolation

Takeuchi, T., Miyasaka, N., Tatsuki, Y., Yano, T., Yoshinari, T., Abe, T., et al. (2011). Baseline Tumour Necrosis Factor Alpha Levels Predict the Necessity for Dose Escalation of Infliximab Therapy in Patients with Rheumatoid Arthritis. *Ann. Rheum. Dis.* 70, 1208–1215. doi:10.1136/ard.2011.153023

Ternant, D., Ducourau, E., Perdriger, A., Corondan, A., le Goff, B., Devauchelle-Pensec, V., et al. (2013). Relationship between Inflammation and Infliximab Pharmacokinetics in Rheumatoid Arthritis. *Br. J. Clin. Pharmacol.* 78, 118–128. doi:10.1111/bcp.12313

Thompson, P. A., Rosner, G. L., Matthay, K. K., Moore, T. B., Bomgaars, L. R., Ellis, K. J., et al. (2009). Impact of Body Composition on Pharmacokinetics of Doxorubicin in Children: A Glaser Pediatric Research Network Study. *Cancer Chemother. Pharmacol.* 64, 243–251. doi:10.1007/s00280-008-0854-z

Tremoulet, A., Le, J., Poindexter, B., Sullivan, J. E., Laughon, M., Delmore, P., et al. (2014). Characterization of the Population Pharmacokinetics of Ampicillin in Neonates Using an Opportunistic Study Design. *Antimicrob. Agents Chemother.* 58, 3013–3020. doi:10.1128/AAC.02374-13

Ulvestad, M., Skottheim, I. B., Jakobsen, G. S., Bremer, S., Molden, E., Åsberg, A., et al. (2013). Impact of OATP1B1, MDR1, and CYP3A4 Expression in Liver and Intestine on Interpatient Pharmacokinetic Variability of Atorvastatin in Obese Subjects. *Clin. Pharmacol. Ther.* 93, 275–282. doi:10.1038/clpt.2012.261

U.S. Food and Drug Administration (2014). General Considerations for Pediatric Studies for Drugs and Biological Products – Draft Guidance for Industry. Available at: https://www.fda.gov/media/90358/download (Accessed Oct 31, 2021).

van Rongen, A., Brill, M. J. E., Vaughns, J. D., Valitalo, P. A. J., van Dongen, E. P. A., van Ramshorst, B., et al. (2018). Higher Midazolam Clearance in Obese Adolescents Compared with Morbidly Obese Adults. *Clin. Pharmacokinet.* 57, 601–611. doi:10.1007/s40262-017-0579-4

van Rongen, A., Vaughns, J. D., Moorthy, G. S., Barrett, J. S., Knibbe, C. A. J., and van den Anker, J. N. (2015). Population Pharmacokinetics of Midazolam and its Metabolites in Overweight and Obese Adolescents. *Br. J. Clin. Pharmacol.* 80, 1185–1196. doi:10.1111/bcp.12693

Vasan, R. S. (2003). Cardiac Function and Obesity. *Heart* 89, 1127–1129. doi:10.1136/heart.89.10.1127

Vaughns, J. D., Conklin, L. S., Long, Y., Zheng, P., Faruque, F., Green, D. J., et al. (2018). Obesity and Pediatric Drug Development. *J. Clin. Pharmacol.* 58, 650–661. doi:10.1002/jcph.1054

Vugmeyster, Y., Xu, X., Theil, F.-P., Khawli, L. A., and Leach, M. W. (2012). Pharmacokinetics and Toxicology of Therapeutic Proteins: Advances and Challenges. *World J. Biol. Chem.* 3, 73–92. doi:10.4331/wjbc.v3.i4.73

Williams, K., Thomson, D., Seto, I., Contopoulos-Ioannidis, D. G., Ioannidis, J. P., Curtis, S., et al. (2012). Standard 6: Age Groups for Pediatric Trials. *Pediatrics* 129, S153–S160. doi:10.1542/peds.2012-0055I

Wolbink, G. J., Voskuyl, A. E., Lems, W. F., de Groot, E., Nurmohamed, M. T., Tak, P. P., et al. (2005). Relationship between Serum Trough Infliximab Levels, Pretreatment C Reactive Protein Levels, and Clinical Response to Infliximab Treatment in Patients with Rheumatoid Arthritis. *Ann. Rheum. Dis.* 64, 704–707. doi:10.1136/ard.2004.030452

World Health Organization (2016). *Report of the Commission on Ending Childhood Obesity*. Geneva, Switzerland: WHO Doc Prod Serv. https://apps. who. int/iris/bitstream/handle/10665/204176/97892 41510 066_ eng. pdf (Accessed Nov 14, 2020).

Young, J. F., Luecke, R. H., Pearce, B. A., Lee, T., Ahn, H., Baek, S., et al. (2009). Human Organ/tissue Growth Algorithms that Include Obese Individuals and Black/white Population Organ Weight Similarities from Autopsy Data. *J. Toxicol. Environ. Heal. - Part. A. Curr. Issues* 72, 527–540. doi:10.1080/15287390802647203

**Conflict of Interest:** DG receives research support from Nabriva Therapeutics through a contract with The University of North Carolina at Chapel Hill. In addition, DG serves as a consultant for Tellus Therapeutics, focusing on neonatal drug development.

The remaining author declares that the research was conducted in the absence of any commercial or financial relationships that could be construed as a potential conflict of interest. This article reflects the views of the authors and should not be construed to represent FDA's views or policies.

The handling editor declared a past collaboration with one of the authors (DG).

**Publisher's Note:** All claims expressed in this article are solely those of the authors and do not necessarily represent those of their affiliated organizations, or those of the publisher, the editors and the reviewers. Any product that may be evaluated in this article, or claim that may be made by its manufacturer, is not guaranteed or endorsed by the publisher.

frontiers in Pharmacology

ORIGINAL RESEARCH
published: 17 March 2022
doi: 10.3389/fphar.2022.817276

# External Evaluation of Risperidone Population Pharmacokinetic Models Using Opportunistic Pediatric Data

*Eleni Karatza[1†], Samit Ganguly[1,2†], Chi D. Hornik[3†], William J. Muller[4†], Amira Al-Uzri[5], Laura James[6], Stephen J. Balevic[3†], Daniel Gonzalez[1*†] and On Behalf of the Best Pharmaceuticals for Children Act–Pediatric Trials Network Steering Committee**

[1]Division of Pharmacotherapy and Experimental Therapeutics, UNC Eshelman School of Pharmacy, The University of North Carolina at Chapel Hill, Chapel Hill, NC, United States, [2]Regeneron Pharmaceuticals, Inc., Tarrytown, NY, United States, [3]Duke Clinical Research Institute, Durham, NC, United States, [4]Ann and Robert H. Lurie Children's Hospital of Chicago, Chicago, IL, United States, [5]Oregon Health and Science University, Portland, OR, United States, [6]Arkansas Children's Hospital Research Institute and the University of Arkansas for Medical Sciences, Little Rock, AR, United States

Risperidone is approved to treat schizophrenia in adolescents and autistic disorder and bipolar mania in children and adolescents. It is also used off-label in younger children for various psychiatric disorders. Several population pharmacokinetic models of risperidone and 9-OH-risperidone have been published. The objectives of this study were to assess whether opportunistically collected pediatric data can be used to evaluate risperidone population pharmacokinetic models externally and to identify a robust model for precision dosing in children. A total of 103 concentrations of risperidone and 112 concentrations of 9-OH-risperidone, collected from 62 pediatric patients (0.16–16.8 years of age), were used in the present study. The predictive performance of five published population pharmacokinetic models (four joint parent-metabolite models and one parent only) was assessed for accuracy and precision of the predictions using statistical criteria, goodness of fit plots, prediction-corrected visual predictive checks (pcVPCs), and normalized prediction distribution errors (NPDEs). The tested models produced similarly precise predictions (Root Mean Square Error [RMSE]) ranging from 0.021 to 0.027 nmol/ml for risperidone and 0.053–0.065 nmol/ml for 9-OH-risperidone). However, one of the models (a one-compartment mixture model with clearance estimated for three subpopulations) developed with a rich dataset presented fewer biases (Mean Percent Error [MPE, %] of 1.0% *vs*. 101.4, 146.9, 260.4, and 292.4%) for risperidone. In contrast, a model developed with fewer data and a more similar population to the one used for the external evaluation presented fewer biases for 9-OH-risperidone (MPE: 17% *vs*. 69.9, 47.8, and 82.9%). None of the models evaluated seemed to be generalizable to the population used in this analysis. All the models had a modest predictive performance, potentially suggesting that sources of inter-individual variability were not entirely captured and that opportunistic data from a highly heterogeneous population are likely not the most appropriate data to evaluate risperidone models externally.

**Keywords: risperidone, pediatrics, pharmacokinetics, precision dosing, population modeling**

OPEN ACCESS

***Edited by:***
*Jeffrey Scott Barrett, Critical Path Institute, United States*

***Reviewed by:***
*Laura B. Ramsey, Cincinnati Children's Hospital Medical Center, United States*
*Sílvia M. Illamola, University of Minnesota Twin Cities, United States*

***Correspondence:**
*Daniel Gonzalez*
*daniel.gonzalez@unc.edu*

***†ORCID:***
*Eleni Karatza*
*https://orcid.org/0000-0001-8406-4121*
*Stephen J. Balevic*
*https://orcid.org/0000-0002-4016-1680*
*Samit Ganguly*
*https://orcid.org/0000-0002-3037-1959*
*Daniel Gonzalez*
*https://orcid.org/0000-0001-5522-5686*
*Chi D. Hornik*
*https://orcid.org/0000-0002-7656-3657*
*William J. Muller*
*https://orcid.org/0000-0001-7690-0695*

***Specialty section:***
*This article was submitted to Obstetric and Pediatric Pharmacology, a section of the journal Frontiers in Pharmacology*

***Received:*** *17 November 2021*
***Accepted:*** *31 January 2022*
***Published:*** *17 March 2022*

***Citation:***
*Karatza E, Ganguly S, Hornik CD, Muller WJ, Al-Uzri A, James L, Balevic SJ and Gonzalez D (2022) External Evaluation of Risperidone Population Pharmacokinetic Models Using Opportunistic Pediatric Data. Front. Pharmacol. 13:817276. doi: 10.3389/fphar.2022.817276*

## INTRODUCTION

Risperidone is the most frequently prescribed atypical antipsychotic in the pediatric population (Halfdanarson et al., 2017). It is an antagonist of serotoninergic, dopaminergic, adrenergic, and histaminergic receptors (Chopko et al., 2018). In the United States, risperidone is indicated for use in the pediatric population for the treatment of irritability associated with autistic disorder (5–16 years of age), bipolar disorder (10–17 years of age), and schizophrenia (13–17 years of age) (Risperdal® package insert, 2009). In addition, risperidone is frequently used off-label (including in pediatric patients below 2 years of age) for the management of delirium in the pediatric intensive care unit (PICU), and in children greater than 5 years of age to treat post-traumatic stress disorder, Tourette syndrome, and agitation associated with delirium (Campbell et al., 2020; Liviskie and McPherson, 2021). Risperidone has also been demonstrated to be an efficacious option for the management of attention-deficit/hyperactivity disorder and various other psychiatric disorders associated with anxiety and irritability in children (Eapen and Gururaj, 2005; Jensen et al., 2007; Biederman et al., 2008; Arnold et al., 2015; Lee et al., 2018). Risperidone use is associated with dose and duration-dependent adverse effects, including weight gain, extrapyramidal symptoms, prolactin elevation, sedation, and QTc interval prolongation (Vanwong et al., 2020; Kloosterboer et al., 2021).

Risperidone is extensively metabolized by cytochrome P450 (CYP) 2D6 and 3A4, leading to the formation of its active metabolite 9-OH-risperidone. Most of the drug is excreted as metabolites in the urine (65%) and the feces (14%), while only 5% is recovered unchanged in the urine (Sheehan et al., 2010; Saibi et al., 2012; Kneller et al., 2020; Kneller and Hempel, 2020). There is large inter-and intra- individual variability in risperidone's plasma concentrations, which has been attributed primarily to genetic polymorphisms in *CYP2D6* and secondarily to age, renal and hepatic function, disease status, and comedications (Livingston, 1994; Sheehan et al., 2010; Saibi et al., 2012; Mauri et al., 2018; Kneller et al., 2020; Kneller and Hempel, 2020). Despite its wide usage, a therapeutic window has not yet been established. Only recently, a range of 15–25 μg/L plasma concentrations, has been proposed as a plausible therapeutic window for the treatment of ADHD of a 10-year-old child receiving risperidone for over 3 months without comedications (Kloosterboer et al., 2021). Risperidone's large variability in plasma concentrations is anticipated to influence its efficacy and toxicity profile. Population pharmacokinetic (PK) models may offer an approach to identify sources of inter-individual variability and to inform precision dosing that would support efficacy for the use of risperidone in children (Medhasi et al., 2016; Kloosterboer et al., 2021).

A model with acceptable predictive performance is needed to guide precision dosing. The vast majority of population PK models of risperidone and 9-OH-risperidone have been developed using data from adult populations (Vermeulen et al., 2007; Feng et al., 2008; Locatelli et al., 2010; Yoo et al., 2012; Vandenberghe et al., 2015; Ji et al., 2016), while only three pediatric population PK models have been developed (Thyssen et al., 2010; Sherwin et al., 2012; Kloosterboer et al., 2021). In most cases, the disposition of both risperidone and its active metabolite was characterized with a one-compartment model. To account for the high variability in risperidone concentrations, mixture models were applied to estimate clearance for multiple subpopulations or *CYP2D6* genotype was included in the model as a covariate (Locatelli et al., 2010; Yoo et al., 2012; Vandenberghe et al., 2015). Other covariates that were identified to impact risperidone or 9-OH-risperidone PK were age and weight. More specifically, 9-OH-risperidone's clearance was shown to decrease with increasing age in adult populations (Feng et al., 2008; Vandenberghe et al., 2015). Also, weight was used for allometric scaling of the clearance and volume of distribution in all the models developed with pediatric data, accounting for changes in body size (Thyssen et al., 2010; Sherwin et al., 2012; Kloosterboer et al., 2021).

Models intended for precision dosing should undergo an extensive internal and external evaluation to ensure their reliability for drug dosing optimization. The most stringent method to effectively assess the predictive performance and generalizability of a population PK model in other populations is the external evaluation (Hwang et al., 2017; US FDA, 2019; Cheng et al., 2021). However, in most cases, only an internal evaluation is carried out during population PK model development (Hwang et al., 2017; Wu et al., 2021). Only one of the population PK models developed for risperidone and 9-OH-risperidone has been externally evaluated, using PK data collected in adults (Ji et al., 2016).

Opportunistic data (i.e., data collected during routine clinical care without retrieving samples solely for research purposes) have helped develop population PK models to support dosing selection in pediatrics (Gonzalez et al., 2014; Ge et al., 2020). The present study aimed to assess if sparse opportunistic data from a highly heterogeneous pediatric population can be used to perform an external evaluation of published models for risperidone. Secondarily, this study aimed to explore which of the published models of risperidone and 9-OH-risperidone is more generalizable to other populations and thus can be used for precision dosing.

## MATERIALS AND METHODS

### Data Collection

The plasma concentrations of risperidone and 9-OH-risperidone used for the present external evaluation analysis were collected through the Pediatric Trials Network (PTN) Pharmacokinetics of Understudied Drugs Administered to Children Per Standard of Care trial (POPS; Clinical Trials. gov # NCT01431326). POPS is a multicenter, prospective study of the PK of understudied drugs, including risperidone, administered to children (<21 years of age) per standard of care, as administered by their treating caregiver. The study protocol was reviewed and approved by the institutional review boards of Duke University (coordinating center) and all participating study sites. All participants and participant parents/legal guardians provided written informed consent or assent, as applicable. Exclusion criteria included

**TABLE 1 |** Population demographics and clinical characteristics of the patients in the external evaluation dataset.

| Characteristic | Median (range) |
|---|---|
| Bodyweight (kg) (*n* = 62) | 18.7 (3.64–129) |
| Post-natal age at first PK draw (years) (*n* = 62) | 4.67 (0.16–16.8) |
| Postmenstrual age at first PK draw (weeks) (*n* = 62) | 283 (45–916) |
| Direct Bilirubin (mg/dl) (*n* = 8) | 0.45 (0.0–4.4) |
| Total Bilirubin (mg/dl) (*n* = 18) | 0.40 (0.1–5.6) |
| Serum Creatinine (mg/dl) (*n* = 48) | 0.39 (0.1–0.8) |
| AST (U/L) (*n* = 19) | 35 (12–517) |
| ALT (U/L) (*n* = 20) | 30.5 (12–289) |
| ALB (g/dl) (*n* = 23) | 3.4 (2.3–4.9) |
| — | Number (%) patients |
| Sex | — |
| Male | 45 (73) |
| Female | 17 (27) |
| Age Group | — |
| Group 1: 31 days ≤ PNA <2 years | 23 (37) |
| Group 2: 2 years ≤ PNA <13 years | 29 (47) |
| Group 3: 13 years ≤ PNA <17 years | 10 (16) |
| RACE | — |
| White | 47 (76) |
| Black or African American | 9 (15) |
| Unknown or not reported | 2 (3) |
| American Indian or Alaska Native | 1 (2) |
| Native Hawaiian or Pacific Islander | 1 (2) |
| Multiple Races | 2 (3) |
| Obesity status (BMI ≥ 95th percentile) at enrollment | — |
| Not Obese | 17 (27) |
| Obese (≥95th percentile) | 26 (34) |
| Unknown/Unevaluable[a] | 24 (39) |
| Indication | — |
| ADHD | 4 (6) |
| Bipolar disorder | 3 (5) |
| Autistic disorder | 5 (8) |
| Behavior disorder | 4 (6) |
| Anxiety | 6 (10) |
| Other[a] | 14 (23) |
| Agitation | 10 (16) |
| Delirium | 16 (26) |
| Route of administration | — |
| Oral | 30 (48) |
| Nasogastric/Orogastric | 9 (15) |
| Nasojejunal | 1 (2) |
| Transpyloric | 7 (11) |
| Gastrostomy Tube | 6 (10) |
| Jejunostomy Tube | 2 (3) |
| Multiple | 7 (11) |
| Formulation | — |
| Solution | 40 (65) |
| Tablet | 22 (35) |

[a]*Other included patients with one of the following conditions or combination of conditions: Angelman's syndrome, irritability, sleep dysfunction, delirium and agitation, depression, sedation, psychotic episode, anxiety, or depression.*

known pregnancy, as determined by interview or testing, if available.

Depending on the patient's age and clinical condition, risperidone was administered through various routes, namely oral, nasogastric/orogastric, nasojejunal, transpyloric, gastrostomy tube, and jejunostomy tube. In addition, different formulations, such as solution and tablet, were used.

Blood samples were collected in ethylenediaminetetraacetic acid (EDTA) containing tubes during clinical laboratory collections or following a specific collection for study purposes. Plasma was separated by centrifugation (2,000 g) for 10 min at 4°C and stored at −70°C or colder within 8 h of collection. Given that this was a standard of care study, dosing and sampling schemes varied between subjects. In the study protocol, recommended PK sampling windows were provided, but PK samples collected with a standard of care laboratory assessment were also acceptable. Standard of care laboratory assessments (e.g., comprehensive metabolic panel) were recorded if collected within 72 h of a study dose of the drug.

## Analytical Method

Plasma samples were analyzed using a validated liquid chromatography method with tandem mass spectrometric detection (LC-MS/MS) by Frontage Laboratories (Exton, PA). Risperidone and its metabolite were extracted by protein precipitation using acetonitrile. Reversed-phase high-performance liquid chromatography (HPLC) separation was achieved using a Phenomenex Kinetex ® PFP column (50 × 3 mm, 2.6 micron). A gradient of two mobile phases was used with phase A consisting of 5 mM ammonium formate and 0.02% formic acid in water and acetonitrile 50/50 v/v and phase B consisting of 5 mM ammonium formate and 0.02% formic acid in water and acetonitrile 2/98 v/v. MS/MS detection was set at mass transitions of m/z 411.2→191.2 for risperidone and m/z 427.2 → 207.2 for 9-OH-risperidone. The lower limit of quantitation (LLOQ) for risperidone and 9-OH-risperidone was 0.100 ng/ml. The linear range of the method was 0.100–100 ng/ml for both compounds. Sample freeze-thaw stability was demonstrated for three cycles (freeze at −70°C and thaw to room temperature).

## Models Under Evaluation

A literature search was performed in PubMed using search terms as "risperidone," "pharmacokinetics," and "population model." Inclusion criteria applied for selecting studies for the external evaluation analysis were studies where risperidone was administered orally and studies with relatively large sample sizes (at least 40 patients included). The published results of the model's internal evaluation were considered.

A total of nine population PK models were identified to meet the above criteria (Vermeulen et al., 2007; Feng et al., 2008; Locatelli et al., 2010; Thyssen et al., 2010; Sherwin et al., 2012; Yoo et al., 2012; Vandenberghe et al., 2015; Ji et al., 2016; Kloosterboer et al., 2021). Three models used pediatric data (Thyssen et al., 2010; Sherwin et al., 2012; Kloosterboer et al., 2021), while the rest were developed with data from adults (Vermeulen et al., 2007; Feng et al., 2008; Locatelli et al., 2010; Yoo et al., 2012; Vandenberghe et al., 2015; Ji et al., 2016). As *CYP2D6* genotyping data were not available in our dataset (POPS study), for this external evaluation analysis, three models that included *CYP2D6* genotype as a covariate were excluded (Locatelli et al., 2010; Yoo et al., 2012; Vandenberghe et al., 2015). Similarly, one study where co-administration of carbamazepine was found as a covariate significantly altering clearance was excluded (Vermeulen et al., 2007).

As the study's primary aim was to evaluate population PK models developed in pediatric populations externally, all the

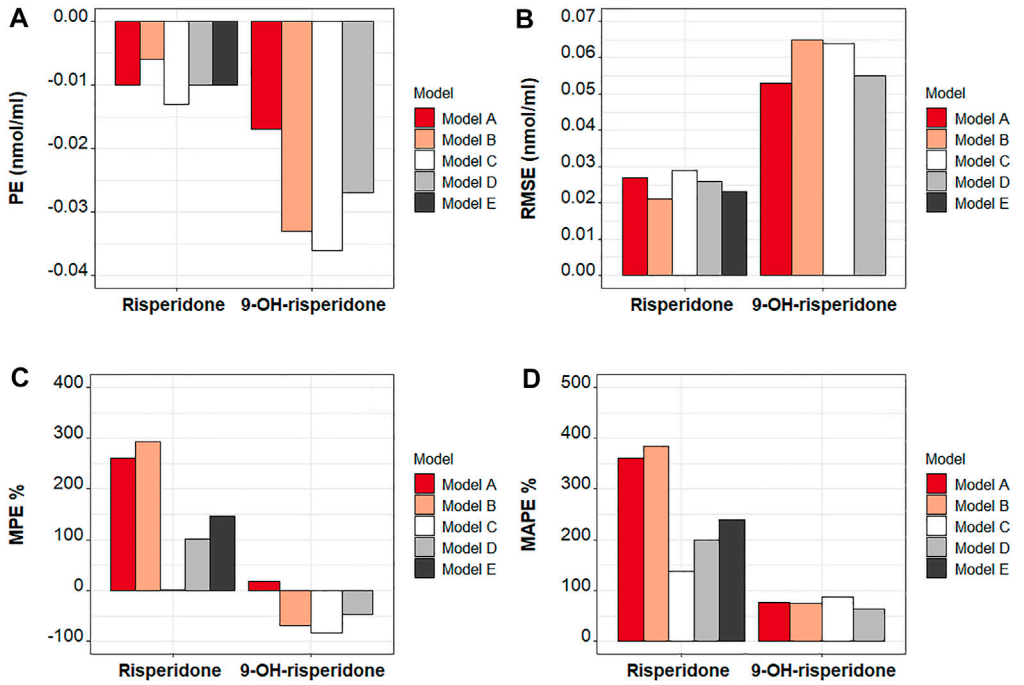


**FIGURE 1 |** Comparison of quantitative measures of bias and precision among the models included in the external evaluation analysis. Model **(A)**: Kloosterboer et al., 2021; Model **(B)**: Sherwin et al., 2012; Model **(C)**: Feng et al., 2008; Model **(D)**: Feng et al., 2008 with allometric scaling; and Model E: Thyssen et al., 2010. Precision was evaluated using the mean prediction error (PE) and the root mean square error (RMSE). Bias were evaluated using the mean percent error (MPE) and the mean absolute percent error (MAPE).

models developed with pediatric data (Thyssen et al., 2010; Sherwin et al., 2012; Kloosterboer et al., 2021) were included. The only model developed using solely adult data that was included in the present analysis was the model developed by Feng et al., 2008. This model was included as it was developed with the largest number of observations for both compounds (1,236 concentrations of risperidone and 1,236 concentrations of 9-OH risperidone) obtained from a large (490 patients) and highly heterogeneous population (18–93 years old and 42–187 kg of weight). In addition, the model developed by Feng et al., 2008 was used as a basis by Sherwin et al., 2012 to develop a model using only data from a pediartic population. More precisely, Sherwin et al., 2012 used the same structure and number of parameters as the model developed by Feng et al., 2008. A summary of the models included in the external evaluation analyses is provided in **Supplementary Table 1**.

As only data from adults were used for model development by Feng et al., 2008, this model was evaluated as reported, as well as after inclusion of bodyweight-dependent allometric scaling on clearance (fixed exponent: 0.75) and volume of distribution (fixed exponent: 1) of risperidone and 9-OH-risperidone. Therefore, the models evaluated were Model A: Kloosterboer et al., 2021; Model B: Sherwin et al., 2012; Model C: Feng et al., 2008; Model D: Feng et al., 2008 with allometric scaling; and Model E: Thyssen et al., 2010.

## External Evaluation

All the models included in the external evaluation analysis were joint parent-metabolite models, except for the model developed by Thyssen et al., 2010 where only risperidone concentrations were modeled (**Supplementary Table 1**). As most models were simultaneously predicting risperidone and 9-OH-risperidone's PK, the plasma concentrations collected and the dose administered were expressed in nmol/mL and nmol, respectively, after dividing by the molecular weight of risperidone (410.485 g/mol) or 9-OH-risperidone (425.91 g/mol).

The additive component of the evaluated error models was expressed in nmol/ml after correcting the reported value in ng/mL with the molecular weight. All the covariates included in the evaluated models were available in our dataset, allowing for a fair evaluation of inter-individual variability (**Supplementary Table 1**). In the model developed by Thyssen et al., data from various studies were included. Different parameters were estimated for two groups of studies depending on the clinical trial design and sampling scheme. The parameters used for the external evaluation were retrieved for the group of studies that included pediatric patients. In addition, as the model was developed with log-transformed concentrations, the model was also evaluated using log-transformed data. In the model developed by Kloosterboer et al., a different residual error model was used for samples obtained with the dried blood spot technique versus plasma samples. Only the latter error model was used for performing the evaluation as no dried blood spot samples were included in the evaluation dataset. Finally, for the models where a multimodal distribution (mixture model) was assumed for some parameters, the total probability in the population belonging to each subpopulation

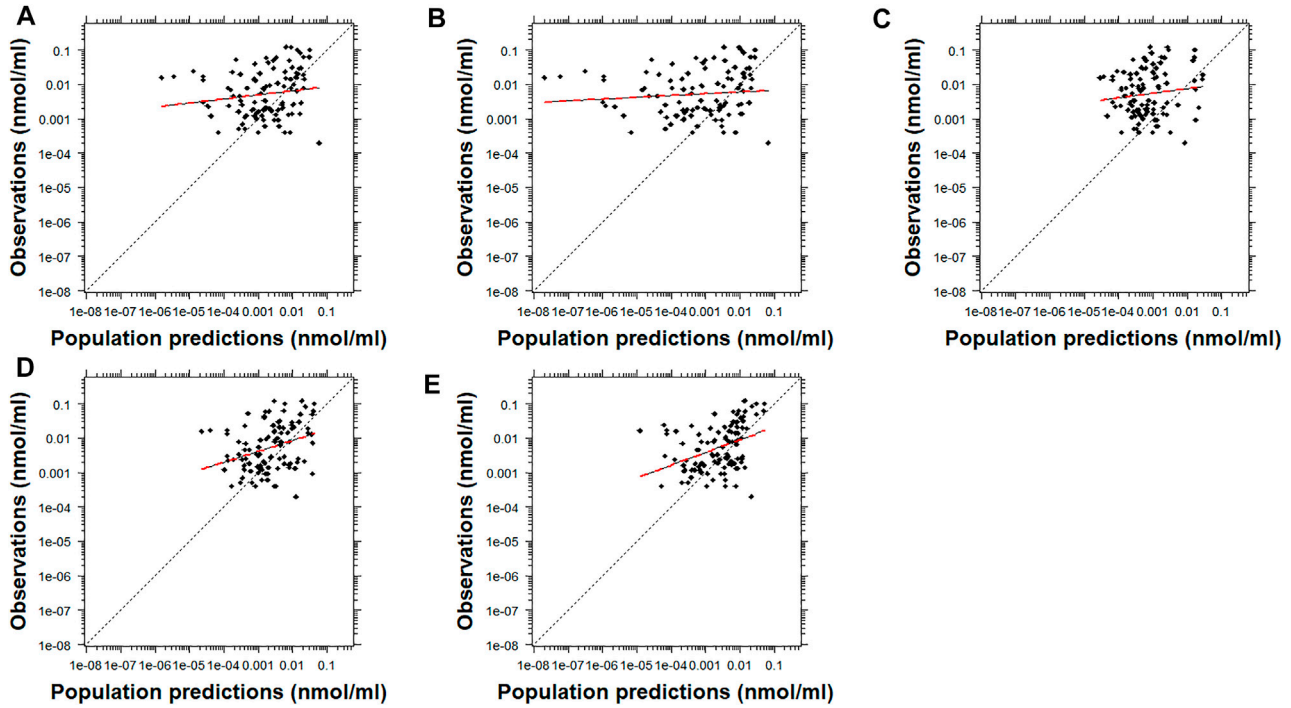


**FIGURE 2 |** Population predicted concentrations versus observations for risperidone. Model **(A)**: Kloosterboer et al., 2021; Model **(B)**: Sherwin et al., 2012; Model **(C)**: Feng et al., 2008; Model **(D)**: Feng et al., 2008 with allometric scaling; and Model **(E)**: Thyssen et al., 2010. The dashed black and dashed red lines represent the line of identity and the least-squares regression curve, respectively.

was fixed, like the rest of the model population parameters, to the value estimated in the respective study. Despite keeping all the parameters fixed, the individual probability of belonging to each subpopulation was estimated for each patient, taking into consideration the respective observations (Carlsson et al., 2009).

The models were implemented using the ADVAN6 subroutine in NONMEM version 7.4 (Icon Development Solutions, Ellicott City, MD, United States). Data manipulation, analysis, and visualization were performed using R (version 4.1.0) and RStudio (version 1.4.1717). The R packages lattice, latticeExtra, and gridExtra were used for preparing the goodness of fit plots (GOF) (Sarkar, 2008; Auguie, 2017; Sarkar and Andrews, 2019).

The external evaluation consisted of two parts. In the first part, the observations (i.e., the concentrations in the external dataset) were compared to the predictions obtained using each model (predictions-based diagnostics). In the second part, 1,000 simulations were performed with each model under evaluation (simulation-based diagnostics). The prediction-corrected visual predictive checks (pcVPCs) were generated by overlaying the observations on the prediction interval of the simulations. In addition, the normalized prediction distribution errors (NPDE) were calculated. The pcVPCs and NPDE are simulation-based diagnostics typically used for the external evaluation of population models (Comets et al., 2008; Bergstrand et al., 2011; Hwang et al., 2017; Nguyen et al., 2017; Cheng et al., 2021).

The observations (OBS) were compared to the population predictions (PRED) to assess the precision and accuracy of the predictions produced by each model. The precision was evaluated using the mean prediction error (PE) and the root mean square error (RMSE) as shown in **Eqs. 1**, **2**. To assess the biases produced by each model, the mean percent error (MPE) and the mean absolute percent error (MAPE) were computed (**Equations 3**, **4**).

$$\boldsymbol{PE} = \frac{1}{\mathrm{N}}\sum_{i=1}^{N}(\mathrm{PREDi} - \mathrm{OBSi}) \tag{1}$$

$$\boldsymbol{RMSE} = \sqrt{\frac{1}{\mathrm{N}}\sum_{i=1}^{N}(\mathrm{PREDi} - \mathrm{OBSi})^2} \tag{2}$$

$$\boldsymbol{MPE} = \frac{100}{\mathrm{N}}\sum_{i=1}^{N}\left(\frac{\mathrm{PREDi} - \mathrm{OBSi}}{\mathrm{OBSi}}\right) \tag{3}$$

$$\boldsymbol{MAPE} = \frac{100}{\mathrm{N}}\sum_{i=1}^{N}\left(\left|\frac{\mathrm{PREDi} - \mathrm{OBSi}}{\mathrm{OBSi}}\right|\right) \tag{4}$$

pcVPCs were generated using the Perl-speaks-NONMEM tool kit (PsN tool kit; version 3.6.2; Uppsala Pharmacometrics, Uppsala, Sweden) and the R package "xpose4" using 1,000 simulated samples. After retrieving 1,000 simulations using the model under evaluation with NONMEM $SIM subroutine, the NPDE were computed using the R package "npde" (Comets et al., 2008). The NPDE were evaluated statistically (Shapiro–Wilks test for normality, Fisher test for the difference of variance from 1 and t-test for the difference of mean from 0) and visually (histogram

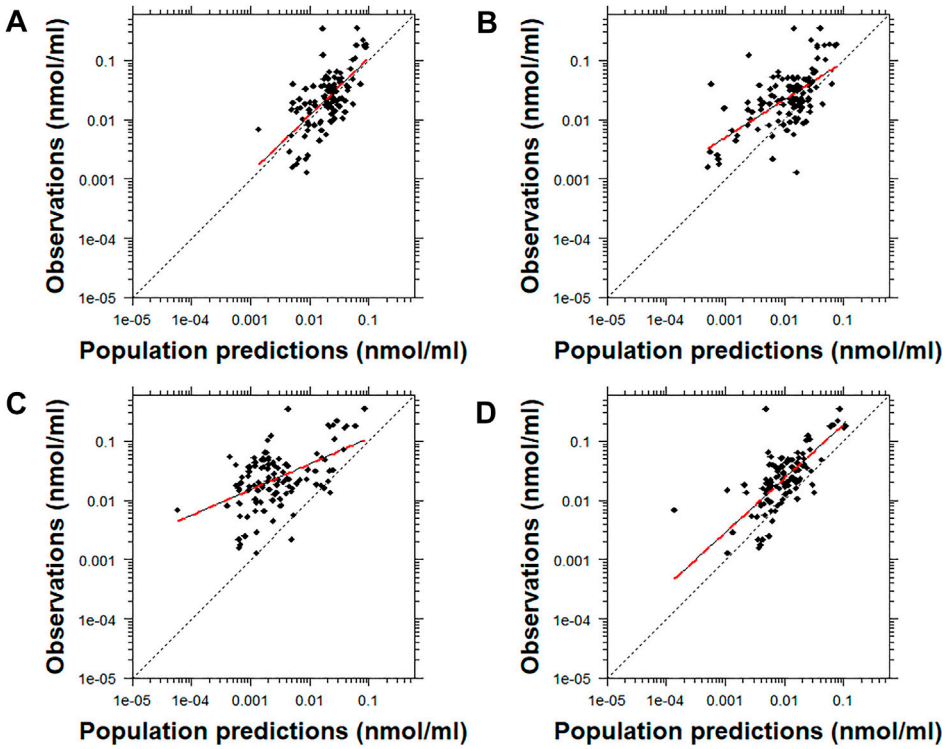


**FIGURE 3 |** Population predicted concentrations versus observations for the metabolite, 9-OH risperidone. Model **(A)**: Kloosterboer et al., 2021; Model **(B)**: Sherwin et al., 2012; Model **(C)**: Feng et al., 2008; and Model **(D)**: Feng et al., 2008 with allometric scaling. The dashed black and dashed red lines represent the line of identity and the least-squares regression curve, respectively.

of the NPDEs, Q-Q plot, NPDE versus PRED and NPDE versus time) (Comets et al., 2008).

# RESULTS

## Study Sample

A summary of the demographic characteristics of the 62 patients included in the study is presented in **Table 1**. Among the patients, three had undergone surgery and were on extracorporeal membrane oxygenation (ECMO) support; two were receiving a vasopressor, four hydromorphone, two linezolid, and one metoclopramide. The median (range) number of doses of risperidone recorded per patient during the study was 9 (1–43). The median (range) dose of risperidone administered was 0.250 mg (0.05–2 mg) or 0.017 mg/kg (0.003–0.068). The median (range) daily dose of risperidone administered was 0.450 mg (0.05–6) or 0.025 mg/kg (0.004–0.102).

A total of 103 concentrations of risperidone and 112 concentrations of 9-OH-risperidone were quantified and included in the study. The median (range) number of observations per subject was 1 (1–7), both for risperidone and 9-OH-risperidone. A total of 10 concentrations of risperidone and one concentration of 9-OH-risperidone were below the quantification limit (BQL) in the present dataset. However, none of the models externally evaluated reported or modeled the probability of data being BQL using the M3 or M4 Beal methods. Therefore, the BQL data collected in this analysis could not be used, but all the quantifiable concentrations were included.

## External Evaluation

The predictive performance of the five published models was initially assessed in terms of the precision of the predictions obtained using RMSE and PE (**Figures 1A,B**) and the biases produced using the MAPE and the MPE (**Figures 1C,D**). The precision of the predictions was similar among the models tested. However, slightly more precise predictions were obtained for risperidone with Model B and secondarily Model D and Model E. For 9-OH-risperidone, Model A and secondarily Model D resulted in more precise predictions. In contrast, there were significant differences among the models in terms of bias. For risperidone, the MPE had a positive value for all the models tested, indicating that the models tended to underestimate the observations (**Figure 1C**). Model C was observed to have a lower bias than the other models, with the MPE% being almost zero. Secondarily, Model D presented less bias than the other models evaluated (**Figures 1C,D**). For 9-OH-risperidone, the opposite trend was noted, as most of the models tested tended to overestimate the observations, apart from Model A that slightly underestimated the observations (**Figure 1C**). Considering the MPE and MAPE for 9-OH-risperidone, Models A, B, and D produced similar bias (**Figures 1C,D**).

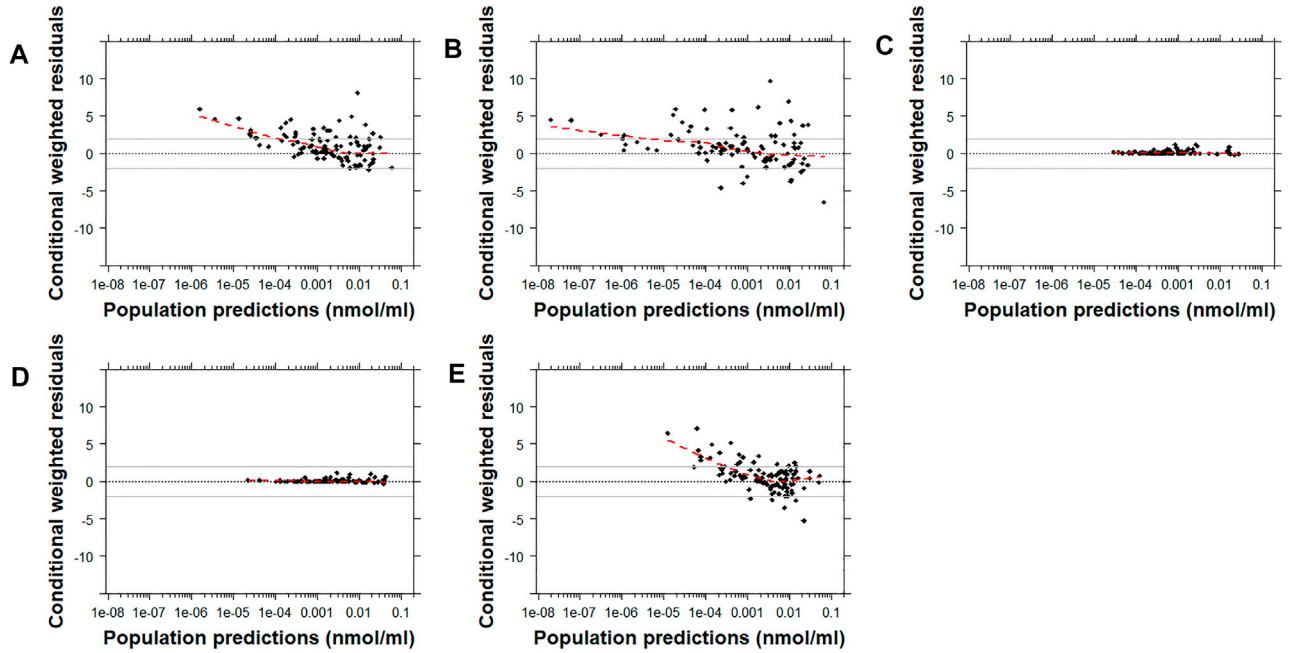


**FIGURE 4 |** Conditional weighted residuals (CWRES) versus population predictions for risperidone plotted on a log scale. Model **(A)**: Kloosterboer et al., 2021; Model **(B)**: Sherwin et al., 2012; Model **(C)**: Feng et al., 2008; Model **(D)**: Feng et al., 2008 with allometric scaling; and Model **(E)**: Thyssen et al., 2010. The dashed black line corresponds to a CWRES of zero. The solid grey lines correspond to CWRES values of 2 and −2. The dashed red line corresponds to the locally-weighted scatterplot smoothing curve (LOWESS).

After visual inspection of the PRED-versus-OBS plots, it was noted that Model D and Model E resulted in a better performance for risperidone (**Figure 2**). In comparison, Model A resulted in a better performance for 9-OH-risperidone (**Figure 3**). Especially for the parent compound, clear trends were noted with all the models under-predicting the observations (**Figure 2).**

Similarly, the conditional weighted residuals (CWRES)-versus-PRED and CWRES-versus-time after the first dose plots demonstrated that the lower observed concentrations of risperidone were generally under-predicted by most models except for Models C and D (**Figure 4** and **Supplementary Figures 1, 7**). The CWRES-versus-PRED and CWRES-versus-time after the first dose plots generated for 9-OH-risperidone demonstrated that Model A, C, and D performed similarly well, with only a few points deviating. At the same time, Model B resulted in non-normally distributed residuals (**Figure 5** and **Supplementary Figures 2, 8**).

For risperidone, the pcVPC plots showed that all the models had a similar predictive performance (**Figure 6** and **Supplementary Figure 9**). Model B demonstrated the lowest percentage of points outside the 95% prediction interval (4.9% [5 points]) followed by Model E, Model C, Model A, and Model D (11.7% [12 points], 18.4% [19 points], 21.4% [22 points], 26.2% [27 points], respectively). While there was a higher number of points outside the prediction interval with Model C and Model D than Model E or Model B, the distance of the points from the higher or the lower bound of the 95% prediction interval was much lower. **Supplementary Figure 3** shows the pcVPCs in a non-log-transformed scale.

For 9-OH-risperidone, the pcVPC plots showed that Models A, C, and D had a similar predictive performance with only 0.9% (1 point), 0.9% (1 point), 1.8% (2 points) of points outside the 95% prediction interval, respectively. In contrast, Model B presented a less adequate predictive performance with 20.5% (23 points) outside the 95% prediction interval (**Figure 7** and **Supplementary Figure 10**).

Hypothesis tests and normality plots performed with the NPDEs generated using 1,000 simulations with each model under evaluation showed that the NPDEs were not normally distributed with a mean of 0 and a variance of 1, with any of the models evaluated (**Supplementary Figure 4**).

The presence of age-related differences in the models' misspecification was also explored for both risperidone (**Supplementary Figure 5**) and 9-OH-risperidone (**Supplementary Figure 6**). In most cases, greater misspecification was observed in children below 2 years of age and secondarily below 6 years for risperidone. No age-related trend was noted for 9-OH-risperidone.

## DISCUSSION

The predictive performance of five models was evaluated using standard measures of model fitness and goodness-of-fit plots. To our knowledge, this is the first published external evaluation analysis of risperidone and 9-OH-risperidone performed using pediatric data. Despite the high reliability of external evaluation to ensure the predictive capacity of a model (US FDA, 2019;

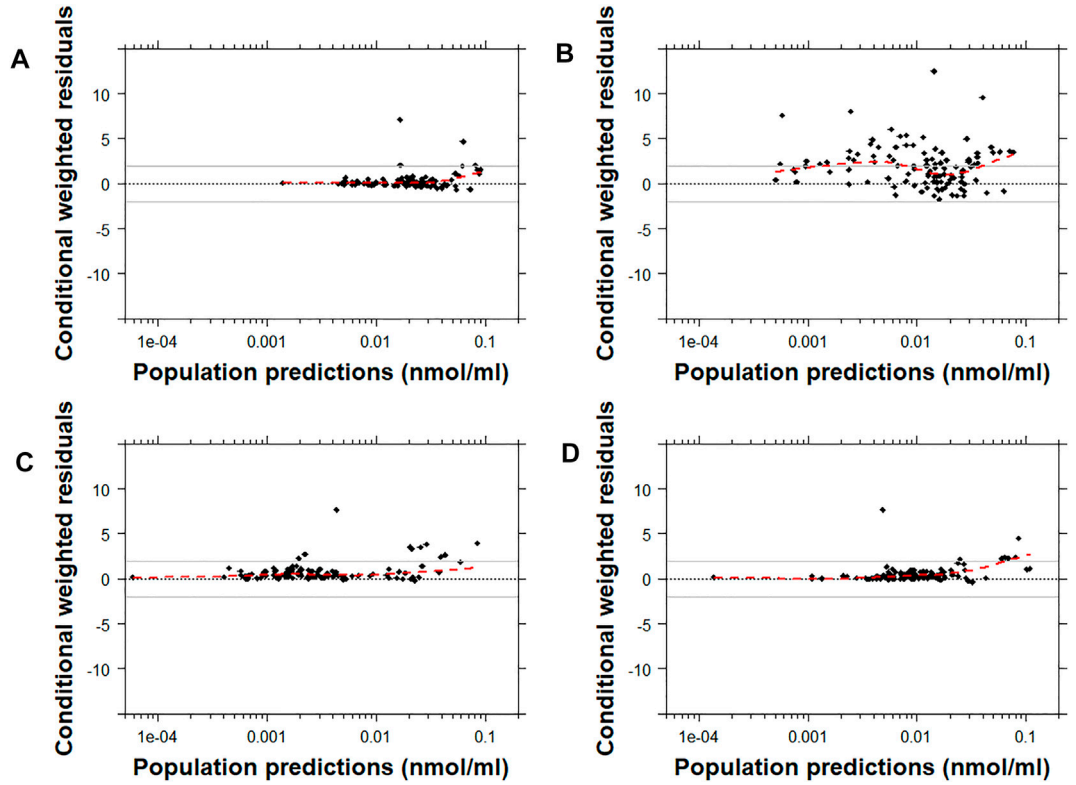


**FIGURE 5 |** Conditional weighted residuals versus populations predictions for 9-OH risperidone plotted on a log scale. Model **(A)**: Kloosterboer et al., 2021; Model **(B)**: Sherwin et al., 2012; Model **(C)**: Feng et al., 2008; and Model **(D)**: Feng et al., 2008 with allometric scaling. The dashed black line corresponds to a CWRES of zero. The solid grey lines correspond to CWRES values of 2 and -2. The dashed red line corresponds to the locally-weighted scatterplot smoothing curve (LOWESS).

Cheng et al., 2021), this type of evaluation is rarely performed with pediatric data, primarily due to the difficulty of obtaining samples from this vulnerable population. However, this study was made possible as opportunistic data from routine clinical care were collected without burdening the patients with additional blood draws. Given the scarcity of clinical data in infants, children, and adolescents to guide the dosing of risperidone, it is of great importance to assess if the developed models have a good extrapolation to these populations.

The present analysis aimed to externally evaluate population PK models developed in pediatric populations. The only model included that was developed using data only from adults was the model developed by Feng et al., 2008. This model was included because it was developed using the largest number of observations for both the parent and the metabolite. It has never been externally evaluated previously. Also, its structure informed the development of a model with pediatric data (Sherwin et al., 2012). By including the model developed by Feng et al., 2008 in the present analysis, we also aimed to indirectly compare these two models with the same structure and understand if developing the model in children offers a significant advantage compared to developing it in a large number of adults. As a result, a model previously developed in adults by Ji et al., 2016, that had been externally evaluated, was not included in the present analysis.

Many challenges were encountered during the assessment of the results of this analysis due to the inherent variability of risperidone and 9-OH risperidone PK, the significant differences in the models evaluated (**Supplementary Table 1**), and the populations used for the development of the models and their evaluation. The findings obtained by prediction-based diagnostics and the pcVPC, a simulation-based diagnostic that provides a direct visual comparison between predicted and observed data, generally agreed. Computation of the NPDE, another simulation-based diagnostic, provides information on the accuracy of the predictive performance of a model. However, none of the models tested produced normally distributed NPDE with a mean of zero and variance of one. This probably can be attributed to the general trend of the models to significantly under-predict risperidone (**Figures 1**, **2**) and to over-predict 9-OH-risperidone concentrations (**Figures 1**, **3**). In addition, it should be noted that the NPDE is probably the stringent and most objective diagnostic for model evaluation (Comets et al., 2008; Nguyen et al., 2017).

The model developed by Kloosterboer et al. (Model A) presented the best performance for 9-OH-risperidone, while for risperidone, it presented a relatively modest performance. This model was a 2-compartment model for the parent combined with a 1-compartment for the metabolite, with first-order absorption with lag-time, which did not assume different

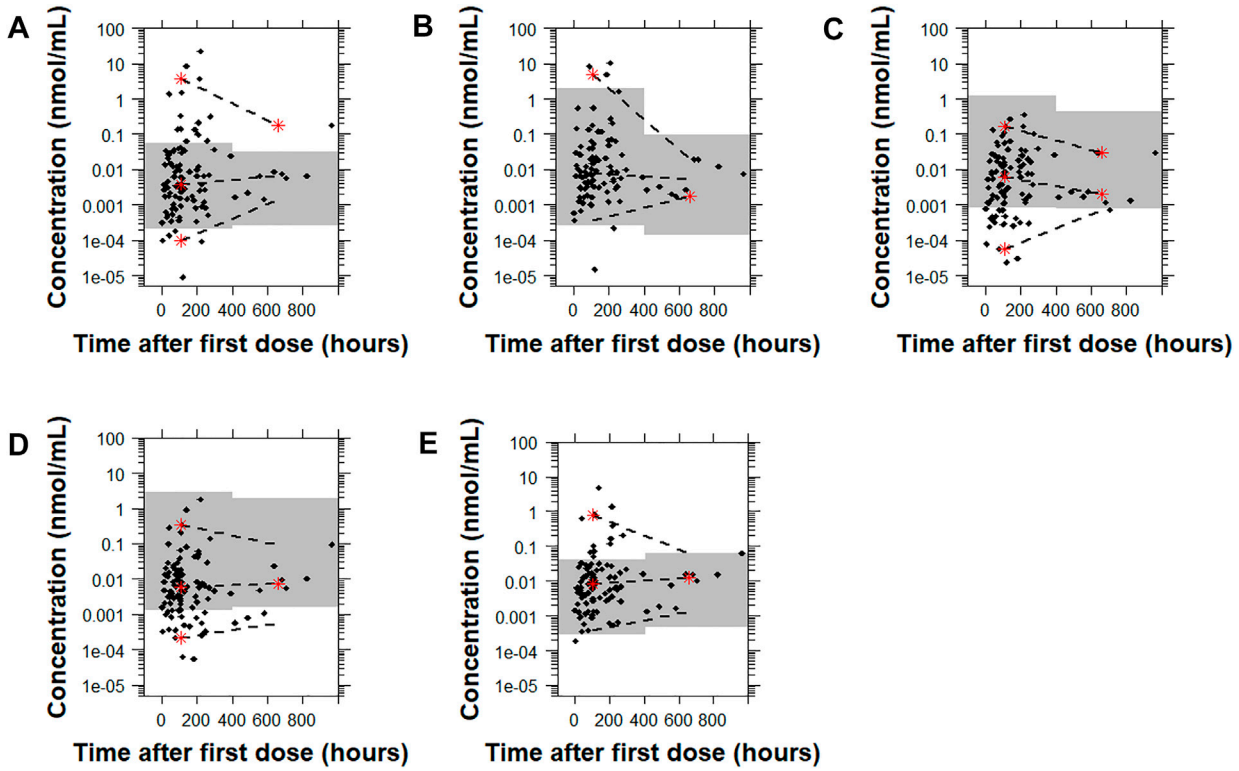


**FIGURE 6 |** Prediction-corrected visual predictive checks (pcVPCs) of the observed data overlaid on the predictions obtained by performing 1,000 simulations with each risperidone population pharmacokinetic model. Model **(A)**: Kloosterboer et al., 2021; Model **(B)**: Sherwin et al., 2012; Model **(C)**: Feng et al., 2008; Model **(D)**: Feng et al., 2008 with allometric scaling; and Model **(E)**: Thyssen et al., 2010. All pcVPC plots are based on the time after the first dose. The dashed lines represent the 5th, 50th, and 95th percentiles for the observed data, and the gray shaded regions are the 95% prediction interval for the predicted concentrations. The red stars indicate outlying percentiles of the observed data from the prediction interval. The *y* axis is in log-transformed scale. The *x* axis represents the time after first recorded dose. A sample that was collected later than 1,000 h after the first recorded dose was omitted from the graphs to improve visualization. The point was within the prediction interval for all of the models tested except for Model A.

subpopulations of risperidone clearance. The large variability in risperidone's PK is mainly attributed to *CYP2D6* genetic polymorphisms affecting its clearance (Sheehan et al., 2010; Kneller et al., 2020; Kneller and Hampel, 2020). Thus, the fact that this source of variability was not accounted for in this model influenced the model's performance leading to the estimation of population parameters that were less generalizable to other populations. Since the 9-OH-risperidone metabolite is not extensively metabolized and is primarily renally excreted (Vermeir et al., 2008), its primary sources of variability are age and weight (Feng et al., 2008; Kloosterboer et al., 2021). Thus, the excellent predictive performance of Model A for 9-OH-risperidone may be explained by the fact that the model was developed exclusively with data from pediatric patients and included patients with obesity, making it the most similar dataset to the one used for the external evaluation in terms of demographic characteristics of the patients. It should be noted that the dataset used by Sherwin et al., 2012 (Model B) also included exclusively pediatric patients (3–18 years old) and was developed with a similar number of observations. However, the two models had significantly different structures, with Model A requiring much fewer parameters than Model B, potentially contributing to a more accurate estimation of the population parameters, especially those describing the PK of the metabolite.

Three of the models compared [Model B, C and D (Feng et al., 2008 and Sherwin et al., 2012)] had the same structure: a 1-compartment model for the parent and 1-compartment for the metabolite, with first-order absorption, and multimodal risperidone clearance and fraction metabolized (including three subpopulations: poor, intermediate and normal metabolizers). Feng et al. developed a model (Model C [no allometric scaling] and Model D [allometric scaling included]) with data from 490 adult patients (1,236 observations for risperidone and 1,236 for its active metabolite), while Sherwin et al. developed a model (Model B) with data from 41 pediatric patients (163 observations for risperidone and 334 for its active metabolite). The fact that Model B considered the multimodal clearance and was developed using data from a more similar population to the one used for the external evaluation led to the model producing slightly more precise predictions for risperidone (**Figures 1A,B** and **6**). However, the same trend was not present for the metabolite. In addition, overall, based on the other metrics evaluated (MPE%, MAPE%, GOF plots), this model presented significant biases for both the parent and the

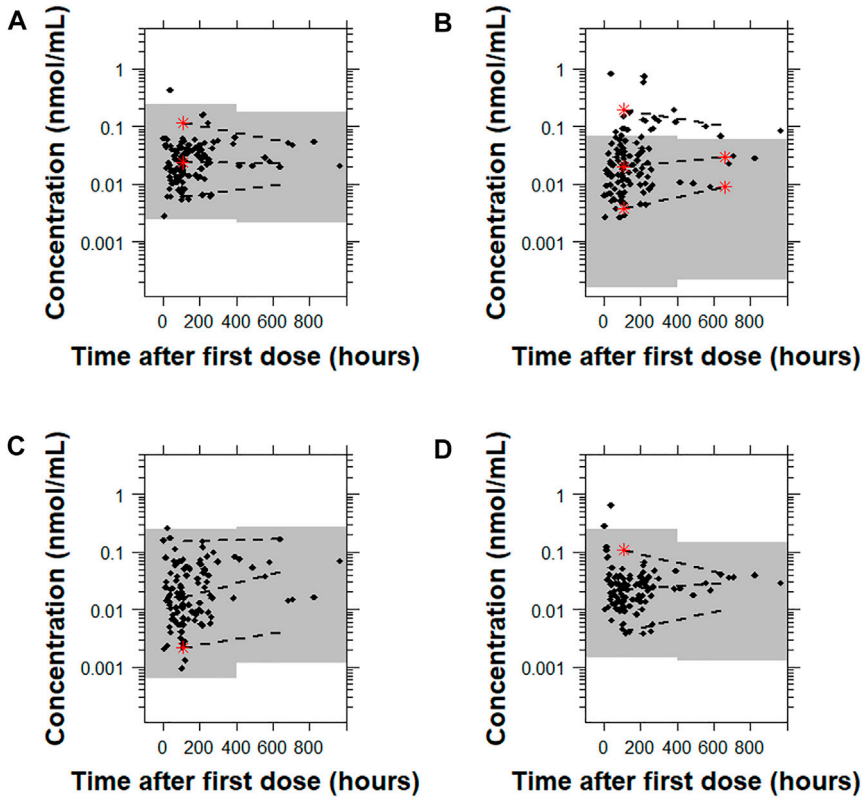


**FIGURE 7 |** Prediction-corrected visual predictive checks (pcVPCs) where the observed data are overlaid on the predictions obtained by performing 1,000 simulations with each model for 9-OH risperidone. Model **(A)**: Kloosterboer et al., 2021; Model **(B)**: Sherwin et al., 2012; Model **(C)**: Feng et al., 2008; and Model **(D)**: Feng et al., 2008 with allometric scaling. All pcVPC plots are based on the time after the first dose. The dashed lines are the 5th, 50th, and 95th percentiles for the observed data, and the gray shaded regions represent the 95% prediction interval for the predicted concentrations. The red stars indicate outlying percentiles of the observed data from the prediction interval. The *x* axis represents the time after first recorded dose. A sample that was collected later than 1,000 h after the first recorded dose was omitted from the graphs to improve visualization. The point was within the prediction interval for all of the models tested.

metabolite (**Figures 1C,D**, **2** and **3**). An explanation for this could be that the model was developed with a relatively small sample size that was also highly heterogeneous (age range: 3–18 years old and weight range: 16–110 kg). In addition, the fraction metabolized for the intermediate metabolizers was fixed to the value of 1 due to estimation difficulties. In contrast, for the normal and the poor metabolizers, the fraction metabolized was estimated at 0.13 and 0.16, respectively. Even though this assumption was also made by Feng et al., possibly due to the availability of a larger number of observations obtained from many patients, a more accurate estimation of the model parameters was made possible. Especially in the case of mixture models, a large sample size is needed to characterize all the subpopulations adequately, and ideally, patients should be monitored for an extended period (Carlsson et al., 2009).

The inclusion of allometric scaling in the model developed by Feng et al., 2008 (Model D) improved the precision of the predictions for risperidone and 9-OH-risperidone while slightly increasing the bias for risperidone but decreasing it for 9-OH-risperidone (**Figure 1**). In addition, it improved the PRED-versus-OBS plots (**Figures 2**, **3**), as it considered body-weight differences of the pediatric population used for external model evaluation compared to the adult data used for model development. Overall, as Model D showed an adequate performance for risperidone and 9-OH-risperidone, it was considered the model with the best performance for our independent pediatric data set.

The last model [Model E (Thyssen et al.)] evaluated was a 2-compartment model with first-order absorption with a lag time, and multimodal risperidone clearance (including two subpopulations) developed using data from 780 adults and children (3,436 observations for risperidone). Overall, this model showed good predictive performance; however, even though it was developed with the largest number of observations, Models C and D (Feng et al., 2008) slightly outperformed it. This might be because, in the model developed by Thyssen et al., only two subpopulations (poor and normal metabolizers) were considered instead of three (poor, intermediate, and normal metabolizers), which is more reflective of the CYP2D6 phenotypes (Kneller and Hampel, 2020). Also, in the model developed by Feng et al., parent and metabolite data were modeled simultaneously, potentially resulting in a better-informed model compared to the model of Thyssen et al., where only the parent compound was modeled.

This study has several limitations. Given the importance of *CYP2D6* genotype on risperidone PK (PharmGKB, 2021), probably one of the most significant limitations of the study is the fact that *CYP2D6* genotype data were not available in the study dataset. As a result, none of the models evaluated included genotype as a covariate. As *CYP2D6* genotype would account for a large part of the variability noted in risperidone's clearance and 9-OH-risperidone concentrations, models with a better performance might have been identified. Also, within each model evaluated a different number of subpopulations was assumed. Another limitation was that none of the models considered accounted for the probability of ultrarapid metabolizers (Caudle et al., 2020). Therefore, a different proportion of patients within each subpopulation could have contributed to discrepancies between the model predictions and the observations.

The other limitations of our study were due to the heterogeneity of the opportunistic dataset used for the external evaluation. First, there were notable differences in the demographic and clinical characteristics of the children enrolled in the study (**Table 1**), including age (0.16–17 years of age) and weight (3.64–129 kg) that are known to exert a significant impact on risperidone's PK (Aichhorn et al., 2005; Kloosterboer et al., 2021). Based on the ontogeny of CYP2D6, the relative activity of the enzyme is significantly lower in neonates compared to adults (Stevens et al., 2008; van Groen et al., 2021). As a result, the models' tendency to under-predict parent concentrations might be explained by the fact that 37% of the data included in the dataset used for external evaluation were obtained from patients below 2 years of age. This is also supported by **Supplementary Figure 5**, which clearly shows the significant impact of maturation on risperidone PK. There is a clear trend of all the models to underpredict the concentration in children below 2 years of age and even below 6 years of age. In contrast, for 9-OH-risperidone, no such trend was noted (**Supplementary Figure 6**), potentially indicating that its route of elimination is less dependent on maturation.

Despite the known effect of ECMO on the PK of some drugs (Sutiman et al., 2020), the measurements obtained from three patients (5%) on ECMO were included in the analysis. The decision to include these patients in the analysis was made after ensuring that the PEs obtained for these subjects were not different from the average PE estimated for the respective model. Thus, their inclusion was considered a more conservative approach. Similarly, data obtained from a patient receiving metoclopramide concomitantly, a known inhibitor of CYP2D6 (Livezey et al., 2014), were not excluded. Also, different formulations of risperidone were administered through various routes, which could account for some differences noted between the observed data and the models evaluated. Last, different analytical methods were applied to quantify the concentrations of risperidone and 9-OH-risperidone, with different LLOQs, among the studies (**Supplementary Table 1**).

Despite these shortcomings, this analysis demonstrates the importance of externally evaluating population PK models to assess their generalizability in pediatric populations, especially when these models are intended to guide drug dosing. The external evaluation analyses identified a comparatively better model, while the main factors explaining the high inter-individual variability of risperidone and 9-OH-risperidone were confirmed. As risperidone seems to follow a multimodal clearance, a large amount of data is needed to build a robust and generalizable model and validate it externally. Based on the present analysis results, none of the models evaluated seemed to be generalizable to the population used in this analysis. Thus, a future direction could be establishing a database combining risperidone and 9-OH-risperidone data collected in clinical trials performed so far and during therapeutic drug monitoring. This data could inform the development and evaluation of population PK models designed to guide safe and effective risperidone dosing in the pediatric population.

## THE BEST ACT – PEDIATRIC TRIALS NETWORK STEERING COMMITTEE*

**PTN Steering Committee Members:** Daniel K. Benjamin Jr., Christoph Hornik, Kanecia Zimmerman, Phyllis Kennel, and Rose Beci, Duke Clinical Research Institute, Durham, NC; Chi Dang Hornik, Duke University Medical Center, Durham, NC; Gregory L. Kearns, Scottsdale, AZ; Matthew Laughon, University of North Carolina at Chapel Hill, Chapel Hill, NC; Ian M. Paul, Penn State College of Medicine, Hershey, PA; Janice Sullivan, University of Louisville, Louisville, KY; Kelly Wade, Children's Hospital of Philadelphia, Philadelphia, PA; Paula Delmore, Wichita Medical Research and Education Foundation, Wichita, KS.

**The Eunice Kennedy Shriver National Institute of Child Health and Human Development (NICHD):** Perdita Taylor-Zapata and June Lee.

**The Emmes Company, LLC (Data Coordinating Center):** Ravinder Anand, Gaurav Sharma, Gina Simone, Kim Kaneshige, and Lawrence Taylor.

**PTN Publications Committee:** Chaired by Thomas Green, Ann and Robert H. Lurie Children's Hospital of Chicago, Chicago, IL.

**The Pediatric Trials Network (PTN) risperidone principal investigators (PIs) are as follows:** Assaf Harofeh Medical Center, Tel Aviv, Israel: Matitiahu Berkovitch (PI); University Hospitals Case Medical Center, Cleveland, OH: David Speicher, (PI); Ann and Robert H. Lurie Childrens Hospital of Chicago, Chicago, IL: William Muller (PI) and Ram Yogev (previous PI); Childrens Hospital of Eastern Ontario, Ottawa, ON: Daniela Pohl (PI), Thierry Lacaze (previous PI), Roger Zemek (previous PI) and Hugh McMullan (previous PI); Children's Hospital of Wisconsin, Milwaukee, WI: Nathan Thompson (PI) and Beth Drolet (previous PI); Duke University Medical Center Durham, NC: Chi Dang Hornik (PI) and Kevin Watt (previous PI); Alfred I. duPont Hospital for Children/Nemours, Wilmington, DE: Marisa Meyer (PI) and Glenn Stryjeuski (previous PI); Indiana University, Indianapolis, IN: Gregory Sokol (PI), Brenda Poindexter (previous PI) and Scott Denne (previous PI); Oregon Health and Science University, Portland, Oregon: Amira Al-Uzri (PI); University of Arkansas for Medical Sciences, Little Rock, Arkansas.: Laura James (PI); University of Florida—Jacksonville, Jacksonville, FL:

Mobeen Rathore (PI); University of Louisville-Kosair Charities Pediatric Clinical Research Unit, Louisville, KY: Janice Sullivan (PI); The University of Maryland Hospital, Baltimore, MD: Caissa Baker-Smith (PI) and Susan Mendley (previous PI); University of North Carolina- Chapel Hill, Chapel Hill, NC: Matt Laughon (PI); and Wesley Medical Center, Wichita, KS: Paula Delmore (previous PI) and Barry Bloom (PI).

## DATA AVAILABILITY STATEMENT

To help expand the knowledge base for pediatric medicine, the Pediatric Trials Network is pleased to share data from its completed and published studies with interested investigators. For requests, please contact: PTN-Program-Manager@dm.duke.edu.

## ETHICS STATEMENT

The study protocol was reviewed and approved by the institutional review boards of Duke University (coordinating center) and all participating study sites. Written informed consent to participate in this study was provided by the participants' legal guardian/next of kin.

## AUTHOR CONTRIBUTIONS

EK and DG designed the study. EK and SG analyzed the data. EK, SG, CH, WM, AA-U, LJ, SB, and DG performed the research. EK and DG wrote the manuscript.

## FUNDING

This work was funded under the National Institute of Child Health and Human Development (NICHD) contract (HHSN275201000003I) for the Pediatric Trials Network (PI: Danny Benjamin). EK was funded through a UNC/GSK Pharmacokinetics/Pharmacodynamics Post-Doctoral Fellowship. DG receives salary support for research from the NICHD (5R01HD096435-03, 1R01HD102949-01A1, and HHSN275201000003I). The content is solely the authors' responsibility and does not necessarily represent the official views of the National Institutes of Health.

## SUPPLEMENTARY MATERIAL

The Supplementary Material for this article can be found online at: https://www.frontiersin.org/articles/10.3389/fphar.2022.817276/full#supplementary-material

## REFERENCES

Aichhorn, W., Weiss, U., Marksteiner, J., Kemmler, G., Walch, T., Zernig, G., et al. (2005). Influence of Age and Gender on Risperidone Plasma Concentrations. *J. Psychopharmacol.* 19 (4), 395–401. doi:10.1177/0269881105053306

Arnold, L. E., Gadow, K. D., Farmer, C. A., Findling, R. L., Bukstein, O., Molina, B. S., et al. (2015). Comorbid Anxiety and Social Avoidance in Treatment of Severe Childhood Aggression: Response to Adding Risperidone to Stimulant and Parent Training; Mediation of Disruptive Symptom Response. *J. Child. Adolesc. Psychopharmacol.* 25 (3), 203–212. doi:10.1089/cap.2014.0104

Auguie, B. (2017). gridExtra: Miscellaneous Functions for "Grid" Graphics. R package version 2.3. https://CRAN.R-project.org/package=gridExtra.

Bergstrand, M., Hooker, A. C., Wallin, J. E., and Karlsson, M. O. (2011). Prediction-corrected Visual Predictive Checks for Diagnosing Nonlinear Mixed-Effects Models. *AAPS J.* 13 (2), 143–151. doi:10.1208/s12248-011-9255-z

Biederman, J., Hammerness, P., Doyle, R., Joshi, G., Aleardi, M., and Mick, E. (2008). Risperidone Treatment for ADHD in Children and Adolescents with Bipolar Disorder. *Neuropsychiatr. Dis. Treat.* 4 (1), 203–207. doi:10.2147/ndt.s1992

Campbell, C. T., Grey, E., Munoz-Pareja, J., and Manasco, K. B. (2020). An Evaluation of Risperidone Dosing for Pediatric Delirium in Children Less Than or Equal to 2 Years of Age. *Ann. Pharmacother.* 54 (5), 464–469. doi:10.1177/1060028019891969

Carlsson, K. C., Savić, R. M., Hooker, A. C., and Karlsson, M. O. (2009). Modeling Subpopulations with the $MIXTURE Subroutine in NONMEM: Finding the Individual Probability of Belonging to a Subpopulation for the Use in Model Analysis and Improved Decision Making. *AAPS J.* 11 (1), 148–154. doi:10.1208/s12248-009-9093-4

Caudle, K. E., Sangkuhl, K., Whirl-Carrillo, M., Swen, J. J., Haidar, C. E., Klein, T. E., et al. (2020). Standardizing CYP2D6 Genotype to Phenotype Translation: Consensus Recommendations from the Clinical Pharmacogenetics Implementation Consortium and Dutch Pharmacogenetics Working Group. *Clin. Transl Sci.* 13 (1), 116–124. doi:10.1111/cts.12692

Cheng, Y., Wang, C. Y., Li, Z. R., Pan, Y., Liu, M. B., and Jiao, Z. (2021). Can Population Pharmacokinetics of Antibiotics Be Extrapolated? Implications of External Evaluations. *Clin. Pharmacokinet.* 60 (1), 53–68. doi:10.1007/s40262-020-00937-4

Comets, E., Brendel, K., and Mentré, F. (2008). Computing Normalised Prediction Distribution Errors to Evaluate Nonlinear Mixed-Effect Models: the Npde Add-On Package for R. *Comput. Methods Programs Biomed.* 90 (2), 154–166. doi:10.1016/j.cmpb.2007.12.002

Eapen, V., and Gururaj, A. K. (2005). Risperidone Treatment in 12 Children with Developmental Disorders and Attention-Deficit/hyperactivity Disorder. *Prim. Care Companion J. Clin. Psychiatry* 7 (5), 221–224. doi:10.4088/pcc.v07n0502

Feng, Y., Pollock, B. G., Coley, K., Marder, S., Miller, D., Kirshner, M., et al. (2008). Population Pharmacokinetic Analysis for Risperidone Using Highly Sparse Sampling Measurements from the CATIE Study. *Br. J. Clin. Pharmacol.* 66 (5), 629–639. doi:10.1111/j.1365-2125.2008.03276.x

Ge, S., Mendley, S. R., Gerhart, J. G., Melloni, C., Hornik, C. P., Sullivan, J. E., et al. (2020). Best Pharmaceuticals for Children Act - Pediatric Trials Network Steering Committee. Population Pharmacokinetics of Metoclopramide in Infants, Children, and Adolescents. *Clin. Transl. Sci.* 13 (6), 1189–1198. doi:10.1111/cts.12803

Gonzalez, D., Melloni, C., Yogev, R., Poindexter, B. B., Mendley, S. R., Delmore, P., et al. (2014). Best Pharmaceuticals for Children Act – Pediatric Trials Network Administrative Core Committee. Use of Opportunistic Clinical Data and a Population Pharmacokinetic Model to Support Dosing of Clindamycin for Premature Infants to Adolescents. *Clin. Pharmacol. Ther.* 96 (4), 429–437. doi:10.1038/clpt.2014.134

Hálfdánarson, Ó., Zoëga, H., Aagaard, L., Bernardo, M., Brandt, L., Fusté, A. C., et al. (2017). International Trends in Antipsychotic Use: A Study in 16 Countries, 2005-2014. *Eur. Neuropsychopharmacol.* 27 (10), 1064–1076. doi:10.1016/j.euroneuro.2017.07.001

Hwang, M. F., Beechinor, R. J., Wade, K. C., Benjamin, D. K., Jr, Smith, P. B., Hornik, C. P., et al. (2017). External Evaluation of Two Fluconazole Infant Population Pharmacokinetic Models. *Antimicrob. Agents Chemother.* 61 (12), e01352–17. doi:10.1128/AAC.01352-17

Jensen, P. S., Buitelaar, J., Pandina, G. J., Binder, C., and Haas, M. (2007). Management of Psychiatric Disorders in Children and Adolescents with Atypical Antipsychotics: a Systematic Review of Published Clinical Trials. *Eur. Child. Adolesc. Psychiatry* 16 (2), 104–120. doi:10.1007/s00787-006-0580-1

Ji, S., Shang, D., Wu, K., Li, A., Li, X., Deng, C., et al. (2016). Population Pharmacokinetic-Pharmacodynamic (PopPK/PD) Modeling of Risperidone and its Active Metabolite in Chinese Schizophrenia Patients. *Int. J. Clin. Pharmacol. Ther.* 54 (5), 378–389. doi:10.5414/CP202498

Kloosterboer, S. M., de Winter, B. C. M., Reichart, C. G., Kouijzer, M. E. J., de Kroon, M. M. J., van Daalen, E., et al. (2021). Risperidone Plasma Concentrations Are Associated with Side Effects and Effectiveness in Children and Adolescents with Autism Spectrum Disorder. *Br. J. Clin. Pharmacol.* 87 (3), 1069–1081. doi:10.1111/bcp.14465

Kneller, L. A., Abad-Santos, F., and Hempel, G. (2020). Physiologically Based Pharmacokinetic Modelling to Describe the Pharmacokinetics of Risperidone and 9-Hydroxyrisperidone According to Cytochrome P450 2D6 Phenotypes. *Clin. Pharmacokinet.* 59 (1), 51–65. doi:10.1007/s40262-019-00793-x

Kneller, L. A., and Hempel, G. (2020). Modelling Age-Related Changes in the Pharmacokinetics of Risperidone and 9-Hydroxyrisperidone in Different CYP2D6 Phenotypes Using a Physiologically Based Pharmacokinetic Approach. *Pharm. Res.* 37 (6), 110. doi:10.1007/s11095-020-02843-7

Lee, E. S., Vidal, C., and Findling, R. L. (2018). A Focused Review on the Treatment of Pediatric Patients with Atypical Antipsychotics. *J. Child. Adolesc. Psychopharmacol.* 28 (9), 582–605. doi:10.1089/cap.2018.0037

Livezey, M. R., Briggs, E. D., Bolles, A. K., Nagy, L. D., Fujiwara, R., and Furge, L. L. (2014). Metoclopramide Is Metabolized by CYP2D6 and Is a Reversible Inhibitor, but Not Inactivator, of CYP2D6. *Xenobiotica* 44 (4), 309–319. doi:10.3109/00498254.2013.835885

Livingston, M. G. (1994). Risperidone. *The Lancet* 343 (8895), 457–460. doi:10.1016/S0140-6736(94)92696-4

Liviskie, C., and McPherson, C. (2021). Delirium in the NICU: Risk or Reality? *Neonatal. Netw.* 40 (2), 103–112. doi:10.1891/0730-0832/11-T-727

Locatelli, I., Kastelic, M., Koprivsek, J., Kores-Plesnicar, B., Mrhar, A., Dolzan, V., et al. (2010). A Population Pharmacokinetic Evaluation of the Influence of CYP2D6 Genotype on Risperidone Metabolism in Patients with Acute Episode of Schizophrenia. *Eur. J. Pharm. Sci.* 41 (2), 289–298. doi:10.1016/j.ejps.2010.06.016

Mauri, M. C., Paletta, S., Di Pace, C., Reggiori, A., Cirnigliaro, G., Valli, I., et al. (2018). Clinical Pharmacokinetics of Atypical Antipsychotics: An Update. *Clin. Pharmacokinet.* 57 (12), 1493–1528. doi:10.1007/s40262-018-0664-3

Medhasi, S., Pinthong, D., Pasomsub, E., Vanwong, N., Ngamsamut, N., Puangpetch, A., et al. (2016). Pharmacogenomic Study Reveals New Variants of Drug Metabolizing Enzyme and Transporter Genes Associated with Steady-State Plasma Concentrations of Risperidone and 9-Hydroxyrisperidone in Thai Autism Spectrum Disorder Patients. *Front. Pharmacol.* 7, 475. doi:10.3389/fphar.2016.00475

Nguyen, T. H. T., Mouksassi, M. S., Holford, N., Al-Huniti, N., Freedman, I., Hooker, A. C., et al. (2017). Model Evaluation Group of the International Society of Pharmacometrics (ISoP) Best Practice Committee Model Evaluation of Continuous Data Pharmacometric Models: Metrics and Graphics. *CPT Pharmacometrics Syst. Pharmacol.* 6 (2), 87–109. doi:10.1002/psp4.12161

PharmGKB (2021). Annotation of DPWG Guideline for Risperidone and CYP2D6. https://www.pharmgkb.org/chemical/PA451257/guidelineAnnotation/PA166104943 (Accessed December, 2021).

Risperdal® package insert (2009). Ortho-McNeil-Janssen Pharmaceuticals, Inc. Titusville, NJ. https://www.accessdata.fda.gov/drugsatfda_docs/label/2009/020272s056,020588s044,021346s033,021444s03lbl.pdf (Accessed June, 2021).

Saibi, Y., Sato, H., and Tachiki, H. (2012). Developing In Vitro-In Vivo Correlation of Risperidone Immediate Release Tablet. *AAPS PharmSciTech* 13 (3), 890–895. doi:10.1208/s12249-012-9814-3

Sarkar, D., and Andrews, F. (2019). *latticeExtra: Extra Graphical Utilities Based on Lattice*. R package version 0.6-29. Available at: https://cran.r-project.org/web/packages/latticeExtra/index.html.

Sarkar, D. (2008). *Lattice: Multivariate Data Visualization with R*. New York: Springer.

Sheehan, J. J., Sliwa, J. K., Amatniek, J. C., Grinspan, A., and Canuso, C. M. (2010). Atypical Antipsychotic Metabolism and Excretion. *Curr. Drug Metab.* 11 (6), 516–525. doi:10.2174/138920010791636202

Sherwin, C. M., Saldaña, S. N., Bies, R. R., Aman, M. G., and Vinks, A. A. (2012). Population Pharmacokinetic Modeling of Risperidone and 9-hydroxyrisperidone to Estimate CYP2D6 Subpopulations in Children and Adolescents. *Ther. Drug Moni.* 34 (5), 535–544. doi:10.1097/FTD.0b013e318261c240

Stevens, J. C., Marsh, S. A., Zaya, M. J., Regina, K. J., Divakaran, K., Le, M., et al. (2008). Developmental Changes in Human Liver CYP2D6 Expression. *Drug Metab. Dispos.* 36 (8), 1587–1593. doi:10.1124/dmd.108.021873

Sutiman, N., Koh, J. C., Watt, K., Hornik, C., Murphy, B., Chan, Y. H., et al. (2020). Pharmacokinetics Alterations in Critically Ill Pediatric Patients on Extracorporeal Membrane Oxygenation: A Systematic Review. *Front. Pediatr.* 8, 260. doi:10.3389/fped.2020.00260

Thyssen, A., Vermeulen, A., Fuseau, E., Fabre, M. A., and Mannaert, E. (2010). Population Pharmacokinetics of Oral Risperidone in Children, Adolescents and Adults with Psychiatric Disorders. *Clin. Pharmacokinet.* 49 (7), 465–478. doi:10.2165/11531730-000000000-00000

US FDA (2019). Population Pharmacokinetics: Guidance for Industry (Draft Guidance). https://www.fda.gov/media/128793/download (Accessed Jun, 2021).

van Groen, B. D., Nicolaï, J., Kuik, A. C., Van Cruchten, S., van Peer, E., Smits, A., et al. (2021). Ontogeny of Hepatic Transporters and Drug-Metabolizing Enzymes in Humans and in Nonclinical Species. *Pharmacol. Rev.* 73 (2), 597–678. doi:10.1124/pharmrev.120.000071

Vandenberghe, F., Guidi, M., Choong, E., von Gunten, A., Conus, P., Csajka, C., et al. (2015). Genetics-Based Population Pharmacokinetics and Pharmacodynamics of Risperidone in a Psychiatric Cohort. *Clin. Pharmacokinet.* 54 (12), 1259–1272. doi:10.1007/s40262-015-0289-8

Vanwong, N., Ngamsamut, N., Nuntamool, N., Hongkaew, Y., Sukprasong, R., Puangpetch, A., et al. (2020). Risperidone-Induced Obesity in Children and Adolescents with Autism Spectrum Disorder: Genetic and Clinical Risk Factors. *Front. Pharmacol.* 11, 565074. doi:10.3389/fphar.2020.565074

Vermeir, M., Naessens, I., Remmerie, B., Mannens, G., Hendrickx, J., Sterkens, P., et al. (2008). Absorption, Metabolism, and Excretion of Paliperidone, a New Monoaminergic Antagonist, in Humans. *Drug Metab. Dispos.* 36 (4), 769–779. doi:10.1124/dmd.107.018275

Vermeulen, A., Piotrovsky, V., and Ludwig, E. A. (2007). Population Pharmacokinetics of Risperidone and 9-hydroxyrisperidone in Patients with Acute Episodes Associated with Bipolar I Disorder. *J. Pharmacokinet. Pharmacodyn.* 34 (2), 183–206. doi:10.1007/s10928-006-9040-2

Wu, Y., Cohen-Wolkowiez, M., Hornik, C. P., Gerhart, J. G., Autmizguine, J., Cobbaert, M., et al. (2021). Best Pharmaceuticals for Children Act—Pediatric Trials Network Steering Committee External Evaluation of Two Pediatric Population Pharmacokinetics Models of Oral Trimethoprim and Sulfamethoxazole. *Antimicrob. Agents Chemother.* 65 (7), e0214920. doi:10.1128/AAC.02149-210.1128/aac.02149-20

Yoo, H. D., Cho, H. Y., Lee, S. N., Yoon, H., and Lee, Y. B. (2012). Population Pharmacokinetic Analysis of Risperidone and 9-hydroxyrisperidone with Genetic Polymorphisms of CYP2D6 and ABCB1. *J. Pharmacokinet. Pharmacodyn.* 39 (4), 329–341. doi:10.1007/s10928-012-9253-5

**Conflict of Interest:** EK received funding from GlaxoSmithKline (GSK) through a University of North Carolina at Chapel Hill (UNC)/GSK Pharmacokinetics/Pharmacodynamics Post-Doctoral Fellowship.

SG is employed by Regeneron Pharmaceuticals, Inc. SJB receives support from the National Institutes of Health (NIH), US Food and Drug Administration, Patient Centered Outcomes Research Institute, the Rheumatology Research Foundation's Scientist Development Award, the Childhood Arthritis and Rheumatology Research Alliance, and consulting for UCB. DG receives research support from Nabriva Therapeutics through a contract with The University of North Carolina at Chapel Hill. In addition, DG serves as a consultant for Tellus Therapeutics, focusing on neonatal drug development.

The remaining authors declare that the research was conducted in the absence of any commercial or financial relationships that could be construed as a potential conflict of interest.

**Publisher's Note:** All claims expressed in this article are solely those of the authors and do not necessarily represent those of their affiliated organizations, or those of the publisher, the editors and the reviewers. Any product that may be evaluated in this article, orclaim that may be made by its manufacturer, is not guaranteed or endorsed by the publisher.

frontiers in Pharmacology

BRIEF RESEARCH REPORT
published: 17 March 2022
doi: 10.3389/fphar.2022.819590

# Exploring Dried Blood Spot Cortisol Concentrations as an Alternative for Monitoring Pediatric Adrenal Insufficiency Patients: A Model-Based Analysis

*Viktoria Stachanow[1,2], Uta Neumann[3], Oliver Blankenstein[3,4], Davide Bindellini[1,2], Johanna Melin[1,2], Richard Ross[5], Martin J. Whitaker[5], Wilhelm Huisinga[6], Robin Michelet[1*†] and Charlotte Kloft[1†]*

[1]Department of Clinical Pharmacy and Biochemistry, Institute of Pharmacy, Freie Universitaet Berlin, Berlin, Germany, [2]Graduate Research Training Program PharMetrX, Berlin, Germany, [3]Pediatric Endocrinology, Charité-Universitätsmedizin, Berlin, Germany, [4]Labor Berlin, Charité Vivantes GmbH, Berlin, Germany, [5]Diurnal Limited, Cardiff, United Kingdom, [6]Institute of Mathematics, Universität Potsdam, Potsdam, Germany

OPEN ACCESS

**Edited by:**
Catherine M. T Sherwin,
Wright State University, United States

**Reviewed by:**
Gregory Thomas Knipp,
Purdue University, United States
Kit Wun Kathy Cheung,
Genentech, Inc., United States

***Correspondence:**
Robin Michelet
robin.michelet@fu-berlin.de

[†]These authors share senior authorship

**Specialty section:**
This article was submitted to Obstetric and Pediatric Pharmacology, a section of the journal Frontiers in Pharmacology

**Received:** 21 November 2021
**Accepted:** 26 January 2022
**Published:** 17 March 2022

**Citation:**
Stachanow V, Neumann U, Blankenstein O, Bindellini D, Melin J, Ross R, Whitaker MJ, Huisinga W, Michelet R and Kloft C (2022) Exploring Dried Blood Spot Cortisol Concentrations as an Alternative for Monitoring Pediatric Adrenal Insufficiency Patients: A Model-Based Analysis. Front. Pharmacol. 13:819590. doi: 10.3389/fphar.2022.819590

Congenital adrenal hyperplasia (CAH) is the most common form of adrenal insufficiency in childhood; it requires cortisol replacement therapy with hydrocortisone (HC, synthetic cortisol) from birth and therapy monitoring for successful treatment. In children, the less invasive dried blood spot (DBS) sampling with whole blood including red blood cells (RBCs) provides an advantageous alternative to plasma sampling. Potential differences in binding/association processes between plasma and DBS however need to be considered to correctly interpret DBS measurements for therapy monitoring. While capillary DBS samples would be used in clinical practice, venous cortisol DBS samples from children with adrenal insufficiency were analyzed due to data availability and to directly compare and thus understand potential differences between venous DBS and plasma. A previously published HC plasma pharmacokinetic (PK) model was extended by leveraging these DBS concentrations. In addition to previously characterized binding of cortisol to albumin (linear process) and corticosteroid-binding globulin (CBG; saturable process), DBS data enabled the characterization of a linear cortisol association with RBCs, and thereby providing a quantitative link between DBS and plasma cortisol concentrations. The ratio between the observed cortisol plasma and DBS concentrations varies highly from 2 to 8. Deterministic simulations of the different cortisol binding/association fractions demonstrated that with higher blood cortisol concentrations, saturation of cortisol binding to CBG was observed, leading to an increase in all other cortisol binding fractions. In conclusion, a mathematical PK model was developed which links DBS measurements to plasma exposure and thus allows for quantitative interpretation of measurements of DBS samples.

**Keywords: adrenal insufficiency, cortisol, dried blood spots, pediatrics, pharmacokinetics, binding, association, red blood cells**

## INTRODUCTION

Congenital adrenal hyperplasia (CAH) is a group of rare autosomal recessive diseases, which are characterized by largely decreased or absent cortisol biosynthesis. In 90–95% of cases, a deficiency of the 21-hydroxylase enzyme is the cause for CAH (Podgórski et al., 2018; Balsamo et al., 2020). A major complication in patients is an adrenal crisis which may even lead to death. Other symptoms of CAH include virilization, hirsutism, premature adrenarche, and premature ending of longitudinal growth due to an overproduction of androgens and possible life-threatening electrolyte imbalance due to the underproduction of mineralocorticoids (Merke and Bornstein, 2005).

The treatment of CAH requires life-long cortisol replacement therapy. The recommended glucocorticoid for pediatric CAH patients is hydrocortisone (HC, name of synthetic cortisol) due to its short half-life and lower risk for adverse events (Oprea et al., 2019). To mimic the circadian rhythm of cortisol biosynthesis, oral administration of 10–15 mg/m$^2$ hydrocortisone daily is recommended, divided into two to three doses, and with the highest dose in the morning (Kamoun et al., 2013; Khattab and Marshall, 2019; Dabas et al., 2020). It is essential to monitor cortisol replacement in CAH patients frequently and adjust dosages according to the patients' individual needs, based on the body surface area, laboratory parameters, and symptoms evaluation (Bornstein et al., 2016) as too high or too low cortisol exposure can cause adverse events, such as Cushing's syndrome, and or lead to an adrenal crisis (Merke and Bornstein, 2005).

Dried blood spot (DBS) samples have been used since the 1960s to perform newborn screenings for diseases such as phenylketonuria (Moat et al., 2020). Currently, because of technological development allowing for more specific and sensitive specimen analysis, DBS has been exploited to monitor CAH patients (Moat et al., 2020). DBS sampling consists of dropping small volumes of whole blood drops (approximately 20 µl) collected via a fingerpick on a cellulose-based sampling paper. Therefore, this sampling procedure is simpler and less invasive than traditional plasma sampling. It is thus of great advantage for the pediatric population because of their vulnerability and limited blood volume (Qasrawi et al., 2021). DBS sampling provides additional benefits such as higher analyte stability, allowing storage at room temperature, and easy transportation (Edelbroek et al., 2009; Wilhelm et al., 2014).

To evaluate the applicability of DBS sampling, it is essential to understand the relationship between cortisol DBS concentrations, and plasma concentrations. Cortisol has complex PK with saturable binding to corticosteroid-binding globulin (CBG) and linear binding to albumin which previously has been identified using a nonlinear mixed-effects (NLME) HC PK model [(Melin et al., 2017; Michelet et al., 2020)]. Moreover, cortisol is known to associate with RBCs (Lentjes and Romijn, 1999). This is of special interest for interpreting DBS samples as these are whole blood samples containing RBCs. The aim of this analysis was to explore and quantify the relationship between venous DBS cortisol concentrations and plasma cortisol concentrations by characterizing the association of cortisol with RBCs; which is the first step towards the use and interpretation of DBS samples for monitoring pediatric CAH patients.

## METHODS

### Data

A previously published NLME HC PK model based on cortisol plasma data from healthy adults and pediatric patients (Melin et al., 2017; Michelet et al., 2020) served as the starting point for our analysis. The model leveraged data from 1) rich plasma sampling ($n$ = 1,482 total cortisol concentrations) in a phase 1 study (Whitaker et al., 2015) with 30 healthy adult subjects, whose cortisol biosynthesis was suppressed with dexamethasone, and who received a single dose of 0.5 mg up to 20 mg of the pediatric HC formulation Alkindi® (hydrocortisone granules in capsules for opening) (Diurnal Europe B.V., Netherlands).

Additionally, the model leveraged 2) sparse phase 3 cortisol plasma data from 24 pediatric adrenal insufficiency (AI) patients receiving their regular HC-morning dose of Alkindi®, ranging from 1 to 4 mg (Neumann et al., 2018; Melin et al., 2020; Michelet et al., 2020). The pediatric patients were divided into three different cohorts according to their age groups: Young children ($n$ = 12, 2–6 years), infants ($n$ = 6, 28 days-2 years), and term neonates ($n$ = 6: 0–28 days). The pediatric total cortisol plasma concentrations were measured prior to dose and 1 and 4 h post-dose in all cohorts. In neonates and infants, the sampling was ethically limited to these 3 times due to the lower total blood volume, whereas in the children cohort, blood sampling at 2 additional times between 30 and 90 h post-dose was allowed as well as at time to $C_{min}$ ($t_{min}$).

To expand this model, simultaneously collected venous total cortisol DBS samples, obtained from the pediatric patients in the phase 3 study, were included. Both total cortisol concentrations in plasma (Whitaker et al., 2015; Melin et al., 2017; Michelet et al., 2020) and in DBS ($n$ = 106 each) were quantified by liquid chromatography with tandem mass spectrometry detection (LC-MS/MS). Linearity, accuracy, and precision were tested for DBS cortisol quantification with the respective acceptance criteria being met according to the guideline on bioanalytical method validation of the European Medicines Agency (European Medicines Agency, 2012).

### Graphical Evaluation of Plasma Versus DBS Cortisol Concentrations

The relationship between the pediatric total cortisol concentrations in plasma and DBS was graphically evaluated based on concentration–time profiles, plotting plasma versus DBS cortisol concentrations and graphically investigating the plasma/DBS ratio as a function of the cortisol concentration, and the cortisol concentration dependency of the plasma/DBS cortisol concentration ratio. The graphical analysis was performed using R (3.6.0) and R Studio (1.3.1056) (R Core Team, 2019; RStudio Team, 2020).

## Pharmacokinetic Model Development and Evaluation

The previously published NLME HC PK model, based on adult and pediatric plasma cortisol data, was a two-compartment PK model describing saturable absorption (Michaelis–Menten type) and a plasma protein binding model considering both nonlinear binding to CBG and linear binding to albumin. An underlying constant cortisol baseline was estimated for the adult data, whereas for the pediatric cortisol data, the baseline was modeled using the individual measured pre-dose concentration. For baseline cortisol concentrations below the lower limit of quantification (LLOQ), a baseline concentration was estimated with the same interindividual variability as the observed pre-dose concentrations above LLOQ (Melin et al., 2020; Michelet et al., 2020).

Body weight was included as an influential factor using theory-based allometric scaling with fixed exponents of 0.75 and 1 on the clearance parameters (CL and Q) and on the volumes of distribution ($V_c$ and $V_p$), respectively, to account for differences in the body size within the pooled dataset. No other covariates besides body weight were evaluated in the structural plasma PK model. Interindividual variability (IIV) was modeled, assuming the structural model parameters to follow a log-normal distribution, and residual unexplained variability (RUV) was modeled following a proportional residual error model (Melin et al., 2020; Michelet et al., 2020).

Based on this PK model structure and modeling approach, the published HC PK model was further developed by extending the underlying data with the pediatric DBS cortisol concentrations. Implemented cortisol binding processes were extended by the association of cortisol with RBCs which were all assumed to contain hemoglobin. For the model development, NONMEM (7.4.3, ICON, Dublin, Ireland, Development Solutions, Ellicott City, MD, United States) and Perl-speaks-NONMEM (3.4.2, Uppsala University, Uppsala, Sweden), embedded in the workbench Pirana (version 2.9.6), were used (Bauer, 2010; Keizer et al., 2013). The appropriateness of the PK model was evaluated based on standard model diagnostics, for example, the difference of the objective function value (dOFV, best fit = maximum likelihood = minimum OFV) and goodness-of-fit (GOF) plots (Mould and Upton, 2012, 2013). Model performance was evaluated using visual predictive checks (VPCs, n = 1,000 simulations) (Bergstrand et al., 2011) (see the **Supplementary Material**) and sampling importance resampling (SIR, with 1,000, 1,000, 1,000, 2,000, and 2,000 samples and 200, 400, 500, 1,000, and 1,000 resamples) (Dosne et al., 2017).

## Simulation of Cortisol Binding Species

The final and evaluated PK model allowed simulating the fractions of the three different binding/association species of cortisol (specific binding to CBG, non-specific binding to albumin, and non-specific association with RBCs) and the unbound cortisol fraction. One individual representing the children/infants age group and one individual representing neonates were virtually dosed with 7 mg HC each; the concentrations of the binding species and cortisol whole blood concentrations were simulated over 6 h [deterministic simulations using NONMEM (7.4.3)].

# RESULTS

## Data

Of the pediatric plasma and DBS concentrations, 17.9% ($n$ = 19 of 106, LLOQ = 14.1 nmol/L) and 0.94% ($n$ = 1 of 106, LLOQ = 1.8 nmol/L) were below the LLOQ, respectively. All adult total cortisol plasma concentrations were above the LLOQ. As in the previously published model, all BLQ observations were discarded so that 87 pediatric plasma samples and 105 pediatric DBS samples remained for the subsequent graphical analysis, modeling, and simulation analysis.

## Graphical Evaluation of Plasma Versus DBS Cortisol Concentrations

Measured plasma cortisol concentrations were considerably higher than DBS cortisol concentrations with ratios with a very high variability, ranging from approximately 2 to 8 (**Figure 1A**). The relationship between total cortisol concentrations in plasma and DBS was nonlinear (**Figure 1B**), where the plasma/DBS cortisol concentration ratio decreased with higher cortisol concentrations, reaching the lowest ratio at the highest concentrations. Regarding the ratio and slope, the data shown in **Figure 1B** could be divided into 2 groups, with DBS concentrations ranging from 0 to 200 nmol/L and from 200 to 800 nmol/L. When observing cortisol DBS concentrations from 0 to 200 nmol/L ($n$ = 83, **Figure 1A**), the plasma/DBS cortisol concentration ratio ranges widely from 1.62 up to 8.01, with a median of 5.17. With higher concentrations ($n$ = 4), which were only observed in the neonatal age group, the concentration ratio decreases to a median value of 2.41 (range 1.88–3.51). The comparison of DBS concentration ranges from 0 to 100 nmol/L and from 100 to 200 nmol/L showed no significant difference in plasma/DBS cortisol concentration ratios.

## Pharmacokinetic Model Development and Evaluation

Since the association of cortisol with RBCs is described as a linear process in the literature (Lentjes and Romijn, 1999), a linear association constant $K_{aRBC}$ was estimated. An additional compartment describing cortisol bound to RBCs was implemented, and an additional apparent volume ($V_{delta}$) was estimated, with the whole blood volume being defined as the sum of $V_c$ and $V_{delta}$. Similarly, to the pediatric plasma cortisol baseline ($BASE_{child,\ pla}$), a pediatric DBS cortisol baseline ($BASE_{child,\ DBS}$) was implemented, and based on pre-dose observations or was estimated if no observation was present. $BASE_{child,\ pla}$ was used as an initial value of the central plasma concentration, whereas $BASE_{child,\ RBC}$ represented cortisol bound to RBCs at baseline and was described in amounts (nmol) as $A_{BASERBC} = A_{BASEchild,\ DBS} - A_{BASEchild,\ pla}$ (**Figure 2**). The underlying model equations can be found in the **Supplementary Material**.

Since higher cortisol concentrations, leading to relatively higher cortisol DBS concentrations, were only observed in the neonatal cohort, "age group" was evaluated as a dichotomous categorical covariate, that is, the influential factor ("children/infants" and "neonates") on the estimated $V_{delta}$. The inclusion of this

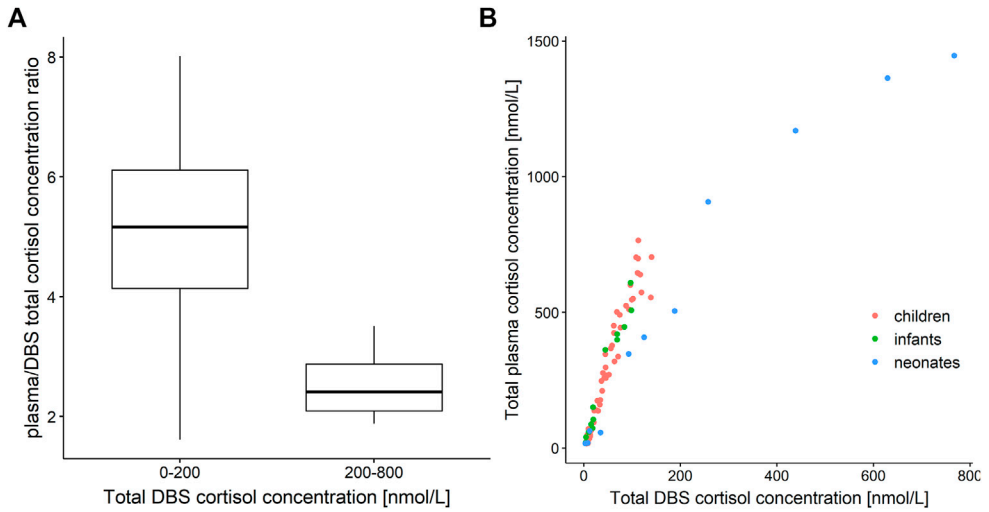


**FIGURE 1 | (A)** Boxplot of plasma/dried blood spot (DBS) cortisol concentration ratio versus cortisol DBS concentration ranges of 0–200 nmol/L ($n$ = 83) and 200–800 nmol/L ($n$ = 4). **(B)** Total cortisol concentration in plasma versus total cortisol concentration in dried blood spots (DBS). Red: children, green: infants, blue: neonates.

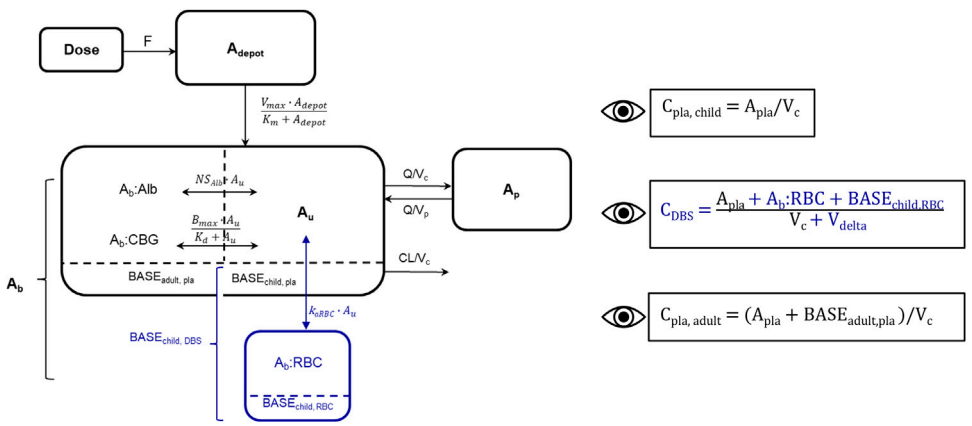


**FIGURE 2 |** Schematic representation of developed cortisol PK model including adult plasma data and pediatric plasma and dried blood spot (DBS) data, blue: new DBS-related compartments/parameters/data. Bioavailability (F), amount in depot compartment ($A_{depot}$), maximum absorption rate ($V_{max}$), amount in depot compartment resulting in half of $V_{max}$ ($K_m$), amount bound ($A_b$), amount bound to albumin ($A_b$:Alb), amount associated to red blood cells ($A_b$:RBC), unbound amount ($A_u$), amount bound to corticosteroid-binding globulin ($A_b$:CBG), linear non-specific parameter for albumin binding ($NS_{Alb}$) and association to red blood cells ($k_{aRBC}$), maximum binding capacity ($B_{max}$), equilibrium dissociation constant ($K_d$), intercompartmental clearance (Q), peripheral volume of distribution ($V_p$), cortisol plama baseline of dexamethasone suppressed healthy adults ($BASE_{adult, pla}$), cortisol plasma baseline of children ($BASE_{child, pla}$), cortisol DBS baseline of children ($BASE_{child, DBS}$), cortisol associated to red blood cells at baseline in children ($BASE_{child, RBC}$). The dashed line divides the central compartment into the $A_b$ and $A_u$ subcompartments, respectively. Eyes next to equations indicate observed concentrations: Pediatric plasma ($C_{pla, child}$) and DBS ($C_{DBS}$) concentrations, adult plasma concentrations ($C_{pla, adult}$), volume of red blood cell compartment ($V_{delta}$).

covariate resulted in −47.06 dOFV and explained more than two-thirds (69.1%) of the interindividual variability (IIV) of $V_{delta}$ (before: 196% CV, after: 60.6% CV). Age was tested as a covariate on $V_{delta}$, with exponential and fractional changes from the median age, and resulted in an OFV drop of −23.0 and of −6.3, explaining 20 and 27% of the $V_{delta}$ IIV, respectively. Given the higher reduction of IIV and the limited neonatal data, the two age groups were chosen and kept in the model as the simplest and thus most appropriate covariate.

**Table 1** shows the parameter estimates and the SIR medians and 95% confidence intervals (CI) of the final PK model including adult plasma cortisol data and pediatric plasma and DBS cortisol data. The resulting $V_{delta}$ for children/infants was 11.1 L compared to 1.05 L in neonates, corresponding to 0.82 L/kg and 0.29 L/kg for children + infants and for neonates, respectively. The linear binding/association

**TABLE 1 |** Parameter estimates with sampling importance resampling (SIR) median and 95% confidence intervals (CI) of developed cortisol pharmacokinetic (PK) model including adult plasma data and pediatric plasma and dried blood spot (DBS) data.

| Parameter | SIR median [95% CI] |
|---|---|
| Structural model | |
| CL [L/h] | 400 [289–549] |
| $V_c$ [L] | 10.6 [7.99–14.0] |
| Q [L/h] | 160 [90.4–268] |
| $V_p$ [L] | 124 [80.7–178] |
| $K_m$ [nmol] | 4,810* |
| $V_{max}$ [nmol/h] | 21,388 [13,888–31,463] |
| F [–] | 1* |
| $K_d$ [nM] | 9.71* |
| $NS_{Alb}$ [–] | 4.15* |
| $K_{aRBC}$ [–] | 6.62 [1.95–13.4] |
| $V_{delta,\ children+infants}$ [L] | 11.1 [7.05–18.8] |
| $V_{delta,\ neonates}$ [L] | 1.05 [0.50–1.80] |
| $BASE_{adult,\ pla}$ [nM] | 15.2 [11.1–20.7] |
| $BASE_{child,\ pla}$ [nM] | 9.41 [3.32–16.7] |
| $BASE_{child,\ DBS}$ [nM] | 4.22 [1.10–7.60] |
| Interindividual variability | |
| ωCL, %CV | 25.8 [14.9–35.8] |
| $\omega K_m$, %CV | 55.7 [31.1–75.5] |
| $\omega V_{max}$, %CV | 46.5 [30.1–65.5] |
| ωF, %CV | 36.1 [20.4–49.4] |
| $\omega V_{delta}$, %CV | 43.4 [27.5–62.2] |
| $\omega BASE_{adult,pla}$, %CV | 35.3 [23.5–47.4] |
| $\omega BASE_{child,pla\ and\ DBS}$, %CV | 131.1* |
| Residual variability | |
| $\sigma_{exp}$ [CV%] | 14.4 [13.2–16.0] |

*Clearance (CL), central volume of distribution ($V_c$), intercompartmental clearance (Q), peripheral volume of distribution ($V_p$), amount in depot compartment resulting in half of Vmax (Km), maximum absorption rate ($V_{max}$), bioavailability (F), equilibrium dissociation constant ($K_d$), linear non-specific parameter for albumin binding and association to red blood cells ($NS_{Alb}$ and $k_{aRBC}$), volume of red blood cell compartment ($V_{delta}$), plasma cortisol baseline in adults ($BASE_{adult,\ pla}$), plasma cortisol baseline in children ($BASE_{child,\ pla}$), dried blood spot cortisol baseline in children ($BASE_{child,\ DBS}$). For $BASE_{child,\ pla}$ and $BASE_{child,\ DBS}$ a common interindividual variability was fixed, residual variability was estimated as an additive error on a logarithmic scale.*
**fixed parameter.*

parameters of cortisol to albumin ($NS_{Alb}$) and RBCs ($K_{aRBC}$) resulted in 4.15 and 6.62, respectively. The predominant binding partner was CBG, with a fixed $K_d$ of 9.71 nmol/L, indicating the unbound cortisol concentration at 50% of $B_{max}$. The estimates for the pediatric plasma and DBS cortisol baselines were 9.41 nmol/L and 4.22 nmol/L, respectively.

The 95% CIs for the parameter estimates resulting from the SIR show good precision of the parameter estimates. Standard model evaluations, that is, GOF plots and VPCs showed that the adult and pediatric plasma and the pediatric DBS concentrations were adequately described by the final PK model (see the **Supplementary Material**).

## Simulation of Cortisol Binding Species

Simulated whole blood cortisol concentrations of children/infants (**Figure 3A**) and of neonates (**Figure 3B**) were based on the PK model with the two different $V_{deltas}$ of the respective age groups based on a dose of 7 mg HC. The fractions of the simulated cortisol species (%) against the whole blood concentration demonstrated the substantial decrease in the cortisol fraction bound to CBG with higher total cortisol concentrations due to the saturation of the binding process. The fraction bound to CBG decreased from approximately 90% at 1.8 nmol/L (LLOQ; i.e., shortly after drug intake) to 45 and 22% at the highest simulated whole blood cortisol concentrations for children/infants (180 nmol/L = Cmax, maximum concentration) and neonates (820 nmol/L = Cmax), respectively. Consequently, a substantial increase was observed for the fraction unbound (children/infants: from 1.7 to 9.0%; neonates: from 1.6 to 13%), the fraction bound to albumin (children/infants: from 7.0 to 37%; neonates: from 6.8 to 53%), and the fraction associated with RBCs (children/infants: from 1.9 to 8.3%; neonates: from 1.9 to 12%).

# DISCUSSION

Leveraging cortisol concentrations from adult plasma data and pediatric plasma and DBS data, we successfully established a quantitative link between pediatric total plasma cortisol concentrations and pediatric total DBS cortisol concentrations by extending a published NLME HC PK model based on adult and pediatric plasma cortisol data with pediatric DBS concentrations.

The inclusion of the whole blood DBS cortisol data into the model allowed to quantitatively characterize cortisol association with RBCs by a linear, non-specific association process, in addition to cortisol binding to CBG, and to albumin. Since the linear association of cortisol with RBCs was only described in adults (Lentjes and Romijn, 1999) and generally a saturation of this process should not be expected due to the abundance of RBCs in all age groups, we assumed that these findings also apply to children. A corresponding RBC-associated cortisol compartment was added to the PK model and RBC volumes were successfully estimated for the neonatal age group and for children/infants. With the age group implemented as a covariate on $V_{delta}$, the $V_{delta}$ estimate (1.05 L) for neonates was considerably lower than the estimated $V_{delta}$ for children/infants (11.1 L) (**Table 1**) and thereby, as an apparent volume of distribution, accounting for the lower plasma/DBS concentration ratio which was observed for neonates.

The estimates for the pediatric baselines in plasma and DBS were reasonably low and close to respective LLOQs. Overall, the inclusion of the pediatric cortisol DBS data barely changed the plasma-related parameter estimates, which were taken from the previous model, whereas the additional DBS-related parameters resulted in plausible estimates.

For a better comparison of $K_{aRBC}$ (6.62) with the other two binding parameters $K_d$ (9.71 nmol/L) and $NS_{Alb}$ (4.15), the PK model was applied to simulate the fractions of cortisol bound to CBG, to albumin, and associated with RBCs. As already expected from the graphical analysis, with increasing cortisol concentrations the ratio between cortisol plasma and DBS concentrations decreased. The simulation results supported this finding, due to the saturation of the nonlinear binding between cortisol and CBG and thus higher availability of unbound cortisol to be associated with RBCs. The simulated fraction of cortisol bound to CBG decreased by 75% in neonates (from 90 to 22%) compared to a decrease of 50% in children/infants (from 90 to 45%). Consequently, a considerably higher

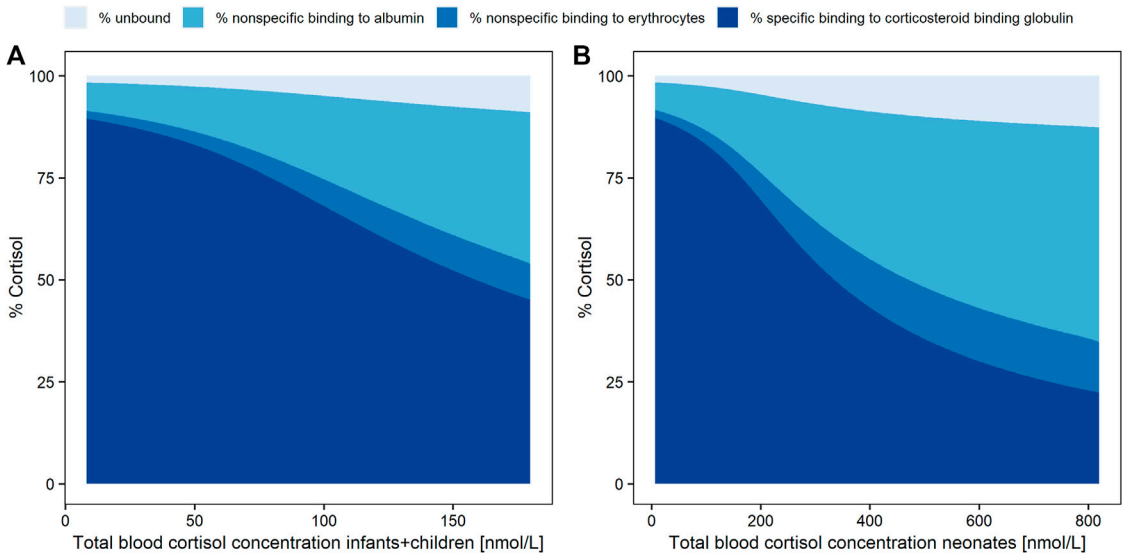


**FIGURE 3 |** Simulated cortisol concentration fractions (%) as unbound (pale blue), with nonspecific linear binding to albumin (light blue), nonspecific linear binding to red blood cells (middle blue) or specific nonlinear binding (dark blue) to corticosteroid binding globulin, over total whole blood (dried blood spot) concentration (LLOQ = 1.8 nmol/L to Cmax) in infants and children **(A)** and neonates **(B)**.

amount of free cortisol became available for binding to albumin or association with RBCs. At the highest simulated whole blood cortisol concentrations, 45% more cortisol is associated with RBCs in neonates (12% at 820 nmol/L Cmax) compared to children/infants (8.3% at 180 nmol/L Cmax). These considerably different simulated fractions of cortisol associated with RBCs could partly explain the highly variable plasma/DBS concentration ratios which were observed in the graphical analysis for the two age groups. The higher cortisol concentrations were only observed in neonates due to a higher dose relative to body weight in the phase 3 trial, which was mimicked in the simulations by dosing both age groups with the same HC dose. Since the simulations were deterministic, that is, did not include interindividual variability, simulations with 4 mg (**Supplementary Figure S3**), which was the maximum single dose given in the phase 3 study, resulted in maximum concentrations lower than the ones observed in the phase 3 study (767.5 nmol/L and 141 nmol/L for neonates and children + infants, respectively). Thus, to ensure simulated total blood cortisol concentrations representing the full range of observed concentrations, the simulation dose was increased to 7 mg. It was assumed that the plasma/DBS concentration ratio depends on the overall cortisol concentration. The high cortisol concentrations observed in neonates were the result of a relatively higher HC dose given in the phase 3 study to avoid underdosing in this highly vulnerable cohort. To further explain the high variability observed in the plasma/DBS concentration ratio, more data are required to investigate whether, besides the concentration dependency, there is also, for example, an age dependency for the ratio.

The graphical investigation of the plasma/DBS cortisol concentration ratio leads to the conclusion that with the observed DBS cortisol concentrations ranging from 0 to 200 nmol/L and from 200 to 800 nmol/L, the corresponding plasma cortisol concentrations are higher than DBS concentrations by a factor of 5 and 2.5, respectively. However, this finding should be confirmed with a richer dataset, especially in the higher concentration range where only four neonatal samples were available, before being considered as a rule of thumb when DBS cortisol sampling is used for clinical monitoring in pediatric adrenal insufficiency patients.

As the cortisol concentration data from the pediatric population were sparse in general, the PK model should be re-evaluated with more plasma and DBS cortisol data to confirm the conclusions of our current analysis. A regression equation based on simulations from the updated PK model could then be identified to enable the calculation of plasma cortisol concentrations from measured DBS cortisol concentrations, opening the opportunity to routinely use and interpret DBS sampling for monitoring this vulnerable patient population. As this analysis is based on data from patients aged from 0 to 6 years, the applicability of the PK model to children older than 6 years can be investigated in future with respective available data. The PK in adolescents aged 12 to 18 years can be assumed to be similar to adult HC PK and binding kinetics as it was found in published pharmacokinetic analyses (Bonner et al., 2021).

Furthermore, the DBS data used in this analysis were venous whole blood concentrations, whereas in clinical practice capillary whole blood is obtained for DBS sampling. It is therefore important to re-evaluate the comparability of venous and capillary whole blood cortisol concentrations. Moreover, the underlying mechanism behind cortisol being associated with RBCs is still unknown, and it should be investigated if cortisol associated with RBCs is biologically active due to its low affinity to RBCs (Lentjes and Romijn, 1999). Thus, further *in vitro* studies are needed to elucidate the underlying mechanisms of

the RBC-associated processes (e.g., adsorption and uptake) qualitatively and quantitatively.

## DATA AVAILABILITY STATEMENT

The original contributions presented in the study are included in the article/**Supplementary Material**; further inquiries can be directed to the corresponding author.

## ETHICS STATEMENT

The studies involving human participants were reviewed and approved by the Local Ethics Committee at Charite Berlin (study nr 15/0375-EK 15). Written informed consent to participate in this study was provided by the participants' legal guardian/next of kin.

## AUTHOR CONTRIBUTIONS

Conceptualization: VS, RM, and CK; formal analysis: VS; data collection: UN, OB, RR, and MW; writing—original draft preparation: VS and DB; writing—review and editing: all authors; and visualization: VS; supervision: RM and CK. All authors have read and approved final version for publication.

## FUNDING

The modeling and simulation work described here was carried out under a Cooperation Agreement between Freie Universitaet and Diurnal funded by Diurnal Lt, based on a clinical trial designed by Diurnal and Charite Berlin.

## ACKNOWLEDGMENTS

The authors acknowledge the High-Performance Computing Service of ZEDAT at Freie Universitaet Berlin (https://www.zedat.fu-berlin.de/HPC/Home) for computing time. We acknowledge the support by the Open Access Publication Initiative of Freie Universität Berlin.

## SUPPLEMENTARY MATERIAL

The Supplementary Material for this article can be found online at: https://www.frontiersin.org/articles/10.3389/fphar.2022.819590/full#supplementary-material

## REFERENCES

Balsamo, A., Baronio, F., Ortolano, R., Menabo, S., Baldazzi, L., di Natale, V., et al. (2020). Congenital Adrenal Hyperplasias Presenting in the Newborn and Young Infant. *Front. Pediatr.* 8, 864. doi:10.3389/FPED.2020.593315/BIBTEX

Bauer, R. (2010). *NONMEM Users Guide: Introduction to NONMEM 7*. Ellicott City, MD: ICON Development Solutions Ellicott City, MD, 1–61. Available at: ftp://nonmem.iconplc.com/Public/nonmem7/Release_Notes_Plus/nm720.pdf.

Bergstrand, M., Hooker, A. C., Wallin, J. E., and Karlsson, M. O. (2011). Prediction-Corrected Visual Predictive Checks for Diagnosing Nonlinear Mixed-Effects Models. *AAPS J.* 13, 143–151. doi:10.1208/s12248-011-9255-z

Bonner, J. J., Burt, H., Johnson, T. N., Whitaker, M. J., Porter, J., and Ross, R. J. (2021). Development and Verification of an Endogenous PBPK Model to Inform Hydrocortisone Replacement Dosing in Children and Adults with Cortisol Deficiency. *Eur. J. Pharm. Sci.* 165, 105913. doi:10.1016/j.ejps.2021.105913

Bornstein, S. R., Allolio, B., Arlt, W., Barthel, A., Don-Wauchope, A., Hammer, G. D., et al. (2016). Diagnosis and Treatment of Primary Adrenal Insufficiency: An Endocrine Society Clinical Practice Guideline. *J. Clin. Endocrinol. Metab.* 101, 364–389. doi:10.1210/JC.2015-1710

Dabas, A., Vats, P., Sharma, R., Singh, P., Seth, A., Jain, V., et al. (2020). Management of Infants with Congenital Adrenal Hyperplasia. *Indian Pediatr.* 57, 159–164. doi:10.1007/s13312-020-1735-8

Dosne, A. G., Bergstrand, M., and Karlsson, M. O. (2017). An Automated Sampling Importance Resampling Procedure for Estimating Parameter Uncertainty. *J. Pharmacokinet. Pharmacodyn.* 44, 509–520. doi:10.1007/s10928-017-9542-0

Edelbroek, P. M., van der Heijden, J., and Stolk, L. M. (2009). Dried Blood Spot Methods in Therapeutic Drug Monitoring: Methods, Assays, and Pitfalls. *Ther. Drug Monit.* 31, 327–336. doi:10.1097/FTD.0B013E31819E91CE

European Medicines Agency (2012). *Guideline on Bioanalytical Method Validation*.

Kamoun, M., Feki, M. M., Sfar, M. H., and Abid, M. (2013). Congenital Adrenal Hyperplasia: Treatment and Outcomes. *Indian J. Endocrinol. Metab.* 17, S14–S17. doi:10.4103/2230-8210.119491

Keizer, R. J., Karlsson, M. O., and Hooker, A. (2013). Modeling and Simulation Workbench for NONMEM: Tutorial on Pirana, PsN, and Xpose. *CPT Pharmacometrics Syst. Pharmacol.* 2, e50. doi:10.1038/psp.2013.24

Khattab, A., and Marshall, I. (2019). Management of Congenital Adrenal Hyperplasia: beyond Conventional Glucocorticoid Therapy. *Curr. Opin. Pediatr.* 31, 550–554. doi:10.1097/MOP.0000000000000780

Lentjes, E. G., and Romijn, F. H. (1999). Temperature-dependent Cortisol Distribution Among the Blood Compartments in Man. *J. Clin. Endocrinol. Metab.* 84, 682–687. doi:10.1210/jcem.84.2.5461

Melin, J., Parra-Guillen, Z. P., Michelet, R., Truong, T., Huisinga, W., Hartung, N., et al. (2020). Pharmacokinetic/Pharmacodynamic Evaluation of Hydrocortisone Therapy in Pediatric Patients with Congenital Adrenal Hyperplasia. *J. Clin. Endocrinol. Metab.* 105. doi:10.1210/clinem/dgaa071

Melin, J., Parra-Guillen, Z. P., Hartung, N., Huisinga, W., Ross, R. J., Whitaker, M. J., et al. (2017). Predicting Cortisol Exposure from Paediatric Hydrocortisone Formulation Using a Semi-mechanistic Pharmacokinetic Model Established in Healthy Adults. *Clin. Pharmacokinet.* 57, 515–527. doi:10.1007/s40262-017-0575-8

Merke, D. P., and Bornstein, S. R. (2005). Congenital Adrenal Hyperplasia. *Lancet* 365, 2125–2136. doi:10.1016/S0140-6736(05)66736-0

Michelet, R., Melin, J., Parra-Guillen, Z. P., Neumann, U., Whitaker, J. M., Stachanow, V., et al. (2020). Paediatric Population Pharmacokinetic Modelling to Assess Hydrocortisone Replacement Dosing Regimens in Young Children. *Eur. J. Endocrinol.* 183, 357–368. doi:10.1530/EJE-20-0231

Moat, S. J., George, R. S., and Carling, R. S. (20202020). Use of Dried Blood Spot Specimens to Monitor Patients with Inherited Metabolic Disorders. *Int. J. Neonatal. Screen.* 6, 26. doi:10.3390/IJNS6020026

Mould, D. R., and Upton, R. N. (2012). Basic Concepts in Population Modeling, Simulation, and Model-Based Drug Development. *CPT Pharmacometrics Syst. Pharmacol.* 1, e6. doi:10.1038/psp.2012.4

Mould, D. R., and Upton, R. N. (2013). Basic Concepts in Population Modeling, Simulation, and Model-Based Drug Development-Part 2: Introduction to Pharmacokinetic Modeling Methods. *CPT Pharmacometrics Syst. Pharmacol.* 2, e38. doi:10.1038/psp.2013.14

Neumann, U., Whitaker, M. J., Wiegand, S., Krude, H., Porter, J., Davies, M., et al. (2018). Absorption and Tolerability of Taste-Masked Hydrocortisone Granules in Neonates, Infants and Children under 6 Years of Age with Adrenal Insufficiency. *Clin. Endocrinol. (Oxf)* 88, 21–29. doi:10.1111/cen.13447

Oprea, A., Bonnet, N. C. G., Pollé, O., and Lysy, P. A. (2019). Novel Insights into Glucocorticoid Replacement Therapy for Pediatric and Adult Adrenal Insufficiency. *Ther. Adv. Endocrinol. Metab.* 10, 2042018818821294. doi:10.1177/2042018818821294

Podgórski, R., Aebisher, D., Stompor, M., Podgórska, D., and Mazur, A. (2018). Congenital Adrenal Hyperplasia: Clinical Symptoms and Diagnostic Methods. *Acta Biochim. Pol.* 65, 25–33. doi:10.18388/ABP.2017_2343

Qasrawi, D. O., Boyd, J. M., and Sadrzadeh, S. M. H. (2021). Measuring Steroids from Dried Blood Spots Using Tandem Mass Spectrometry to Diagnose Congenital Adrenal Hyperplasia. *Clin. Chim. Acta* 520, 202–207. doi:10.1016/J.CCA.2021.06.005

R Core Team (2019). R: A Language and Environment for Statistical Computing. Available at: https://www.R-project.org/ (Accessed November 21, 2021).

RStudio Team (2020). *RStudio*. Boston, MA: Integrated Development Environment for R.

Whitaker, M. J., Spielmann, S., Digweed, D., Huatan, H., Eckland, D., Johnson, T. N., et al. (2015). Development and Testing in Healthy Adults of Oral Hydrocortisone Granules with Taste Masking for the Treatment of Neonates and Infants with Adrenal Insufficiency. *J. Clin. Endocrinol. Metab.* 100, 1681–1688. doi:10.1210/jc.2014-4060

Wilhelm, A. J., den Burger, J. C., and Swart, E. L. (2014). Therapeutic Drug Monitoring by Dried Blood Spot: Progress to Date and Future Directions. *Clin. Pharmacokinet.* 53, 961–973. doi:10.1007/S40262-014-0177-7/TABLES/2

**Conflict of Interest:** The modeling and simulation work described here was carried out under a Cooperation Agreement between Freie Universitaet and Diurnal funded by Diurnal Lt, based on a clinical trial designed by Diurnal and Charite Berlin. The manuscript writing was done by all involved parties, that is, Freie Universitaet Berlin, Diurnal Lt, University of Potsdam and Charite Berlin.

The remaining authors declare that the research was conducted in the absence of any commercial or financial relationships that could be construed as a potential conflict of interest.

frontiers | Frontiers in Pharmacology

ORIGINAL RESEARCH
published: 06 April 2022
doi: 10.3389/fphar.2022.802974

# Maternal Exposure to Polychlorinated Biphenyls and Asthma, Allergic Rhinitis and Atopic Dermatitis in the Offspring: The Environmental Health Fund Birth Cohort

*Maya Berlin[1,2], Hadar Flor-Hirsch[1], Elkana Kohn[1], Anna Brik[1], Rimona Keidar[3], Ayelet Livne[3], Ronella Marom[4], Amit Ovental[4], Dror Mandel[4], Ronit Lubetzky[4], Pam Factor-Litvak[5], Josef Tovbin[6], Moshe Betser[6], Miki Moskovich[6], Ariela Hazan[1], Malka Britzi[7], Itai Gueta[8], Matitiahu Berkovitch[1]*, Ilan Matok[2] and Uri Hamiel[9]*

[1]*Clinical Pharmacology and Toxicology Unit, Shamir Medical Center (Assaf Harofeh), Affiliated to Sackler Faculty of Medicine, Tel-Aviv University, Tel Aviv, Israel,* [2]*Division of Clinical Pharmacy, Institute for Drug Research, School of Pharmacy, Faculty of Medicine, Hebrew University of Jerusalem, Jerusalem, Israel,* [3]*Department of Neonatology, Shamir Medical Center (Assaf Harofeh), Affiliated to Sackler Faculty of Medicine, Tel-Aviv University, Tel Aviv, Israel,* [4]*Departments of Neonatology and Pediatrics, Dana Dwek Children's Hospital, Tel Aviv Medical Center, Affiliated to Sackler Faculty of Medicine, Tel-Aviv University, Tel Aviv, Israel,* [5]*Department of Epidemiology, Mailman School of Public Health, Columbia University, New York, NY, United States,* [6]*Division of Obstetrics and Gynecology, Shamir Medical Center (Assaf Harofeh), Affiliated to Sackler Faculty of Medicine, Tel-Aviv University, Tel Aviv, Israel,* [7]*Residues Lab, Kimron Veterinary Institute, Beit-Dagan, Israel,* [8]*The Institute of Clinical Pharmacology and Toxicology, Department of Medicine, Sheba Medical Center, Affiliated to Sackler Faculty of Medicine, Tel-Aviv University, Tel Aviv, Israel,* [9]*Department of Pediatrics, Shamir Medical Center (Assaf Harofeh), Zerifin, Affiliated to Sackler Faculty of Medicine, Tel-Aviv University, Tel Aviv, Israel*

OPEN ACCESS

**Edited by:**
*Catherine M. T. Sherwin, Wright State University, United States*

**Reviewed by:**
*Yaron Finkelstein, University of Toronto, Canada*
*Laurent Azoulay, McGill University, Canada*

***Correspondence:**
*Matitiahu Berkovitch*
*mberkovitch@shamir.gov.il*

**Specialty section:**
*This article was submitted to Obstetric and Pediatric Pharmacology, a section of the journal Frontiers in Pharmacology*

**Received:** *27 October 2021*
**Accepted:** *07 March 2022*
**Published:** *06 April 2022*

**Citation:**
*Berlin M, Flor-Hirsch H, Kohn E, Brik A, Keidar R, Livne A, Marom R, Ovental A, Mandel D, Lubetzky R, Factor-Litvak P, Tovbin J, Betser M, Moskovich M, Hazan A, Britzi M, Gueta I, Berkovitch M, Matok I and Hamiel U (2022) Maternal Exposure to Polychlorinated Biphenyls and Asthma, Allergic Rhinitis and Atopic Dermatitis in the Offspring: The Environmental Health Fund Birth Cohort. Front. Pharmacol. 13:802974. doi: 10.3389/fphar.2022.802974*

**Background:** Polychlorinated biphenyls (PCBs) are persistent organic pollutants banned for use worldwide. Due to their biodegradation resistance, they accumulate along the food chain and in the environment. Maternal exposure to PCBs may affect the fetus and the infant. PCBs are immunotoxic and may damage the developing immune system. PCBs are associated with elevated IgE antibodies in cord blood and are considered to be predictive of atopic reactions. Several studies on the association between prenatal exposure to PCBs and atopic reactions were previously published, albeit with conflicting results.

**Objectives:** To examine the association between maternal PCBs levels and atopic reactions in their offspring.

**Methods:** During the years 2013–2015, a prospective birth cohort was recruited at the delivery rooms of Shamir Medical Center (Assaf Harofeh) and "Dana Dwek" Children's Hospital. Four PCBs congeners were investigated: PCBs 118, 138, 153, and 180. In 2019, when children reached the age of 4–6 years, mothers were interviewed using the ISAAC questionnaire to assess symptoms of atopic reactions, including asthma, allergic rhinitis, and atopic dermatitis.

**Results:** One hundred and fifty mother-child dyads were analyzed. No significant differences were found in the median serum PCBs concentrations of each studied congener or total PCBs for asthma, allergic rhinitis, atopic dermatitis diagnosis, or

parent-reported symptoms. No association was found between exposure to total PCBs and the risk for asthma symptoms or diagnosis, adjusted to maternal age and family member with atopic condition: aOR = 0.94, 95%CI: (0.88; 0.99). No association was observed between each studied PCB congener and asthma symptoms or diagnosis. The same results were found also for other studied outcomes—allergic rhinitis and atopic dermatitis.

**Conclusion:** Our study joins a series of previous studies that attempt to shed light on environmental exposures *in utero* as influencing factors for atopic conditions in children. Our results reflect the complexity of the pathophysiology of these phenomena. No relationship between maternal serum PCBs levels was demonstrated for asthma, allergic rhinitis, or atopic dermatitis. However, additional multi-participant studies, with longer, spanning into later pediatric age follow up are needed.

**Keywords: polychlorinated biphenyls (PCBs), endocrine-disrupting chemicals (EDCs), allergy, asthma, atopic dermatitis, pregnancy, allergic rhinitis**

## INTRODUCTION

Atopic conditions are complex traits, most probably caused by an interaction of multiple disease susceptibility genes and environmental factors (Sengler et al., 2002). During the last century prevalence of atopic conditions has been on the rise. Numerous studies link exposure to various domestic and industrial environmental pollutants with bronchial wheezing and atopic morbidity (Masoli et al., 2004; Pope and Dockery, 2006; Clark et al., 2010; WHO Regional Office for Europe, 2013). Several studies in Israel have found an association between exposure to such environmental pollutants and childhood asthma and respiratory morbidity (Portnov et al., 2012; Greenberg et al., 2015; Greenberg et al., 2019).

Polychlorinated biphenyls (PCBs) are a large family of persistent organic pollutants, industrial chemicals, once used widely as non-flammable lubricants and insulators. This family of PCBs is considered as one of the most dominant pollutants worldwide (Agency for Toxic Substances and Disease Registry, 2000; Bergman et al., 2012). PCBs were banned from production in late 1970 in the United States and from 2001 worldwide by the Stockholm Convention on Persistent Organic Pollutants (United Nations Environment Programme, 2018). However, their chemical properties, such as a long half-life and fat solubility, cause them to be preserved in soil, water, and food chain, and consequently in human tissues (Domingo, 2012). PCBs are readily absorbed from the environment into the food chain, rendering human and animal exposure ubiquitous. Human exposure is mainly through consuming fatty foods like fish, meat, and dairy products (Freels et al., 2007; Fernández-González et al., 2015). PCBs 118, 138, 153, 180 are among the most frequently detected congeners in human adipose tissue and represent long-lasting exposure (Bonefeld-Jørgensen et al., 2001; Freels et al., 2007; Müllerová and Kopecký, 2007; Domingo, 2012). PCBs 138, 153, and 180 have the highest detection frequencies in the US population and contributed to 80% of the total PCBs in human serum (Faroon and Ruiz, 2015).

Several studies have found an association between exposure to PCBs and their effects on the immune system (Hertz-Picciotto et al., 2008). Epidemiologically, an increase in the rate of upper respiratory tract infections was demonstrated (Dallaire et al., 2004). At the pathophysiological level, changes in thymus development, changes in levels and differentiation of lymphocytes of the various subtypes, an increase in Immunoglobulin E (IgE) antibody levels in the umbilical cord, and a decrease in antibody production in response to childhood vaccines are described in association with PCBs exposure (Reichrtová et al., 1999; Weisglas-Kuperus et al., 2000; Belles-Isles et al., 2002; Heilmann et al., 2006). IgE antibody levels in the umbilical cord were found to be a predictor of atopic predisposition (Liptay et al., 1992). A recent study showed that serum aryl hydrocarbon receptor (AhR) bioactivities were increased with specific PCB congeners (Park et al., 2017). AhR activation was positively correlated with atopic dermatitis (Hidaka et al., 2017). It has been hypothesized that prenatal exposure to PCBs may be linked to atopic phenomena. Maternal PCBs levels were positively associated with upper respiratory tract in infections during the first year of life (Stølevik et al., 2013). Children exposed in-utero to persistent organic pollutants (POPs) such as organochlorine pesticides and PCBs have an increased risk of asthma, wheezing and eczema (Hansen et al., 2014; Mamane et al., 2015; Parker-Lalomio et al., 2017). There is a complex interaction between the environmental exposures acting during the early stages of development and genetic susceptibility that might contribute to asthma and allergy (Kahr et al., 2015; Morales and Duffy, 2019). Studies attempting to answer this question yielded conflicting results (Smit et al., 2015; Hansen et al., 2016; Parker-Lalomio et al., 2017).

There are prominent developmental events *in utero*, leading to critical windows for susceptibility to immunotoxic effects. Pregnant women and the fetus, infants, and children are most vulnerable to low-dosage environmental exposure. There is growing evidence of adverse effects of environmental exposure on reproduction, pre and post-natal development (Sharpe and Irvine, 2004; Di Renzo et al., 2015; Teysseire et al., 2019). As a lipophilic substance, PCBs can be transferred through the placenta and during breastfeeding to increase children's body

burden. Therefore, children are exposed to PCBs starting from conception, during pregnancy and lactation, and the exposure continues throughout lifetime (Sly and Flack, 2008).

This study aimed to examine the possible relationship between prenatal background exposure to PCBs and the prevalence of atopic phenomena in children from a birth cohort of Israeli mothers and children.

# MATERIAL AND METHODS

## Study Population

We used data collected from a birth cohort recruited at Shamir Medical Center (Assaf Harofe) and "Dana Dwek" Children's Hospital, Tel Aviv Medical Center. Complete details of this birth cohort have been presented elsewhere (Sheinberg et al., 2020; Berlin et al., 2021).

Briefly, from January 2013 through April 2015, 263 mother-father-newborn triads were recruited. The women recruited for the study were asked to participate during attendance in the delivery room. Data on social and demographic characteristics and lifestyle variables from both the father and mother were obtained through a detailed questionnaire. Data on occupation, residential history, diet, hobbies, and detailed health history were also collected. At the delivery room, blood and urine samples were collected from mothers and fathers.

Birth weight, length, and head circumference were measured three times using standard research procedures. Birth weight was adjusted to gestational age at birth and infant's sex and classified according to percentile values derived from the Israeli Perinatal survey (Dollberg et al., 2005).

All participants signed informed consent. The study was performed according to the Declaration of Helsinki, and the Institutional Review Board approved the protocol (The World Medical Association, 2018).

## Data Extraction

The database included 263 mother-newborn dyads. Due to budget limitations, we measured concentrations of 4 PCBs from maternal blood of 183 mothers who gave birth at Shamir Medical Center (Assaf Harofeh). On average, included and excluded dyads were similar in potential confounders such as birth weight, length of gestation, and maternal age (Sheinberg et al., 2020; Berlin et al., 2021).

Cases of women with twin pregnancies ($N$ = 2), premature delivery (<37 weeks) ($N$ = 8), and incomplete details ($N$ = 3) were excluded.

We retrieved data on 170 dyads for which serum PCBs measurements were obtained. Data on maternal demographics, exposures, lifestyle, and labor were extracted as well as newborn anthropometrics and measurements.

Maternal laboratory test results obtained during delivery included 4 PCB congeners, total cholesterol, and triglycerides.

A follow-up questionnaire was sent out to participants between April 2019 and October 2019, when the children were 4–6 years old. Mothers were contacted to evaluate the prevalence of atopic phenomena among their offspring. The atopic symptoms were assessed using—the International Study of Asthma and Allergies in Childhood ("ISAAC") questionnaire, (Asher et al., 1995), previously validated and implemented to assess the prevalence and severity of asthma and allergic reactions in children (Romano-Zelekha et al., 2007; Raherison et al., 2019; Jøhnk et al., 2020). The questionnaire includes modules to assess asthma, allergic rhinitis, and atopic dermatitis.

The outcomes of asthma, allergic rhinitis, and atopic dermatitis were classified as doctor-diagnosed or parent-reported. Parent-reported asthma symptoms were defined as children with one of the following symptoms: wheezing or shortness of breath in the past year or use of inhalations in the past year. Parent-reported symptoms of allergic rhinitis were defined as children with one of the following symptoms: chronic rhinitis occurring not as part of an acute infection in the last year or use of nasal sprays in the previous year. Parent-reported symptoms of atopic dermatitis were defined as children with one of the following symptoms: a persistent itchy rash in the past year or use of topical preparations in the past year.

The questionnaire was translated into Hebrew, and questions were added regarding general medical conditions and the presence of possible confounders such as smoking by one of the family members; child's births order in the family; rural/urban living environment; pet in the family home; and atopy among nuclear family members.

## Sample Analysis

All samples were processed, aliquoted, and frozen at -80°C until analysis. PCBs were measured at the Centre de Toxicologie du Quebec. Congeners 118 (2,3′,4,4′,5-pentachlorobiphenyl), 138 (2,2′,3,4,4′,5′-hexachlorobiphenyl), 153 (2,2′,4,4′,5,5′-hexachlorobiphenyl), and 180 (2,2′,3,4,4′,5,5′-heptachlorobiphenyl) were measured. All measures were performed using GC/MS at INSPEQ, at the Arctic Monitoring and Assessment Programme Ring Test for Persistent Organic Pollutants in Human Serum (AMAP), organized and managed by the Centre de Toxicologie du Québec (CTQ).

The lower limit of quantification (LOQ) was 10 ng/L. For statistical analysis purposes, values below LOQ were assigned with the value of LOQ/$\sqrt{2}$. All the samples were above the LOQ for PCB 153. There were 11 samples with levels below the LOQ: PCB 118—six samples, PCB 118 + 138—one sample, PCB 118 + 180—one sample.

PCBs were measured in 200 randomly selected samples. Seventeen of the 200 samples were duplicates. The correlations between the duplicates were 0.996, 0.997, 1, and 0.997 for congeners 118, 138, 153, and 180, respectively. Where duplicate samples were measured, a mean of the two measures was taken.

PCBs were reported as the wet weight. We normalized the concentrations using the following equation, which adjusts chemical per gram of total lipids (lipid weight, ng chemical/g total lipid) (Schisterman et al., 2005).

Total lipids (TL) were estimated using the formula (Bernert et al., 2007; Bergonzi et al., 2009):

$$\mathrm{TL}(\mathrm{g/L}) = 2.27 \times \mathrm{TC}(\mathrm{g/L}) + \mathrm{TG}(\mathrm{g/L}) + 0.623$$

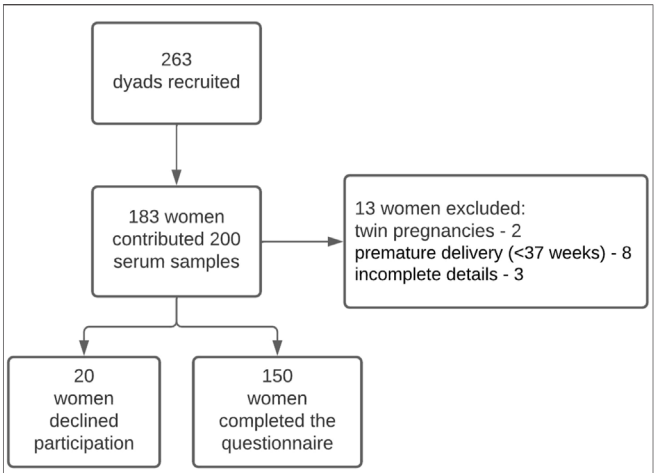


**FIGURE 1 |** Flowchart of study population.

where TL—total lipids, TC—total cholesterol, TG—triglycerides.

Maternal total cholesterol and triglycerides were measured in the Shamir (Assaf Harofeh) biochemistry lab using standard methods. The enzymatic method was used to quantitatively determine cholesterol and triglycerides in human serum and plasma on Roche/Hitachi Cobas c systems.

## Statistical Analysis

Continuous variables are presented as mean and standard deviation (±SD) or median and interquartile range (IQR). Continuous variables were compared between groups using the Kruskal Wallis test or Mann-Whitney test. Categorical variables were compared using the Chi-square test, or Fisher's exact test, as appropriate.

Spearman correlation coefficients were calculated to assess the correlation between continuous variables of the mother and the newborn and PCBs level variables.

Logistic regression models were constructed and OR and 95% CI were calculated. The models were adjusted for potential confounders: maternal age and family member with asthma/atopic condition. PCBs levels used were adjusted to serum lipids. In order to perform the regression analysis and to increase the sample size for each outcome, the studied outcomes (asthma, allergic rhinitis and atopic dermatitis) were combined into 3 groups—children with symptoms and/or with diagnosis.

All statistical tests were two-sided, and $p < 0.05$ was considered statistically significant. SPSS software (IBMS SPSS Statistics for Windows, Version 25, IBM Corp, Armonk, New York, United States) was used for all statistical analyses.

# RESULTS

## Subjects' Characteristics

One hundred and fifty mothers-newborn dyads completed the questionnaire and were included in the final analysis, **Figure 1** presents the flowchart of the study population. Maternal and newborn characteristics of those included in the final analysis and those who refused participation in the study are presented in **Table 1**. The only observed difference between the groups was that newborns included in the study had higher birth weight and birth percentile as compared to those who refused to answer the questionnaire, 3,200 (2,900–3,478) g vs. 2,875 (2,640–3,337) g, *p*-value = 0.03, birth percentile 53 (34–75) vs. 33 (12–70.75), *p*-value = 0.02.

When comparing maternal, neonatal, and demographic characteristics between children with and without a diagnosis of studied outcomes, no statistically significant difference was found in most of the parameters, such as maternal age at childbirth, gestational age, birth weight percentile, current weight percentile, order of the child in the family, sex (male), smoker in the immediate family, rural living environment and presence of a household pet (**Supplementary Tables S1–S6**).

We found that 5% ($N = 8$) of the children were diagnosed with asthma. Parent-reported symptoms of asthma had 16% ($N = 24$) of children. Six children (4%) were diagnosed with allergic rhinitis, but for 21 children (14%), parents reported having allergic rhinitis symptoms. The prevalence of atopic dermatitis diagnosis was 13% ($N = 19$), and symptoms of atopic dermatitis were reported in 14 children (9%).

## Maternal Serum Polychlorinated Biphenyls Levels and Offsprings' Allergic Outcomes

Statistical analysis was performed to examine the correlation between maternal PCB levels at birth and the other characteristics. Two associations were found to be statistically

**TABLE 1 |** Selected maternal and child characteristics in the EHF-Assaf-Harofeh-Ichilov birth cohort, Israel, 2013–2015, comparing those included ($n = 150$) with those refused to answer the questionnaire ($n = 20$).

| | Included *N* = 150 | Refused participation *N* = 20 | *p*-value |
|---|---|---|---|
| Maternal age at childbirth (years) | 32 (30–36) | 30.5 (29–35.5) | 0.33 |
| Maternal education (years) | 16 (14–17) | 16 (12.25–17) | 0.58 |
| Gestational age (weeks) | 39 (38–40) | 39 (38–40) | 0.71 |
| Birth weight (g) | 3,200 (2,900–3,478) | 2,875 (2,640–3,337) | **0.03** |
| Birth weight percentile | 53 (34–75) | 33 (12–70.75) | **0.02** |
| Child sex—male (N, %) | 79 (52.7%) | 8 (40%) | 0.28 |

*Values presented as median and IQR, unless otherwise specified.*
***Bold**: p-value<0.05.*

**TABLE 2 |** Spearman rank correlations of PCBs (lipid adj.) and maternal age and education in the EHF-Assaf-Harofeh-Ichilov birth cohort, Israel, 2013–2015 ($n$ = 150).

| | Maternal age | Maternal education |
|---|---|---|
| PCB 118 (ng/g lipids) | 0.33 | 0.31 |
| PCB 138 (ng/g lipids) | 0.33 | 0.32 |
| PCB 153 (ng/g lipids) | 0.41 | 0.30 |
| PCB 180 (ng/g lipids) | 0.63 | 0.37 |
| Sum PCBs (ng/g lipids) | 0.45 | 0.33 |

*p-value <0.01 (for all results presented).*

significant—maternal age and maternal education, the effect size was 0.45 ($p < 0.01$) and 0.33 ($p < 0.01$) for total PCBs, respectively (**Table 2**). Moderate-strong association was found between maternal age at birth and every studied congener—PCB 118–0.33, PCB 138—0.33, PCB 153—0.41, PCB 180—0.63, with $p$-value for all results <0.01. The association between the maternal education and studied PCBs was moderate—PCB 118—0.31, PCB 138—0.32, PCB 153—0.30, PCB 180—0.33, with $p$-value for all results <0.01 (**Table 2**).

We compared serum PCBs concentration (lipid-adjusted) in mothers of children with an allergic outcome to serum concentration in mothers without allergic outcome (**Table 3**). No significant differences were found in the median serum PCBs concentrations of 4 studied congeners or total PCBs for asthma, allergic rhinitis, atopic dermatitis diagnosis, or parent-reported symptoms.

## The Association Between Maternal Serum Polychlorinated Biphenyls Levels and Asthma, Allergic Rhinitis and Atopic Dermatitis Diagnosis and/or Symptoms

We divided the serum PCBs concentration in tertiles, defined as concentrations in the lowest third, middle third, and highest third. Then compared the number of children with allergic conditions between first and second tertiles vs. the third tertile of maternal lipid-adjusted PCBs serum concentration (**Table 4**). No significant differences were found for asthma diagnosis or parent-reported symptoms. The same results were observed for allergic rhinitis diagnosis. A statistically significant difference was observed for PCB 118 in children with parent-reported allergic rhinitis when comparing the first and second tertile to the third tertile—18 vs. 6%, $p$-value = 0.05 (**Table 4**). A significantly higher percentage of children with atopic dermatitis diagnosis was observed in the third tertile of total PCBs—20.4 vs. 8.9% (in the first and second tertiles), $p$-value = 0.05. The same results were observed for the PCB 153. When comparing the parent-reported symptoms for atopic dermatitis–the same results were observed with a $p$-value toward significance. For total PCBs: 16.3 vs. 5.9% (third tertile vs. first and second tertiles), $p$-value = 0.07, the same results were obtained for PCB 153 and PCB 180 (**Table 4**).

**TABLE 3 |** Maternal median (IQR) serum PCBs concentration (lipid adjusted) among offspring with or without allergic outcomes.

| | — | Sum PCBs | P | PCB 118 | P | PCB 138 | P | PCB 153 | P | PCB 180 | P |
|---|---|---|---|---|---|---|---|---|---|---|---|
| Asthma diagnosed | with 8 | 11.71 (9.19; 20.57) | 0.29 | 1.93 (1.74; 2.13) | 0.12 | 2.95 (2.16; 4.36) | 0.36 | 4.19 (3.22; 7.73) | 0.3 | 3.26 (2.06; 6.65) | 0.48 |
| | w/o 142 | 15.03 (11.76; 19.99) | | 2.31 (1.85; 3.05) | | 3.36 (2.53; 4.81) | | 5.39 (4.10; 7.27) | | 3.72 (2.69; 5.39) | |
| Asthma symptoms | with 24 | 12.92 (10.01; 18.49) | 0.10 | 2.07 (1.63; 2.73) | 0.1 | 2.87 (2.16; 4.18) | 0.13 | 4.47 (3.46; 6.84) | 0.07 | 3.34 (2.25; 4.69) | 0.16 |
| | w/o 126 | 15.14 (12.02; 21.56) | | 2.31 (1.87; 3.17) | | 3.39 (2.61; 4.9) | | 5.48 (4.23; 7.73) | | 3.9 (2.71; 5.61) | |
| Allergic rhinitis diagnosed | with 6 | 15.18 (9.66; 31.03) | 0.90 | 1.93 (1.39; 4.54) | 0.42 | 3.9 (2.13; 7.11) | 0.82 | 5.77 (3.59; 11.95) | 0.79 | 3.7 (2.24; 8.16) | 0.92 |
| | w/o 144 | 14.69 (11.26; 19.64) | | 2.28 (1.82; 3.04) | | 3.31 (2.52; 4.63) | | 5.38 (3.9; 7.12) | | 3.69 (2.69; 5.38) | |
| Allergic rhinitis symptoms | with 21 | 14.48 (10.03; 20.56) | 0.61 | 1.97 (1.73; 2.54) | 0.15 | 3.22 (2.29; 4.68) | 0.65 | 5.38 (3.59; 7.68) | 0.68 | 3.26 (2.26; 5.13) | 0.51 |
| | w/o 129 | 14.75 (11.71; 20.29) | | 2.31 (1.84; 3.11) | | 3.34 (2.52; 4.84) | | 5.38 (4.04; 7.39) | | 3.75 (2.75; 5.42) | |
| Atopic dermatitis diagnosed | with 19 | 20.88 (12.59; 33.08) | 0.19 | 2.52 (1.81; 4.67) | 0.21 | 4.09 (2.25; 7.45) | 0.15 | 7.73 (4.45; 12.25) | 0.16 | 4.68 (2.48; 8.39) | 0.30 |
| | w/o 131 | 14.60 (11.15; 19.09) | | 2.24 (1.81; 2.94) | | 3.27 (2.52; 4.48) | | 5.21 (3.85; 6.90) | | 3.69 (2.69; 5.01) | |
| Atopic dermatitis symptoms | with 14 | 21.09 (12.46; 38.06) | 0.14 | 2.39 (1.89; 4.77) | 0.31 | 4.41 (2.75; 7.86) | 0.14 | 7.79 (4.49; 14.37) | 0.12 | 5.79 (2.64; 10.51) | 0.08 |
| | w/o 136 | 14.63 (10.97; 19.14) | | 2.25 (1.79; 2.97) | | 3.28 (2.51; 4.49) | | 5.38 (3.82; 6.93) | | 3.62 (2.68; 5.01) | |

*PCBs, polychlorinated biphenyls presented in (ng/g lipids).*
*IQR, interquartile range.*
*P—p-value.*
*w/o—without.*

**TABLE 4 |** Comparison of number of children with allergic conditions, between first + second tertiles vs. third tertile of maternal lipid adjusted PCBs serum concentration.

| | Sum PCBs | | | PCB 118 | | | PCB 138 | | | PCB 153 | | | PCB 180 | | |
|---|---|---|---|---|---|---|---|---|---|---|---|---|---|---|---|
| | 1 + 2 | 3d | P | 1 + 2 | 3d | P | 1 + 2 | 3d | P | 1 + 2 | 3d | P | 1 + 2 | 3d | P |
| Asthma diagnosed | 5.9% (6) | 4.1% (2) | 1.0 | 7% (7) | 2% (1) | 0.27 | 6% (6) | 4% (2) | 0.72 | 5.9% (6) | 4.1% (2) | 1.0 | 5.9% (6) | 4.1% (2) | 1.0 |
| Asthma symptoms | 17.8% (18) | 12.2% (6) | 0.38 | 18% (18) | 12% (6) | 0.35 | 17% (17) | 14% (7) | 0.64 | 17.8% (18) | 12.2% (6) | 0.38 | 17.8% (18) | 12.2% (6) | 0.38 |
| Allergic rhinitis diagnosed | 4.0% (4) | 4.1% (4) | 1.0 | 5% (5) | 2% (1) | 0.66 | 3% (3) | 6% (3) | 0.4 | 4% (4) | 4.1% (4) | 1.0 | 4% (4) | 4.1% (4) | 1.0 |
| Allergic rhinitis symptoms | 13.9% (14) | 14.3% (7) | 0.94 | 18% (18) | 6% (3) | **0.05** | 14% (14) | 14% (7) | 1.0 | 12.9% (13) | 16.3% (8) | 0.57 | 13.9% (14) | 14.3% (7) | 0.94 |
| Atopic dermatitis diagnosed | 8.9% (9) | 20.4% (10) | **0.05** | 10% (10) | 18% (9) | 0.17 | 10% (10) | 18% (9) | 0.17 | 8.9% (9) | 20.4% (10) | **0.05** | 9.9% (10) | 18.4% (9) | 0.14 |
| Atopic dermatitis symptoms | 5.9% (6) | 16.3% (8) | **0.07** | 8% (8) | 12% (6) | 0.55 | 7% (7) | 14% (7) | 0.23 | 5.9% (6) | 16.3% (8) | **0.07** | 5.9% (6) | 16.3% (8) | **0.07** |

*Values presented as % (N).*
*PCBs, polychlorinated biphenyls.*
*P—p-value.*
*Bold: p-value toward significance.*
*1 + 2 - first and second tertiles.*
*3d—third tertile.*

**TABLE 5 |** The association between PCBs (lipid-adjusted) serum levels and asthma, allergic rhinitis and atopic dermatitis diagnosis and/or symptoms.

| | N | Sum PCBs | | PCB 118 | | PCB 138 | | PCB 153 | | PCB 180 | |
|---|---|---|---|---|---|---|---|---|---|---|---|
| | | OR crude | aOR CI 95% | OR crude | aOR CI 95% | OR crude | aOR CI 95% | OR crude | aOR CI 95% | OR crude | aOR CI 95% |
| Asthma symptoms and/or diagnosis | 26 | 0.96 (0.91; 1.01) | 0.94 (0.88; 0.99) | 0.74 (0.51; 1.08) | 0.67 (0.45; 1.01) | 0.86 (0.69; 1.07) | 0.8 (0.63; 1.02) | 0.91 (0.8; 1.04) | 0.86 (0.74; 1.01) | 0.88 (0.73; 1.06) | 0.74 (0.57; 0.97) |
| Allergic rhinitis symptoms and/or diagnosis | 22 | 0.99 (0.95; 1.03) | 0.98 (0.94; 1.03) | 0.91 (0.64; 1.21) | 0.88 (0.65; 1.2) | 0.96 (0.81; 1.13) | 0.94 (0.78; 1.12) | 0.98 (0.89; 1.07) | 0.96 (0.87; 1.07) | 0.94 (0.8; 1.1) | 0.89 (0.72; 1.1) |
| Atopic dermatitis symptoms and/or diagnosis | 21 | 1.02 (0.99; 1.04) | 1.01 (0.98; 1.04) | 1.16 (0.96; 1.4) | 1.11 (0.9; 1.36) | 1.07 (0.96; 1.2) | 1.04 (0.91; 1.18) | 1.03 (0.97; 1.09) | 1.01 (0.94; 1.08) | 1.07 (0.97; 1.18) | 1.01 (0.9; 1.14) |

*PCBs, polychlorinated biphenyls presented in (ng/g lipids).*
*aOR, adjusted odd ratio for maternal age, family member with asthma/atopic condition.*
*CI 95% - 95% confidence interval.*

The studied outcomes (asthma, allergic rhinitis and atopic dermatitis) were combined into 3 groups—children with symptoms and/or with diagnosis to increase the sample size. No association was found between exposure to Sum PCBs and the risk for asthma symptoms and/or diagnosis, crude: OR = 0.96, 95%CI: (0.91; 1.01) or adjusted to maternal age and family member with atopic condition: aOR = 0.94, 95%CI: (0.88; 0.99) (**Table 5**). No association was observed between each studied PCB congener and asthma symptoms or diagnosis. The same results were found also for other studied outcomes—allergic rhinitis and atopic dermatitis (**Table 5**).

## DISCUSSION

In this prospective birth cohort study of 150 mothers-newborns dyads, we aimed to evaluate the possible associations between background exposure to PCB congeners (118, 138, 153, and 180) and children's allergic conditions. We found that a significantly higher percentage of children with atopic dermatitis diagnosis or parent-reported symptoms of atopic dermatitis were detected in the third tertile of maternal serum levels of total PCBs, PCB 153 and PCB 180. There were no statistically significant associations between prenatal PCBs exposure and asthma or allergic rhinitis in the offspring aged 4–6 years. However, after performing the logistic regression and adjusting the analysis for maternal age and family member with atopic condition, no association was found for each of the atopic conditions—asthma, allergic rhinitis and atopic dermatitis.

The prevalence of symptoms of asthma, allergic rhinitis, and atopic dermatitis in the last 12 months in our study (16, 14, 9.3%, respectively) is comparable to those previously reported in an Israeli national study conducted using the same questionnaires from 2003 (13.8, 10.5, 8.7%) (Romano-Zelekha et al., 2007). The higher rates in our study could be attributed to the lower age in our study (4–6 vs. 12–13 years). Additionally, contrary to our study, the aforementioned study used self-report of diagnosis to define the disease and not self-report of symptoms. Data from

other industrialized countries based on Phase 3 of ISSAC studies also indicate prevalence rates of allergic rhinitis ranging around 15% (Björkstén et al., 2008).

In our study, children with atopic dermatitis diagnosis or symptoms were located in higher tertile of the studied PCBs. There was no statistically significant difference in the median maternal serum levels of PCBs in children with or without diagnosis or parent-reported symptoms of atopic dermatitis. However, the median levels of total PCBs were still much higher in groups with diagnosis or symptoms of atopic dermatitis—20.88 (12.59; 33.08) ng/g lipids vs. 14.60 (11.15; 19.09) ng/g lipids for diagnosis and 21.09 (12.46; 38.06) ng/g lipids vs. 14.63 (10.97; 19.14) ng/g lipids for symptoms of atopic dermatitis. Aside from genetic factors, the recent dramatic increase in the prevalence of atopic dermatitis in low- and middle-income countries strongly suggests that environmental factors may play an essential role in the pathogenesis of atopic dermatitis (Narla and Silverberg, 2020). The role of maternal exposure to PCBs in atopic dermatitis is unclear.

A previous retrospective study showed that reported prenatal exposure to PCBs increased the odds for eczema/hay fever [OR 3.29 (1.54–7.04)] (Parker-Lalomio et al., 2017). In mice, maternal exposure to DEHP during neonatal periods was found to accelerate atopic dermatitis-like skin lesions related to mite allergen in male offspring, possibly via T helper 2 (TH2)-dominant responses (Yanagisawa et al., 2008). Another study did not find a correlation between levels of environmental chemical contaminants in maternal serum in pregnancy and childhood rates of eczema at 5–9 years (Hansen et al., 2016). In contrast, some studies showed prenatal PCB exposures were inversely associated with a history of atopic dermatitis (Grandjean et al., 2010; Ochiai et al., 2014). A cross-sectional study conducted amongst Japanese adults found exposure to certain PCBs (dioxins) associated with a reduced risk of atopic dermatitis (Nakamoto et al., 2013).

Similar to atopic dermatitis, studies assessing the role of maternal exposure to PCBs in wheezing/asthma and allergic rhinitis show conflicting results (Björkstén et al., 2008; Grandjean et al., 2010; Smit et al., 2015; Parker-Lalomio et al., 2017). It is possible that due to multiple confounders, different PCBs examined, different methods and timing of testing, and relatively small cohorts, results in various studies are conflicting.

Atopic dermatitis is considered the first manifestation of the atopic march, and therefore relatively young age of questioning in our study could be related to the underdiagnosis of children who will later present with other atopic phenomena (Yang et al., 2020).

The birth weight and birth percentile of the newborns included in the analysis were higher as compared to the refusal group (**Table 1**). This is a potentially selection bias. However, the birthweight was within the normal range in both groups (appropriate for gestational age). Furthermore, the refusal group included a small number of newborns ($N$ = 20), as compared to the study group ($N$ = 150).

Our study has several strengths. It is a prospective birth cohort study with a high response rate in the study's second phase. Analysis based on patient-reported symptoms could very well be more representative of actual prevalence, as the underdiagnosis of atopic conditions is reported in resource-rich and developing countries (Brożek et al., 2013; Esteban et al., 2014; Jacobs et al., 2014; Krajewska-Wojtys et al., 2016; Aaron et al., 2018; Yang et al., 2019). PCBs 118, 138, 153, 180 are among the most frequently detected congeners in white adipose tissue (Müllerová and Kopecký, 2007), and those specific PCBs were tested in our cohort. As the information collected relies on self-reporting, it is subject to recall bias. To minimize this bias, we considered information from the last year before the data collection date to include patients in the atopic groups, which could have resulted in over including some children who had acute rather than chronic conditions in the atopic groups. On the other hand, children with acute conditions, common in younger children, whose symptoms later did not persist were not included in the atopic groups, strengthening the analysis.

## CONCLUSION

This study demonstrated that children with atopic dermatitis diagnosis or symptoms are located at higher tertile of maternal PCBs level. No similar relationship was demonstrated for asthma or allergic rhinitis. The logistic regression adjusted for maternal age and family member with atopic condition, found no association for each of the atopic conditions—asthma, allergic rhinitis and atopic dermatitis. Additional multi-participant studies, with longer, spanning into later pediatric age follow up are needed to examine the possible effects of other environmental pollutants on the prevalence of atopic phenomena. Our research joins a series of previous studies that attempt to shed light on environmental exposures in utero as influencing factors for atopic conditions in children; as in previous studies, the results reflect the complexity of the pathophysiology of these phenomena.

## DATA AVAILABILITY STATEMENT

The raw data supporting the conclusion of this article will be made available by the authors, without undue reservation.

## ETHICS STATEMENT

The studies involving human participants were reviewed and approved by the Shamir (Assaf Harofeh) IRB. Written informed consent to participate in this study was provided by the participant or participants' legal guardian.

## AUTHOR CONTRIBUTIONS

The Author Contributions statement describes the contributions of individual authors referred to by their

initials and, in doing so, all authors agree to be accountable for the content of the work: substantial contributions to the conception or design of the work; or the acquisition, analysis or interpretation of data for the work—MyB, HF-H, EK, AB, RK, AL, RM, AO, JT, MsB, MM, PF-L, AH, MlB, MtB, IG, IM, and UH. Drafting the work or revising it critically for important intellectual content—MyB, HF-H, DM, RL, PFL, MtB, IM, and UH. Agree to be accountable for all aspects of the work in ensuring that questions related to the accuracy or integrity of any part of the work are appropriately investigated and resolved—MyB, MtB, and UH.

## FUNDING

This work was supported by the Environment and Health Fund (EHF)—Grant No. RGA1202.

## SUPPLEMENTARY MATERIAL

The Supplementary Material for this article can be found online at: https://www.frontiersin.org/articles/10.3389/fphar.2022.802974/full#supplementary-material

## REFERENCES


Aaron, S. D., Boulet, L. P., Reddel, H. K., and Gershon, A. S. (2018). Underdiagnosis and Overdiagnosis of Asthma. *Am. J. Respir. Crit. Care Med.* 198 (8), 1012–1020. doi:10.1164/rccm.201804-0682CI

Agency for Toxic Substances and Disease Registry (2000). *Toxicological Profile for Polychlorinated Biphenyls (PCBS) - Update*. Atlanta, Georgia.

Asher, M. I., Keil, U., Anderson, H. R., Beasley, R., Crane, J., Martinez, F., et al. (1995). International Study of Asthma and Allergies in Childhood (ISAAC): Rationale and Methods. *Eur. Respir. J.* 8 (3), 483–491. doi:10.1183/09031936.95.08030483

Belles-Isles, M., Ayotte, P., Dewailly, E., Weber, J. P., and Roy, R. (2002). Cord Blood Lymphocyte Functions in Newborns from A Remote Maritime Population Exposed to Organochlorines and Methylmercury. *J. Toxicol. Environ. Health A.* 65 (2), 165–182. doi:10.1080/152873902753396794

Bergman, Å., Heindel, J., Jobling, S., Kidd, K., and Zoeller, R. T. (2012). State-of-the-science of Endocrine Disrupting Chemicals. *Toxicol. Lett.* 211, S3.

Bergonzi, R., De Palma, G., Tomasi, C., Ricossa, M. C., and Apostoli, P. (2009). Evaluation of Different Methods to Determine Total Serum Lipids for Normalization of Circulating Organochlorine Compounds. *Int. Arch. Occup. Environ. Health* 82 (10), 1241–1247. doi:10.1007/s00420-009-0426-5

Berlin, M., Barchel, D., Brik, A., Kohn, E., Livne, A., Keidar, R., et al. (2021). Maternal and Newborn Thyroid Hormone, and the Association with Polychlorinated Biphenyls (PCBs) Burden: The EHF (Environmental Health Fund) Birth Cohort. *Front. Pediatr.* 9, 705395. doi:10.3389/fped.2021.705395

Bernert, J. T., Turner, W. E., Patterson, D. G., and Needham, L. L. (2007). Calculation of Serum "Total Lipid" Concentrations for the Adjustment of Persistent Organohalogen Toxicant Measurements in Human Samples. *Chemosphere* 68 (5), 824–831. doi:10.1016/j.chemosphere.2007.02.043

Björkstén, B., Clayton, T., Ellwood, P., Stewart, A., and Strachan, D. (2008). Worldwide Time Trends for Symptoms of Rhinitis and Conjunctivitis: Phase III of the International Study of Asthma and Allergies in Childhood. *Pediatr. Allergy Immunol.* 19 (2), 110–124. doi:10.1111/j.1399-3038.2007.00601.x

Bonefeld-Jørgensen, E. C., Andersen, H. R., Rasmussen, T. H., Vinggaard, A. M., Bonefeld-Jørgensen, E. C., Andersen, H. R., et al. (2001). Effect of Highly Bioaccumulated Polychlorinated Biphenyl Congeners on Estrogen and Androgen Receptor Activity. *Toxicology* 158 (3), 141–153. doi:10.1016/s0300-483x(00)00368-1

Brożek, G. M., Farnik, M., Lawson, J., and Zejda, J. E. (2013). Underdiagnosis of Childhood Asthma: A Comparison of Survey Estimates to Clinical Evaluation. *Int. J. Occup. Med. Environ. Health* 26 (6), 900–909. doi:10.2478/s13382-013-0162-7

Clark, N. A., Demers, P. A., Karr, C. J., Koehoorn, M., Lencar, C., Tamburic, L., et al. (2010). Effect of Early Life Exposure to Air Pollution on Development of Childhood Asthma. *Environ. Health Perspect.* 118 (2), 284–290. doi:10.1289/ehp.0900916

Dallaire, F., Dewailly, E., Muckle, G., Vézina, C., Jacobson, S. W., Jacobson, J. L., et al. (2004). Acute Infections and Environmental Exposure to Organochlorines in Inuit Infants from Nunavik. *Environ. Health Perspect.* 112 (14), 1359–1365. doi:10.1289/ehp.7255

Di Renzo, G. C., Conry, J. A., Blake, J., Defrancesco, M. S., Denicola, N., Martin, J. N., et al. (2015). International Federation of Gynecology and Obstetrics Opinion on Reproductive Health Impacts of Exposure to Toxic Environmental Chemicals. *Int. J. Gynaecol. Obstet.* 131 (3), 219–225. doi:10.1016/j.ijgo.2015.09.002

Dollberg, S., Haklai, Z., Mimouni, F. B., Gorfein, I., and Gordon, E. S. (2005). Birthweight Standards in the Live-Born Population in Israel. *Isr. Med. Assoc. J.* 7, 311–314.

Domingo, J. L. (2012). Polybrominated Diphenyl Ethers in Food and Human Dietary Exposure: A Review of the Recent Scientific Literature. *Food Chem. Toxicol.* 50, 238–249. doi:10.1016/j.fct.2011.11.004

Esteban, C. A., Klein, R. B., Kopel, S. J., McQuaid, E. L., Fritz, G. K., Seifer, R., et al. (2014). Underdiagnosed and Undertreated Allergic Rhinitis in Urban School-Aged Children with Asthma. *Pediatr. Allergy Immunol. Pulmonol* 27 (2), 75–81. doi:10.1089/ped.2014.0344

Faroon, O., and Ruiz, P. (2015). Polychlorinated Biphenyls: New Evidence from the Last Decade. *Toxicol. Ind. Health* 32 (11), 1825–1847. doi:10.1177/0748233715587849

Fernández-González, R., Yebra-Pimentel, I., Martínez-Carballo, E., and Simal-Gándara, J. (2015). A Critical Review about Human Exposure to Polychlorinated Dibenzo-P-Dioxins (PCDDs), Polychlorinated Dibenzofurans (PCDFs) and Polychlorinated Biphenyls (PCBs) through Foods. *Crit. Rev. Food Sci. Nutr.* 55 (11), 1590–1617. doi:10.1080/10408398.2012.710279

Freels, S., Chary, L. K., Turyk, M., Piorkowski, J., Mallin, K., Dimos, J., et al. (2007). Congener Profiles of Occupational PCB Exposure versus PCB Exposure from Fish Consumption. *Chemosphere* 69 (3), 435–443. doi:10.1016/j.chemosphere.2007.04.087

Grandjean, P., Poulsen, L. K., Heilmann, C., Steuerwald, U., and Weihe, P. (2010). Allergy and Sensitization during Childhood Associated with Prenatal and Lactational Exposure to marine Pollutants. *Environ. Health Perspect.* 118 (10), 1429–1433. doi:10.1289/ehp.1002289

Greenberg, N., Carel, R., and Portnov, B. A. (2015). Air Pollution and Respiratory Morbidity in Israel: A Review of Accumulated Empiric Evidence. *Isr. Med. Assoc. J.* 17 (7), 445–450.

Greenberg, N., Carel, R. S., Dubnov, J., Derazne, E., and Portnov, B. A. (2019). Prevalence of Asthma Among Young Men Residing in Urban Areas with Different Sources of Air Pollution. *Isr. Med. Assoc. J.* 21 (12), 785–789.

Hansen, S., Strøm, M., Olsen, S. F., Dahl, R., Hoffmann, H. J., Granström, C., et al. (2016). Prenatal Exposure to Persistent Organic Pollutants and Offspring Allergic Sensitization and Lung Function at 20 Years of Age. *Clin. Exp. Allergy* 46 (2), 329–336. doi:10.1111/cea.12631

Hansen, S., Strøm, M., Olsen, S. F., Maslova, E., Rantakokko, P., Kiviranta, H., et al. (2014). Maternal Concentrations of Persistent Organochlorine Pollutants and the Risk of Asthma in Offspring: Results from a Prospective Cohort with 20 Years of Follow-Up. *Environ. Health Perspect.* 122 (1), 93–99. doi:10.1289/ehp.1206397

Heilmann, C., Grandjean, P., Weihe, P., Nielsen, F., and Budtz-Jørgensen, E. (2006). Reduced Antibody Responses to Vaccinations in Children Exposed to Polychlorinated Biphenyls. *Plos Med.* 3 (8), e311. doi:10.1371/journal.pmed.0030311

Hertz-Picciotto, I., Park, H.-Y., Dostal, M., Kocan, A., Trnovec, T., and Sram, R. (2008). Prenatal Exposures to Persistent and Non-persistent Organic Compounds and Effects on Immune System Development. *Basic Clin. Pharmacol. Toxicol.* 102, 146–154. doi:10.1111/j.1742-7843.2007.00190.x

Hidaka, T., Ogawa, E., Kobayashi, E. H., Suzuki, T., Funayama, R., Nagashima, T., et al. (2017). The Aryl Hydrocarbon Receptor AhR Links Atopic Dermatitis and Air Pollution via Induction of the Neurotrophic Factor Artemin. *Nat. Immunol.* 18 (1), 64–73. doi:10.1038/ni.3614

Jacobs, T. S., Forno, E., Brehm, J. M., Acosta-Pérez, E., Han, Y. Y., Blatter, J., et al. (2014). Underdiagnosis of Allergic Rhinitis in Underserved Children. *J. Allergy Clin. Immunol.* 134 (3), 737–e6. doi:10.1016/j.jaci.2014.03.028

Jøhnk, C., Høst, A., Husby, S., Schoeters, G., Timmermann, C. A. G., Kyhl, H. B., et al. (2020). Maternal Phthalate Exposure and Asthma, Rhinitis and Eczema in

552 Children Aged 5 years; a Prospective Cohort Study. *Environ. Heal* 19 (1), 1–10. doi:10.1186/s12940-020-00586-x

Kahr, N., Naeser, V., Stensballe, L. G., Kyvik, K. O., Skytthe, A., Backer, V., et al. (2015). Gene-environment Interaction in Atopic Diseases: a Population-Based Twin Study of Early-Life Exposures. *Clin. Respir. J.* 9 (1), 79–86. doi:10.1111/crj.12110

Krajewska-Wojtys, A., Jarzab, J., Gawlik, R., and Bozek, A. (2016). Local Allergic Rhinitis to Pollens Is Underdiagnosed in Young Patients. *Am. J. Rhinol Allergy* 30 (6), 198–201. doi:10.2500/ajra.2016.30.4369

Liptay, S., Bauer, C. P., Grübl, A., Franz, R., and Emmrich, P. (1992). Natural History of Atopic Disease in Early Childhood: Is Cord Blood IgE a Prognostic Factor? A Preliminary Report. *Clin. Pediatr. (Phila)* 31 (4), 241–246. doi:10.1177/000992289203100411

Mamane, A., Raherison, C., Tessier, J. F., Baldi, I., and Bouvier, G. (2015). Environmental Exposure to Pesticides and Respiratory Health. *Eur. Respir. Rev.* 24 (137), 462–473. doi:10.1183/16000617.00006114

Masoli, M., Fabian, D., Holt, S., and Beasley, R. (2004). The Global burden of Asthma: Executive Summary of the GINA Dissemination Committee Report. *Allergy* 59 (5), 469–478. doi:10.1111/j.1398-9995.2004.00526.x

Morales, E., and Duffy, D. (2019). Genetics and Gene-Environment Interactions in Childhood and Adult Onset Asthma. *Front. Pediatr.* 7, 499. doi:10.3389/fped.2019.00499

Müllerová, D., and Kopecký, J. (2007). White Adipose Tissue: Storage and Effector Site for Environmental Pollutants. *Physiol. Res.* 56, 375–381. doi:10.33549/physiolres.931022

Nakamoto, M., Arisawa, K., Uemura, H., Katsuura, S., Takami, H., Sawachika, F., et al. (2013). Association between Blood Levels of PCDDs/PCDFs/dioxin-like PCBs and History of Allergic and Other Diseases in the Japanese Population. *Int. Arch. Occup. Environ. Health* 86 (8), 849–859. doi:10.1007/s00420-012-0819-8

Narla, S., and Silverberg, J. I. (2020). The Role of Environmental Exposures in Atopic Dermatitis. *Curr. Allergy Asthma Rep.* 20 (12), 74. doi:10.1007/s11882-020-00971-z

Ochiai, S., Shimojo, N., Yuka, I., Watanabe, M., Matsuno, Y., Suzuki, S., et al. (2014). A Pilot Study for Foetal Exposure to Multiple Persistent Organic Pollutants and the Development of Infant Atopic Dermatitis in Modern Japanese Society. *Chemosphere* 94, 48–52. doi:10.1016/j.chemosphere.2013.09.009

Park, W. H., Kang, S., Lee, H. K., Salihovic, S., Bavel, B. V., Lind, P. M., et al. (2017). Relationships between Serum-Induced AhR Bioactivity or Mitochondrial Inhibition and Circulating Polychlorinated Biphenyls (PCBs). *Sci. Rep.* 7 (1), 9383. doi:10.1038/s41598-017-09774-1

Parker-Lalomio, M., McCann, K., Piorkowski, J., Freels, S., and Persky, V. W. (2017). Prenatal Exposure to Polychlorinated Biphenyls and Asthma, Eczema/hay Fever, and Frequent Ear Infections. *J. Asthma* 55 (10), 1105–1115. doi:10.1080/02770903.2017.1396470

Pope, C. A., and Dockery, D. W. (2006). Health Effects of Fine Particulate Air Pollution: Lines that Connect. *J. Air Waste Manag. Assoc.* 56 (6), 709–742. doi:10.1080/10473289.2006.10464485

Portnov, B. A., Reiser, B., Karkabi, K., Cohen-Kastel, O., and Dubnov, J. (2012). High Prevalence of Childhood Asthma in Northern Israel Is Linked to Air Pollution by Particulate Matter: Evidence from GIS Analysis and Bayesian Model Averaging. *Int. J. Environ. Health Res.* 22 (3), 249–269. doi:10.1080/09603123.2011.634387

Raherison, C., Baldi, I., Pouquet, M., Berteaud, E., Moesch, C., Bouvier, G., et al. (2019). Pesticides Exposure by Air in Vineyard Rural Area and Respiratory Health in Children: A Pilot Study. *Environ. Res.* 169, 189–195. doi:10.1016/j.envres.2018.11.002

Reichrtová, E., Ciznár, P., Prachar, V., Palkovicová, L., and Veningerová, M. (1999). Cord Serum Immunoglobulin E Related to the Environmental Contamination of Human Placentas with Organochlorine Compounds. *Environ. Health Perspect.* 107 (11), 895–899.

Romano-Zelekha, O., Graif, Y., Garty, B. Z., Livne, I., Green, M. S., and Shohat, T. (2007). Trends in the Prevalence of Asthma Symptoms and Allergic Diseases in Israeli Adolescents: Results from a National Survey 2003 and Comparison with 1997. *J. Asthma* 44 (5), 365–369. doi:10.1080/02770900701363983

Schisterman, E. F., Whitcomb, B. W., Louis, G. M., and Louis, T. A. (2005). Lipid Adjustment in the Analysis of Environmental Contaminants and Human Health Risks. *Environ. Health Perspect.* 113 (7), 853–857. doi:10.1289/ehp.7640

Sengler, C., Lau, S., Wahn, U., and Nickel, R. (2002). Interactions between Genes and Environmental Factors in Asthma and Atopy: New Developments. *Respir. Res.* 3 (1), 7. doi:10.1186/rr179

Sharpe, R. M., and Irvine, D. S. (2004). How strong Is the Evidence of a Link between Environmental Chemicals and Adverse Effects on Human Reproductive Health? *BMJ* 328 (7437), 447–451. doi:10.1136/bmj.328.7437.447

Sheinberg, R., Siegel, E. L., Keidar, R., Mandel, D., Lubetzky, R., Kohn, E., et al. (2020). Associations between Intrauterine Exposure to Polychlorinated Biphenyls on Neonatal Ano-Genital Distance. *Reprod. Toxicol.* 96, 67–75. doi:10.1016/j.reprotox.2020.06.005

Sly, P. D., and Flack, F. (2008). Susceptibility of Children to Environmental Pollutants. *Ann. N. Y Acad. Sci.* 1140, 163–183. doi:10.1196/annals.1454.017

Smit, L. A., Lenters, V., Høyer, B. B., Lindh, C. H., Pedersen, H. S., Liermontova, I., et al. (2015). Prenatal Exposure to Environmental Chemical Contaminants and Asthma and Eczema in School-Age Children. *Allergy* 70 (6), 653–660. doi:10.1111/all.12605

Stølevik, S. B., Nygaard, U. C., Namork, E., Haugen, M., Meltzer, H. M., Alexander, J., et al. (2013). Prenatal Exposure to Polychlorinated Biphenyls and Dioxins from the Maternal Diet May Be Associated with Immunosuppressive Effects that Persist into Early Childhood. *Food Chem. Toxicol.* 51 (1), 165–172. doi:10.1016/j.fct.2012.09.027

Teysseire, R., Brochard, P., Sentilhes, L., and Delva, F. (2019). Identification and Prioritization of Environmental Reproductive Hazards: A First Step in Establishing Environmental Perinatal Care. *Int. J. Environ. Res. Public Health* 16 (3), 366. doi:10.3390/ijerph16030366

The World Medical Association (2018). WMA Declaration of Helsinki – Ethical Principles for Medical Research Involving Human Subjects. Available at: https://www.wma.net/policies-post/wma-declaration-of-helsinki-ethical-principles-for-medical-research-involving-human-subjects/ (Accessed September 20, 2020).

United Nations Environment Programme (UNEP) (2018). *Stockholm Convention on Persistent Organic Pollutants (POPs)*. Secr Stock Conv. Revised in 2018.

Weisglas-Kuperus, N., Patandin, S., Berbers, G. A., Sas, T. C., Mulder, P. G., Sauer, P. J., et al. (2000). Immunologic Effects of Background Exposure to Polychlorinated Biphenyls and Dioxins in Dutch Preschool Children. *Environ. Health Perspect.* 108 (12), 1203–1207. doi:10.1289/ehp.001081203

Who Regional Office for Europe (2013). *Review of Evidence on Health Aspects of Air Pollution – REVIHAAP Project: Final Technical Report*. World Health Organization.

Yanagisawa, R., Takano, H., Inoue, K., Koike, E., Sadakane, K., and Ichinose, T. (2008). Effects of Maternal Exposure to Di-(2-ethylhexyl) Phthalate during Fetal And/or Neonatal Periods on Atopic Dermatitis in Male Offspring. *Environ. Health Perspect.* 116 (9), 1136–1141. doi:10.1289/ehp.11191

Yang, G., Han, Y. Y., Forno, E., Acosta-Pérez, E., Colón-Semidey, A., Alvarez, M., et al. (2019). Under-diagnosis of Atopic Dermatitis in Puerto Rican Children. *World Allergy Organ. J.* 12 (1), 100003. doi:10.1016/j.waojou.2018.11.003

Yang, L., Fu, J., and Zhou, Y. (2020). Research Progress in Atopic March. *Front. Immunol.* 11, 1907. doi:10.3389/fimmu.2020.01907

**Conflict of Interest:** The authors declare that the research was conducted in the absence of any commercial or financial relationships that could be construed as a potential conflict of interest.

**Publisher's Note:** All claims expressed in this article are solely those of the authors and do not necessarily represent those of their affiliated organizations, or those of the publisher, the editors and the reviewers. Any product that may be evaluated in this article, or claim that may be made by its manufacturer, is not guaranteed or endorsed by the publisher.

frontiers | Frontiers in Pharmacology

ORIGINAL RESEARCH
published: 05 May 2022
doi: 10.3389/fphar.2022.818952

# Serum Metabonomics Reveals Key Metabolites in Different Types of Childhood Short Stature

*Guoyou Chen[1†], Jinming Wang[2†], Yisi Jing[3], Chunxiang Li[3], Wenyue Zhang[3], Shuang Yang[3], Ye Song[3], Xin Wang[3], Jincheng Liu[1], Dejun Yu[3]* and Zhichun Xu[3]**

[1]Daqing Campus, Harbin Medical University, Daqing, China, [2]Gynecology Department, Dating Oil Field General Hospital, Daqing, China, [3]Fifth Affiliated Hospital, Harbin Medical University, Daqing, China

Nowadays, short stature (SS) in childhood is a common condition encountered by pediatricians, with an increase in not just a few families. Various studies related to the variations in key metabolites and their biological mechanisms that lead to SS have increased our understanding of the pathophysiology of the disease. However, little is known about the role of metabolite variation in different types of childhood SS that influence these biological processes and whether the understanding of the key metabolites from different types of childhood SS would predict the disease progression better. We performed a systematic investigation using the metabonomics method and studied the correlation between the three groups, namely, the control, idiopathic short stature (ISS), and short stature due to growth hormone deficiency (GHD). We observed that three pathways (viz., purine metabolism, sphingolipid signaling pathway, and sphingolipid metabolism) were significantly enriched in childhood SS. Moreover, we reported that two short peptides (Thr Val Leu Thr Ser and Trp Ile Lys) might play a significant role in childhood SS. Various metabolites in different pathways including 9,10-DiHOME, 12-HETE, 12(13)-EpOME, arachidonic acid methyl ester, glycerophospho-N-arachidonoyl ethanolamine, curvulinic acid (2-acetyl-3,5-dihydroxyphenyl acetic acid), nonanoic acid, and N'-(2,4-dimethylphenyl)-N-methylformamidine in human serum were compared between 60 children diagnosed with SS and 30 normal-height children. More investigations in this area may provide insights and enhance the personalized treatment approaches in clinical practice for SS by elucidating pathophysiology mechanisms of experimental verification.

**Keywords: different types, human serum, metabonomics, key metabolites, childhood short stature (SS)**

OPEN ACCESS

***Edited by:***
*Catherine M. T. Sherwin, Wright State University, United States*

***Reviewed by:***
*Ian James Martins, University of Western Australia, Australia*
*Kathleen Job, The University of Utah, United States*

****Correspondence:***
*Dejun Yu*
*yudejun100@126.com*
*Zhichun Xu*
*xzc286286@126.com*

*†These authors have contributed equally to this work and share first authorship*

***Specialty section:***
*This article was submitted to Obstetric and Pediatric Pharmacology, a section of the journal Frontiers in Pharmacology*

***Received:*** *20 November 2021*
***Accepted:*** *21 March 2022*
***Published:*** *05 May 2022*

***Citation:***
*Chen G, Wang J, Jing Y, Li C, Zhang W, Yang S, Song Y, Wang X, Liu J, Yu D and Xu Z (2022) Serum Metabonomics Reveals Key Metabolites in Different Types of Childhood Short Stature. Front. Pharmacol. 13:818952. doi: 10.3389/fphar.2022.818952*

## INTRODUCTION

In clinical practice, the therapy of childhood short stature (SS) is often confronted by pediatric endocrinologists and is also an intractable problem (Rogol and Hayden, 2014; Smuel and Yeshayahu, 2017; Ma et al., 2019). Almost half of the pediatric visitors come to consult about short stature (Murray et al., 2018). Childhood short stature, which has various causes, can be categorized under normal and pathological conditions (Ma et al., 2019). The normal condition includes familial short stature and constitutional delay of growth. However, various pathological

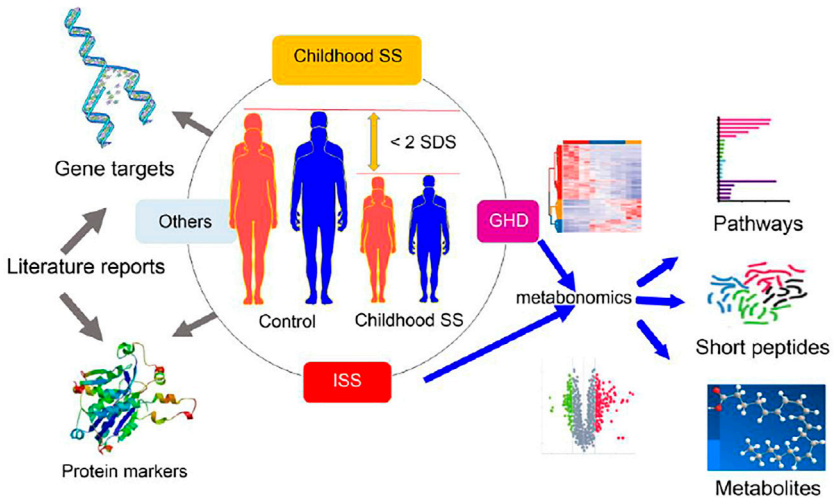


**GRAPHICAL ABSTRACT |** SS, short stature; SDS, standard deviation scores; Control, normal height, *n*=30; ISS, idiopathic short stature *n*=31; GHD, short stature caused by growth hormone deficiency, *n*=29.

factors lead to SS, including Turner syndrome, hypothyroidism, chronic diseases, growth hormone deficiency, and idiopathic short stature (Allen and Cuttler, 2013). Short stature during childhood is easily overlooked and embarrassing, which makes an individual vulnerable to psychological disorders, such as low self-esteem, loneliness, academic and job difficulties, and social immaturity (Kim and Park, 2009). Regrettably, many children with SS remain affected by short stature as they grow old (Ma et al., 2019). For example, the probability of developing preterm birth or stillbirth for pregnant women with SS was seen to be relatively higher (Derraik et al., 2016; Ma et al., 2019). Childhood short stature may be more susceptible to chronic diseases such as obesity and insulin resistance. The inactivation of sirtuin 1 (SIRT1) is connected to the progression of insulin resistance associated with SS. Diabetes in people with short stature may be induced later in life with relevance to sirtuin 1 repression (Martins, 2016; Martins, 2017). Therefore, it becomes necessary and urgent to identify critical targets and mechanisms for childhood short stature.

It has been observed that BMI and growth hormone (GH) were negatively correlated with childhood short stature (Bosy-Westphal et al., 2009; Zhao et al., 2021). SIRT1 is a nicotinamide adenine dinucleotide (NAD)-dependent histone deacetylase that is activated in response to calorie restriction (CR) (Yamamoto and Takahashi, 2018). Further investigation between sirtuins, metabolism, and age-associated diseases has implicated the essential role of activation of SIRT1 (Satoh et al., 2011). SIRT1 regulated the adaptive response of the GH–insulin-like growth factor 1 (IGF-1) axis under particular conditions in the liver (Yamamoto et al., 2013). Therefore, the role of SIRT1 activators may be of critical importance in molecular metabolic processes and the treatment of childhood short stature.

Recent studies have identified some possible protein markers in childhood short stature: bone alkaline phosphatase, collagen markers, apolipoprotein (Apo) A-II, Apo C-I, Apo A-II, serum amyloid A4 (SAA4), and transthyretin (TTR) (Crofton et al., 1996; Hellgren et al., 2008; Decker et al., 2013). The most common cause of

**TABLE 1 |** Personal basic information.

| | Control | ISS | GHD | *P* (ISS *vs.* control) | *P* (GHD *vs.* control) | *P* (ISS *vs.* GHD) |
|---|---|---|---|---|---|---|
| Number | 30 | 31 | 29 | | | |
| Gender | 16 boys | 18 boys | 20 boys | | | |
| | 14 girls | 13 girls | 9 girls | | | |
| Age (years) | 8.5 ± 1.3 | 9.2 ± 2.5 | 7.9 ± 3.1 | 0.225 | 0.098 | 0.12 |
| Height (cm) | 133.4 ± 7.7 | 119.7 ± 13.0 | 113 ± 15.1 | <0.001 | <0.001 | 0.069 |
| Body weight (kg) | 29.5 ± 4.5 | 30.9 ± 12.5 | 28.9 ± 17.2 | 0.572 | 0.852 | 0.609 |
| BMI (kg/m2) | 16.5 ± 0.9 | 21 ± 5.9 | 20.9 ± 6.7 | <0.001 | <0.001 | 0.978 |

*Control, normal height;* n = *30; ISS, idiopathic short stature,* n = *31; GHD, short stature caused by growth hormone deficiency,* n = *29; age (years), height (cm), body weight (kg), BMI (kg/m2): mean ± SD, two-tailed* t *test.*

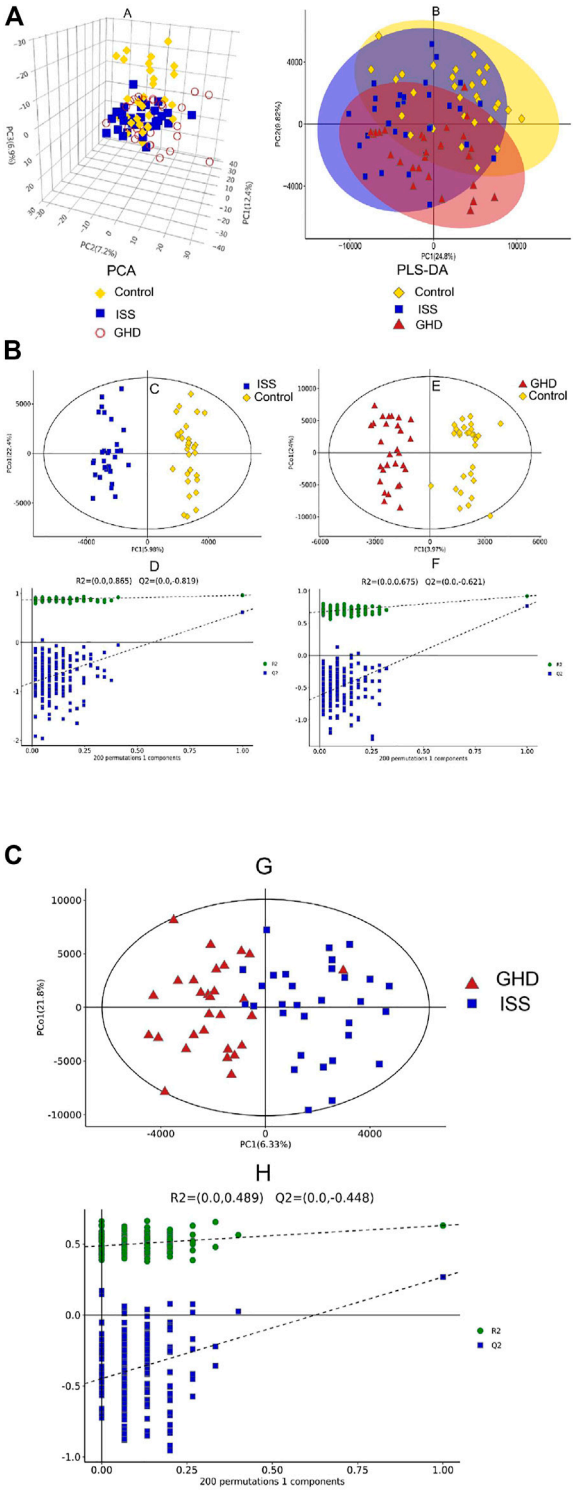


**FIGURE 1 |** Metabolic profiling analysis in different types of childhood short stature. **(A)** Score plot of the samples using the 3D-PCA model. **(B)** Score plot of the samples using PLS-DA model. Control, normal height, $n$ = 30; ISS, idiopathic short stature, $n$ = 31; GHD, short stature of growth hormone deficiency, $n$ = 29. **(C)** OPLS-DA between control group and ISS group. **(D)** Investigate the quality of the OPLS-DA model (control *vs*. ISS) by RPT (response permutation testing). **(E)** OPLS-DA between GHD group and (*Continued*)

**FIGURE 1 |** control group. **(F)** Investigate the quality of the OPLS-DA model (GHD *vs*. control) by RPT (response permutation testing). Control, normal height, $n$ = 30; ISS, idiopathic short stature, $n$ = 31; GHD, short stature of growth hormone deficiency, $n$ = 29. **(G)** OPLS-DA between ISS group and GHD group. **(H)** Investigate the quality of the OPLS-DA model (ISS *vs*. GHD) by RPT (response permutation testing). Control, normal height, $n$ = 30; ISS, idiopathic short stature, $n$ = 31; GHD, short stature of growth hormone deficiency, $n$ = 29.

monogenic short stature is the deficiency of the short-stature homeobox-containing (SHOX) gene (Marchini et al., 2016; Ponomarenko et al., 2020). A study revealed newer mechanistic insights that identified c.1675G > A mutation in receptor tyrosine kinase-like orphan receptor 2 (ROR2) in patients with short stature (Gui et al., 2021). To date, key molecular mechanisms underlying stunted growth and childhood short stature remain equivocal. Meanwhile, a number of children are troubled with SS; it is believed that the knowledge of crucial metabolites will help in rapid diagnosis. Moreover, physiological and pathological mechanisms are also growing significantly and are reliable. Metabonomics is a powerful biological tool commonly used in disease phenotypic studies, which plays a vital role in several aspects such as biomarker discovery, the origin and development of a disease, and the personalized treatment (Nicholson et al., 2005; Huang et al., 2013; Wishart, 2016).

In our study, the serum metabolic profiling of 60 children with SS and 30 normal-height children was investigated using UHPLC-Q-TOF-MS. We explored 10 significant metabolites that are found in human serum in the different types of childhood SS groups (ISS and GHD) compared to the control children group. They were short peptides (Thr Val Leu Thr Ser and Trp Ile Lys and), 9,10-DiHOME, 12-HETE, 12(13)-EpOME, arachidonic acid methyl ester, glycerophospho-N-arachidonoyl ethanolamine, curvulinic acid (2-acetyl-3,5-dihydroxyphenyl acetic acid), nonanoic acid, and N'-(2,4-dimethylphenyl)-N-methylformamidine. These metabolites regulate various pathways, including arachidonic acid metabolism, short peptides metabolism, purine metabolism, sphingolipid signaling pathway, and sphingolipid metabolism in children's body. Our results explore new therapeutic target metabolites based on metabonomics analysis. The key metabolites discovered will be beneficial in rapid clinical diagnosis and individualized treatment of patients with different types of childhood SS.

## MATERIALS AND METHODS

### Sample Collection of Children With Short Stature

All patients were recruited from the Fifth Affiliated Hospital of Harbin Medical University. The Ethics Committee approved the study of the Fifth Affiliated Hospital of Harbin Medical University (KY2018003). In addition, the study to determine

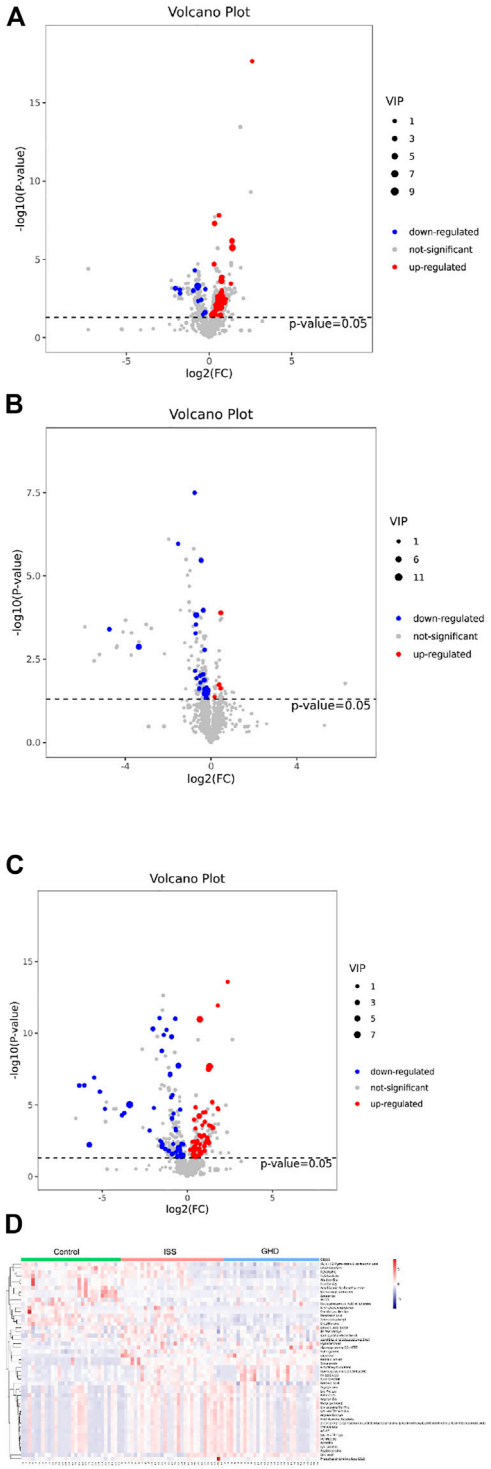


**FIGURE 2 |** Differential metabolites demonstrated by volcano plot and heat map. **(A–C)** represent the metabolites that are downregulated, not significant, or upregulated in different types of childhood short stature. The abscissa is $log_2$ (*FC*), the left ordinate is $-\log_{10}$ (*p – value*), and the right ordinate is VIP (variable important in projection). **(A)** It presents volcano plot ISS *vs*. control. **(B)** It presents volcano plot ISS *vs*. GHD. **(C)** It presents volcano plot GHD *vs*. control. **(D)** It presents a heat map among ISS, GHD, and control. Control, normal height, *n* = 30; ISS, idiopathic short stature, *n* = 31, GHD, short stature of growth hormone deficiency, *n* = 29.

the childhood short stature was diagnosed according to the 2015 edition of Chinese guidelines for childhood short stature prevention and treatment. On the basis of the cause of SS, the childhood short stature groups were strictly divided into two. The two groups that are defined as ISS (31 SSs) and GHD (29 SSs) comprise the short stature children due to idiopathy or the deficiency of growth hormone, respectively. The controls (30 children) were from physical examination screening. Moreover, the serum for non-targeted metabonomics analysis was collected from 60 SS children and 30 controls from June 2018 to September 2019. Sample information is summed up in **Table 1**.

## Non-Targeted Metabonomics Analysis of SSs

The chromatographic separation was performed by ultrahigh-pressure liquid chromatography (UHPLC) (Agilent 1290, United States). For purification, the chromatographic column used was ACQUITY UPLC HSS T3 1.8 μm 2.1 × 100 mm (Waters). The mobile phase included 0.1% formic acid in water (part A) and 0.1% formic acid in acetonitrile (part B) (Zhao et al., 2014). The gradient elution was 5% B kept for 1 min, changed linearly to 10% B within 1 min, then changed linearly to 95% B within 12 min, held for 2 min, finally changed linearly to 5% B within 1 min, and held for 3 min. The analytical column and autosampler temperatures were 35 and 4°C, respectively. The sample volume was 5 μL for each run. The column eluent was directly analyzed from the MS system (Zhao et al., 2014).

In total, 200 μL of serum with four volumes of methanol/acetonitrile (1:1, v/v) was extracted. All the samples were shaken for 30 s and subjected to ultrasound for 10 min. Next, the mixture was incubated at −20°C for 2 h to facilitate the precipitation of protein. The serum supernatant was collected after 15 min of centrifugation at 13,000 *g* and dried under vacuum and 4°C and centrifuged before the MS test. The aliquots were reconstituted in 200 μL of acetonitrile/water (1:1) and were shaken for 30 s. Then each sample supernatant after 15-min centrifugation at 13,000 *g* was collected at a volume of 150 μL and analyzed by a UHPLC system (Agilent 1290, United States) coupled with a Q-TOF system (Agilent 6545, United States). The remaining sample supernatants were mixed to make many quality control (QC) samples. The QC samples were carried out after every 15 serum samples.

Data were obtained with auto MS/MS mode from m/z 50-1100. Collision energies for collision-induced dissociation were 20 and 40 V. MS parameters were set as follows: ion source dry gas temperature was at 320°C, $N_2$ gas flow was 8 L/min, sheath gas temperature was 350°C, sheath gas flow was 12 L/min, and ion spray voltage was 4000 V (positive ion) and 3500 V (negative ion), respectively.

## Data Collection and Analysis

Data files from the Q-TOF-MS system were converted to the .abf format using the Analysis Base File Converter software. Peak detection, chromatogram deconvolution, and other data processing used MSDIAL3.82 software and aligned with the

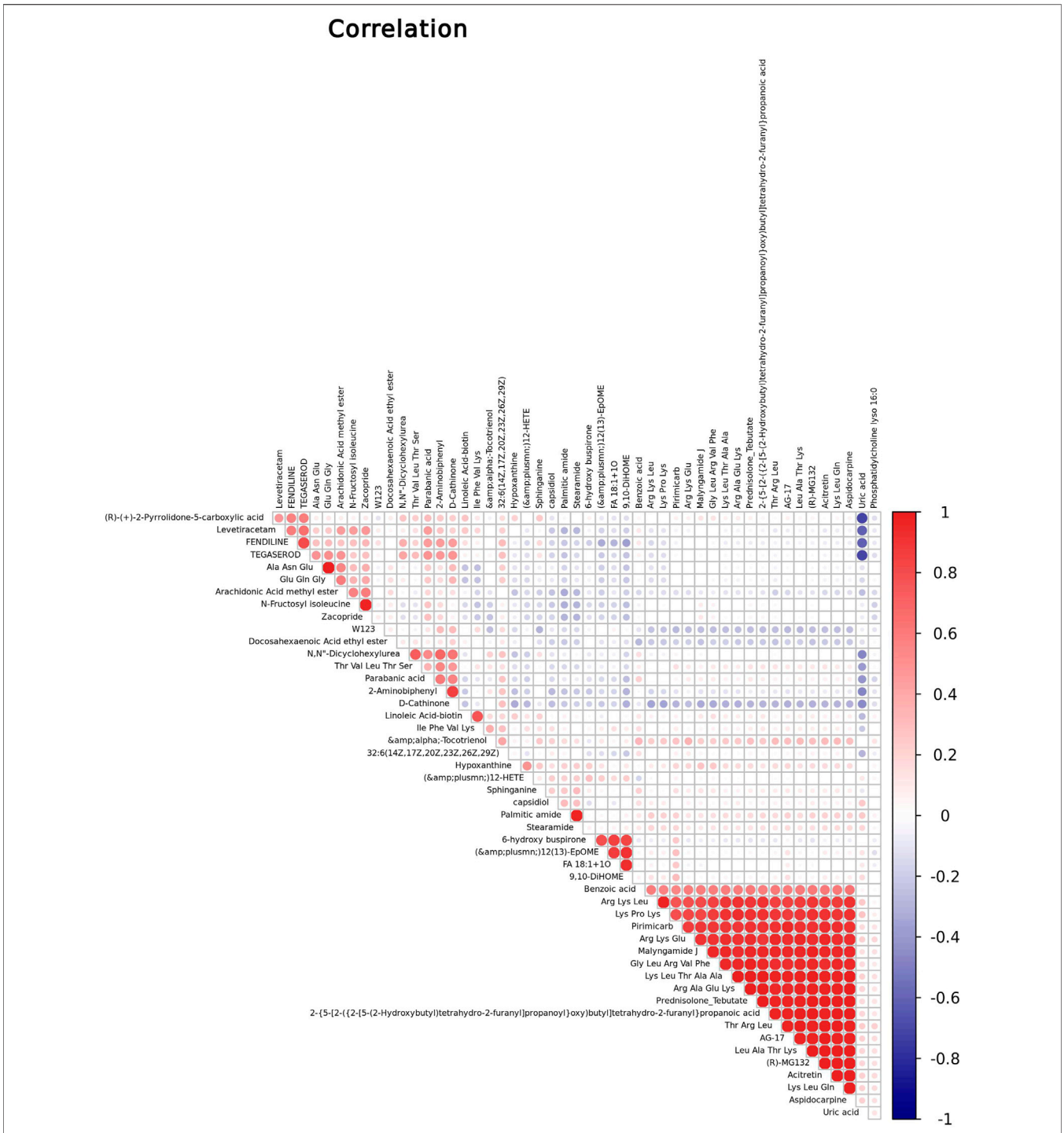


**FIGURE 3 |** Correlation studies of identified metabolites in childhood short stature. Positive and negative correlations are indicated in red and blue, respectively.

following parameters: alignment-MS1, tolerance −0.01Da, retention time tolerance-0.2 min, identification accurate mass tolerance (MS1)-0.005Da, (MS2)-0.05Da, and identification score cutoff −60%. For the identification of key metabolites and metabolic pathways following databases were used: HMDB (http://www.hmdb.ca/), METLIN (http://metlin.scripps.edu/), Massbank (http://www.massbank.jp), and KEGG (http://www.kegg.com/).

Multivariate statistical analysis was performed using SIMCA-P software (version 14.1, Umetrics, Umea, Sweden). Unit variance scaling followed partial least-squares discrimination

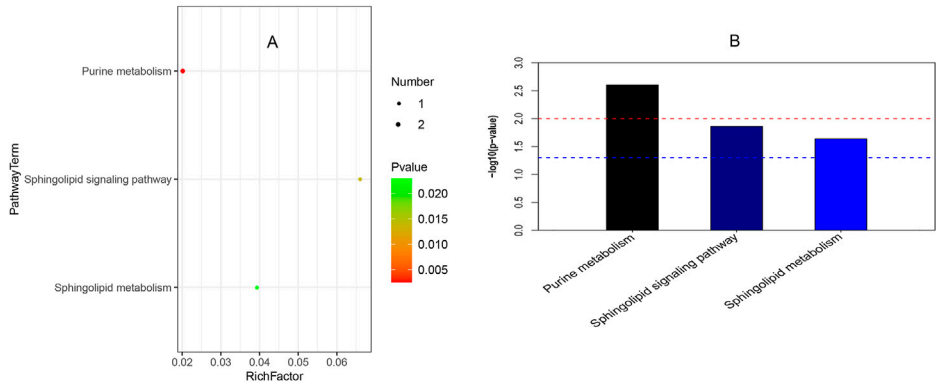


**FIGURE 4 |** Pathway enrichment analysis. **(A)** It shows the bubble chart among ISS, GHD, and control groups. The abscissa is a rich factor (the detailed description was shown in Result 3.4), and the left ordinate is the pathway. **(B)** It presents the bar chart of the three groups. The abscissa is the pathway, and the ordinate is $-\log_{10}(p - value)$. The blue line indicates a *p*-value threshold of 0.05, and the red line indicates a *p*-value threshold of 0.01.

analysis (PCA) and orthogonal partial least-squares discriminant analysis (OPLS-DA), which were applied to distinguish three groups (viz., controls, idiopathic short stature group, and growth hormone deficiency group). A permutation test was used to check the validity and the degree of overfitting for the model. The VIP values of metabolites greater than 1 in non-targeted metabolomics analysis, and all metabolites were performed using the Wilcoxon Mann–Whitney test and identified various metabolites. $p < 0.05$ was considered significant. Meanwhile, the false discovery rate (FDR) was used for multiple comparisons ($p < 0.10$). The ratios of different metabolites between the average of those in normal control samples and the two experimental groups were calculated, and MeV version 4.5.1 software was used to illustrate the relationship between the different metabolites. Raw data are shown in **Supplementary Table S1**.

# RESULTS

## Metabonomics Analysis in Two Different Types of Childhood Short Stature by UHPLC-TOF-MS

To explore the critical metabolites in serum metabolism of different types of childhood short stature, the metabolic profiles of serum in different groups (ISS and GHD groups) were analyzed by UHPLC-TOF-MS. Data were analyzed by SIMCA-P software. 3D PCA (principal components analysis) and PLS-DA (partial least-squares discrimination analysis) were demonstrated (**Figure 1A**). Orthogonal PLS-DA (OPLS-DA) was performed to explore further the risk metabolites in each group (**Figure 1B**). A clear differentiation was shown between the ISS and control groups, GHD and control groups, and ISS and GHD groups (Figure S1). All OPLS-DA models were reliable because none of the permutation tests had no overfitting. Many critical metabolites and multiple metabolic pathways had been explored in the serum of different types of childhood short stature.

## Visualization of Differential Metabolites Using Volcano Plot and Heat Map

We investigated differential metabolites between the control group and two types of short stature group (**Figures 2A–C**). Compared with normal-height children, fourteen metabolites were downregulated, and 53 were upregulated in ISS (**Figure 2A**). Meanwhile, 50 metabolites were downregulated, and 63 were upregulated in the short stature of GHD (**Figure 2C**). Furthermore, we focused on 33 differential metabolites between the ISS and GHD groups (**Figure 2B**), including 27 downregulated and five upregulated metabolites. At the same time, the heat map revealed differential expression of metabolites among the control, ISS, and GHD groups. These findings revealed that specific metabolites played significant roles in the progression of different childhood SS.

## Metabolite–Metabolite Correlation Analysis Among Identified Metabolites

We performed Pearson correlation coefficient analysis to understand further the interrelationship among identified metabolites in childhood short stature. **Figure 3** shows the correlation between the top 50 differential metabolites. For instance, Thr Val Leu Thr Ser, one of the oligopeptides, shows a significant positive correlation with 2-aminobiphenyl and a negative correlation with uric acid.

## KEGG Pathway Enrichment Analysis

**Figure 4** reveals that three pathways (viz., purine metabolism, sphingolipid signaling pathway, and sphingolipid metabolism) were significantly enriched in childhood SS. In **Figure 4A**, the abscissa indicates rich factor originated in the number of differential metabolites in the corresponding metabolic pathway/the number of total metabolites identified in the pathway. The larger the value of the rich factor, the greater the degree of pathway enrichment.

Colors are expressed on a linear scale from green to red with *p* values gradually decreasing. In addition, the greater the bubble, the more metabolites in the pathway. Bar charts in **Figure 4B** show purine metabolism was the most significantly enriched in the three groups.

## Short Peptides Analysis

Short peptides include basic molecular information and are the precursor to life. Researchers have recently developed a greater interest in the field due to its unique features and rosy prospects in innovative bio-therapies [25]. There are 18 short peptides with

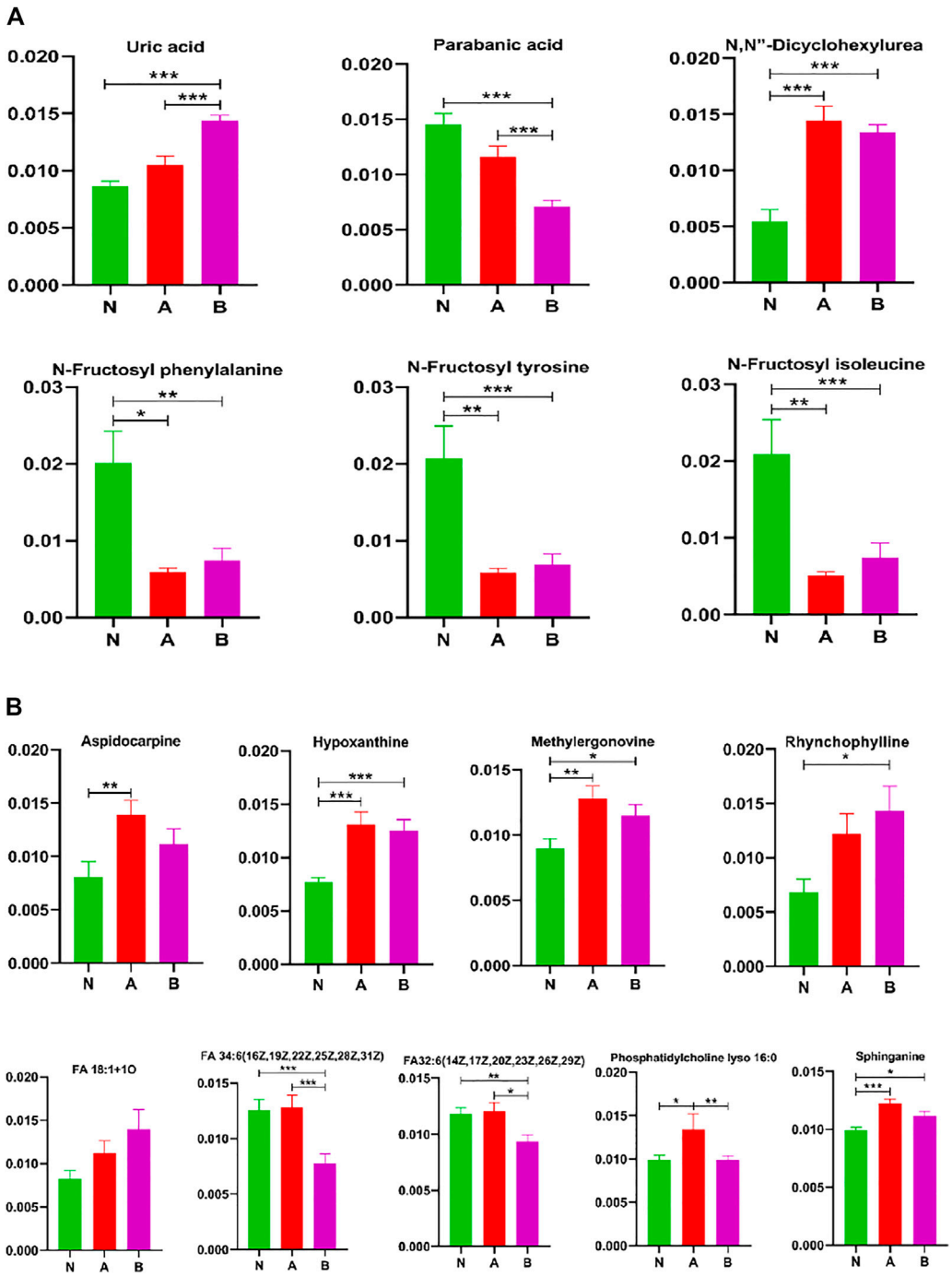


**FIGURE 5 |** Other metabolites analysis in column configuration. Group N, normal height, $n = 30$; group A, ISS, idiopathic short stature, $n = 31$; group B, GHD, short stature of growth hormone deficiency, $n = 29$. All data are mean ± SEM. *$p < 0.05$; **$p < 0.01$; ***$p < 0.001$; two-tailed Mann–Whitney U test.

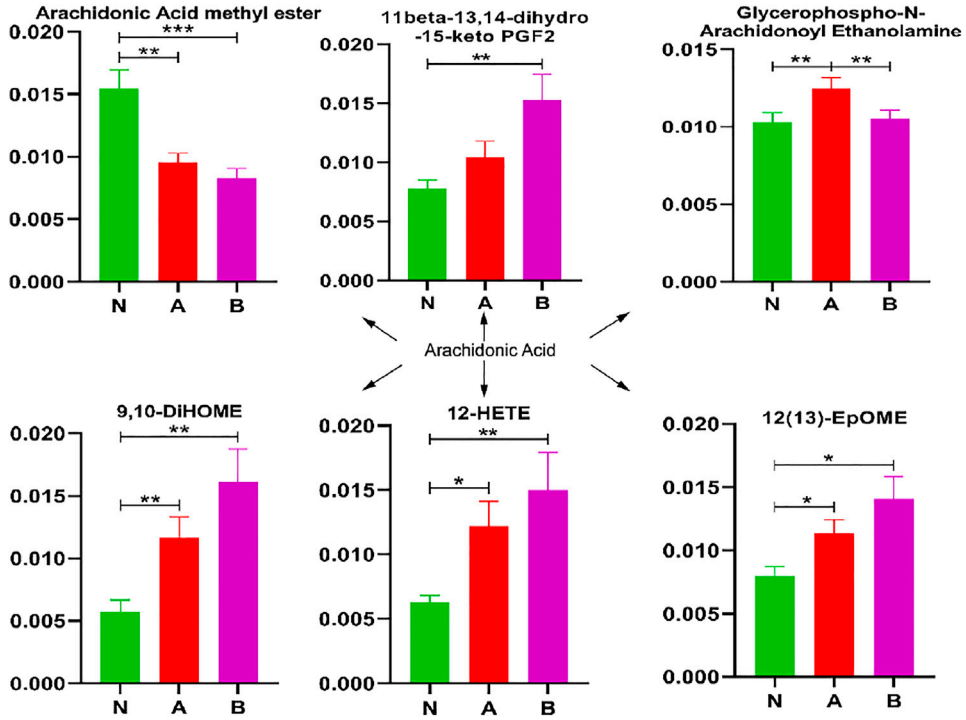


**FIGURE 6 |** Arachidonic acid pathway analysis in column configuration. Group N, normal height, $n = 30$; group A, ISS, idiopathic short stature, $n = 31$; group B, GHD, the short stature due to growth hormone deficiency, $n = 29$. All data are mean ± SEM. $^{*}p < 0.05$; $^{**}p < 0.01$; $^{***}p < 0.001$; two-tailed Mann–Whitney U test.

visible differences between normal-height children (control) and idiopathic short stature (ISS) in **Figure 5**. They are Arg Ala Glu Lys, Arg Lys Glu, Arg Phe Val, Gly Leu Arg Val Phe, lle Phe Val Lys, Leu Ala Thr Lys, Lys Leu Gln, Lys Leu Thr Ala Ala, Lys Pro His, Lys Pro Lys, Lys Ser Gln Lys, Phe Ala Asn Lys, Ser Lys Phe, Thr Arg Leu, Thr Asn Phe Asp, Thr Glu Leu Lys, Trp Ile Lys, Val Ile Asp Lys. Similarly, 16 short peptides have shown a visible difference between normal-height children (control) and short stature caused by the GHD. They are Arg Ala Glu Lys, Arg Lys Leu, Arg Phe Val, Glu Gln Gly, Leu Ala Thr Lys, Lys Leu Gln, Lys Pro His, Lys Pro Lys, Lys Ser Gln Lys, Phe Ala Asn Lys, Ser Lys Phe, Thr Asn Phe Asp, Thr Glu Leu Lys, Thr Val Leu Thr Ser, Trp Ile Lys, and Val Ile Asp Lys. Furthermore, there are merely five short peptides visibly different in ISS and GHD short stature children. They are Arg Lys Leu, Glu Gln Gly, lle Phe Val Lys, Thr Val Leu Thr Ser, and Trp Ile Lys.

We found that the short peptides Thr Val Leu Thr Ser and Trp Ile Lys might significantly affect childhood short stature.

## 3.6 Arachidonic Acid Pathway Analysis

In children with idiopathic short stature or a growth hormone deficiency, 9,10-DiHOME, 12-HETE, and 12 (13)-EpOME significantly increased, whereas arachidonic acid methyl ester was remarkably decreased (**Figure 6**). Glycerophospho-N-arachidonoyl ethanolamine showed markedly elevated levels in children with idiopathic short stature compared to normal-height children or children with growth hormone deficiency. Thus, these metabolites refined our understanding of SS in the arachidonic acid pathway.

## Acids and Acid Amides Metabolites Analysis

To better understand differential metabolites in pubertal children with short stature, acids and acid amides were also analyzed to find the key metabolites that could differentiate between the normal-height group and SS (**Figure 7**). Our results demonstrated that the key metabolites were curvulinic acid, docosahexaenoic acid ethyl ester, nonanoic acid, stearamide, capsidiol, eicosanoyl-EA, N'-(2,4-dimethylphenyl)-N-methylformamidine, N, N-diisopropyl-3-nitrobenzamide, and palmitic amide. Moreover, the compounds such as alpha-tocotrienol, benzoic acid, curvulinic acid, linoleic acid-biotin, nonanoic acid, and N'-(2,4-dimethylphenyl)-N-methylformamidine could discriminate ISS group from normal height subjects or children with the GHD.

It was observed that some metabolites could distinguish subtypes of childhood SS, which were (R)-(+)-2-pyrrolidone-5-carboxylic acid, alpha-tocotrienol, benzoic acid, curvulinic acid, linoleic acid-biotin, nonanoic acid, and N'-(2,4-dimethylphenyl)-N-methylformamidine.

## Analysis of Other Metabolites

While screening differential metabolites, we investigated some interesting compounds like uric acid, lipids, fructose, and others in (**Figure 8**). A series of metabolites (Yusupov et al., 2017) could differentiate between the normal-height group and childhood SS, that is, N, N-dicyclohexylurea, N-fructosyl isoleucine, N-fructosyl phenylalanine, N-fructosyl tyrosine, methylergonovine,

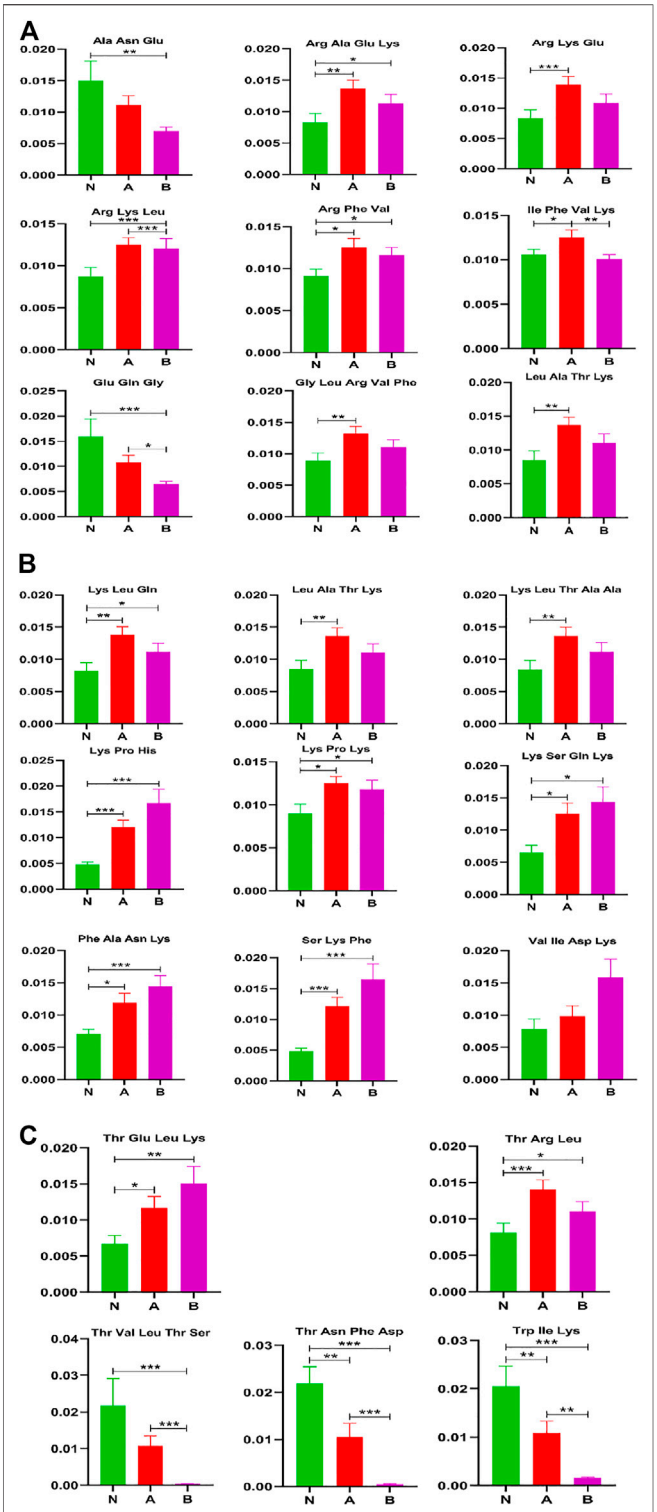


**FIGURE 7 |** Acids and acid amides metabolite(s) analysis in column configuration. Group N, normal height, $n = 30$; group A, ISS, idiopathic short stature, $n = 31$; group B, GHD, short stature of growth hormone deficiency, $n = 29$. All data are mean ± SEM. $^{*}p < 0.05$; $^{**}p < 0.01$; $^{***}p < 0.001$; two-tailed Mann–Whitney U test.

hypoxanthine, and sphinganine. Moreover, phosphatidylcholine lyso 16:0 could discriminate ISS from normal-height subjects or children with growth hormone deficiency. We also discovered some metabolites could identify subtypes of childhood SS, which were parabanic acid, FA 34:6 (16Z,19Z,22Z,25Z,28Z,31Z), and FA32:6 (14Z,17Z,20Z,23Z,26Z,29Z).

## DISCUSSION

The most significant difference between the species is the size of the individual (Klingseisen and Jackson, 2011). However, the mechanisms behind childhood short stature's pathogenic processes remain poorly understood. Early diagnosis and identification of key metabolites of childhood SS will lead to the reasonable treatment and understanding of the mechanism behind the progression of the disease. Our study investigates the key metabolites between different types of childhood SS and normal height children by UHPLC-MS-MS.

Our study revealed that purine metabolism, sphingolipid signaling pathway, and sphingolipid metabolism were significantly enriched in ISS, childhood SS with GHD, and normal-height children (**Figure 4**). Several studies involving the anti-aging gene SIRT1 have suggested that SIRT1 is involved in regulating growth hormone and sphingolipid metabolism with relevance in neurodegeneration. Therefore, it has been suggested that SIRT1 plays a critical role in the hypothalamic–pituitary axis, regulation of metabolism, aging, and longevity (Satoh et al., 2011; Yamamoto and Takahashi, 2018).

Some studies have observed that purine metabolism plays a vital role in energy metabolism (Esther et al., 2015). Since uric acid is the final product and an essential index of purine metabolism (Si et al., 2020), we found that increased uric acid could discriminate idiopathic short stature among the ISS, GHD, and control groups (**Figure 8**). Moreover, hypoxanthine could distinguish childhood SS from normal height children, as observed in **Figure 8**. Changed sphingolipid metabolism might result in sensory neuron damage (Chen et al., 2015). In recent years, some evidence has also suggested that sphingolipid dysregulation plays a pivotal role in the pathogenesis of many brain disorders (Bourgognon et al., 2018). Growth hormone secreted from the pituitary gland is closely related to childhood SS. The primary reasons for GH secretion level changes with age were associated with the transformation in the pituitary gene expression of GH and the GHRH receptor together with a decrease in hypothalamic GHRH (Sonntag et al., 1980; Corpas et al., 1993; Chapman et al., 1997; Degli Uberti et al., 1997; Russell-Aulet et al., 1999; Rosen, 2000; Frutos et al., 2007; Weigent, 2013). Our results showed that sphinganine could distinguish between childhood SS and normal height children. In addition, sphingolipid metabolites have also been shown to regulate arachidonic acid (AA) metabolism (Zhang et al., 2021). As shown in **Figure 6**, similarly, our results have revealed that the AA pathway contributes to childhood SS development and progression.

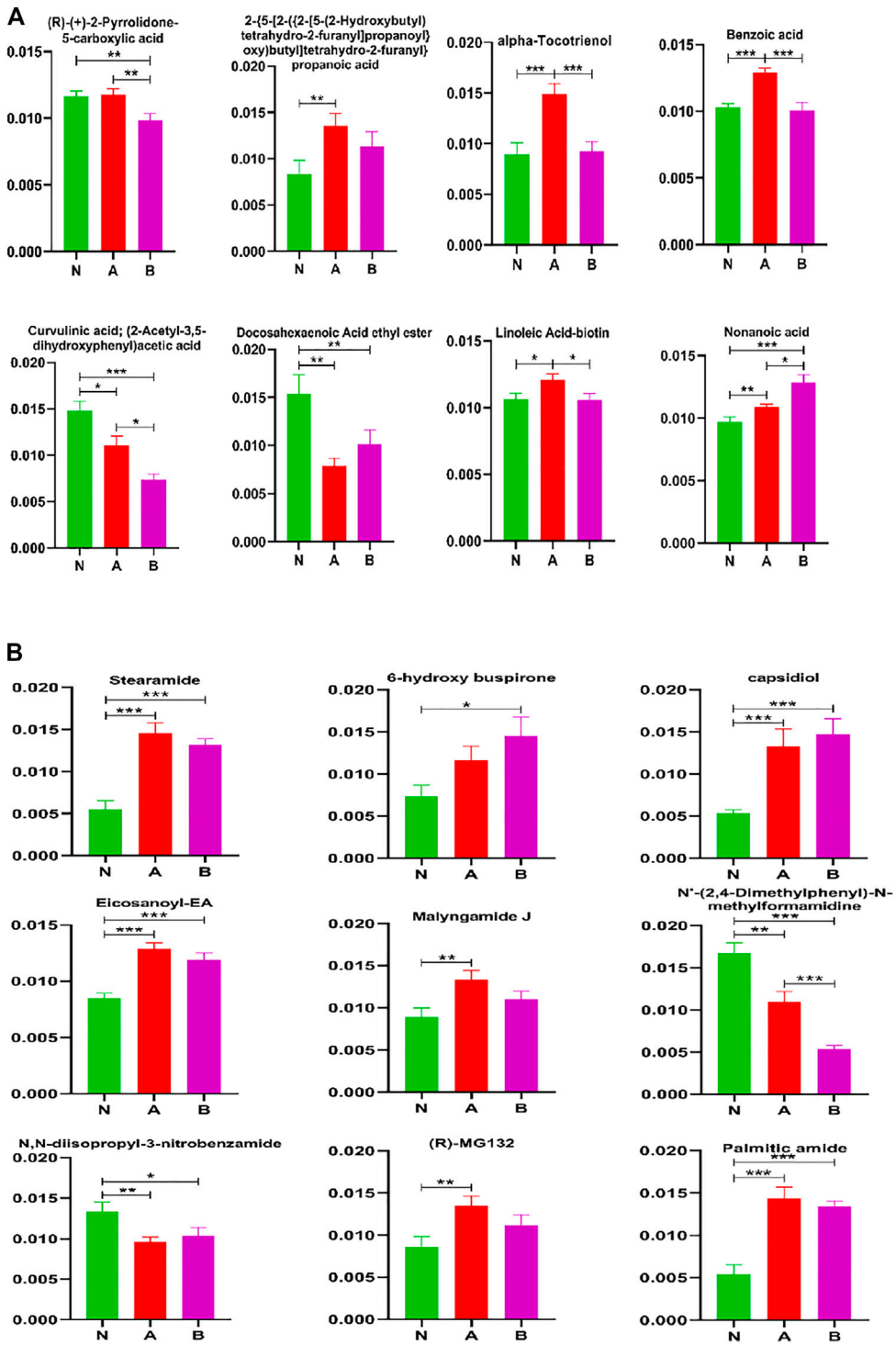


**FIGURE 8 |** Other metabolites analysis in column configuration. Group N, normal height, $n = 30$; group A, ISS, idiopathic short stature, $n = 31$; group B, GHD, short stature of growth hormone deficiency, $n = 29$. All data are mean ± SEM. *$p < 0.05$; **$p < 0.01$; ***$p < 0.001$; two-tailed Mann–Whitney U test.

Short peptides play an important role in the immune system and are responsible for transmitting most immunological information (Parhiz et al., 2013). Some short peptides (2–20 amino acids) are partially obtained by enzymatic hydrolysis of proteins and are important bioactive peptides (Zhang et al., 2019). In recent years, short peptides have been of considerable interest in the branch of biology, chemistry, and medicine for their unique structural and functional diversity (Apostolopoulos et al., 2021). Reports showed that

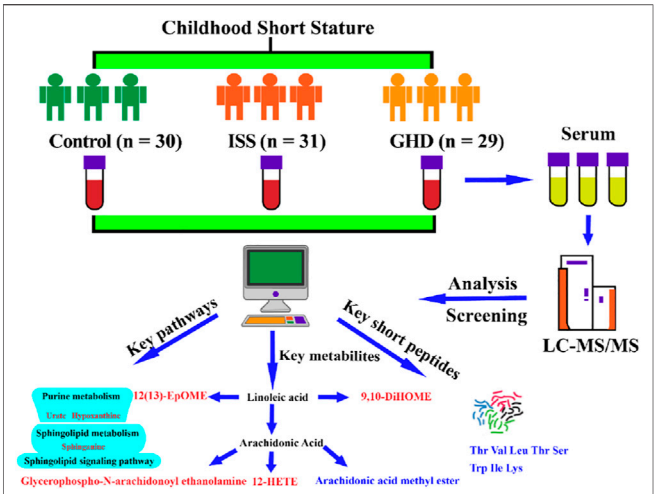


**FIGURE 9 |** Control, normal height, $n = 30$; ISS, idiopathic short stature, $n = 31$; GHD, short stature of growth hormone deficiency, $n = 29$. Significance was increased relative to the controls indicated in red, and significance was decreased relative to the controls indicated in blue. All data are of the two-tailed Mann–Whitney U test.

short peptides have relevance in many diseases, including neurodegenerative diseases (Jang et al., 2016), Alzheimer's (Perez-Garmendia and Gevorkian, 2013; Soudy et al., 2019), and rheumatoid arthritis (Turesson et al., 2007; Ruiz-Ortiz De Arrizabaleta et al., 2011) and also has many therapeutic effects (New et al., 2014; Tatman et al., 2016; Baig et al., 2018; Horsley et al., 2020). Our results demonstrated that 18 short peptides could visibly differentiate between the control and ISS groups, as well as 16 short peptides could clearly distinguish the control from the GHD group, and six short peptides can distinguish ISS from the GHD group (**Figure 5**). These findings necessitate further investigation and may serve as the starting point for developing new therapeutics for childhood SS.

Our study also detected a number of acids, acid amides, lipids, fructose, and other metabolites, indicating their involvement in the process of childhood SS (**Figures 6-8**). The 16 metabolites that could differentiate between the normal height group and childhood SS were curvulinic acid, docosahexaenoic acid ethyl ester, nonanoic acid, stearamide, capsidiol, eicosanoyl-EA, N'-(2,4-dimethylphenyl)-N-methylformamidine, N,N-diisopropyl-3-nitrobenzamide, palmitic amide, N,N-dicyclohexylurea, N-fructosyl isoleucine, N-fructosyl phenylalanine, N-fructosyl tyrosine, methylergonovine, hypoxanthine, and sphinganine. Furthermore, the seven compounds that could discriminate ISS from normal-height subjects or childhood SS with GHD were alpha-tocotrienol, benzoic acid, curvulinic acid, linoleic acid-biotin, nonanoic acid, N'-(2,4-dimethylphenyl)-N-methylformamidine, and phosphatidylcholine lyso 16:0.

Our study has also revealed that 10 metabolites could distinguish subtypes of childhood SS, which were (R)-(+)-2-pyrrolidone-5-carboxylic acid, alpha-tocotrienol, benzoic acid, curvulinic acid, linoleic acid-biotin, nonanoic acid, parabanic acid, FA 34:6 (16Z,19Z,22Z,25Z,28Z,31Z) FA32:6 (14Z,17Z,20Z,23Z,26Z,29Z), and N'-(2,4-dimethylphenyl)-N-methylformamidine. However, in order to achieve a clear distinction and characterization, optimization of potential biomarker analysis is the most important to understand childhood SS. In our study, the three potential biomarkers, curvulinic acid (2-acetyl-3,5-dihydroxyphenyl acetic acid), nonanoic acid, and N'-(2,4-dimethylphenyl)-N-methylformamidine had apparent changes among the three groups. It has been observed that curvulinic acid originated from the microbial metabolism of polyphenols is widely distributed in organisms (Vázquez-Manjarrez et al., 2020). Polyphenols have been shown to play an essential part in plant development (participating in plant hormone signaling), reproduction, and defense (protecting from pathogens) (Agati et al., 2012; Agati et al., 2013; Zhao et al., 2017). Nonanoic acid is a species of fatty acid and is a group of compounds that can potentially be a consequence of increased cell membrane lysis (Hillyer et al., 2016; Yusupov et al., 2017; Lawson et al., 2019). Some studies have also demonstrated that nonanoic acid had a particular influence on the Poria placenta growth (Kozicki et al., 2019). Some genes can degrade an array of methylated compounds (dimethylamine, methylamine, and N'-(2,4-dimethylphenyl)-N-methylformamidine) to produce either formaldehyde or methyl groups as the intermediates (Huang et al., 2019). Consequently, our study revealed that these three potential biomarkers played vital roles in the development of childhood SS.

There are some limitations of this study that need to be focused and discussed. Even though there were relatively equal numbers of gender and age in each childhood SS group, we were underpowered to evaluate the associated diseases (except for injuries), dietary supplements, and diet differences. Furthermore, the batch samples used for screening key metabolites were relatively modest (normal height, $n = 30$; ISS, $n = 31$; GHD, $n = 29$), although the number of samples met the human metabonomics requirements. Nevertheless, our observations need to be replicated in an independent and enough quantity samples in the future. Moreover, childhood SS could be primarily judged by body height comparison table and instruments (test bone age). We noted that our study was intended to illustrate complementary methods that might improve clinical prediction and help understand childhood SS progression.

## CONCLUSION

In our study, the metabolite changes in ISS and short stature caused by GHD were investigated utilizing UHPLC-Q-TOF-MS-based metabonomics (**Figure 9**). Our data have revealed that three pathways (viz., purine metabolism, sphingolipid signaling pathway, and sphingolipid metabolism) were significantly enriched in childhood SS. Moreover, two short peptides (Thr Val Leu Thr Ser and Trp Ile Lys) may play a vital role in childhood SS. In addition, altered metabolites were involved in the metabolism of 9,10-DiHOME, 12-HETE, and 12 (13)-EpOME, arachidonic acid methyl ester, glycerophospho-N-arachidonoyl ethanolamine, curvulinic acid (2-acetyl-3,5-dihydroxyphenyl acetic acid), nonanoic acid, and N'-(2,4-dimethylphenyl)-N-methylformamidine. Our findings contribute to the understanding of molecular

metabolic processes in childhood short stature and may provide potential clues for the underlying mechanisms that will help treat childhood short stature.

## DATA AVAILABILITY STATEMENT

The original contributions presented in the study are included in the article/**Supplementary Material**; further inquiries can be directed to the corresponding authors.

## ETHICS STATEMENT

This study was approved by the Ethics Committee of Fifth Affiliated Hospital of Harbin Medical University (KY2018003). Written informed consent to participate in this study was provided by the participants' legal guardian/ next of kin.

## AUTHOR CONTRIBUTIONS

GC, DY, and ZX designed the project. GC wrote the manuscript. DY, ZX, YJ, CL, WZ, SY, YS, and XW performed the sample collection. GC and DY performed sample testing. GC and JL carried out the figures. ZX and JW performed the data interpretation. GC and ZX performed the data analysis. DY, ZX, and GC provided funds. GC is the first author. JW is the co-first authors. ZX is the corresponding author. DY is co-corresponding authors. The Fifth Affiliated Hospital of Harbin Medical University is the first unit of the article. All authors were involved in editing the manuscript.

## FUNDING

This work was supported by the Scientific Research Fund of the Fifth Affiliated Hospital of Harbin Medical University of China (Nos. 2018-001 and 2018-002), Daqing City Guiding Science and Technology Project (Nos. zdy-2016-080 and zdy-2020-45), and the Fundamental Research Funds for the Provincial Universities of Hei Long Jiang province (No. JFXN202003).

## SUPPLEMENTARY MATERIAL

The Supplementary Material for this article can be found online at: https://www.frontiersin.org/articles/10.3389/fphar.2022.818952/full#supplementary-material

## REFERENCES

Agati, G., Azzarello, E., Pollastri, S., and Tattini, M. (2012). Flavonoids as Antioxidants in Plants: Location and Functional Significance. *Plant Sci.* 196, 67–76. doi:10.1016/j.plantsci.2012.07.014

Agati, G., Brunetti, C., Di Ferdinando, M., Ferrini, F., Pollastri, S., and Tattini, M. (2013). Functional Roles of Flavonoids in Photoprotection: New Evidence, Lessons from the Past. *Plant Physiol. Biochem.* 72, 35–45. doi:10.1016/j.plaphy.2013.03.014

Allen, D. B., and Cuttler, L. (2013). Clinical Practice. Short Stature in Childhood-Cchallenges and Choices. *N. Engl. J. Med.* 368, 1220–1228. doi:10.1056/NEJMcp1213178

Apostolopoulos, V., Bojarska, J., Chai, T. T., Elnagdy, S., Kaczmarek, K., Matsoukas, J., et al. (2021). A Global Review on Short Peptides: Frontiers and Perspectives. *Molecules* 26, 430. doi:10.3390/molecules26020430

Baig, M. H., Ahmad, K., Rabbani, G., and Choi, I. (2018). Use of Peptides for the Management of Alzheimer's Disease: Diagnosis and Inhibition. *Front. Aging Neurosci.* 10, 21. doi:10.3389/fnagi.2018.00021

Bosy-Westphal, A., Plachta-Danielzik, S., Dörhöfer, R. P., and Müller, M. J. (2009). Short Stature and Obesity: Positive Association in Adults but Inverse Association in Children and Adolescents. *Br. J. Nutr.* 102, 453–461. doi:10.1017/S0007114508190304

Bourgognon, J. M., Spiers, J. G., Scheiblich, H., Antonov, A., Bradley, S. J., Tobin, A. B., et al. (2018). Alterations in Neuronal Metabolism Contribute to the Pathogenesis of Prion Disease. *Cell Death Differ* 25, 1408–1425. doi:10.1038/s41418-018-0148-x

Chapman, I. M., Hartman, M. L., Pezzoli, S. S., Harrell, F. E., Jr., Hintz, R. L., Alberti, K. G., et al. (1997). Effect of Aging on the Sensitivity of Growth Hormone Secretion to Insulin-like Growth Factor-I Negative Feedback. *J. Clin. Endocrinol. Metab.* 82, 2996–3004. doi:10.1210/jcem.82.9.4223

Chen, Y. C., Auer-Grumbach, M., Matsukawa, S., Zitzelsberger, M., Themistocleous, A. C., Strom, T. M., et al. (2015). Transcriptional Regulator PRDM12 Is Essential for Human Pain Perception. *Nat. Genet.* 47, 803–808. doi:10.1038/ng.3308

Corpas, E., Harman, S. M., and Blackman, M. R. (1993). Human Growth Hormone and Human Aging. *Endocr. Rev.* 14, 20–39. doi:10.1210/edrv-14-1-20

Crofton, P. M., Stirling, H. F., Schönau, E., and Kelnar, C. J. (1996). Bone Alkaline Phosphatase and Collagen Markers as Early Predictors of Height Velocity Response to Growth-Promoting Treatments in Short normal Children. *Clin. Endocrinol.* 44, 385–394. doi:10.1046/j.1365-2265.1996.706cn527.x

Decker, R., Andersson, B., Nierop, A. F., Bosaeus, I., Dahlgren, J., Albertsson-Wikland, K., et al. (2013). Protein Markers Predict Body Composition during Growth Hormone Treatment in Short Prepubertal Children. *Clin. Endocrinol. (Oxf)* 79, 675–682. doi:10.1111/cen.12196

Degli Uberti, E. C., Ambrosio, M. R., Cella, S. G., Margutti, A. R., Trasforini, G., Rigamonti, A. E., et al. (1997). Defective Hypothalamic Growth Hormone (GH)-releasing Hormone Activity May Contribute to Declining GH Secretion with Age in Man. *J. Clin. Endocrinol. Metab.* 82, 2885–2888. doi:10.1210/jcem.82.9.4216

Derraik, J. G., Lundgren, M., Cutfield, W. S., and Ahlsson, F. (2016). Maternal Height and Preterm Birth: A Study on 192,432 Swedish Women. *PLoS One* 11, e0154304. doi:10.1371/journal.pone.0154304

Esther, C. R., Coakley, R. D., Henderson, A. G., Zhou, Y. H., Wright, F. A., and Boucher, R. C. (2015). Metabolomic Evaluation of Neutrophilic Airway Inflammation in Cystic Fibrosis. *Chest* 148, 507–515. doi:10.1378/chest.14-1800

Frutos, M. G., Cacicedo, L., Méndez, C. F., Vicent, D., González, M., and Sánchez-Franco, F. (2007). Pituitary Alterations Involved in the Decline of Growth Hormone Gene Expression in the Pituitary of Aging Rats. *J. Gerontol. A. Biol. Sci. Med. Sci.* 62, 585–597. doi:10.1093/gerona/62.6.585

Gui, B., Yu, C., Li, X., Zhao, S., Zhao, H., Yan, Z., et al. (2021). Heterozygous Recurrent Mutations Inducing Dysfunction of ROR2 Gene in Patients with Short Stature. *Front Cel Dev Biol* 9, 661747. doi:10.3389/fcell.2021.661747

Hellgren, G., Andersson, B., Nierop, A. F., Dahlgren, J., Hochberg, Z., and Albertsson-Wikland, K. (2008). A Proteomic Approach Identified Growth Hormone-dependent Nutrition Markers in Children with Idiopathic Short Stature. *Proteome Sci.* 6, 35. doi:10.1186/1477-5956-6-35

Hillyer, K. E., Tumanov, S., Villas-Bôas, S., and Davy, S. K. (2016). Metabolite Profiling of Symbiont and Host during thermal Stress and Bleaching in a Model Cnidarian-Dinoflagellate Symbiosis. *J. Exp. Biol.* 219, 516–527. doi:10.1242/jeb.128660

Horsley, J. R., Jovcevski, B., Wegener, K. L., Yu, J., Pukala, T. L., and Abell, A. D. (2020). Rationally Designed Peptide-Based Inhibitor of Aβ42 Fibril Formation

and Toxicity: a Potential Therapeutic Strategy for Alzheimer's Disease. *Biochem. J.* 477, 2039–2054. doi:10.1042/BCJ20200290

Huang, J., Yu, Z., Groom, J., Cheng, J. F., Tarver, A., Yoshikuni, Y., et al. (2019). Rare Earth Element Alcohol Dehydrogenases Widely Occur Among Globally Distributed, Numerically Abundant and Environmentally Important Microbes. *ISME J.* 13, 2005–2017. doi:10.1038/s41396-019-0414-z

Huang, Q., Tan, Y., Yin, P., Ye, G., Gao, P., Lu, X., et al. (2013). Metabolic Characterization of Hepatocellular Carcinoma Using Nontargeted Tissue Metabolomics. *Cancer Res.* 73, 4992–5002. doi:10.1158/0008-5472.CAN-13-0308

Jang, T. H., Lim, I. H., Kim, C. M., Choi, J. Y., Kim, E. A., Lee, T. J., et al. (2016). Rescuing Neuronal Cell Death by RAIDD- and PIDD- Derived Peptides and its Implications for Therapeutic Intervention in Neurodegenerative Diseases. *Sci. Rep.* 6, 31198. doi:10.1038/srep31198

Kim, B., and Park, M. J. (2009). The Influence of Weight and Height Status on Psychological Problems of Elementary Schoolchildren through Child Behavior Checklist Analysis. *Yonsei Med. J.* 50, 340–344. doi:10.3349/ymj.2009.50.3.340

Klingseisen, A., and Jackson, A. P. (2011). Mechanisms and Pathways of Growth Failure in Primordial Dwarfism. *Genes Dev.* 25, 2011–2024. doi:10.1101/gad.169037

Kozicki, M., Wiejak, A., Piasecki, M., and Abram, A. (2019). Identification of MVOCs Produced by Coniophora puteana and Poria Placenta Growing on WPC Boards by Using Subtraction Mass Spectra. *Int. J. Environ. Res. Public Health* 16, 2499. doi:10.3390/ijerph16142499

Lawson, C. A., Possell, M., Seymour, J. R., Raina, J. B., and Suggett, D. J. (2019). Coral Endosymbionts (Symbiodiniaceae) Emit Species-specific Volatilomes that Shift when Exposed to thermal Stress. *Sci. Rep.* 9, 17395. doi:10.1038/s41598-019-53552-0

Ma, J., Pei, T., Dong, F., Dong, Y., Yang, Z., Chen, J., et al. (2019). Spatial and Demographic Disparities in Short Stature Among School Children Aged 7-18 Years: a Nation-wide Survey in China, 2014. *BMJ Open* 9, e026634. doi:10.1136/bmjopen-2018-026634

Marchini, A., Ogata, T., and Rappold, G. A. (2016). A Track Record on SHOX: From Basic Research to Complex Models and Therapy. *Endocr. Rev.* 37, 417–448. doi:10.1210/er.2016-1036

Martins, I. J. (2016). Anti-Aging Genes Improve Appetite Regulation and Reverse Cell Senescence and Apoptosis in Global Populations. *Adv. Aging Res.* 5, 9–26. doi:10.4236/aar.2016.51002

Martins, I. J. (2017). Single Gene Inactivation with Implications to Diabetes and Multiple Organ Dysfunction Syndrome. *J. Clin. Epigenet* 3, 24. doi:10.21767/2472-1158.100058

Murray, P. G., Clayton, P. E., and Chernausek, S. D. (2018). A Genetic Approach to Evaluation of Short Stature of Undetermined Cause. *Lancet Diabetes Endocrinol.* 6, 564–574. doi:10.1016/S2213-8587(18)30034-2

New, R., Bansal, G. S., Dryjska, M., Bogus, M., Green, P., Feldmann, M., et al. (2014). Design and Optimisation of Bioactive Cyclic Peptides: Generation of a Down-Regulator of TNF Secretion. *Molecules* 19, 21529–21540. doi:10.3390/molecules191221529

Nicholson, J. K., Holmes, E., and Wilson, I. D. (2005). Gut Microorganisms, Mammalian Metabolism and Personalized Health Care. *Nat. Rev. Microbiol.* 3, 431–438. doi:10.1038/nrmicro1152

Parhiz, H., Hashemi, M., Hatefi, A., Shier, W. T., Amel Farzad, S., and Ramezani, M. (2013). Arginine-rich Hydrophobic Polyethylenimine: Potent Agent with Simple Components for Nucleic Acid Delivery. *Int. J. Biol. Macromol* 60, 18–27. doi:10.1016/j.ijbiomac.2013.05.001

Perez-Garmendia, R., and Gevorkian, G. (2013). Pyroglutamate-Modified Amyloid Beta Peptides: Emerging Targets for Alzheimer´s Disease Immunotherapy. *Curr. Neuropharmacol* 11, 491–498. doi:10.2174/1570159X11311050004

Ponomarenko, M., Kleshchev, M., Ponomarenko, P., Chadaeva, I., Sharypova, E., Rasskazov, D., et al. (2020). Disruptive Natural Selection by Male Reproductive Potential Prevents Underexpression of Protein-Coding Genes on the Human Y Chromosome as a Self-Domestication Syndrome. *BMC Genet.* 21, 89. doi:10.1186/s12863-020-00896-6

Rogol, A. D., and Hayden, G. F. (2014). Etiologies and Early Diagnosis of Short Stature and Growth Failure in Children and Adolescents. *J. Pediatr.* 164, S1–S14. e16. doi:10.1016/j.jpeds.2014.02.027

Rosen, C. J. (2000). Growth Hormone and Aging. *Endocrine* 12, 197–201. doi:10.1385/ENDO:12:2:197

Ruiz-Ortiz De Arrizabaleta, E., Grados-Cánovas, D., Teniente-Serra, A., García-López, V., Quirant-Sánchez, B., Holgado, S., et al. (2011). Diagnostic Value of Different Anti-citrullinated Peptides Antibodies in Rheumatoid Arthritis. *J. Transl Med.* 9 (Suppl. 2), P51. doi:10.1186/1479-5876-9-S2-P51

Russell-Aulet, M., Jaffe, C. A., Demott-Friberg, R., and Barkan, A. L. (1999). *In Vivo* semiquantification of Hypothalamic Growth Hormone-Releasing Hormone (GHRH) Output in Humans: Evidence for Relative GHRH Deficiency in Aging. *J. Clin. Endocrinol. Metab.* 84, 3490–3497. doi:10.1210/jcem.84.10.6063

Satoh, A., Stein, L., and Imai, S. (2011). The Role of Mammalian Sirtuins in the Regulation of Metabolism, Aging, and Longevity. *Handb Exp. Pharmacol.* 206, 125–162. doi:10.1007/978-3-642-21631-2_7

Si, Z., Zhou, S., Shen, Z., and Luan, F. (2020). High-Throughput Metabolomics Discovers Metabolic Biomarkers and Pathways to Evaluating the Efficacy and Exploring Potential Mechanisms of Osthole against Osteoporosis Based on UPLC/Q-TOF-MS Coupled with Multivariate Data Analysis. *Front. Pharmacol.* 11, 741. doi:10.3389/fphar.2020.00741

Smuel, K., and Yeshayahu, Y. (2017). "Real-world" Pediatric Endocrine Practice; How Much Is it Influenced by Physician's Gender and Region of Practice. Results of an International Survey. *J. Eval. Clin. Pract.* 23, 866–869. doi:10.1111/jep.12745

Sonntag, W. E., Steger, R. W., Forman, L. J., and Meites, J. (1980). Decreased Pulsatile Release of Growth Hormone in Old Male Rats. *Endocrinology* 107, 1875–1879. doi:10.1210/endo-107-6-1875

Soudy, R., Kimura, R., Patel, A., Fu, W., Kaur, K., Westaway, D., et al. (2019). Short Amylin Receptor Antagonist Peptides Improve Memory Deficits in Alzheimer's Disease Mouse Model. *Sci. Rep.* 9, 10942. doi:10.1038/s41598-019-47255-9

Tatman, P. D., Muhonen, E. G., Wickers, S. T., Gee, A. O., Kim, E. S., and Kim, D. H. (2016). Self-assembling Peptides for Stem Cell and Tissue Engineering. *Biomater. Sci.* 4, 543–554. doi:10.1039/c5bm00550g

Turesson, C., Jacobsson, L. T., Sturfelt, G., Matteson, E. L., Mathsson, L., and Rönnelid, J. (2007). Rheumatoid Factor and Antibodies to Cyclic Citrullinated Peptides Are Associated with Severe Extra-articular Manifestations in Rheumatoid Arthritis. *Ann. Rheum. Dis.* 66, 59–64. doi:10.1136/ard.2006.054445

Vázquez-Manjarrez, N., Ulaszewska, M., Garcia-Aloy, M., Mattivi, F., Praticò, G., Dragsted, L. O., et al. (2020). Biomarkers of Intake for Tropical Fruits. *Genes Nutr.* 15, 11. doi:10.1186/s12263-020-00670-4

Weigent, D. A. (2013). Expression of Lymphocyte-Derived Growth Hormone (GH) and GH-Releasing Hormone Receptors in Aging Rats. *Cell Immunol* 282, 71–78. doi:10.1016/j.cellimm.2013.04.009

Wishart, D. S. (2016). Emerging Applications of Metabolomics in Drug Discovery and Precision Medicine. *Nat. Rev. Drug Discov.* 15, 473–484. doi:10.1038/nrd.2016.32

Yamamoto, M., Iguchi, G., Fukuoka, H., Suda, K., Bando, H., Takahashi, M., et al. (2013). SIRT1 Regulates Adaptive Response of the Growth Hormone--insulin-like Growth Factor-I axis under Fasting Conditions in Liver. *Proc. Natl. Acad. Sci. U S A.* 110, 14948–14953. doi:10.1073/pnas.1220606110

Yamamoto, M., and Takahashi, Y. (2018). The Essential Role of SIRT1 in Hypothalamic-Pituitary Axis. *Front. Endocrinol. (Lausanne)* 9, 605. doi:10.3389/fendo.2018.00605

Yusupov, M., Wende, K., Kupsch, S., Neyts, E. C., Reuter, S., and Bogaerts, A. (2017). Effect of Head Group and Lipid Tail Oxidation in the Cell Membrane Revealed through Integrated Simulations and Experiments. *Sci. Rep.* 7, 5761. doi:10.1038/s41598-017-06412-8

Zhang, N., Tang, C., Ma, Q., Wang, W., Shi, M., Zhou, X., et al. (2021). Comprehensive Serum Metabolic and Proteomic Characterization on Cognitive Dysfunction in Parkinson's Disease. *Ann. Transl Med.* 9, 559. doi:10.21037/atm-20-4583

Zhang, R., Chen, J., Mao, X., Qi, P., and Zhang, X. (2019). Separation and Lipid Inhibition Effects of a Novel Decapeptide from Chlorella Pyenoidose. *Molecules* 24, 3527. doi:10.3390/molecules24193527

Zhao, Q., Chu, Y., Pan, H., Zhang, M., and Ban, B. (2021). Association between Triglyceride Glucose index and Peak Growth Hormone in Children with Short Stature. *Sci. Rep.* 11, 1969. doi:10.1038/s41598-021-81564-2

Zhao, S. Y., Liu, Z. L., Shu, Y. S., Wang, M. L., He, D., Song, Z. Q., et al. (2017). Chemotaxonomic Classification Applied to the Identification of Two Closely-

Related Citrus TCMs Using UPLC-Q-TOF-MS-Based Metabolomics. *Molecules* 22, 1721. doi:10.3390/molecules22101721

Zhao, X., Xu, F., Qi, B., Hao, S., Li, Y., Li, Y., et al. (2014). Serum Metabolomics Study of Polycystic Ovary Syndrome Based on Liquid Chromatography-Mass Spectrometry. *J. Proteome Res.* 13, 1101–1111. doi:10.1021/pr401130w

**Conflict of Interest:** Author JW was employed by Dating Oil Field General Hospital.

The remaining authors declare that the research was conducted in the absence of any commercial or financial relationships that could be construed as a potential conflict of interest.

**Publisher's Note:** All claims expressed in this article are solely those of the authors and do not necessarily represent those of their affiliated organizations, or those of the publisher, the editors, and the reviewers. Any product that may be evaluated in this article, or claim that may be made by its manufacturer, is not guaranteed or endorsed by the publisher.

frontiers | Frontiers in Pediatrics

ORIGINAL RESEARCH
published: 12 May 2022
doi: 10.3389/fped.2022.840710

# Application of a Physiologically Based Pharmacokinetic Approach to Predict Theophylline Pharmacokinetics Using Virtual Non-Pregnant, Pregnant, Fetal, Breast-Feeding, and Neonatal Populations

*Khaled Abduljalil*, Iain Gardner and Masoud Jamei*

*Certara UK Limited (Simcyp Division), Sheffield, United Kingdom*

OPEN ACCESS

**Edited by:**
*Catherine M. T. Sherwin, Wright State University, United States*

**Reviewed by:**
*Robin Michelet, Freie Universität Berlin, Germany*
*Silvia M. Illamola, University of Minnesota Twin Cities, United States*
*Raman Venkataramanan, University of Pittsburgh, United States*
*Saskia N. De Wildt, Radboud University Nijmegen, Netherlands*

***Correspondence:**
*Khaled Abduljalil*
*khaled.abduljalil@certara.com*

**Specialty section:**
*This article was submitted to Obstetric and Pediatric Pharmacology, a section of the journal Frontiers in Pediatrics*

**Received:** *21 December 2021*
**Accepted:** *11 April 2022*
**Published:** *12 May 2022*

**Citation:**
*Abduljalil K, Gardner I and Jamei M (2022) Application of a Physiologically Based Pharmacokinetic Approach to Predict Theophylline Pharmacokinetics Using Virtual Non-Pregnant, Pregnant, Fetal, Breast-Feeding, and Neonatal Populations. Front. Pediatr. 10:840710. doi: 10.3389/fped.2022.840710*

Perinatal pharmacology is influenced by a myriad of physiological variables that are changing dynamically. The influence of these covariates has not been assessed systemically. The objective of this work was to use theophylline as a model drug and to predict its pharmacokinetics before, during (including prediction of the umbilical cord level), and after pregnancy as well as in milk (after single and multiple doses) and in neonates using a physiological-based pharmacokinetic (PBPK) model. Neonatal theophylline exposure from milk consumption was projected in both normal term and preterm subjects. Predicted infant daily doses were calculated using theophylline average and maximum concentration in the milk as well as an estimate of milk consumption. Predicted concentrations and parameters from the PBPK model were compared to the observed data. PBPK predicted theophylline concentrations in non-pregnant and pregnant populations at different gestational weeks were within 2-fold of the observations and the observed concentrations fell within the 5th−95th prediction interval from the PBPK simulations. The PBPK model predicted an average cord-to-maternal plasma ratio of 1.0, which also agrees well with experimental observations. Predicted postpartum theophylline concentration profiles in milk were also in good agreement with observations with a predicted milk-to-plasma ratio of 0.68. For an infant of 2 kg consuming 150 ml of milk per day, the lactation model predicted a relative infant dose (RID) of 12 and 17% using predicted average ($C_{avg,ss}$) and maximum ($C_{max,ss}$) concentration in milk at steady state. The maximum RID of 17% corresponds to an absolute infant daily dose of 1.4 ± 0.5 mg/kg/day. This dose, when administered as 0.233 mg/kg every 4 h, to resemble breastfeeding frequency, resulted in plasma concentrations as high as 3.9 (1.9–6.8) mg/L and 2.8 (1.3–5.3) (5th−95th percentiles) on day 7 in preterm (32 GW) and full-term neonatal populations.

**Keywords: theophylline, pregnancy, feto-placenta, lactation, preterm, PBPK model, breastfeeding, infant dose**

## INTRODUCTION

Pharmacokinetics (PK) are typically influenced by a variety of physiological variables and also can be altered in different pathological states (1, 2). During the perinatal period, drug PK can be affected by a variety of time-varying physiological parameters in the mother and the unborn fetus (3). Immediately after birth few physiological parameters are reverting to the pre-pregnancy status and can affect the maternal drug exposure (4). For many drugs, the impacts of these changes are minimal with most of the PK parameters being within the pre-pregnancy range (5, 6). Drug exposure to neonates after birth may happen during breastfeeding, assuming the drug reaches the milk after maternal intake. The amount of drug delivered to the breastfed neonate varies with variability in maternal physiology and milk composition as well as the breastfeeding style, i.e., frequency and fed amounts (7, 8). Once the drug reaches the neonatal gut or systemic circulation, the exposure in neonates is influenced by the maturation of the drug absorption and disposition processes that are known to vary with the age of the newborn (9–11).

The impact of physiological changes during pregnancy on drug disposition has not always been thoroughly assessed in clinical studies. This leaves open the question of how and to what extent physiological changes can affect the PK of a drug during pregnancy and if knowledge of the physiological changes that occur during pregnancy can be used to provide some insight into potential PK alterations during pregnancy. Information on the expected alteration of drug PK during the perinatal period can be used to guide the initial prescription strategies to protect both the mother and the neonate by aiding the selection of the right dose for the right patient at the right time (12, 13). During breastfeeding, there is a risk of neonatal drug exposure *via* breast milk following maternal drug intake. Milk is a complex fluid, with pH, fat, and protein levels that change over time. The composition of milk and the physicochemical properties of drugs largely determine the extent to which drugs are excreted into the milk (14). The ability to predict neonatal exposure to drugs *via* breast milk (particularly those that are potentially hazardous to neonates) would also be useful in a clinical setting.

Physiologically-based-pharmacokinetic (PBPK) modeling has been widely used to investigate the influence of physiological changes in different subjects or in specific populations on drug disposition (15, 16). The application of PBPK models to predict drug exposure in pregnant women is increasing due to its mechanistic nature. This allows the inclusion of gestational age-related changes in physiological parameters together with information on the physicochemical properties, *in vitro* disposition information (binding, metabolism, permeability, solubility, etc.), and human PK of the drug to be considered in the PBPK model (12). To date, the clinical applications of the PBPK model to predict drug exposure in milk are still very limited. The aim of this work is to develop a PBPK model to describe the pharmacokinetics of theophylline before, during, and after pregnancy, in breast milk, and in neonates. Theophylline is commonly used to treat asthma and apnea of prematurity and was selected as a model drug for this exercise due to the availability of PK data from different perinatal periods.

## MATERIALS AND METHODS

### Workflow

For all predictions of theophylline kinetics in different populations, the Simcyp Simulator (V21) was used. The workflow of the PBPK model implementation was as follows. Firstly, simulations were performed to predict the theophylline PK in non-pregnant subjects. Secondly, the developed theophylline PBPK model in non-pregnant subjects was used to predict the theophylline PK during pregnancy by applying gestational-dependent changes in the physiological parameters of the mother and the fetus. Thirdly, the PBPK model was coupled with a lactation model (14) to predict the drug exposure in maternal plasma and milk (8). Finally, the predicted infant daily dose from the lactation model was used as a dose input for the neonatal PBPK model in neonatal subjects of different ages by accounting for neonatal age-dependent physiology changes (17). This workflow is depicted in **Figure 1**. The results from all simulations were compared to observed clinical data. A total of 20 trials were used in each executed simulation using the reported sample size for each trial to the derived parameters e.g., AUC, Cmax, etc., are reasonable estimates of the parameters and their associated variability in a population. If a clinical study used $< 10$ subjects, we executed the simulation for 10 subjects in 20 trials (200 subjects) to get a better picture of the variability.

### Model Building

The input parameters for the theophylline PBPK model are provided in the **Supplementary Table 1**. The parameters used in the theophylline PBPK model are based on a previously published theophylline PBPK model (3) that was used to simulate theophylline PK in non-pregnant and pregnant women without considering the fetoplacental model or CYP2E1 changes during pregnancy. The absorption was modeled using a first-order absorption model. In the current work, a mechanistic model of oral absorption of theophylline was used with the permeability in different segments of the intestine being predicted from physicochemical properties using a mechanistic permeability approach (18).

Depending on the clinical study the theophylline was dosed in the PBPK model either as a solution or a tablet. After oral administration of theophylline in adult subjects, the bioavailability is ∼100% from uncoated tablet and liquid formulations (19). When tablets were used in the clinical study the solid formulation option was chosen for the PBPK model with dissolution being described using a diffusion layer model (20) with an intrinsic solubility value for theophylline being calculated from the melting point and lipophilicity of the drug [273°C; (21)] (22). The distribution of theophylline into the tissues was described using a full-body PBPK model with tissue partition coefficients (Kps) being predicted according to Rodgers and Rowland (23) with a global tissue scalar of 1.2 to recover reported data after an intravenous dose (24). The elimination of theophylline was described using metabolism (∼85% of systemic clearance) and renal clearance data (∼15% of systemic clearance) (see **Supplementary Table 1**) for a list of input parameters in the PBPK model). The metabolism of

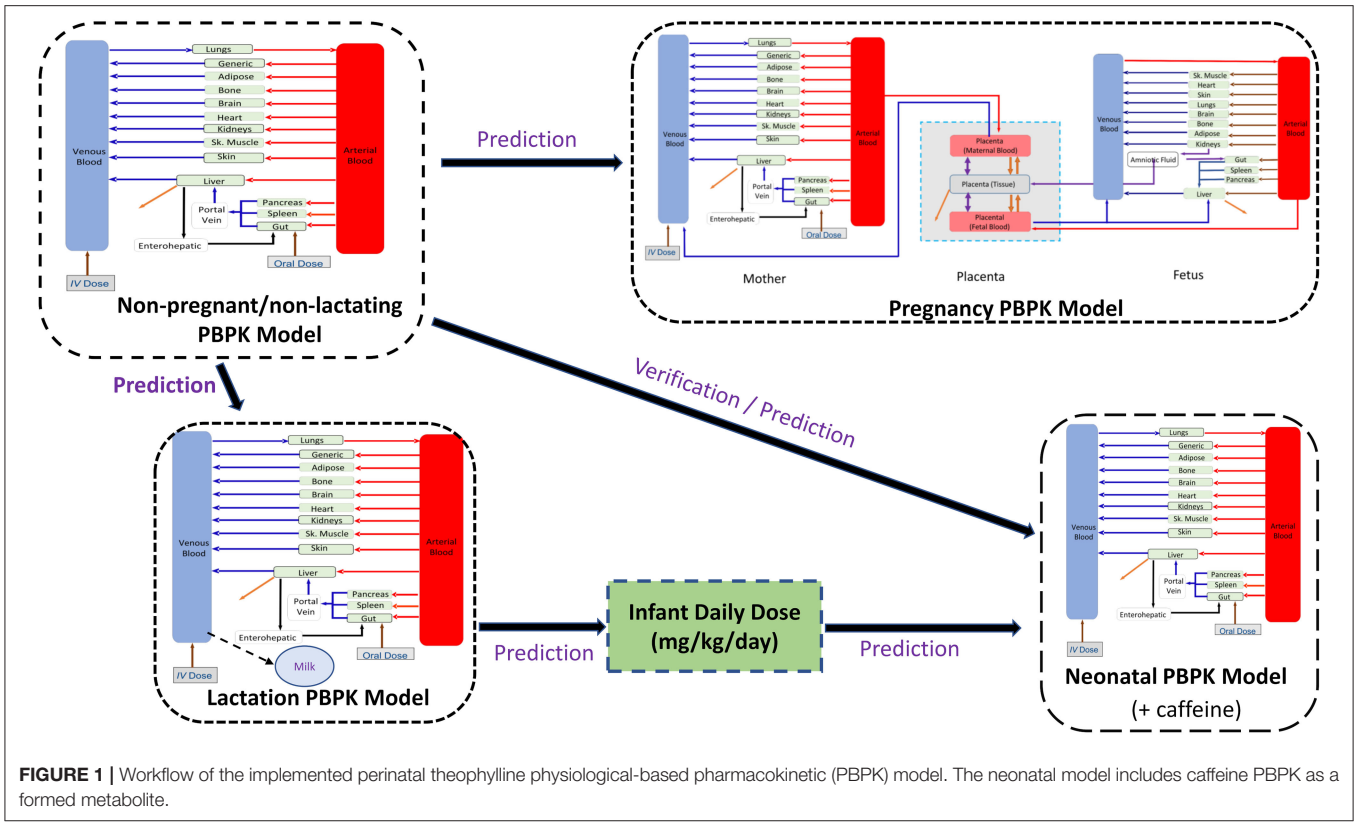


**FIGURE 1 |** Workflow of the implemented perinatal theophylline physiological-based pharmacokinetic (PBPK) model. The neonatal model includes caffeine PBPK as a formed metabolite.

theophylline in non-pregnant subjects was mainly by CYP 1A2 (∼88% of hepatic metabolism) and CYP2E1 (∼12% of hepatic metabolism) with minor contributions (<1%) from CYP2D6 and CYP3A4). Assignment of the contribution of individual CYP isozymes to the metabolism of theophylline was made based on published data (25, 26). The adequacy of these parameters to predict theophylline PK in non-pregnant subjects was assessed by comparison with observed data in non-pregnant populations after intravenous and oral administrations. The compound PBPK model was then used to simulate theophylline PK in the pregnancy, lactation, and neonatal PBPK models. In these simulations, the input parameters for theophylline were not modified with the exception of the inclusion of a metabolic pathway resulting in the formation of caffeine in neonatal subjects that is not observed in adult subjects (27, 28) (**Supplementary Table 1**). In addition, a first-order absorption model was used in the preterm subjects as the mechanistic absorption model used in the other populations has not been implemented in the software for preterm subjects due to a paucity of appropriate physiological gut data to parametrize the more complex absorption model in preterm subjects. Other physiological changes in the PBPK model were accounted for in pregnant women and neonatal subjects (see following sections for details).

## Theophylline PK in Non-Pregnant Population

The following virtual trial settings were used for non-pregnant subjects after either intravenous or oral administrations:

*Trial design NP1* (model building)*:* Single intravenous infusion of 4.5 mg/kg theophylline administered over 30 min (24); 20 trials of 14 (0% women) subjects aged 19–35 years.

*Trial design NP2:* Single intravenous infusion of 7.3 mg/kg theophylline administered over 30 min (19); 20 trials of 20 (50% women) subjects aged 24–57 years.

*Trial design NP3:* Single intravenous infusion of 240 mg theophylline administered over 45 min (29); 20 trials of 10 (100% women) subjects aged 22–26 years.

*Trial design NP4:* Single intravenous infusion of 151.2 mg theophylline administered over 20 min (30); 20 trials of 13 (0% women) subjects aged 20–39 years.

*Trial design NP5:* Single oral doses of 3.4 mg/kg theophylline (31); 20 trials of 10 (56% women) subjects aged 18–36 years.

*Trial design NP6:* Single oral dose of 5 mg/kg theophylline solution (32); 20 trials of 12 subjects (0% women) aged 23–39 years.

*Trial design NP7:* Single oral dose of 5 mg/kg theophylline solution (33); 20 trials of 10 (50% women) subjects aged 22–35 years.

*Trial design NP8:* Single oral dose of 7.6 mg/kg theophylline (19); 20 trials with 10 (50% women) subjects aged 22–57 years in each trial.

*Trial design NP9:* Single ascending oral dose of 125, 250, 375, and 500 mg theophylline tablet (34); 20 trials of 10 (50% women) subjects aged 22–35 years in each trial.

## Theophylline PK During Pregnancy

The changes in maternal physiology during pregnancy have been described in detail previously (3). The main physiological changes affecting the clearance of theophylline during pregnancy are the changes in CYP1A2 and CYP2E1 activity and renal GFR during pregnancy. These changes were described in the PBPK model using the following functions:

$$CYP1A2_{preg} = CYP1A2_{(0)} \left(1 - 0.02552\, GW + 0.0002\, GW^2\right)$$

$$CYP2E1_{preg} = CYP2E1_{(0)} \left(1 + 0.012\, GW + 0.0002\, GW^2\right)$$

$$GFR_{pred}\left(\frac{mL}{\min}\right) = GFR_{(0)} \left(1 + 0.028392\, GW - 0.000502\, GW^2\right)$$

where $CYP1A2_{(0)}$, $CYP2E1_{(0)}$, and $GFR_{(0)}$ are the baseline values in non-pregnant women. Values for individual subjects *i*, are generated from a mean value and %CV using lognormal distribution, GW is the gestational week. These equations, except CYP2E1, have been described previously (3, 35). The change of CYP2E1 activity during pregnancy used in this study was derived based on the difference in the longitudinal *unbound* oral clearance of theophylline observed during pregnancy and the predicted *unbound* clearance from the PBPK model without CYP2E1 changes being incorporated (**Supplementary Figure 1**). Due to the absence of systemic clearance at different gestational weeks, the oral clearance was used as the bioavailability of theophylline was reported to be complete, i.e., F = 1 (19). Exposure in the fetus was simulated to occur *via* a placental permeability-limited model as described previously (36). In the current work, the fetal model was extended to 14 compartments representing various fetal tissues and linked to the maternal full-PBPK model *via* the placenta, which in turn was represented by three compartments (**Figure 1**). Growth of the fetus and fetal tissues, tissue blood flows, and binding proteins were all dynamic within the model according to previously published relationships (37–40). Physiological changes to the placenta, including its size and blood flow on the maternal and fetal sides, were also included in the model (35, 40). More details on the fetoplacental model assumptions and application have been described elsewhere (41).

This maternal-fetal model allows the prediction of fetal exposure. A value for theophylline transplacental clearance ($CL_{PD}$) obtained from an *ex vivo* experiment of 2.59 mL/min/cotyledon (42) was included in the PBPK model to predict umbilical cord exposure. The *in vitro* value was scaled to give a $CL_{PD}$ value in (L/h/g tissue) as described below using the reported cotyledon weight of 22 g reported in the same experiment (42):

$$Placenta\ CL_{PD} = \frac{2.59\ (mL/\min)}{22\ (g)}\ 60/1000 = 0.0071\ L/h/g\ tissue$$

This $CL_{PD}$ of *0.0071 L/h/g tissue* was used as a model input parameter to parametrize the passive diffusion clearances on both sides of the placenta assuming a placental density of 1 g/ml. In addition, to predict the amniotic exposure of theophylline, the fetal renal clearance (*fetal* $CL_R$) was calculated based on fetal GFR of 4.9 ml/min (43) with reference to a typical adult GFR value of 121 mL/min (44) and the adult theophylline renal clearance of 0.31 L/h (see **Supplementary Table 1**) according to the following equation

$$fetal\ CL_R\left(L/h/kg\right) = \left(\frac{Adult\ CL_R\ (L/h)}{Fetal\ Bodyweight(Kg)}\right)\left(\frac{fetal\ GFR\ (mL/min)}{Adult\ GFR\ (mL/min)}\right)$$

Clearances between the fetal tissue and amniotic fluid, as well as fetal swallowing, were accounted for in the fetal PBPK model as described previously (41). The full list of the model input parameters is available in **Supplementary Table 1**.

The following trial designs were set for model prediction during pregnancy to match the clinical studies after oral administration of theophylline:

*Trial design P1:* Multiple oral doses of 259 mg theophylline for 5 days (45); 20 trials of 10 pregnant women aged 19–31 years at 13–19 GWs.

*Trial design P2:* Multiple oral doses of 259 mg theophylline for 5 days (45); 20 trials of 10 pregnant women aged 19–31 years at 23–28 GWs.

*Trial design P3:* Multiple oral doses of 259 mg theophylline for 5 days (45); 20 trials of 10 pregnant women aged 19–31 years at 34–39 GWs.

*Trial design P4:* Multiple oral doses of 259 mg theophylline for 5 days (46); 20 trials of 10 pregnant women aged 20–31 years at 37–40 GWs.

*Trial design P5:* Multiple oral doses of 160 mg theophylline every 6 h for 3 days (47); 20 trials of 10 pregnant women aged 19–31 years at 34–39 GWs.

*Trial design P6:* Multiple oral doses of 100 mg theophylline every 12 h for 3 days (48); 20 trials of 10 pregnant women aged 18–45 years at 40 GWs.

## Theophylline PK During Lactation

Due to an absence of information on the milk composition of the nursing mothers included in the clinical studies, two empirical models (I and II; see below for detailed equations) were used to predict the theophylline milk-to-plasma (M/P) ratio assuming a mature milk composition (8) and the average value of milk:plasma ratio (M/P) was used in the simulations (see Discussion section).

Model I (14, 49):

$$M/P = \frac{fu_p fu_p^{un}}{fu_{mk}^{un}} \frac{1}{fu_{mk}\left(\frac{1}{1+f_{fat}\,(fu_{mk}Papp_{milk}-1)}\right)}$$

Model II (14):

$$\ln M/P = -0.405 + 9.36\,\ln(Mu/Pu) - 0.69\,\ln fu_p - 1.54\,InK$$

where,

$$K = ((1 - f_{fat})/fu_{mk}) + f_{fat} \cdot Papp_{milk}$$
$$Papp_{milk} = 10^{(-0.88+1.29\ LogD_{7.2})}$$

$fu_p$ is the individualized unbound fraction of the drug in the maternal plasma, $f_{fat}$ is the fractional volumes of fat components in the milk, sampled from a population mean of 6.2 g/100 ml of milk and distribution (33% CV) using a lognormal distribution. $LogD_{7.2}$ is the apparent milk fat-to-skimmed milk partition at pH 7.2 (14). This value is predicted from the theophylline octanol-to-water partitioning ratio ($LogP_{o:w}$) accounting for ionization at pH = 7.2. $fu_{mk}$ is the individualized unbound fraction of the drug in the milk calculated using the following equation (50):

$$fu_{mk} = \frac{{fu_p}^{0.448}}{0.000694^{0.448} + {fu_p}^{0.448}}$$

$Mu/Pu$, is the ratio of the unionized fraction of the drug in plasma, $f_p^{un}$, to the unionized fraction of the drug in milk, $f_{mk}^{un}$. $f_p^{un}$, is calculated using the compound pKa(s) and the plasma pH. According to the following equations:

$$f_p^{un} = \frac{1}{1 + 10^{(pKa2-pKa1)} + 10^{(pH_{plasma}-pKa1)} + 10^{(pKa2-pH_{plasma})}}$$

$$f_{mk}^{un} = \frac{1}{1 + 10^{(pKa2-pKa1)} + 10^{(pH_{Milk}-pKa1)} + 10^{(pKa2-pH_{Milk})}}$$

Where the pH of the milk is a physiological parameter (milk pH = 7.0) (8).

Using the average milk to plasma ratio, the milk level of theophylline after single and multiple dosing in the mother was simulated. Predicted infant daily doses were calculated using the predicted theophylline average ($C_{avg,ss}$) and maximum ($C_{max,ss}$) concentration in milk at a steady state.

*Trial design L1:* Multiple oral doses of 259 mg theophylline for 5 days (45); 20 trials of 10 nursing mothers aged 19–31 years in each trial.

*Trial design L2:* Single intravenous dose of 4.25 mg/kg infused over 20 min (51); 20 trials of 10 nursing mothers aged 19–31 years in each trial.

*Trial design L3:* Oral doses of 300 mg theophylline followed by 200 mg after 4 h (52); 20 trials of 12 nursing mothers aged 20–40 years old.

## Theophylline PK in Neonates

For assessment of theophylline neonatal exposure from milk, the calculated infant daily dose was used as an input for the neonatal PBPK model. Simulations were conducted in both full-term and preterm neonatal subjects. The physiology of the preterm PBPK model includes age-dependent changes in physiology, including parameters relevant to theophylline elimination such as renal function, and CYP1A2 ontogeny (53). The ontogeny of CYP2E1 has not been quantified in preterm individuals so the ontogeny in preterm subjects was assumed to be the same as in the full-term subjects (54). Therefore, the following equations were used to describe the age-related changes in theophylline clearance:

$$GFR_{preterm}\ (mL/\min) = 121\left(\frac{PMA^{3.4}}{0.923^{3.4} + PMA^{3.4}}\right)\left(\frac{weight}{70}\right)^{0.75}$$

$$CYP1A2_{preterm}\ (fraction\ of\ adult) = 0.81 + PMA^{5.2}$$

$$CYP2E1_{preterm}\ (fraction\ of\ adult) = \frac{0.99\ x\ (PNA/52)^{0.5}}{0.23^{0.5} + (PNA/52)^{0.5}}$$

where PMA is the postmenstrual age in years, and PNA is the postnatal age in weeks converted to years *via* dividing by 52 weeks.

Theophylline undergoes an additional metabolic process in preterm neonates resulting in the formation of caffeine (27). This metabolic pathway does not occur in adults and the pathway is therefore not included in the adult model. The pathway leading to caffeine formation was accounted for in the preterm neonatal PBPK model as described below with no further ontogeny of the pathway being considered in the liver. A previously verified caffeine PBPK model (53) was included in the preterm neonatal model as a metabolite of theophylline and was used to optimize the intrinsic clearance of theophylline to caffeine by comparison of the simulated with the observed caffeine levels in preterm neonates after intravenous (28) and oral administration (55) of theophylline. A scaling factor of 20-fold for the conversion of theophylline to caffeine in the gut was required to describe the observed exposure of theophylline, but also the formed caffeine checked during the exercise, after oral administration. Sensitivity analysis for this intestinal metabolism scalar is given in **Supplementary Figure 4**. The caffeine metabolite model was retained in the PBPK model for all neonatal simulations. A list of preterm PBPK model inputs for theophylline and caffeine is given in **Supplementary Tables 1**, **2**. To account for fast developmental changes in the preterm physiology, the time-varying covariates option within the Simulator was used (56).

The following simulations were conducted for the neonatal model building and performance verification:

*Trial design N1* (model building)*:* An intravenous loading dose of 5.5 mg/kg theophylline infused over 20 min followed by multiple intravenous doses every 12 h of 1.1 mg/kg infused over 1 h for 7 days (28); 20 trials of 10 (20% women) preterm neonates aged 0–3 postnatal weeks and their gestational weeks ranged between 27 and 32 weeks. The systemic concentration profiles were followed for 14 days from the first dose.

*Trial design N 2:* a single IV bolus of 1.2 mg/kg of theophylline to produce the same initial plasma concentration in the neonatal PBPK model that was observed in the umbilical cord plasma at birth (48); 20 trials of 10 full-term neonates at birth (0 h PNA).

*Trial design N 3:* a single IV infusion of 4 mg/kg theophylline for 20 min (57); 20 trials of 10 (50% women) preterm neonates aged 3–15 days and GWs of 27.5 weeks.

*Trial design N 4* (model building): a loading oral dose of 5 mg/kg theophylline then 1.25mg/kg orally every 6 h (55); 20 trials of 14 (50% women) preterm neonates aged 85 h and their gestational weeks ranged between 25 and 34 weeks.

*Trial design N5:* Single oral dose of 5.6 mg/kg theophylline solution (58); 20 trials of 10 (50% women) preterm neonates aged 0–4 postnatal weeks and their gestational weeks ranged between 29 and 36 weeks.

*Trial design N6*: a loading oral dose of 5 mg/kg theophylline followed by 8 doses of 2.3 mg/kg every 12 h [subject Sch in (58)]; 20 trials of 10 (50% women) preterm neonates aged 2–28 days and 34 gestational weeks. A similar experimental design was used but with 7 doses of 2 mg/kg every 12 h [subject C in (58)].

*Trial design N7:* Multiple oral doses of 1.25 mg/kg theophylline every 6 h (27); 20 trials of 10 (30% women) preterm neonates aged 1–9 days with their gestational weeks ranging between 26 and 33 weeks.

*Trial design N8:* A loading dose of 5 mg/kg theophylline infused over 30 min followed by 1 h-infusion of 1.1 mg/kg/12 h in 28 (A), 32 (B), and 38 (C) GWs neonates at birth. This replicates the study design reported by Bonati et al. (28).

*Trial design N9:* Multiple oral doses of the predicted average infant daily dose divided into 6 daily doses. This dosing pattern resembles the frequency of feeding for breastfed babies. Dosing was repeated for 14 consecutive days; 20 trials of 20 (50% women) neonates at birth, either 28, 32, or 38 GWs (three scenarios). In this trial, a single intravenous loading dose of 4.2 mg/kg (for a 28 GWs group), 4.5 mg/kg (for a 32 GWs group), and 4.8 mg/kg (for a 38 GWs group) was administered over 10 s to produce an initial systemic concentration of 10 mg/L, the same concentration as was observed in the cord plasma at birth.

*Trial design N10:* Multiple oral doses of the predicted maximum infant daily dose divided into 6 daily doses. This dosing pattern resembles the frequency of feeding for breastfed babies. Dosing was repeated for 7 14 consecutive days; 20 trials of 20 (50% women) neonates at birth, either 28, 32, or 38 GWs (three scenarios). A single intravenous loading dose as described in *Trial design N9* was used here as well to give an initial plasma concentration the same as that observed in the cord plasma at birth.

*Trial design N11:* Same design as in *Trial design N10*, but without any loading dose.

## Assessment Criteria

Dependent on data availability, the predicted PK profiles and/or PK parameters were compared with different sets of clinical observations available in the literature. The PBPK model predictions were considered successful and acceptable if the observed PK profile fell within the 95th and 5th percentile of predicted data and the predicted PK parameters fell within 0.5- to 2-fold of the observed data.

# RESULTS

Theophylline simulations for the baseline model in non-pregnant subjects are shown in **Figure 2**. The PBPK model predictions agreed with the observed mean profiles in different studies after intravenous and oral administrations. The predicted mean concentration profile follows the same shape as the observed mean concentration profiles and the observed data fell within the simulated 5th−95th prediction interval. A comparison of the predicted PK parameters in the non-pregnant population with those available from the clinical studies is shown in **Table 1**.

The PBPK model predictions during the different trimesters of pregnancy are shown in **Figure 3**. The predicted data agree with the observed data within the pre-defined success criteria. Limited observed data were available for theophylline exposure during delivery. However, the predicted plasma and umbilical cord concentrations of theophylline during labor agreed with the reported observed concentrations (**Figure 3**). The model predicted a mean cord-to-plasma AUC ratio of 1 ± 0.1 (range: 0.8–1.3) at a steady state. A comparison of the predicted PK parameters during pregnancy with those available from clinical studies is presented in **Table 1**.

Predicted postpartum theophylline concentrations in the maternal plasma were in good agreement with observations (**Figure 4**). Lactation empirical methods predicted different mean M/P ratios (0.49 for Model I and 0.87 for Model II; see **Supplementary Figure 3**), hence the mean value (0.68 ± 0.05) of these predicted ratios was used, which resulted in better. agreement with observations (**Figure 4**). For a preterm infant of 2 kg consuming 150 ml of milk/day, the lactation model predicted a relative infant daily dose (RID) of 12 ± 5% (5th−95th percentiles: 5–20) using milk $C_{avg,ss}$, increasing to a RID of 17 ± 6% (5th−9th percentiles: 9–26) using milk $C_{max,ss}$. These RID values correspond to absolute values of 0.94 ± 0.4 (5th−95th percentiles: 0.4–1.61) mg/kg/day, and 1.4 ± 0.5 (5th−95th percentiles: 0.74–2.1) mg/kg/day for $C_{avg,ss}$ and $C_{max,ss}$ doses, respectively.

The preterm PBPK model replicated the observed exposure of theophylline and its metabolite caffeine after i.v. and oral doses (**Figure 5**). **Figure 6** shows the simulation results for systemic theophylline (and formed caffeine) exposure in neonates (of different gestational weeks) compared to the suggested theophylline therapeutic window for apnea (60). The doses in milk were divided equally into 6 daily oral doses to resemble a 4-h frequency pattern of breastfeeding after birth, i.e., $C_{avg,ss}$ dose was 0.157 mg/kg/4 h and $C_{max,ss}$ dose was 0.233 mg/kg/4 h. The concentration in the cord at birth was included as a baseline exposure to mimic the real clinical situation. Simulations were performed for a duration of 2 weeks. Within the PBPK model, the total doses and physiological parameters (including changes in body weight) were continually updated to account for neonatal growth and development over the 14-day simulation period. Predicted systemic exposure in neonates at birth with either 28, 32, or 38 GWs is shown in **Figure 6**.

In a preterm population of 32 GW at birth the predicted mean concentration of theophylline decreased from 7.7 (6–9.3) to 2.3 (1–4.3) mg/L [mean (5th−95th percentiles)] between day 1 and day 14 in subjects receiving the repeated $C_{avg,ss}$ dose. At the higher $C_{max,ss}$ dose the concentration of theophylline was simulated to decrease from 8.1 (6.3–9.8) to 3.4 (1.5–6.4) mg/L between day 1 and day 14.

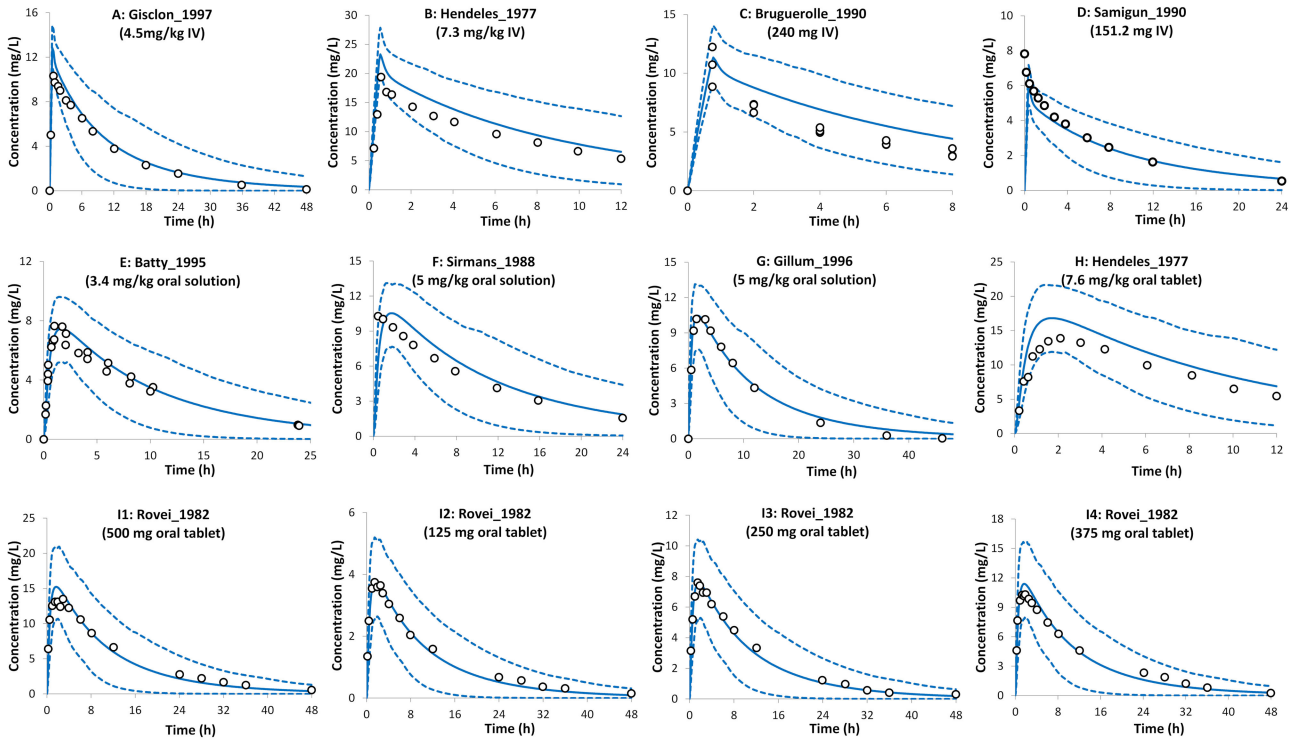


**FIGURE 2 |** Plasma concentration profiles after intravenous infusion and oral administration in the non-pregnant population. Solid lines, predicted means; Dashed lines, 5th and 95th centiles; Circles, observed means. **(A)** *Trial design NP1* (24), **(B)** *Trial design NP2* (19), **(C)** *Trial design NP3* (29), **(D)** *Trial design NP4* (30), **(E)** *Trial design NP5* (31), **(F)** *Trial design NP6* (32), **(G)** *Trial design NP7* (33), **(H)** *Trial design NP8* (19), and **(I1–I4)** *Trial design NP9* (34). See the Method section for trial settings.

## DISCUSSION

This work presented in this manuscript describes the use of a PBPK framework approach to describe the pharmacokinetics of a model drug (theophylline) during the perinatal period. Drug concentrations were predicted in the mother, the unborn fetus, and the neonatal subject post-delivery (**Figure 1**). Theophylline was chosen as a model drug based on the amount of data available for verification of model predictions and because it is often used to treat neonatal apnea.

The perinatal PBPK model presented here adequately predicted the observed exposure and kinetics of theophylline in non-pregnant, pregnant, lactating, and preterm populations. This type of simulation approach using a PBPK model allows drug concentrations to be predicted in populations of individuals that are otherwise difficult to study and also offers the possibility of supplementing sparse samples obtained in vulnerable populations with additional information, facilitating the design of future studies and also developing or refining hypotheses for future testing.

The PBPK model predictions for theophylline PK in the non-pregnant population after oral and intravenous administrations were in good agreement with observed values in different studies of variable dosing levels (**Figure 2** and **Table 1**). All PK parameters were within 2-fold of the observed values and predicted 5th and 95th percentiles for the systemic exposure in plasma including the observed concentration vs. time profiles. The predicted bioavailability in the model was $0.96 \pm 0.03$, which is in agreement with the observed value of $0.99 \pm 0.02$ (19).

The reduction of CYP1A2 activity that occurs during pregnancy (3, 61) together with the increase in renal function and CYP2E1 activity considered within the pregnancy PBPK model adequately described the changes in theophylline pharmacokinetics during the whole gestational period (**Figure 3**). The CYP2E1 activity was calculated to increase by 1.8-fold at term compared to the pre-pregnancy values. The values calculated in this study are in agreement with the observed 1.87-fold (62) and 1.79-fold (63) increase in acetaminophen clearance to its glutathione-derived conjugate in pregnant women at term. Acetaminophen glutathione conjugate formation has been proposed as a marker metabolic pathway for CYP2E1 activity.

The progression of gestation dynamically changes the contribution of the different elimination pathways to the overall clearance of theophylline (see **Supplementary Figure 2**). The pregnancy PBPK model predicted an overall 40% reduction in theophylline clearance at term from the non-pregnant clearance, which agrees with clinical data (**Table 1**). A potential weakness of the developed PBPK model is that no physiological changes to intestinal physiology during pregnancy were considered, however as there was good agreement between the predicted

**TABLE 1 |** Predicted vs. observed theophylline pharmacokinetics (PK) parameters in pre-pregnant, pregnant, breastfeeding, and neonatal populations.

| Population *N* (%Female) | Dose | CL (L/h)[a] | | | AUC (mg*h/L) | | | Cmax (mg/L) | | |
|---|---|---|---|---|---|---|---|---|---|---|
| | | Obs | PRED | Ratio | Obs | PRED | Ratio | Obs | PRED | Ratio |
| Non-Preg 14 (0%) | 4.5 mg/kg–30 min INF (24) | 2.84 ± 0.62 | 3.19 ± 1.8 | 1.12 | 126 ± 30 | 144 ± 72 | 1.14 | 10.7 ± 1.3 | 13.5 ± 1.2 | 1.26 |
| Non-Preg 20 (50%) | 7.3 mg/kg–30 min INF (19) | 2.53 | 3.02 (0.7–11) | 1.19 | 184 (95–287) | 232 (48–716) | 1.26 | NA | 23.3 (18.2–35.4) | NA |
| Non-Preg 9 (100%) | 240 mg–45 min INF (29) | 3.15 | 2.9 ± 1.6 | 0.92 | 76 ± 35 | 103 ± 48 | 1.36 | 10.7 | 11.3 ± 1.5 | 1.06 |
| Non-Preg 13 (0%) | 151.2 mg–20 min INF (30) | 2.8 ± 0.9 | 3.20 ± 1.80 | 1.14 | NA | 60 ± 31 | NA | NA | 6.01 ± 0.68 | NA |
| Non-Preg 9 (55.6%) | 3.4 mg/kg oral solution (31) | 2.96 | 3.2 ± 1.9 | 1.10 | 86.12 | 97.8 ± 48 | 1.14 | NA | 7.62 ± 1.2 | NA |
| Non-Preg 12 (0%) | 5 mg/kg—oral solution (32) | 3.18 ± 0.75 | 3.4 ± 2.0 | 1.06 | 134 ± 34 | 155 ± 79 | 1.15 | NA | 10.3 ± 1.6 | NA |
| Non-Preg 11 (0%) | 5 mg/kg—oral solution (33) | 3.2 ± 0.7 | 3.46 ± 2.1 | 1.08 | 140 ± 24 | 152 ± 79 | 1.09 | 10.9 ± 1.1 | 10.7 ± 1.6 | 0.98 |
| Non-Preg 10 (50%) | 6.7 mg/kg oral tablet (19) | 3.05 | 3.1 ± 1.8 | 1.02 | 173 (88–283) | 231 (54–738) | 1.34 | 15.3 (13–20) | 17.2 (11–23.4) | 1.12 |
| Non-Preg 8 (50%) | 125 mg oral tablet (34) | 2.7 (1.6–3.8) | 3.3 (0.80–10.8) | 1.22 | 52 (31–94) | 48.8 (12.0–157) | 0.94 | 4.1 (3.0–6.7) | 3.86 (2.3–6.7) | 0.94 |
| Non-Preg 8 (50%) | 250 mg oral tablet (34) | 2.54 (1.74–2.98) | 3.3 (0.80–11) | 1.3 | 106 (69–172) | 99 (23–316) | 0.93 | 8.0 (5.0–12.1) | 7.74 (4.5–13.34) | 0.97 |
| Non-Preg 8 (50%) | 375 mg oral tablet (34) | 2.6 (1.8–4.0) | 3.3 (0.80–10.6) | 1.27 | 161 (75–272) | 150 (35–479) | 0.93 | 10.5 (6.7–15.0) | 11.7 (6.81–20.1) | 1.11 |
| Non-Preg 8 (50%) | 500 mg oral tablet (34) | 2.54 (1.61–3.16) | 3.2 (0.78–10.5) | 1.26 | 210 (136–373) | 202 (48–643) | 0.96 | 15.1 (10.7–20.5) | 15.6 (9.1–27) | 1.03 |
| Preg 13–19 GWs 10 (100%) | 259 mg oral solution/12 h (45) | 2.61 ± 0.63 | 2.50 ± 1.3 | 0.96 | 99.23 | 127 ± 57 | 1.28 | NA | 14.6 ± 5.0 | NA |
| Preg 23–28 GWs 10 (100%) | 259 mg oral solution/12 h (45) | 2.85 ± 1.05 | 2.47 ± 1.3 | 0.87 | 90.88 | 131 ± 58 | 1.44 | NA | 14.7 ± 4.8 | NA |
| Preg 34–39 GWs 10 (100%) | 259 mg oral solution/12 h (45) | 2.1 ± 0.49 | 2.2 ± 1.0 | 1.04 | 123.3 | 142 ± 59 | 1.15 | NA | 15.3 ± 4.7 | NA |
| Lactation 10 (100%) | 259 mg oral solution/12 h (45) | 2.16 ± 0.81 | 3.0 ± 1.7 | 1.39 | 120 | 112 ± 55 | 0.93 | NA | 13.5 ± 4.7 | NA |
| Lactation 12 (100%) | 300 mg followed by 200 mg—oral (52) | NA | 3.0 ± 1.7 | NA | NA | NA | NA | NA | 10.5 ± 1.8 | NA |
| Preterm* 9 (30%) GW: 27–31; PNA: 0–1 | 5.5 mg/kg i.v followed by 1.1 mg/kg/12 h i.v. (28) | 14.5[#,a] | 11.2 ± 3.7[#] (4.91–25.3)** | 0.803 | NA | 118 ± 37 (46–233)** | NA | NA | 10.9 ± 3.3 (5.0—20)** | NA |
| Preterm* 6 (NA) GW: 27.5; PNA: 0.5–3 | 4 mg/kg infusion over 20 min (57) | 17.6** (12.1 – 25.9) | 25.9 ± 1.7 (22–31)** | 1.47 | NA | 155 ± 10 (128–184)** | NA | NA | 9.4 ± 0.24 (8.9–10.4)** | NA |
| Preterm* 15 (NA) GW: 25–34; PNA: 1–2 | (NA) (59) | 15.4 ± 6.8[#,a] (3.3–31.4) | 12.5 ± 4.7[#,a] (5.0–34) | 0.81 | NA | 99 ± 35 (32–232)** | NA | NA | 9.3 ± 2.9 (3.7–20)** | NA |
| Preterm* 11 (50%) GW = 32–36; PNA: 0.7–4 | 5.6 mg/kg /8 h oral Solution (58) | 28.3 ± 6.4[a] (20.1–40.1) | 25.9 ± 17.2[a] (6.9–123) | 0.92 | NA | 100 ± 37 (25–235)** | NA | 7 (6.4–8) | 6.8 (2.8–9.0) | 0.90 |

**Preterm: GW, gestational age in weeks; PNA, postnatal age in weeks, [a]preterm clearance unit is mL/h/kg, [#]blood clearance, ** range, NA, not mentioned. For preterm simulations, 50% of simulated subjects were female. For preterm AUC was calculated as the last $AUC_{tau}$.*

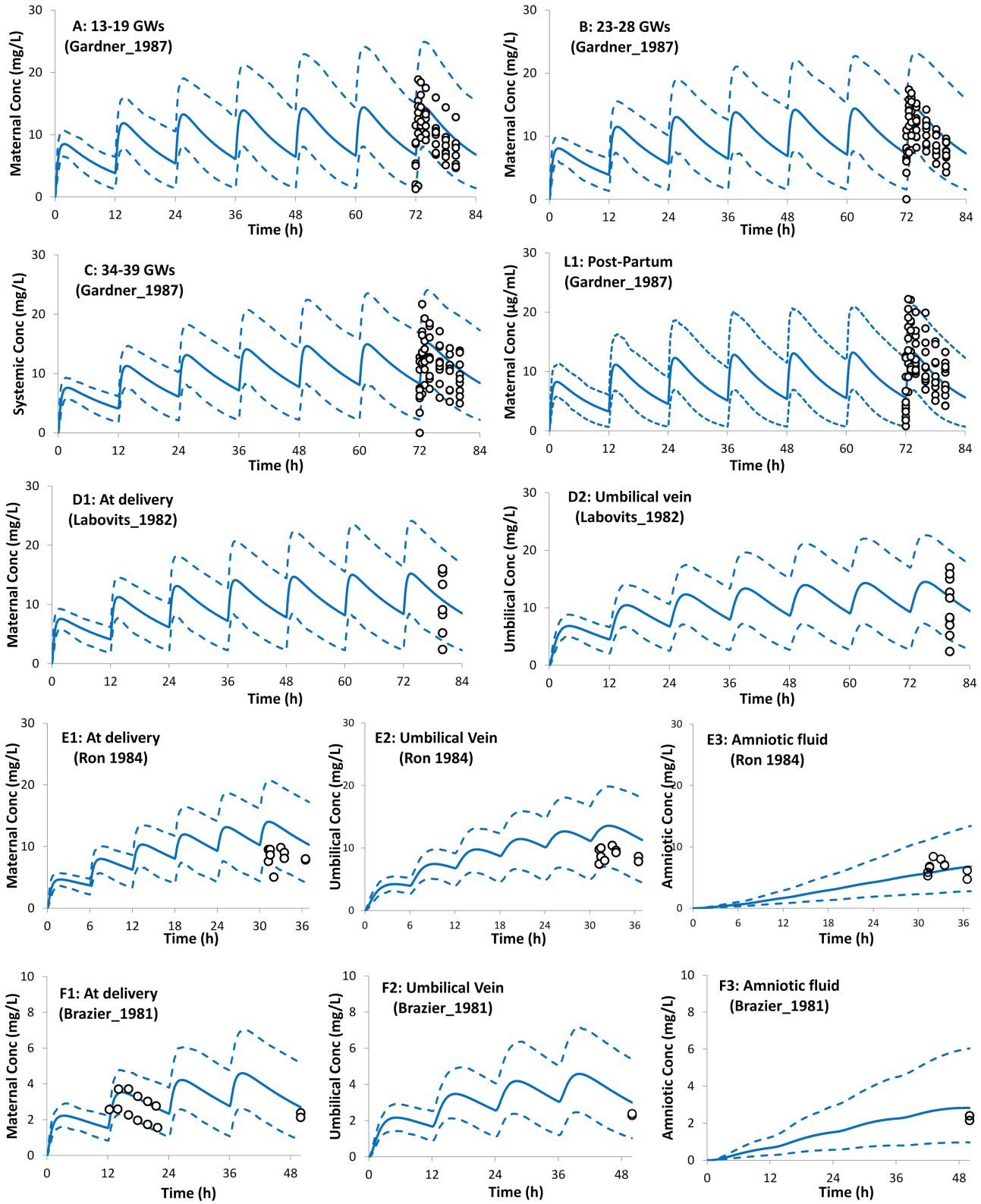


**FIGURE 3 |** Plasma concentration profiles after multiple oral administration in pregnant population during pregnancy and at delivery. Solid lines, predicted means; Dashed lines, 5th and 95th centiles; Circles, individual observations (open, maternal; filled, umbilical cord). Plots representing the following trials: **(A)** *Trial design P1* (45), **(B)** *Trial design P2* (45), **(C)** *Trial design P3* (45), **(L1)** *Trial design L1* (45) added here for comparison (see lactation section), **(D1,D2)** *Trial design P4* (46), **(E1–E3)** *Trial design P5* (47), and **(F1–F3)** *Trial design P6* (48). See the Method section for trial settings.

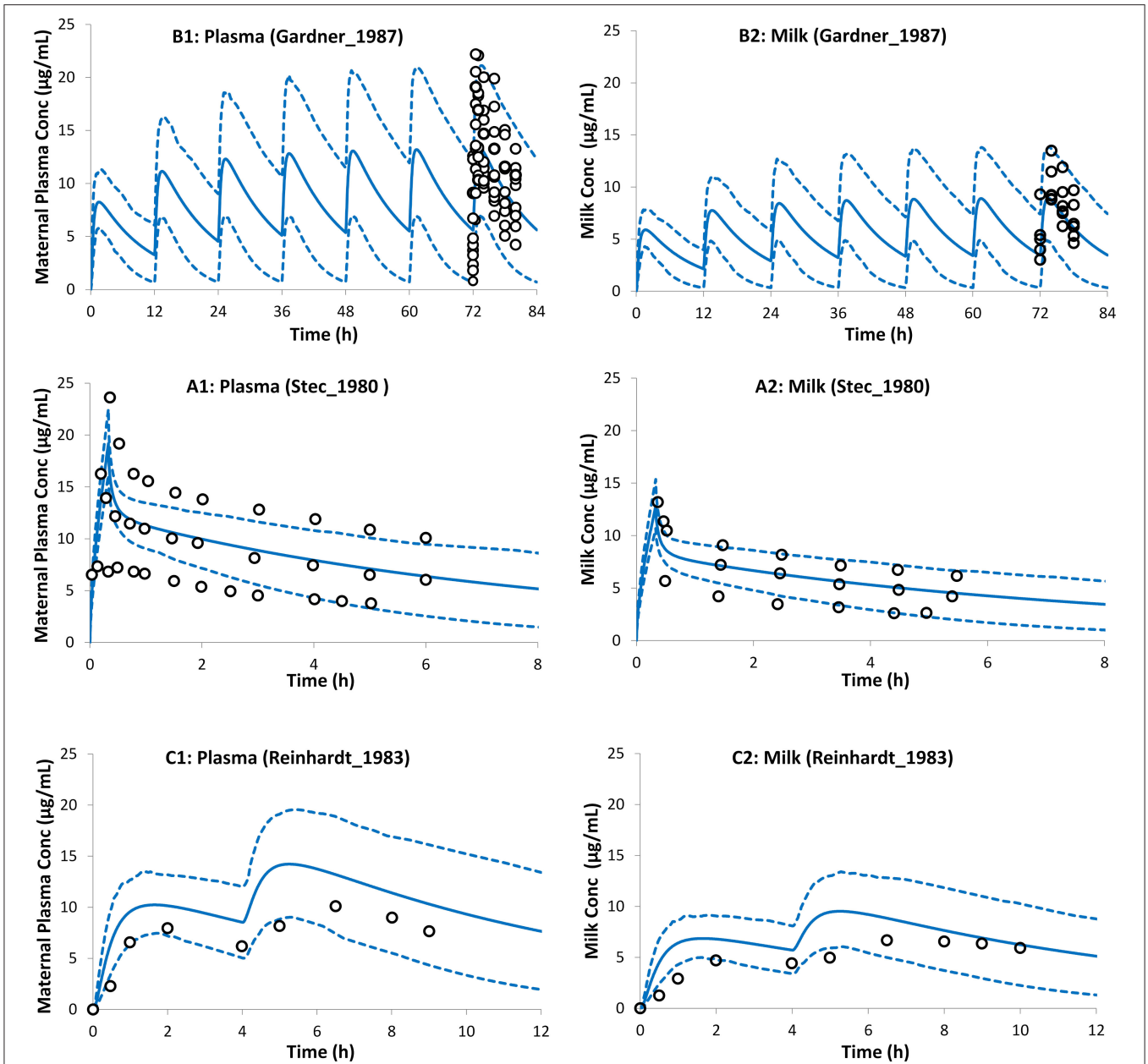


**FIGURE 4 |** Theophylline concentration profiles in maternal plasma (left) and the milk (right). Milk exposure was predicted using the average predicted M/P ratio from both lactation models (see Method section). Solid lines, predicted means; Dashed lines, 5th and 95th centiles; Circles, individual observations (open, maternal; filled, milk). **(A1,A2)** *Trial design L1* (45), **(B1,B2)** *Trial design L2* (51), and **(C1,C2)** *Trial design L3* (52). See the Method section for trial settings.

and observed theophylline concentrations at different gestational weeks Any pregnancy-related changes in intestinal physiology or enzyme levels appear to have minimal impact on theophylline pharmacokinetics. This can be partially explained by the minimal gut metabolism, Fg ∼1, and almost complete bioavailability, F ∼1.0, observed in non-pregnant subjects (19).

**Figure 3** shows that the incorporation of the theophylline transplacental clearance from an *ex vivo* experiment resulted in the adequate prediction of the theophylline umbilical cord level when compared to the observed values. The theophylline PBPK model predicted cord/maternal ratio based on AUC at steady-state is 1.0 (5th−95th percentiles: 0.86–1.2) and ranges from 0.8–1.3 in different virtual individuals. This is in line with the clinically reported ratio of unity from sparse data observed in 2 (64), 6 (65), 10 (47), and 12 (46) subjects at delivery. Because of the high transplacental passage of theophylline, toxicity in neonates at birth has been reported after multiple doses to the mother before delivery (66, 67).

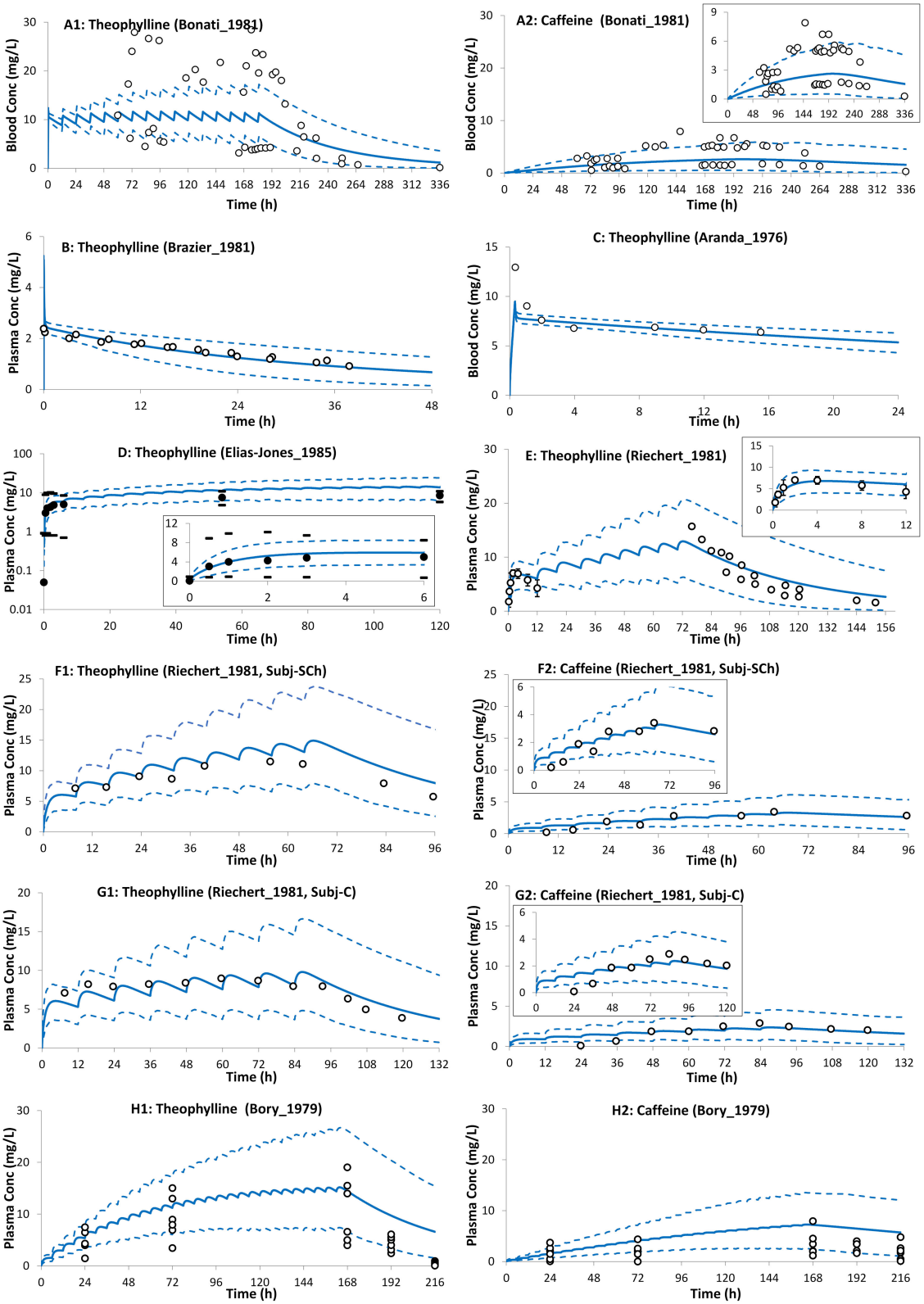


**FIGURE 5 |** Theophylline (and formed caffeine) concentration profiles in neonates after intravenous **(A–C)** and oral **(D–H)** administration of theophylline. Solid lines, predicted means; Dashed lines, 5th and 95th centiles; closed circles, individual observations; closed circles **(D,E)**, mean; dashes associated with observations in **(D)** represent reported ranges, and bars [**(E)**; till 12 h] represent SD. **(A1,A2)** *Trial design N1* (28), **(B)** *Trial design N2* (48), **(C)** *Trial design N3* (57), **(D)** *Trial design N4* (55), **(E)** *Trial design N5* (58), **(F1,F2)** *Trial design N6* (58) subject-Sch, **(G1,G2)** *Trial design N6* (58) subject-C, and **(H1,H2)** *Trial design N7* (27). See the Method section for trial settings.

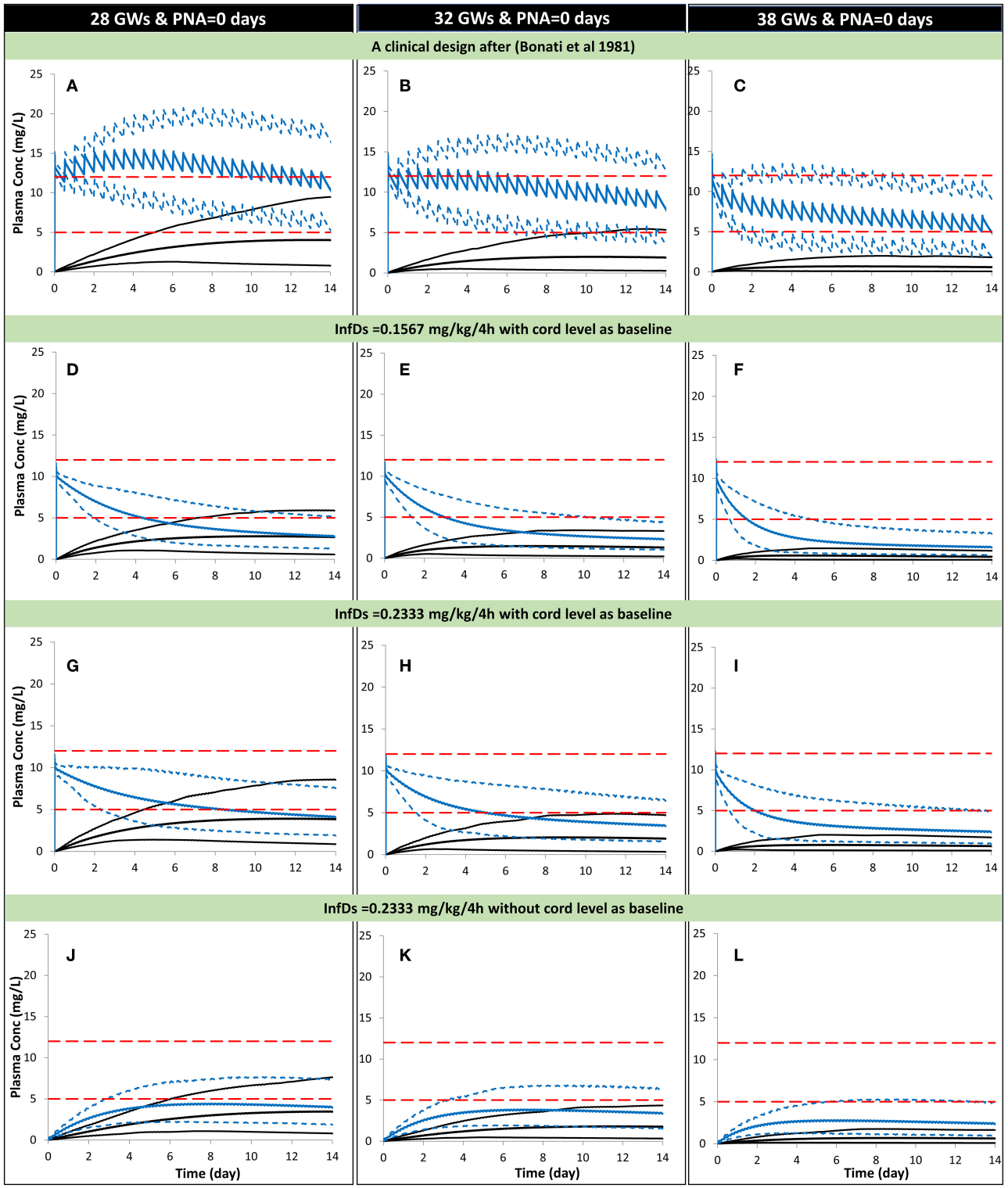


**FIGURE 6 |** Predicted mean (5th–95th percentiles) neonatal theophylline (and formed caffeine) concentration during the first 2 weeks of life with different gestational weeks. Predicted scenarios: The first three plots show, respectively, theophylline exposure in neonates at birth using a dosage of 30-min infusion of 5 mg/kg as a loading dose followed by 1 h-infusion of 1.1 mg/kg/12 h in 28 **(A)**, 32 **(B)**, and 38 **(C)** GWs according to a clinical study (28). Exposure after oral administration of the calculated theophylline infant dose using milk $C_{avg,ss}$ are shown for 28 **(D)**, 32 **(E)**, and 38 **(F)** GW considering the cord level at birth as a baseline. Exposure after oral administration of the calculated theophylline infant dose using milk $C_{max,ss}$ are shown for 28 **(G)**, 32 **(H)**, and 38 **(I)** GW considering the cord level at birth as a baseline.

*(Continued)*

**FIGURE 6 |** Exposure after oral administration of the calculated theophylline infant dose using milk $C_{max,ss}$ are shown for 28 **(J)**, 32 **(K)**, and 38 **(L)** GW without considering the cord level at birth as a baseline. **(A–D)** *Trial design N8*, **(D–F)** *Trial design N9*, **(G–I)** *Trial design N10*, and plo **(J–L)** *Trial design N11*. See the Method section for trial settings. Dashed horizontal lines represent the theophylline therapeutic window for apnea. InfDs, infant dose predicted using the lactation model; GWs, gestational weeks; PNA, postnatal age. The lowest profiles in each plot represent the mean (5th−95th percentiles) for the formed caffeine.

Lactating mothers sometimes need to take medication whilst breastfeeding and are therefore confronted with a difficult choice to either discontinue breastfeeding or stop their medication to avoid potentially harmful effects on their breastfed children. The lack, or even the poor quality, of information about drug safety during lactation can cause confusion, which can result in the early cessation of breastfeeding (68). Different drugs (or environmental chemicals) will carry different levels of risks to the breastfed infant (69). Although these risks should not be exaggerated, since neonates and infants in most cases receive a much lower dose in breast milk, compared to the known safe dose of the same drug administered to them in clinical pediatric wards (70), there is still a possibility that some drugs could be harmful to breastfed children or may have not yet adequately been studied meaning that precautions should be taken. PBPK modeling offers one potential approach to address some of these questions. Another important aspect in this regard is to have quantitative information on drug exposure in breast milk both to verify the performance of PBPK models with a wider spectrum of compounds but also to allow the development of better algorithms with a wider domain of applicability to predict milk concentrations for drugs where quantitative measurements are lacking. Together the PBPK modeling approaches and quantitative information or prediction of milk concentrations have the potential to reduce the confusion and anxiety that lactating women may experience when making decisions about whether or not to take medication during breastfeeding, especially for those nursing mothers who are on chronic medication.

The reported theophylline elimination rate constant for the milk was $0.122 \pm 0.051\ h^{-1}$, which was not significantly different from that in plasma $0.123 \pm 0.041\ h^{-1}$ (52) indicating rapid equilibrium between the two matrices. Two different methods were used to predict the theophylline M/P ratio. These methods resulted in different predicted M/P ratios (0.49 for Model I and 0.87 for Model II; see **Supplementary Figure 3**). As a pragmatic approach the average M/P ratio of the 2 values, i.e., 0.68 (5%CV) was used to calculate the dose in the neonatal PBPK simulation. Studies with a larger set of compounds are needed to determine which of the methods or whether using an average value from the two methods would be the most appropriate approach for *a priori* prediction for a drug where the M/P ratio is unknown.

The average value for the M/P ratio used in the simulations reported here is in line with reported values in the literature from several different sources. For instance, an observed mean M/P ratio of 0.79 was reported by Gardner et al. (45), a range of values 0.6–0.89 was reported by Reinhardt et al. (52), an observed mean value of 0.67 was reported by Stec et al. (51), and a value of $0.57 \pm 0.14$ was reported by Oo et al. (71). The calculated absolute infant dose based on milk $C_{max,ss}$ was 1.4 $\pm$ 0.5 (5th−95th percentiles: 0.74–2.1) mg/kg/day. This dose is less than the loading intravenous dose of 5 mg/kg theophylline (28, 58, 60) and in line with the intravenous maintenance, dose using a 1-h infusion of 1.1 mg/kg/12 h (28) to treat apnea of prematurity. The individual maintenance dose is titrated to individual needs and some neonates may need maintenance doses as high as 4.4 mg/kg per day (60). Although the calculated dose from milk exposure is in line with the maintenance infusion dose used for apnea treatment, accumulation of theophylline can occur, especially in premature infants due to the lower capacity of their CYP1A2 clearance pathway, which can lead to adverse effects.

The neonatal PBPK model adequately described theophylline and its formed metabolite, caffeine, exposure after intravenous infusion, and after oral administration of theophylline (**Figure 5**). In contrast to a previously published theophylline PBPK in preterm neonates (72), the current model applied dynamic change in growth physiology, and utilized ontogeny functions to describe the maturation of CYP1A2 and CYP2E1 enzymes. In addition, the performance of the theophylline PBPK model in neonatal subjects was verified with multiple clinical studies. **Table 1** shows the predicted clearance in preterm subjects. The predicted values agreed with the observed values after intravenous (28, 57) and oral administration of theophylline (58). The contribution of the different elimination pathways to the clearance of theophylline at different gestational and postnatal ages is shown in **Supplementary Figure 5**.

The higher concentrations of caffeine compared to theophylline after the cessation of theophylline therapy were due to the (∼2- to 4-fold) slower elimination and continued formation of caffeine as theophylline was cleared (27, 58, 73). In the developed preterm PBPK model there is a futile recycling process occurring whereby theophylline is methylated to form caffeine that is subsequently demethylated to theophylline by CYP1A2 and CYP2E1.

The theophylline plasma levels in neonates (32GW) were simulated using the PBPK model with the dose based on the milk $C_{avg,ss}$, and $C_{max,ss}$ and the assumption that babies ingest about 150 mL/kg/day and that feeding is split over 6 sessions 4-h apart. Under these assumptions and using a bolus dose to set the initial concentration in neonatal plasma to be the same as the concentration in the cord blood at birth the theophylline concentrations were shown to remain within the therapeutic range for 2–4 days post-birth. The length of time the concentration stayed in the therapeutic range varied with the gestational age due to the elimination mechanisms of theophylline being immature at birth and varying with the gestational age of the neonates.

Within the PBPK model for the neonate subjects, the conversion of theophylline to caffeine was considered. But the

simulations showed that the caffeine levels predicted in the neonatal plasma of individuals who ingested theophylline *via* the milk were too low to exert a significant pharmacological effect. At therapeutic doses such as those used to treat apnea in very premature babies, the caffeine concentrations were at a level that may contribute to the pharmacological effect of theophylline (**Figure 6A**).

The infant's daily dose based on milk $C_{max,ss}$ with an administered volume of 150 mL of milk/day per kg infant bodyweight being ingested was used as a fairly conservative scenario in this analysis. In reality, the nursing mother may not start breastfeeding straight after birth or may not produce 150 mL of milk in the first few days post-partum. As the therapeutic window of theophylline is not well-defined for premature apnea the recommended range defined by Jones and Baillie was used for comparison with the simulated data in this study (60).

The theophylline level in milk or in the neonatal circulation can also be influenced by other intrinsic or extrinsic factors, such as co-medication, and/or disease. The maturation of theophylline elimination with age showed that the theophylline levels decline with age more rapidly in older newborns at 38 GWs compared with those born at 28 GWs (**Figure 6**).

While this work shows a case study of the application of the PBPK model during the perinatal period, there are limitations to the study. No attempt was made to include fetal metabolism in the maternal-fetal PBPK model due to a lack of data to parameterize the fetal metabolism model and verify the performance of the model. The contribution of fetal metabolism to the overall drug elimination is expected to be small for three reasons; (1) the transplacental passage of theophylline is high (cord/maternal ratio is ∼1) (2) the metabolism of theophylline in fetal liver explants (12–20 GWs) was slow ∼1.25 nmol/day (74), and (3) the reported absence of CYP1A2 protein in the fetal and neonatal livers (75). Theophylline PK data in the fetoplacental unit are limited to a few observations during delivery (46–48). There are limitations with the available data in that the dosing history prior to the studied doses at a steady state was not available during pregnancy and lactation. This makes accurate simulation of the clinical studies more difficult as some assumptions need to be made, i.e., the studied dosing regimen at steady-state and formulation was assumed since initiation of therapy (45, 46). In some studies where different subjects were studied after receiving a different number of doses and this information was not available, an average number of doses was assumed (47). The issue with incomplete dosing information was also encountered in some of the lactation studies, where three subjects were studied but only the dose range was reported (51). In another study, only a single profile from the 12 studied subjects was reported for the plasma and milk concentration profiles (52) making a meaningful comparison of the simulated and observed data difficult. In the lactation studies, information on milk pH and fat content were not available necessitating an assumption in the PBPK model that the milk composition was the same as that of mature milk. The lactation model used in this work assumes that a rapid equilibrium of drug concentrations exists between plasma and milk. This assumption was sufficient to describe theophylline exposure in the milk, but for other (more lipophilic) drugs the time course of drug concentrations in plasma and milk may not increase or decrease in parallel, and in these cases, the milk profiles cannot be explained with an assumption of rapid equilibration between the two phases.

The simulations in adult subjects were performed using a mechanistic absorption model (76). Due to a lack of detailed intestinal physiology in the preterm neonate, the same approach could not be used to model the absorption of theophylline in the neonate subjects. Therefore, a first-order absorption model was used in the preterm PBPK model. Although verification of the first-order absorption model in preterm studies was performed it would be preferable to have used the same absorption model for all of the different scenarios that were simulated.

The available preterm PK data were reported without the details of the postnatal and gestational ages for individual subjects and usually subjects with different gestational ages were lumped together in the reported data. This makes it difficult to simulate the studies with matched subjects (in terms of demographics). While there are multiple unpowered studies that have attempted to investigate theophylline pharmacokinetics in preterm individuals, to the best of our knowledge, longitudinal assessments of drug levels in this population after birth with or without considering the contribution of ingested drugs in the milk have not been reported in the literature. A further complication is that the observed data in the literature are usually reported from preterm subjects under treatment and as such the exposure information may also be influenced by co-morbidity and/or comedication factors. For example, the theophylline half-life was reported to be 39.4 h in a group of individuals co-dosed with betamethasone compared to a half-life of 61 h in the control group in two age-matched preterm groups of 29.6 gestational weeks and 1–3 days. Even after a few weeks of treatment, the theophylline half-life remained higher in the control group compared with the betamethasone treatment group, 31 vs. 19 h (77).

## CONCLUSION

A PBPK approach was adopted to evaluate the pharmacokinetics of theophylline from the general population and at different gestational weeks throughout pregnancy as well as in the plasma and milk of lactating women and in plasma from neonatal subjects. Utilizing a PBPK approach in special populations reinforces the utility of PBPK to assess pharmacokinetics in clinical settings where clinical data are limited and can be used to improve study design in these vulnerable populations.

## RESOURCE IDENTIFICATION INITIATIVE

The Simcyp Simulator V21 (Simcyp, RRID:SCR_003944) was used for the assessment of theophylline pharmacokinetics using the PBPK approach.

## DATA AVAILABILITY STATEMENT

The original contributions presented in the study are included in the article/**Supplementary Material**, further inquiries can be directed to the corresponding author/s.

## AUTHOR CONTRIBUTIONS

KA collected the data, analyzed the data, and wrote the manuscript. IG and MJ reviewed the manuscript. All authors contributed to the article and approved the submitted version.

## ACKNOWLEDGMENTS

We thank Eleanor Savill and Anna Kenworthy for their assistance with collecting the references and preparing the manuscript. The authors thank Dr. William J. Jusko (State University of New York, Buffalo) for providing theophylline clinical PK data used for model verification.

## SUPPLEMENTARY MATERIAL

The Supplementary Material for this article can be found online at: https://www.frontiersin.org/articles/10.3389/fped.2022.840710/full#supplementary-material

## REFERENCES

1. Jamei M, Dickinson GL, Rostami-Hodjegan A. A framework for assessing inter-individual variability in pharmacokinetics using virtual human populations and integrating general knowledge of physical chemistry, biology, anatomy, physiology and genetics: a tale of 'bottom-up' vs 'top-down' recognition of covariates. *Drug Metab Pharmacokinet.* (2009) 24:53–75. doi: 10.2133/dmpk.24.53
2. Tan ML, Zhao P, Zhang L, Ho YF, Varma MVS, Neuhoff S, et al. Use of physiologically based pharmacokinetic modeling to evaluate the effect of chronic kidney disease on the disposition of hepatic CYP2C8 and OATP1B drug substrates. *Clin Pharmacol Ther.* (2019) 105:719–29. doi: 10.1002/cpt.1205
3. Abduljalil K, Pansari A, Jamei M. Prediction of maternal pharmacokinetics using physiologically based pharmacokinetic models: assessing the impact of the longitudinal changes in the activity of CYP1A2, CYP2D6 and CYP3A4 enzymes during pregnancy. *J Pharmacokinet Pharmacodyn.* (2020) 47:361–83. doi: 10.1007/s10928-020-09711-2
4. Dallmann A, Himstedt A, Solodenko J, Ince I, Hempel G, Eissing T. Integration of physiological changes during the postpartum period into a PBPK framework and prediction of amoxicillin disposition before and shortly after delivery. *J Pharmacokinet Pharmacodyn.* (2020) 47:341–59. doi: 10.1007/s10928-020-09706-z
5. Robson SC, Boys RJ, Hunter S, Dunlop W. Maternal hemodynamics after normal delivery and delivery complicated by postpartum hemorrhage. *Obstet Gynecol.* (1989) 74:234–9.
6. Polepally AR, Pennell PB, Brundage RC, Stowe ZN, Newport DJ, Viguera AC, et al. Model-based lamotrigine clearance changes during pregnancy: clinical implication. *Ann Clin Transl Neurol.* (2014) 1:99–106. doi: 10.1002/acn3.29
7. Anderson PO, Momper JD. Clinical lactation studies and the role of pharmacokinetic modeling and simulation in predicting drug exposures in breastfed infants. *J Pharmacokinet Pharmacodyn.* (2020) 47:295–304. doi: 10.1007/s10928-020-09676-2
8. Abduljalil K, Pansari A, Ning J, Jamei M. Prediction of drug concentrations in milk during breastfeeding, integrating predictive algorithms within a physiologically-based pharmacokinetic model. *CPT Pharmacometrics Syst Pharmacol.* (2021) 10:878–89. doi: 10.1002/psp4.12662
9. Salem F, Johnson TN, Abduljalil K, Tucker GT, Rostami-Hodjegan A. A re-evaluation and validation of ontogeny functions for cytochrome P450 1A2 and 3A4 based on *in vivo* data. *Clin Pharmacokinet.* (2014) 53:625–36. doi: 10.1007/s40262-014-0140-7
10. Allegaert K, Simons SHP, Tibboel D, Krekels EH, Knibbe CA, van den Anker JN. Non-maturational covariates for dynamic systems pharmacology models in neonates, infants, and children: filling the gaps beyond developmental pharmacology. *Eur J Pharm Sci.* (2017) 109S:S27–31. doi: 10.1016/j.ejps.2017.05.023
11. Johnson TN, Bonner JJ, Tucker GT, Turner DB, Jamei M. Development and applications of a physiologically-based model of paediatric oral drug absorption. *Eur J Pharm Sci.* (2018) 115:57–67. doi: 10.1016/j.ejps.2018.01.009
12. Abduljalil K, Badhan RKS. Drug dosing during pregnancy-opportunities for physiologically based pharmacokinetic models. *J Pharmacokinet Pharmacodyn.* (2020) 47:319–40. doi: 10.1007/s10928-020-09698-w
13. Vinks AA, Barrett JS. Model-informed pediatric drug development: application of pharmacometrics to define the right dose for children. *J Clin Pharmacol.* (2021) 61(Suppl. 1):S52–9. doi: 10.1002/jcph.1841
14. Atkinson HC, Begg EJ. Prediction of drug distribution into human milk from physicochemical characteristics. *Clin Pharmacokinet.* (1990) 18:151–67. doi: 10.2165/00003088-199018020-00005
15. El-Khateeb E, Burkhill S, Murby S, Amirat H, Rostami-Hodjegan A, Ahmad A. Physiological-based pharmacokinetic modeling trends in pharmaceutical drug development over the last 20-years; in-depth analysis of applications, organizations, and platforms. *Biopharm Drug Dispos.* (2021) 42:107–17. doi: 10.1002/bdd.2257
16. Barrett JS, Della Casa Alberighi O, Laer S, Meibohm B. Physiologically based pharmacokinetic (PBPK) modeling in children. *Clin Pharmacol Ther.* (2012) 92:40–9. doi: 10.1038/clpt.2012.64
17. Abduljalil K, Pan X, Pansari A, Jamei M, Johnson TN. A preterm physiologically based pharmacokinetic model. Part I: physiological parameters and model building. *Clin Pharmacokinet.* (2020) 59:485–500. doi: 10.1007/s40262-019-00825-6
18. Pade D, Jamei M, Rostami-Hodjegan A, Turner DB. Application of the MechPeff model to predict passive effective intestinal permeability in the different regions of the rodent small intestine and colon. *Biopharm Drug Dispos.* (2017) 38:94–114. doi: 10.1002/bdd.2072
19. Hendeles L, Weinberger M, Bighley L. Absolute bioavailability of oral theophylline. *Am J Hosp Pharm.* (1977) 34:525–7. doi: 10.1093/ajhp/34.5.525
20. Chirumamilla SK, Banala VT, Jamei M, Turner DB. Mechanistic PBPK modelling to predict the advantage of the salt form of a drug when dosed with acid reducing agents. *Pharmaceutics.* (2021) 13:1169. doi: 10.3390/pharmaceutics13081169
21. PubChem Theophylline. *PubChem*. Available online at: https://pubchem.ncbi.nlm.nih.gov/compound/Theophylline (accessed December 7, 2021).
22. Jain N, Yalkowsky SH. Estimation of the aqueous solubility I: application to organic nonelectrolytes. *J Pharm Sci.* (2001) 90:234–52. doi: 10.1002/1520-6017(200102)90:2andlt;234::AID-JPS14andgt;3.0.CO;2-V
23. Rodgers T, Rowland M. Physiologically based pharmacokinetic modelling 2: predicting the tissue distribution of acids, very weak bases, neutrals and zwitterions. *J Pharm Sci.* (2006) 95:1238–57. doi: 10.1002/jps.20502
24. Gisclon LG, Curtin CR, Fowler CL, Williams RR, Hafkin B, Natarajan J. Absence of a pharmacokinetic interaction between intravenous theophylline and orally administered levofloxacin. *J Clin Pharmacol.* (1997) 37:744–50. doi: 10.1002/j.1552-4604.1997.tb04362.x
25. Ha HR, Chen J, Freiburghaus AU, Follath F. Metabolism of theophylline by cDNA-expressed human cytochromes P-450. *Br J Clin Pharmacol.* (1995) 39:321–6. doi: 10.1111/j.1365-2125.1995.tb04455.x
26. Zhang ZY, Kaminsky LS. Characterization of human cytochromes P450 involved in theophylline 8-hydroxylation. *Biochem Pharmacol.* (1995) 50:205–11. doi: 10.1016/0006-2952(95)00120-O

27. Bory C, Baltassat P, Porthault M, Bethenod M, Frederich A, Aranda JV. Metabolism of theophylline to caffeine in premature newborn infants. *J Pediatr.* (1979) 94:988–93. doi: 10.1016/S0022-3476(79)80246-2
28. Bonati M, Latini R, Marra G, Assael BM, Parini R. Theophylline metabolism during the first month of life and development. *Pediatr Res.* (1981) 15(Pt. 1):304–8. doi: 10.1203/00006450-198104000-00003
29. Bruguerolle B, Toumi M, Faraj F, Vervloet D, Razzouk H. Influence of the menstrual cycle on theophylline pharmacokinetics in asthmatics. *Eur J Clin Pharmacol.* (1990) 39:59–61. doi: 10.1007/BF02657059
30. Samigun, M.ulyono, Santoso B. Lowering of theophylline clearance by isoniazid in slow and rapid acetylators. *Br J Clin Pharmacol.* (1990) 29:570–3. doi: 10.1111/j.1365-2125.1990.tb03681.x
31. Batty KT, Davis TM, Ilett KF, Dusci LJ, Langton SR. The effect of ciprofloxacin on theophylline pharmacokinetics in healthy subjects. *Br J Clin Pharmacol.* (1995) 39:305–11. doi: 10.1111/j.1365-2125.1995.tb04453.x
32. Sirmans SM, Pieper JA, Lalonde RL, Smith DG, Self TH. Effect of calcium channel blockers on theophylline disposition. *Clin Pharmacol Ther.* (1988) 44:29–34. doi: 10.1038/clpt.1988.108
33. Gillum JG, Sesler JM, Bruzzese VL, Israel DS, Polk RE. Induction of theophylline clearance by rifampin and rifabutin in healthy male volunteers. *Antimicrob Agents Chemother.* (1996) 40:1866–9. doi: 10.1128/AAC.40.8.1866
34. Rovei V, Chanoine F, Strolin Benedetti M. Pharmacokinetics of theophylline: a dose-range study. *Br J Clin Pharmacol.* (1982) 14:769–78. doi: 10.1111/j.1365-2125.1982.tb02035.x
35. Abduljalil K, Furness P, Johnson TN, Rostami-Hodjegan A, Soltani H. Anatomical, physiological and metabolic changes with gestational age during normal pregnancy: a database for parameters required in physiologically based pharmacokinetic modelling. *Clin Pharmacokinet.* (2012) 51:365–96. doi: 10.2165/11597440-000000000-00000
36. Zhang Z, Unadkat JD. Development of a novel maternal-fetal physiologically based pharmacokinetic model II: verification of the model for passive placental permeability drugs. *Drug Metab Dispos.* (2017) 45:939–46. doi: 10.1124/dmd.116.073957
37. Abduljalil K, Johnson TN, Rostami-Hodjegan A. Fetal physiologically-based pharmacokinetic models: systems information on fetal biometry and gross composition. *Clin Pharmacokinet.* (2018) 57:1149–71. doi: 10.1007/s40262-017-0618-1
38. Abduljalil K, Jamei M, Johnson TN. Fetal physiologically based pharmacokinetic models: systems information on the growth and composition of fetal organs. *Clin Pharmacokinet.* (2019) 58:235–62. doi: 10.1007/s40262-018-0685-y
39. Abduljalil K, Jamei M, Johnson TN. Fetal physiologically based pharmacokinetic models: systems information on fetal blood components and binding proteins. *Clin Pharmacokinet.* (2020) 59:629–42. doi: 10.1007/s40262-019-00836-3
40. Abduljalil K, Pan X, Clayton R, Johnson TN, Jamei M. Fetal physiologically based pharmacokinetic models: systems information on fetal cardiac output and its distribution to different organs during development. *Clin Pharmacokinet.* (2021) 60:741–57. doi: 10.1007/s40262-020-00973-0
41. Abduljalil K, Pansari A, Ning J, Jamei M. Prediction of maternal and fetal acyclovir, emtricitabine, lamivudine, and metformin concentrations during pregnancy using a physiologically based pharmacokinetic modeling approach. *Clin Pharmacokinet.* (2022) doi: 10.1007/s40262-021-01103-0
42. Omarini D, Barzago MM, Bortolotti A, Lucchini G, Stellari F, Efrati S, et al. Placental transfer of theophylline in an *in vitro* closed perfusion system of human placenta isolated lobule. *Eur J Drug Metab Pharmacokinet.* (1993) 18:369–74. doi: 10.1007/BF03190187
43. Ezuruike U, Blenkinsop A, Pansari A, Abduljalil K. Quantification of fetal renal function using fetal urine production rate and its reflection on the amniotic and fetal creatinine levels during pregnancy. *Front Pediatr.* (2022) 10:841495. doi: 10.3389/fped.2022.841495
44. Rhodin MM, Anderson BJ, Peters AM, Coulthard MG, Wilkins B, Cole M, et al. Human renal function maturation: a quantitative description using weight and postmenstrual age. *Pediatr Nephrol.* (2009) 24:67–76. doi: 10.1007/s00467-008-0997-5
45. Gardner MJ, Schatz M, Cousins L, Zeiger R, Middleton E, Jusko WJ. Longitudinal effects of pregnancy on the pharmacokinetics of theophylline. *Eur J Clin Pharmacol.* (1987) 32:289–95. doi: 10.1007/BF00607577
46. Labovitz E, Spector S. Placental theophylline transfer in pregnant asthmatics. *JAMA.* (1982) 247:786–8. doi: 10.1001/jama.1982.03320310034024
47. Ron M, Hochner-Celnikier D, Menczel J, Palti Z, Kidroni G. Maternal-fetal transfer of aminophylline. *Acta Obstet Gynecol Scand.* (1984) 63:217–8. doi: 10.3109/00016348409155499
48. Brazier JL, Salle B. Conversion of theophylline to caffeine by the human fetus. *Semin Perinatol.* (1981) 5:315–20.
49. Fleishaker JC, Desai N, McNamara PJ. Factors affecting the milk-to-plasma drug concentration ratio in lactating women: physical interactions with protein and fat. *J Pharm Sci.* (1987) 76:189–93. doi: 10.1002/jps.2600760302
50. Atkinson HC, Begg EJ, Darlow BA. Drugs in human milk. Clinical pharmacokinetic considerations. *Clin Pharmacokinet.* (1988) 14:217–40. doi: 10.2165/00003088-198814040-00003
51. Stec GP, Greenberger P, Ruo TI, Henthorn T, Morita Y, Atkinson J Jr., et al. Kinetics of theophylline transfer to breast milk. *Clin Pharmacol Ther.* (1980) 28:404–8. doi: 10.1038/clpt.1980.180
52. Reinhardt D, Richter O, Brandenburg G. [Pharmacokinetics of drugs from the breast-feeding mother passing into the body of the infant, using theophylline as an example]. *Monatsschr Kinderheilkd.* (1983) 131:66–70.
53. Abduljalil K, Pan X, Pansari A, Jamei M, Johnson TN. Preterm physiologically based pharmacokinetic model. Part II: applications of the model to predict drug pharmacokinetics in the preterm population. *Clin Pharmacokinet.* (2020) 59:501–18. doi: 10.1007/s40262-019-00827-4
54. Tateishi T, Nakura H, Asoh M, Watanabe M, Tanaka M, Kumai T, et al. A comparison of hepatic cytochrome P450 protein expression between infancy and postinfancy. *Life Sci.* (1997) 61:2567–74. doi: 10.1016/S0024-3205(97)01011-4
55. Elias-Jones AC, Dhillon S, Greenough A. The efficacy of oral theophylline in ventilated premature infants. *Early Hum Dev.* (1985) 12:9–14. doi: 10.1016/0378-3782(85)90131-8
56. Abduljalil K, Jamei M, Rostami-Hodjegan A, Johnson TN. Changes in individual drug-independent system parameters during virtual paediatric pharmacokinetic trials: introducing time-varying physiology into a paediatric PBPK model. *AAPS J.* (2014) 16:568–76. doi: 10.1208/s12248-014-9592-9
57. Aranda JV, Sitar DS, Parsons WD, Loughnan PM, Neims AH. Pharmacokinetic aspects of theophylline in premature newborns. *N Engl J Med.* (1976) 295:413–16. doi: 10.1056/NEJM197608192950803
58. Riechert M, Lipowsky G, Stockl H, Stiegler H. [Pharmacokinetics of theophylline and caffeine in premature infants with apnea (author's transl)]. *Monatsschr Kinderheilkd.* (1981) 129:697–702.
59. Gal P, Boer HR, Toback J, Wells TJ, Erkan NV. Effect of asphyxia on theophylline clearance in newborns. *South Med J.* (1982) 75:836–8. doi: 10.1097/00007611-198207000-00017
60. Jones RA, Baillie E. Dosage schedule for intravenous aminophylline in apnoea of prematurity, based on pharmacokinetic studies. *Arch Dis Child.* (1979) 54:190–3. doi: 10.1136/adc.54.3.190
61. Tracy TS, Venkataramanan R, Glover DD, Caritis SN, National Institute for Child H, Human Development Network of Maternal-Fetal-Medicine U. Temporal changes in drug metabolism (CYP1A2, CYP2D6 and CYP3A Activity) during pregnancy. *Am J Obstet Gynecol.* (2005) 192:633–9. doi: 10.1016/j.ajog.2004.08.030
62. Miners JO, Robson RA, Birkett DJ. Paracetamol metabolism in pregnancy. *Br J Clin Pharmacol.* (1986) 22:359–62. doi: 10.1111/j.1365-2125.1986.tb02901.x
63. Kulo A, Peeters MY, Allegaert K, Smits A, de Hoon J, Verbesselt R, et al. Pharmacokinetics of paracetamol and its metabolites in women at delivery and post-partum. *Br J Clin Pharmacol.* (2013) 75:850–60. doi: 10.1111/j.1365-2125.2012.04402.x
64. Arwood LL, Dasta JF, Friedman C. Placental transfer of theophylline: two case reports. *Pediatrics.* (1979) 63:844–6. doi: 10.1542/peds.63.6.844
65. Romero R, Kadar N, Gonzales Govea F, Hobbins JC. Pharmacokinetics of intravenous theophylline in pregnant patients at term. *Am J Perinatol.* (1983) 1:31–5. doi: 10.1055/s-2007-1000048
66. Yeh TF, Pildes RS. Transplacental aminophylline toxicity in a neonate. *Lancet.* (1977) 1:910. doi: 10.1016/S0140-6736(77)91240-5
67. Agarwal HS, Nanavati RN, Bhagwat MS, Kabra NS, Udani RH. Transplancental aminophylline toxicity. *Indian Pediatr.* (1998) 35:467–70.

68. McClatchey AK, Shield A, Cheong LH, Ferguson SL, Cooper GM, Kyle GJ. Why does the need for medication become a barrier to breastfeeding? A narrative review. *Women Birth.* (2018) 31:362–6. doi: 10.1016/j.wombi.2017.12.004
69. Beauchamp GA, Hendrickson RG, Horowitz BZ, Spyker DA. Exposures through breast milk: an analysis of exposure and information calls to U.S. Poison Centers, 2001-2017. *Breastfeed Med.* (2019) 14:508–12. doi: 10.1089/bfm.2019.0075
70. Anderson PO, Manoguerra AS, Valdes V. A review of adverse reactions in infants from medications in breastmilk. *Clin Pediatr.* (2016) 55:236–44. doi: 10.1177/0009922815594586
71. Oo CY, Burgio DE, Kuhn RC, Desai N, McNamara PJ. Pharmacokinetics of caffeine and its demethylated metabolites in lactation: predictions of milk to serum concentration ratios. *Pharm Res.* (1995) 12:313–16. doi: 10.1023/A:1016207832591
72. Ginsberg G, Hattis D, Russ A, Sonawane B. Physiologically based pharmacokinetic (PBPK) modeling of caffeine and theophylline in neonates and adults: implications for assessing children's risks from environmental agents. *J Toxicol Environ Health A.* (2004) 67:297–329. doi: 10.1080/15287390490273550
73. Aranda JV, Turmen T, Sasyniuk BI. Pharmacokinetics of diuretics and methylxanthines in the neonate. *Eur J Clin Pharmacol.* (1980) 18:55–63. doi: 10.1007/BF00561479
74. Aranda JV, Louridas AT, Vitullo BB, Thom P, Aldridge A, Haber R. Metabolism of theophylline to caffeine in human fetal liver. *Science.* (1979) 206:1319–21. doi: 10.1126/science.515734
75. Sonnier M, Cresteil T. Delayed ontogenesis of CYP1A2 in the human liver. *Eur J Biochem.* (1998) 251:893–8. doi: 10.1046/j.1432-1327.1998.2510893.x
76. Jamei M, Turner D, Yang J, Neuhoff S, Polak S, Rostami-Hodjegan A, et al. Population-based mechanistic prediction of oral drug absorption. *AAPS J.* (2009) 11:225–37. doi: 10.1208/s12248-009-9099-y
77. Baird-Lambert J, Doyle PE, Thomas D, Jager-Roman E, Cvejic M, Buchanan N. Theophylline metabolism in preterm neonates during the first weeks of life. *Dev Pharmacol Ther.* (1984) 7:239–44. doi: 10.1159/000457170


**Conflict of Interest:** KA, IG, and MJ are paid employees of Certara UK Limited (Simcyp Division) and may hold shares in Certara.

frontiers | Frontiers in Pharmacology

ORIGINAL RESEARCH
published: 11 August 2022
doi: 10.3389/fphar.2022.842548

# Leveraging Predictive Pharmacometrics-Based Algorithms to Enhance Perinatal Care —Application to Neonatal Jaundice

*Gilbert Koch*[1,2]*, *Melanie Wilbaux*[1], *Severin Kasser*[3], *Kai Schumacher*[4], *Britta Steffens*[1,2], *Sven Wellmann*[2,3,4†] and *Marc Pfister*[1,2†]

[1]Pediatric Pharmacology and Pharmacometrics, University Children's Hospital Basel (UKBB), University of Basel, Basel, Switzerland, [2]NeoPrediX AG, Basel, Switzerland, [3]Division of Neonatology, University Children's Hospital Basel (UKBB), University of Basel, Basel, Switzerland, [4]Department of Neonatology, Hospital St. Hedwig of the Order of St. John of God, University Children's Hospital Regensburg (KUNO), University of Regensburg, Regensburg, Germany

OPEN ACCESS

**Edited by:**
Catherine M. T. Sherwin,
Wright State University, United States

**Reviewed by:**
Claudio Tiribelli,
Italian Liver Foundation ONLUS, Italy
Kathleen Job,
The University of Utah, United States
Giovanna Bertini,
Careggi University Hospital, Italy

***Correspondence:**
Gilbert Koch
gilbert.koch@ukbb.ch

[†]These authors have contributed equally to this work and share last authorship

**Specialty section:**
This article was submitted to Obstetric and Pediatric Pharmacology, a section of the journal Frontiers in Pharmacology

**Received:** 23 December 2021
**Accepted:** 16 June 2022
**Published:** 11 August 2022

**Citation:**
Koch G, Wilbaux M, Kasser S, Schumacher K, Steffens B, Wellmann S and Pfister M (2022) Leveraging Predictive Pharmacometrics-Based Algorithms to Enhance Perinatal Care—Application to Neonatal Jaundice. Front. Pharmacol. 13:842548. doi: 10.3389/fphar.2022.842548

The field of medicine is undergoing a fundamental change, transforming towards a modern data-driven patient-oriented approach. This paradigm shift also affects perinatal medicine as predictive algorithms and artificial intelligence are applied to enhance and individualize maternal, neonatal and perinatal care. Here, we introduce a pharmacometrics-based mathematical-statistical computer program (PMX-based algorithm) focusing on hyperbilirubinemia, a medical condition affecting half of all newborns. Independent datasets from two different centers consisting of total serum bilirubin measurements were utilized for model development (342 neonates, 1,478 bilirubin measurements) and validation (1,101 neonates, 3,081 bilirubin measurements), respectively. The mathematical-statistical structure of the PMX-based algorithm is a differential equation in the context of non-linear mixed effects modeling, together with Empirical Bayesian Estimation to predict bilirubin kinetics for a new patient. Several clinically relevant prediction scenarios were validated, i.e., prediction up to 24 h based on one bilirubin measurement, and prediction up to 48 h based on two bilirubin measurements. The PMX-based algorithm can be applied in two different clinical scenarios. First, bilirubin kinetics can be predicted up to 24 h based on one single bilirubin measurement with a median relative (absolute) prediction difference of 8.5% (median absolute prediction difference 17.4 µmol/l), and sensitivity and specificity of 95.7 and 96.3%, respectively. Second, bilirubin kinetics can be predicted up to 48 h based on two bilirubin measurements with a median relative (absolute) prediction difference of 9.2% (median absolute prediction difference 21.5 µmol/l), and sensitivity and specificity of 93.0 and 92.1%, respectively. In contrast to currently available nomogram-based static bilirubin stratification, the PMX-based algorithm presented here is a dynamic approach predicting individual bilirubin kinetics up to 48 h, an intelligent, predictive algorithm that can be incorporated in a clinical decision support tool. Such clinical decision support tools have the potential to benefit perinatal medicine facilitating personalized care of mothers and their born and unborn infants.

**Keywords: algorithm, prediction, jaundice, hyperbilirubinemia, mechanism-based modeling**

## INTRODUCTION

The field of medicine is undergoing a fundamental change in which artificial intelligence is connecting with diagnostic instruments, patient information systems and therapy management enabling unforeseen opportunities in transforming the health system towards a modern data-driven patient-oriented approach (Rajkomar et al., 2019). This paradigm shift also affects perinatal medicine as predictive algorithms and artificial intelligence are applied to enhance and individualize maternal, neonatal and perinatal care, with the goal not only to predict mortality (Mangold et al., 2021) but also to facilitate therapeutic decisions for our most vulnerable patients, fetuses and newborns, and their mothers.

In this work, we discuss a predictive algorithm in neonatology, with initial focus on hyperbilirubinemia, a medical condition affecting half of all newborns. Hyperbilirubinemia is a condition defined as elevated serum or plasma bilirubin levels above the reference range of the laboratory, and it is due to disorders or immaturity of bilirubin metabolism. In neonates, transient jaundice is a normal part of postnatal transition (Dennery et al., 2001). Bilirubin has strong antioxidant properties but when reaching too high levels, bilirubin can cross the blood-brain barrier and might cause bilirubin-induced neurotoxicity, of which kernicterus is the most dangerous form (Watchko and Tiribelli, 2013). Thus, medical screening of all neonates for hyperbilirubinemia is recommended to commence prompt therapy, namely phototherapy, once certain thresholds are crossed to prevent neurological complications (Watchko and Tiribelli, 2013). Up to 10% of neonates experience rebound hyperbilirubinemia, requiring re-initiation of treatment (So and Khurshid, 2021), and making hyperbilirubinemia the major reason for re-hospitalization in the first year of life (Schiltz et al., 2014).

Currently, static population-based nomograms for the assessment of neonatal hyperbilirubinemia are applied in daily clinical practice (Dennery et al., 2001). These nomograms are based on percentiles of bilirubin values at a given age in hours and classify neonates into risk groups. More recent risk stratification approaches include additional clinical factors for the prediction of neonatal hyperbilirubinemia shortly after birth (Castillo et al., 2018) or before discharge (Han et al., 2015). Even though approaches for risk stratification provide clinicians with a guideline for their assessment, adherence is only 50% due to cumbersome documentation (Tartaglia et al., 2013; Sampurna et al., 2018). Moreover, it has been found that health care professional noncompliance with best practices is the main reason for kernicterus in countries with highest health care standards (Alkén et al., 2019). Nomogram-based methods are overly general and do not provide an individual prediction of what will happen. Therefore, we aim for personalized prediction by identifying neonates at risk for clinically relevant hyperbilirubinemia more accurately, thus preventing the development of severe neonatal jaundice as well as overtreatment and unnecessary hospital stays.

Machine learning (ML) methods are computationally powerful tools for the analysis of large and heterogeneous datasets almost in real time (Koch et al., 2020a). Such methods can be applied for discriminating between classes or patient populations (e.g. high *vs*. low risk patient; treatment required yes or no) by identifying relevant variables (features) of interest. As such we recently developed a ML-based tool to predict the probability of whether a neonate will need a phototherapy treatment or not within the next 48 h (Daunhawer et al., 2019). Although this ML tool provides an innovative risk assessment regarding phototherapy requirement, this algorithm does not predict the dynamics of bilirubin kinetics, i.e., this ML algorithm is not able to predict bilirubin levels up to 24 h or 48 h.

Complementary to our previously published ML-based algorithm, we present a predictive PMX-based algorithm (Koch et al., 2020b) that computes individual bilirubin kinetics up to 48 h. The PMX-based algorithm is intended for non-intensive care units to facilitate and optimize management of neonates with jaundice supporting clinical decisions such as 1) is an additional bilirubin measurement necessary? 2) can the neonate be discharged home? 3) can a neonate at risk for clinically relevant hyperbilirubinemia be identified early?

This manuscript has five objectives. First, we describe the development of the PMX-based algorithm. Second, we define clinically relevant scenarios, i.e., prediction up to 24 h based on one bilirubin measurement, and prediction up to 48 h based on two or more bilirubin measurements, and validate the prediction of developed PMX-based algorithm, which is the main goal of this manuscript. An appropriate external validation is a crucial step to perform predictions at the individual patient level. Third, we carry out stress test of this algorithm with increased prediction horizons up to 60 h. Fourth, we assess the sensitivity and specificity of the developed algorithm to evaluate performance relevant to clinical practice in neonatology. Further, we discuss opportunities and challenges of applying "intelligent" ML-, artificial neural networks (ANN)- and PMX-based algorithms in the field of perinatal medicine.

## METHODS

This section is structured as follows. First, we explain the magnitude of total serum bilirubin (TSB) measurement errors in clinical practice. Second, we present the study patient populations applied for development and validation of the PMX-based algorithm. Third, we describe the development of the PMX-based algorithm to characterize postnatal bilirubin kinetics. Fourth, we present the development of the PMX-based algorithm to predict individual bilirubin kinetics. Fifth, we outline the validation procedure of the developed PMX-based algorithm. Sixth, we provide information on applied software for descriptive statistics, algorithm development and validation.

### Magnitude of Total Serum Bilirubin Measurement Errors in Clinical Practice

TSB measurements are subject to considerable intra- and inter-individual variability due to biological factors and measurement

**TABLE 1 |** Key characteristics of the dataset for algorithm development (Basel, Switzerland) and validation (Regensburg, Germany). Values are presented as follows: Median [Q1, Q3] (Min, Max).

| Gestational Age (week + day) | Weight at Birth (gram) | Delivery Mode (C-section *vs.* Vaginal Delivery) | Postnatal hour of Last Bilirubin Measurement |
|---|---|---|---|
| Basel, Switzerland (342 neonates with 1,478 bilirubin values, average 4.3 values per neonate) | | | |
| 37 + 6 [34 + 1, 39 + 5] (32 + 0, 42 + 5) | 2,500 [1,950, 3,400] (1,050, 5,520) | 179 C.S. 163 Vaginal | 77 [56,124] (1, 411) |
| Regensburg, Germany (1,101 neonates, 3,081 bilirubin values, average 2.8 values per neonate) | | | |
| 38 + 2 [36 + 2, 39 + 6] (24 + 0, 42 + 2) | 3,085 [2,532, 3,580] (520, 5,015) | 620 C.S. 481 Vaginal | 87.2 [63.0, 115.3] (1, 359) |

errors related to clinical practice and laboratory measurements. Van Imhoff et al. (van Imhoff et al., 2011) showed that the inter-laboratory variability was up to a CV of 14.1%. Hence, anticipated magnitude of variability associated with TSB measurements in clinical practice is expected to be of the order of 5–15%.

## Study Patients

### Dataset for PMX-Based Algorithm Development

The dataset for model development (University Children's Hospital Basel, Basel, Switzerland) comprises TSB measurements from neonates admitted directly after birth to the neonatal unit due to varying reasons such as respiratory morbidity, birth complications, infection, mild prematurity and feeding problems. None of the neonates suffered from inherited diseases such as glucose-6-phosphate dehydrogenase (G6PDH) deficiency. All neonates included in this study had an inconspicuous neurological status, including those with values in the further course exceeding 15 mg/dl. The bilirubin measurements prior to phototherapy available in this dataset and used for model development consisted of 1,478 measurements from 342 patients, see **Table 1** for more details. All bilirubin measurements were performed as total bilirubin using an ABL800 FLEX blood gas analyzer (Radiometer Medical ApS, Denmark). The study was approved by the Institutional Review Board (EKNZ:BASEC 2018-00053).

### Dataset for External PMX-Based Algorithm Validation

The dataset for external algorithm validation (University Children's Hospital Regensburg, Hospital St. Hedwig of the Order of St. John, Regensburg, Germany) comprises TSB measurements in two clinical settings: 1) 80% healthy neonates staying with their mothers after birth until discharge home (the majority) or until admission to the neonatal unit because of significant neonatal hyperbilirubinemia or other reasons, 2) 20% neonates admitted after birth to the neonatal unit due to varying reasons such as respiratory diseases, birth complications, infection, mild prematurity and feeding problems. The goal was to apply and validate the PMX-based algorithm in these two clinical settings to cover various neonatal medical conditions and a wide range of postnatal bilirubin time courses. Some neonates suffered from blood group incompatibility; details of which were not reported. All neonates included in this study had an inconspicuous neurological status, including those with values in the further course exceeding 15 mg/dl. Of note, healthy neonates staying with their mothers after birth obtained the bilirubin check together with the mandatory metabolic screening at day 2 or 3 of life. Timing of bilirubin measurement was individualized based on medical or practical factors representing clinical workflow in a perinatal center. Bilirubin measurements prior to phototherapy in this dataset were utilized for model validation, see **Table 1** for more details. All bilirubin measurements were performed as total bilirubin utilizing a Bilimeter 3D (Pfaff medical GmbH, Germany). The study was approved by the ethics commission of the University of Regensburg (21-2,518-104).

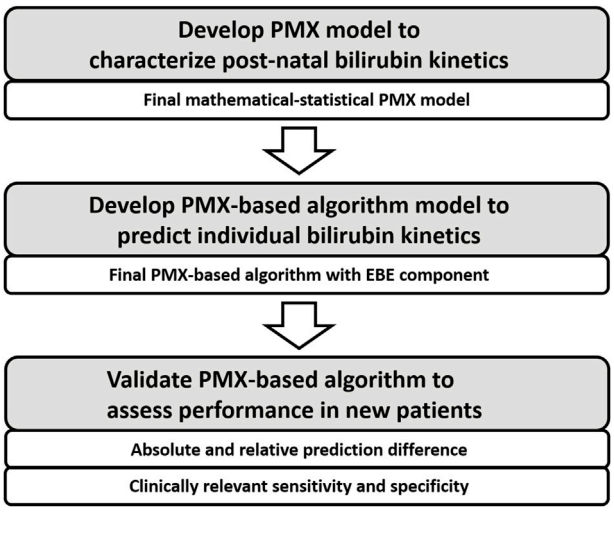


**FIGURE 1 |** Workflow of the three components for model development and validation.

## Development of PMX Model to Characterize Postnatal Bilirubin Kinetics

In this section, the development process of the PMX-based algorithm to characterize individual bilirubin kinetics is presented, compare **Figure 1**. First, develop structure of the mathematical-statistical PMX model to characterize postnatal bilirubin kinetics based on physiological mechanisms. Second, apply a non-linear mixed effects modeling approach (Lavielle, 2014) to fit the dataset for development to estimate the fixed and random effects resulting in the mathematical-statistical model.

### Structure of Mathematical Model to Characterize Bilirubin Kinetics

In healthy individuals beyond the neonatal period, most physiological processes are in an equilibrium, i.e., in balance between production and elimination. Consequently, this results

in constant bilirubin levels. For neonates shortly after birth, the equilibria of many processes are not yet reached due to maturation. Hence, bilirubin production might be increased, and elimination might be reduced during the first days of life, leading to elevated bilirubin levels. This physiological principle of bilirubin levels $B(t)$ is modeled with a differential equation consisting of a zero-order production term $k_{prod}$ and a first-order elimination term $k_{elim}$ (Dayneka et al., 1993; Koch et al., 2013; Koch and Schropp, 2018)

$$\frac{d}{dt}B(t) = k_{prod}(t,\theta,c,\beta) - k_{elim}(t,\theta,c,\beta)\cdot B(t), \quad B(0) = B^0 \tag{1}$$

where $t$ is postnatal age (PNA), $B^0$ is the initial condition (i.e., a parameter for bilirubin level at birth), $\theta$ the structural model parameters, $c$ the covariates (i.e., patient characteristics such as birth weight, gestational age and delivery mode) and $\beta$ the parameters characterizing the covariate effect on the model parameters. The detailed mathematical model structure is part of a broader active patent (Koch et al., 2020b) where more information on **Eq. (1)** can be found. The structural model parameters are summarized in

$$\Theta = (\theta, B^0).$$

### Data Fitting and Development of Mathematical-Statistical Model

The non-linear mixed effects modeling approach was applied for data fitting and parameter estimation. Briefly, structural model parameters have a population value $\Theta_{pop}$ (also called fixed effect or typical value) describing the average patient in the population. To characterize an individual neonate in the population, individual model parameters are drawn from a normal distribution with covariance matrix $\Omega$ (called random effects). The normal distribution is further transformed to a log-normal distribution to allow log-normally distributed individual model parameters, see (Lavielle, 2014) for more technical details. In addition, the parameter $\beta$ characterizing covariate effects is estimated. Typically, only covariate effects that show 1) a statistically significant effect, 2) a reduced objective function value, 3) a reduced variability of the random effects, and 4) are clinically relevant and routinely available in clinical practice, are included. Finally, the developed mathematical-statistical model is given by **Eq. (1)** together with fixed and random effects

$$\rho = \left(\Theta_{pop}, \Omega, \beta\right) \tag{2}$$

## Development of PMX-Based Algorithm to Predict Individual Bilirubin Kinetics

In this section, the development process of the PMX-based algorithm to predict individual bilirubin kinetics is presented, compare **Figure 1**. The final PMX-based algorithm with an Empirical Bayesian Estimation (EBE) component is applied to predict the individual bilirubin kinetics for a new patient.

### Final PMX-Based Algorithm to Predict Individual Bilirubin Kinetics

The mathematical-statistical model defined by (**Eqs 1**, **2**) is the final (trained) model based on the dataset applied for development. To predict the bilirubin kinetics for a new patient, EBE, also known as Maximum A Posteriori Estimation (Bassett and Deride, 2019), is applied. The EBE utilizes **Eq. (1)** and the prior information stored in $\rho$ **Eq. (2)** about the population applied for model development and training, and estimates the individual model parameters $\hat{\Theta}_i$ for a new patient by minimizing

$$\hat{\Theta}_i = \text{argmin}\left\{-2\log p\left(\Theta_i | w_i; \rho\right)\right\} \tag{3}$$

based on the new individual bilirubin measurements $w_i$ and patient characteristics. These estimated individual model parameters $\hat{\Theta}_i$ are then utilized to perform the individual prediction of bilirubin kinetics.

### Implementation of PMX-Based Algorithm

Model development was performed in the NLME software The Monolix Suite 2020 (Lixoft, Orsay, France). Since The Monolix Suite 2020 is a commercial software that does not allow application in app- or web-based tools, the developed mathematical-statistical model (**Eqs 1**, **2**) and the EBE **Eq. (3)** was re-implemented in Matlab 2021 (MathWorks, Natick, MA, USA).

## Validation of PMX-Based Algorithm

In this section, the application and validation of the PMX-based algorithm is presented. First, definitions of the different validation scenarios and some input rules are shown. Second, validation metrics are given, including the absolute und relative prediction difference as well as clinically relevant sensitivity and specificity, compare **Figure 1**. Third, the construction of validation datasets is briefly discussed.

### Definition of Validation Scenarios and Input Rules

In the following, clinically relevant validation scenarios are defined for prediction horizons up to 24 and 48 h. To provide a *stress test* for the PMX-based algorithm, additional validation scenarios with longer prediction horizons were also included.

#### *Definition of Validation Scenario 1: Prediction up to 24 h Based on One TSB Measurement*

PMX-based algorithm predicts for one TSB measurement the bilirubin kinetics for up to 24 h with respect to the time point of the measurement.

#### *Definition of Validation Scenario 2a: Prediction up to 48 h Based on Two TSB Measurements*

PMX-based algorithm predicts for two TSB measurements the bilirubin kinetics for up to 48 h with respect to the time point of the second measurement.

### *Definition of Validation Scenario 2b: Prediction up to 48 h Based on Two or More TSB Measurements*

PMX-based algorithm predicts for two or more TSB measurements the bilirubin kinetics for up to 48 h with respect to the time point of the last measurement.

### *Definition of Stress Test Scenarios With Longer Prediction Horizon*

The prediction horizon for one TSB measurement (validation scenario 1) was extended by an additional 6 h, i.e., for a total prediction of up to 30 h. The prediction horizon for two, (validation scenario 2a), or two or more (validation scenario 2b) TSB measurements were extended by an additional 12 h, i.e., for a total prediction of up to 60 h.

### *Definition of Input Rules Regarding Postnatal Age*

The time point of the first TSB measurement must be between ≥ 8 and ≤ 72 h of PNA. All further time points of TSB measurements must be between ≥ 24 and ≤ 96 h of PNA. The PNA distance between successive measurements must be ≥ 8 h.

## Definition of Validation Metrics

### *Definition of Absolute Prediction Difference and Relative Prediction Difference*

The absolute prediction difference (p.d.) between predicted bilirubin level $B_{pred}$ and measured (observed) bilirubin level $B_{obs}$ was defined as

$$p.d. = \left| B_{pred} - B_{obs} \right| \tag{4}$$

The relative (absolute) prediction difference (r.p.d.) in percent was defined as

$$r.p.d. = \frac{\left| B_{pred} - B_{obs} \right|}{B_{obs}} \cdot 100 \tag{5}$$

### *Definition of Clinically Relevant Sensitivity and Specificity*

For validation, e.g., of diagnostic tests and algorithms with a binary outcome, statistical measures such as sensitivity and specificity are essential. As such we define these performance measures for our developed PMX-based algorithm in the context of a clinically relevant bilirubin threshold in neonatology. The phototherapy limit for the most vulnerable late preterm and term born neonates is 15 mg/dl (equals to 250 µmol/l) when older than 72 h (Bhutani, 2011). As such this bilirubin level has been set as the threshold to evaluate the performance of the PMX-based predictive algorithm. It should be noted that a bilirubin level > 250 µmol/l is considered clinically relevant, requiring appropriate monitoring and management. Moreover, for a neonate with hyperbilirubinemia, an under-prediction with a value below the threshold would possibly lead to inadequate therapeutic management depending on the magnitude of under-prediction. Taking into account variability in the prediction, e.g., caused by measurement errors, an acceptance range for the prediction difference $B_{pred} - B_{obs}$ is defined by applying the Bland-Altman method (Altman and Bland, 1983) with 5th and 95th percentile of the standard normal distribution (corresponding to 90% limits of agreement):

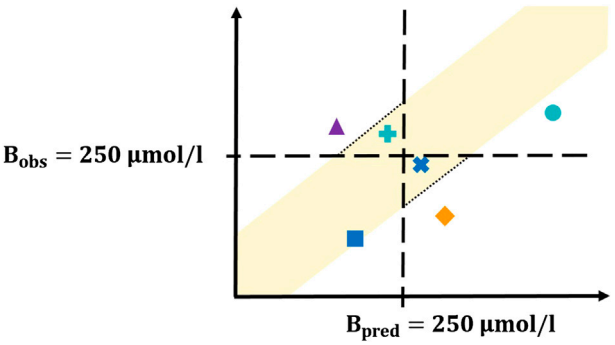


**FIGURE 2 |** Concept plot for sensitivity/specificity calculation. The four different colors correspond to the four possible test results. The yellow shaded area corresponds to the acceptance range, the turquoise dot and plus represent the true positives, the blue square and cross display the true negatives, the orange diamond corresponds to the false positives and the purple triangle represents the false negatives. Detailed explanation is provided in the main text.

$$acceptance\ range = \left[ MW_{diff} - 1.6449 \cdot SD_{diff},\ MW_{diff} + 1.6449 \cdot SD_{diff} \right]$$

where $MW_{diff}$ is the mean of the prediction differences, and $SD_{diff}$ is the standard deviation of the prediction differences.

This defines a criterion for clinically interchangeably measurements and allows for characterizing accepted true positives or accepted true negatives, respectively.

The following terms are defined:

1) True positive: Neonate with hyperbilirubinemia (i.e., observed bilirubin level > 250 µmol/l) either with a predicted bilirubin level > 250 µmol/l or with both a predicted bilirubin level ≤ 250 µmol/l and a prediction difference within the acceptance range (accepted true positive)
2) True negative: Neonate without hyperbilirubinemia (i.e., observed bilirubin level ≤ 250 µmol/l) either with a predicted bilirubin level ≤ 250 µmol/l or with both a predicted bilirubin level > 250 µmol/l and a prediction difference within the acceptance range (accepted true negative)
3) False positive: Neonate without hyperbilirubinemia with a predicted bilirubin level > 250 µmol/l but with a prediction difference above the upper limit of the acceptance range
4) False negative: Neonate with hyperbilirubinemia with a predicted bilirubin level ≤ 250 µmol/l but with a prediction difference below the lower limit of the acceptance range

Based on these terms, sensitivity and specificity measures were calculated. The four situations (test results) (i)-(iv) are conceptually visualized in **Figure 2** and explained in the following. The black dashed horizontal and vertical lines

correspond to a bilirubin level of 250 µmol/l. The yellow shaded area displays the acceptance range. Situation (i), the area of true positives, is shown with turquoise shapes. The dot represents a neonate with hyperbilirubinemia with $B_{pred} > 250$ µmol/l and the plus represents a neonate with hyperbilirubinemia with $B_{pred} \leq 250$ µmol/l but with a prediction difference in the acceptance range, indicated by the black dotted line. For the true negatives, situation (ii), the analogous situation is given in blue. The square corresponds to a neonate without hyperbilirubinemia with $B_{pred} \leq 250$ µmol/l and the cross corresponds to a neonate without hyperbilirubinemia with $B_{pred} > 250$ µmol/l but with a prediction difference within the acceptance range, again indicated by the black dotted line. The two remaining situations are the false positives, situation (iii), displayed with orange diamonds, and the false negatives, situation (iv), displayed with purple triangles.

### Construction of Validation Datasets

The initial number of neonates in the validation dataset was $n$ = 1,101. After deletion of patients with exactly one bilirubin measurement and patients with partially missing values, n = 892 neonates were available for the validation data set.

#### *Construction of Validation Datasets for One Measurement (Scenario 1) With Prediction Horizon up to 24 h*

From the $n$ = 892 neonates, eligible neonates for this scenario were selected as follows. The first bilirubin measurement served as user input based on the input rules regarding PNA. Time point of the second measurement was tested to determine whether it fulfills the ≤24 h PNA distance with respect to the first measurement. If yes, all additional measurements were deleted, and this neonate is identified as eligible for the validation dataset, if, in addition all other input rules are met as well. This resulted in a validation dataset which consists of $n$ = 236 neonates. Please note that the second measurement is the bilirubin level that will be predicted. In addition, a stress test validation dataset with a prediction horizon up to 30 h instead of 24 h was similarly constructed resulting in $n$ = 387 neonates.

#### *Construction of Validation Datasets for Two (Scenario 2a) and Two or More (Scenario 2b) Measurements With Prediction Horizon up to 48 h*

In these scenarios, only neonates with three or more measurements were eligible. Construction of validation datasets was a step-by-step procedure. First, the PNA distance between the second and the last measurement was computed. Second, if this PNA distance fulfills ≤48 h, then this measurement was selected to be predicted. If the PNA distance is larger, the last measurement was rejected and the PNA distance between the second and the second last measurement was computed, and the procedure was repeated. For the validation datasets with two bilirubin measurements, all measurements between the second and the measurement selected to be predicted were deleted. For the validation datasets with two or more bilirubin measurements, these values were kept. Finally, all input rules were tested and neonates that do not fulfill the input rules were deleted. The final validation sets for scenario 2a (two bilirubin measurements) consist of $n$ = 119 neonates and for scenario 2b (two or more bilirubin measurements) consist of $n$ = 111 neonates. The stress test validation datasets for two or two or more bilirubin measurements with a prediction horizon up to 60 h was constructed with a similar procedure resulting in $n$ = 132 and $n$ = 122 neonates, respectively.

## Software Applied for Descriptive Statistics, Algorithm Development and Validation

Descriptive statistical analysis was carried out in R 3.6.0 (R core team, Vienna, Austria). Non-linear mixed effects modeling for model development was performed in The Monolix Suite 2020 (Lixoft, Orsay, France). Construction of validation datasets was performed in R. Model validation was conducted in Matlab 2021 (MathWorks, Natick, MA, USA). A-posteriori data visualization was implemented in R and Matlab.

# RESULTS

This section is structured as follows. First, results of the PMX-based algorithm development is presented. Second, results of the external validation are shown.

## Development of PMX-Based Algorithm to Predict Individual Bilirubin Kinetics

Development of the PMX-based algorithm to predict individual bilirubin kinetics is presented. First, results regarding data fitting and model parameter estimation are briefly given. Second, the verification of the EBE implementation in Matlab is shown.

### Data Fitting and Model Parameter Estimation (Fixed and Random Effects)

The mathematical model **Eq. (1)** was fitted to the dataset for model development resulting in estimates for the fixed and random effects, as well as covariate effects **Eq. (2)**. Several covariates such as gestational age, sex, delivery mode, Apgar scores, arterial pH, weight (at birth and progression), hemoglobin, sodium, hematocrit, feeding (formula, mother milk), Rh blood group system and blood type of mother and neonate, and maternal factors were tested, compare (Daunhawer et al., 2019) and see **Supplementary Table S1** in the supplemental material for more details. Weight at birth (continuous), gestational age (continuous) and delivery mode (categorical) were statistically significant covariates and included in the final model with typical PMX covariate approaches. The observation vs. prediction plot of the mathematical-statistical model (**Eqs 1**, **2**) with dataset for model development is shown in **Figure 3.**

### Verification of EBE Implementation in Matlab

To verify the EBE implementation in Matlab, each individual neonate from the dataset for model development was re-fitted in Matlab and individual model parameter estimates were

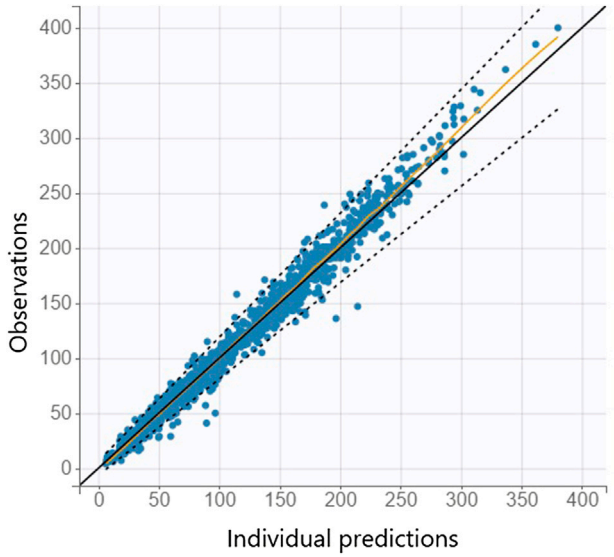


**FIGURE 3 |** Individual observation vs. prediction plot is shown from the mathematical-statistical model based on the dataset for model development where the orange line indicates the spline and dashed lines the 90% prediction interval.

compared with the results from *Monolix*. Since the model parameters have different magnitudes, the percent difference over all model parameters was calculated. Comparison of model parameters obtained from Monolix and Matlab showed a median maximal discrepancy of 0.48% caused by non-identical, but structurally similar numerical algorithms applied in both software programs, as well as internal tolerances and termination criteria settings.

## External Validation of the PMX-Based Algorithm

Results of the external validation for scenarios 1, 2a, and 2b as well as the stress test validation are presented as follows. In **Table 2**, median of the relative (absolute) prediction difference, median of the absolute prediction difference, and the sensitivity and specificity are shown. Observation versus prediction plots for scenario 1 (one measurement with prediction horizon up to 24 h) and scenario 2a (two measurements with prediction horizon up to 48 h) are shown in **Figure 4**.

# DISCUSSION

As perinatal medicine is undergoing a fundamental change transforming towards a modern data-driven patient-oriented approach new tools that will predict the dynamics of biomarkers for an individual fetus or newborn will become increasingly important in maternal, neonatal and perinatal care. We developed PMX-based algorithms to optimize and individualize dosing of therapeutics in the field of perinatal medicine (Wilbaux et al., 2016a; Wilbaux et al., 2016b; Koch et al., 2017; Nekka et al., 2017; van Donge et al., 2018; Dallmann et al., 2019; van Donge et al., 2019; Wilbaux et al., 2019; van Donge et al., 2020a; van Donge et al., 2020b; Koch et al., 2020c; Dao et al., 2020; Samiee-Zafarghandy et al., 2022). It is time to go beyond classical pharmacological applications and develop algorithms condensing the wealth of clinical data and physiology knowledge into predictive tools coping with the dynamics of biomarkers for an individual fetus or neonate.

These tools can be developed based on various methods, such as PMX-based mathematical-statistical computer models, machine learning (ML) or other artificial intelligence (AI) methods such as artificial neural networks (ANNs). In the following, PMX, ML and ANN approaches are discussed with focus on our perinatal case study.

The undisputed major advantage of ML methods is its computational efficiency in handling big data (Koch et al., 2020a). Large amounts of input features can be processed regarding its relationship with a dependent variable, e.g., a labeled (supervised) binary outcome. On one hand this allows large amounts of input features to be screened, e.g., patient characteristics, for their relevance, but on the other hand the ML-based tool is solely data-driven. Recently, we developed a ML-based tool to predict the probability whether a neonate will need a phototherapy treatment or not within the next 48 h (Daunhawer et al., 2019). Almost 50 features were screened resulting in a relevant subset of only four, which suffices for a strong predictive performance (Daunhawer et al., 2019). Although such ML-based tool provides an innovative risk assessment regarding phototherapy requirement, it does not predict the dynamics of bilirubin kinetics. In addition, ML methods are not pre-destined to represent physiological mechanisms. Hence, we consider ML as a powerful tool e.g., in pre-screening large amounts of input features and in developing diagnostic tools where dynamic aspects of the dependent variable are not of primary importance.

**TABLE 2 |** For each scenario (including the stress tests), the median of relative (absolute) prediction difference (r.p.d.) **Eq. (5)**, the median of absolute prediction difference (p.d) **Eq. (4)**, and the sensitivity and specificity are presented.

| Scenario | Median of r.p.d. in Percent (%) | Median of p.d. mg/dl (μmol/l) | Sensitivity/Specificity | Prediction Horizon |
|---|---|---|---|---|
| Scenario 1 (one TSB meas.) | 8.5% | 1.0 mg/dl (17.4 μmol/l) | 95.7%/96.3% | Up to 24 h |
| Scenario 1 (one TSB meas. stress test) | 7.9% | 0.9 mg/dl (15.7 μmol/l) | 92.5%/97.5% | Up to 30 h |
| Scenario 2a (two TSB meas.) | 9.2% | 1.3 mg/dl (21.5 μmol/l) | 93.0%/92.1% | Up to 48 h |
| Scenario 2a (two TSB meas. stress test) | 9.9% | 1.3 mg/dl (22.3 μmol/l) | 91.7%/94.0% | Up to 60 h |
| Scenario 2b (two or more TSB meas.) | 8.8% | 1.2 mg/dl (20.5 μmol/l) | 94.6%/93.2% | Up to 48 h |
| Scenario 2b (two or more TSB meas. stress test) | 9.3% | 1.3 mg/dl (21.8 μmol/l) | 92.7%/93.8% | Up to 60 h |

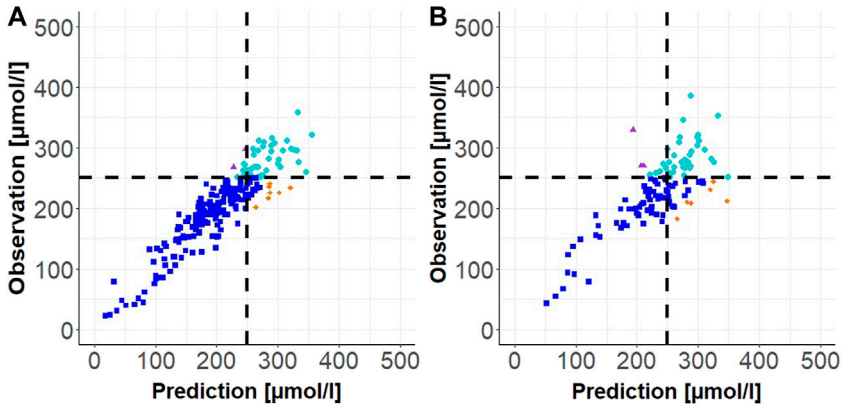


**FIGURE 4 |** Individual observation vs. prediction plot for Scenario 1 (one TSB measurement) in **(A)** and for Scenario 2a (two TSB measurements) in **(B)**. The dashed black lines correspond to the phototherapy limit of 250 $\mu$mol/l; turquoise dots display true positives, blue squares display true negatives, orange diamonds display false positives and purple triangles display false negatives.

AI methods, such as ANNs, have become popular to analyze data from various fields as ANNs can approximate any function up to a certain accuracy (Hornik et al., 1989). At first glance, this sounds like the perfect tool to learn any kind of behavior. Although this is true in theory, an ANN is solely data-driven, i.e., anything the ANN will learn arises from the analysis dataset which can have essential fundamental consequences. An enormous amount of data may be required covering all possible situations. What ANNs do not see, will not be learned, and may not be accurately predicted. Another issue with ANNs is its black-box property, which makes it almost impossible to understand why a trained ANN looks the way it does. This in turn can limit acceptance of ANN-based algorithms by care givers in clinical practice.

The developed PMX-based algorithm presented in this paper includes known physiology-based, biological, and clinical facts (Bonate, 2006; Koch et al., 2013; Gabrielsson, 2017). As an example, neonates undergo strong maturation processes during the first days and even weeks of life. We think it is "intelligent" to incorporate such scientific, medical understanding into our computer models. Our PMX-based algorithm predicts bilirubin kinetics over time up to 48 h. Hence, not only an answer for a specific question is available for the clinician (Koch et al., 2020a), but the entire bilirubin kinetics is revealed and provided. In addition, due to the availability of the predicted bilirubin kinetics, different clinical end points of interest can be defined in an a-posteriori step, e.g., prediction up to 24 h, 48 h or even longer prediction horizons, as presented in this paper. Moreover, clinically relevant binary end points such as prediction above or below a certain threshold, can be defined, as presented in the sensitivity and specificity computations.

Discussed PMX-, ML- and ANN-based methods have in common that an external validation, i.e., a dataset from another medical center, is necessary before application in clinical practice. The major goal of this paper was to present an external validation of the PMX-based algorithm based on a dataset that was not available during algorithm development. In addition to typical validation procedures in pharmacometrics (Lavielle, 2014), we applied the statistical concept of sensitivity and specificity for the external validation of the PMX-based algorithm. This is to demonstrate that one can translate PMX-based algorithms that forecast dynamics of biomarker responses or disease progression into simplified algorithms that predict a binary outcome.

The developed, predictive PMX-based algorithm was applied in two different clinically relevant scenarios in neonatology. In the first scenario, bilirubin kinetics is predicted up to 24 h into the future based on a single bilirubin measurement with a median relative (absolute) prediction difference of 8.5% (median absolute prediction difference 17.4 µmol/l), and sensitivity and specificity of 95.7 and 96.3%, respectively. In the second scenario, bilirubin kinetics is predicted up to 48 h into the future based on two bilirubin measurements with a median relative (absolute) prediction difference of 9.2% (median absolute prediction difference 21.5 µmol/l), and sensitivity and specificity of 93.0 and 92.1%, respectively. Moreover, a scenario with two or more bilirubin measurements and various stress tests based on increasing the prediction horizon were also performed. In all these cases, similar values regarding the applied validation metrics were obtained.

Recently, the PMX-based algorithm has even been validated with three additional external, independent datasets: 1) clinical dataset from Greece consisting of neonates with transcutaneous bilirubin (TcB) measurements only, 2) clinical dataset from Germany consisting of neonates with TSB only, TcB only, or combinations of TSB and TcB measurements, and 3) clinical dataset from Kenya, Africa, consisting of neonates with TSB and TcB measurements. Results from these additional external validation studies will be published in the near future.

Until now, best practice has been to plot measured bilirubin values to given nomograms in a paper or electronic-based fashion to identify the current level of patients' jaundice status. Then, for estimating individual risk of a given neonate and to provide a recommendation for next measures, including further bilirubin controls or specific therapy management steps, various clinical

parameters need to been considered by the responsible health care provider. As long as the neonatal patient is hospitalized anyway there is only the medical challenge. In contrast, once there is no other reason for keeping the patient in hospital or the patient is already in the outpatient service, clinical decision making becomes even more demanding as additional organizational, economic and legal challenges may arise (Brown et al., 2021). However, there are no randomized and quasi-randomized studies available specifically addressing bilirubin therapy, namely home-versus hospital-based phototherapy (Malwade and Jardine, 2014).

Our intelligent PMX-based algorithm for prediction of bilirubin kinetics is based on differential equations that characterize maturation processes and other balance properties and are then trained and validated on large datasets. PMX-based algorithms can complement "artificial intelligence" such as ML- and ANN-based approaches in perinatal medicine. PMX-based algorithms leverage and integrate scientific, medical knowledge with intelligent learning from clinical data. Our developed intelligent algorithm for bilirubin level prediction will be incorporated in a clinical decision support tool with the goal to further optimize and individualize treatment of preterm and term neonates, our most vulnerable patients. The presented case of hyperbilirubinemia illustrates the potential of intelligent, predictive ML-, ANN- or PMX-based algorithms in neonatology.

There are numerous opportunities for such clinical decision support tools to further enhance and personalize care of mothers and their unborn and born children. Neonatal jaundice is just one of many medical conditions affecting newborn babies. There are many other diseases in fetuses, neonates and their mothers rooted in the specific dynamics of pregnancy and transition from intra-uterine to extra-uterine life (Evers and Wellmann, 2016). In contrast to adult medicine where health is defined as a continuum and the absence of physical and mental degradation, in perinatal medicine, health is a matter of cycles, growth, development and maturation processes. As such intelligent algorithms and tools designed for predicting medical conditions in perinatal medicine must address these specific properties.

## DATA AVAILABILITY STATEMENT

The raw data supporting the conclusions of this article will be made available by the authors, without undue reservation.

## ETHICS STATEMENT

The studies involving human participants were reviewed and approved by University of Basel (EKNZ:BASEC 2018-00053) and University of Regensburg (21-2518-104). Written informed consent to participate in this study was provided by the participants' legal guardian/next of kin.

## AUTHOR CONTRIBUTIONS

Participated in research design and data collection: SK, KS, MP, and SW. Performed data analysis: GK, MW, BS, and MP. Wrote or contributed to the writing of the manuscript: GK, BS, SW, and MP.

## SUPPLEMENTARY MATERIAL

The Supplementary Material for this article can be found online at: https://www.frontiersin.org/articles/10.3389/fphar.2022.842548/full#supplementary-material

## REFERENCES


Alkén, J., Håkansson, S., Ekéus, C., Gustafson, P., and Norman, M. (2019). Rates of Extreme Neonatal Hyperbilirubinemia and Kernicterus in Children and Adherence to National Guidelines for Screening, Diagnosis, and Treatment in Sweden. *JAMA Netw. Open* 2 (3), e190858. doi:10.1001/jamanetworkopen.2019.0858

Altman, D. G., and Bland, J. M. (1983). Measurement in Medicine: the Analysis of Method Comparison Studies. *Statistician* 32 (3), 307–317. doi:10.2307/2987937

Bassett, R., and Deride, J. (2019). Maximum A Posteriori Estimators as a Limit of Bayes Estimators. *Math. Program.* 174, 129–144. doi:10.1007/s10107-018-1241-0

Bhutani, V. K. (2011). Phototherapy to Prevent Severe Neonatal Hyperbilirubinemia in the Newborn Infant 35 or More Weeks of Gestation. *Pediatrics* 128 (4), e1046–52. doi:10.1542/peds.2011-1494

Bonate, P. (2006). *Pharmacokinetic-pharmacodynamic Modeling and Simulation*. New York: Springer.

Brown, S., Small, R., Faber, B., Krastev, A., and Davis, P. (2021). Early Postnatal Discharge from Hospital for Healthy Mothers and Term Infants. *Cochrane Database Syst. Rev.* 6, CD002958. doi:10.1002/14651858.CD002958

Castillo, A., Grogan, T. R., Wegrzyn, G. H., Ly, K. V., Walker, V. P., and Calkins, K. L. (2018). Umbilical Cord Blood Bilirubins, Gestational Age, and Maternal Race Predict Neonatal Hyperbilirubinemia. *PLoS One* 13 (6), e0197888. doi:10.1371/journal.pone.0197888

Dallmann, A., van den Anker, J., Pfister, M., and Koch, G. (2019). Characterization of Maternal and Neonatal Pharmacokinetic Behavior of Ceftazidime. *J. Clin. Pharmacol.* 59 (1), 74–82. doi:10.1002/jcph.1294

Dao, K., Guidi, M., André, P., Giannoni, E., Basterrechea, S., Zhao, W., et al. (2020). Optimisation of Vancomycin Exposure in Neonates Based on the Best Level of Evidence. *Pharmacol. Res.* 154, 104278. doi:10.1016/j.phrs.2019.104278

Daunhawer, I., Kasser, S., Koch, G., Sieber, L., Cakal, H., Tütsch, J., et al. (2019). Enhanced Early Prediction of Clinically Relevant Neonatal Hyperbilirubinemia with Machine Learning. *Pediatr. Res.* 86 (1), 122–127. doi:10.1038/s41390-019-0384-x

Dayneka, N. L., Garg, V., and Jusko, W. J. (1993). Comparison of Four Basic Models of Indirect Pharmacodynamic Responses. *J. Pharmacokinet. Biopharm.* 21 (4), 457–478. doi:10.1007/BF01061691

Dennery, P. A., Seidman, D. S., and Stevenson, D. K. (2001). Neonatal Hyperbilirubinemia. *N. Engl. J. Med.* 344 (8), 581–590. doi:10.1056/NEJM200102223440807

Evers, K. S., and Wellmann, S. (2016). Arginine Vasopressin and Copeptin in Perinatology. *Front. Pediatr.* 4, 75. doi:10.3389/fped.2016.00075

Gabrielsson, M. D. W. (2017). *Pharmacokinetic and Pharmacodynamic Data Analysis*. 5 ed. Sweden: Swedish Pharmaceutical Press.

Han, S., Yu, Z., Liu, L., Wang, J., Wei, Q., Jiang, C., et al. (2015). A Model for Predicting Significant Hyperbilirubinemia in Neonates from China. *Pediatrics* 136 (4), e896–905. doi:10.1542/peds.2014-4058

Hornik, K., Stinchcombe, M., and White, H. (1989). Multilayer Feedforward Networks Are Universal Approximators. *Neural Netw.* 2, 359–366. doi:10.1016/0893-6080(89)90020-8

Koch, G., Pfister, M., Daunhawer, I., Wilbaux, M., Wellmann, S., and Vogt, J. E. (2020a). Pharmacometrics and Machine Learning Partner to Advance Clinical Data Analysis. *Clin. Pharmacol. Ther.* 107 (4), 926–933. doi:10.1002/cpt.1774

Koch, G., Schönfeld, N., Jost, K., Atkinson, A., Schulzke, S. M., Pfister, M., et al. (2020c). Caffeine Preserves Quiet Sleep in Preterm Neonates. *Pharmacol. Res. Perspect.* 8 (3), e00596. doi:10.1002/prp2.596

Koch, G., and Schropp, J. (2018). Delayed Logistic Indirect Response Models: Realization of Oscillating Behavior. *J. Pharmacokinet. Pharmacodyn.* 45 (1), 49–58. doi:10.1007/s10928-017-9563-8

Koch, G., and Schropp, J. (2013). "Mathematical Concepts in Pharmacokinetics and Pharmacodynamics with Application to Tumor Growth," in *Nonautonomous Dynamical Systems in the Life Sciences*. Editors P. Kloeden and C. Pötzsche (Switzerland: Sprinter International). doi:10.1007/978-3-319-03080-7_7

Koch, G., Schropp, J., and Pfister, M. (2017). Facilitate Treatment Adjustment after Overdosing: Another Step toward 21st-Century Medicine. *J. Clin. Pharmacol.* 57 (6), 704–711. doi:10.1002/jcph.852

Koch, G., Wellmann, S., Pfister, M., Kasser, S., and Wilbaux, M. (2020b). *Method and Computer Program for Predicting Bilirubin Levels in Neonates*. European Patent Office, EP3688473B1. Patent.

Lavielle, M. (2014). *Mixed Effects Models for the Population Approach: Models, Tasks, Methods and Tools*. Boca Raton, London, New York: Chapman & Hall.

Malwade, U. S., and Jardine, L. A. (2014). Home- versus Hospital-Based Phototherapy for the Treatment of Non-haemolytic Jaundice in Infants at More Than 37 Weeks' Gestation. *Cochrane Database Syst. Rev.* 6 (6), CD010212. doi:10.1002/14651858.CD010212

Mangold, C., Zoretic, S., Thallapureddy, K., Moreira, A., Chorath, K., and Moreira, A. (2021). Machine Learning Models for Predicting Neonatal Mortality: A Systematic Review. *Neonatology* 118 (4), 394–405. doi:10.1159/000516891

Nekka, F., Csajka, C., Wilbaux, M., Sanduja, S., Li, J., and Pfister, M. (2017). Pharmacometrics-based Decision Tools Facilitate mHealth Implementation. *Expert Rev. Clin. Pharmacol.* 10 (1), 39–46. doi:10.1080/17512433.2017.1251837

Rajkomar, A., Dean, J., and Kohane, I. (2019). Machine Learning in Medicine. *N. Engl. J. Med.* 380 (14), 1347–1358. doi:10.1056/NEJMra1814259

Samiee-Zafarghandy, S., van Donge, T., Fusch, G., Pfister, M., Jacob, G., Atkinson, A., et al. (2022). Novel Strategy to Personalise Use of Ibuprofen for Closure of Patent Ductus Arteriosus in Preterm Neonates. *Arch. Dis. Child.* 107 (1), 86–91. doi:10.1136/archdischild-2020-321381

Sampurna, M. T. A., Ratnasari, K. A., Etika, R., Hulzebos, C. V., Dijk, P. H., Bos, A. F., et al. (2018). Adherence to Hyperbilirubinemia Guidelines by Midwives, General Practitioners, and Pediatricians in Indonesia. *PLoS One* 13 (4), e0196076. doi:10.1371/journal.pone.0196076

Schiltz, N. K., Finkelstein Rosenthal, B., Crowley, M. A., Koroukian, S. M., Nevar, A., Meropol, S. B., et al. (2014). Rehospitalization during the First Year of Life by Insurance Status. *Clin. Pediatr. (Phila)* 53 (9), 845–853. doi:10.1177/0009922814536924

So, V., and Khurshid, F. (2021). Treatment Practices and Implementation of Guidelines for Hyperbilirubinemia and Rebound Hyperbilirubinemia. *J. Neonatal Perinat. Med.* 15 (2), 335–343. doi:10.3233/NPM-210781

Tartaglia, K. M., Campbell, J., Shaniuk, P., and McClead, R. E. (2013). A Quality Project to Improve Compliance with AAP Guidelines for Inpatient Management of Neonatal Hyperbilirubinemia. *Hosp. Pediatr.* 3 (3), 251–257. doi:10.1542/hpeds.2012-0103

van Donge, T., Bielicki, J. A., van den Anker, J., and Pfister, M. (2018). Key Components for Antibiotic Dose Optimization of Sepsis in Neonates and Infants. *Front. Pediatr.* 6, 325. doi:10.3389/fped.2018.00325

van Donge, T., Evers, K., Koch, G., van den Anker, J., and Pfister, M. (2020). Clinical Pharmacology and Pharmacometrics to Better Understand Physiological Changes during Pregnancy and Neonatal Life. *Handb. Exp. Pharmacol.* 261, 325–337. doi:10.1007/164_2019_210

van Donge, T., Fuchs, A., Leroux, S., Pfister, M., Rodieux, F., Atkinson, A., et al. (2020). Amoxicillin Dosing Regimens for the Treatment of Neonatal Sepsis: Balancing Efficacy and Neurotoxicity. *Neonatology* 117 (5), 1–9. doi:10.1159/000509751

van Donge, T., Samiee-Zafarghandy, S., Pfister, M., Koch, G., Kalani, M., Bordbar, A., et al. (2019). Methadone Dosing Strategies in Preterm Neonates Can Be Simplified. *Br. J. Clin. Pharmacol.* 85 (6), 1348–1356. doi:10.1111/bcp.13906

van Imhoff, D. E., Dijk, P. H., Weykamp, C. W., Cobbaert, C. M., Hulzebos, C. V., and Group, B. A. S. (2011). Measurements of Neonatal Bilirubin and Albumin Concentrations: a Need for Improvement and Quality Control. *Eur. J. Pediatr.* 170 (8), 977–982. doi:10.1007/s00431-010-1383-4

Watchko, J. F., and Tiribelli, C. (2013). Bilirubin-induced Neurologic Damage-Mmechanisms and Management Approaches. *N. Engl. J. Med.* 369 (21), 2021–2030. doi:10.1056/NEJMra1308124

Wilbaux, M., Fuchs, A., Samardzic, J., Rodieux, F., Csajka, C., Allegaert, K., et al. (2016). Pharmacometric Approaches to Personalize Use of Primarily Renally Eliminated Antibiotics in Preterm and Term Neonates. *J. Clin. Pharmacol.* 56 (8), 909–935. doi:10.1002/jcph.705

Wilbaux, M., Kasser, S., Gromann, J., Mancino, I., Coscia, T., Lapaire, O., et al. (2019). Personalized Weight Change Prediction in the First Week of Life. *Clin. Nutr.* 38 (2), 689–696. doi:10.1016/j.clnu.2018.04.001

Wilbaux, M., Kasser, S., Wellmann, S., Lapaire, O., van den Anker, J. N., and Pfister, M. (2016). Characterizing and Forecasting Individual Weight Changes in Term Neonates. *J. Pediatr.* 173, 101–e10. doi:10.1016/j.jpeds.2016.02.044

**Conflict of Interest:** GK, BS, SW, and MP are part-time employed by NeoPrediX.

The remaining authors declare that the research was conducted in the absence of any commercial or financial relationships that could be construed as a potential conflict of interest.

**Publisher's Note:** All claims expressed in this article are solely those of the authors and do not necessarily represent those of their affiliated organizations, or those of the publisher, the editors and the reviewers. Any product that may be evaluated in this article, or claim that may be made by its manufacturer, is not guaranteed or endorsed by the publisher.

# Advantages of publishing in Frontiers

**OPEN ACCESS**
Articles are free to read for greatest visibility and readership

**FAST PUBLICATION**
Around 90 days from submission to decision

**HIGH QUALITY PEER-REVIEW**
Rigorous, collaborative, and constructive peer-review

**TRANSPARENT PEER-REVIEW**
Editors and reviewers acknowledged by name on published articles

**Frontiers**
Avenue du Tribunal-Fédéral 34
1005 Lausanne | Switzerland

**Visit us:** www.frontiersin.org
**Contact us:** frontiersin.org/about/contact

**REPRODUCIBILITY OF RESEARCH**
Support open data and methods to enhance research reproducibility

**DIGITAL PUBLISHING**
Articles designed for optimal readership across devices

**FOLLOW US**
@frontiersin

**IMPACT METRICS**
Advanced article metrics track visibility across digital media

**EXTENSIVE PROMOTION**
Marketing and promotion of impactful research

**LOOP RESEARCH NETWORK**
Our network increases your article's readership